Molecular heterogeneity of rodent and human histamine H and H receptors

Shenton, Fiona C.

A thesis submitted to Durham University in accordance with the requirements for the degree of Doctor of Philosophy March 2007

Molecular Heterogeneity of Rodent and Human Histamine H_3 and H_4 Receptors

Fiona C. Shenton

School of Biological and Biomedical Sciences

Durham University

ABSTRACT

Histamine receptors H_3 and H_4 are classic G-protein coupled receptors (GPCRs) and are potential therapeutic targets for a number of CNS pathologies and inflammatory diseases, respectively. They are highly related both in terms of protein sequence and gene structure, and are likely to share key molecular pharmacological features. Pharmacological heterogeneity between and within species has hindered efforts to bring H_3R directed drugs to the clinic. Possible mechanisms underlying this variability are the subject of these investigations. Current opinion on GPCRs suggests that many function as obligate dimers or higher oligomers. In addition alternative splicing of H_3 and H_4R cDNA generates splice variants which result in the potential expression of different receptor isoforms. Two common human H_3R isoforms expressed in the basal ganglia are the focus of this thesis: the full length $H_{3\,(445)}$ isoform and the shorter $H_{3\,(329)}$ isoform. For the human H_4 receptor only two isoforms have been identified to date. These are drastically truncated versions of the full length receptor. Many of the H_3 isoforms and both the H_4 isoforms appear to be non-functional with respect to ligand binding and signalling. To determine whether these attributes could be a source of receptor heterogeneity, five major hypotheses have been addressed: 1. Human H_3 and H_4 receptors are able to homo-oligomerise; 2. Human H_3 and H_4 receptors are able to hetero-oligomerise with their respective splice variants; 3. Splice variants can act as dominant negative regulatory subunits; 4. N-glycosylation is a prerequisite for receptor dimerisation; 5. H_3 and H_4 histamine receptors are both expressed in brain and subserve distinct functions.

A new panel of anti- H_3R and H_4R specific antibodies have been generated, and used as immunological probes to test the thesis hypotheses using a combination of biochemical,

biophysical and pharmacological techniques. Cross-linking experiments suggested the presence of human and rodent H_3R and human H_4R homo-oligomers, further corroborated by FRET analysis for the hH_3R, and by both nickel column purification and BRET in the case of the hH_4R. FRET experiments also provided evidence for the existence of hetero-oligomers, consisting of the full length receptor with a respective shorter isoform. Neither of the truncated hH_4 isoforms can bind or transduce a signal. The effect of the two isoforms on surface expression of the full length receptor was investigated using the surface biotinylation technique. Results confirmed that the shorter isoforms decreased the surface expression of the full length $hH_{4\ (390)}$ isoform in line with the effects of the two isoforms on the number of [^{3}H] histamine binding sites. Both the human H_3 and H_4 receptors are modestly N-glycosylated, however N-glycosylation is not a prerequisite for receptor dimerisation. In the case of the H_3 receptor preventing glycosylation has only a modest effect on ligand binding to the receptor.

In conclusion, variability in the level of homo- and hetero-oligomerisation and propensity for N-glycosylation may contribute to H_3 and H_4 receptor heterogeneity. Furthermore shorter isoforms are able to act as dominant negative subunits which would have profound functional consequences on both H_3 and H_4 receptors *in vivo*. This study also provides the first evidence that both the H_3 and H_4 receptors are expressed in the human and rodent brain.

CANDIDATES DECLARATION

I confirm that no part of the materials presented has previously been submitted for a degree in this or any other University. If materials have been generated through joint work, my independent contribution has been clearly indicated. In all other cases, materials from the work of others has been clearly indicated, acknowledged and quotations and paraphrases indicated.

ACKNOWLEDGEMENTS

I am a relative newcomer to neuroscience but was immediately gripped by a field where science is so intimately bound up with what it means to be human. There are many people who I would like to thank for making my PhD thesis an enjoyable and rewarding experience. First and foremost my supervisor Dr Paul Chazot for giving me the opportunity to do a PhD, an ambition put on hold for many years while balancing a career with a young family. Paul succeeded in striking the balance between being approachable without micro-managing, I always felt free to ask questions – even stupid ones! My colleagues: Becca Sheahan, Sawsan Abuhamdah, Heather Chaffey, Andrea Bradford and others, have made working in the lab easy and fun. Undergraduate project students: Farah Ahmed, Jenny Parten and Nicola Abassah, carried out some of the immunohistochemistry under my supervision, all three did an excellent job.

Also thank you to Richard van Rijn and Prof Rob Leurs (Amsterdam Centre for Drug Research, Vrije University), who have been our close collaborators in much of the work, especially in exploring the functional implications of histamine receptor oligomersiation. In the course of our PhDs Richard and I did an exchange visit to learn new techniques and further our research. Despite being a much bigger laboratory than my own, the atmosphere at the Vrije was very friendly; it was also a stimulating and exciting place to work with a truly international mix of young scientists.

The association with Prof Rob Leurs laboratory came about through a small but long established research society, the European Histamine Research Society (EHRS) whose

annual meetings I have attended for the last three years with the help of travel bursaries. The EHRS began as a rather small club, it has managed to maintain that feel while at the same time being very welcoming and encouraging to new members. The meetings have all been great fun and have been the start of several successful collaborations.

Dr Keri Cannon and Dr Dorrit Dijkstra have both allowed me to show immunofluorescence images using our anti-H_3 and anti- H_4 antibodies in mouse brain slices and on human monocytes respectively. Prof Francis Cogé supplied the human H_3R clones, Prof Rob Leurs the human H_4R clones, Prof Tim Lovenberg provided brains from both wild type and H_3R knockout mice. These gifts reflect the spirit of generosity and openness which I have encountered throughout.

My family have mostly ignored my doing a PhD which on reflection has probably been a good thing! But thank you Steve for sticking with me for the final push and your usual sound advice on putting things plainly. My parents have, as always, been brilliant - whenever there were just too many balls in the air I knew I could rely on them.

CONTENTS

ABSTRACT i

CANDIDATES DECLARATION iii

ACKNOWLEDGEMENTS iv

CONTENTS vi

CHAPTER 1

INTRODUCTION

1. Histamine and the histaminergic system 1

Fig. 1.1 The Histaminergic System 3

2. Histamine receptors 4

2.1 The first histamine receptors: H_1 and H_2 5

2.2 The histamine H_3 receptor 7

2.2.1 Anatomical distribution 8

2.2.2 Auto- and hetero-receptors: matching anatomy and functional data 10

2.2.3 H_3 receptor structure and signalling 11 - 18

a) Splice variants generate receptor isoforms

Fig. 1.2 Reported human H_3R isoforms

b) Genetic polymorphism

c) Signalling pathways

d) Effector mechanisms

e) Constitutive activity

2.2.4 Histamine H_3 receptor pharmacology 19

a) Agonists 19

Fig. 1.3 Imidazole-containing histamine H_3 receptor agonists

Table 1.1 Affinities of human H_3R agonists and selectivity over H_4R 21

b) Antagonists 22

i) Imidazole-containing antagonists 22

Fig. 1.4 Imidazole-containing histamine H_3 Receptor antagonists 22

Table 1.2 Affinities of human H_3R antagonists and selectivity over H_4R 24

ii) Non-imidazole antagonists 24

2.2.5 Pharmacological heterogeneity 24 - 30

a) Cross-species heterogeneity

b) Evidence for amino acids at key sites being responsible for inter-species differences

c) Heterogeneity within species

d) Evidence for different splice variants exhibiting distinct pharmacologies

2.2.6 *In vivo* role of histamine H_3 receptors 31 – 39

a) Arousal

b) Homeostasis

i) Fluid intake

ii) Food intake

iii) Cardiovascular control

c) Cognition, learning and memory

d) Pain and stress

2.2.7 Potential H_3R targeted therapies 39

2.3 The histamine H_4 receptor 40

2.3.1 Cloning 40

2.3.2 Anatomical distribution 41

2.3.3 Signal transduction 42

2.3.4 Pharmacology 43

2.3.5 *In vivo* role of histamine H_4 receptor 45

2.3.6 Potential H_4R targeted therapies 47

3. GPCR dimerisation 48 – 55

a) Homo-dimerisation

b) Hetero-dimerisation

c) Mechanism of dimerisation

Fig. 1.5 Comparison of contact dimers and domain-swapped dimers

d) Possible role of GPCR dimers

3.1 GPCR interactions with other proteins 56

3.2 Post-translational changes and GPCR function 57

4. Conclusions and Aims 58

CHAPTER 2

MATERIALS AND GENERAL METHODS

2.1 Source of materials 61

2.2 Instruments and equipment 66

2.3 Preparation of standard solutions 68

2.4 General methods 69

2.4.1 Membrane preparation for immunoblotting 69

2.4.2 Determination of protein concentration 70

2.4.3 SDS-polyacrylamide gel electrophoresis 70

2.4.3.1 Preparation of resolving gel 71

2.4.3.2 Chloroform/methanol method for protein precipitation and preparation of protein samples for SDS-PAGE 71

2.4.3.3 SDS-polyacrylamide gel electrophoresis 72

2.4.4 Immunoblotting 72

2.4.5 Transformation of competent *E. coli* cells 74

2.4.6 Glycerol stocks of transformed competent *E. Coli* cells 74

2.4.7 Amplification and preparation of plasmid DNA 75

2.4.7.1 Preparation of small scale culture of plasmid DNA 75

2.4.7.2 Preparation of large scale culture of plasmid DNA 75

2.4.7.3 Harvesting the large scale culture and purification of plasmid DNA using QIAGEN™ Plasmid Maxi-Kit 75

2.4.7.4 Quantification and determination of purity of the DNA yield 76

CHAPTER 3

DEVELOPMENT AND CHARACTERISATION OF NOVEL ANTI-H_3 RECEPTOR ISOFORM SPECIFIC ANTIBODIES

3.1 OBJECTIVES 77

3.2 INTRODUCTION 77

Fig 3.1 Schematic organization of the human H_3 histamine receptor gene and cDNA 79

Fig 3.2 The amino acid sequences of the full length rat and human H_3 receptor isoforms 82 - 84

3.3 METHODS 85

3.3.1 Choice of peptide sequences 85

3.3.2 Antibody production 86

3.3.3 The 3-maleimdobenzoic acid N-hydroxysuccinimide (MBS) ester method of coupling peptides to carrier proteins 86

3.3.4 Inoculation procedure 87

3.3.5 Affinity purification 87

3.3.5.1 Coupling of peptides to sepharose beads via sulphydryl groups 87

3.3.5.2 Peptide affinity purification of antibodies 88

3.3.6 Culture and transfection of HEK (Human Embryonic Kidney) 293 cells 89

3.3.6.1 Preparation of DMEM/F12 media + L-glutamine 89

3.3.6.2 Subculturing of HEK 293 cells 89

3.3.6.3 Preparation of new stocks of HEK 293 cells 90

3.3.6.4 Lipofectamine PLUS transfection method 90

3.3.6.5 Harvesting and membrane preparation of HEK 293 cells 91

3.3.7 Immunoblots 91

3.3.7.1 Preparation of resolving gel 92

3.3.7.2 Preparation of protein samples for SDS-PAGE 92

3.3.7.3 SDS-PAGE 93

3.3.7.4 Immunoblotting 93

3.3.8 Immunohistochemical analysis 95

3.3.8.1 Peptide block to confirm antibody specificity 96

3.4 RESULTS 97

3.4.1 Determination of antibody concentration following peptide affinity purification 97

Fig 3.3 A representative elution profile 98

Table 3.1 Concentrations of antibodies purified from different Bleeds of immunized rabbits 98

3.4.2 Immunoblotting analysis of anti-H_3 receptor antibodies against recombinant rat and human H_3 receptor isoforms expressed in HEK 293 cells 99

3.4.2.1 Isoform specificity of the rH_{3C} (268-277) antibody 99

Fig 3.4 Immunoblot showing rH_{3C} (268-277) antibody reactivity against rat H_3 receptor isoforms expressed in HEK 293 cells 100

Fig 3.5 Immunoblot of three different FLAG tagged human H_3 receptor isoforms probed with anti-FLAG antibody and antibodies raised to peptide sequence rH_3 (268 – 277) 101

Fig 3.6 Anti-rH_{3C} (268 – 277) from different rabbits and different bleeds used against human isoforms 102

3.4.3 Purified antibodies from rabbits immunised with peptide sequences unique to human H_3 365, 415 and 329 isoforms failed to detect their particular isoforms when tested in immunoblots 103

Fig 3.7 Immunoblot of human H_3 receptor isoforms expressed in HEK 293 cells probed with antibodies or immune sera from rabbits immunized with three different H_3 receptor peptide sequences 104

3.4.4 The anti-rat H_3 (268 – 277)/anti-$hH_{3\ (445)}$ was able to detect native H_3R in both rodent and human brain 105

Table 3.2 Summary of immunoreactive species detected in rat forebrain using pan anti-H_3(346-358) and anti-rat H_3(268-277)/anti-$hH_{3(445)}$ 105

Table 3.3 Summary of immunoreactive species detected in human putamen using pan anti-H_3(346-358) and anti-rat H_3(268-277)/anti-$hH_{3(445)}$ 106

Fig 3.8 Rat forebrain probed with pan anti-H_3R and

anti-rH$_3$ (268-277) /anti-hH$_{3\ (445)}$ antibody 107

Fig 3.9 Human putamen probed with pan anti-H$_3$R and anti-r H$_3$(268-277)/anti-hH$_{3(445)}$ antibody 108

3.4.5 The anti-hH$_{3\ (445)}$ identified bands in immunoblots of wild type (H$_3$R +/+) mouse brain which were not evident in brain from H$_3$R knockout (H$_3$R -/-) mice 109

Table 3.10 Summary of results comparing protein species detected in KO and WT mouse brain using anti-rat H$_3$ (268 – 277)/anti-hH$_{3\ (445)}$ 109

Fig 3.10 Immunoblot using anti-hH$_{3\ (445)}$ to compare H$_3$ receptor immunoreactivity in H$_3$R -/- (KO) mice with wild type (WT) mice 110

3.4.6 Immunohistochemical studies using anti- rH$_{3C}$/anti-hH$_{3\ (445)}$antibody to compare immunoreactivity in H$_3$R -/- (KO) mice with wild type (WT) mice clearly demonstrated the specificity of this antibody 111

Table 3.5a) IHC: Pan anti-H$_3$ receptor antibody, summary of some key brain structures 112

Table 3.5b) IHC: Anti- rH$_{3A/3C}$ / hH$_{3\ (445)}$ antibody, summary of some key brain structures 113

Fig 3.11 Comparing anti-hH$_3$(445) immunoreactivity in H$_3$ +/+ (wild type) mice with H$_3$ -/- (knockout) mice in selected key brain structures 114 - 116

Fig 3.12 Immunofluorescent detection of H$_3$ immunoreactivity in striatum and substantia nigra pars reticulata comparing

H_3+/+ (wild type) mice with H_3-/- (knockout) 117

3.5 DISCUSSION 118

CHAPTER 4

EVIDENCE FOR HUMAN AND RODENT H_3 RECEPTOR OLIGOMERS: BIOCHEMICAL AND BIOPHYSICAL APPROACHES

4.1 OBJECTIVES 125

4.2 INTRODUCTION 125

4.3 METHODS 128

4.3.1 Chemical cross-linking 128

4.3.2 *tr*-FRET 129

Fig 4.1 Schematic representation of tr-FRET to show H_3R homo-dimers 130

Fig 4.2 Schematic representation of tr-FRET to show H_3R hetro-dimers 131

4.4 RESULTS 134

4.4.1 Chemical cross-linking studies show rH_{3A} dimers but not rH_{3C} dimers 134

Table 4.1 Summary of protein species detected following chemical cross-linking of rat $H_{3\,(A)}$ and $H_{3\,(C)}$ isoforms 134

Fig 4.3 Cross-linking of recombinant rat H_3R expressed in HEK 293 cells 135

4.4.2 Chemical cross-linking enhances both $hH_3R_{(445)}$ and $hH_3R_{(329)}$ homo-dimers 135

Fig 4.4 a) Cross-linking of human $H_3R_{(445)}$ expressed in HEK 293 cells 137

Fig 4.4 b) Cross-linking of human FLAG-$H_{3(445)}$ expressed in HEK 29 cells probed with anti-FLAG and anti-$hH_{3(445)}$ 138

Fig 4.4 c) Graph to show densitometric evaluation of $hH_3R_{(445)}$ immunoreactivity in the presence of increasing cross-linker concentration 138

Fig 4.5 a) Cross-linking of human $H_3R_{(329)}$ expressed in HEK 293 cells 139

Fig 4.5 b) Graph to show densitometric evaluation of FLAG- $hH_3R_{(329)}$ immunoreactivity in the presence of increasing cross-linker concentration 140

4.4.3 FRET studies confirmed the presence of rat $H_3R_{(A)}$ homo-dimers 141

Fig 4.6 FRET studies confirm the presence of full length rat $H_3R_{(A)}$ dimers adapted from Bakker et al, 2006 141

4.4.4 FRET assays confirmed the presence of human H_3 receptor homo-dimers and provided evidence for the existence of 329/445 hetero-dimers 142

Fig 4.7 Homo-oligomerisation of the $hH_{3\,(329)}$ and $hH_{3\,(445)}R$ isoforms 143

Fig 4.8 Hetero-oligomerisation of the $hH_{3\,(329)}$ and $hH_{3\,(445)}R$ isoforms 144

Fig 4.9 Demonstration of hetero-oligomerisation of the $hH_{3\,(329)}$ and $hH_{3\,(445)}R$ isoforms 145

4.5 DISCUSSION 146

CHAPTER 5

DEVELOPMENT OF THE FIRST ANTI-HUMAN H_4 RECEPTOR ANTIBODIES: DEMONSTRATION OF THE EXISTANCE OF THE H_4R IN THE HUMAN BRAIN AND H_4R HOMO- AND HETERO-OLIGOMERS

5.1 OBJECTIVES 150

5.2 INTRODUCTION 150

Fig 5.1 Schematic organisation of the H_4R gene 152

5.3 METHODS 155

5.3.1 Production of human PHA blasts 155

5.3.2 Immunoprecipitation to confirm the selectivity of the H_4R antibody 156

5.3.3 Immunohistochemistry (IHC) 156

5.3.4 Receptor immobilisation on a nickel column 157

Fig 5.2 Scematic representation of nickel column purification 158

5.3.5 Bioluminescence Resonance Energy Transfer (BRET) 159

Fig 5.3 Schematic representation of the BRET assay 160

5.3.5.1 BRET ratio 161

5.3.6 Immunoprecipitation to investigate hetero-dimerisation 161

5.3.7 Surface bioyinylation – H_4 isoforms 162

5.4 RESULTS 163

5.4.1 Choice of peptide sequences 163

Fig 5.4 Full length amino acid sequence of the hH_4R with

the sequences of the immunising peptides highlighted 164

5.4.2 Antibody yields 165

5.4.3 The antibody was able to detect human H_4R expressed in HEK 293 cells 165

Fig 5.5 Anti-H_4 (374-390) and anti-FLAG immunoreactivity are coincident 166

5.4.4 Immunoprecipitation of recombinantly expressed HA-H_4Rs from HEK 293 cells 166

Fig 5.6 The anti-H_4R antibodies recognize anti-HA immunoprecipitated HA-H_4Rs 168

5.4.5 The antibody was specific for hH_4R expressed in HEK 293 cells 168

Fig 5.7 Characterisation of specific polyclonal hH_4R antibodies 169

5.4.6 The polyclonal H_4R antibodies are able to detect specific immunoreactivity in native tissue, including human and rat brain 170

Fig 5.8 Immunoblot using anti-$H_{4\ (374\text{-}390)}$ Receptor to probe human and rat brain 171

5.4.7 The anti-$H_{4\ (374\text{-}390)}$ identified H_4R protein in human spleen lysates and tissue sections 171

Fig 5.9 Anti-$H_{4(374\text{-}390)}$ reacts with human H_4R in spleen lysate and tissue sections 172

5.4.8 The anti-$H_{4(374\text{-}390)}$antibody also worked well as a probe to identify hH_4R on human monocytes using fluorescence activated cell-sorting (FACS) 173

Fig 5.10 Staining of human monocytes with anti-H_4 (374-390)R 173

5.4.9 The existence of heterogeneously expressed H_4R homo-dimers 174

5.4.10 Cross-linking of H_4Rs 174

Fig 5.11 Cross-linking evidence for hH_4R dimmers and higher oligomers 175

5.4.11 HA-H_4Rs associate with c-myc-H_4R-his_{10} 175

Fig 5.12 Nickel column purification of H_4R homo-oligomers 176

5.4.12 BRET shows homo-oligomerisation of hH_4Rs 176

Table 5.1 Average BRET ratios confirming the formation of H_4R homo-dimers in COS-7 cell membranes 177

Fig 5.13 Average BRET ratios confirming the formation of H_4R homo-dimers in COS-7 cell membranes 178

5.4.13 Immunoprecipitation confirms the presence of hH_4R hetero-dimerisation 178

Fig 5.14 Immunoprecipitation evidence for $hH_{4\,(390)}$ receptor interaction with hH_4 receptor isoforms, $hH_{4\,(302)}$ and $hH_{4\,(67)}$ 180

5.4.14 Surface labelling experiments confirm that the shorter hH_4 isoforms are expressed at the cell surface 181

Fig 5.15 Surface labelling of hH_4 receptor isoforms 181

5.4.15 The shorter hH_4 isoforms reduce surface expression of the full length $hH_{4\,(390)}$ receptor 182

Fig 5.16 Surface Labelling of $hH_{4\,(390)}$: effect of isoforms 183

Table 5.2 Densitometric evaluation of surface expression of

$hH_4R_{(390)}$ in the presence of the three different isoforms:

390 itself and the shortened splice variants 302 and 67 183

Fig 5.17 a) The two truncated H_4R isoforms dose dependently reduce surface expression of the full length $hH_{4\,(390)}$ isoform 184

Fig 5.17 b) Densitometric quantification of surface expression of $hH_{4\,(390)}$ following co-expression with the shorter H_4 isoforms 185

5.5 DISCUSSION 186

CHAPTER 6

THE ROLE OF N-GLYCOSYLATION IN DIMERISATION AND PHARMACOLOGY OF H_3 AND H_4 RECEPTORS

6.1 OBJECTIVES 193

6.2 INTRODUCTION 193

Fig 6.1 Putative sites of N-glycosylation 194

6.3 METHODS 196

6.3.1 Tunicamycin experiments with recombinant H_3 and H_4 receptors 196

6.3.2 Deglycosylation of native H_4 receptor 196

6.3.3 Specific binding of [^{3}H]-clobenpropit to recombinant H_3 receptors 196

6.4 RESULTS 198

6.4.1 Human H_3 receptors are N-glycosylated and prevention of N-glycosylation does not have a major effect upon [^{3}H]-clobenpropit binding to the hH_3 445 receptor 198

Fig 6.2 N-glycosylation inhibition of the human $H_{3\ (445)}$ receptor 200

6.4.2 Biochemical evidence that the hH_4R is an N-glycosylated homo-dimer 201

Fig 6.3 The effect of inhibition of glycosylation on the expression of human H_4R in HEK 293 cells 202

Fig 6.4 Deglycosylation of human H_4R expressed in HEK 293 cells 203

Fig 6.5 Deglycosylation of H_4R in human blast cells 204

6.5 DISCUSSION 205

CHAPTER 7

GENERAL DISCUSSION

1) Human H_3 and H_4 receptors are able to homo-oligomerise 212

2) Human H_3 and H_4 receptors are able to hetero-oligomerise with their respective splice variants 213

3) Splice variants can act as dominant negative regulatory subunits 213

4) N-glycosylation is a prerequisite for receptor dimerisation 214

5) H_3 and H_4 histamine receptors are both expressed in brain and subserve distinct functions 215

REFERENCES 222

APPENDIX

PUBLICATIONS

LAY SUMMARY

CHAPTER 1

INTRODUCTION

1. Histamine and the histaminergic system

Histamine is a basic amine formed from the amino acid L-histidine by histidine decarboxylase, a reaction which can be blocked for experimental purposes by the enzyme inhibitor α-fluoromethylhistidine (α-FMH).

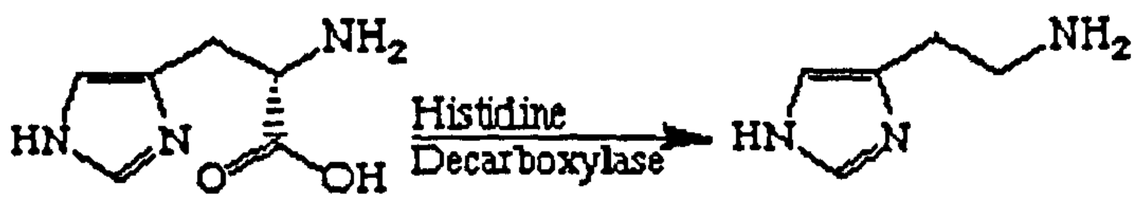

Histidine Histamine

It is metabolized to N-methylhistamine by an N-methyl-transferase or to imidazole acetic acid by diamine oxidase. The N-methylhistamine can be further metabolized to N-methyl-imidazole acetic acid by monoamine oxidase.

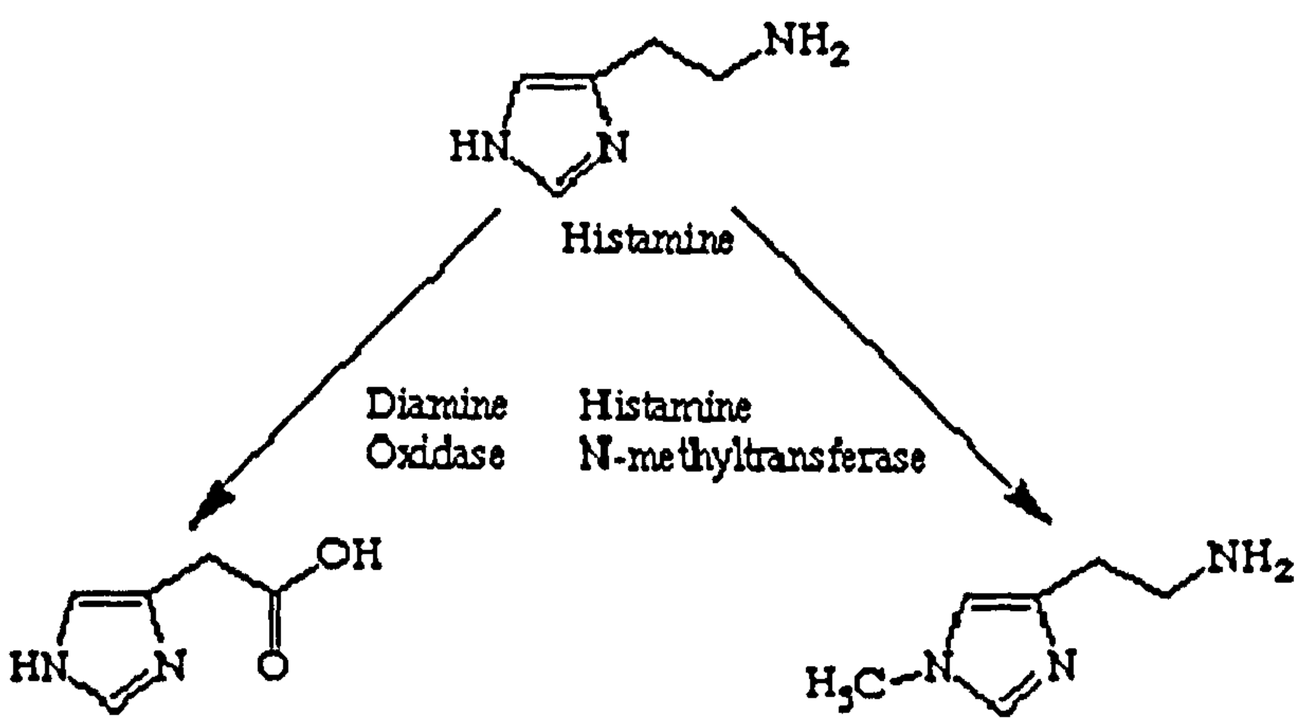

Imidazole acetic acid N-Methylhistamine

It is found in most tissues of the body but is present in high concentrations in the lungs and the skin and in particularly high concentrations in the gastrointestinal tract. It is found mainly in mast cells and basophils, associated with heparin, but non-mast-cell histamine occurs in 'histaminocytes' in the stomach and in histaminergic neurons

in the brain (Parsons & Ganellin, 2006). Most of the early studies describing the biological action of histamine in the periphery were carried out by Sir Henry Dale and colleagues in the early 1930s. Anti-histamines were developed as successful therapies for allergic and inflammatory conditions. It was soon recognized that classical anti-histamines had a sedative action and were therefore affecting the CNS. Evidence for a role for histamine in brain aminergic systems began to accumulate (Green, J.P. in *Handbook of Neurochemistry*, 1970) and lesion studies (Garbarg *et al*, 1974) identified the approximate source of brain histamine. Knowing where histamine is found in the brain and the effects it has on different brain areas is crucial to gaining an understanding of its function. There are many similarities between the histaminergic system and the other three aminergic systems i.e. the serotonergic, dopaminergic and noradrenergic systems. All four of these systems consist of small groups of neurons with widespread projection networks to most brain areas and the spinal cord. This is compatible with their having a broad modulatory effect on neuronal function. Specificity of action is achieved by the different brain regions from which they receive input and by the distinct distribution of receptor subtypes in target regions. The central histamine system is involved in many CNS functions: arousal, activation of the sympathetic nervous system, stress-related release of hormones from the pituitary and of central aminergic neurotransmitters, anti-nociception, water retention and suppression of eating. Histamine is synthesized and transported in the brains of almost all animal species and the histaminergic system is phylogenetically highly conserved (Haas & Panula, 2003). In vertebrates the tuberomamillary nucleus (TMN), which is part of the posterior hypothalamus, is the soul source of histaminergic neurons and their projections (Fig. 1.1). In all mammals the cerebral cortex, amygdala, substantia nigra and striatum receive moderate or dense histaminergic

innervation (Watanabe *et al,* 1984; Inagaki *et al*, 1988; Panula *et al*, 1989). The density of projections into the hippocampus (Panula *et al*, 1989; Greene *et al*,1990; Brown *et al*, 2001) and thalamus (McCormick & Williamson, 1989; McCormick, 1992; Pape & McCormick, 1995) varies, and the retina and spinal cord also receive histaminergic input. Afferent projections to the TMN come from many different areas. Major sources are the infralimbic cortex, lateral septum and preoptic nucleus (Ericson *et al*, 1991). The brainstem innervation derives mainly from adrenergic cell groups C1-C3, noradrenergic groups A1-A3 and from serotonergic groups B5-B9. By contrast the locus coeruleus and the dopaminergic groups of the substantia nigra and ventral tegmental area send only a few fibres to the TMN (Ericson *et al*, 1989).

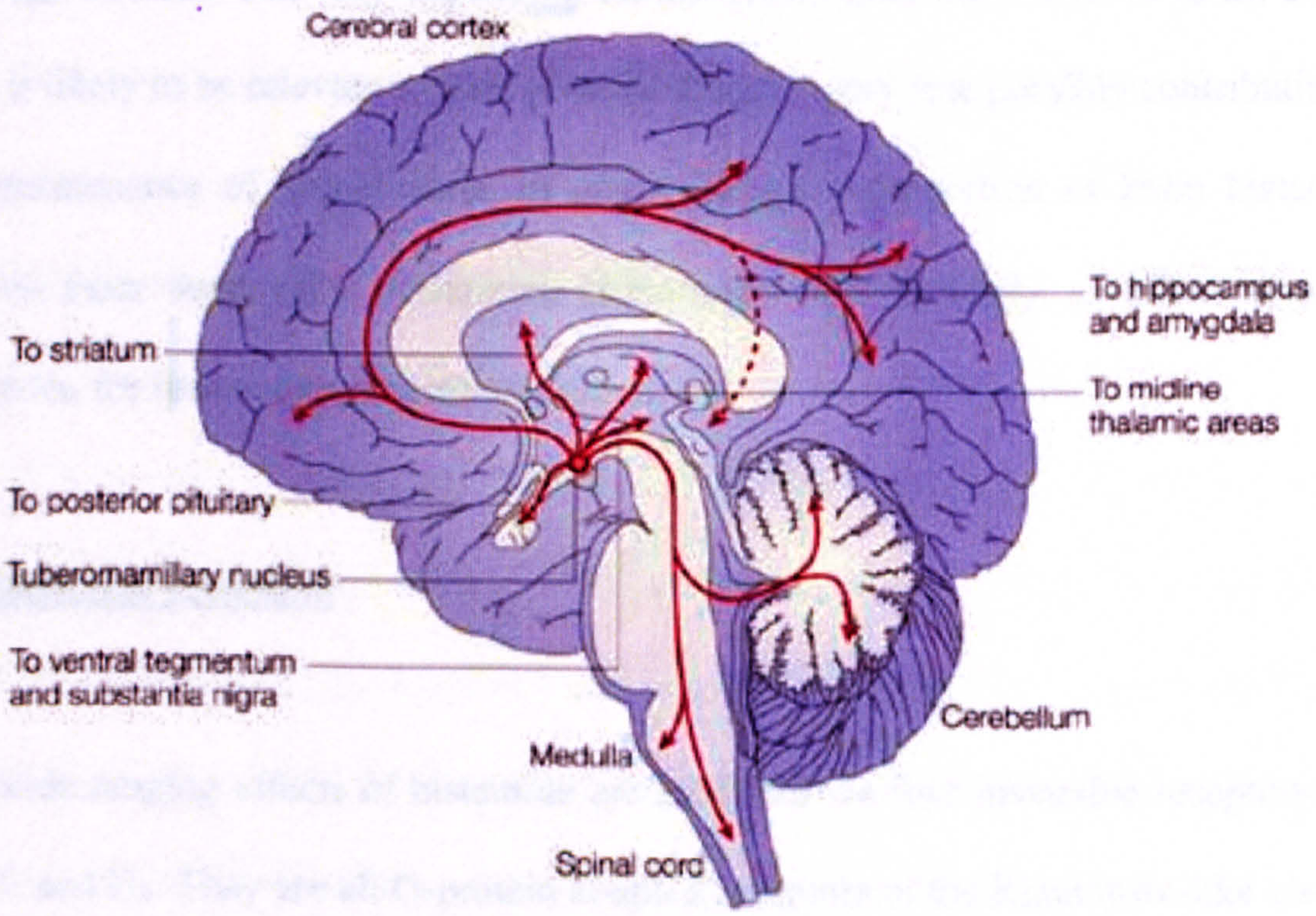

Haas & Panula, 2003

Fig 1.1 The Histaminergic System

The TMN neurons contain several other neurotransmitters and modulators besides histamine. Glutamic acid decarboxylase the γ-aminobutyric acid (GABA) synthesizing enzyme and GABA itself are found in many TMN neurons. This may have functional significance because TMN neurons extend widely throughout the CNS so that they could mediate general inhibition. The neuropeptides galanin, thyrotropin releasing hormone, proenkephalin-derived peptides and substance P are also found in subsets of histamine producing TMN neurons, although their function here is not known (Staines *et al*, 1986; Airaksinen & Panula, 1988). Most TMN neurons also express adenosine deaminase (ADA), the enzyme that converts adenosine to inosine (Staines *et al*, 1986; Senba *et al*, 1991).

Histaminergic neurons are pacemakers that fire at a slow regular rate (below 3Hz), although this rate can vary depending on the behavioural state (Brown *et al*, 2001). This is likely to be relevant to their presumed modulatory role possibly contributing to the maintenance of homeostasis. In many species a proportion of brain histamine derives from mast cells. Histamine from mast cells is likely to affect neuronal receptors, for instance during inflammation.

2 . Histamine receptors

The wide ranging effects of histamine are mediated via four histamine receptors: H_1, H_2, H_3 and H_4. They are all G-protein coupled receptors of the Rhodopsin-like class A type. H_1, H_2 and H_3 are all prominently expressed in the brain. The most recently described receptor H_4 has so far been detected predominantly in the periphery. The H_1 and H_2 receptors mostly excite neurons or potentiate excitatory inputs whereas H_3 is

an inhibitory receptor. Histamine can also modulate currents gated by the glutamate N-methyl-D-aspartate (NMDA) receptor (Haas, 1984). Since the H_3 and H_4 receptors are the subject of this thesis the H_1 and H_2 receptors are covered in less detail here. However they are both important receptors in the brain, in addition some of the effects of H_3R stimulation result from a reduction in histamine activation at H_1 and H_2 receptors.

2.1 The first histamine receptors: H_1 and H_2

The first classical anti-histamines antagonized the effects of histamine on a range of smooth muscles. From these compounds drugs were developed to treat various allergic disorders such as hay fever, allergic rhinitis and urticaria. However these anti-histamines failed to inhibit some of the actions of histamine, suggesting that there were at least two types of receptors sensitive to histamine (Ashford *et al*, 1949).

H_1R distribution in different animal tissues has been mapped with the use of selective radioligands one of the first being [^{3}H]-mepyramine. In addition to the brain it is found in a wide variety of tissues including: smooth muscle from airways, gastrointestinal tract, genitourinary system, and the cardiovascular system; adrenal medulla; endothelial cells and lymphocytes (Hill *et al*, 1990). In human brain, higher densities of H_1R are found in neocortex, hippocampus, nucleus accumbens, thalamus and posterior hypothalamus, whereas cerebellum and basal ganglia show lower densities (Martinez-Mir *et al*, 1990; Villemagne *et al*, 1991; Yanai *et al*, 1992). The H_1R influences eating, drinking and thermoregulation (Brown *et al*; 2001). It may also be involved in learning and memory (Knoche *et al*, 2003; Dai *et al*, 2007).

H_2R was first described in the periphery where it modulates smooth muscle and gastric acid secretion (Black *et al*, 1972). H_2R antagonists are widely prescribed to control excessive gastric acid secretion. It is also found in cardiac tissue and on immune cells, where it has been shown to negatively regulate histamine release and a number of cell functions such as antibody synthesis in B cells, and T cell proliferation (reviewed by Hill *et al*, 1990; Chand & Eyre, 1994). [^{125}I]iodoaminopotentidine has been used for autoradiographic mapping of H_2R in mammalian brain where it is widely distributed. Highest densities are found in the basal ganglia, hippocampus, amygdala and cerebral cortex. Lowest densities are detected in cerebellum and hypothalamus (Traiffort *et al*, 1992; Vizuete *et al*, 1997; Honrubia *et al*, 2000). Overall the effect of H_2R activation on neurons is most often excitatory (Chen *et al*, 2003; Chen *et al*, 2005; Tang *et al*, 2007). As with the H_1R, there is evidence for H_2R playing a part in learning and memory (Dai *et al*, 2007).

The H_1 and H_2 receptors were both cloned in 1991 (Yamishita *et al*, 1991 and Gantz *et al*, 1991 respectively). The gene for the human H_1 is located on chromosome 3 (Leconiat *et al*, 1994). The receptor signals through G proteins of the $G_{q/11}$ subtype which stimulate the phopholipase C, diacyl glycerol (DAG), inositol triphosphate (IP_3) pathway (Leurs *et al*, 1994). DAG activates protein kinase C (PKC), whilst IP_3 releases calcium from intracellular stores. H_1R activation can also lead to the formation of arachidonic acid (AA), probably through the action of phospholipase A_2 (Leurs *et al*, 1994) and to the formation of cGMP (Richelson, 1978). The cGMP formation may arise from an increase in intracellular calcium $[Ca]_i$ leading to activation of nitric oxide synthase, production of nitric oxide (NO) and subsequent stimulation of guanylate cyclase. Therefore H_1R activation may be able to modulate

presynaptic transmitter release as both AA and NO have been proposed to act as retrograde messengers, however such modulation has yet to be shown. H_1R stimulation can indirectly generate cAMP by substances acting at receptors coupled to G_s G proteins (Baudry *et al*, 1975; Daum *et al*, 1982; Leurs *et al*, 1994) e.g. histamine acting at H_2R or adenosine acting at the A_2R.

The H_2R shares 28% homology with the H_1R. The gene for H_2R is located on human chromosome 5 (Traiffort *et al*, 1995). It is a GPCR which mostly couples through G_s G proteins, activation of which leads to stimulation of adenylyl cyclase and production of the second messenger cAMP (Baudry *et al*, 1975; Hegstrand *et al*, 1976). The major pathway is activation of cAMP dependent protein kinase A (PKA). PKA can phosphorylate a range of target regulatory proteins in the cytosol or in the cell membrane, alternatively it can translocate to the cell membrane and activate the transcription factor cAMP response element binding (CREB) protein.

2.2 Histamine H_3 receptor

The H_3R was first identified by Arrang *et al*, 1983, describing auto-inhibition of brain histamine release via a novel histamine receptor. It is pharmacologically distinct from the H_1 and H_2 receptors.

2.2.1 Anatomical distribution

Autoradiographic studies with the H_3R selective ligand [^{3}H]R-(α)-methylhistamine have shown the presence of specific binding in several rat brain regions (Arrang *et al*, 1987), particularly cerebral cortex, striatum, hippocampus, olfactory nucleus, and the bed nuclei of the stria terminalis, which receive ascending histaminergic projections from the magnocellular nuclei of the posterior hypothalamus. H_3R have also been visualised in human brain and the brain of nonhuman primates (Martinez-Mir *et al*, 1990).

More recently a detailed mapping of the H_3R and its gene transcripts has been carried out in the rat brain (Pillot *et al*, 2002) The distribution of H_3R mRNA in rat brain was compared in the same animals with [^{125}I]iodoproxyfan binding, a selective radioligand. The signal was quantified or rated and compared for each probe to identify the neuronal populations expressing the receptor. This study (Pillot *et al*, 2002) is unique in its' meticulous comparison of mRNA with the distribution of H_3R protein in the same animals, thus providing evidence for the presence of receptors on many neuronal perikarya, dendrites and projections. Strong mRNA signal was detected in intermediate and deep layers of the cerebral cortex, while binding (i.e. corresponding to H_3R protein) was high in all layers except layer V. High binding in layer IV, combined with high levels of message in thalamic nuclei, suggest the presence of H_3R as hetero-receptors on thalamocortical projections. Strong mRNA signal but low binding was detected in distinct regions of the hippocampal structure, therefore the H_3R appears to be present on projections pf pyramidal cells of the CA1 and CA3 regions. In the basal ganglia high binding was found in the striatal complex

and the olfactory tubercles. H_3R mRNA in cortical layer V may code for H_3R hetero-receptors on cotricostriatal neurons. In addition message in the substantia nigra pars compacta was compatible with the presence of H_3R on nigrostriatal afferents. Message in the caudate putamen and nucleus accumbens suggests striatal H_3 receptors on both the direct and indirect movement pathways. In the amygdala levels of binding and mRNA were uniformly high. In the thalamus binding detected in some association nuclei may be on neurons emanating from deep cortical layers. However, low binding in most nuclei combined with a strong mRNA signal suggests that the majority of the H_3 receptors are on thalamic projections. The pattern of binding and mRNA signal reported in the lower brain stem i.e. high mRNA signal but negligible binding, is compatible with the presence of presynaptic H_3 receptors regulating noradrenaline (Schlicker *et al*, 1989) and serotonin release (Schlicker *et al*, 1988). In the cerebellum there was negligible binding but high levels of message, suggesting the presence of receptors on efferent projections. The distribution of the H_3R both at the structural and cellular level is critical to understanding of its' physiological role. Immunological identification of the H_3R protein in mouse brain (Chazot *et al*, 2001) was generally in concordance with the ligand-autoradiographical data from both the above study and that described in mouse forebrain (Cumming *et al*, 1994).

H_3R mRNA and protein is also found in some non-brain tissues including skin, dorsal root ganglia (Cannon *et al*, 2007), stomach, intestines (Chazot *et al*, 2007) and brown adipose tissue (Karlstedt *et al*, 2003). H_3R mRNA was detected in a wide range of tissues from developing rats (Heron *et al*, 2001) with highest expression in the central and peripheral nervous system, adipose tissue, skin, thymus, respiratory and tongue epithelia. Expression in some areas was found to be developmentally regulated.

2.2.2 Auto- and hetero-receptors: matching anatomy and functional data

The new H_3 receptor was shown initially to inhibit histamine release and synthesis (Arrang *et al*, 1983). Subsequently H_3R have been found to function as both auto- and hetero-receptors inhibiting the release of many other transmitters including glutamate (Brown & Reymann, 1996), GABA (Garcia *et al*, 1997), noradrenaline (Schlicker *et al*, 1989), dopamine (Schlicker *et al*, 1993), acetylcholine (Arrang *et al*, 1995), serotonin (Schlicker *et al*, 1988) and various peptides (Hill *et al*, 1997). It is this property together with its' widespread CNS distribution which has generated such great interest in the H_3R as a potential therapeutic target.

Differential responses to $GABA_A$ or H_3 receptor antagonists suggest the existence of distinct subpopulations among histaminergic neurons (Giannoni *et al*, 2006). Using dual probe microdialysis, with one electrode in the TMN and a second electrode in different histaminergic projection sites, the effects of administration of either an H_3 or $GABA_A$ antagonist (thioperamide or bicuculline respectively) on the target region were compared. Results confirmed that both GABA and HA tonically modulate HA neuronal activity. The different responses evoked by intra-TMN administration of either thioperamide or bicuculline on HA release in distinct projection areas suggested the presence of functionally distinct HA neuronal populations. Our group in collaboration with. teams at Oxford and Florence Universities have new data showing neurons in the rat TMN double stained for GABA (anti-GAD_{67} antibody) and H_3R (anti-H_3R antibody). Although modest in numbers, there was clear evidence of GAD-positive neurons expressing H_3R. There were a large number of neurons which were H_3R positive but GAD negative, and GAD positive and H_3R negative, confirming

significant heterogeneity of TMN neurons (Appendix). Using a combination of pharmacological and physiological approaches other examples of heterogeneity have been described including differences in histaminergic and orexinergic neurons in relation to $GABA_A$ receptors subunit composition (Haas *et al*, 2006), and evidence for distinct control by H_3R of dopamine release in the substantia nigra (SNr) and prefrontal cortex (PFC) – brain regions which differ in the origin of their dopaminergic innervation (Garduño-Torres *et al*, 2006). In superfused rat SNr slices depolarisation-evoked [^{3}H]-dopamine release was diminished by the H_3R agonist immepip. In contrast, immepip failed to affect [^{3}H]-dopamine release from PFC synaptosomes. This same group showed the presence of H_3R coupled to $G_{\alpha i/o}$ proteins on thalamic nerve terminals, activation of these H_3 receptors modulated glutamatergic, but not GABAergic transmission.

2.2.3 H_3 receptor structure and signalling

In 1983 the first evidence for an additional histamine receptor, the H_3R, was obtained (Arrang *et al*, 1983). However, it was not cloned until 1999 (Lovenberg *et al*, 1999). This was largely because it shares only 22 and 20% homology with H_1R and H_2R respectively so genomic searches based on sequence homology proved unsuccessful. Indeed it was finally cloned from a human thalamus cDNA library using a potential GPCR-related sequence tag (EST) sequence with homology to α_2 adrenergic receptors. The gene is located on human chromosome 20 (Tardivel-Lacombe *et al*, 2001; Cogé *et al*, 2001), it encodes a gene of 445 amino acids.

The H_3R belongs to superfamily 1 of the seven transmembrane (TM) domain containing receptors that couple to G-proteins. This family includes those receptors activated by small ligands, such as biogenic amines; larger peptide ligands and glycoprotein hormones. In common with other family members, H_3 receptors are characterised by unique sequence motifs (Leurs *et al*, 2000) as follows:

DRY (DRF for the H_3R) or ERW motif at the interface of TM3 and intracellular loop 2; the NPXXY motif in TM7 (NPVLY in all H_3R so far); conserved aspartates at positions 80 in TM2 and 114 in TM3; conserved tryptophan residues W174 and W371 in TM4 and TM6 respectively; conserved prolines P210 and P373 in TM5 and TM6 respectively; and a conserved asparagine N404 in TM7. Other features of the H_3R common to many GPCRs include putative disulphide bridge sites between the first and second cysteine residues (C107 and C188 on extracellular loops 1 and 2 respectively, Leurs *et al*, 2000); and potential sites for palmitoylation (C428 near the carboxy terminus) and N-linked glycosylation (N11). Sites for phosphorylation by protein kinases have been identified in all three intracellular loops: at serines S63 or S64 (first intracellular loop), serine S141 and threonine T149 (second intracellular loop), and at serines S310, S319, S341, S343 or threonines T314 and T345 (third intracellular loop) (Leurs *et al*, 2000).

Publication of the human H_3R gene sequence lead quickly to the cloning of the rat (Lovenberg *et al*, 2000) and guinea-pig (Tardivel-Lacombe *et al*, 2000) H_3 receptor orthologues. The sequence of the mouse receptor has also been published (Genbank Accession nos. NP598610; AY044153; NM133849, Koyama *et al*, 2002; AY142145, Chen *et al*, 2002) and further characterised (Chen *et al*, 2003). Abbott Laboratories have cloned the monkey H_3 receptor (Accession no. AY231164, Yao *et al*, 2003a) and

obtained partial peptide sequences for the canine receptor (Accession nos. AY231165 and AY231166, Witte *et al*, 2003). Comparison of all these sequences shows a high degree of homology. Approximately 92% of the amino acids are conserved across the five species whose complete sequences are available. By contrast, other than modest homology to the H_4 receptors (Hough, 2001), the H_3R does not show a high degree of homology to any other known or orphan GPCR.

a) Splice variants generate receptor isoforms

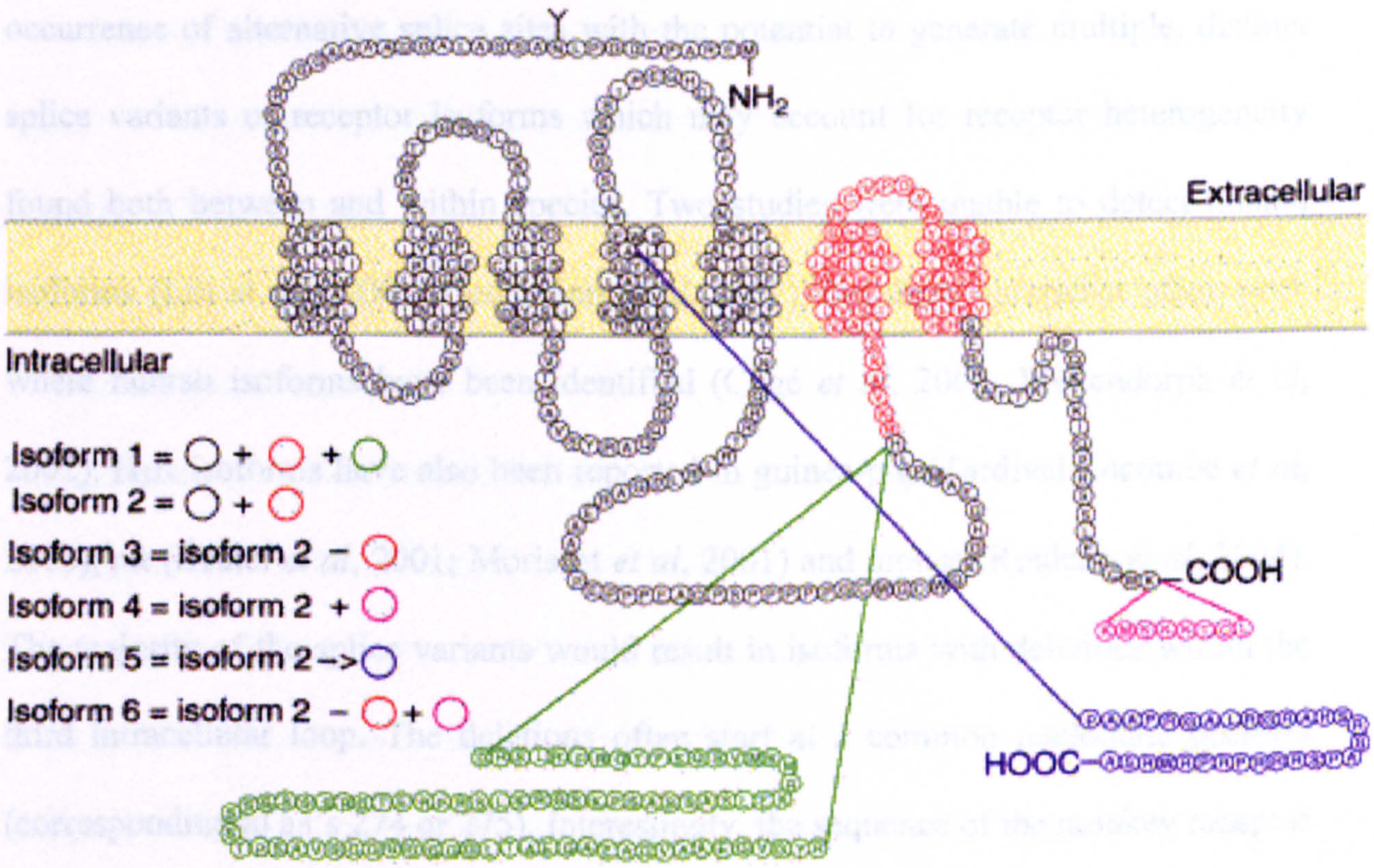

Fig.1.2 Reported human histamine H_3 receptor isoforms (Dave Weiner, Acadia Pharmaceuticals, San Diego, CA, USA). Isoform 1 is similar to that previously reported by Lovenberg *et al*, 1999, whereas isoform 2 has an 80-amino-acid deletion in the third intracellular loop. This deletion is combined with an 8-amino-acid longer C-tail (isoform 4). Isoform 3 contains a deletion of 144 amino acids, which includes the 80-amino-acid deletion of isoform 2 but also eliminates transmembrane domain (TM) 6 and TM7. This deletion is also found in combination with the eight additional amino acids in the C-terminal tail (isoform 6). Finally, isoform 5 is generated as a result of a 409-nucleotide deletion and a frameshift. This results in a protein with a deleted TM4 and TM5, and a new 30-amino acid C-terminus. *The figure was kindly provided by Kim Retra (Leiden/Amsterdam Center for Drug Research, Vrije Universiteit, The Netherlands).*

The genes coding for many GPCRs lack introns, however several introns have been found in the H_3R gene. Two different studies of the human gene (Tardivel-Lacombe *et al*, 2001; Wiedemann *et al*, 2002) suggest a gene with three exons and two introns. However Cogé (Cogé *et al*, 2001) reported a gene with a minimum of four exons and three introns (Fig 3.1, Chapter 3). In addition their analysis suggests the possibility of a fourth intron which would split exon 4 in two. A further exon may result in an additional 8 amino acids in the carboxy terminus of the human H_3R (Itadani *et al*, 2001 European Patent Application, # EP 1, 142, 909, A1) thus generating a protein 453 aa's long. The consequence of these diverse exon/intron junctions, is the occurrence of alternative splice sites with the potential to generate multiple, distinct splice variants or receptor isoforms which may account for receptor heterogeneity found both between and within species. Two studies were unable to detect human isoforms (Liu *et al*, 2000; Wiedemann *et al*, 2002), but these contradict other work where human isoforms have been identified (Cogé *et al*, 2001; Wellendorph *et al*, 2002). H_3R isoforms have also been reported in guinea-pig (Tardivel-Lacombe *et al*, 2000), rat (Drutel *et al*, 2001; Morisset *et al*, 2001) and mouse (Rouleau *et al*, 2004). The majority of the splice variants would result in isoforms with deletions within the third intracellular loop. The deletions often start at a common nucleotide position (corresponding to aa's 274 or 275). Interestingly, the sequence of the monkey receptor at this putative splice site differs from the other species and expression of splice isoforms of the monkey receptor has not been detected (Yao *et al*, 2003). The mechanisms regulating alternative splicing of the H_3R gene remain to be investigated.

It is unlikely that all the possible splice variants are actually expressed as protein. Furthermore, receptors with deletions in regions thought to be important in ligand

binding and/or signal transduction may not be functional in respect of those two particular properties. However these truncated versions might still be physiologically relevant if they alter the expression levels or functioning of the native receptor, either directly or indirectly by their interactions with other cellular proteins. There is indeed evidence that this occurs (Bakker *et al*, 2006), although the underlying mechanism is still a matter for speculation. Oligomerisation of GPCR's is a topic on which there is presently a great deal of debate. Most GPCR's studied to date appear to be able to oligomerise but whether this happens in native tissue and what its' functional significance might be remains unknown (see section **3**). The potential for receptor cross-talk and a role in regulatory mechanisms such as receptor trafficking is currently an active area of research for these important receptors. This topic will be a focus of a large part of this thesis.

b) Genetic polymorphism

Independent publications and GenBank submissions of human H_3R sequences have either glutamic acid (Accession nos. XM009561, AB019000 and AB045369) or aspartic acid (AF363791) at position 19 (Hancock *et al*, 2003). Wiedemann *et al*, 2002 have identified a polymorphism at position 280 (A to V) in a patient with Shy-Drager syndrome, a disease characterised by neuronal degeneration and autonomic failure. Abbott Laboratories have confirmed this finding and identified another polymorphism at amino acid 197 (cysteine for phenylalanine, Yao *et al*, unpublished). Similarly genetic polymorphism has been reported in the rat H_3 receptor, with several single amino acid substitutions in intracellular loop 3 (Cogé *et al*, 2001). Polymorphic sites may also be present in the mouse where complete sequences (Cogé *et al*, 2001b; Chen *et al*, 2003) differ from the partial mouse sequence (Goodearl *et al*, 1999

International Patent Application # WO 99/28470.). Other polymorphic sites may remain to be discovered in both these and other species.

c) Signalling pathways

Even before the H_3R was cloned there was evidence for it coupling to $G_{i/o}$, that is to the inhibitory class of G proteins shown by the pertussis-toxin (PTX) sensitivity of H_3R agonist-dependent [^{35}S]GTPγS binding in the rat brain (Clark & Hill, 1996; Laitinen & Jokinen, 1998). This was confirmed by Lovenberg *et al* when they cloned the receptor in 1999. Our laboratory provided the first evidence for a direct interaction of native H_3 receptors in rat striatum with the $G_{\alpha i3}$ protein (Victoria Hann PhD Thesis, 2003). A number of studies have consistently linked both human and rat recombinant H_3R to the adenylyl cyclase system (Lovenberg *et al*, 1999, 2000; Wieland *et al*, 2001; Morisset *et al*, 2000; Uveges *et al*, 2002; Cogé *et al*; 2001; Gomez-Ramirez *et al*, 2002). Effects on adenylyl cyclase have also been shown for various H_3R isoforms using cAMP-dependent reporter systems (Drutel *et al*, 2001). Drutel and colleagues identified cDNA's of three functional rH_3 isoforms which they termed H_{3A}, H_{3B} and H_{3C} and one non-functional truncated receptor H_{3T}. H_{3A} was the full length clone of 445 aa whereas H_{3B} and H_{3C} both had deletions within the 3rd intracellular loop. This study was the first to demonstrate coupling of all three isoforms to the P44/P42 mitogen activated protein kinase (MAPK) cascade, again in a PTX-sensitive manner. None of the isoforms coupled to phospholipase C. The MAPK pathway is believed to be important in neuronal plasticity and is activated in hippocampal LTP (English & Sweatt, 1996). The H_3 receptor has been shown to play a role in learning and memory, therefore these results suggest a possible mechanism. New signalling pathways, also with significance for neuronal survival and memory consolidation, have recently been

reported. In transfected SK-N-MC cells the hH_3R 445 isoform modulates the activity of the Akt/Glycogen synthase kinase 3β (GSK-3β) axis both in a constitutive and an agonist-dependent manner (Bongers *et al*, EHRS 2006; Bongers *et al*, 2007). The H_3R mediated activation of the protein kinase Akt can be inhibited by the H_3R inverse agonist thioperamide as well as by wortmannin and pertussis toxin (PTX), suggesting that Akt activation occurs via a $G_{i/o}$-mediated activation of phosphoinositide-3-kinase (PI-3-K). H_3R activation also leads to phosphorylation of GSK-3β, which acts downstream of Akt and plays an important role in brain neuronal development and function. In rat embryonic day (ED) 17 cortical neurons H_3R activation phosphorylates Ser^{473} Akt in a time-dependent manner (Mariottini *et al*, EHRS 2006). Akt activation, besides promoting neuronal survival, regulates synaptic strength and is critical for memory consolidation and retrieval.

d) Effector mechanisms: H_3R and calcium channels

H_3R have been shown to be coupled to $G_{i/o}$ and high voltage activated calcium ion (Ca^{2+}) channels. An important physiological role of H_3R activation may be a reduction in Ca^{2+} ion influx. Mobilisation of Ca^{2+} ions is important in neurotransmitter release. Therefore a direct G-protein mediated inhibition of presynaptic calcium channels appears to be the most likely mechanism underlying inhibition of neurotransmitter release by H_3R activation. In dissociated TM neurons H_3R activation suppressed N- and P-type calcium channels via a pertussis toxin-sensitive G-protein (Takeshita *et al*, 1998). The increase in noradrenaline release in myocardial ischaemia can be ameliorated by addition of an H_3 agonist (Levi & Smith, 2000) and is a direct effect of reduced intracellular Ca^{2+} (Silver *et al*, 2001).

e) Constitutive activity

An important property of the H_3R is that it demonstrates a high level of constitutive activity, this means that at least a proportion of the receptor population is active even in the absence of histamine. Constitutive activation of GPCR's was first reported by Lefkowitz *et al*, 1993 when they produced a mutant α_{1B}-adrenoceptor which was able to generate an inositol phosphate accumulation in the absence of agonist. The H_3R naturally contains within the C-terminal region of its' third intracellular loop the residues that are normally mutated into a GPCR to make it constitutively active. Noting this Morisset *et al*, 2000 carried out a series of experiments to demonstrate that the H_3R is indeed constitutively active and importantly produced the first evidence that this is also the case in native tissue. This has significant implications for the way in which the H_3R may be regulated *in vivo*. It also means that many so-called antagonists are more properly thought of as inverse-agonists. Neutral antagonists simply inactivate a receptor, whereas an inverse-agonist has highest affinity for the receptor in its inactive conformation. Thus an inverse-agonist stabilises the receptor in a form that is not coupled to its respective G-protein.

2.2.4 Histamine H_3 receptor pharmacology

a) Agonists

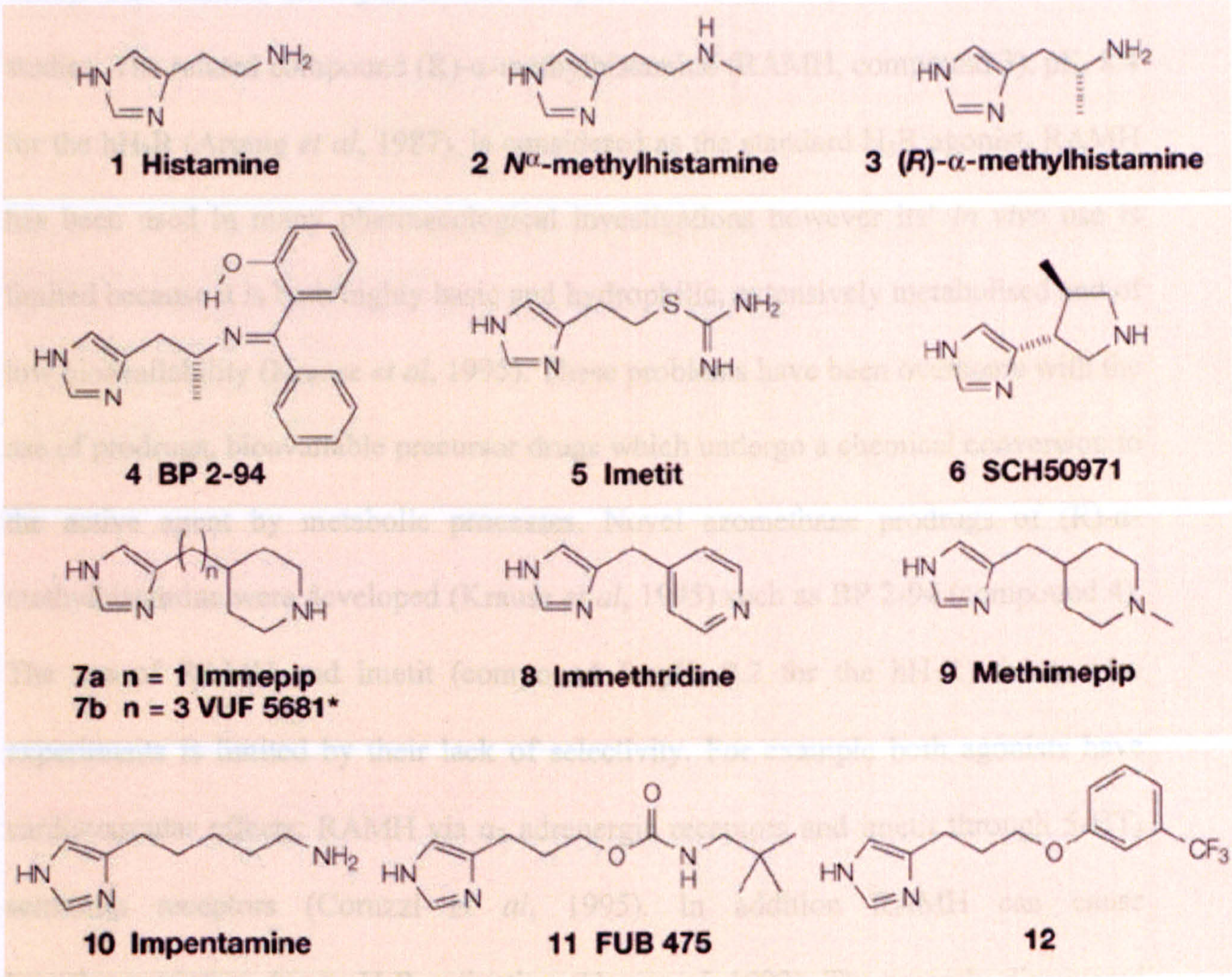

(Leurs *et al*, 2005)

Figure 1.3 Imidazole-containing histamine H_3 receptor agonists.

*This compound is not an agonist, but a neutral antagonist.

So far all H_3R agonists are very similar to histamine (compound 1, Fig 1.3) and contain a 4(5)-substituted imidazole ring. Replacements of this moiety and/or attachments to the imidazole ring eliminate H_3R activity (Leurs *et al*, 1995; de Esch & Belzar, 2004). However, small structural changes to the imidazole side chain of histamine have resulted in very potent and selective H_3R agonists. Methylation of the

basic amine group of histamine generates N-α- methylhistamine (compound 2), an H_3R agonist that is about three times more active than histamine itself (Lipp *et al*, 1995). The tritiated analogue of this compound is frequently used in H_3R binding studies. The related compound (R)-α-methylhistamine (RAMH, compound 3), pK_i 8.4 for the hH_3R (Arrang *et al*, 1987), is considered as the standard H_3R agonist. RAMH has been used in many pharmacological investigations however its' *in vivo* use is limited because it is both highly basic and hydrophilic, extensively metabolised and of low bioavailability (Krause *et al*, 1995). These problems have been overcome with the use of prodrugs, bioavailable precursor drugs which undergo a chemical conversion to the active agent by metabolic processes. Novel azomethane prodrugs of (R)-α-methylhistamine were developed (Krause *et al*, 1995) such as BP 2-94 (compound 4). The use of RAMH and imetit (compound 5, pK_i 9.2 for the hH_3R) for *in vivo* experiments is limited by their lack of selectivity. For example both agonists have cardiovascular effects: RAMH via α_2 adrenergic receptors and imetit through 5-HT_3 serotonin receptors (Coruzzi *et al*, 1995). In addition RAMH can cause bronchconstriction due to H_1R activation (Hey *et al*, 1992). The recently discovered H_4R can be activated by H_3R agonists such as immepip (compound 7a, pK_i 9.6 for the hH_3R), RAMH and imetit (see section **2.3.4**). The selectivity of these agonists for H_3 over the related H_4R is only 27-55 fold (Hough, 2001). An immepip analogue (compound 8, immethridine) has recently been produced (Leurs *et al*, 2005). Immethridine is slightly less active than immepip at the H_3R but shows a 300-fold selectivity for this receptor compared with H_4R (Kitbunnadaj *et al*, 2004). Methimepip (compound 9) has both high affinity for the H_3R (pK_i 9 hH_3R) and 2000-fold selectivity over the hH_4R (Kitbunnadaj *et al*, 2004; Leurs *et al*, 2005).

Compound No See Fig 1.3	Name	pK_i at native hH_3R	Selectivity over hH_4R
1	Histamine	8.59[a]	1.5[d]
2	NAMH	9.41[a]	46[d]
3	RAMH	8.41[a]	200[d]
5	Imetit	9.67[a]	9[d]
7	Immepip	9.58[a]	23[d]
8	Immethridine	9.07[b]	300[b]
9	Methimepip	9.0[c]	2000[c]

Table 1.1 Affinities to hH_3R and selectivity over hH_4R of imidazole-containing histamine H_3 receptor agonists

NAMH = N-α-methylhistamine; RAMH = R-α-methylhistamine

[a] Ireland-Denny *et al*, 2001

[b] Kitbunnadaj *et al*, 2004

[c] Kitbunnadaj *et al*, 2005

[d] Liu *et al*, 2001

b) Antagonists

i) Imidazole-containing antagonists

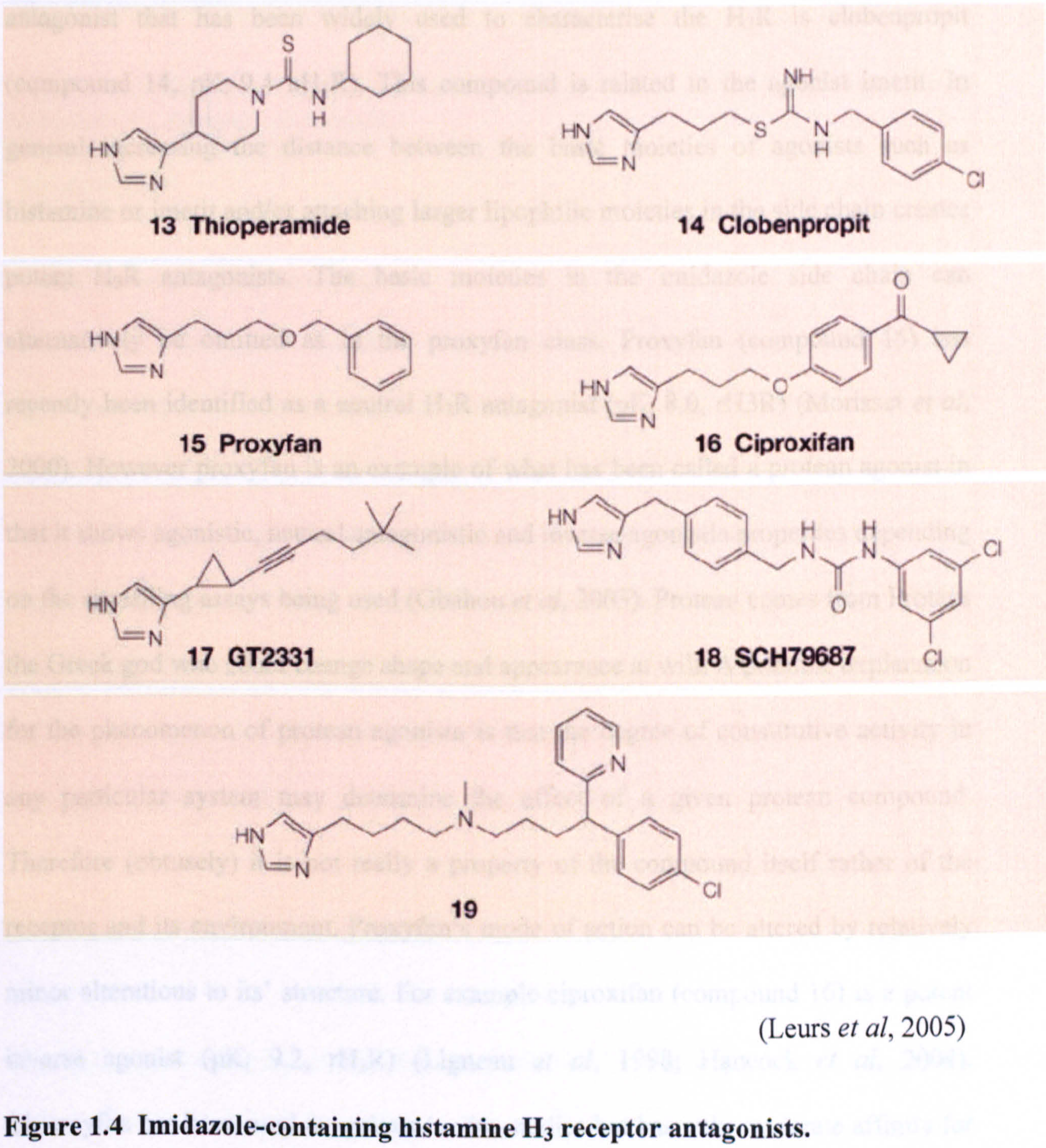

(Leurs *et al*, 2005)

Figure 1.4 Imidazole-containing histamine H_3 receptor antagonists.

Thioperamide (compound 13, Fig 1.4) was for many years the reference H_3 antagonist since it was the first potent antagonist to lack activity at H_1 and H_2 receptors (Arrang *et al*, 1987). It is now more accurately described as an inverse agonist. It shows high affinity for the rat H_3R (pK_i 8.4) but is less active at the hH_3R (pK_i 7.2) (Lovenberg *et*

al, 2000) In addition it has high activity at the hH_4R (pK_i 7.3), the rat 5-HT_3 serotonin receptor (pK_i 5.6) and α_{2A} adrenergic receptor (pK_i 6.9) and the human α_{2C} adrenergic receptor (pK_i 6.5) (Esbenshade *et al*, 2003). Another early imidazole-containing H_3R antagonist that has been widely used to characterise the H_3R is clobenpropit (compound 14, pK_i 9.4 hH_3R). This compound is related to the agonist imetit. In general increasing the distance between the basic moieties of agonists such as histamine or imetit and/or attaching larger lipophilic moieties in the side chain creates potent H_3R antagonists. The basic moieties in the imidazole side chain can alternatively be omitted as in the proxyfan class. Proxyfan (compound 15) has recently been identified as a neutral H_3R antagonist (pK_i 8.0, rH3R) (Morisset *et al*, 2000). However proxyfan is an example of what has been called a protean agonist in that it shows agonistic, neutral antagonistic and inverse agonistic properties depending on the signalling assays being used (Gbahou *et al*, 2003). Protean comes from Proteus the Greek god who could change shape and appearance at will. A possible explanation for the phenomenon of protean agonism is that the degree of constitutive activity in any particular system may determine the effect of a given protean compound. Therefore (obtusely) it is not really a property of the compound itself rather of the receptor and its environment. Proxyfan's mode of action can be altered by relatively minor alterations to its' structure. For example ciproxifan (compound 16) is a potent inverse agonist (pK_i 9.2, rH_3R) (Ligneau *et al*, 1998; Hancock *et al*, 2004). Ciproxyfan has been used in various *in vivo* studies but has only moderate affinity for the human H_3R (pK_i 6.99), in addition it shows moderate activity at a number of other important receptors (Ebenshade *et al*, 2003). An important characteristic of the H_3R antagonists is that there is evidence for considerable inter-species variability (Ireland-Denny *et al*, 2001).

Compound No See Fig 1.4	Name	pK_i at native human H_3R[a]	pK_i at native rat H_3R[a]	Selectivity over hH_4R[b]
13	Thioperamide	7.13	8.1	0
14	Clobenpropit	9.08	9.38	21
16	Ciproxyfan	6.99	9.15	0

Table 1.2 Affinities to hH_3R and selectivity over hH_4R of imidazole-containing histamine H_3 receptor antagonists

[a] Ireland-Denny *et al*, 2001
[b] Liu *et al*,.2001

ii) Non-imidazole H_3R antagonists

Most of the imidazole-containing antagonists (thioperamide, clobenpropit and ciproxifan) have the disadvantage of interacting with cytochrome P450. Therefore much effort has been put into developing non-imidazole H_3R antagonists (Leurs *et al*, 2005) and it is these latest compounds which hold most promise as future drugs, e.g. potential anti-obesity drugs A-423579 and NNC 0038-000-1202 from Abbott Laboratories and Novo Nordisk respectively (Hancock *et al*, 2004; Malmlof *et al*, 2007 respectively) and ABT-239 from Abbott Laboratories as a possible treatment for Alzheimer's Disease (Fox *et al*, 2004; Esbenshade *et al*, 2004).

2.2.5 Pharmacological heterogeneity

Pharmacological heterogeneity of H_3 receptors both within and between species has long been a conundrum. Cloning of the H_3R has lead to far more detailed understanding of its structure. Receptor polymorphisms and the possibility of multiple receptor isoforms are likely to underlie at least some of this diversity (Hancock *et al*, 2003). There is accumulating evidence for differential distribution of splice variants in different brain regions in human (Cogé *et al*, 2001; Wellendorph *et al*, 2002), rat

(Drutel *et al*, 2001; Morisset *et al*, 2001) and mouse (Rouleau *et al*, 2004). Interestingly expression of the different isoforms within the CNS varied in key areas involved in regulation of sensory, endocrine, cognitive and motor functions. It should be emphasised that studies mapping native distribution of splice variants rely solely on detecting expression of mRNA. So far it has not been possible to directly probe protein expression, an issue addressed for the first time in this thesis.

a) Cross-species heterogeneity

Radioligand binding (RLB) studies and functional assays have been used to compare the pharmacology of native H_3 receptors across species. Several histamine homologues have different effects on noradrenaline release in mouse cortex compared with their effect on neurogenic contractions in guinea pig jejunum (Leurs *et al*, 1996). This could also be accounted for by H_3R heterogeneity between tissues. In the same study different potencies for several compounds were found when comparing guinea pig functional assays with rat brain radioligand binding. Comparing antagonist potencies (thioperamide or ciproxifan) to modulate [^{3}H]-histamine release from human and rat cortex or in other functional or radioligand binding studies, lower potencies at human receptors were described for these antagonists but not for agonists (review by Schwartz *et al*, 2001). Cross-species studies of radioligand binding to rat cortex, [^{3}H]-noradrenaline release in mouse cortex, or reversal of H_3R agonist induced inhibition of electrically produced contractions of guinea pig intestine were performed with a series of imidazole-based ligands related to iodoproxyfan (Schlicker *et al*, 1996) as well as compounds related to immepip and imetit (Alves-Rodrigues *et al*, 2001). In the latter study an immepip analogue VUF4929 showed a nearly 20fold increase in affinity to block guinea pig jejunal contraction than to antagonise

noradrenaline release in rat cortices, while a reversed agonist potency order (10fold) was observed for immepip. Somewhat surprisingly a better correlation was found when comparing antagonist potencies between guinea pig and rat radioligand binding affinities than when comparing rat binding affinities to apparent blocking potencies in the mouse (Schlicker *et al*, 1996). It is now known from studies on the pharmacology of cloned receptors that the protein sequences in the mouse and the rat are identical at key sites shown to be important in determining binding affinity.

Inter-species potency differences for antagonist compounds were also suggested by radioligand binding competition assays carried out in rat, monkey and human cortices. The affinity of thioperamide was significantly lower in primates compared to the rodent (West *et al*, 1999).

By contrast, comparing human saphenous vein to guinea pig ileum showed no big differences in the antagonist potencies of either thioperamde or clobenpropit (Valentine *et al*, 1999).

b) Evidence for amino acids at key sites being responsible for inter-species differences

Extensive comparison of native receptors in radioligand binding and functional assays also confirmed distinct cross-species pharmacology which could be explained by amino acid differences between human, canine, rat and guinea-pig receptors (Ireland-Denny *et al*, 2001). Most agonists were nearly equipotent at cloned human, cloned rat or native rat cortical receptors. However the antagonist thioperamide had a 10-fold lower affinity at the cloned human receptor compared to the cloned rat receptor.

Clobenpropit on the other hand was nearly equipotent at human and rat receptors in both radioligand binding and cAMP based functional assays (Ireland-Denny *et al*, 2001; Lovenberg *et al*, 2000). Ligneau *et al*, 2000 obtained similar results for both thioperamide and ciproxifan reporting 9-fold and 12-fold lower affinities respectively at cloned human H_3R compared with the cloned rat receptor. As in the previous study clobenpropit was found to be approximately equipotent at the two receptors. By contrast the situation was reversed for the antagonist potency of FUB(349) with affinity at the human receptor 6-fold greater than at the rat receptor.

Similar evidence of interspecies heterogeneity has been reported in radioligand binding assays with the antagonist A-304121 (Hancock *et al*, 2003). Comparing affinities at rat and human cortices with guinea pig ileum the order was as follows: rat 30-fold > guinea pig 300-fold > human. Ligneau *et al*, 2000 demonstrated that key amino acids are responsible for these species differences. They mutated rat receptors either at a single site V122A or doubly V122A together with A119T, effectively turning the rat receptor into the human equivalent. The single mutation produced a 5-fold decrease in the affinity of ciproxifan binding while the double mutation resulted in an 18-fold decrease making the mutated rat receptor pharmacologically identical to the human receptor. In analogous studies (Yao *et al*, 2003) used recombinant technology to ligate the N terminus through TM3 of the human receptor to TM4 through to the carboxy terminus of the rat receptor. Subsequent pharmacological analysis confirmed TM3 as being critical for the affinity of several species-selective ligands. The importance of the amino acids at positions 119 and 122 in affinity of the binding domain of ciproxifan, thioperamide and several non-imidazole antagonists was also established.

Previously cited studies (Schlicker *et al*, 1996) showed a higher correlation between antagonist potencies for 16 iodoproxifan analogues in the guinea pig ileum assay and rat radioligand binding affinities than between rat binding affinities and antagonist potencies in mouse perfusion studies measuring radiolabeled noradrenaline release from cortical slices. This is surprising because it is now known that rat and mouse receptors are identical at positions 119 and 122 in TM3, whereas guinea pig has threonine and valine at these positions. However these differences could reflect differential tissue distribution of H_3R isoforms since receptors in guinea pig ileum are being compared with receptors found in mouse cortical slices. In general the findings relating key sites in TM3 to particular pharmacological profiles has been confirmed in several other species (review by Hancock *et al*, 2003).

c) Heterogeneity within species

Pharmacological data has since the 1990's pointed to H_3R heterogeneity and the possibility of receptor subtypes. Different classes of binding site were defined in rat cortical membranes (West *et al*, 1990a) having either slow or fast off rates for [^{3}H]-R-α-methyl histamine (RAMH). These same workers described high (rat H_{3A}) and low (rat H_{3B}) affinity sites in rat brain slices using the inverse agonists thioperamide and burimamide (West *et al*, 1990b). Other studies in rat are broadly in agreement with these initial findings (Arrang *et al*, 1990; Jansen *et al*, 1994).

The rank order of potency for thioperamide, impromidine and burimamide, in experiments to block H_3R-agonist inhibition of sympathetic-elicited hypertension in the guinea-pig, were found to reflect that described at the rat H_{3B} site (Hey *et al*, 1992). These findings were used to make a case for the physiological relevance of the

low affinity site. However these results should be interpreted with care since the rat and guinea pig receptors are pharmacologically different. Conversely Schlicker *et al*, 1992 proposed that control of CNS noradrenaline in the mouse cortex was mediated via the high affinity H_{3A} site. Potency orders for several H_3R ligands to regulate potassium-stimulated [H^3]-acetylcholine release from preloaded slices of rat entorhinal cortex also suggested subtype heterogeneity (Clapham & Kilpatrick, 1992). Nevertheless other workers (Schlicker *et al*, 1996; Brown *et al*, 1996) were unable to obtain radioligand binding data in support of high and low affinity states in either rat or guinea pig tissues.

Thus far it has not proved possible to conclusively distinguish between distinct high and low affinity sites on the same receptor, different states arising from modulation of agonist affinity due to the receptor being coupled/uncoupled to G protein (or possibly in a constitutively active conformation), or the expression of different receptor subtypes in different tissues within the same species for which there is some evidence (Harper *et al*,1999; Cogé *et al*, 2001; Ebenshade *et al*, 2005). Conceivably all these mechanisms may contribute in some manner to the observed heterogeneity within species.

d) Evidence for different splice variants exhibiting distinct pharmacologies

With recognition of the existence of splice variants it was obvious to ask whether different affinity states might reflect potency differences between receptor isoforms. A 5-fold difference in affinity of thioperamide (39 and 199nM) for human isoform 1 (445) compared with isoform 2 (365) was reported by Wellendorph *et al*, 2002. However other studies failed to show affinity differences for ciproxifan, thioperamide

or clobenpropit at these two isoforms (Cogé *et al*, 2001), although this was not surprising for clobenpropit where no differences are observed in native rat tissue either. Abbott Laboratories also found no differences for thioperamide at these isoforms. Large potency differences were not found for a series of antagonists in either radioligand binding or functional assays (review by Hancock *et al*, 2003). By contrast other workers (Morisset *et al*, 2001) found thioperamide more potent at the shorter isoforms of the rat receptor (445< 413< 397). Likewise clobenpropit and ciproxifan were 5-fold more potent at the shorter isoforms, although FUB465 and proxifan were more potent at 445, as were the agonists histamine and imetit. These findings are in agreement with those of Drutel *et al*, 2001. In conclusion several studies, although not all, support lower potencies and affinities for full length compared with shorter isoforms – both for antagonists and agonists. However these differences appear modest compared with first reports of possible receptor subtypes referred to as H_{3A} and H_{3B} (West *et al*, 1990 a and b).

A further source of pharmacological heterogeneity may be the co-expression of different receptor isoforms. The pharmacology of the full length rat H_3R is altered by the presence of shorter isoforms (Bakker *et al*, 2006). Heterogeneous co-expression of the $rH_{(3A)}$ with the $rH_{(3D)}$ isoform resulted in the intracellular retention of the $rH_{(3A)}$ and reduced $rH_{(3A)}$ functionality. This study investigates whether human H_3 and H_4 isoforms could play a similar regulatory role.

2.2.6 *In vivo* role of histamine H_3 receptors

As alluded to earlier histamine and the histaminergic system appear to be important in nervous system regulation and behaviour. Roles in arousal, attention and homeostatic mechanisms are well documented (review by Brown *et al*, 2001). In the following section the main focus will be on current evidence for the involvement of the H_3 receptor in these areas.

a) Arousal

Lesions in the TMN and the adjacent posterior hypothalamus lead to hypersomnia (Lin *et al*, 1989). Firing of histaminergic neurons mirrors the sleep/wake cycle and histamine release in the prefrontal cortex is correlated to waking (Sakai *et al*, 1990). Mice lacking brain histamine are unable to stay awake when high vigilance is needed (Parmentier *et al*, 2002). As H_3 receptors can function as auto-receptors controlling histaminergic transmission it is not surprising that there is both pharmacological and behavioural data which provides evidence for their involvement in the sleep/wake cycle. H_3R antagonists lead to increased levels of brain histamine which in turn increase wakefulness. H_3R -/- mice are insensitive to the wake-promoting effects of the H_3R antagonist thioperamide (Toyota *et al*, 2002), confirming the role of the H_3R as a mediator of wakefulness. Interestingly there was no evidence for an increase in arousal in H_3R -/- mice. Several possible explanations could account for this (Chazot & Shenton, 2004) reflecting the complexity of the interactions both within the histaminergic system itself and between this system and other transmitter circuits. As discussed later H_3R blockade might also improve vigilance and cognitive responses.

b) Homeostasis

Pharmacological studies support a role for histamine in homeostatic mechanisms involving the hypothalamus. These include fluid balance, eating, thermoregulation and cardiovascular regulation.

i) Fluid intake

Histamine injected into the cerebral ventricles of hypothalamic sites leads to an increase in drinking. At the same time this results in an increase in vasopressin levels and a decrease in urine output mediated via both H_1 and H_2R (Brown *et al*, 2001). Dehydration–induced vasopressin release is also strongly depressed by blockade of histamine synthesis by α-FMH (an inhibitor of histamine synthesis), activation of presynaptic H_3R or antagonism of postsynaptic histamine receptors (Kjaer *et al*, 1994).

ii) Food intake

There is consistent evidence for histamine involvement in eating. Increased brain histamine following i.c.v. injection or loading with the precursor L-histidine, or application of thioperamide, leads to decreased feeding (Brown *et al*, 2001). Conversely α-FMH or antagonists of H_1R lead to increased feeding (Brown *et al*, 2001). H_3 -/- mice manifest a mild obese phenotype (Takahashi *et al*, 2002) characterised by increased body weight, food intake and adiposity and decreased energy expenditure. The anorexigenic effect of thioperamide is not seen in these mice. Studies in the Siberian hamster have shown an involvement of the H_3R in regulation of food intake related to hibernation. Catabolism of intra-abdominal fat reserves is one of the most striking physiological adaptations to winter hibernation. A screen of gene

expression revealed that H_3R mRNA in the dorsomedial posterior hypothalamic nucleus is photoperiodically regulated, with significantly lower expression associated with weight loss when the hamsters were switched from a long to short photoperiod (Barrett *et al*, 2005).

iii) Cardiovascular control

H_3R have been identified as inhibitory hetero-receptors in cardiac adrenergic nerve endings and H_3R activation decreases carrier-mediated noradrenaline release in guinea-pig and human heart (Silver *et al*, 2001). Silver *et al*, 2001 demonstrated that stimulation of H_3R on H_3R transfected SKNMC neuroblastoma cells inhibited the Na^+/H^+ exchanger which is pivotal to the transport of noradrenaline across the cell membrane. This study focussed on the possibility of H_3R activation limiting the excessive release of noradrenaline during protracted myocardial ischaemia and thus having a cardioprotective effect. The role of the H_3R on adrenergic neurons under normal physiological conditions was not explored.

c) Cognition, learning and memory

Cognition is a complex of multiple integrated neurological and behavioural activities in which arousal and attention are very important. The central histaminergic system is known to play a role in cognition, learning and memory. Histaminergic neurons innervate structures which are important in cognition including the basal forebrain, cerebral cortex, cingulate cortices, amygdala, and thalamus through cholinergic projections to the hippocampus. The excitatory action of histamine on some of these projection sites is well documented (Brown *et al*, 2001). Direct or indirect activation of brain histamine has been shown to have procognitive effects (reviewed by Passani

et al, 2000). For example increases in brain histamine improve social memory in rats whereas decreases have a detrimental effect (Prast *et al*, 1996). Interactions of histamine with the N-methyl-D-aspartate (NMDA) receptor polyamine site (Witkin & Nelson review, 2004) and evidence of histamine-induced facilitation of long-term potentiation in rat hippocampal slices (Selbach *et al*, 1997) also support a role for histamine in cognition.

Decrease in levels and/or function of acetylcholine in the brain are thought to be a major factor in age related cognitive decline. Increased levels of histaminergic activity in aging human brain (Prell *et al*, 1991) and increased levels of histamine in rat brain with age (Onodera *et al*, 1992) may play a part in decreased acetylcholine uptake and function. H_3R antagonists may be able to prevent the reductions in acetylcholine release and cognition brought about by histamine (Blandina *et al*, 1996; Orsette *et al*, 2002; Bacciottini *et al*, 2002).

H_3R antagonists have been shown to have procognitive effects in animal models (Passani *et al*, 2000) and to prevent impairments in cognitive performance caused by scopolamine (cholinergic antagonist), MK-801 (NMDA antagonist) or age (Miyazaki *et al*, 1995; Blandina *et al*, 1996; Onodera *et al*, 1998; Giovannini *et al*, 1999; Molinengo *et al*, 1999). This suggests that H_3R antagonists may be more effective in enhancing cognition in impaired systems or systems under stress.

H_3 -/- mice showed insensitivity to the amnesic effects of scopolamine in passive avoidance conditioning (Toyota *et al*, 2002). Interestingly the H_3 -/- mice were not insensitive to scopolamine in a second model, the open field habituation test. The fact

that the H_3 -/- mice were sensitive to the effect of scopolamine only in an aversion model may indicate a specific role for the H_3R in memory formation associated with painful or unpleasant stimuli. H_3 -/- mice showed enhanced spatial learning and memory in the Barnes maze (Rizk *et al*, 2004). In this same study H_3 -/- mice showed reduced measures of fear avoidance in limited models involving exploratory behaviour and avoidable fear-provoking stimuli. However, the effects of acute H_3R blockade on fear avoidance and cognition (Bongers *et al*, 2004) were found to differ markedly from the effects of constitutive H_3R deficiency seen in H_3 -/- mice. Whereas measures of fear in tests involving exploratory behaviour and avoidable fear-provoking stimuli were increased after acute H_3R blockade, they were unchanged in constitutive H_3R deficiency. Therefore the use of H_3 antagonists to treat cognitive impairments should be very carefully evaluated.

Conversely H_3R agonists generally impair cognitive performance. Pre-training (Blandina *et al*, 1996) but not post-training (Giovannini *et al*, 1999) administration of RAMH or imetit impaired the performance of rats in object recognition and passive avoidance. In the pre-training study impairment of performance was produced at agonist doses which decreased the release of acetylcholine *in vivo*. These data suggest that the H_3R might preferentially influence learning rather than already acquired behaviours, although other findings show that H_3R antagonists can also facilitate learned behaviours. The H_3 agonist immepip produced cognitive deficits in tests of olfactory and social memory, whereas thioperamide had the opposite effect (Prast *et al*, 1996).

However the above observations are by no means universal. H_3 agonists have been reported to improve cognition. RAMH improved spatial learning in a water maze (Smith *et al*, 1994). Possibly specific neuronal circuits underlie spatial learning which relies on hippocampal function in contrast to attentional functions or episodic memory functions, and these may involve different regulatory mechanisms. Similarly H_3 antagonists do not show efficacy in all animal models of cognition (Miyazaki *et al*, 1995; Miyazaki *et al*, 1997; Kirkby *et al*, 1996). Under conditions where neither thioperamide nor VU9153 showed improvement in object recognition and passive avoidance tests when administered before training to normal animals, both compounds attenuated scopolamine deficits (Giovannini *et al*, 1999). However, in similar experiments (Molinengo *et al*, 1999) it was found that H_3 antagonists could improve the performance of both normal and scopolamine treated mice. It should be noted that the Giovannini experiments were carried out in rats, not mice. Also thioperamide can reverse cognitive impairment produced by means other than just cholinergic blockade (ie resulting from scopolamine treatment). A cognitive deficit produced by the NMDA receptor ion channel antagonist MK-801 could be improved by administration of thioperamide (Chen *et al*, 1999; Huang *et al*, 2004).

With regard to these apparent anomalies in the experimental evidence linking the H_3R with cognition it should be remembered that there are many factors which may impinge on the final outcome:

- the time of administration of the drug may be important, that is before, during or after training or different combinations of all three

- the behavioural state both before and during testing, for example fearful or aroused, may be important. As histamine levels and histaminergic activity is tightly linked to the sleep/wake cycle this should also be taken into account
- as mentioned earlier H_3R antagonists may be more effective at improving impaired cognition or learning under stress
- the effects on cognition are dose-dependent and the dose-effect curves are typically NOT monophasic. The lack of linearity could be due to the multiple central activities of H_3R ligands.
- the effects are mediated via several different systems and receptors including: cholinergic system, NMDA receptors, H_1R and H_2R.
- different brain regions may be differentially affected
- effects may be different in different species.
- the ligands used vary in their H_3 selectivity, some of them do not exclusively target the H_3R

d) Pain and Stress

A large number of studies have examined the role of the central histamine system in modulating the perception of pain. Whilst peripheral histamine is involved in the stimulation of nociceptive fibres it appears that central histamine is important in anti-nociception (Hough, 1988; Chazot & Shenton, 2004). Histamine when administered icv can elicit either anti-nociceptive or hypernociceptive effects depending on the site of injection and the dose in a number of rodent models (Chung *et al*, 1984; Glick & Crane, 1978; Malmberg-Aiello *et al*, 1994). Other strategies of increasing brain histamine, including application of L-histidine, the H_3R antagonist thioperamide, and the catabolism inhibitor metoprine, have all resulted in anti-nociception (Malmberg-

Aiello *et al*, 1994). Both H_1 and H_2R antagonists when applied icv or into the periaquaductal gray have been shown to block histamine induced anti-nociception (Bhattacharya & Parmar, 1985; Thoburn *et al*, 1994; Lamberti *et al*, 1996). Recent work with KO mice has further implicated the postsynaptic H_1 and H_2 receptors in pain transmission. H_1 -/- mice showed significantly fewer nociceptive responses in a wide range of pain models, including the hot plate tail flick, tail pressure, formalin, capsaicin and abdominal constriction tests (Mobarakeh *et al*, 2000). Nociceptive responses in H_2 -/- mice are similarly reduced, it appears that H_1 and H_2 receptors function cooperatively to modulate pain perception in the CNS (Mobarakeh *et al*, 2006). The H_3R also plays a role in nociception. Neither RAMH nor thioperamide alone elicited any anti-nociceptive effect upon thermal or chemical tests. However thioperamide reduced the effects of morphine in the tail-emersion model, while RAMH enhanced its effects in the hot-plate test (Owen *et al*, 1994). This illustrates the integration of the opioid and histaminergic systems in certain pain states. H_3R -/- mice are refractory to the nociceptive effects of thioperamide (Cannon & Hough, 2005). Initial studies indicated that the anti-nociceptive action of H_3R agonists might result from inhibition of transmission by sensory C fibres at peripheral loci. However recent immunohistochemical studies (Cannon *et al*, 2006 in press) is at odds with these findings. A case can be made for H_3R-containing, ASIC3-expressing, deep dermal fibres being involved in mechanical nociceptive transmission. In addition H_3R- containing, deep dermal, peptidergic Aδ fibres have been identified. These fibres lie close to the adventitial layers of arterioles suggesting that they may be involved in regulating blood flow ((Fundin *et al*, 1997). During injury H_3R containing deep dermal , perivascular fibres could contribute to the pain and inflammation (Chazot & Shenton, 2004).

A note of caution should be added here in that the most recently discovered H_4R is also an important mediator of inflammatory responses (see later). Since some of the drugs hitherto considered selective for the H_3R are now known to have at least some activity against this latest histamine receptor, findings of past studies may need to be re-evaluated.

As outlined in section 1.1, histamine acting on the hypothalamus affects the release of many hormones from the pituitary gland. The hypothalamic-pituitary-adrenal axis (HPA axis) constitutes a major part of the neuroendocrine system that controls reactions to stress and regulates various body processes including digestion, the immune system, mood and sexuality, and energy usage. Species from humans to the most ancient organisms share components of the HPA axis. It is the mechanism for a set of interactions among glands, hormones and parts of the mid-brain that mediate a general adaptation response. Since histamine has a key role in learning and memory as well as homeostasis during times of stress or threat, a persuasive case has been made for the physiological role of histamine and the histaminergic system as a danger response system (Brown *et al*, 2001).

2.2.7 Potential H_3R targeted therapies

Taken together with the physiological role of histamine and the histaminergic system, the anatomical distribution of the H_3R and its modulation of key transmitter systems, as discussed above; strongly suggests that this receptor may be a potential therapeutic target in a broad range of diseases and disorders. Current areas of interest are in the treatment of cognitive deficits (Leurs *et al*, 2005; Hancock, 2006), dementias

(Medhurst *et al*, 2007) and psychoses (Akhtar *et al*, 2006); movement disorders (Gomez-Ramirez *et al*; 2006); sleep disorders (Leurs *et al*; 2005); obesity (Hancock, 2006); migraine (Millan-Guerrero *et al*; 2003) and gastric inflammatory pain (Coruzzi *et al*, 2007; Coruzzi *et al*, EHRS 2007); epilepsy (Yokoyama et al, 1993; Vohora et al, 2000; Kakinoki et al, 1998; Yoshida et al, 2000; Chazot & Hann, 2001); cerebral ischaemia (Lozada *et al*; 2005) and cardiac arrhythmias (Levi & Smith, 2000).

2.3 Histamine H_4 Receptor

2.3.1 Cloning

After the cloning of the human H_3 receptor in 1999 (Lovenberg *et al*, 1999) two separate groups used homology studies to identify and clone the latest human histamine H_4 receptor within the following year (Oda *et al*, 2000; Nakamura *et al*, 2000). The gene encoding the H_4 receptor is on human chromosome 18, spans >20.6 kb and has a similar intron-exon arrangement to the H_3R gene (Cogé *et al*, 2001). The H_4 receptor is expressed predominantly in bone marrow, eosinophils and mast cells. There is mounting evidence for its presence in some brain areas although there may be important species differences (see section **2.3.2** below). The H_4R shows considerable homology with the H_3R (58% for the transmembrane regions, but 34-35% overall) (Nguyen *et al*, 2001). There is substantial variation between species, with only 65-70% homology across human, mouse, rat and guinea-pig H_4 receptors (Liu *et al*, 2001) (see also section **2.3.4**). This is in contrast to the H_3R which is approximately 92% conserved across species (Liu *et al*, 2001). Reflecting their dissimilarity H_4 receptors have different pharmacological profiles. H_4R from humans

and guinea pigs have high affinity for histamine (5nM), whereas the affinity of the rat H_4R is 136nM. The rat H_4R is also less sensitive to other H_4R ligands (Liu *et al*, 2001).

This 390-residue GPCR is encoded by three exons. The similarity between the H_4 and H_3 gene structure and organisation suggests that multiple H_4R isoforms might exist and indeed two isoforms have recently been reported (van Rijn *et al*, 2007 submitted). The first, $H_4R_{(302)}$, lacks exon 2 which results in a deletion of 88 amino acids between TM2 and TM4. The second, $H_4R_{(67)}$, is a truncated receptor containing only the first 67 amino acids of the full length receptor.

2.3.2 Anatomical distribution

Mapping of anatomical distribution of H_4 receptors is hampered by the fact that the receptor appears to be expressed at low levels in most tissues. In addition expression levels may be altered by the activation state of the cell. It is expressed predominantly in bone marrow, eosinophils and mast cells. The tissue distribution of this receptor has been profiled in a range of human (using RT-PCR) and mouse (using in situ hybridisation) tissues (Zhu *et al*, 2001). In human tissues H_4R expression was most abundant in bone marrow and lung. It was expressed at a high level in human neutrophils. Interestingly receptor expression was higher in resting mononuclear cells, $CD4^+$ T cells, and $CD8^+$ T cells than in the activated cells. Very low levels of expression were found in resting and activated $CD19^+$ B cells and resting $CD14^+$ monocytes. In mouse tissue H_4R was detected in the hippocampal formation, particularly in the granular cell layer of the dentate gyrus and the pyramidal cell layer,

but not in the rest of the brain or other tissues such as skeletal muscle, fat, heart, liver, spleen, thymus, lymph node, adrenal gland, spinal cord or kidney. Another study using *in situ* hybridisation reported expression of the H_4R in both adult and embryonic rat brain where it was speculated to contribute to the migration of developing neurons (Lozada *et al*, EHRS 2004). Immunohistochemistry has shown that H_4 receptors are present in nerves from the human nasal mucosa (Nakaya *et al*, 2004). This thesis addresses the hypothesis that the H_4 receptor is expressed in the rat and human brain and may play a distinct role to the H_3R within the CNS.

2.3.3 Signal transduction

The H_4R is coupled mainly to $G_{i/o}$ proteins. Heterologous expression of H_4R leads to a pertussis-toxin-sensitive decrease in the forskolin-induced production of cAMP and the inhibition of downstream events such as cAMP responsive element-binding protein (CREB)-dependent gene transcription (Oda *et al*, 2000; Nakamura *et al*, 2000; Zhu *et al*, 2001; Liu *et al*, 2001). In addition in stably transfected HEK293 cells, H_4R stimulation leads to the pertussis-toxin-sensitive activation of downstream mitogen-activated protein (MAP) kinase pathways (Morse *et al*, 2001). As with most $G_{i/o}$-coupled GPCRs, H_4R activation increases [^{35}S]GTPγS binding (Morse *et al*, 2001). Furthermore increased basal levels of [^{35}S]GTPγS binding seen in H_4R transfected cells compared with non-transfected cells indicates that the H_4R is constitutively active, as already observed in the other histamine receptor subtypes. Histamine mediated activation of either endogenous H_4R in mast cells (Hofstra *et al*, 2003) or H_4R stably expressed in L1.2 cells (Nakayama *et al*, 2004) results in a Ca^{2+} response. Histamine-induced Ca^{2+} signalling is also described in eosinophils (Buckland *et al*,

2003). Both $G_{i/o}$ proteins and phospholipase C (PLC) are involved in histamine-induced calcium mobilization and chemotaxis in mast cells, because these responses were completely inhibited by pertussis toxin and the PLC inhibitor U73122. These observations suggest that phospholipase C is activated via Gβγ subunits dissociating from $G_{i/o}$ proteins following H_4R activation. The Ca^{2+} response in mast cells is probably linked to cellular chemotaxis because histamine-induced mast-cell chemotaxis shows similar sensitivity to pertussis toxin and U73122. In addition there is evidence for H_4R down-regulation of both STAT1 (Horr *et al*, 2006) and STAT6 (Michel *et al*, 2007) in sensitised human lymphocytes. The Jak/Stat pathway is involved in responses to many cytokines. Dimerisation of cytokine receptors occurs when the cytokine binds, this attracts a cytosolic tyrosine kinase unit (Jak) which associates with the dimer. Among the targets for phosphorylation by the receptor-Jak complex are a family of transcription factors (Stats). Phosphorylation leads to activation of the Stat which then migrates to the nucleus and activates gene expression. H_4R activation may down regulate the transcription activity of STAT6 by influencing cleavage of the transcription activation domain (TAD) (Michel *et al*, EHRS 2007).

2.3.4 Pharmacology

In view of the high homology between the H_3 and H_4 receptors in the transmembrane regions it is not surprising that several H_3 ligands also activate the H_4R. Amongst this group are the agonists immepip (H_4R K_i 9nM) (Liu *et al*, 2001), imetit (H_4R K_i 5nM) (Nguyen *et al*, 2001) and RAMH (H_4R K_i 146nM) (Jablonowski *et al*, 2003). In addition the H_4R is **activated** by the H_2/H_3R antagonist burimamide (H_4R K_i 180nM)

(Jablonowski *et al*, 2003) and the H_3R antagonist clobenpropit (H_4R K_i 13nM) (Liu *et al*, 2001). Thioperamide the prototypical inverse agonist at H_3R is also an inverse agonist at H_4R (H_4R K_i 27nM) (Jablonowski *et al*, 2003). Consequently these compounds can no longer be considered to be H_3R selective. However newer H_3R ligands such as the agonists immethridine and methimmepip (Kitbunnadaj *et al*, 2004 and 2005 respectively), and the non-imidazole H_3R antagonists JNJ6379490 and A349821 (Shah *et al*, 2002 and Faghih *et al*, 2003 respectively) have wide margins of selectivity making them useful research tools for the future. In addition other compounds with better H_4R selectivity, both agonists (Hashimoto *et al*, 2003; Lim *et al*, 2006) and antagonists (Jablonowski *et al*, 2003; Thurmond *et al*, 2004; Terzioglu *et al*, 2004), are showing promise. Interestingly the neuroleptic clozapine has also been shown to activate the H_4R (Oda *et al*, 2000). It is possible that H_4R activation may underlie the serious drug-induced agranulocytosis which clozapine can sometimes cause (Krupp & Barnes, 1992; Alphs & Anand, 1999). In addition, given preliminary evidence for some H_4R expression in the brain, it is possible that it may play a part in the therapeutic action of clozapine.

Full details of the H_4R ligand-binding site are yet to be described. The binding pocket for histamine is formed by transmembrane domains TM3, TM5 and TM6 (Shin *et al*, 2002). Not surprisingly it has characteristics common to the binding sites of other aminergic GPCR's (Shi & Javitch, 2002). A cluster of highly conserved aromatic residues in TM6, which faces the binding site, is thought to be involved in receptor binding and activation. Amino acid differences at key sites within the binding pocket are likely to account for differences in the affinity of histamine for the different

histamine receptors. Histamine shows increased affinity for H_3R and H_4R compared with H_1 and H_2 receptors.

As alluded to earlier (section **2.3.1**) there are considerable species differences in pharmacology of the H_4R (Liu *et al*, 2001). In a recent study chimeric receptors of the human and mouse H_4R were constructed to address the molecular basis for the different affinity of histamine at these two receptors (Lim, EHRS 2007). The second extracellular loop of the H_4R was found to be responsible. An important additional finding of this study was the possibility that the widely used human H_4R antagonist JNJ7777120 (Jablonowski *et al*, 2003) may not afterall be an antagonist at the rat H_4R, this requires further investigation.

2.3.5 *In vivo* role of histamine H_4 receptor

Several studies support a role for H_4 receptors in chemotaxis of immune cells, including human monocyte-derived dendritic cells and eosinophils (Gutzmer *et a*l, 2005; Buckland *et al*, 2003; Ling *et al*, 2004; O'Reilly *et al*, 2002), and most recently in human monocytes (Dijkstra *et al*, in press). H_4 receptor stimulation leads to actin polymerisation which is a key step in the polarisation and subsequent shape change of the cell which drives chemotaxis (Buckland *et al*, 2003). Most leukocyte attractants also affect the function and expression of adhesion molecules which are important for interactions with the microvascular epithelium. In line with its chemoattractant effects, histamine upregulates CD11b and CD54 in eosinophils (Buckland *et al*, 2003; Ling *et al*, 2004). Histamine also induces migration of mast cells *in vivo*. Histamine inhalation leads to an increase in the total number of mast cells in the trachea of mice

(Thurmond *et al*, 2004). These increases are mediated via H_4 receptors as demonstrated by the ability of H_4R antagonists to inhibit the migration. The H_4R also has a role in the secretion of IL-16 from $CD8^+$ T cells (Gantner *et al*, 2002). IL-16 is produced by several cell types and is a chemoattractant for $CD4^+$ T cells. Stimulation of both H_4 and H_2R appears to be necessary for this effect because inhibitors of either block the response. Furthermore H_4R modulation of $CD4^+$ T cell activation and Th2 responses has been described in a murine asthma model (Dunford *et al*, 2006). In this study blockade of the H_4R on dendritic cells lead to decreases in cytokine and chemokine production and limited their ability to induce Th2 responses. The monocyte fraction of peripheral blood mononuclear cells, where H_4R have most recently been demonstrated (Dijkstra *et al*, 2007 in press), contain direct precursors of dendritic cells and skin associated macrophages. Stimulation of H_4R on monocytes (Dijkstra *et al*, 2007 in press) lead to an inhibition of the production of the chemokine CCL2 which resulted in a decrease in monocyte recruitment.

The widespread expression of H_4 receptors on immune cells including mast cells, eosinophils and monocytes, together with their ability to mediate chemotaxis and influence the secretion of some chemokines; suggests a role for the H_4R in inflammation and immune responses. The increase in vascular permeability caused by histamine is mediated through its action at H_1R. However H_4 receptors appear to be responsible for other well documented inflammatory events. H_4R antagonists block neutrophilia in pleurisy models and peritonitis induced by zymosan (Thurmond *et al*, 2004; Takeshita *et al*, 2003). It should be noted that the maximum inhibition achieved in these two models is only about 50%, implying that H_4 activation is not the sole mechanism underlying the response. *In vivo* inhibition of neutrophilia is unlikely to

result from a direct effect on neutrophils (Takeshita *et al*, 2004; Thurmond *et al*, 2004), it could be that H_4R antagonists reduce the level of other neutrophil chemoattractants.

Histamine has an important role in the development of several cell types mediated via the different histamine receptors. Recent investigations demonstrate that the H_4R plays a critical role in dendritic cell (DC) differentiation and also regulates cytokine production by these cells (Jelinek *et al*, EHRS 2005). Thymic selection and T cell development also appear to be influenced by the H_4R (Pállinger *et al*, EHRS 2005). In addition there is evidence for H_4R involvement in placental development (Szewczyk *et al*, 2007).

2.3.6 Potential H_4R targeted therapies

Considering the putative *in vivo* role of H_4R in mediating certain aspects of inflammatory responses, H_4R selective drugs might prove beneficial in the treatment of some allergic (Daugherty, 2004) and inflammatory conditions (de Esch *et al*, 2005; Lim *et al*, 2006). Selective H_4R antagonists significantly inhibited both paw oedema and thermal hyperalgesia induced by subplantar injection of carrageenan in the rat (Coruzzi *et al*, 2007). Importantly these activities were not associated with gastric damage, which is an unwanted side effect of many commonly used non-steroidal anti-inflammatories (NSAIDs).

In addition H_4R mediated influences on cell differentiation suggest cancer therapies could be an area of interest. Preliminary evidence for H_4R involvement has been

reported for colon cancer (Cianchi *et al*, 2005; Darvas *et al*, EHRS 2007), pancreatic carcinoma (Martin *et al*, EHRS 2007) and mammary carcinogenesis (Medina *et al*, 2006).

3. GPCR Oligomerisation

The subject of GPCR oligomerisation is currently attracting great interest. Since the early 1990s, evidence has been growing not only for the existence of GPCR oligomers but also for their functional significance (George *et al*, 2002; Hill, 2006). The terms oligomer and dimer have been used interchangeably here, although strictly speaking a dimer consists of only two units, while an oligomer may be two or more. Experiments making use of GPCR chimeras whereby co-expression of two individually nonfunctional receptors could restore functionality (α_2/M_3 and M_3/α_2 chimeras Maggio *et al*, 1993) were among the first to demonstrate the potential for dimerisation. More recently biophysical techniques such as Fluorescent Resonance Energy Transfer (FRET) and Bioluminescent Resonance Energy Transfer (BRET) have provided evidence that oligomers exist in living cells (Bulenger *et al*, 2005). In these assays close proximity between donor and acceptor fluorophore tagged receptors allows excitation of the acceptor which results in a fluorescent emission.

One of the most well known demonstrations of a receptor hetero-dimer being essential for function is provided by studies of $GABA_BR1$ and $GABA_BR2$ (Marshall *et al*, 1999). $GABA_BR2$ is necessary for the successful trafficking and expression of receptors at the cell surface, $GABA_BR1$ is essential for ligand binding (Jones *et al*, 1998). A further compelling example is provided by sweet and unami (savoury) taste

receptors. These receptors are coded for by three genes T1R1, T1R2 and T1R3. Two of the three genes need to be expressed in order to give a functional receptor (Zhao *et al*, 2003). The T1R1/T1R3 combination codes for the unami receptor while T1R2/T1R3 results in the expression of sweet taste receptors (Nelson *et al*, 2001). Therefore the receptor binding site is clearly altered by the presence of either the T1R1 or the T1R2 subunit.

Both the $GABA_B$ and the taste receptors belong to the GPCR class C family of GPCRs, however there is also support for dimerisation in the rhodopsin-like class A GPCRs, to which the histamine receptors all belong. Impressive atomic force microscopy images have been published of rhodopsin homo-dimers in native retinal discs (Fotiadis *et al*, 2003). Furthermore the 3D structure of rhodopsin (Palczewski *et al*, 2000) and heterotrimeric G proteins (Sondek *et al*, 1996; Lambright *et al*, 1996) suggests that a 2:1 (GPCR:G protein) stoichiometry is necessary for receptor/G protein coupling. Direct proof of this has come from neutron-scattering experiments on the solubilised receptor for leukotriene B_4 (BLT_1R) (Baneres & Parello, 2003). A pentameric assembly was demonstrated in the presence of agonist, consisting of a $BLTR_1$ dimer coupled to a trimeric G protein.

Here emphasis will be given to functional evidence for class A GPCR dimers, suggestive of a potential *in vivo* role.

a) Homo-dimerisation

Functional roles for homo-dimers have been implicated in a number of investigations (Brady & Limbird, 2002). The level of dimerisation of mouse δ opioid receptors

expressed in CHO cells was found to be agonist dependent (Cvejic & Devi, 1997). Increasing the agonist concentration brought about an increase in the level of dimers and a concomitant decrease in receptor monomers. Morphine, however, did not affect the levels of either form. Since morphine, unlike other opioid agonists, does not induce receptor internalization, this may suggest a relationship between the ability of agonists to reduce the levels of dimer and to induce receptor internalization. At odds with these findings levels of human δ opioid receptor homo-dimers constitutively expressed in HEK293 cells were not affected by either agonist or inverse-agonist (McVey *et al*, 2001). A peptide derived from TM6 of the β_2- adrenoceptor (AR) was able to inhibit the formation of homo-dimers (Hebert *et al*, 1996). Importantly this same peptide was able to inhibit agonist-promoted stimulation of adenylyl cyclase activity. Agonist binding was found to stabilise dimers, whereas inverse agonist favoured formation of the monomer. Therefore interconversion between monomeric and dimeric states could be important for biological activity. In agreement with these observations, agonist was shown to increase the BRET signal generated by the formation of β_2-AR homo-dimers in whole cells (Angers *et al*, 2000). Using photoincorporation of radiolabelled ligands selective for dopamine D2 receptors, spiperone was shown to target monomers whereas nemonapride was incorporated into both monomers and dimers (Ng *et al*, 1996).

b) Hetero-dimerisation

Hetero-dimerisation between κ and δ opioid receptors results in pharmacology quite distinct from that of the individual component receptors (Jordan & Devi, 1999). Recently an opioid agonist, 6'-guanidinonaltrindole (6'-GNTI), which is selective for κ/δ opioid hetero-dimers has been described (Waldhoer *et al*, 2005). Importantly this

study demonstrated the potential for tissue selective drug-targeting based on GPCR dimerisation. 6'-GNTI induces analgesia only when it is administered in the spinal cord but not in the brain, suggesting tissue specific expression of κ/δ opioid hetero-dimers. Many class A GPCRs do not reach the cell surface in heterologous expression systems (Minneman, 2006). This "technical inconvenience" has been turned to advantage in experiments to investigate the combinations of receptor subunits which facilitate receptor expression at the cell surface. Within the α_1-AR subfamily, α_{1D}-ARs are almost entirely intracellular (Chalothorn *et al*, 2002). However co-expression of α_{1D}-ARs with α_{1B}-ARs leads to quantitative surface expression of the α_{1D}-AR subtype (Hague *et al*, 2004). Consistent with this, α_{1D}-ARs are expressed on the cell surface when they are transfected into DDT1 smooth muscle cells which endogenously express α_{1B}-ARs (Han *et al*, 1992); while in rat aortic smooth muscle cells, which do not endogenously express α_{1B}-ARs, they remain intracellular (Hague *et al*, 2004). Olfactory receptors (ORs) make up about half of the entire human GPCR family, in common with other class A GPCRs many of them are not trafficked to the cell surface in heterologous expression systems. However co-expression of the mouse M71-OR with the β_2-AR subtype in HEK293 cells leads to a substantial translocation of functional M71-ORs to the cell membrane (Hague *et al*, 2004). Importantly, in this same study, *in situ* hybridisation showed extensive co-localisation of M71-OR with β_2-AR mRNA in mouse olfactory epithelium. Interestingly all *Drosophila* olfactory neurons express two ORs: one specific to a particular olfactory neuron while the other (OR83b) is ubiquitously expressed in most olfactory neurons (Larsson *et al*, 2004). Without OR83b specific ORs do not localise to appropriate dendritic compartments and the neurons are not stimulated by odour in electrophysiological assays.

Furthermore flies lacking OR83b do not respond to odour in behavioural experiments (Larsson *et al*, 2004).

c) Mechanism of dimerisation

The manner in which GPCRs dimerise has not been resolved and given the diversity of GPCR structures even within any one class it is unlikely that there is a universal mechanism. Initial studies for family A GPCRs implicated involvement of both N (Abdalla *et al*, 1999) and C (Cvejic & Devi, 1997) termini in receptor dimerisation. However more recently the focus has been on the TM helices. Several studies have used peptides with sequences corresponding to the predicted site of interaction to disrupt dimers. For example a peptide matching a sequence in TM6 of β_2-ARs abolished immunoreactive species of a size compatible with homo-dimers (Hebert *et al*, 1996). Similarly putative dopamine D2 receptor homo-dimer immunoreactivity was removed by peptides directed at sequences in TM6 and TM7 (Ng *et al*, 1996). Characterisation of the yeast alpha factor receptor (a receptor for the alpha-mating pheromone in the yeast *Saccharomyces cerevisiae*) has identified a GXXXG dimerisation motif in TM1 (Overton *et al*, 2003). This same sequence is present in the TM regions of many GPCRs. It is also found within the H_3R sequence (GALAG) although here it is in the extra-cellular N-terminus. Mutation and truncation studies with α_1-AR subtypes (Hague *et al*, 2004) suggest the hydrophobic core and/or intra/extracellular loops are the sites of interaction between dimer components. However data on the importance of different regions and motifs has sometimes been conflicting (Milligan *et al*, 2004) and this may indicate that there are multiple sites and no common mechanism involved in these interactions.

Two types of inter-molecular association have been proposed for GPCR homo-oligomers: disulphide bonds and TM-domain interactions. Homo-oligomers of several class A GPCRs can be dissociated using reducing agents (George *et al*, 2002), suggesting that a disulphide linkage is important for oligomer formation. Interestingly, this is not detected in all receptors (including the histamine H_3 and H_4Rs, from our own observations), and the complete dissociation by a reducing agent of all receptor dimers to receptor monomers is not always seen, even in receptors that are sensitive to this treatment. Therefore other interactions besides disulphide bonds appear to be involved. As described above there is increasing evidence for TM-domain interactions. Computer models of adrenoceptors have indicated that GPCRs might undergo a process known as "domain swapping" (Gouldson *et al*, 2000). Domain swapping has been shown to occur in the oligomerisation of several other proteins (Bennett *et al*, 1994) and it could explain the rescue of binding seen in experiments where ligand binding is restored by the co-expression of two nonbinding GPCR mutants, with mutations in different TM domains both involved in the binding site (Maggio *et al*, 1993,1996; Monnot *et al*, 1996). There is however some evidence against domain swapping, not least that in class A GPCRs the TM domains appear to be arranged in a tightly packed hydrophobic bundle, rendering folding rearrangements unlikely. Photoaffinity labelling of the cholesystokinin receptor failed to demonstrate domain swapping in cholesystokinin oligomerisation (Hadac *et al*, 1999); and functional rescue was not seen on co-expression of full length vasopressin V2 receptors containing the R181C (TM4) and the Y280C (TM6) missense mutations (Schulz et al, 2000). Therefore "contact" oligomers have been proposed, as an alternative arrangement (Fig 1.5)

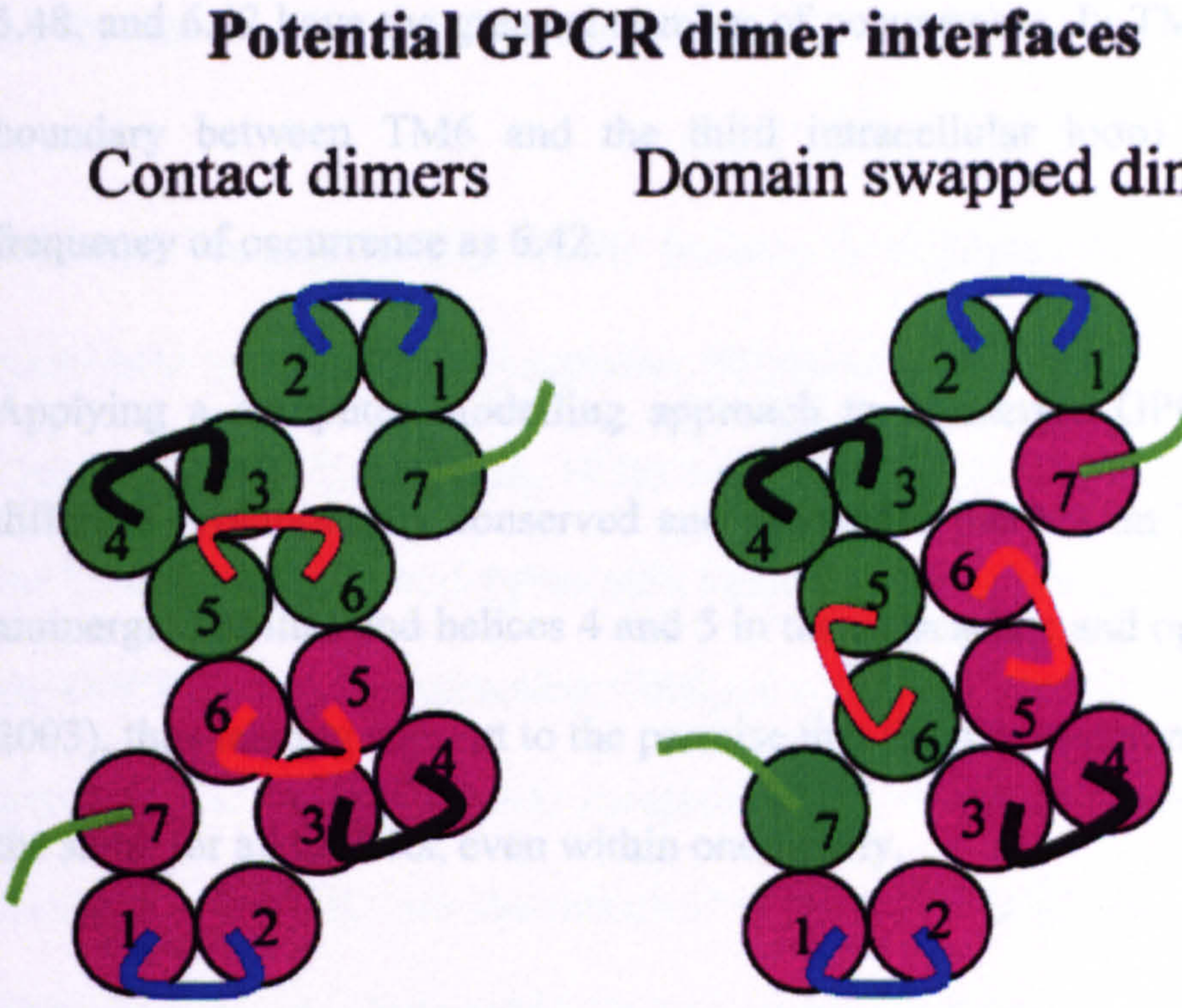

Fig 1.5 Comparison of contact dimers and domain-swapped dimers

In practice it may often not be possible to distinguish between these two different configurations (Gouldson *et al*, 2000), and it is quite likely that they are not mutually exclusive.

Bioinformatics techniques are increasingly being used to predict dimer and oligomer interfaces. These techniques begin with multiple sequence alignments and share the assumption that proteins that are evolutionarily related probably share common structural and functional features corresponding to detectable patterns in their sequences (Reggio, 2006).

The occurrence of lipid-exposed residues in predictions from bioinformatics methods has been analysed and used to search for dimerization/oligomerization interfaces of GPCRs (Filizola & Weinstein, 2005). Residues most frequently identified cluster in TM helices 4 – 6. Among the residues identified within each of these 3 helices, 4.58,

5.48, and 6.42 have the greatest number of occurrences. In TM6, residue 6.30 (at the boundary between TM6 and the third intracellular loop) had nearly the same frequency of occurrence as 6.42.

Applying a computer modelling approach to aminergic GPCR sequences revealed different evolutionarily conserved and accessible patches on TM helices 4-6 in most aminergic families and helices 4 and 5 in the muscarinic and opsin family (Soyer *et al*, 2003), thus lending support to the premise that the dimerisation mechanism may not be the same for all GPCRs, even within one family.

d) Possible role of GPCR dimers

The physiological role of receptor dimerisation is still largely unknown. GPCR's are important because they usually play a regulatory role, modulating all known physiological processes in mammals. The nature of ligand-GPCR-effector interactions is such that it is uniquely amenable to adjustments and fine tuning. This is because the responses are relatively slow and involve multiple steps and interactions, providing many opportunities for continual adjustment. Dimerisation provides another means of moderating a response and tailoring it to meet continually changing external demands. Several possible mechanisms can be envisaged (e.g. facilitating cell surface expression) and there is growing evidence for some of them as alluded to above. Dimerisation may serve the same or different purposes depending on the receptors in question.

3.1 GPCR interactions with other proteins

It is now understood that GPCR function is regulated by interacactions with other membrane and intracellular proteins. Receptor inactivation is brought about by GPCR kinases (GRKs) (Lefkowitz, 1993) which phosphorylate serine/threonine residues in the C-terminus, followed by arrestin binding (Zuckerman *et al*, 1985). Arrestins block the GPCR/G protein interaction. GRKs are receptor specific and mainly phosphorylate activated i.e. agonist bound, receptors. This is called homologous desensitisation. Arrestins and GRKs are also involved in endocytosis of receptors and cell signalling. They can act as "adaptors" linking receptors both to endocytic machinery and signalling proteins (Ferguson, 2001).

Receptor Activity Modifying Proteins (RAMPS) are a family of membrane proteins that bind GPCRs and alter their function. It was found that the receptor for a neuropeptide (calcitonin gene-related peptide: CGRP) lacked activity without the presence of another membrane bound protein, since designated RAMP1 (McLatchie *et al*, 1998). Surprisingly this same receptor when complexed with a different RAMP (RAMP2) shows specificity for a completely different peptide, therefore specificity is conferred by the RAMP rather than the GPCR. It is not known how widespread this form of regulation is.

Many more multidomain scaffolding proteins and accessory/chaperone proteins have now been identified. These provide a broad range of mechanisms for ligand recognition, signalling, receptor regulation and trafficking (reviewed by Brady & Limbird, 2002), an exhaustive account will not be provided here.

3.2 Post-translational changes and GPCR function

Post-translational modifications of proteins involved in cell signalling are important to their function. Two of the most common are palmitoylation and glycosylation. Palmitoylation is a covalent attachment of palmitic acid to one or more cysteine residues via a hydroxylamine-labile thioester bond. Glycosylation is the addition of saccharides either via the amide nitrogen of asparagines (N-linked glycosylation) or the hydroxyl oxygen of serine and threonine residues (O-linked glycosylation). The effects of both have been investigated for several GPCRs (Palmitoylation review: Qanbar & Bouvier, 2003; Glycosylation review: Duvernay *et al*, 2005).

Studies of the palmitoylation sites of rhodopsin (Moench *et al*, 1994) revealed that anchoring of the palmitates in the membrane results in the formation of a fourth cytoplasmic loop. However palmitoylation has been reported to regulate a range of other functions in different family members. In the vasopressin V_{1a} receptor palmitoylation status controls both phosphorylation and sequestration of the receptor, furthermore palmitoylation, phosphorylation and sequestration are all regulated by agonist (Hawtin *et al*, 2001). Palmitoylation of the human endothelin$_B$ receptor is critical for G-protein coupling (Okamoto *et al*,1997), while in the vasopressin V2R palmitoylation enhances cell surface expression (Sadeghi *et al*, 1997).

Since O-glycosylation lacks a consensus site it has proved more difficult to study, therefore most of the literature relates to N-glycosylation which occurs exclusively at the consensus site NXS/T. The involvement of glycosylation in modulating GPCR targeting to the cell surface varies among different GPCRs. N-linked glycosylation of

the angiotensin II type 1 receptor (AT1R) is an absolute requirement for cell surface expression (Deslauriers *et al*, 1999). By contrast, although mutation of the two glycosylation sites on β_2-AR leads to a significant decrease in plasma membrane expression, receptor function is not greatly affected (Rands *et al*, 1990). In the case of the histamine H_2R removal of glycosylation sites does not prevent their cell surface expression (Fukushima *et al*, 1995). The molecular mechanism by which glycosylation is able to regulate GPCR maturation and export trafficking is unclear and is unlikely to be the same for all receptors. There is evidence to suggest that the glycosylation state might determine which Rab GTPase is activated and thereby direct the pathway by which the receptor is trafficked from one compartment to another (Wu *et al*, 2003; Filipeanu *et al*, 2004). The Rab family is part of the Ras superfamily of small GTPases. The different Rab GTPases are located on the cytosolic face of specific intracellular membranes, where they function as regulators of distinct steps in membrane traffic pathways. In the GTP-bound form, the Rab GTPases recruit specific sets of effector proteins onto membranes. Through their effectors, Rab GTPases regulate vesicle formation, actin- and tubulin-dependent vesicle movement, and membrane fusion. Finally a recent study has shown that receptor sialylation and N-glycosylation participate with disulphide bonding in the stabilisation of human bradykinin B2 receptor dimers at the cell surface (Michineau *et al*, 2005).

4. Conclusions and Aims

The biology of histamine and its receptors is complex. Histamine is available in many parts of the body and receptor distribution is widespread. In the periphery histamine is a mediator in inflammatory and immune reactions, it also controls vascular permeability, gastric acid secretion and smooth muscle contraction. In the CNS

histamine appears to play a key role in important homeostatic mechanisms regulating arousal, the sleep/wake cycle, feeding behaviour, learning and memory, and responses to stressful or painful stimuli. It interacts with a myriad of other receptors and chemical messengers so that the final outcome is an integrated response to multiple influences. The age of molecular biology has seen an extraordinarily rapid increase in our knowledge of all the components involved in cell signalling. Despite this our ability to predict the effect of manipulating a particular receptor in a whole animal is still extremely limited in many cases and this is exemplified in responses to H_3 receptor ligands. Cloning of the H_3 receptor has provided insights into possible mechanisms underlying experimental observations. The possibility of multiple splice site variants with differential tissue distribution, pharmacology and signalling is one confounding factor. Another is the multifaceted nature of GPCR signalling and regulation. GPCR's appear to operate by interacting with a range of other proteins, thus enabling them to act as modulators responding flexibly over time to changing stimuli. There is a growing consensus that GPCR function as dimers or higher oligomers and this is likely to be important both in signalling and receptor regulation. Furthermore the significance of post-translational changes such as glycosylation to receptor function is gaining recognition.

While cloning of the H_3 receptor has lead to a rapid increase in our understanding of its structure and function, tools to exclusively demonstrate expression of H_3 receptor protein are limited. Our laboratory was the first to develop a specific anti-H_3R antibody (Chazot & Hann, 2001). This antibody has been used to map H_3R distribution in rodent brain and further characterise the receptor. In the light of current thinking on GPCR biology the aim of this PhD project was as follows: First, to

develop further anti-H_3 receptor isoform specific antibodies with which to map the expression of H_3R isoforms in native tissue; and second to use these antibodies as probes to investigate potential sources of receptor heterogeneity, in particular oligomerisation and glycosylation. An additional aim was to generate the first anti-H_4 receptor antibody following our previously successful anti-H_3R strategy, and to use this antibody in studies to characterise the histamine H_4 receptor.

Hypotheses to address relating to the human H_3 and H_4 histamine receptors:

1) H_3 and H_4 receptors are able to homo-oligomerise
2) H_3 and H_4 receptors are able to hetero-oligomerise with their respective splice variants
3) Splice variants can act as dominant negative regulatory subunits
4) N-glycosylation is a prerequisite for receptor dimerisation
5) H_3 and H_4 histamine receptors are both expressed in brain and subserve distinct functions

CHAPTER 2

MATERIALS AND GENERAL METHODS

2.1 Source of materials

2.1.1 Sigma-Aldridge chemical company (Poole, Dorset, UK)

N-2-hydroxyethylpiperazine-N'-2-ethane sulphonic acid (HEPES).

Thyroglobulin.

Folin-ciolcalteau phenol reagent.

Pre-stained molecular weight markers (molecular weight range 30 - 220 kDa).

Tween – 20.

p-coumaric acid.

Luminol.

Hydrogen peroxide (30% v/v).

Kodak D-19 developer.

Kodak fixer.

Ampicillin.

Agarose.

Teriffic broth.

Agar.

Dulbecco's modified eagle medium/F12 containing L-glutamine.

Dulbecco's modified eagle medium/F12.

7.5% (w/v) Sodium bicarbonate.

Penicillin (500I U/ml) / streptomycin (500µg/ml) solution.

Sodium hydroxide.

Trypsin 0.5g, EDTA 0.2g per litre of Hanks.

Ethylenediaminetetracetic acid (EDTA).

Ethylenebis(oxyethylenenitrilo)tetracetic acid (EGTA).

Metyrapone.

Glutaraldehyde.

Sodium phosphate

3-maleimimdobenzoic acid N-hydroxysuccinimide ester (MBS).

Freund's adjuvant complete.

Freund's adjuvant incomplete.

CH-sepharose beads.

Tris (hydroxymethyl) methylamine.

Sodium azide.

Sodium phosphate.

Diaminobenzidine tablets.

Triton X-100.

Anti-β-actin

Anti-FLAG M2 monoclonal antibody (Product code F3165)

Dithiothreitol (DTT).

Poly(ethyleneimine) solution.

Dialysis tubing (visking size 11/4'').

Bis (sulfosuccinimidyl) suberate.

Sodium dodecyl sulphate (SDS).

β-mercaptoethanol.

Albumin bovine fraction V powder

Acrylamide/bis-acrylamide 30%

Bromophenol blue

Streptavidin beads

2.1.2 BDH laboratory supplies (Leicestershire, UK)

N,N,N',N'-teramethylethylenediamine (TEMED).

Amonium persulphate.

Methanol.

Chloroform.

Glycerol.

Isopropanol.

Ethanol.

Dimethyl sulphoxide (DMSO).

Sodium hydrogen carbonate.

Potassium phosphate.

Hydrochloric acid.

Citric acid.

Sodium chloride.

Acetic acid.

DPX mountant.

Potassium chloride.

Diethylamine.

2.1.3 Cambrex Bio Science (Verviers, Belgium)

Foetal calf serum.

2.1.4 Promega Ltd (Southampton, UK)

VECTASTAIN® ABC kit.

HB101 Competent *E.coli* cells.

2.1.5 Amersham International (Aylesbury, Bucks, UK)

Blotting paper.

Nitrocellulose.

Hyperfilm™.

HRP linked secondary antibody- rabbit.

HRP linked secondary antibody-mouse.

Binding filters.

2.1.6 Tocris (Bristol, UK)

Thioperamide.

Iodophenpropit.

(R)-(-)-α-Methylhistamine dihydrobromide.

2.1.7 Boehringer mannheim GMBH (Lewes, Sussex, UK)

N-glycosidase F^*, recombinant.

2.1.8 Immune systems (Bristol, UK)

Histamine H_3R peptides

Rat histamine $H_{3\,C}$ (268 – 277) EAMPLHRGSK-Cys

a sequence specific to the i3 region in the rat H_{3C} isoform

2.1.9 Sigma-Genosys (Cambridge, UK)

Histamine H_3R peptides

P1:	human $H_{3\ 365}$ (270 – 279)	i3 just before TM6	CMPLHRKVAKS
P2:	human $H_{3\ 415}$ (229 – 238)	i3	CTRLRLKGHGE
P3:	human $H_{3\ 329\ \Delta 13}$ (222 – 231)	TM5 i3	CYLNIQSFTQR

Sequences specific to the i3 region of the respective isoforms

human $H_{3\ 220}$ (211 – 220)	Isoform 5	CRRPRPRWRSA

Histamine H_4R peptides

Chazot 3 human H_4 (374 – 390)	C-terminal	CIKKQPLPSQHSRSVSS
Chazot 4 human H_4 (251 – 266)	C-terminal	CERRRRKSSLMFSSRTK

2.1.10 QIAGEN Ltd (Dorking, Surrey, UK)

QIAGEN® plasmid maxi kit.

2.1.11 Calbiochem (Nottingham, UK)

Protease inhibitor cocktail, Set III

2.1.12 Pierce (Rockford, UK)

Sulpho-NHS-SS-Biotin

2.1.13 Miscellaneous

[^{3}H]-clobenpropit, 43Ci/mmol, 99% purity James Black Foundation.

H_3R -/- mouse material (US Patent 7151200) a gift from Prof Tim Lovenberg

Human putamen prepared for SDS-PAGE gift from Dr Margaret Piggott, Newcastle University

pCI neo $H_{3\ (445)}$ construct was a gift from Prof Tim Lovenberg.

Human H_3R cDNA C-terminally labelled with FLAG a gift from Prof Francis Cogé:

$hH_{3\ (445)}$/pc DNA 3.1 (-)

$hH_{3\ (365)}$/pc DNA 3.1 (-)

$hH_{3\ (329)}$/pc DNA 3.1 D-V5-His-TOPO

Human H_4R cDNA a gift from Prof Rob Leurs

Anti-haemagglutinin antibody a gift from Prof Rob Leurs

Human embryonic kidney (HEK) 293 cells from the European collection of cell cultures, Salisbury, Wilts.

2.2 Instruments and Equipment

Spectrophotometry: Jenway Genova spectrophotometer

Centrifuges: A sorval RC5C centrifuge was used with a GS-3 fixed angle rotor (for large volumes >400ml). A Biofuge fresco Heraeus (Kendro Laboratory Products) was used for all volumes less than 1.5ml.

Incubators: shaking incubator, cell incubator Shel Lab (Sheldon Manufacturing Inc.).

Orbital shaker: Stuart scientific 505.

Water bath: Nüve bath.

Heating block: QBT2 heating block (Grant).

Hot plate: FALC

Stirrer: Bibby Sterilin

Rocker: Grant-Bio PMR-30

Balances: Milligram amounts were weighed using a Mettler Toledo classic. All other amounts were weighed using a Scouts Pro balance (Ohous).

Electrophoresis equipment: Polyacrylamide gels were cast in a Hoefer SE 245 dual gel caster using gel plates of 10x8cm, electrophoresis was performed using a Hoefer mini-vertical gel electrophoresis unit SE260 and transferred using a Hoefer TE 22 tank transfer unit, power was from an Electrophoresis Power Supply EPS 301, all supplied by Amersham Biosciences.

Radioligand binding equipment: Bound radioactivity was collected using a Brandel cell harvester. Radioactivity was counted using a TriCarb 1600TR Liquid Scintillation Analyser (Packard).

Microscopes: Nikon Eclipse E400 used for Immunohistochemistry and cells.

Photography: Nikon digital camera Coolpix E950 used for Immunohistochemistry. Kodak camera for agarose gels.

Other equipment: Immunoblotting cassette, pH meter was a Mettler Toledo MP220, automatic pipetteman

Glassware, plastics and disposables: Hamilton syringe. Dounce glass/glass homogeniser. Cell scrapers, 250ml sterile cell culture flasks, petri dishes and sterile pipettes from Greiner. Sterile filters: 0.2μm Sartorius Sartolab- V150 filter unit. Microtitre plates. Cryogenic vials. Sterile pipettes and 250ml sterile filter lid cell culture flasks from Bibby sterilin. Falcon tubes. Columns. Filters for radioligand binding, Whatman GF/B filters, radioligand binding tubes, Eppendorf tubes, pipette tips, syringes from SLS, UK.

2.3 Preparation of standard solutions

2.3.1 Lowry reagent A:

2% (w/v) sodium carbonate, 0.1M sodium hydroxide and 5% (w/v) SDS.

2.3.2 Lowry reagent B:

2% (w/v) sodium potassium tartrate.

2.3.3 Lowry reagent C:

1% (w/v) copper sulphate.

2.3.4 Stacking gel buffer:

0.5M Tris-glycine, pH 6.8, containing 8mM EDTA and 0.4% (w/v) SDS.

2.3.5 Resolving gel buffer:

50mM Tris, 384mM glycine, 1.8mM EDTA and 0.1% (w/v) SDS pH 8.8.

2.3.6 Stock acrylamide:

30% (v/v) acrylamide and N,N'-methylenebisacrlyamide

2.3.7 Electrode buffer:

50mM Tris, 384mM glycine, 1.8mM EDTA and 0.1% (w/v) SDS pH 8.8.

2.3.8 Sample buffer:

30mM sodium hydrogen phosphate, pH 7.0, 30% (v/v) glycerol, 0.05% (v/v) bromophenol blue and 7.5% (w/v) SDS.

.2.3.9 Pre-stained molecular weight markers:

Pre-stained standards (protein molecular weight range 6.5-200 KDa, Sigma), stored in sample buffer, section 2.3.8.

2.3.10 Transfer buffer:

25mM Tris, pH 8.4, 192mM glycine and 20% (v/v) methanol.

2.3.11 TEE buffer:

50mM Tris-citrate pH 7.1, containing 5mM EDTA and 5mM EGTA.

2.3.12 Phosphate buffered saline (PBS):

0.01M sodium hydrogen phosphate, 1.7mM potassium hydrogen phosphate, pH 7.4, 137mM sodium chloride, 107mM potassium chloride.

2.3.13 Tris buffered saline (TBS):

50mM Tris-HCl, pH 7.4.

2.3.14 HEPES buffered saline (HBS):

280mM sodium chloride and 1M sodium hydrogen phosphate pH7.12.

2.3.15 Tris/EDTA (TE) buffer:

10mM Tris, 1mM EDTA, pH8.0

2.3.16 TBE buffer:

0.9M Tris, 0.9M boric acid and 40mM EDTA.

2.3.17 Homogenisation buffer:

50mM Tris-HCl pH 7.4, containing 5mM EDTA and 5mM EGTA.

2.4 General methods

2.4.1 Membrane Preparation for Immunoblotting

Either adult Wistar rats or adult mice strain C57B6 were stunned and decapitated. The required brain tissue was dissected and kept cool on ice. The tissue was then homogenised in ice-cold homogenisation buffer (section 2.3.17) supplemented with 320mM sucrose using a dounce glass/glass homogeniser. Membrane debris was pelleted by spinning the homogenate at 1,200 x g, 4°C for 10 minutes. The supernatant was transferred to a clean JA20 centrifuge tube, the volume was made up

to 10 ml with homogenisation buffer + sucrose and it was spun at 20,000 x g, 4°C for 30 minutes. The supernatant was discarded and the pellet briefly drained before resuspension in homogenisation buffer (without sucrose), 5ml of buffer for every gram of starting material. The homogenate was stored in 100µl aliquots at –20°C.

2.4.2 Determination of Protein Concentration

The protein concentration was determined using the method of Lowry *et al.*, (1951) employing bovine serum albumin (BSA) as the standard protein. A stock solution of BSA (10 mg/ml) was serially diluted in water, to give a range of standard BSA concentrations from 0 to 100 µg/ml. Lowry reagent A (section 2.3.1), Lowry reagent B (section 2.3.2) and Lowry reagent C (section 2.3.3) were mixed in a volume ratio of A (50): B (1): C (1). To both the BSA standards and the unknown protein samples (50 µl) 0.5 ml of the mixture of reagent A, B and C was added, each sample was vortexed and incubated at room temperature for 10 minutes. All samples were assayed in triplicate. On the addition of 50 µl of Folin-Ciocalteau phenol reagent (1 M, 1:1 mix of Folin reagent and water) each sample was mixed and incubated at room temperature for 30 minutes. The reaction was terminated by the addition of 500µl of water. The O.D. at λ = 750 nm was determined for each sample using a Jenway Genova spectrophotometer.

A calibration curve was plotted of O.D. at λ = 750 nm for the BSA samples. This was then used to determine the unknown protein concentration.

2.4.3 SDS-Polyacrylamide Gel Electrophoresis

Immunoblotting was carried out essentially as described by Duggan *et al.*, (1991), using SDS/PAGE in 7.5% polyacrylamide mini-slab gels under reducing conditions.

2.4.3.1 Preparation of Resolving Gel

The resolving gel (7.5 %) was prepared by mixing water (6 ml) with resolving gel buffer (section 2.3.5), TEMED (6 µl), stock acrylamide (section 2.3.6) (3 ml), and 10 % (w/v) ammonium persulphate (APS) (60µl). The polyacrylamide solution was immediately poured into a Hoefer SE 245 dual gel caster, using 2 gel plates of 10 x 8 cm and spacers of 1 mm width. Saturated water/butanol solution (100 µl) was added over the top of each gel. The gels were covered with parafilm and were allowed to polymerise for 60 minutes at room temperature. Gels were individually wrapped in tissue and stored in electrode buffer (section 2.3.7) at 4°C until use.

2.4.3.2 Chloroform/methanol Method for Protein Precipitation and Preparation of Protein Samples for SDS-PAGE

Protein samples for SDS-PAGE were precipitated using chloroform/methanol precipitation described as follows. To the protein samples (25-50 µg), methanol (4 vol) was added and the samples were vortexed and centrifuged at room temperature at 18,000xg for 1 minute. Chloroform (1 vol) was added to the samples, which were vortexed and centrifuged at 18,000xg at room temperature for 1minute. To each of the samples water (3 vol) was added which were again vortexed and centrifuged at room temperature at 13000 rpm for 1 minute. The upper layer was carefully discarded and methanol (1 vol) was added to each of the samples. The samples were centrifuged at 18,000xg at room temperature for 4 minutes. The supernatant was removed and the samples were air-dried. The dried protein pellet was resuspended by vortexing in sample buffer (section 2.3.8), 200mM DTT (2 µl) and water to a final volume of 15

µl. The samples were boiled in a water bath for 5 minutes and then centrifuged at 18,000xg for 30 seconds at room temperature before analysis by SDS- PAGE.

2.4.3.3 SDS-Polyacrylamide Gel Electrophoresis

The resolving mini-slab gel was clamped into a Hoefer mini-vertical gel electrophoresis unit SE260. The stacking gel was prepared by mixing water (2.3 ml) with stacking gel buffer (section 2.3.4) (1 ml), stock acrylamide (section 2.3.6) (650 µl) and TEMED (5 µl) and 10% (w/v) ammonium persulphate (80 µl) was added to the stacking gel solution and this was immediately poured into the mini-slab gel above the resolving gel. A welled comb was inserted into the stacking gel. After the polymerisation of the gel, the comb was carefully removed and the wells were washed with water. Electrode buffer (section 2.3.7) (~ 300 ml) was poured into the wells and into the base of the electrophoresis unit. Protein samples (15 µl) and pre-stained standards (protein molecular weight range of 200-6.5 kDa,) (15 µl) were loaded into the wells of the stacking gel using a Hamilton syringe. Electrophoresis was carried out at a constant current of 15 mA for ~2 h until the appropriate pre-stained molecular weight marker (25 kDa) was at the bottom of the gel.

2.4.4 Immunoblotting

After SDS-PAGE (section 2.4.3.3), the proteins from the gels were transferred to nitrocellulose membranes. A transfer cassette sandwich was constructed with the following order of components each of which had been pre-equilibrated in transfer buffer (section 2.3.10) sponge, two sheets of blotting paper and nitrocellulose membrane. The SDS-PAGE gel, two sheets of blotting paper and a final piece of sponge were added to the transfer cassette sandwich. On the addition of each

component to the transfer cassette air bubbles were carefully removed by pressing each layer with a test tube. Proteins were transferred at a constant voltage of 50 V for 2.5 hours using a Hoefer TE 22 tank transfer unit containing transfer buffer kept cool with ice and ice packs.

Following the transfer of the proteins, the nitrocellulose membrane was briefly rinsed with TBS (section 2.3.13) and incubated with blocking buffer which was TBS, containing 5 % (w/v) dried milk and 0.02 % (v/v) Tween-20 (15 ml) for 1 hour at room temperature with gentle shaking. After blocking of the non-specific antibody sites the nitrocellulose membranes were washed with ~10 ml of TBS. The appropriate affinity-purified primary antibodies were diluted in incubation buffer, which was TBS, pH 7.4 containing 2.5 % (w/v) dried milk to working concentrations (0.25-5 µg/ml). The nitrocellulose membranes were incubated with the diluted primary antibody solution (10 ml) for 1 hour at room temperature, or overnight at 4°C with gentle shaking.

After incubation with the primary antibody the nitrocellulose membranes were washed four times in wash buffer containing, TBS, containing, 2.5 % (w/v) dried milk and 0.2 % (v/v) Tween-20 (10 ml) at 10 minute intervals with gentle shaking at room temperature. Nitrocellulose membranes were then incubated with horseradish peroxidase (HRP) labelled secondary antibody, either anti-rabbit or anti-mouse depending on what the primary antibody was raised in, at a dilution of 1/2000 in incubation buffer (10 ml). The membrane was incubated for 1 hour at room temperature with gentle shaking. The unbound secondary antibody was removed by washing the membrane as described above. The nitrocellulose membrane was drained of excess wash buffer and briefly rinsed in TBS. Immunoreactive bands on the nitrocellulose membranes were developed by processing in a solution containing, 68

mM p-coumaric acid (100 µl), 1.25 mM luminol (10 ml) and 30 % H_2O_2 (6 µl) for 1 minute at room temperature. After removal of the reagents the immunoblot was wrapped in cling film, and placed in a film cassette. The immunoblot was exposed to Hyperfilm™ for various times (1-5 minutes). The film was then developed in Kodak D-19 Developer until the immunoreactive bands were visible and fixed in Kodak Unifix for 5 minutes at room temperature.

2.4.5 Transformation of competent *E. Coli* Cells

This method was performed essentially as described by Dagert and Ehrlich (1979).

For the transformation of competent *E. coli* cells, a frozen aliquot (100µl) of HB101 competent cells were removed from –80°C and thawed on ice for 5 minutes. The appropriate plasmid DNA (20 ng/µl) was added to the competent cells (100 µl) and mixed gently. The cell mixture was then incubated on ice for 30 minutes and heat-shocked by placing in a water bath at 42°C for 60 seconds. After 2 minutes incubation on ice, Terrific broth (section 2.1.1) (900 µl) was added to the transformed cells. Following a 1 hr incubation in an orbital shaker at 250xg, 37°C the cell suspension (100 µl) was plated onto culture plates prepared with 1.5 % (w/v) agar in terrific broth containing ampicillin (50 µg/ml). The culture plates were incubated at 37°C for 18-20 h in an inverted position.

2.4.6 Glycerol Stocks of transformed Competent *E. Coli* Cells

Transformed competent *E. Coli* cell stocks were prepared by mixing 500µl of Terrific broth supplemented with 50% (v/v) sterile glycerol and 50µg/ml ampicillin with 500µl of the small overnight culture (section 2.4.7.1). The cell culture mixture was immediately added to a cryogenic vial and stored at –80°C until use.

2.4.7 Amplification and preparation of Plasmid DNA

2.4.7.1 Preparation of Small-Scale Culture of Plasmid DNA

Terrific broth (10 ml) containing ampicillin (50 μg/ml) was added to a sterile 50 ml Falcon tube and inoculated with one isolated colony from the culture plate (section 2.4.5) using a sterile loop. The small culture was incubated for 18-20 hours in an orbital shaker at 250xg, 37°C.

2.4.7.2 Preparation of Large - Scale Culture of Plasmid DNA

Terrific broth (500 ml) containing ampicillin (50 μg/ml) was inoculated with 3ml of the small overnight culture (section 2.4.7.1) in a sterile 500 ml flask. The large culture was incubated for 18-20 hours in an orbital shaker at 250xg, 37°C.

2.4.7.3 Harvesting the Large Scale Culture and Purification of Plasmid DNA Using QIAGEN™ Plasmid Maxi-Kit

E. Coli cells were harvested by transferring the large overnight culture (section 2.4.7.2) into two ice- cold centrifuge tubes, and centrifuged at 6500xg for 10 minutes at 4°C. The supernatant was discarded and the remaining pellet was resuspended in ice-cold P1 buffer (10ml). Bacteria containing the plasmid were then lysed by the addition of P2 Buffer (10ml) mixed by gentle inversion and incubated at room temperature for 5 minutes. The mixture was then neutralised with chilled P3 buffer (10ml) mixed by gentle inversion and incubated on ice for 20 minutes. The solution was then centrifuged at 14000xg for 30 minutes at 4°C and the clear lysate was removed into fresh tube.

A QIAGEN™ 500 tip was equilibrated with QBT buffer (10ml). The lysate was gently poured onto the column and allowed to pass through the column under gravity flow. The column was washed twice with QC buffer (30ml), then QF buffer (15ml) was added to the column to elute the plasmid DNA. Ice-cold isopropanol (0.7vol) (10.5ml) was added to the eluted DNA and the solution was centrifuged at 14000xg for 30 minutes at 4°C. The remaining pellet was carefully washed with ice-cold ethanol (1ml) and air-dried for approximately 30 minutes. The purified DNA was dissolved in TE buffer (section 2.3.15) (500µl) and stored at 4°C until the purity and yield of the DNA was calculated.

2.4.7.4 Quantification and determination of Purity of the DNA Yield :

The purity of plasmid DNA was determined by measuring the OD at $\lambda = 260$ nm and $\lambda = 280$ nm (Sambrook *et al.,* 1989). The ratio of the optical densities at $\lambda = 260$ nm and $\lambda = 280$ nm ($OD_{\lambda} = 260$ nm / $OD_{\lambda} = 280$ nm) should be within the range 1.8 – 2.0 for pure plasmid DNA. The plasmid DNA concentration was determined by measuring the O.D. at $\lambda = 260$ nm. An O.D. = 1 corresponds to ~50 µg/µl for double standard DNA (dsDNA).

The DNA was then diluted to a final concentration of 1µg/ml in TE buffer and stored in 100µl aliquots at –20°C until use. Once thawed DNA was stored at 4°C.

. CHAPTER 3

DEVELOPMENT AND CHARACTERIZATION OF NOVEL ANTI-H_3 RECEPTOR ISOFORM SPECIFIC ANTIBODIES

3.1 OBJECTIVES

Develop and characterise novel anti-H_3 receptor isoform specific antibodies, and map the distribution of H_3 receptor isoforms in the brain.

3.2 INTRODUCTION

Due to lower than expected homology with histamine receptors H_1 and H_2, the H_3 receptor was not cloned until 1999 (Lovenberg *et al*, 1999) more than a decade after it was first described (Arrang *et al*, 1983). It was discovered as part of an effort to identify orphan GPCR's. Lovenberg and colleagues identified a partial clone (GPCR97) that had significant homology to biogenic amine receptors. The GPCR97 clone was used to probe a human thalamus library, which resulted in the isolation of a full-length clone encoding a putative G protein- coupled receptor. Homology analysis showed the highest similarity to M_2 muscarinic acetylcholine receptors and overall low homology to all other biogenic amine receptors. Transfection of GPCR97 into a variety of cell lines conferred an ability to inhibit forskolin-stimulated cAMP formation in response to histamine, but not to acetylcholine or any other biogenic amine. Subsequent analysis revealed a pharmacological profile practically indistinguishable from that for the histamine H_3 receptor.

In two analyses of the human gene (Tardivel-Lacombe *et al*, 2001; Wiedemann *et al*, 2002) a 1063 base pair (bp) intron beginning 250 nucleotides downstream of the start

codon (corresponding to aa 84) and another 1564 bp intron at position 417 (corresponding to aa 139) suggests a gene with three exons and two introns. By contrast Cogé (Cogé *et al*, 2001; see Fig 3.1) has put forward a gene having a minimum of four exons and three introns. In their analysis the coding region is interrupted by introns of 1062, 1565 and 240 bp. A further exon may result in an additional 8 amino acids at the C-terminus, leading to a protein of 453 aa (Nakamura *et al*, 2000). The result of these diverse exon/intron junctions is the occurrence of alternative splicing to generate multiple splice variants which may potentially lead to several receptor isoforms.

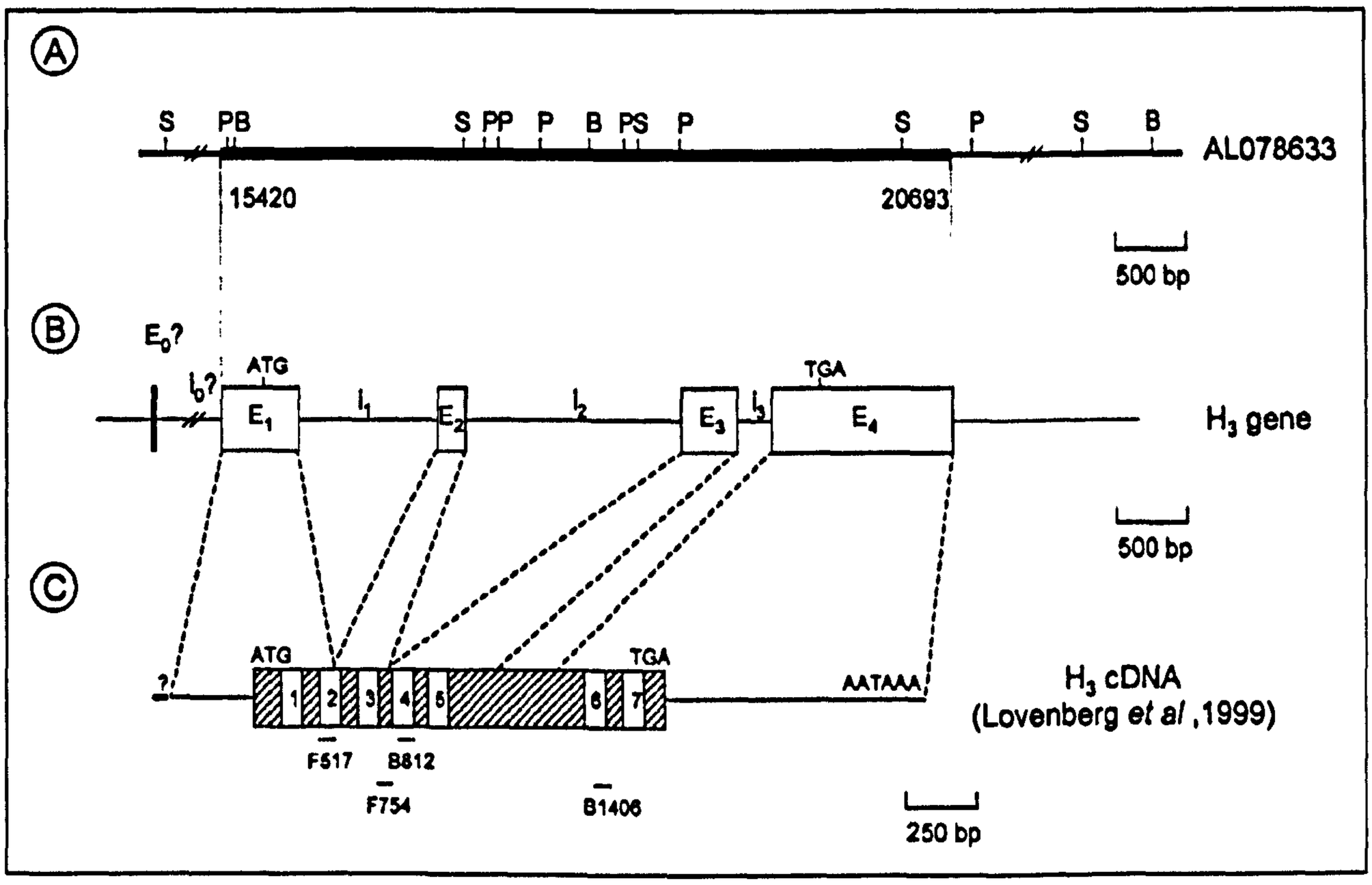

Cogé *et al*, 2001

Fig 3.1 Schematic organisation of the human H_3 histamine receptor gene and cDNA

(**A**) Restriction map of the genomic DNA fragment from human chromosome 20 (accession number AL078633). B, *Bam*HI; P, *Pst*I; S, *Sac*I. (**B**) Schematic structure of the H_3 gene with the location of exons (E_{1-4}) shown by boxes and the location of introns (I_{1-3}) shown by horizontal lines. The exons are numbered from the 5′ end of the gene with exon E_1 containing the first ATG codon. The initiation (ATG) and termination (TGA) codons are indicated. Exon E_0 and intron i_0 were deduced from the H_3 receptor cDNA described by Lovenberg *et al*. (Lovenberg *et al*, 1999), but are not confirmed. (**C**) Structure of the human H_3-receptor cDNA. The coding region is shown by boxes and the 5′- and 3′-UTRs are shown by horizontal lines. The putative TMs (1–7) are mentioned in the coding region. The translation initiation site (ATG), the termination site (TGA) and the polyadenylation signal sequence (AATAAA) are indicated. The forward (F) and reverse (B) primers used for RT-PCR analysis are shown under the cDNA structure.

The cloning of the H_3 receptor has initiated a new era in histamine research. In particular the recognition of the existence of multiple H_3 receptor isoforms has opened up possibilities to account for the pharmacological heterogeneity in H_3 receptors, within and across species, which has long been recognised. The reasons for this heterogeneity are complex and not fully understood. In all species tested so far the full

length H_3 receptor encodes a polypeptide of 445 amino acids (predicted polypeptide Mr 47,000). Shorter isoforms with deletions predominantly in the third intracellular loop domain have also been identified (predicted polypeptide Mr range 35,000-45,000). While the full length clone is found in most abundance in the CNS in all species studied so far, there is regional variation in the distribution of the different isoforms (Harper *et al*, 1999; Cogé *et al*, 2001; Sogawa *et al*, 2004; Ebenshade *et al*, EHRS abstract, 2005). This has given rise to speculation that H_3 heterogeneity could underlie different activities and functions of H_3 receptors in specific brain areas.

The evidence for heterogeneity in anatomical distribution is based mostly on the distribution pattern of mRNA coding for the various isoforms. Note that these splicing events yield potentially **different** protein sequences in rodents and man. In order to define the importance of H_3 receptor heterogeneity, specific immunological probes are required. Our laboratory has developed the first anti-H_3 receptor antibodies (Chazot *et al*, 2001; Cannon *et al*, 2007; Victoria Hann PhD thesis, 2004). The first two antibodies were raised against human H_3 receptor sequences common to most human and rodent isoforms: anti-H_3 (346-358) and anti-H_3 (175-187) (see Fig 3.2 rat and human isoform sequences). They both detected two specific immunoreactive protein species (Mr 68,000 and 93,000) which were suppressed by prior incubation with their respective peptide antigens, in many adult rat and mouse brain regions. These species are most likely derived from dimeric and/or glycosylated versions of the receptor. In an attempt to generate an antibody specific to the rat H_{3C} (397) isoform a peptide sequence was chosen which spanned the deletion within the third ic loop (see Fig 3.2 A) and B) rat isoform sequences) and would therefore be unique to this isoform. When tested against three of the major human and rat isoforms heterologously expressed in

HEK 293 cells namely $hH_{3\ (445)}$, $hH_{3\ (365)}$ and $hH_{3\ (329)}$; $rH3_{A\ (445)}$, $rH3_{B\ (413)}$ and $rH3_{C\ (397)}$, the antibody was found to be selective for both the full length human and rat isoforms $hH_{3\ (445)}$ and $rH_{3A\ (445)}$, as well as the expected $rH_{3C\ (397)}$ isoform. Furthermore it detected protein species in both human and rodent (mouse and rat) native tissue. Therefore this antibody was used to map the distribution of the H_3R in mouse brain slices and to compare the immunoreactivity obtained with this 445 specific antibody to that previously described with the pan-specific H_3R antibody. In addition it was used to further characterize both the human and the rat H_3R as described in subsequent chapters. Antibodies specific for three of the other major human H_3R isoforms were also sought with peptide sequences unique to the 415, 365, and 329 ΔI3 human H_3R isoforms (see Fig 3.2 human isoform sequences). Finally a peptide sequence unique to human $H_{3\ 220}$ was chosen (Wellendorph *et al*, 2002, Isoform 5). Human $H_{3\ (220)}$ has a 170-306 deletion plus a frame shift and a novel stop codon, so that the C terminus is exclusive to that isoform. Therefore the last 10 amino acids were selected.

Herein are described the methods for preparing the peptides for immunization, the immunization procedure, antibody purification and the experiments performed to check the individual antibody specificity. Results of immunohistochemical analysis using the human/rodent antibody in mouse brain slices from both wildtype (WT) and H_3R -/- (H_3R KO) mice (kind gift of Prof Tim Lovenberg, Johnson & Johnson) are also presented.

A) Full length Rat H_{3A} sequence

```
  1 merappdglm nasgtlagea aaaggargfs aawtavlaal mallivatvl gnalvmlafv
 61 adsslrtqnn ffllnlaisd flvgafcipl yvpyvltgrw tfgrglcklw lvvdyllcas
121 svfnivlisy drflsvtrav syraqqgdtr ravrkmalvw vlafllygpa ilsweylsgg
181 ssipeghcya effynwyfli tastlefftp flsvtffnls iylniqrrtr lrldggreag
241 pepppdaqps pppappscwg cwpkghgeam plhrygvgea gpgveageaa lgggsgggaa
301 asptsssgss srgterprsl krgskpsass aslekrmkmv sqsitqrfrl srdkkvaksl
361 aiivsifglc wapytllmii raachgrcip dywyetsfwl lwansavnpv lyplchysfr
421 raftkllcpq klkvqphgsl eqcwk
```

B) Rat sequence showing rH_{3C} deletion **(deletion red and in bold)**

Peptide sequence used to immunise rabbit blue and underlined

```
  1 merappdglm nasgtlagea aaaggargfs aawtavlaal mallivatvl gnalvmlafv
 61 adsslrtqnn ffllnlaisd flvgafcipl yvpyvltgrw tfgrglcklw lvvdyllcas
121 svfnivlisy drflsvtrav syraqqgdtr ravrkmalvw vlafllygpa ilsweylsgg
181 ssipeghcya effynwyfli tastlefftp flsvtffnls iylniqrrtr lrldggreag
241 pepppdaqps pppappscwg cwpkghgeam plhrygvgea gpgveageaa lgggsgggaa
301 asptsssgss srgterprsl krgskpsass aslekrmkmv sqsitqrfrl srdkkvaksl
361 aiivsifglc wapytllmii raachgrcip dywyetsfwl lwansavnpv lyplchysfr
421 raftkllcpq klkvqphgsl eqcwk
```

C) Full length Human $H_{3\ (445)}$

Peptide sequences used to generate first pan anti-H_3R antibodies blue and underlined

```
  1 merappdgpl nasgalagda aaaggargfs aawtavlaal mallivatvl gnalvmlafv
 61 adsslrtqnn ffllnlaisd flvgafcipl yvpyvltgrw tfgrglcklw lvvdyllcts
121 safnivlisy drflsvtrav syraqqgdtr ravrkmllvw vlafllygpa ilsweylsgg
181 ssipeghcya effynwyfli tastlefftp flsvtffnls iylniqrrtr lrldgareaa
241 gpepppeaqp sppppgcwg cwqkghgeam plhrygvgea avgaeageat lgggggggsv
301 asptsssgss srgterprsl krgskpsass aslekrmkmv sqsftqrfrl srdrkvaksl
361 avivsifglc wapytllmii raachghcvp dywyetsfwl lwansavnpv lyplchhsfr
421 raftkllcpq klkiqphssl ehcwk
```

D) Human sequence showing $H_{3\ (365)}$ deletion **(deletion red and in bold)**

Peptide sequence used to immunise rabbit blue and underlined (P1)

```
  1 merappdgpl nasgalagda aaaggargfs aawtavlaal mallivatvl gnalvmlafv
 61 adsslrtqnn ffllnlaisd flvgafcipl yvpyvltgrw tfgrglcklw lvvdyllcts
121 safnivlisy drflsvtrav syraqqgdtr ravrkmllvw vlafllygpa ilsweylsgg
181 ssipeghcya effynwyfli tastlefftp flsvtffnls iylniqrrtr lrldgareaa
241 gpepppeaqp sppppgcwg cwqkghgeam plhrygvgea avgaeageat lgggggggsv
301 asptsssgss srgterprsl krgskpsass aslekrmkmv sqsftqrfrl srdrkvaksl
361 avivsifglc wapytllmii raachghcvp dywyetsfwl lwansavnpv lyplchhsfr
421 raftkllcpq klkiqphssl ehcwk
```

E) Human sequence showing $H_{3\ (415)}$ deletion **(deletion red and in bold)**

Peptide sequence used to immunise rabbit blue and underlined (P2)

```
  1 merappdgpl nasgalagda aaaggargfs aawtavlaal mallivatvl gnalvmlafv
 61 adsslrtqnn ffllnlaisd flvgafcipl yvpyvltgrw tfgrglcklw lvvdyllcts
121 safnivlisy drflsvtrav syraqqgdtr ravrkmllvw vlafllygpa ilsweylsgg
181 ssipeghcya effynwyfli tastlefftp flsvtffnls iylniqrrtr lrldgareaa
241 gpepppeaqp sppppgcwg cwqkghgeam plhrygvgea avgaeageat lgggggggsv
301 asptsssgss srgterprsl krgskpsass aslekrmkmv sqsftqrfrl srdrkvaksl
361 avivsifglc wapytllmii raachghcvp dywyetsfwl lwansavnpv lyplchhsfr
421 raftkllcpq klkiqphssl ehcwk
```

F) Human sequence showing $H_{3\ (329\ \Delta i3)}$ deletion **(deletion red and in bold)**

Peptide sequence used to immunise rabbit blue and underlined (P3)

```
  1 merappdgpl nasgalagda aaaggargfs aawtavlaal mallivatvl gnalvmlafv
 61 adsslrtqnn ffllnlaisd flvgafcipl yvpyvltgrw tfgrglcklw lvvdyllcts
121 safnivlisy drflsvtrav syraqqgdtr ravrkmllvw vlafllygpa ilsweylsgg
181 ssipeghcya effynwyfli tastlefftp flsvtffnls iylniqrrtr lrldgareaa
241 gpepppeaqp sppppgcwg cwqkghgeam plhrygvgea avgaeageat lgggggggsv
301 asptsssgss srgterprsl krgskpsass aslekrmkmv sqsftqrfrl srdrkvaksl
361 avivsifglc wapytllmii raachghcvp dywyetsfwl lwansavnpv lyplchhsfr
421 raftkllcpq klkiqphssl ehcwk
```

Fig 3.2 The amino acid sequences of the full length rat and human H_3 receptor isoforms are shown, with the deletions giving rise to the shorter isoforms and the peptide sequences used to generate specific antibodies to those isoforms

3.3 METHODS

3.3.1 Choice of peptide sequences

The following peptide sequences were chosen for the short peptides used to immunize the rabbits. The choice was made based on their specificity: that is being unique to that particular receptor isoform, and likely immunogenicity. See Fig 3.2 showing the full length aa sequences of each isoform with the sequences of the immunizing peptide underlined. A cysteine residue was added to one end of each sequence so that the peptide could be coupled to the carrier protein thyroglobulin (see below).

First antibody

rH_{3C} (268 – 277) EAMPLHRGSK-Cys

a sequence specific to the i3 region in the rat H_{3C} isoform

Subsequent three antibodies: P1, P2, P3

P1:	$hH_{3\ (365)}$ (270 – 279)	i3 just before TM6	CMPLHRKVAKS
P2:	$hH_{3\ (415)}$ (229 – 238)	i3	CTRLRLKGHGE
P3:	$hH_{3\ (329\ \Delta I3)}$ (222 – 231)	TM5 i3	CYLNIQSFTQR

Sequences specific to the i3 region of the respective isoforms

Also hH_3 – 5 (Wellendorph *et al*, 2002; Isoform 5) (aa 211 – 220) CRRPRPRWRSA (but this antibody has yet to be purified and characterised)

3.3.2 Antibody production

As the peptide on its own is too small to stimulate an immune response it is coupled to a large immunogenic carrier protein, in this case thyroglobulin, before injection into the rabbit. Serum was collected and purified using peptide-affinity chromatography.

3.3.3 The 3-Maleimimdobenzoic Acid N-hydroxysuccinimide Ester (MBS) Method of Coupling peptides to Carrier Proteins

This method was performed essentially as described previously (Duggan *et al*, 1991) and was used to conjugate the peptide to the carrier protein thyroglobulin through its carboxyl-terminal cysteine residue.

Thyroglobulin was dissolved in 10mM KH_2PO_4, 10mM Na_2HPO_4 buffer pH 7.2 to a final concentration of 20mg/ml. This preparation was then dialysed against 500ml of the same buffer overnight at 4°C. 50µl of the buffer was added to 4mg (200µl) of dialysed carrier protein. The carrier protein was then activated by dropwise addition of 85µl stock MBS (3mg/ml MBS in N,N-dimethylformamide) and incubated at room temperature for 30 minutes with shaking. The activated carrier was separated from free MBS by dialysis against 50mM KH_2PO_4, 50mM Na_2HPO_4 buffer pH 6.0, for 2 hours at room temperature, 2 X 1 litre changes. 1ml of 4mg/ml peptide dissolved in 10mM KH_2PO_4, 10mM Na_2HPO_4 buffer pH 7.2 was added to the dialysed activated carrier protein and incubated overnight at room temperature with gentle mixing. The peptide conjugate was then separated from the uncoupled peptide by dialysis against PBS for a total of 4 hours at 4°C, 4 X 500ml changes. The dialysed peptide protein conjugate was diluted with PBS to a final concentration of 1mg/ml and stored in 100µl aliquots at -20 °C.

3.3.4 Inoculation procedure

Routinely, 200µl of sterile PBS was mixed with 100µg (100µl) of freshly thawed peptide-carrier protein conjugate, and emulsified with an equal volume of Freund's Adjuvant. This preparation was then injected intramuscularly into both hind legs of a Dutch rabbit. The primary immunisation was performed with complete Freund's Adjuvant, for subsequent immunisations, at 1 month intervals, incomplete Freund's Adjuvant was used. Rabbits were bled from the marginal ear vein 7-10 days following the booster injections, 10-15ml of blood was collected. Blood was allowed to stand at room temperature for 2 hours, then clot contraction was allowed to occur over 16 hours at 4°C. Cellular material was removed by centrifugation at 12000g for 10 minutes at 4°C, and the serum was stored in 1ml aliquots at -20 °C. All procedures were performed in accordance with the Animals (Scientific Procedures) Act 1986 (PPL 602/657).

3.3.5 Affinity purification

3.3.5.1 Coupling of peptides to sepharose beads via sulphydryl groups

This method was carried out as described formerly (Duggan *et al*, 1991) and was used to couple the peptide to activated thiol-sepharose beads via its C-terminal cysteine residue.

0.35g of activated thiol-sepharose was allowed to swell in 100ml water for 15 minutes at room temperature. The swollen sepharose was placed in a 25ml column and washed with 100ml of 0.1M Tris-HCl pH8.0, containing 0.3M NaCl, 1mM EDTA. It was then drained until just 2/3ml of the buffer remained. 1ml of 5mg/ml peptide dissolved in the same buffer was added to the sepharose and incubated with gentle shaking for 2 hours at room temperature. The reaction was terminated by draining the column and washing

the sepharose with 10ml of 0.1M citric acid pH 4.5. Next all remaining unreacted thiol groups on the sepharose were blocked by incubation with 3ml of 1mM β-mercaptoethanol in 0.1M citric acid pH 4.5 for 1 hour at room temperature. The blocking reaction was terminated by washing with 25ml 0.1M citric acid pH 4.5. Finally the sepharose column was equilibrated with 25ml PBS and stored in 10ml PBS containing 0.02% (w/v) sodium azide, at 4°C until use.

3.3.5.2 Peptide affinity purification of antibodies

For the purification of anti-peptide polyclonal antibodies a sepharose column (1ml) linked to the appropriate peptide was equilibrated with 100mls of TBS. 4ml of immune serum was applied to the column followed by incubation either for 2 hours at room temperature or overnight at 4°C, with gentle mixing. Unbound immune serum was drained from the column, the column was then washed with 100mls TBS. The bound antibody was eluted from the column with 10mls of 50mM glycine/HCl pH 2.3. The eluate was collected in 10 X 1ml fractions. Each 1ml fraction was collected into a microtube containing 1M Tris (15µl) to neutralise the contents to a final pH of 7.4. For each fraction the O.D. at λ = 280nm was determined and the protein concentration calculated using the Beer Lambert law,

$C = A / \epsilon L$

Where,

C, is the protein concentration of the antibody

A, is the absorbance at $\lambda = 280$nm

ϵ, is the molar extinction coefficient

L, is the path length

The fractions containing the highest protein concentrations were pooled and dialysed against 500mls TBS overnight at 4°C. The affinity column was regenerated with 100mls of TBS and stored in 10mls TBS containing 0.02% (w/v) sodium azide at 4°C until later use.

3.3.6 Culture and transfection of HEK (Human Embryonic Kidney) 293 cells

3.3.6.1 Preparation of DMEM/F12 media + L-glutamine

All procedures were performed under sterile conditions. Powdered Dulbecco's Modified Eagle Medium/F12 (DMEM/F12 1:1 mixture) (15g/l) containing L-glutamine (0.0365g/l) and 15mM N-2-hydroxyethylpoiperazine-N'-2-ethane sulphonic acid (HEPES) was mixed with sterile water (800ml). The mixture was supplemented with 10% (v/v) foetal calf serum (FCS), 40ml of 7.5% (w/v) $NaHCO_3$ (final conc. 3.0g/l) and penicillin (500 IU/ml)/ streptomycin (500µg/ml) solution (20ml). The pH of the media was adjusted to pH 7.6 using 10M NaOH and the final volume made up to 1 litre with sterile water. The media was filter sterilised using a 0.2µm Sartorius Sartolab-V150 filter unit and stored at 4°C until use.

3.3.6.2 Subculturing of HEK 293 cells

HEK 293 cells were grown in in DMEM/F12 media containing L-glutamine in 250 ml Greiner culture flasks at 37°C in 5% CO_2 in a Sanyo incubator. Every 7 days the cells were subcultured. Sterile PBS for washing, fresh media and trypsin-EDTA were all prewarmed to 37°C. The old media was removed and the cells washed with 10ml of prewarmed, sterile PBS. 2ml of trypsin-EDTA was added to the cells, following a 1 minute incubation at 37°C, the cells were resuspended in 10 ml of fresh media by

gentle pipetting up and down. 2ml of the cell suspension was added to a new flask along with a further 10 ml of fresh media. The flask was then returned to the incubator.

3.3.6.3 Preparation of new stocks of HEK 293 cells

The old media was removed from a flask of HEK 293 cells and the cells washed with 10 ml sterile PBS. Following a 1 minute trypsinisation with 4 ml trypsin-EDTA covering the cells for 1 minute at 37°C, the cells were resupended in 20 ml fresh media. The cells were pelleted by centrifugation at 200g for 5 minutes at 4°C. The pellet was resuspended in 4.8 ml of media supplemented with 0.6ml of FCS and 0.6ml dimethylsuphoxide (DMSO). The cell suspension was immediately divided into three cryogenic vials and stored at –80°C for 24 hours before transfer to liquid nitrogen.

For the preparation of a new culture a single cryogenic vial of frozen HEK 293 cells was thawed at 37°C. The cells were pelleted by centrifugation at 200g for 5 minutes at 4°C and resuspended in 15 ml fresh media. The cells were added to a tissue culture flask for culture at 37°C in 5% CO_2.

3.3.6.4 LipofectaminePLUS transfection method

cDNA for transfection:	$hH_{3\ (445)}$ FLAG, $hH_{3\ (365)}$ FLAG, $hH_{3\ (329)}$ FLAG
	$rH_{3A\ (445)}$ $rH_{3B\ (413)}$, $rH_{3C\ (397)}$
cDNA vector:	pcDNA 3.1

The LipofectaminePlus method (Tucker *et al*, 2003) was utilised. Briefly for each cDNA clone mixtures were produced in two microtubes: tube 1 contained 2µg cDNA, 6µl of lipofectaminePLUS reagent and 150µl of Optimem-I media (Gibco); tube 2 contained 5µl lipofectamine reagent and 150µl of Optimem-I media. The mixtures were incubated at room temperature for 15 minutes after which the contents of tube 2

were added to tube 1 followed by a further 5 minute incubation. In the meantime the HEK 293 cells at 50-80% confluence in 2ml petri dishes were washed three times with Optimem-I media. At the end of the second incubation period the contents of tube 1 were made up to 1.5ml with Optimem-I media and added to the washed HEK 293 cells. The cells were incubated at 37°C for 6 hours. The transfection mixture was then removed and replaced with ordinary growth media. The cells were harvested after a further 48 hours growth. They were homogenised and aliquots stored frozen at -20°C prior to immunoblotting.

3.3.6.5 Harvesting and membrane preparation of HEK 293 cells

Transfected HEK cells were harvested 48 hours post transfection. The culture media were removed and replaced with 1ml of ice-cold homogenisation buffer (50mM Tris-HCl pH 7.4, 5 mM EDTA, 5 mM EGTA). Cells were scraped off the bottom of the petri dish using Greiner cell scrapers. The resuspended cells were transferred to a dounce glass/glass homogeniser on ice glass and homogenised with at least 30 strokes of the plunger. The homogenate was placed in a microtube and spun down for 5 minutes at 18000g in a benchtop microfuge at 4°C. The supernatant was removed and replaced with another 1 ml of ice cold homogenisation buffer. The cells were resuspended and rehomogenised as before in the dounce glass/glass homogeniser. After the second homogenisation the homogenate was divided into 100µl aliquots and stored in microtubes at -20°C.

3.3.7 Immunoblots

Sodium dodecyl sulphate polyacrylamide gel electrophoresis (SDS-PAGE) was carried out using either 6% or 7.5 % polyacrylamide slab gels under reducing conditions.

Immunoblots were probed either with anti-FLAG antibody in the case of the human H_3R clones epitope tagged with FLAG, or with the appropriate rabbit anti-H_3R antibody.

3.3.7.1 Preparation of resolving gel

The resolving gel (6% or 7.5%) was prepared by mixing water (6.6 or 6ml) with resolving gel buffer (3ml), stock acrylamide (2.4 or 3ml), TEMED (6µl) and 10% (w/v) ammonium persulphate (APS) (60µl). The polyacrylamide mixture was poured immediately into a Hoefer™ SE 245 dual gel caster, for 8 X 9 cm gels of 1 mm thickness. The top of each gel was covered with saturated water/butanol solution (100µl). The gels were covered with parafilm and allowed to polymerise for 60 minutes at room temperature. The tops of the gels were rinsed with water, then they were individually wrapped in tissue soaked in electrode buffer and stored in sealed plastic bags at 4°C until use.

3.3.7.2 Preparation of protein samples for SDS-PAGE

100µl aliquots of homogenised cells were thawed and pelleted by spinning for 1 minute at 18000g in a benchtop microfuge. The supernatant was removed and the cells resupended in 15µl sample buffer containing 100mM Dithiothreitol (DTT). The samples were boiled in a water bath for 5 minutes and then centrifuged at 18000g for 30 seconds. The samples were then vortexed briefly and applied to the gel. Rodent brain material was prepared as described in section 2.4.1. Human putamen was supplied in Laemmli buffer ready prepared for SDS-PAGE (gift from Dr Margaret Piggott, Newcastle University).

3.3.7.3 SDS-PAGE

The resolving mini-slab gel was clamped into a Hoefer™ SE 260 mini-vertical gel electrophoresis unit. The stacking gel was prepared by mixing water (2.3ml) with stacking gel buffer (1ml), stock acrylamide (650µl), TEMED (5µl) and 10% (w/v) ammonium persulphate (APS) (80µl). This mixture was poured immediately onto the resolving gel. A welled comb was inserted into the stacking gel. Following polymerisation of the gel (after about 15 minutes) the comb was carefully removed and the wells washed with water. Electrode buffer (approximately 300ml) was poured into the wells, the space behind the gel and into the base of the electrophoresis tank. Protein samples (15µl) and pre-stained molecular weight markers (15µl) were loaded into the wells of the stacking gel using a Hamilton syringe. Initially electrophoresis was carried out at a constant current of 10mA, increasing to 15mA after the first 30 minutes. The gel was run for approximately 2 hours in total until the lowest pre-stained molecular weight marker was at the bottom of the gel.

3.3.7.4 Immunoblotting

After SDS-PAGE the proteins from the gels were transferred to nitrocellulose membranes. A transfer cassette sandwich was constructed with the following order of components each of which had been pre-equilibrated in transfer buffer: layer of sponge, two sheets of blotting paper, nitrocellulose membrane, gel, another two sheets of blotting paper and a final piece of sponge. As each layer of the sandwich was added care was taken to roll out any air bubbles with a clean test tube. Proteins were transferred at a constant voltage of 50V for 2.5 hours using a Hoefer™ TE 22 tank transfer unit containing transfer buffer. The buffer was kept cool by strapping two ice packs to the front and back of the tank and constant, steady stirring throughout the run.

Following the transfer of the proteins the nitrocellulose membrane was rinsed briefly with TBS and incubated with blocking buffer consisting of TBS containing 5% (w/v) dried milk and 0.2% (v/v) Tween-20 (15ml), for 1 hour at room temperature with gentle mixing. After blocking of membrane sites capable of nonspecific protein binding, blocking buffer was removed and replaced with the primary antibody diluted appropriately in incubation buffer which was TBS containing 2.5% (w/v) dried milk (10ml). Peptide specific antibodies were usually used at a final protein concentration of 0.5 - 2μg/ml (occasionally up to 5μg/ml was used), while the anti-FLAG antibody was used at a 1:5000 dilution. The incubation was carried out overnight at 4°C with gentle mixing. Following incubation in primary antibody nitrocellulose membranes were given 4 X 10 minute washes in 10ml wash buffer made up of TBS containing 2.5% (w/v) dried milk and 0.2% (v/v) Tween-20. The washes were carried out at room temperature with gentle mixing. The membranes were then incubated with horseradish peroxidase (HRP) labelled secondary antibody, either anti-rabbit (for the peptide specific antibodies) or anti-mouse (for the monoclonal anti-FLAG antibodies), at a dilution of 1:2000 in incubation buffer (10ml). The membrane was incubated with the secondary antibody for 1 hour at room temperature with gentle mixing. Unbound secondary antibody was removed by washing the membrane as before. The nitrocellulose membrane was drained of wash buffer and rinsed briefly in TBS. Immunoreactive bands on the membrane were developed by processing in 1.25 mM luminol (10ml) containing 68mM p-coumaric acid (100μl) and 30% H_2O_2 (6μl). The reaction was allowed to take place over 1 minute at room temperature. The membrane was then removed from the reaction mixture, gently blotted, wrapped in cling film and placed in a film cassette. In the dark the sealed membrane was covered with a piece of Hyperfilm™, the film cassette was shut and the film exposed to the immunoblot for a

period of between 1 to 5 minutes. The film was then developed in Kodak D-19 Developer. When the immunoreactive bands were visible the film was rinsed briefly in tap water before fixing in Kodak Unifix for 5 minutes.

3.3.8 Immunohistochemical analysis

Immunohistochemical analysis was carried out by conventional procedures as described previously (Thompson *et al*, 1992). Briefly adult mouse brains (wild-type and H_3 (-/-) animals kindly provided by Professor LB Hough, NY, USA) (Toyota *et al*, 2002 and US Patent 7151200) were perfusion-fixed with 4% (w/v) paraformaldehyde, 0.05% (v/v) glutaraldehyde in 0.1M phosphate buffer, pH 7.4. Brains were removed, post-fixed overnight and then cryoprotectd by incubation in 30% (w/v) sucrose in 0.01M phosphate buffer, pH 7.4, at 4°C for 48h. The tissue was then frozen in isopentane (-80°C), and coronal sections (20μm thick) were cut on a cryostat. Free-floating sections were initially treated with 10% (v/v) methanolic and 3% (v/v) hydrogen peroxide in 50mM TBS, pH 7.4, for 10 min to quench endogenous peroxidase activity. Sections were incubated in TBS, 0.2% (w/v) glycine and 0.2% (v/v) Tween-20, for 15 min to mop up residual unreacted aldehyde groups from the fixative. Non-specific, antibody binding sites on the tissue were blocked by incubating with either goat or foetal calf serum (2%, v/v) in TBS/Tween-20 (0.2%, v/v) for 60 minutes. Sections were then incubated overnight at 4°C in anti-H_3 445 antibody at a final concentration of 0.1μg/ml in goat or foetal calf serum/TBS (1% serum, v/v). After washing three times in 1% serum/TBS antibody binding was detected by means of the Vectastain ABC Elite kit. The biotin linked, anti-rabbit, secondary antibody was followed by a streptavidin-horse radish peroxidase (HRP) complex. The immune reaction was visualised using 3,3'-diaminobenzidine tetrahydrochloride as the HRP

substrate. Antibody specifity was confirmed by means of a peptide block test (see below). In addition a control was carried out where the primary anti-H_3 445 antibody was left out. This was to rule out nonspecific binding of the secondary antibody to the slice.

3.3.8.1 Peptide block to confirm antibody specificity

In order to confirm that immunoreactivity detected either in blots or in immunohistochemical analysis was specific to the amino acid sequence of the immunizing peptide, a peptide block was carried out in which the antibody was incubated overnight at 4°C with an equal volume of the relevant peptide. The peptide concentration during this incubation was 500µg/ml well in excess of that needed to completely block the antibody and therefore prevent it from binding to equivalent sites in an immunoblot or on a tissue slice in IHC analysis. For the test the antibody dilution was adjusted to take account of the initial 1:2 dilution with peptide. Bands or immunstaining persisting after the antibody block were considered to be due to nonspecific antibody binding.

3.4 RESULTS

3.4.1 Determination of antibody concentration following peptide affinity purification

Immunization with a peptide coupled to a carrier protein will elicit antibodies to both the peptide sequence and the carrier protein. Affinity purification of the serum is undertaken to separate the antibodies specific to the peptide from those that react with the carrier protein. The pure peptide is coupled to sepharose beads which are then placed in a column. The rabbit serum is incubated with the peptide coupled beads under conditions which allow specific peptide antibodies to bind to the peptide on the sepharose column. Following washing to remove all the serum proteins which may have adhered nonspecifically to the beads the anti-peptide antibodies are eluted off in 1 millilitre fractions. The optical density (OD) at λ=280nm was measured for each fraction and those two or three fractions giving the highest OD value, and thus having the greatest protein concentration were pooled and dialysed overnight against PBS. After dialysis the final protein concentration in the pooled fractions was calculated according to the following formula:

$$OD_{280} \text{ pooled fractions} / 1.35 = \text{protein concentration mg/ml}$$

Finally, approx. 0.05% (w/v) sodium azide was added and the purified antibody stored at 4°C for future use.

Concentrations in the range of 83 - 354 μg of purified antibody/ml of immune serum were obtained. The following graph (Fig.3.3) shows a representative series of OD's from eluted column fractions.

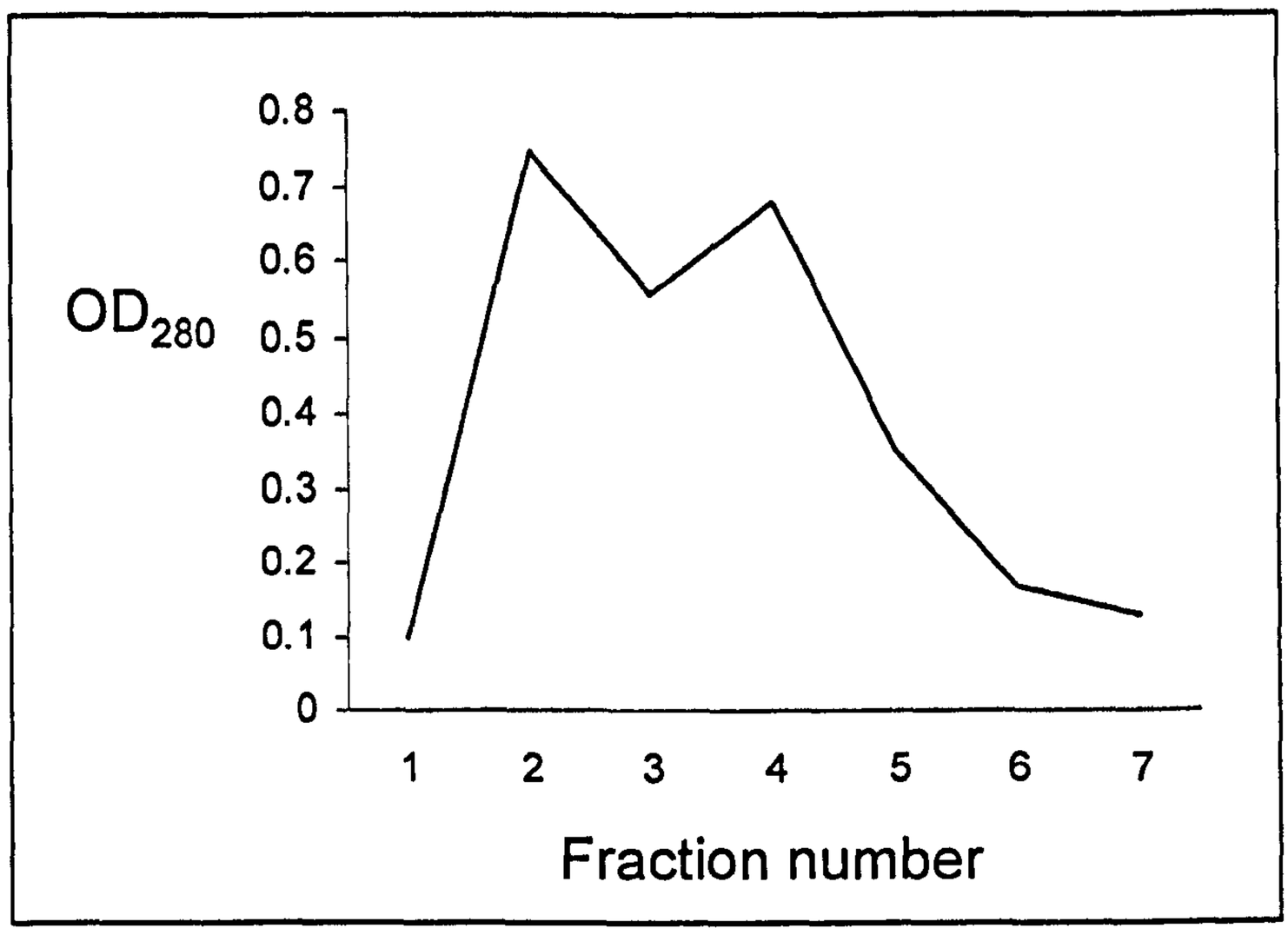

Fig 3.3 A representative elution profile

Column fractions 2-4 were chosen on this occasion.

Table 3.1 shows the concentrations of antibodies purified from different bleeds of immunized rabbits

rH_{3C} (268 – 277) EAMPLHRGSK-Cys

Rabbit	Bleed 1	Bleed 2	Bleed 4
12MY	-	-	163 µg/ml
13MY	137 µg/ml	150 µg/ml	-
15MY	244 µg/ml	-	148 µg/ml

Subsequent three antibodies: P1, P2, P3

P1:	$hH_{3\ (365)}$ (270 – 279)	i3 just before TM6	CMPLHRKVAKS
P2:	$hH_{3\ (415)}$ (229 – 238)	i3	CTRLRLKGHGE
P3:	$hH_{3\ (329)}$ ΔI3 (222 – 231)	TM5 i3	CYLNIQSFTQR

Sequences specific to the i3 region of the respective isoforms

	Bleed 1	Bleed 2
P1	83 µg/ml	195 µg/ml
P2	failed	-
P3	354 µg/ml	215 µg/ml

For unknown reasons the affinity column used to purify P2 serum failed in that all the elution fractions were of a similar low absorbance: around 0.020. For subsequent immunoblots the whole serum was used in the hope that specific antibody might nonetheless be present. However no specific immunoreactivity could be detected with this serum.

3.4.2 Immunoblotting analysis of anti-H_3 receptor antibodies against recombinant rat and human H_3 receptor isoforms expressed in HEK 293 cells

3.4.2.1 Isoform specificity of the rH_{3C} (268 – 277) antibody

rH_{3C} (268 – 277) EAMPLHRGSK-Cys

Sequence specific to the i3 region in the rat H_{3C} isoform. This antibody was shown to be selective for the rat H_{3A} and rat H_{3C} isoforms (Fig 3.4) and the human $H_{3\ (445)}$ isoform (Fig 3.5). Antibodies purified from different rabbits and different bleeds consistently showed the same $H_{3\ (445)}$ selectivity (Fig 3.6).

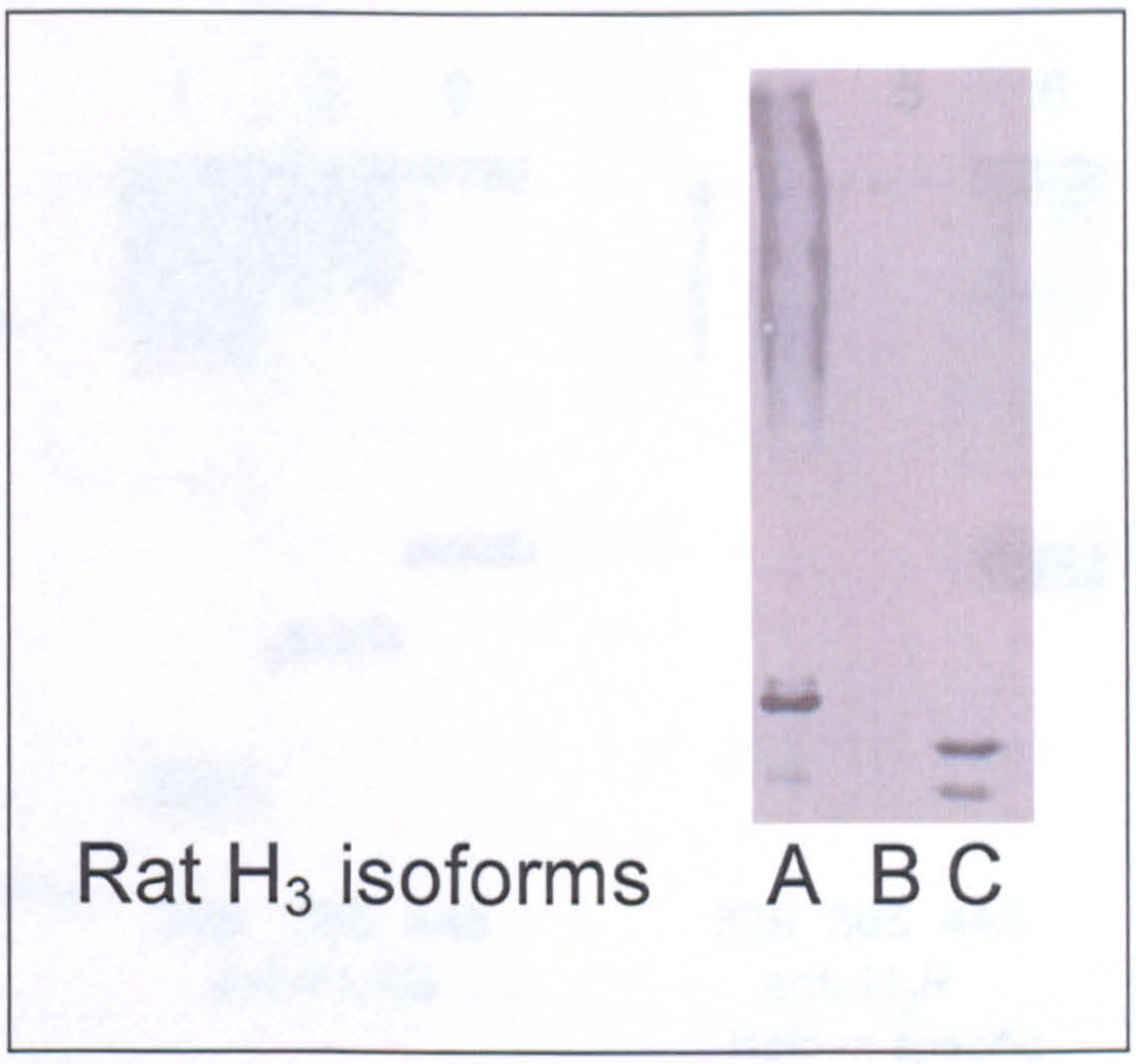

Fig. 3.4 Immunoblot showing rH_{3C} (268-277) antibody reactivity against rat H_3 receptor isoforms expressed in HEK 293 cells

HEK 293 cells transfected with three of the major rat H_3R isoforms $rH_{3A}/rH_{3\ (445)}$, $rH_{3B}/rH_{3\ (413)}$ and $rH_{3C}/rH_{3\ (397)}$ were homogenized and run out on an SDS-PAGE gel as described previously. Anti-$hH_{3\ (445)}$ (268 – 277) antibody (purified from first bleed of rabbit 15MY) was used at a final concentration of 1 μg/ml. The antibody was selective for the rat A and C isoforms, no reactivity being evident for isoform B. Notably, higher molecular weight species were detected in the rH_{3A} lane but were not evident for the rH_{3C} isoform. Representative blot from at least 10 experiments.

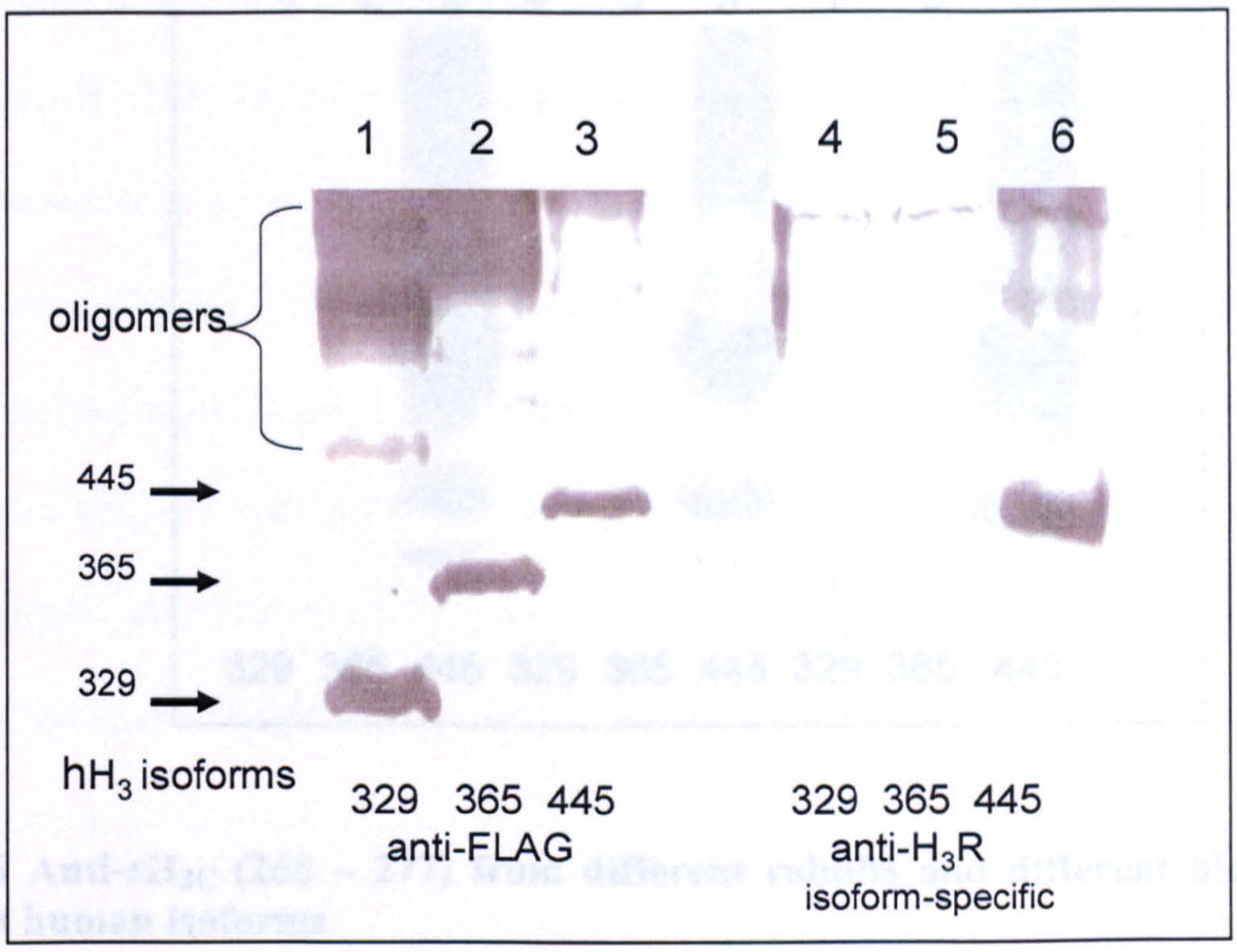

Fig. 3.5 Immunoblot of three different FLAG tagged human H_3 receptor isoforms probed with anti-FLAG antibody (Lanes 1-3) and antibodies raised to peptide sequence rH_3 (268 - 277) (Lanes 4-6)

Homogenates of HEK 293 cells transfected with three different human H_3 receptor isoforms (329, 365 and 445) all epitope tagged with FLAG were prepared. Cell homogenates were loaded (approximately 50 μg of protein/well) onto a 7.5% PAGE gel. Identical samples were run on the left and right hand sides of the gel. Following separation the proteins were transferred to a nitrocellulose membrane which was then divided vertically between the two sets of samples. The left hand side was probed with a monoclonal mouse anti-FLAG antibody (dilution 1:5000) and the right hand side with affinity purified anti-H_3 receptor antibody (first bleed from rabbit 15MY) at a final concentration of 1 μg/ml. The FLAG antibody clearly reacts with all three isoforms with monomeric species running at Mr 33,000; 36,500 and 44,500 as expected. By contrast the anti-H_3 receptor antibody is selective for the full length 445 isoform with negligible reactivity against the two shorter isoforms. In both blots, there is clear evidence of higher molecular weight species, most prominently with the 329 isoform. Representative blot from at least 10 similar experiments.

Recombinant cells expressing FLAG tagged human H_3 receptors

Lanes 1 and 4, HEK 293 cells expressing $hH_{3\ (329)}$ receptor; Lanes 2 and 5, HEK 293 cells expressing $hH_{3\ (365)}$ receptor; Lanes 3 and 6, HEK 293 cells expressing $hH_{3\ (445)}$ receptor

Lanes 1-3 were probed with anti-FLAG 1:5000; Lanes 4-6 were probed with anti rH_3 (268-277) at 1 μg/ml.

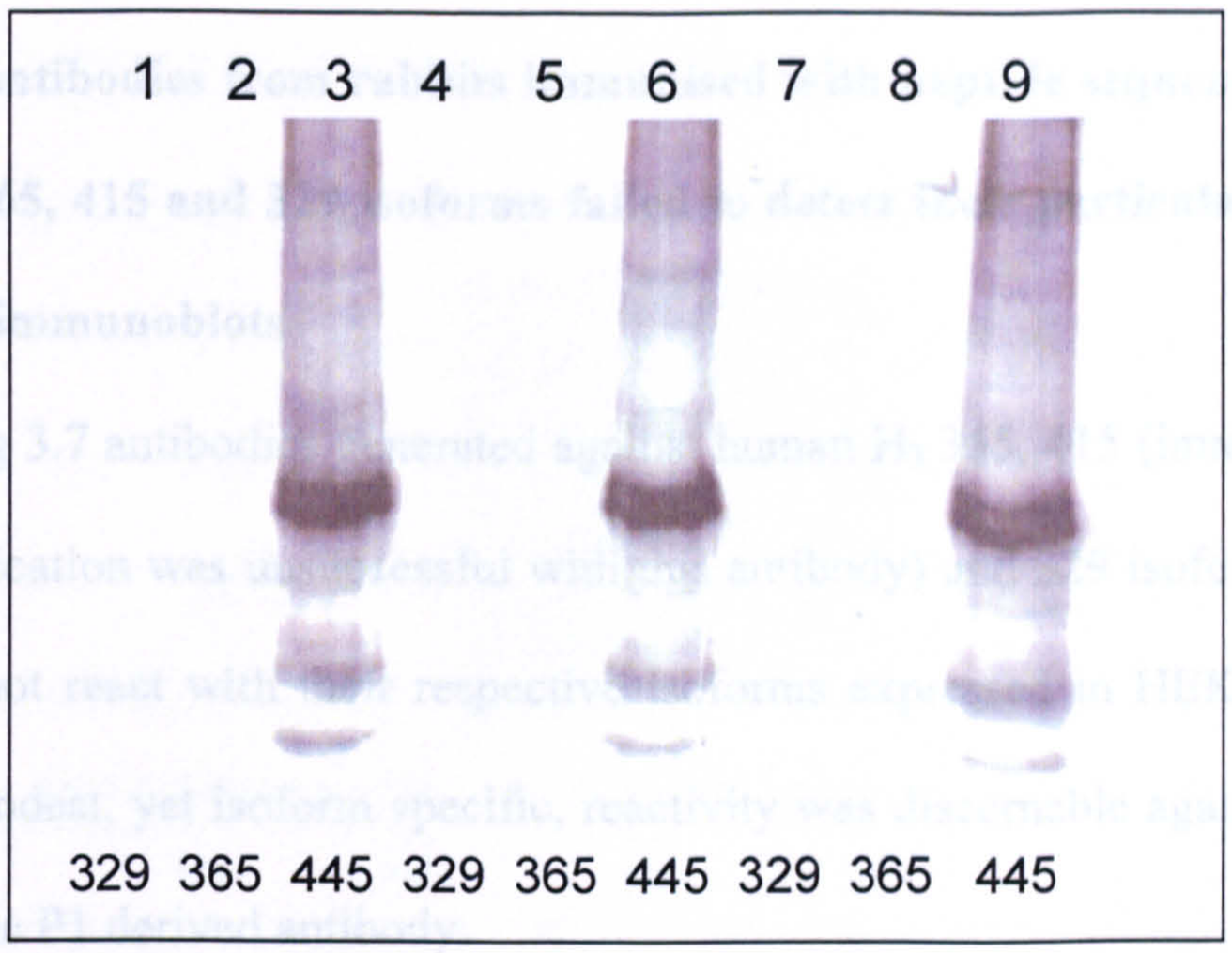

Fig 3.6 Anti-rH_{3C} (268 – 277) from different rabbits and different bleeds used against human isoforms

Fig 3.6 shows a similar blot to the one described above to test the purified antibodies from different rabbits, and different bleeds from the same rabbit all immunized with the rH_{3C} (268 – 277) peptide sequence. All three antibodies show selectivity for the full length hH_3 ($_{445}$) isoform. The monomer is detected as a strong band running at Mr 44,500, in addition higher molecular weight species are clearly evident as before.

Recombinant cells expressing FLAG tagged human H_3 receptors
Lanes 1, 4 and 7, HEK 293 cells expressing h$H_{3\ (329)}$ receptor; Lanes 2, 5 and 8, HEK 293 cells expressing h$H_{3\ (365)}$ receptor; Lanes 3, 6 and 9, HEK 293 cells expressing h$H_{3\ (445)}$ receptor

Antibodies from different rabbits and bleeds immunized with rH_3 (268-277)(1μg/ml)
Lanes 1-3, rabbit 15MY, Bleed 4; Lanes 4-6, rabbit 12MY, Bleed 4; Lanes 7-9, rabbit 15MY, Bleed 1

3.4.3 Purified antibodies from rabbits immunised with peptide sequences unique to human H_3 365, 415 and 329 isoforms failed to detect their particular isoforms when tested in immunoblots

As shown in Fig 3.7 antibodies generated against human H_3 365, 415 (immune serum as affinity purification was unsuccessful with this antibody) and 329 isoform specific sequences did not react with their respective isoforms expressed in HEK 293 cells. Interestingly, modest, yet isoform specific, reactivity was discernable against the 329 isoform using the P1 derived antibody.

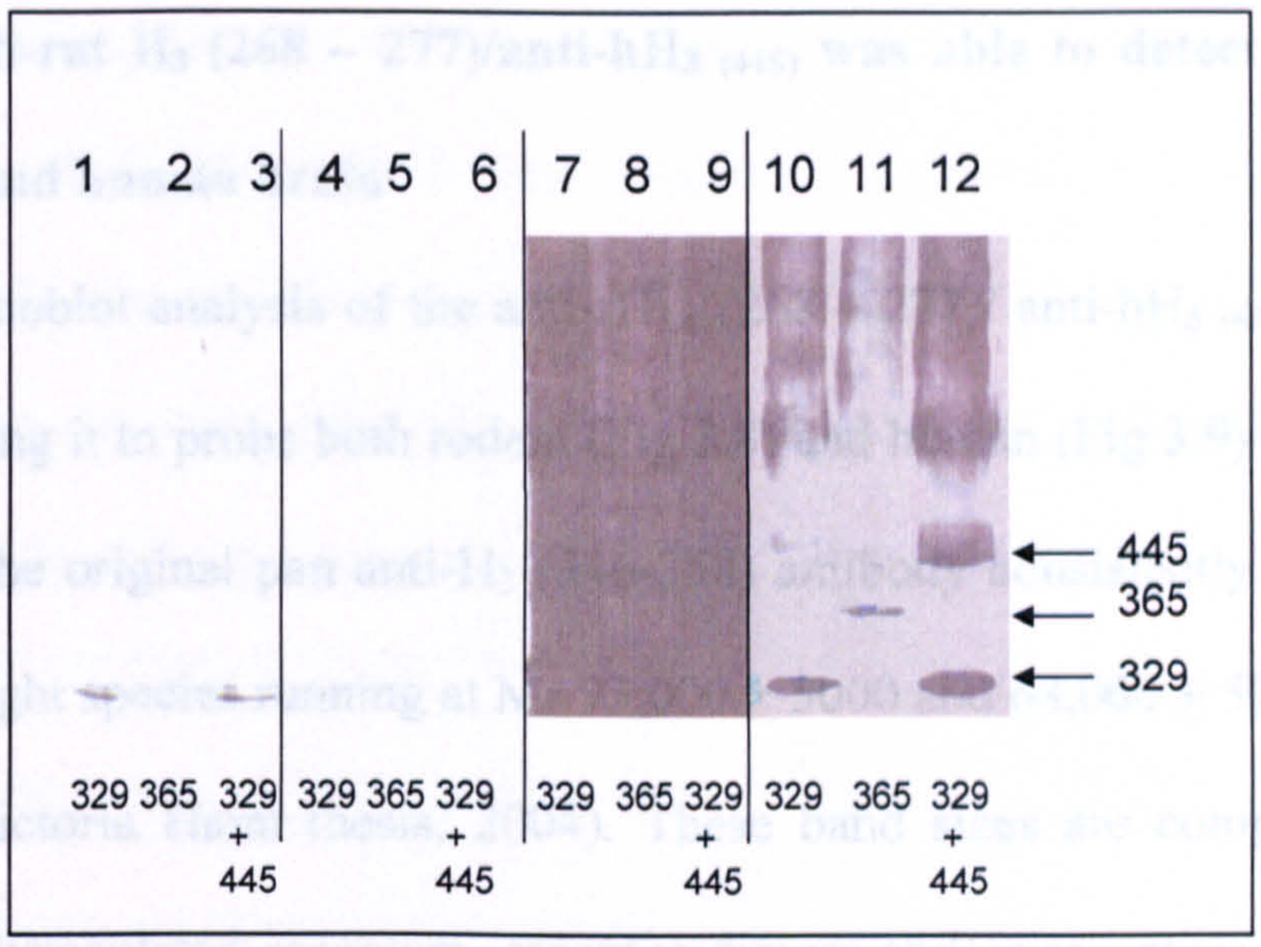

Fig 3.7 Immunoblot of human H_3 receptor isoforms expressed in HEK 293 cells probed with antibodies or immune sera from rabbits immunized with three different H_3 receptor peptide sequences.

Homogenates of HEK 293 cells transfected with three different human H_3 receptor isoforms (329, 365 and 329 + 445 co-transfected) all epitope tagged with FLAG were prepared and run on an SDS-PAGE gel as previously described. Three replicates from three independent transfections were run in parallel on the same gel. Following separation, the proteins were transferred to a nitrocellulose membrane which was then divided vertically between the three sets of samples. Each strip of nitrocellulose was probed with either purified antibody or serum from the second bleed of immunized rabbits.

Lanes 10-12 are a reprobe of lanes 4-6 using a monoclonal mouse anti-FLAG antibody at a 1:5000 dilution to detect each of the FLAG tagged isoforms and thereby confirm their position on the blot. The FLAG antibody clearly reacts with all three isoforms with monomeric species running at Mr 33,000; 36,500 and 44,500 as expected. Modest immunoreactivity corresponding to the 329 isoform is seen in Lanes 1 and 3. No specific immunoreactivity was detected by either the purified antibody or the immune serum from the other two rabbits.

Recombinant cells expressing FLAG tagged human H_3 receptors

Lanes 1, 4, 7 and 10 HEK 293 cells expressing $hH_{3\,(329)}$ receptor; Lanes 2, 5, 8 and 11 HEK 293 cells expressing $hH_{3\,(365)}$ receptor; Lanes 3, 6, 9 and 12 HEK 293 cells co-expressing $hH_{3\,(329)}$ and $hH_{3\,(445)}$ receptors

Antibodies or immune sera

Lanes 1-3, Antibodies from rabbit immunized with $H_{3\,(365)}$ sequence 5µg/ml; Lanes 4-6, Antibodies from rabbit immunized with $H_{3\,(329\ \Delta I3)}$ sequence 5µg/ml; Lanes 7-9, Immune serum from rabbit immunized with $H_{3\,(415)}$ sequence 20µl/8ml; Lanes 10-12, Anti-FLAG antibody 1:15000

3.4.4 The anti-rat H_3 (268 – 277)/anti-h$H_{3\ (445)}$ was able to detect native H_3R in both rodent and human brain

Further immunoblot analysis of the anti-rH_{3A} (268 – 277)/ anti-h$H_{3\ (445)}$ antibody was carried out using it to probe both rodent (Fig 3.8) and human (Fig 3.9) native tissue. In rat forebrain the original pan anti-H_3 (346-358) antibody consistently detected higher molecular weight species running at Mr 93,000 ± 5000 and 68,000 ± 5000 as described previously (Victoria Hann thesis, 2004). These band sizes are compatible with the presence of glycosylated receptors, receptor dimers and/or receptors associated with other proteins. Using the new anti-rat H_3 (268 – 277)/anti-h$H_{3\ (445)}$ antibody (from rabbit 15MY Bleed 1) bands of a size suggestive of receptor monomers were most frequent as summarised in Table 3.2 below. However using antibody purified from a different rabbit (13MY) a higher molecular weight species at Mr 83,000 ± 3000 was noted on a couple of occasions (2/4 repeats). The anti-rat H_3 (268 – 277)/anti-h$H_{3\ (445)}$ antibody used for all the following experiments in this thesis was that purified from rabbit 15MY Bleed 1. The putative monomeric species were frequently diffuse and/or gave the appearance of doublets or triplets, again consistent with glycosylated forms of the receptor (see chapter 6).

anti-rat H_3 (268 – 277)/anti-h$H_{3\ (445)}$
60,000 ± 2000 (3/6 repeats)
49,000 ± 2000 (6/6 repeats)
38,000 ± 2000 (6/6 repeats)

Table 3.2 Summary of immunoreactive species detected in rat forebrain using anti-rat H_3 (268 – 277)/anti-h$H_{3\ (445)}$ (Rabbit 15MY Bleed 1)

Sizes are Mr values with the range for 6 replicate blots from n > 4 rat brain preparations.

Similarly in human putamen, a doublet at Mr 90,000 ± 3000 and a higher molecular weight species Mr 99,000 ± 3000 were detected (5 individuals, 4 replicate blots). In the same samples the original pan anti-H_3R antibody identified multiple bands at Mr 103,000 ± 4000; 76,000 ± 6000; 64,000 ± 3000 and 51,000 ± 1000) (5 individuals, 4 replicate blots, Fig 3.9). A summary is set out in Table 3.3 below.

Pan anti-H_3	**anti-rat H_3 (268 – 277)/anti-h$H_{3\ (445)}$**
103,000 ± 4000	99,000 ± 3000
	Doublet 90,000 ± 3000
76,000 ± 6000	
64,000 ± 3000	
51,000 ± 1000	

Table 3.3 Summary of immunoreactive species detected in human putamen using pan anti-H_3 (346-358) and anti-rat H_3 (268 – 277)/anti-h$H_{3\ (445)}$

Sizes are Mr values with the range for 4 replicate blots from n = 5 individuals.

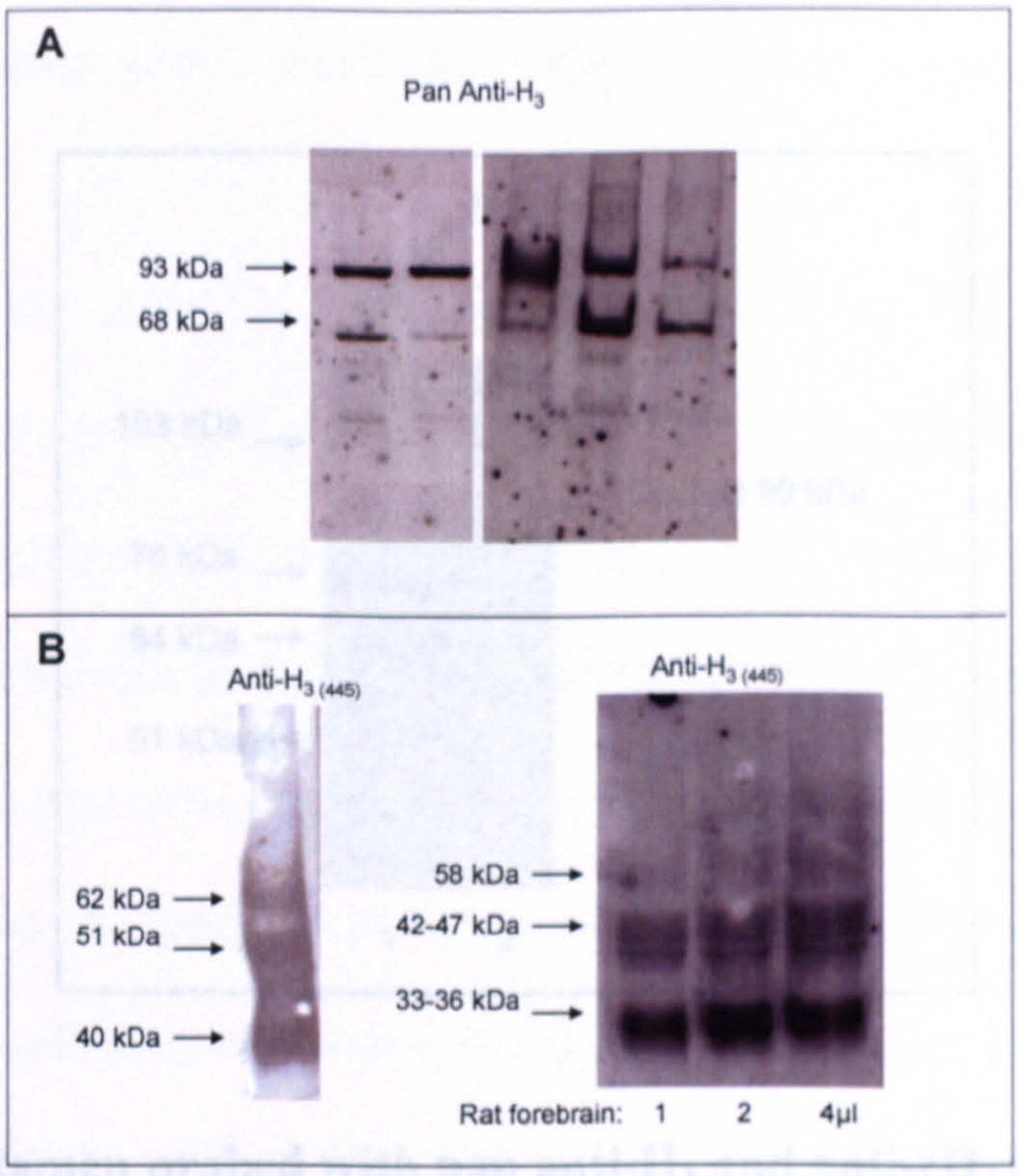

Fig 3.8 Rat forebrain probed with pan anti-H_3 and anti-rH_3 (268-277)/ antihH_3 (445)

Each lane was loaded with approximately 40 µg of rat forebrain (20 µg/µl). Panel **A** shows representative blots from numerous (n > 10) experiments using the pan anti-H_3 antibody (1-2 µg/ml). Two major bands were consistently detected at Mr 93,000 ± 5000 and 68,000 ± 5000.

In panel **B** the anti-rH_3 (268-277)/ anti-h$H_{3\ (445)}$ antibody from rabbit 15MY Bleed 1 was used at 1 µg/ml. Two representative blots are shown from a total of six replicates. Major immunoreactive species ran at Mr 60,000 ± 2000 (3/6 repeats); 49,000 ± 2000 (6/6 repeats) and 38, 000 ± 2000 (6/6 repeats). On most of the blots bands were either diffuse or appeared as doublets or triplets compatible with the occurrence of glycosylated receptors (see chapter 6).

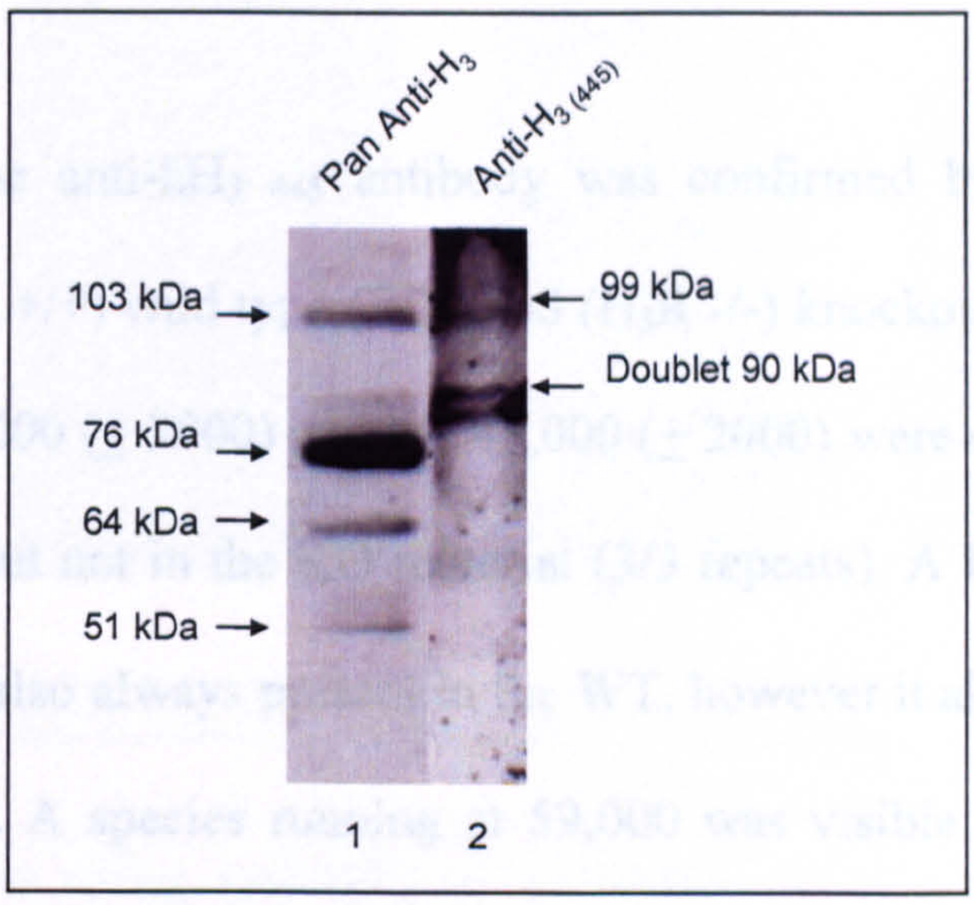

Fig 3.9 Human putamen probed with pan anti-H_3 and anti-rH_3 (268-277)/ antihH_3 (445)

The anti-$rH_{3A/C}$/anti-$hH_{3\ (445)}$ antibody was used to probe human putamen. Immunoreactivity of this new antibody (Lane 2) was compared with that of our previously described pan anti-H_3 antibody (Lane 1). The blot shown is typical of results from 5 individuals, repeated on 4 occasions. The pan anti-H_3 antibody detected species running at Mr 103,000 ± 4000; 76,000 ± 6000; 64,000 ± 3000 and 51,000 ± 1000); whereas the anti-$hH_{3\ 445}$ antibody identified a doublet at 90,000 ± 3000 and a higher molecular weight species Mr 99,000 ± 3000 (5 individuals, 4 replicates). Human putamen 50 µg both lanes, probed with: Lane 1 pan anti-H_3 R 5µg/ml, incubated for 72 hours at 4°C; Lane 2 anti-$rH_{3A/C}$/ anti-$hH_{3\ (445)}$ 2µg/ml, incubated for 72 hours at 4°C.

3.4.5 The anti-r$H_{3A/C}$/ anti-h$H_{3\ (445)}$ identified bands in immunoblots of (H_3R +/+) wild type mouse brain which were not evident in brain from (H_3R -/-) knockout mice

The specificity of the anti-h$H_{3\ 445}$ antibody was confirmed by using it to probe immunoblots of (H_3R +/+) wild type (WT) and (H_3R -/-) knockout (KO) mouse brain. Two bands at Mr 50,000 (± 2000) and Mr 44,000 (± 2000) were consistently detected in WT mouse brain but not in the KO material (3/3 repeats). A further species at Mr 40,000 (± 2000) was also always present in the WT, however it also appeared twice in the KO (2/3 repeats). A species running at 59,000 was visible once in the KO but never in the WT; in addition a band at approximately 88,000 was evident once in both the KO and the WT (1/3 repeats.) The findings are summarised in Table 3.4. Possible explanations for these results are explored in the discussion.

Protein species Mr	WT	KO
50,000 (± 2000)	++ (3/3 repeats)*	–
44,000 (± 2000)	+ (3/3 repeats)	–
40,000 (± 2000)	++ (3/3 repeats)*	+/± (2/3); – (1/3)

* Possibly equivalent to bands detected in rat forebrain at Mr 49,000 (± 2000) and 38,000 (± 2000).

Table 3.4 Summary of results comparing immunoreactive species present in KO and WT mouse brain using anti-rat H_3 (268 – 277)/anti-h$H_{3\ (445)}$

Sizes are Mr values with the range for 3 replicate blots.

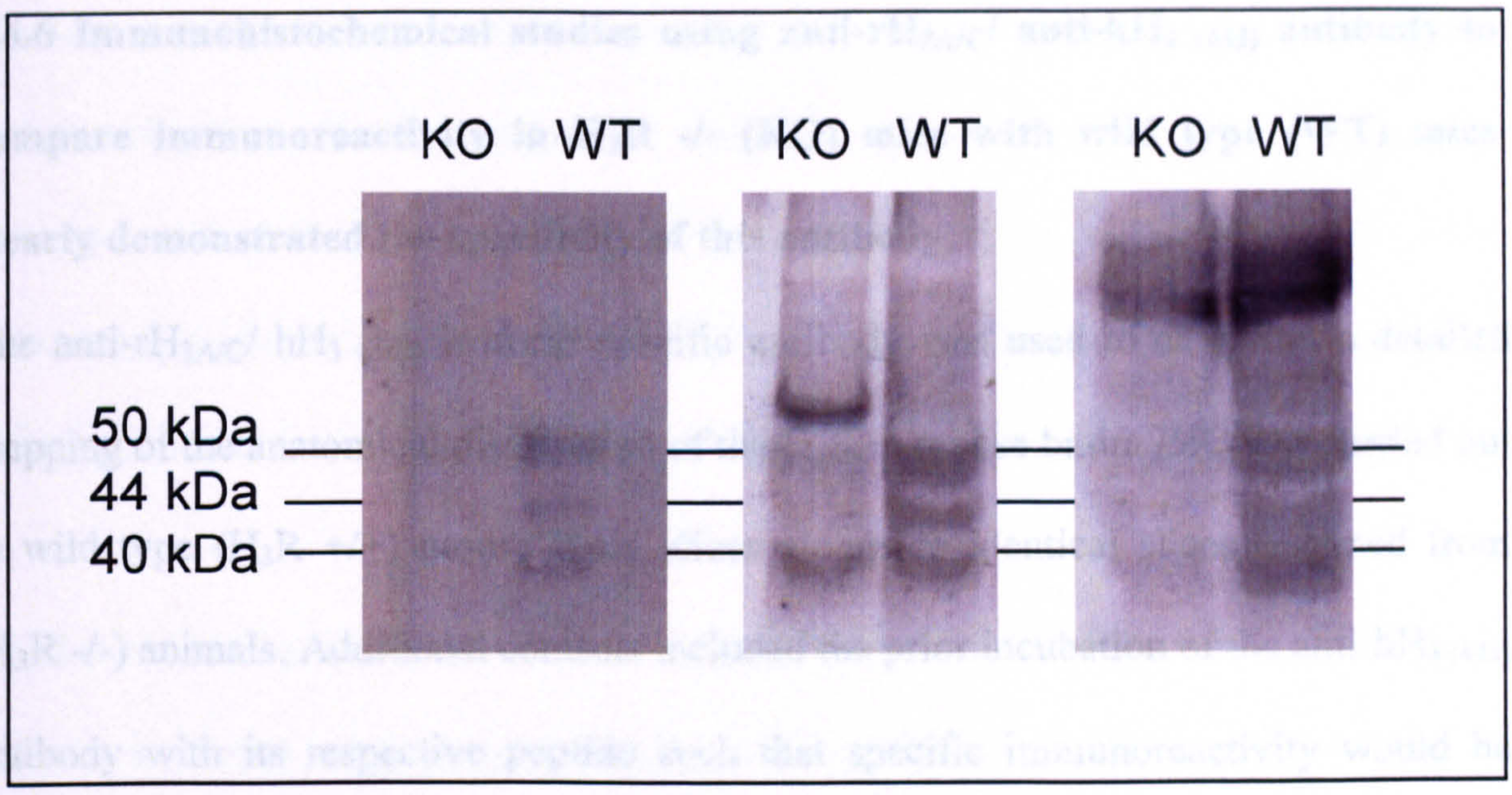

Fig 3.10 Immunoblot using anti-r$H_{3A/C}$/ anti-h$H_{3\ (445)}$ to compare H_3 receptor immunoreactivity in H_3R -/- knockout (KO) mice with H_3R +/+ wild type (WT) mice

KO and WT mouse forebrain (10 μg protein) was probed in parallel with anti-r$H_{3A/C}$/ h$H_{3\ (445)}$ R used at 1μg/ml. Two bands at Mr 50,000 ± 2000 and 44,000 ± 2000 were consistently detected in WT but not in KO material (3/3 repeats). A band at 40,000 ± 2 000 was also detected in WT on 3/3 occasions however it also appeared once in the KO material. A species running at 59,000 was detected once in the KO lane but never in the WT, while a high molecular weight band at approximately 88,000 was seen once in both KO and WT. After each immunoblot the nitrocellulose sheet was stained with Ponceau S to confirm that the total protein loading was the same for both the KO and WT lanes.

3.4.6 Immunohistochemical studies using anti-$rH_{3A/C}$/ anti-$hH_{3\ (445)}$ antibody to compare immunoreactivity in H_3R -/- (KO) mice with wild type (WT) mice clearly demonstrated the specificity of this antibody

The anti-$rH_{3A/C}$/ $hH_{3\ (445)}$ isoform specific antibody was used to carry out a detailed mapping of the anatomical distribution of the H_3R in mouse brain. IHC was carried out in wild type (H_3R +/+) mouse brain slices alongside identical slices obtained from (H_3R -/-) animals. Additional controls included the prior incubation of the anti-$hH_{3\ (445)}$ antibody with its respective peptide such that specific immunoreactivity would be blocked. To achieve this, the primary antibody was incubated with the peptide at a final concentration of 500µg/ml overnight at 4°C. For use the antibody/peptide mixture was diluted such that the final antibody concentration was the same as for the unblocked antibody. As a second control IHC was carried out with the secondary antibody alone.

Immunohistochemical (IHC) studies in the mouse

A descriptive summary of the immunoreactivity in selected brain regions is shown in Tables 3.5 a) and b) for both wild type and H_3R -/- mice. Table a) and b) show results using the pan anti-H_3R (346-358) antibody and the isoform specific anti-$rH_{3A/C}$/ anti-$hH_{3\ (445)}$ antibody, respectively. The data are from three different mice and the findings are in agreement with those from an independent laboratory using our antibodies to screen at least four further WT and KO animals (Dr Keri Cannon, Johnson & Johnson). Intensity of staining has been graded 0 – 4, with 0 being equivalent to background and 4 representing intense labelling. The strongest specific staining (that is not present in knockout animals) was seen in cortical laminae II, somatosensory cortex, piriform cortex, and the amygdaloid complex (Fig 3.11). Moderate reactivity

was also noted in the str terminalis, str: caudate putamen, fimbria of the hippocampus and the cingulum. Weak non-specific reactivity was observed in some of the brain structures of knockout animals using the anti-$rH_{3A/C}$/ anti-$hH_{3\ (445)}$ antibody (Fig 3.11). This non-specific staining was not seen with an immunofluorescence detection system using rhodamine linked anti-rabbit secondary antibodies (Fig 3.12).

The background strain of the H_3R -/- mice is C5731/6J (US Patent no. 7151200). In contrast to results using the pan anti-H_3 (346 – 358) in B6C3Fe mice (Chazot *et al*, 2001), there was negligible immunostaining in the deeper cortical layers and little detectable signal above background in the CA1, CA2 and CA3 regions of the hippocampus. In B6C3Fe mouse brain slices pan anti-H_3 (346 – 358) immunoreactivity was detected in cortical layers II and V, and in the CA3 region of the hippocampus (Chazot *et al*, 2001).

Table 3.5 a) Summary of some key brain structures using pan-H_3 receptor antibody

Tissue	H_3R +/+	H_3R -/-
Striatum	+3-4	0
Sunstantia nigra	+3	0
S1/S2 cortex	+3-4	+1
Cingulate cortex	+3	0
Entorhinal cortex	+3	0
Thalamus	+3	0
Amygdaloid complex	+3-4	0
Hippocampus CA1	0-1	0-1
Medial septal cortex	0	0

Table 3.5 b) Summary of some key brain structures using anti- $rH_{3A/3C}$ / $hH_{3\ (445)}$ antibody

Tissue	H_3R +/+	H_3R -/-
Substantia nigra	+4	+1
Striatum	+3	+1
Cingulum	+3	+2
Somatosensory cortex	+3	0
Fimbria of the hippocampus	+3	+2
Hippo: CA1/CA2/CA3	0	0
Cortex layer II	+4	0
Piriform cortex	+4	0
Str terminalis	+4	+1
Amygdaloid complex: ACo, PLCo	+4	0

Data are from n = 3 mice of each type

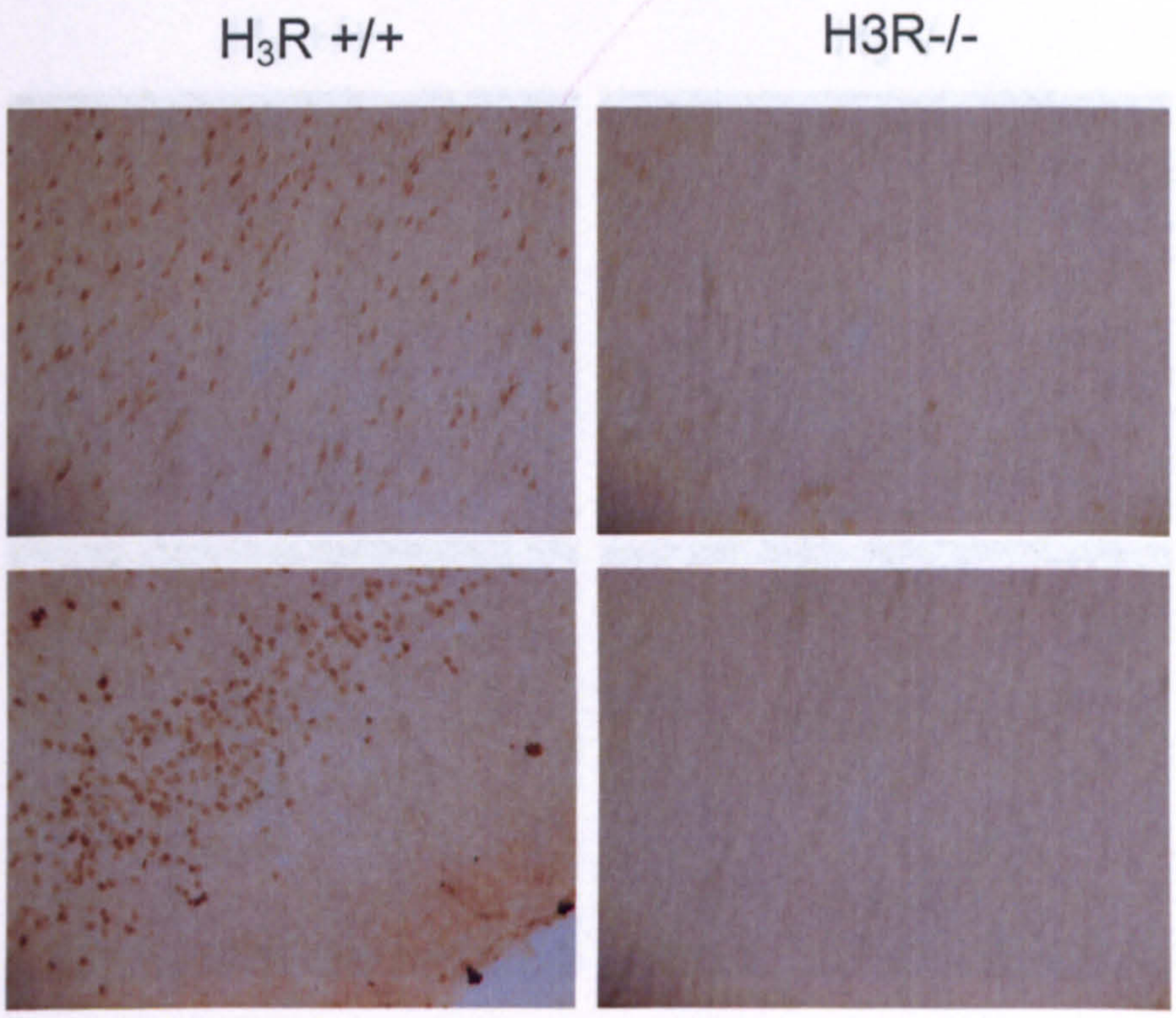

Fig 3.11 Comparing anti-r$H_{3\ A/C}$/ anti-h$H_{3\ (445)}$ immunoreactivity in H_3 +/+ (wildtype) mice with H_3 -/- (knockout) mice in selected key brain structures

Immunostaining of mouse 20μm coronal brain slice (x 200) using anti-hH_3 (445) at 0.1 μg/ml.

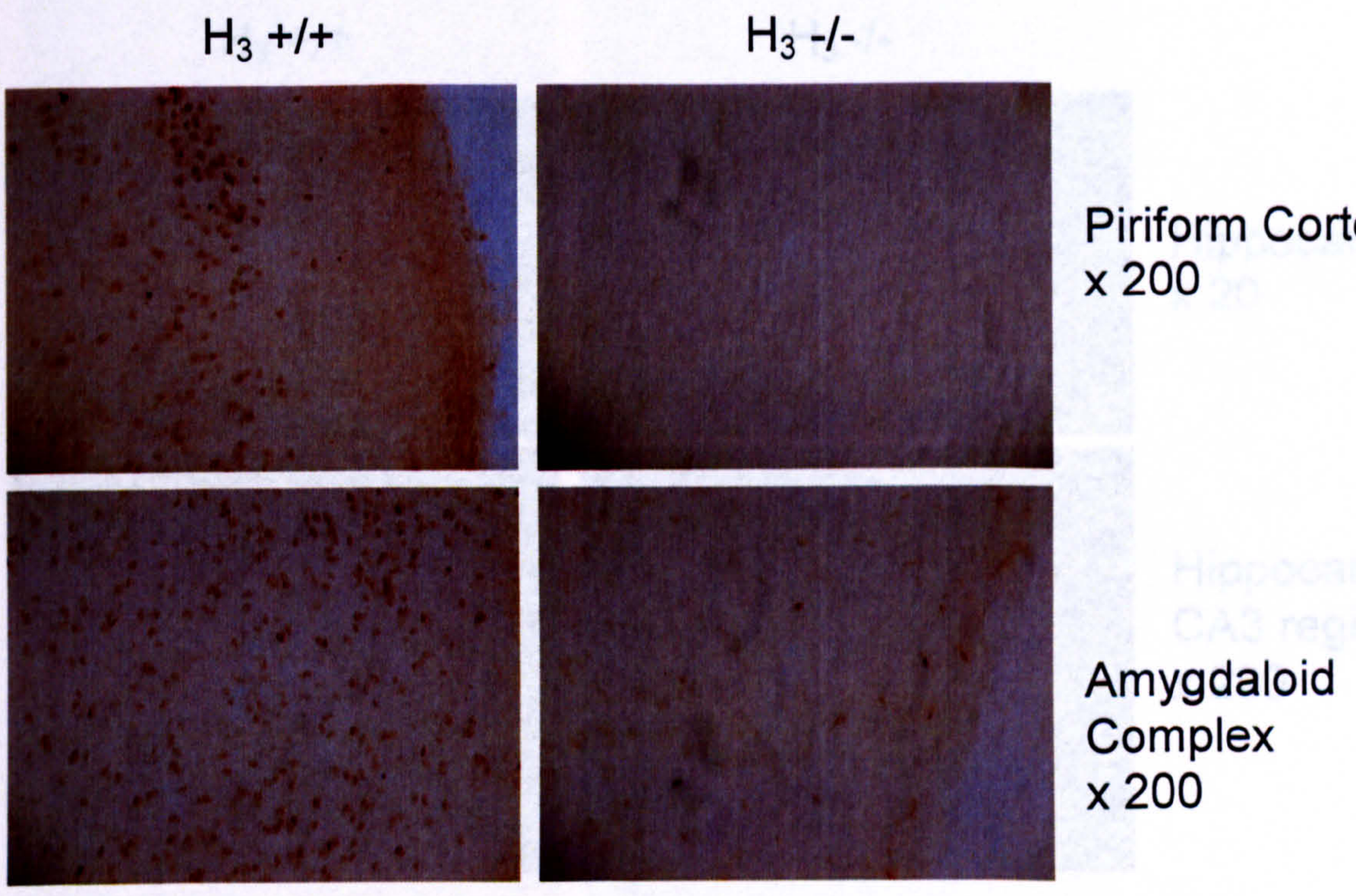

Fig 3.11 Comparing anti-r$H_{3A/3C}$ /anti-h$H_{3\ (445)}$ immunoreactivity in H_3 +/+ (wildtype) mice with H_3 -/- (knockout) mice in selected key brain structures

Immunostaining of mouse 20μm coronal brain slice (x 200) using anti-hH_3 (445) at 0.1 μg/ml.

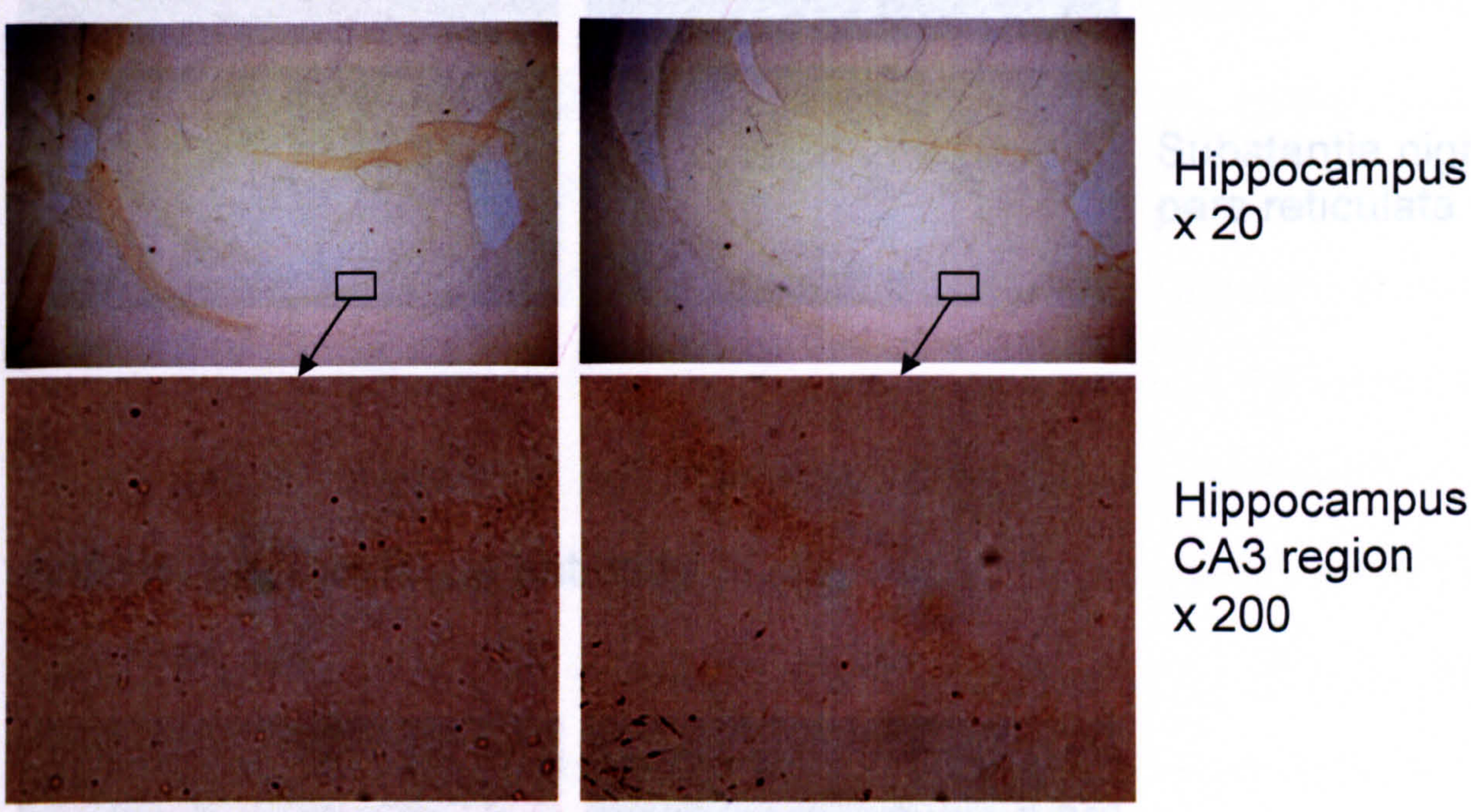

Fig 3.11 Comparing anti-r$H_{3A/3C}$ /anti-h$H_{3\ (445)}$ immunoreactivity in H_3 +/+ (wildtype) mice with H_3 -/- (knockout) mice in selected key brain structures

Immunostaining in the hippocampal formation of a mouse 20 μm coronal brain slice (x 20 and x 200), using anti-hH_3 (445) at 0.1 μg/ml.

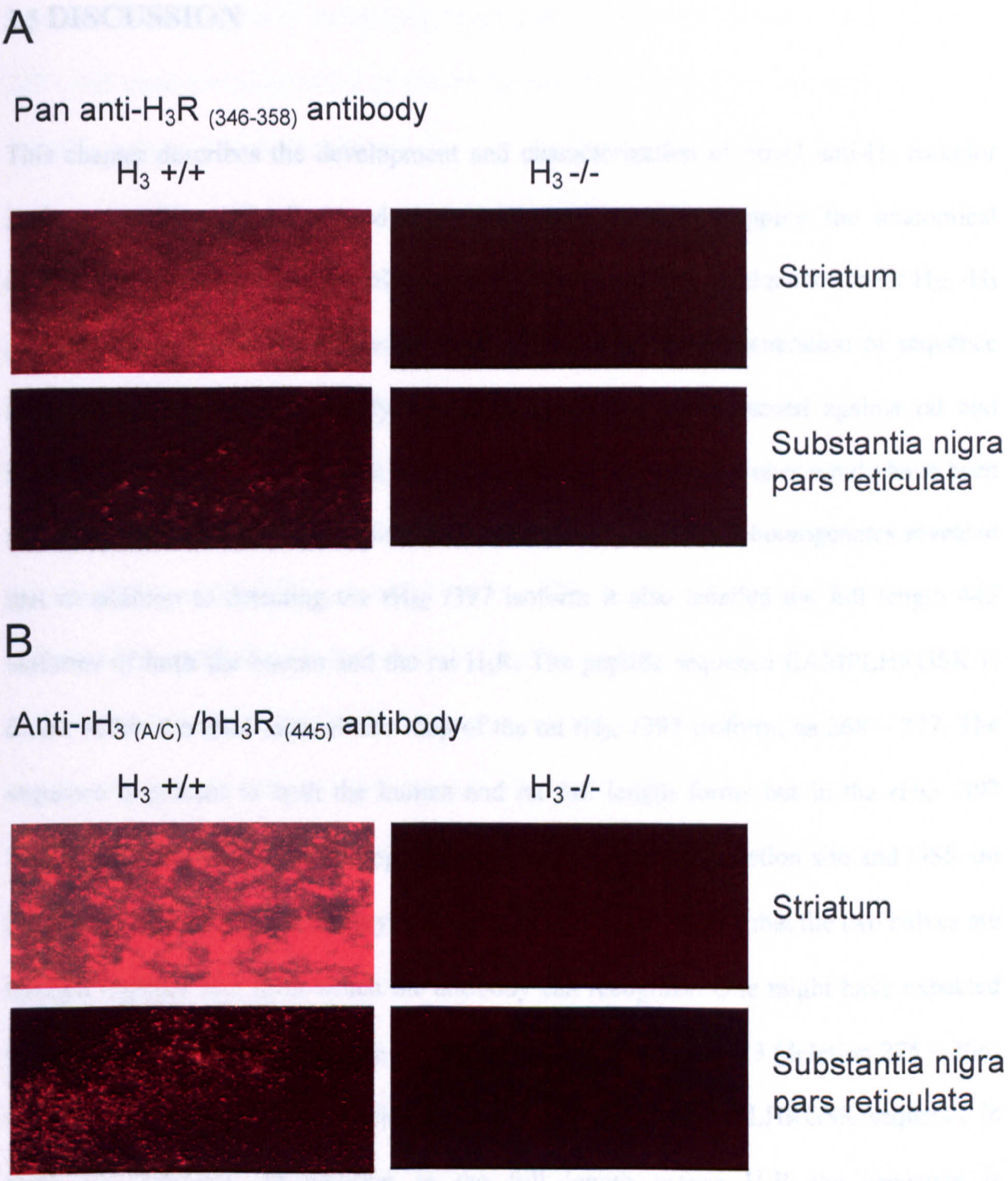

Fig 3.12 Immunofluorescent detection of H_3 immunoreactivity in striatum and substantia nigra pars reticulata comparing H_3 +/+ (wild type) mice with H_3 -/- (knockout) mice

A Pan anti-H_3R (346-358) antibody, **B** Anti-$rH_{3A/3C}$ /anti-hH_3R (445) antibody in coronal mouse brain slices (x 100).
Reproduced with kind permission of Dr Keri Cannon

3.5 DISCUSSION

This chapter describes the development and characterization of novel anti-H_3 receptor isoform specific antibodies, and their preliminary use in mapping the anatomical distribution of the H_3R in mammalian brain. A peptide sequence unique to the rat H_{3C} /$H_{3\,(397)}$ isoform was chosen and used to immunise rabbits for the generation of sequence specific antibodies. The antibody was affinity purified and screened against rat and human H_3R isoforms expressed in HEK 293 cells, (Note: mouse clones would have been used but were not available at this time). Immunoblotting of cell homogenates revealed that in addition to detecting the rH_{3C} /397 isoform it also labelled the full length 445 isoforms of **both** the human and the rat H_3R. The peptide sequence EAMPLHRGSK is found within the third intracellular loop of the rat rH_{3C} /397 isoform, aa 268 – 277. The sequence is present in both the human and rat full length forms but in the rH_{3C} /397 isoform it is split: EAMPLHR appearing on the 5' side of the deletion site and GSK on the 3' side. Presumably the tertiary structure of the receptor is such that the two halves are brought together in a form which the antibody can recognize. One might have expected the antibody to react with $hH_{3\,(365)}$ (deletion 275-354) and rH_{3B} /413 (deletion 275 – 306) since only the last two amino acids are missing from the EAMPLHRGSK sequence in these two isoforms. In addition in the full length mouse H_3R the sequence is EAMPLHR**YGV**, with the last three amino acids being different from the immunising peptide, nevertheless specific anti-H_3R immunostaining was detected with both the pan anti-H_3 and the anti-$rH_{3A/3C}$ /anti-$hH_3R_{\,(445)}$ in mouse brain slices. However, the tertiary structure of the $hH_{3\,(365)}$ and rH_{3B} /413 may have been unfavourable, with the peptide

sequence not accessible to the antibody within these isoforms. The $hH_{3\ (329\ \Delta IC)}$ (deletion 227 -342) does not possess any of this particular peptide sequence and, as expected, no reactivity was seen with this clone.

The presence of higher molecular weight species even under the strong reducing and detergent conditions under which the gels were run indicates the possible presence of robust dimers or higher oligomers in addition to the monomer. However, the molecular weights of the higher bands were not all compatible with multiples of the H_3 receptor monomer. At least two explanations might account for this: firstly, anomalous running of the oligomers possibly due to post-translational changes, eg. glycosylation, and secondly other cellular proteins could be robustly interacting with the H_3 receptor. Results obtained with recombinant proteins should be interpreted with caution. The receptor is not being expressed in its natural environment and receptor levels are generally higher than in native tissue. However, higher molecular weight species were also observed in immunoblots of native tissue, especially in the human material; suggesting that this is indeed a real phenomenon. Immunoreactivity in human putamen was investigated because high levels of H_3R mRNA have been reported in this brain structure for human (Cogé *et al*, 2001), rat (Pillot *et al*, 2002) and mouse (Rouleau *et al*, 2004). Furthermore it is of interest as a key region in voluntary movement. In the Pillot study the mRNA signal was matched with strong ligand binding, indicative of H_3R protein expression. Evidence for message coding for several different isoforms in addition to the full length isoform was found in both human and mouse cortex (Cogé *et al*, 2001 and Rouleau *et al*, 2004, respectively), a brain area which sends projections to the striatum which includes

the putamen. Message for several isoforms was also found in the striatum itself in the Rouleau study. In agreement with these reports both the pan anti-H_3R and the anti-rat H_3 (268 – 277)/anti-$hH_{3\ (445)}$ antibody identified multiple bands in human putamen, both putative monomers (with the pan anti-H_3R) and higher molecular weight species (with both antibodies). Interestingly, in immunoblots of rodent brain higher molecular weight species were seldom seen, suggesting there may be species differences in oligomer stability. However the data from these experiments are limited because the material was from only a small number of animals (n = 3). There was some indication that the different isoforms may differ in their potential to oligomerise and/or interact with other proteins. With rat isoform $H_{3C}/397$ expressed in HEK 293 cells, higher molecular weight species were less apparent than with the full length $rH_{3A}/445$ isoform. The evidence for H_3R oligomers is further investigated in Chapter 4.

Attempts were made to generate antibodies against three more human H_3R isoforms using an identical strategy, however these met with only limited success. However, one of these antibodies appears to selectively recognise the 329 isoform with moderate affinity. This requires further investigation.

The rH_{3C} (268 – 277)/$hH_{3\ (445)}$ antibody was used to map the anatomical distribution of the H_3R in mouse brain slices. Immunohistochemical (IHC) studies using wild-type and H_3R -/- mice (Lovenberg, Johnson and Johnson, US Patent no. 7151200) showed a marked reduction in immunoreactivity in the knockout animals compared to the wild type, demonstrating the specificity of the new antibody. In this investigation only material from

three animals was available to us, however the findings are in agreement with an extensive IHC study using our antibodies and the same H_3R -/- animals, an immunofluorescent detection system was used on this occasion (see Fig 3.12, Cannon *et al*, 2007). The immunoreactivity in wild type animals was similar for both the original pan anti-H_3 (346-358) antibody and the new isoform selective antibody. The findings also confirmed those of a previous study using the pan anti-H_3 (346-358) antibody (Chazot *et al*, 2001) to map the anatomical distribution of the H_3R in mouse brain slices; with the exception of cortex layer V which showed moderate/strong staining in the first study but only light staining in the present investigation, and the hippocampus (regions CA1-CA3 and dentate gyrus) where there was some moderate reactivity, not found here. It is possible that these minor differences might be accounted for by the fact that different mouse strains were used (B6C3Fe, Chazot *et al*, 2001; C5731/6J in this study), however further work is necessary to validate these observations and confirm their reproducibility. IHC using the anti-$rH_{3C}/hH_{3\ (445)}$ antibody demonstrated clear specific immunoreactivity in substantia nigra, cortical laminae II, somatosensory cortex, piriform cortex, and the amygdaloid complex. Moderate reactivity was also noted in the striatum, str terminalis, fimbria of the hippocampus and the cingulum. Background labelling was evident in some brain areas in knockout animals, notably the fimbria of the hippocampus and cingulum, and to a lesser degree in the striatum; nevertheless it was at a lower level than in equivalent areas from wild type mice. This background labelling was not apparent using an immunofluorescent detection system e.g. basal ganglia (Fig 3.12). However in immunoblots comparing mouse brain homogenates from WT and KO the animals there was an indication of some immunoreactivity in the KO material (Fig 3.10). In the H_3R -/-

mice the H_3R gene is disrupted by homologous recombination (US Patent no. 7151200). A 0.7 kb region covering part of the first intron and the 5' end of the second exon is replaced. Although the gene is rendered non-functional by this disruption with no detectable [^{3}H]-RAMH binding in KO animals (Toyota *et al*, 2002; US Patent no. 7151200) there could possibly be some low level expression of non-functional H_3R protein remaining. The staining might be entirely non-specific but this is unlikely because the peptide block experiment wherein the antibody was pre-incubated with its respective peptide completely removed the reactivity, therefore demonstrating that the antibody is binding to that particular peptide sequence. Alternatively the sequence might occur in other proteins in this region which are not H_3R. However a standard BLAST screen performed as described previously (Chazot *et al*, 2001) yielded no mammalian brain protein hits. Such proteins could conceivably be other histamine receptor subtypes not yet identified. Although there is evidence for the most recently discovered histamine H_4 receptor subtype in both human brain (Cogé *et al*, 2001) and mouse brain (Zhu *et al*, 2001) cross-reactivity with this particular receptor is unlikely. The EAMPLHRGSK sequence is not found within the H_4R aa sequence and the anti-rH_{3C}/h$H_{3\ (445)}$ antibody does not detect recombinant H_4R expressed in HEK 293 cells.

Specific immunoreactivity in the amygdaloid complex could be of significance in that this area of the brain is known to be involved in fear and memory. The H_3 receptor appears to play a role in memory in some experimental models. It was found using the passive avoidance model, that H_3R -/- mice learned as normal, but were insensitive to the amnesia-inducing effects of the muscarinic antagonist scopolamine (Toyota *et al*, 2002).

This is in agreement with studies where H_3 receptor antagonists have been shown to have the same effect on scopolamine-induced memory deficits (Giovannini *et al*, 1999). Interestingly, the H_3R -/- mice were not insensitive to scopolamine in the open field habituation test, which measures memory as the habituation of exploratory activity in a new environment. The fact that H_3 -/- mice were only insensitive to the effects of scopolamine in an aversion model may point to a specific role for the H_3 receptor in memory formation associated with painful stimuli.

The high expression in the basal ganglia, particularly in the substantia nigra, is consistent with recent double labelling confocal studies using these H_3 receptor antibodies (Appendix). These have shown that the H_3 receptor is expressed on minor subpopulations of GABA-ergic neurons in the sustantia nigra and frontal cortex, and furthermore on subpopulations of histaminergic neurons in the tubermammilary nucleus, which suggests distinct control of output neurons to other brain regions by the H_3 receptor (unpublished findings, see Appendix).

In conclusion a novel anti-H_3R antibody was generated which was selective for two rat isoforms: rH_{3A} and rH_{3C} and only for the human $hH_{3\,(445)}$ isoform. This antibody was used to further characterise rodent and human H_3R in both heterologous and native tissue. In addition it was used to map the distribution of these isoforms in mouse brain. Two potential sources of receptor heterogeneity are indicated by these results. Firstly there was clear evidence of higher molecular weight species on immunoblots. These could be accounted for by any or all of the following: receptor oligomers, the receptor associated

with other cellular proteins, and/or post-translational changes. Secondly different isoforms may vary in their propensity to form homo and hetero-oligomers (see Chapter 4); for example in contrast to the rH_{3A} isoform, higher molecular weight species were not evident with the rH_{3C} following heterologous expression in HEK 293 cells. There could also be interspecies differences in receptor oligomersisation in native tissue, higher molecular weight species were rarely detected in rodent brain using the rH_{3C} (268 – 277)/$hH_{3\ (445)}$ antibody in contrast to observations in human putamen. In the following chapter the presence of human and rat H_3R oligomers will be investigated and its' relevance to receptor heterogeneity and function will be discussed. Note chapter 4 will also take advantage of the subtype selectivity of the new antibody for the full length human H_3 receptor.

CHAPTER 4

EVIDENCE FOR HUMAN AND RODENT H_3 RECEPTOR OLIGOMERS: BIOCHEMICAL AND BIOPHYSICAL APPROACHES

4.1 OBJECTIVES

Investigate oligomer formation, both homo-oligomers between the same isoforms and the possibility of hetero-oligomers consisting of splice variants of the receptor.

4.2 INTRODUCTION

Oligomerisation of histamine receptors has been demonstrated for the H_1R (Carillo *et al*, 2003; Bakker *et al*, 2004), the H_2R (Fukushima *et al*, 1997), rat H_3R (Bakker *et al*, 2006; Shenton *et al*, 2005) and the H_4R (Chapter 5 and van Rijn *et al*, 2006). In H_1 receptors transiently expressed in COS-7 cells, Bakker and colleagues (Bakker *et al*, 2004) demonstrated the presence of domain swapped H_1 receptor dimers in which there was a reciprocal exchange of TM domains 6 and 7.

Heterogeneity in the pharmacology of the H_3 receptor both between and within species is well documented (see chapter 1) and the reasons for it are likely to be complex. The existence of several H_3 receptor isoforms in all mammalian species studied so far and their differential distribution within brain regions could in theory provide potential mechanisms for generating this heterogeneity. Multiple receptor isoforms generated by differential splicing of receptor RNA have been reported for other GPCRs (reviewed by Bockaert & Pin, 1999). However the functional relevance of these splice variants is

largely unknown. A variant of the gonadotrophin-releasing hormone receptor (GNRHR) impairs receptor signalling possibly by preventing proper trafficking of the full length GNRHR (Grosse *et* al, 1997). A non-functional transmembrane truncated variant of the arginine vasopressin V2 receptor (AVPR2) co-expressed with the full length AVPR2 acted as a negative regulator of normal AVPR2 function (Zhu & Wess, 1998). The truncated isoform reduced both the surface expression of the full length receptor and the maximum cAMP resonse induced by ligand stimulation. Thromboxane A (2) is a potent mediator of inflammation, vasoconstriction and oxidative stress. Its receptor (TP) is expressed as two alternatively spliced isoforms alpha and beta. TP alpha does not undergo constitutive or agonist-induced endocytosis when co-expressd with TP beta (Laroche *et al*, 2005). Co-transfection of vasoactive intestinal peptide (VIP) receptor ($VPAC_2$) with a short deletion (SD) splice variant SD $VPAC_2$, leads to a decreased VIP enhancement of IL-4 production by Th2 cells compared with the full length $VPAC_2$ receptor alone (Huang *et al*, 2006). The evidence suggested a competitive interaction between the two isoforms in the same signalling pathway, with the SD $VPAC_2$ isoform inhibiting the increase of nuclear levels of transcription factors. However hetero-oligomerisation was not investigated in this study.

In the case of rat H_3 receptors, our group and colleagues have provided evidence for truncated rH_3 isoforms acting as dominant negative hetero-dimers which impede the expression of the full length rH_{3A} isoform at the cell surface (Bakker *et al*, 2006). Therefore the evidence to date tends to suggest a potential negative regulatory role for GPCR splice variants.

As described in chapter 3 and previously in the laboratory (Chazot *et al*, 2001; Victoria Hann PhD thesis, 2004) immunoblots of both recombinant and native **rat** H_3R provided evidence for robust oligomers (insensitive to 200mM DTT). The purpose of the experiments described in this chapter was to confirm the existence of **human** H_3R homo- and hetero-dimers (ie dimerisation between different isoforms) when expressed in HEK 293 cells. The studies focussed on the full length 445 H_3 isoform and another major isoform the 329 ΔIC. mRNA coding for both these isoforms is abundant within human brain and they appear to exist together in some important brain regions (Cogé *et al*, 2001). In order to address the question as to whether the H_3R is capable of forming both homo- and hetero-oligomers (ie oligomers between different splice variants), different approaches were used: a) biochemical, using a chemical cross-linking technique to stabilise putative homo-dimers, and b) biophysical, using Fluorescent Resonance Energy Transfer (FRET) to confirm the presence of both homo- and hetero-dimers within the cell membrane.

4.3 METHODS

Culture and transfection of HEK 293 cells

Harvesting and membrane preparation of HEK 293 cells for blotting

Lowry assay for protein estimation

Immunoblotting

Chloroform/ methanol protein extraction

All as described in Chapters 2 and 3.

In addition to the usual sample preparation described in Chapter 3, a method involving incubation of the sample with urea at 4°C was used (Gazi *et al*, 2003) which was found to enhance the visualisation of higher oligomers. For this method, the sample buffer was as follows: 100mM Tris-HCl pH 6.8, 4% SDS, 0.2% bromophenol blue, 20% glycerol and 8% urea. The sample was dissolved in 13 µl of this sample buffer plus 2µl of 1.5M DTT (giving a final DTT concentration of 200mM). Following a 2 – 4 hour incubation period at 4°C, the sample was subjected to standard gel electrophoresis. Where a particularly clean preparation was required the protein was occasionally extracted using a standard chloroform/ methanol method.

4.3.1 Chemical cross-linking

HEK 293 cells were transfected with either rat or human H_3R cDNAs. The human isoforms were both epitope tagged with FLAG (Cogé *et al*, 2001). Two days post-transfection, the cells were harvested and homogenised, homogenates were then incubated with increasing concentrations of the irreversible chemical cross-linker bis(sulphosuccinimidyl) suberate sodium salt (BS_3). This involves the covalent

coupling of proteins via primary amine bonds. The cross-linking method was adapted from that of Haugeto *et al*,1996. Aliquots of transfected HEK cells were pelleted, the suspension buffer was removed and replaced with 150µl cross-linking buffer (150mM NaCl, 100mM Na-HEPES, 5mM EDTA pH7.5, 5mM DTT) to give a final protein concentration of approx. 5mg/ml. The BS_3 was dissolved in 20mM HCl to give a 100mM stock solution. The stock was added at doubling dilutions to nine tubes of resuspended cells to give final cross-linker concentrations ranging from 0 to 4mM. The tubes were incubated at room temperature with continual mixing for 12 minutes after which they were spun down at 10000rpm for 5mins, the cross-linking mixture was removed and the pellet prepared for immunoblotting either in the usual way or using the method outlined above, using sample buffer plus urea at 4°C. The blots were carried out on 6% PAGE gels following cross-linking to allow larger molecular weight species to be resolved on the gel. Either anti-FLAG antibody or the new anti-$H_{3\ (445)}$ specific antibody described in Chapter 3 was used as the primary antibody. As reported in Chapter 3 the latter antibody was selective for the $hH_{3\ (445)}$ isoform and the rat H_{3A} and H_{3C} isoforms, but not the hH_3 (365), hH_3 329 or rH_{3B}.

Immunoblots were quantified by densitometry using NIH ImageJ in the linear range of the film. Optical density values were normalised to respective background as described previously (Chazot *et al*, 2002).

4.3.2 *tr*-FRET

This method uses differential labelling of membrane receptors with a donor (europium 3+) and an acceptor (allophycocyanin APC) fluorophore and the subsequent transfer of resonance energy from one to the other provided the two receptors are close enough

together. If the two receptors are within 100Å of each other in the membrane, excitation of the Eu^{3+} fluorophore will result in resonance energy transfer to the APC fluorophore which will emit fluorescence at 665nm (Fig 4.1 Schematic representation of FRET for homo-dimers). In order to demonstrate the presence of hetero-oligomers a slightly different strategy was necessary (Fig 4.2 Schematic representation of FRET for hetero-dimers).

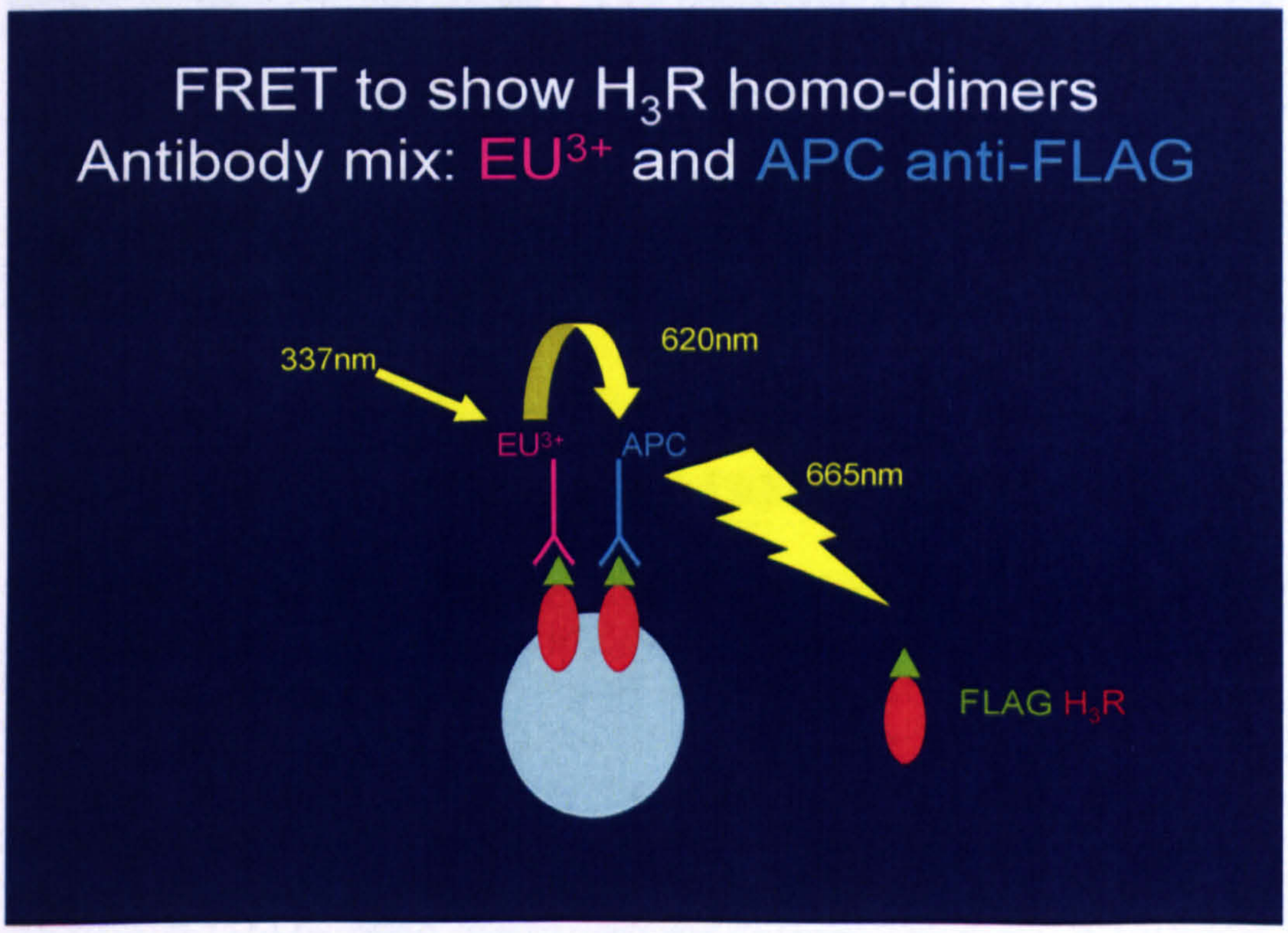

Fig 4.1 Schematic representation of *tr*-FRET to show H_3R homo-dimers.

HEK 293 cells were transfected with an H_3R isoform epitope tagged with FLAG. The transfected cells were incubated with a mixture of Eu^{3+} labelled- and allophycocyanin (APC) labelled-anti-FLAG antibodies. Excitation of the Eu^{3+} fluorophore with a 337nm wavelength generates an emission at 620nm. If an APC labelled antibody bound to an adjacent receptor is within 100Å range, resonance energy transfer can occur. The ensuing 665nm emission thus indicates the formation of receptor homo-oligomers within the cell membrane.

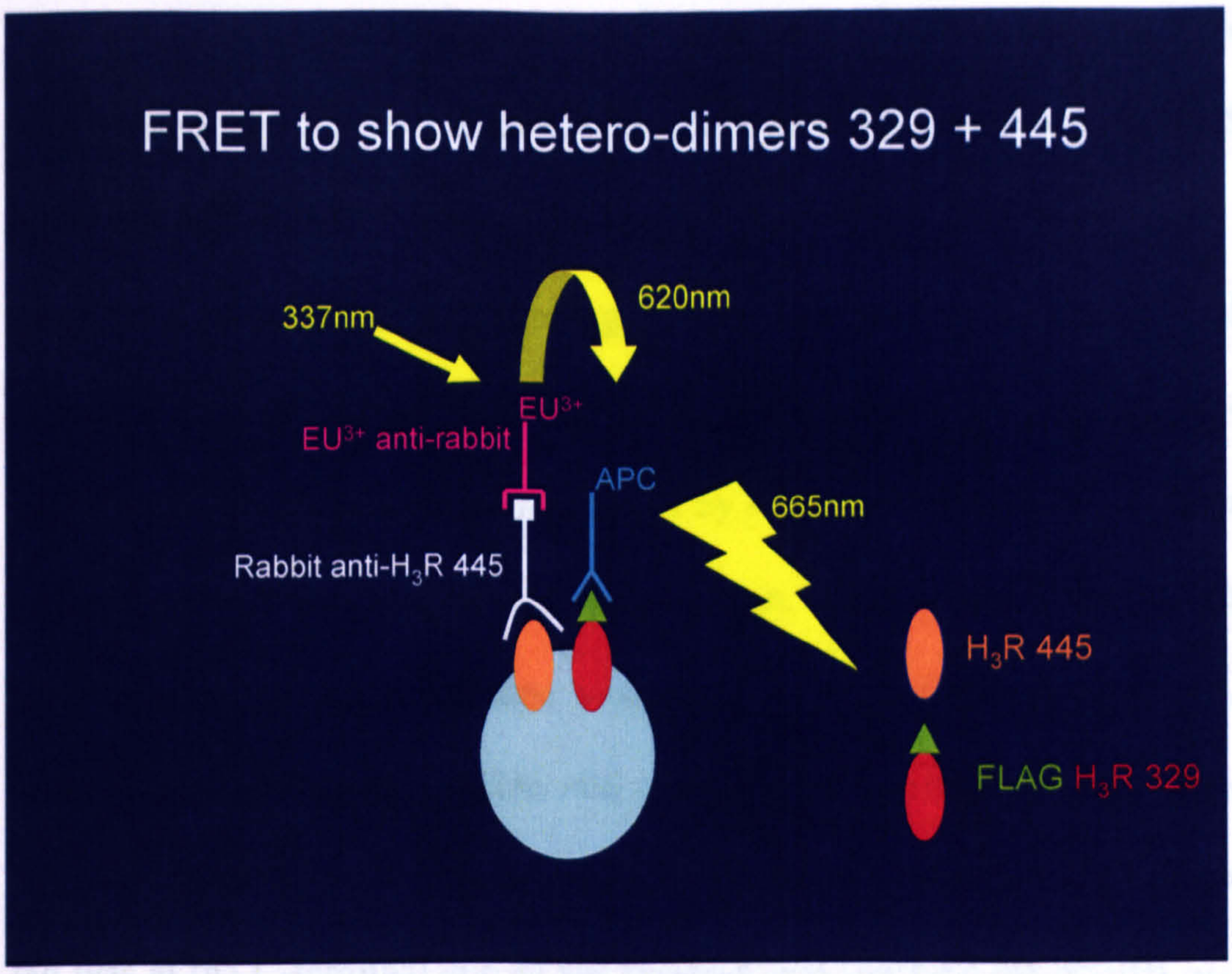

Fig 4.2 Schematic representation of *tr*-FRET to show H_3R hetero-dimers.

HEK 293 cells were co-transfected with $H_{3\,(329)}$ and $H_{3\,(445)}R$ isoforms The 329 isoform is epitope tagged with FLAG whereas the 445 isoform is untagged. The transfected cells were incubated with a rabbit anti-$hH_{3\,(445)}R$ selective antibody (Chapter 3) initially. Following washing steps the cells are then incubated with a mixture of Eu^{3+} labelled anti-rabbit and allophycocyanin (APC) labelled-anti-FLAG antibodies. Excitation of the Eu^{3+} fluorophore bound via the rabbit anti-$hH_{3\,(445)}R$ to a 445 isoform, generates an emission at 620nm. If an APC labelled antibody bound to an adjacent 329 receptor is within 100Å range, resonance energy transfer can occur. The ensuing 665nm emission thus indicates the formation of receptor hetero-oligomers within the cell membrane.

For the homo-dimer experiment HEK-293 cells were individually transfected with either the 329 isoform or the 445 isoform both epitope tagged with FLAG. For the hetero-dimer experiment cells co-transfected with FLAG tagged 329 and untagged 445 isoforms were used. The *tr*-FRET assay was adapted from that described previously by Bakker *et al*, 2006. Bakker used whole cells, however as the antibodies used here were all directed to intracellular portions of the receptor, it was necessary to disrupt the cells in order to allow the antibodies access to the relevant epitopes. Two days post-

transfection, cells were harvested and suspended in PBS containing 50% FCS (v/v). Suspensions of 1.5 x 10^6 cells/ml were made for cells transfected with 329 alone, 445 alone or 329 + 445 (untagged) together. Additional batches of cells individually transfected with 329 or 445 (untagged) were prepared at 0.75 x 10^6 cells/ml. These latter cells were mixed 1:1 and used as a control for the hetero-dimerisation experiment. The cells were homogenised by sonication and the membranes purified by passage through a Sephadex G25 mini-column. Passage through the column results in the formation of cell membrane vesicles, it was assumed that 50% of the vesicles would have the receptors inside out, i.e. with the C-terminal tail on the extracellular side, and 50% in the correct orientation. This step was necessary because the FLAG tag was at the C-terminal end of the receptor and likewise the anti-$H_{3\ (445)}$ antibody is directed towards the 3ic, which is also intracellar. Each column contained 0.5ml packed volume of Sephadex G25 pre-swelled in milliQ water. A total volume of 0.5ml of homogenised cells was added to the column, once this had run through a further 0.5ml of the PBS/FCS diluent was added to elute the disrupted membranes from the column as vesicles. Eluted vesicles were pelleted and the PBS/FCS removed. The vesicles were then resuspended in 300µl of fresh PBS/FCS containing the fluorophore labelled antibodies. For the homo-dimer experiment a combination of both europium 3+ (Eu^{3+})-labelled and allophycocyanin (APC)-labelled anti-FLAG antibodies was used, at 0.8nM and 8nM concentrations respectively. Control vesicles were incubated with Eu^{3+}-labelled anti-FLAG (0.8nM) alone. Vesicles were incubated in the dark for two hours, at room temperature on a rotating wheel; after which they were washed twice with PBS. The final pellet was resuspended in 150 µl PBS and this was split into three 50µl samples on transfer to three wells of a 384-microtiter plate. Energy transfer was measured by exciting the Eu^{3+} at 320nm and monitoring the allophycocyanin

emission for 500μs at 665nm using a Novostar (BMG Labtechnologies) configured for *tr*-fluorescence after a 100 μs delay. For the hetero-dimer experiment cells co-transfected with 329 + 445 (untagged) were used and the control was a 1:1 mixture of cells (329 transfected cells mixed with 445(untagged) transfected cells). Following column separation these vesicles were pelleted and then resuspended in rabbit anti-hH_3 $_{(445)}$ specific antibody at 1μg/ml. After the initial 2 hour incubation the primary antibody was removed and replaced with either Eu^{3+}-labelled anti-rabbit alone (only for the co-transfected cells) or a mixture of Eu^{3+}-labelled anti-rabbit and APC-labelled anti-FLAG for both the co-transfected cells and the cell mixture. The fluorophore labelled antibodies were used at the same concentrations as in the homo-dimer experiment. Following an additional two hour incubation period, the energy transfer was measured as before. All tests and controls were performed in triplicate. These experiments were performed on 3-4 separate occasions with similar results.

4.4 RESULTS

4.4.1 Chemical cross-linking studies show rat $H_{3\,(A)}$ dimers and $H_{3\,(C)}$ dimers

In the rat full length $H_{3\,(A)}$ isoform increasing concentrations of the cross-linker (0 – 0.25 mM) clearly showed increasing levels of higher molecular weight species compatible with the presence of receptor dimers and higher oligomers. In addition to the monomer, proteins running at Mr > 173,000; 133,000 and 89,000 $\pm$ 3000 were evident (summarised in Table 4.1). These increased in intensity in the presence of cross-linker while the bands corresponding to the monomers tended to decrease. By contrast the shorter $H_{3\,(C)}$ isoform did not appear to form higher molecular weight species so readily (Fig 4.3).

Rat $H_{3\,(A)}$ isoform	Rat $H_{3\,(C)}$ isoform
>173,000	
133,000	
89,000 $\pm$ 3000	
47,000 doublet	39,000 doublet
32,000	< 32,000

Table 4.1 Summary of protein species detected following chemical cross-linking of rat $H_{3\,(A)}$ and $H_{3\,(C)}$ isoforms

Mr values for protein species identified in replicate experiments from two independent transfections. Putative dimeric/ oligomeric species are shown in red.

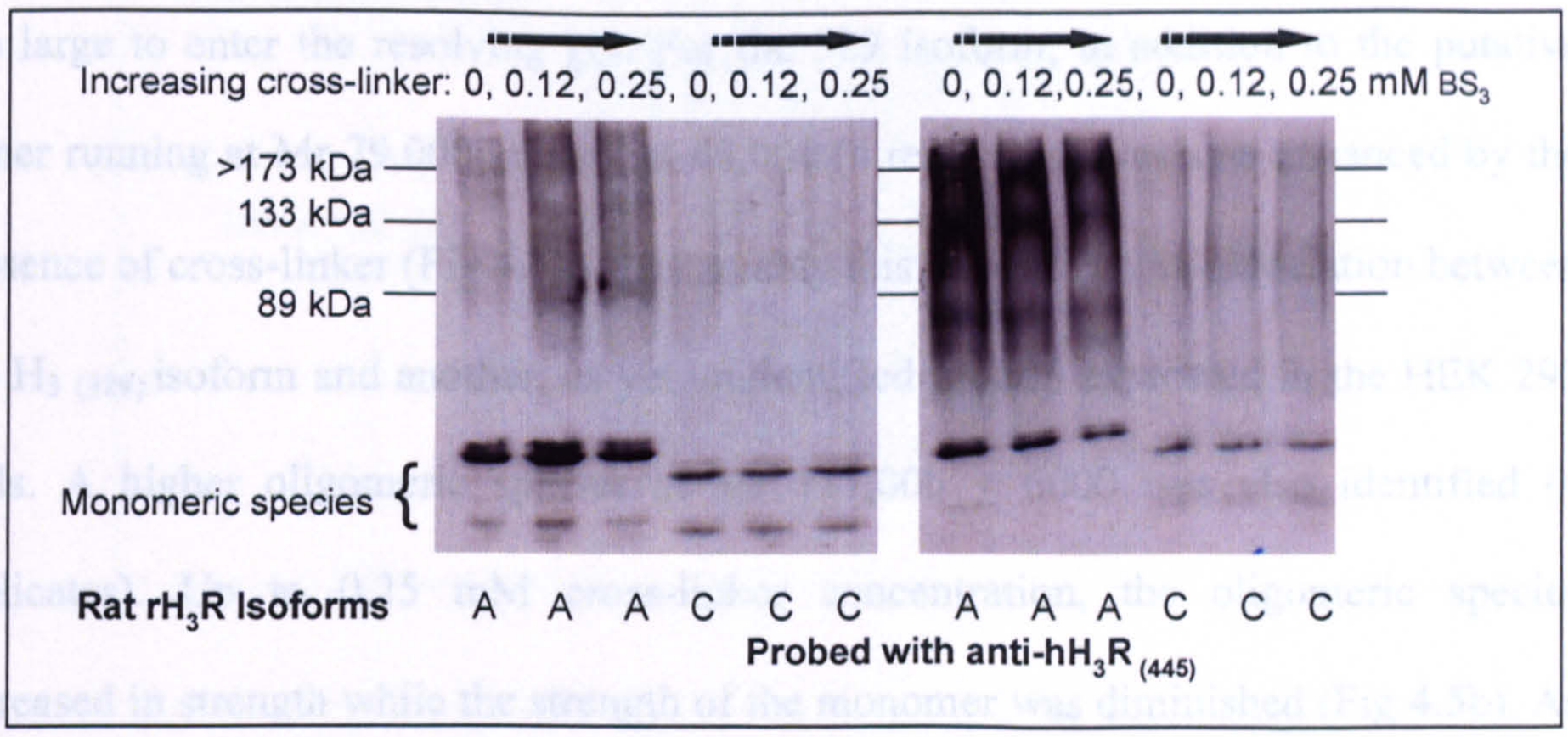

Fig 4.3 Cross-linking of recombinant rat H_3R expressed in HEK 293 cells

HEK 293 cells were transfected with either the rat $H_3R_{(A)}$ or $H_3R_{(C)}$ isoforms. Two days post-transfection the cells were harvested and homogenized. Homogenates were pelleted and the suspension buffer replaced with 150µl cross-linking buffer (150mM NaCl, 100mM Na-HEPES, 5mM EDTA pH 7.5, 5mM DTT) to give a final protein concentration of approx. 5mg/ml. Homogenates were incubated with increasing concentrations of the cross-linker BS_3 (0, 0.12 and 0.25 mM) for 12 minutes at room temperature, with continual mixing. Following this they were spun down at 10000 rpm for 5mins, the cross-linking mixture was removed and the pellet prepared for immunoblotting. The blots were carried out using 6% PAGE gels following cross-linking to allow larger molecular weight species to be resolved on the gel. Two blots are shown, which are replicate experiments from two independent transfections.

4.4.2 Chemical cross-linking enhances both $hH_3R_{(445)}$ and $hH_3R_{(329)}$ homo-dimers

Using the chemical cross-linking technique, higher oligomers were demonstrated for both the human full length $H_3R_{(445)}$ isoform and the $hH_3R_{(329)}$ isoform expressed in HEK 293 cells. With the $hH_3R_{(329)}$ isoform higher oligomers were clearly evident even in the absence of cross-linker. For the 445 isoform the dimeric species running at Mr 106,000 (3 replicates: twice probed with anti-$hH_{3\,(445)}$ Fig 4.4a, once probed with anti-FLAG Fig 4.4b) increased in strength while the strength of the monomer was diminished as the cross-linker concentration increased from 0 – 0.25mM (Fig 4.4c). Above 1mM cross-linker concentration the monomer and higher oligomers were

removed altogether, presumably because the receptors were all converted to oligomers too large to enter the resolving gel. For the 329 isoform, in addition to the putative dimer running at Mr 79,000; a band at 48,000 (4 replicates) was also enhanced by the presence of cross-linker (Fig 4.5a). Presumably this arises from an association between the $H_{3\ (329)}$ isoform and another, as yet unidentified protein expressed in the HEK 293 cells. A higher oligomeric species at Mr 117,000 $\pm$ 6000 was also identified (4 replicates). Up to 0.25 mM cross-linker concentration, the oligomeric species increased in strength while the strength of the monomer was diminished (Fig 4.5b). As with the full length isoform, above 1mM cross-linker concentration the monomer and higher oligomers were removed altogether.

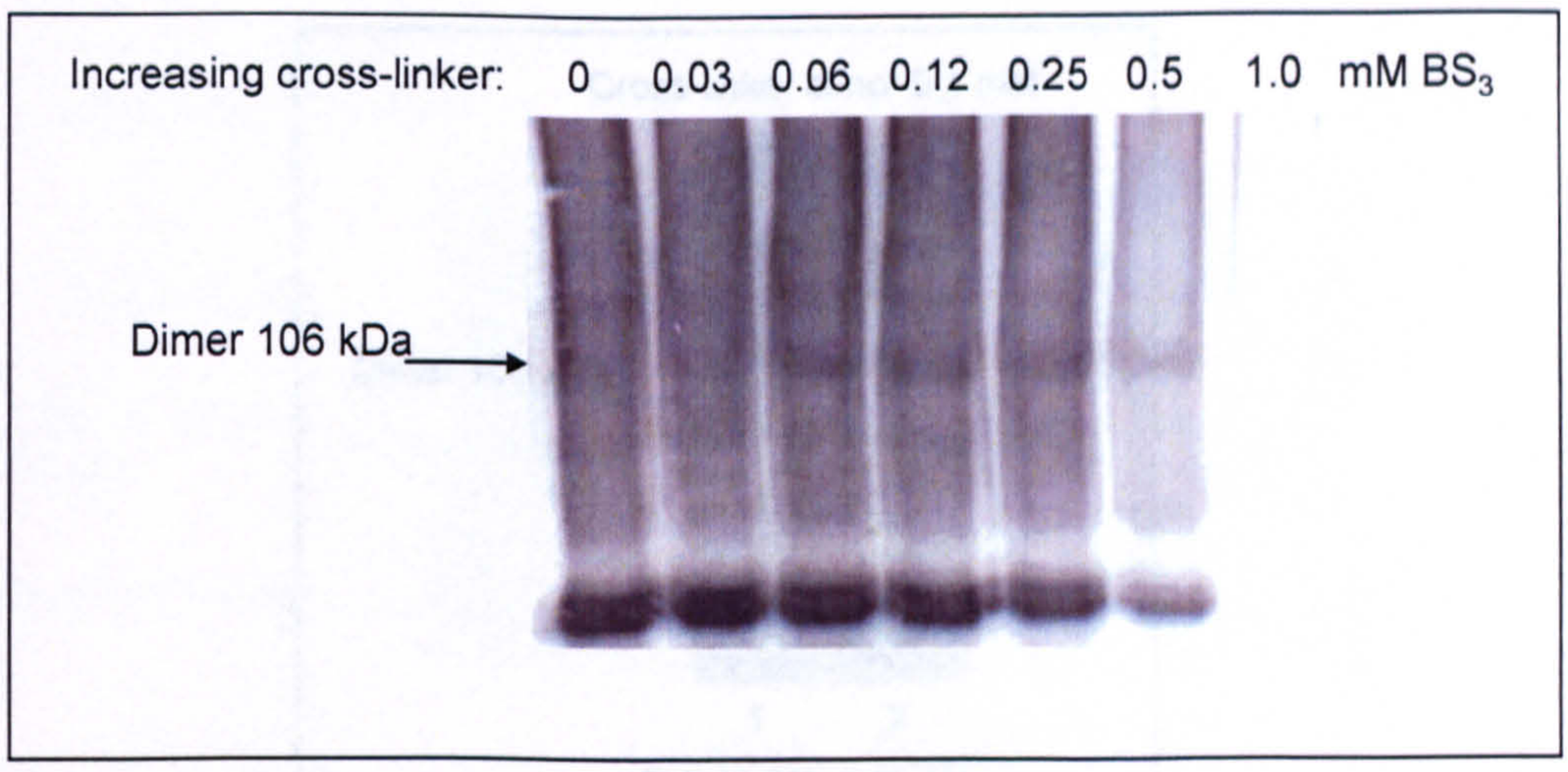

Fig 4.4 a) Cross-linking of human $H_3R_{(445)}$ expressed in HEK 293 cells

HEK 293 cells were transfected with either the human $H_3R_{(445)}$ full length isoform. Two days post transfection the cells were harvested and homogenized. Homogenates were pelleted and the suspension buffer replaced with 150µl cross-linking buffer (150mM NaCl, 100mM Na-HEPES, 5mM EDTA pH7.5, 5mM DTT) to give a final protein concentration of approx. 5mg/ml. Homogenates were incubated with the cross-linker BS_3 at different concentrations at room temperature with continual mixing for 12 minutes. The samples were spun down at 10000rpm for 5min, the cross-linking mixture was removed and the pellet prepared for immunoblotting. The blots were carried out on 6% PAGE gels following cross-linking to allow larger molecular weight species to be resolved on the gel. Lane 1 Control, no cross-linker; Lanes 2-7: 0.03, 0.06, 0.12, 0.25, 0.5, 1 mM BS_3. Probed with anti-$hH_{3\ (445)}$ at 1µg/ml. One representative immunoblot from 3 replicate experiments.

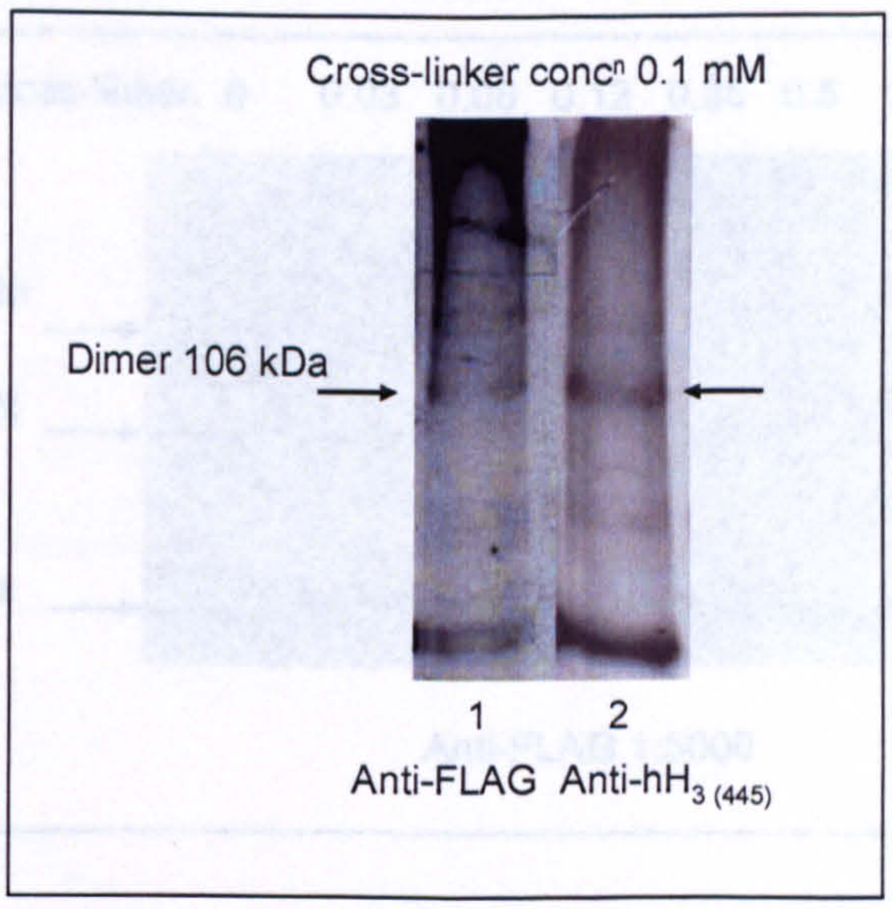

Fig 4.4 b) Cross-linking of human FLAG-$H_3R_{(445)}$ expressed in HEK 293 cells probed with anti-FLAG and anti-$hH_{3\ (445)}$

Chemical cross-linking carried out as described above on cells transfected with human FLAG-$H_3R_{(445)}$. Lanes 1 and 2 probed with anti-FLAG antibody (1:5000) and anti-$hH_{3\ (445)}$ at 1μg/ml, respectively.

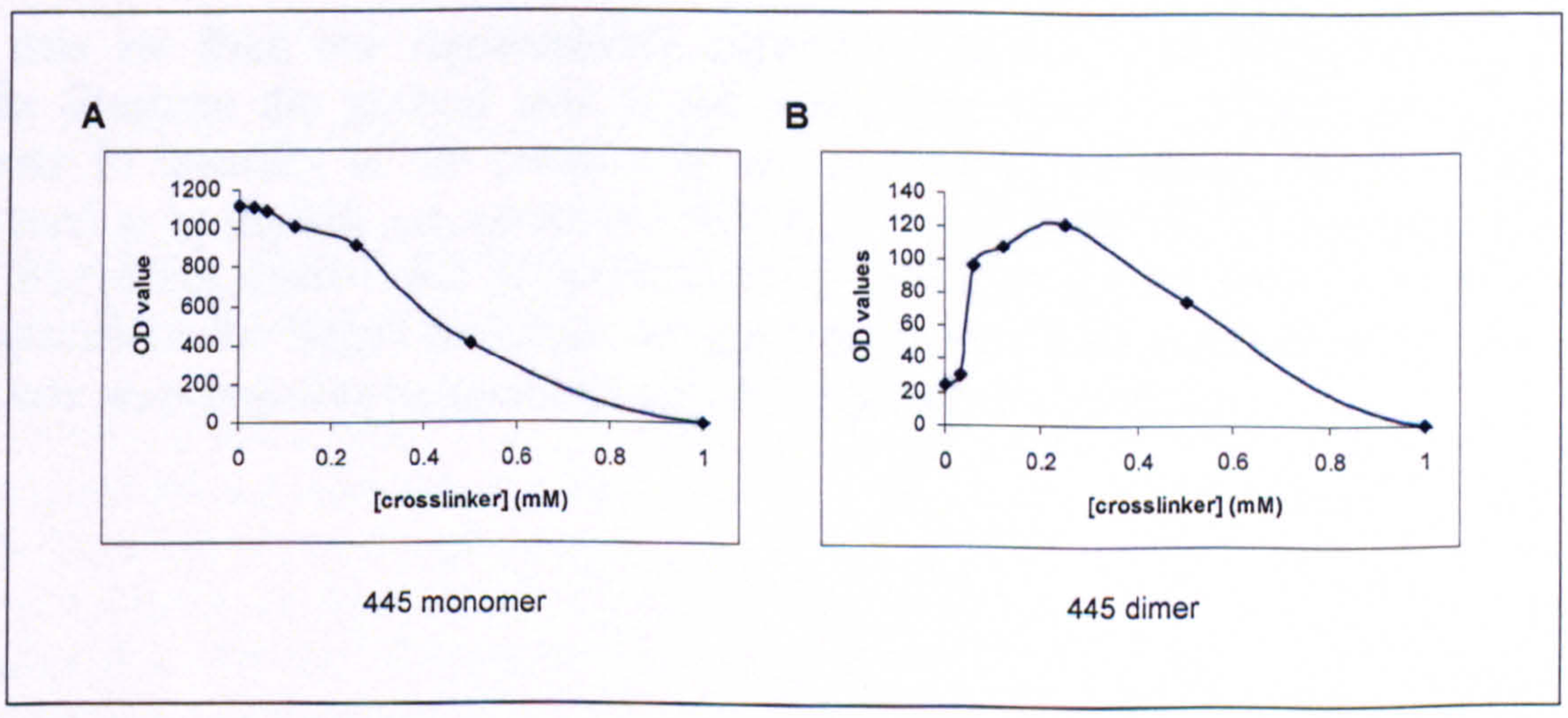

Fig 4.4 c) Graph to show densitometric evaluation of $hH_3R_{(445)}$ immunoreactivity in the presence of increasing cross-linker concentration

The data are from one representative experiment as described in Fig 4.4 a). The graphs illustrate the gradual loss of the monomeric species (A) and concomitant increase in intensity of the putative dimer (B) with increasing cross-linker concentration up to 0.25 mM. At greater cross-linker concentrations the higher oligomeric species were also diminished. Graphs are from one representative immunoblot out of 3 replicate experiments.

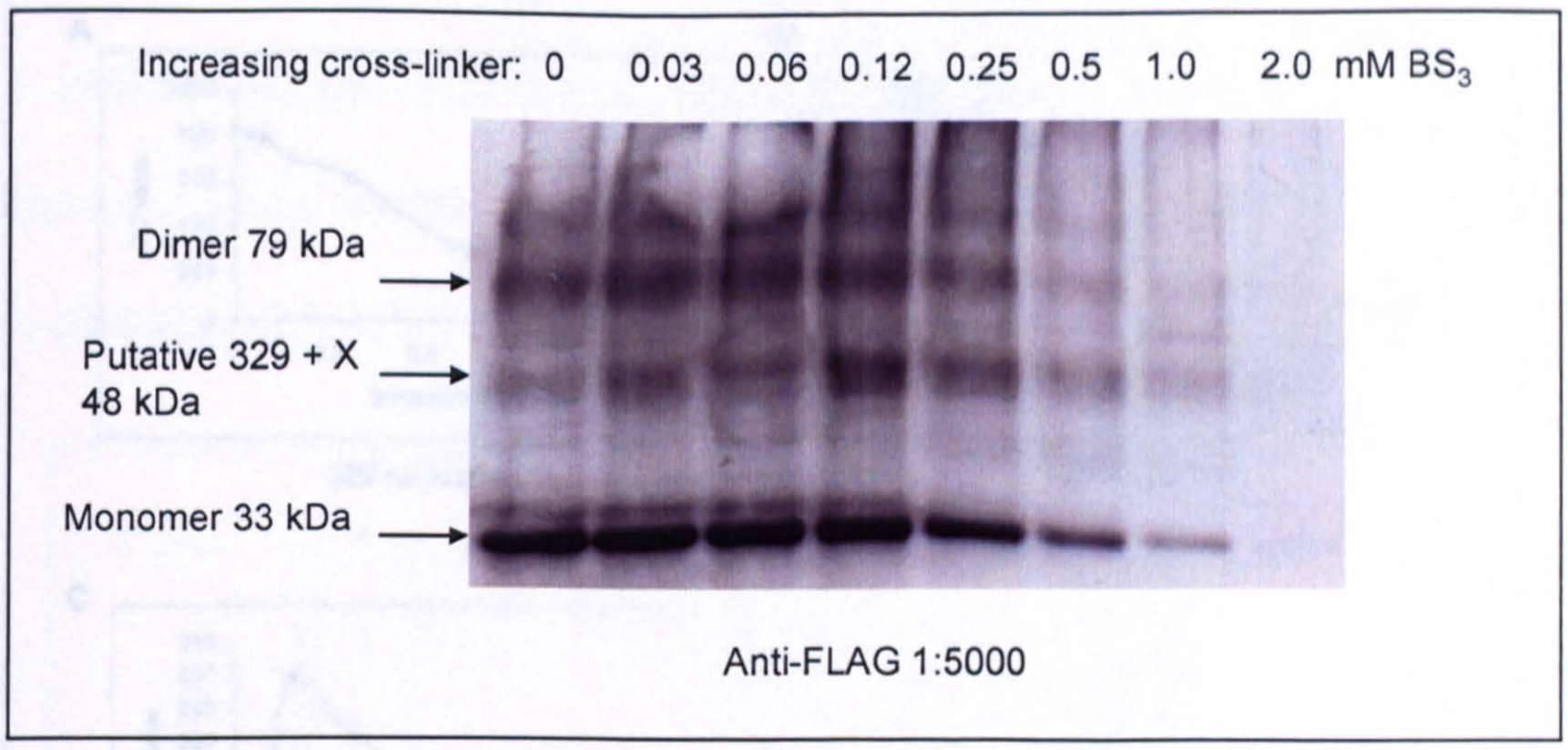

Fig 4.5 a) Cross-linking of human $H_3R_{(329)}$ expressed in HEK 293 cells

Cross-linking experiment carried out as described for the human $H_3R_{(445)}$ isoform. The $H_3R_{(329)}$ cDNA was C-terminally tagged with FLAG, therefore mouse anti-FLAG antibody was used as the primary antibody for the immunoblot.
Lane 1 Control, no cross-linker; Lanes 2-8: 0.03, 0.06, 0.12, 0.25, 0.5, 1, 2 mM BS_3.
One representative immunoblot from 3 replicate experiments.

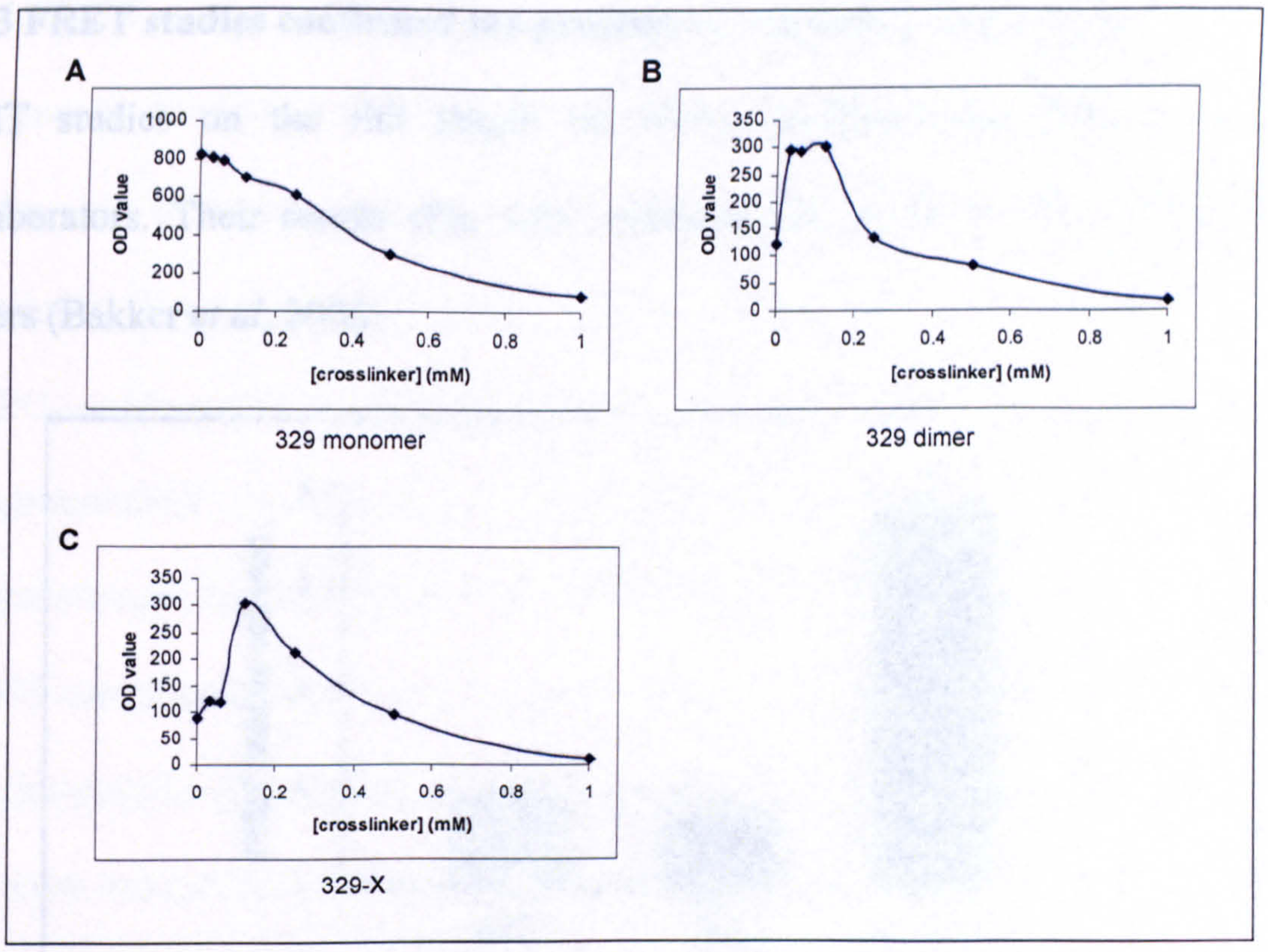

Fig 4.5 b) Graph to show densitometric evaluation of FLAG-h$H_3R_{(329)}$ immunoreactivity in the presence of increasing cross-linker concentration

The data are from one representative experiment as described in Fig 4.5 a). The graphs illustrate the gradual loss of the monomeric species (A) and concomitant increase in intensity of the putative dimer (B) and an additional species (329-X) presumed to be the $hH_{3\,(329)}$ associated with an as yet unidentified cellular protein (C), with increasing cross-linker concentration up to 0.25 mM. At greater cross-linker concentrations the higher molecular weight species were also diminished. Graphs are from one representative immunoblot out of 3 replicate experiments.

4.4.3 FRET studies confirmed the presence of rat $H_3R_{(A)}$ homo-dimers

FRET studies on the full length rat $H_3R_{(A)}$ isoform were performed by our collaborators. Their results (Fig 4.6) confirmed the presence of rat $H_3R_{(A)}$ homo-dimers (Bakker *et al*, 2006).

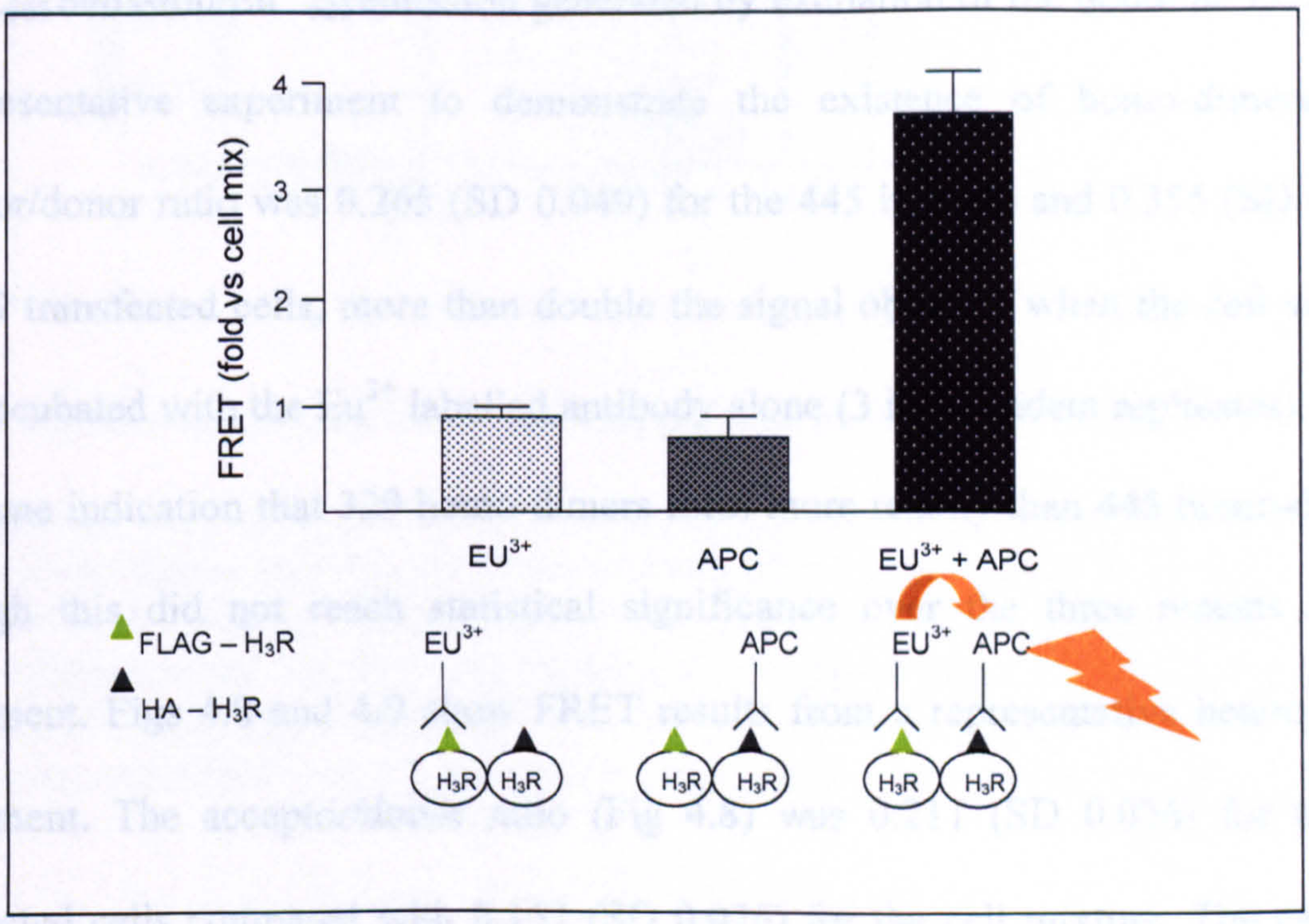

Fig 4.6 FRET studies confirm the presence of full length rat $H_3R_{(A)}$ dimers adapted from Bakker *et al*, 2006

Cells co-transfected with FLAG tagged and Haemagluttinin (HA) tagged $rH_{3(A)}R$ were homogenised and then incubated either with fluorophore Europium 3+ (Eu^{3+}) labelled anti-FLAG or allophycocyanin (APC) XL665 labelled anti-HA separately, or with a mixture of both antibodies together. Excitation at 337nm stimulates an emission from the Eu^{3+} fluorophore. Resonance energy can be transferred to the APC fluorophore providing it is wthin a distance of 100Å. The Eu^{3+} anti-FLAG/ APC anti-HA mixture resulted in an approximately three fold increase in the APC_{665} emission, confirming the presence of $rH_{3(A)}$ homo-oligomers. Results are expressed as the cell fold increase in signal (that is the APC_{665} emission from co-transfected cells divided by the APC_{665} resulting from a 1:1 mixture of cells transfected individually with FLAG- $rH_{3(A)}$ and HA- $rH_{3(A)}$).

4.4.4 FRET assays confirmed the presence of human H_3 receptor homo-dimers and provided evidence for the existence of 329/445 hetero-dimers.

Herein, we assessed whether human H_3 receptor isoforms homo- and hetero-oligomerise. Fig 4.7 shows the FRET signal expressed as the acceptor/donor ratio (that is APC_{665} emission/$Eu^{3+}{}_{620}$ emission generated by excitation of the donor at 337nm) in a representative experiment to demonstrate the existence of homo-dimers. The acceptor/donor ratio was 0.265 (SD 0.049) for the 445 isoform and 0.355 (SD 0.054) for 329 transfected cells, more than double the signal obtained when the cell vesicles were incubated with the Eu^{3+} labelled antibody alone (3 independent replicates). There was some indication that 329 homo-dimers form more readily than 445 homo-dimers, although this did not reach statistical significance over the three repeats of the experiment. Figs 4.8 and 4.9 show FRET results from a representative hetero-dimer experiment. The acceptor/donor ratio (Fig 4.8) was 0.211 (SD 0.026) for the co-transfected cells compared with 0.152 (SD 0.026) for the cell mixture. The cell fold increase in signal (that is the co-transfected APC_{665} emission divided by the cell mixture APC_{665} emission) (Fig 4.9) was 1.594 (3 independent replicates). The fact that the acceptor/donor ratio was less than that seen for the homo-dimers may suggest that hetero-dimers form less frequently than homo-dimers, however it is not possible to make a direct comparison as the assay methods were not identical.

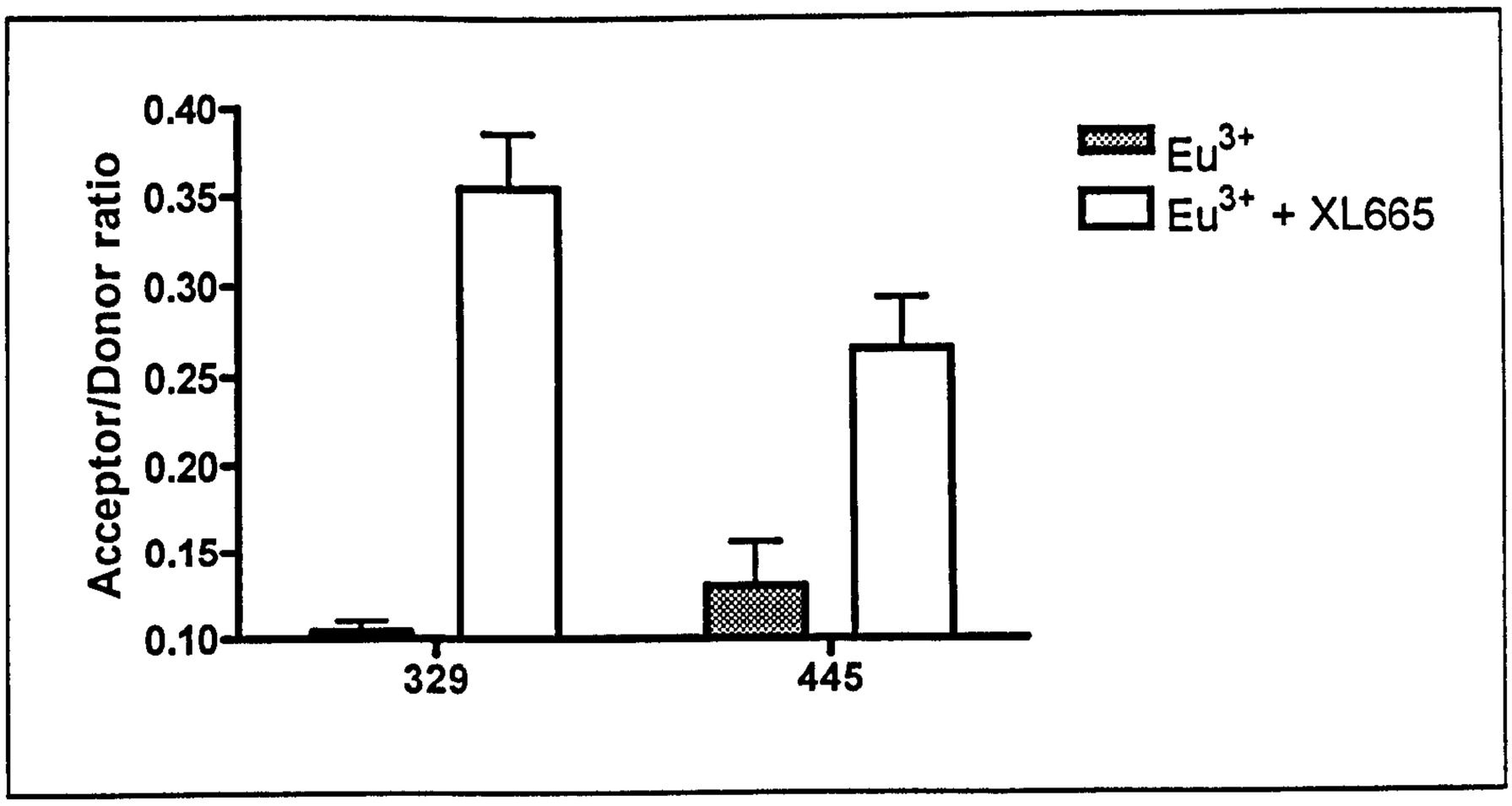

Fig 4.7 Homo-oligomerisation of the $hH_{3\,(329)}$ and $hH_{3\,(445)}$R isoforms.

Homogenates derived from HEK-293 cells transfected with either the $hH_{3\,(329)}$ or $hH_{3\,(445)}$R epitope tagged with FLAG were prepared. The homogenates were incubated for two hours with either Eu^{3+} labelled anti-FLAG antibody alone (filled bars, Eu^{3+}) or with a mixture of Eu^{3+} labelled anti-FLAG and Allophycocyanin (APC) XL665 labelled anti-FLAG (open bars, Eu^{3+} + XL665). Data shown are from a representative experiment, replicated in n = 3 independent experiments with similar results.

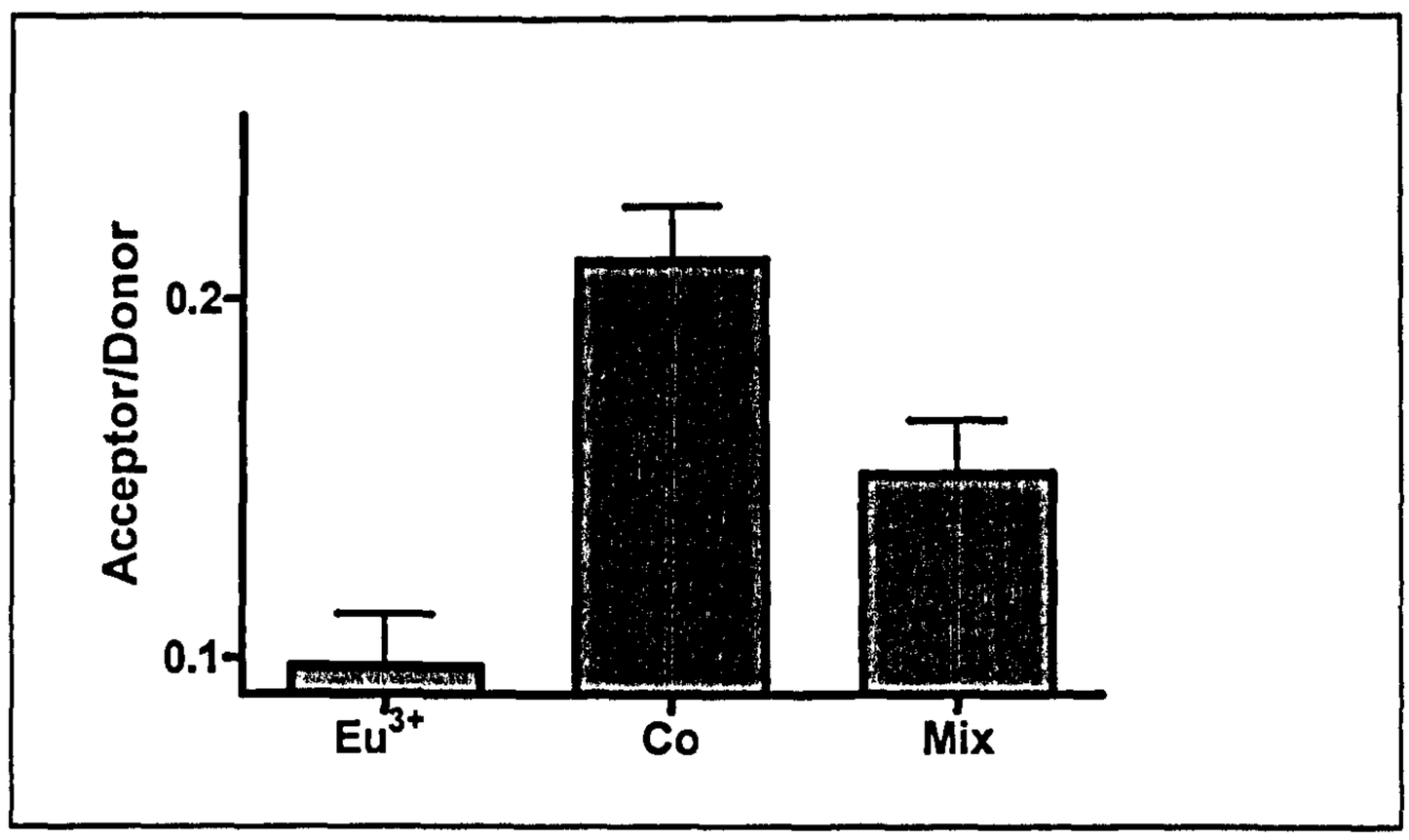

Fig 4.8 Hetero-oligomerisation of the $hH_{3\,(329)}$ and $hH_{3\,(445)}R$ isoforms.

Homogenates from HEK-293 cells co-transfected with FLAG-tagged $hH_{3\,(329)}$ and untagged $hH_{3\,(445)}R$ (Co) were prepared. A mixture of cells transfected individually with the FLAG-329 and 445 isoforms (Mix) was used as a control. The homogenates were incubated for two hours with rabbit anti- $hH_{3\,(445)}R$ antibody, they were then washed and incubated for a further two hours with a mixture of Eu^{3+} labelled anti-FLAG and Allophycocyanin XL665 labelled anti-FLAG antibodies. As an additional control, half of the co-transfected homogenates were incubated with Eu^{3+} labelled anti-FLAG antibody alone (Eu^{3+}) rather than the antibody mixture. The *tr*-FRET signal is expressed as the Acceptor/Donor ratio (that is APC_{665} emission/$Eu^{3+}{}_{620}$ emission generated by excitation of the donor at 337nm). Data shown are from a representative experiment, replicated in n = 3 independent experiments with similar results.

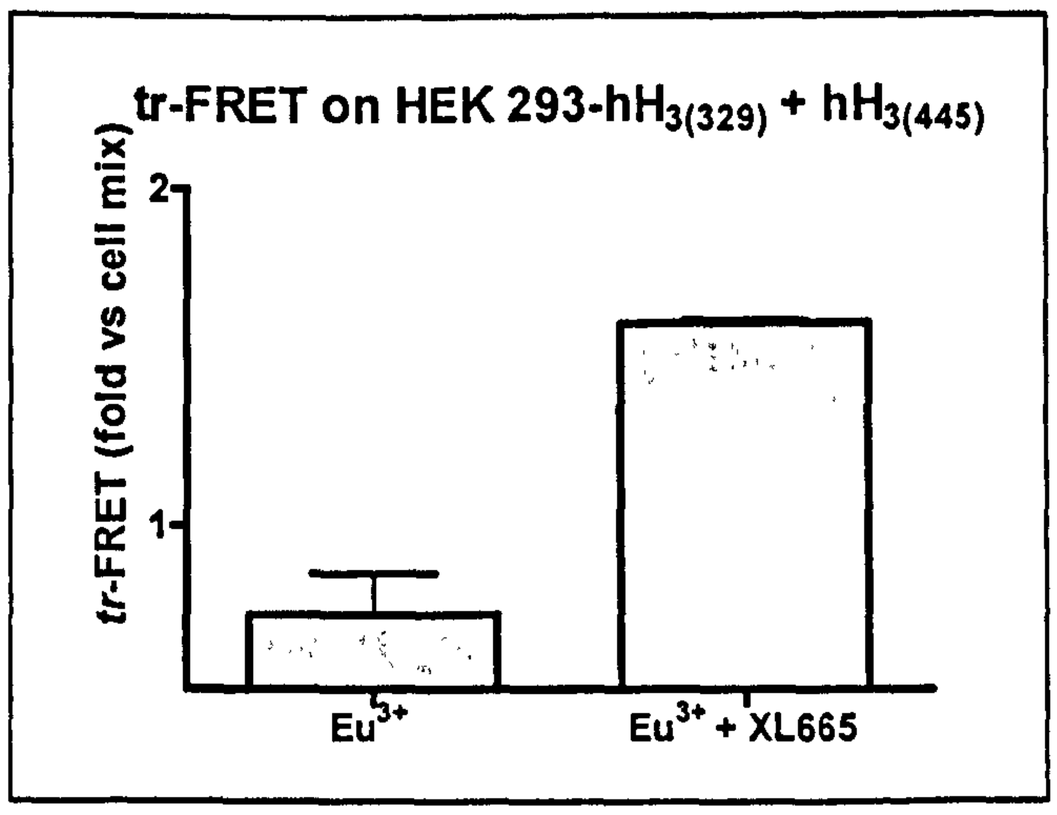

Fig 4.9 Demonstration of hetero-oligomerisation of the $hH_{3\,(329)}$ and $hH_{3\,(445)}$R isoforms.

Data from the same experiment as Fig 4.8 above, expressed as the cell fold-increase in signal (co-transfected APC_{665} emission divided by the cell mixture APC_{665} emission).

4.5 DISCUSSION

There is a growing consensus that many GPCRs, possibly all of them, function as dimers or higher molecular weight oligomers. Immunoblots of native rat and human brain tissue, probed with our anti-H_3R specific antibodies showed multiple bands (see Figs 3.8 and 3.9 respectively, Chapter 3) suggesting that H_3Rs are commonly present as oligomers. Similarly in blots of hH_3R isoforms expressed in HEK 293 cells higher molecular weight species were apparent.

Here two different approaches were used to study H_3R oligomer formation: chemical cross-linking and *tr*-FRET, biochemical and biophysical techniques respectively. A criticism of chemical cross-linking studies is that the formation of protein aggregates can potentially give false positive results. The reducing agent dithiothreitol (DTT) is included in the cross-linking buffer (section 4.3.1) in order to prevent this, in addition both DTT and the detergent SDS are present in the sample buffer (section 2.3.8). The *tr*-FRET data was also in agreement with the cross-linking evidence. *Time resolved* (*tr*)-FRET is used to ensure that shorter-lived endogenous fluorescence is extinguished before the longer lasting FRET signal is measured. Homo-oligomerisation between the same isoforms, and hetero-oligomerisation between different isoforms were both investigated. The human $H_{3\ (445)}$ and $H_{3\ (329)}$ isoforms are both major isoforms with mRNA expressed in many important brain regions. Although they show differential expression there are some key brain areas such as the basal ganglia where they are found together, therefore the question of hetero-oligomersiation between these two isoforms may be of physiological relevance.

Using the chemical cross-linking method homo-dimers were clearly demonstrated for the rat $H_{3\,(A)}$, and both the human $H_{3\,(445)}$ and $H_{3\,(329)}$ isoforms. By contrast rat $H_{3\,(C)}$ dimers were not so obvious. Even in the absence of cross-linker $hH_{3\,(329)}$ dimers were evident and these were enhanced by increasing concentrations of the cross-linker. Taken together these findings suggest that there could be differences in the potential for different isoforms to form robust homo-oligomers, ranging from the $rH_{3\,(C)}$ where dimers may be either absent or only very weakly expressed through to the $hH_{3\,(329)}$ where dimers appear to be constitutively expressed. However care should be taken not to over interpret results from recombinant systems, receptors are being expressed in a foreign environment at much higher levels than would normally be the case.

With the $H_{3\,(329)}$ isoform a species running at Mr 48,000 was also enhanced by the presence of the cross-linker, in addition to the Mr 79,000 species (compatible with the size of the putative dimer). Presumably the monomer is associating with a different, as yet unidentified cellular protein. In addition to this distinct Mr 48,000 species material of higher molecular weight is clearly visible with both the human isoforms, and to a lesser extent with the rat isoforms, even in the absence of cross-linker. While acknowledging the caveat that this is an artificial expression system, it is likely that GPCRs associate with a variety of cell proteins (Bermack & Zhou, 2001), the identities and functional significance of which remain to be unravelled.

Tr-FRET assays confirmed the presence of H_3R homo-dimers in cell membranes, since resonance energy transfer between fluorophore labelled H_3R receptors was able to occur. Rat H_{3A} dimers have been shown previously (Bakker *et al*, 2006), however the rH_{3C} isoform was not included in this study. *Tr*-FRET on the human isoforms gave

clear evidence of $H_{3\ (445)}$ and $H_{3\ (329)}$ homo-dimers, and hetero-dimerisation between the 329 and 445. Although statistical significance was not achieved, the trend suggested that 329 homo-dimers may form more readily than 445 dimers, in agreement with the cross-linking observations. Hetero-dimerisation appeared to be at a lower level than for homo-dimerisation, however further studies would be needed to confirm this as the FRET technique was modified slightly in order to be able to distinguish hetero- from homo-dimers, and therefore the results are not directly comparable.

Preliminary pharmacological studies indicated that while the $hH_{3\ (329)}$ isoform did not itself bind [^{3}H]-clobenpropit, it reduced binding of the radioligand to the full length $hH_{3\ (445)}$ isoform in co-transfected cells. These findings remain to be validated and are therefore not shown here. If verified this suggests that the shorter isoform may play a negative regulatory role similar to that described for truncated rat H_3R isoforms (Bakker *et al*, 2006).

In conclusion rat and human H_3R isoforms can form both homo- and hetero-dimers, and this is likely to contribute to the observed H_3 receptor heterogeneity. The potential to dimerise may be variable with some isoforms less likely to form robust dimers (rH_{3C}) and others more commonly found as dimers (rH_{3A}). In this study, the effect of histamine on oligomerisation was not investigated. Nevertheless in both recombinant systems and native tissue, oligomers were clearly evident (Figs 3.4 and 3.5 recombinant; Figs 3.8, 3.9 native, Chapter 3), even in the absence of histamine. Furthermore, van Rijn and colleagues (van Rijn *et al*, 2006) failed to show any effect of H_4R agonists on oligomerisation. However, results from other studies looking at the

effects of ligand binding on GPCR oligomerisation have been inconsistent (Angers *et al*, 2002; George *et al*, 2002; Pfleger & Eidne, 2005).

In Chapter 5, we investigate the highly related H_4 histamine receptor to compare the structural properties to the H_3 receptors. To this end, the first immunological probes were developed and characterised. The first evidence for the expression of the H_4 receptor in the rat and human brain is provided, and immunobiochemical and biophysical studies demonstrate that H_4 homo- and hetero-oligomerisation can occur. The influence of H_4 receptor isoforms upon the full length receptor is investigated to address the overall hypothesis "*Expression of histamine receptor isoforms act as regulatory mechanisms to control central histaminergic function"*

CHAPTER 5

DEVELOPMENT OF THE FIRST ANTI-HUMAN H_4 RECEPTOR ANTIBODIES: DEMONSTRATION OF THE EXISTANCE OF THE H_4R IN THE HUMAN BRAIN AND H_4R HOMO- AND HETERO-OLIGOMERS

5.1 OBJECTIVES

Develop new anti-HUMAN H_4 receptor antibodies and investigate the possibility of brain H_4 receptors, homo- and hetero-oligomerisation of H_4 receptor isoforms and dominant negative effects of $H_{4\ (302)}$ and $H_{4\ (67)}$ isoforms.

5.2 INTRODUCTION

The discovery of the most recent histamine receptor, histamine H_4R, followed shortly after the successful cloning of the human H_3R in 1999 (Lovenberg *et al*, 1999). Using sequence information from the human H_3R, several independent groups identified homologous GPCR sequences in the human-genome databases. In 2000, the hH_4R was cloned from foetus and leukocyte cDNA (Oda *et al*, 2000; Nakamura *et al*, 2000 respectively). Since then six other laboratories have reported the same finding (reviewed in de Esch *et al*, 2005). The H_4R gene is on chromosome 18, it spans more than 20.6 kilobases and has a similar structure to the H_3R (Fig 5.1 Cogé *et al*, 2001) The H_4R is 390 amino acids long and contains three exons coding for amino acids 1-64, 65- 119 and 120-390. It is found at high levels in bone marrow, eosinophils and mast cells (Oda *et al*, 2000; Nakamura *et al*, 2000; Zhu *et al*, 2001; Nguyen *et al*, 2001; Morse *et al*, 2001; Liu *et al*, 2001; O'Reilly *et al*, 2002). However, although Zhu and co-workers found H_4R mRNA expression to be highest in peripheral blood

mononuclear cell tissues such as bone marrow and lung, they also identified it expressed in mouse hippocampus. H_4R mRNA has also been reported in both adult and embryonic rat brain (Lozada *et al*, abstract, EHRS 2004). Using RT-PCR, expression of H_4R mRNA was found in several human brain regions (Cogé *et* a*l*, 2001). Expression was highest in cerebellum and hippocampus, no message was detected in either cerebral cortex or the raphe nuclei. Whether the H_4R is expressed on immune cell infiltrates into the brain or on brain tissue itself is not yet known.

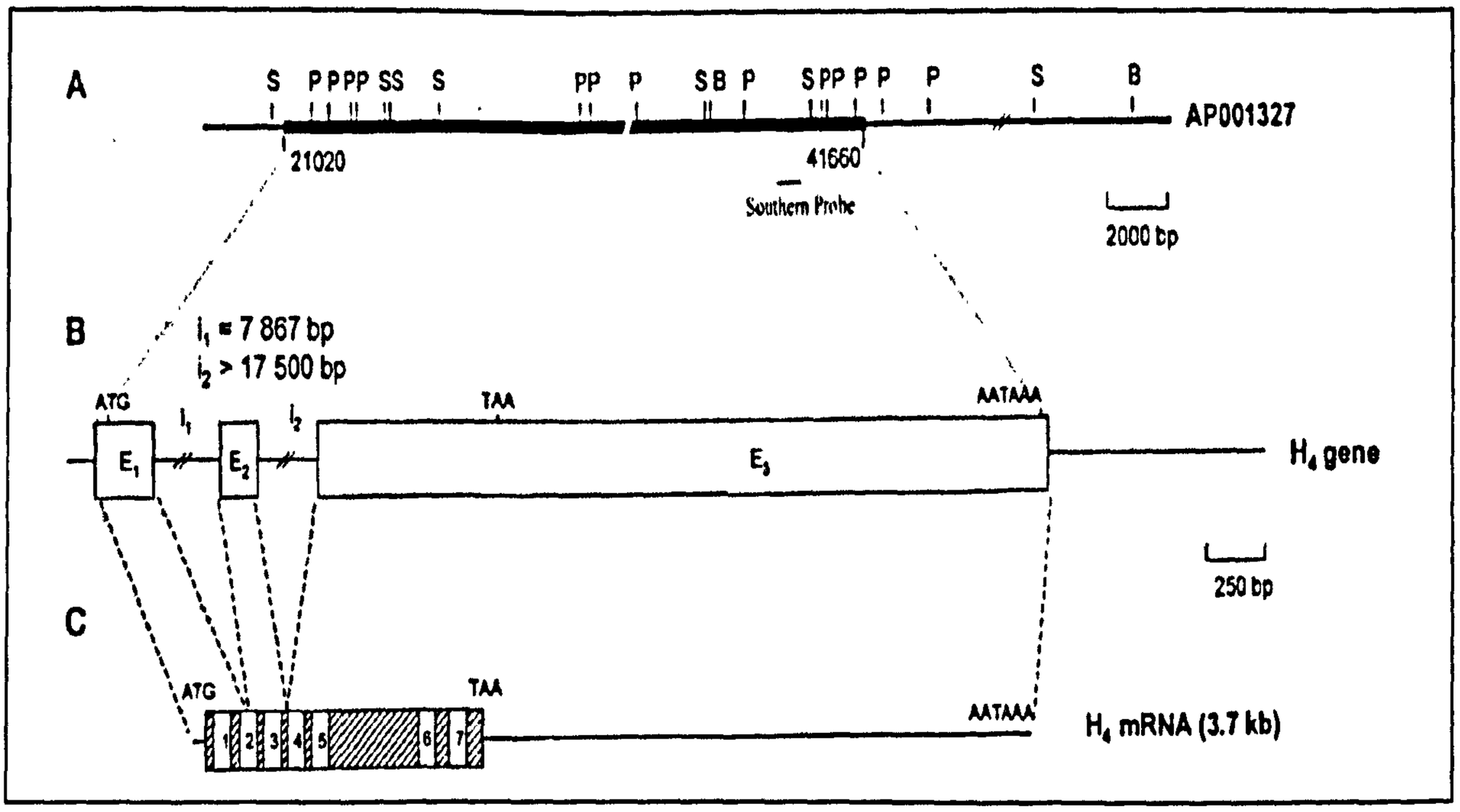

Cogé *et al*, 2001

Fig 5.1 Schematic organisation of the H_4R gene

Restriction map of the genomic DNA fragment from the human chromosome 18 (Accession number AP001327); B, *Bam*HI; P, *Pst*I; S, *Sac*I. (B) Schematic structure of the H_4-receptor gene with the exons (E_{1-3}) shown by boxes and the introns (I_{1-2}) shown by horizontal lines. The exons are numbered from the gene 5'-end with exon E_1 containing the first ATG codon. (C) Structure of the human H_4-receptor cDNA. The coding region is shown by boxes and the 5'- and 3'- untranslated regions by horizontal lines. The putative transmembrane domains (1-7) are mentioned in the coding region. The translation initiation site (ATG), the termination site (TAA) and the polyadenylation signal sequence (AATAAA) are indicated.

The similarity between the H_3R and H_4R genes suggests that, as with the H_3R, alternative splicing could result in different H_4R isoforms. The first two hH_4R isoforms: h$H_{4\ (302)}$ lacking TM regions 3 and 4, and h$H_{4\ (67)}$ consisting of only the first two TM regions, have recently been described by our collaborators (van Rijn *et al*, submitted). These isoforms are unable to bind either histamine or a selective H_4R antagonist, JNJ7777120; neither do they transduce signal. Nevertheless, they may play a regulatory role since they reduce the level of histamine binding to H_4 (390) by 55% (302 isoform) and 30% (67 isoform). Since mRNA message coding for these two

splice variants is coexpressed in a number of white blood cell types along with message for the full length $H_{4\ (390)}$ receptor, there is the potential for hetero-oligomerisation in native tissue. The published amino acid sequence of the human H_4R shows it to be a class A rhodopsin-like GPCR, as are the other histamine receptors. The sequence from Oda's laboratory differs from the other reported sequences and the genomic sequence (Genbank Accession number AC007922) (Zhu *et al*, 2001). The three different amino acids V138A, R206H and R253Q could be polymorphic H_4R variants but these discrepancies need to be validated.

Based on the preliminary published report(s) of H_4R mRNA expressed in mammalian brain and the similarity between the H_3R and the H_4R; our previously successful strategy for generating H_3R selective antibodies (described in Chapter 3) was used to develop specific anti-hH_4R antibodies.

This chapter describes the development and characterisation of a novel anti-human H_4R antibody. The specificity of the antibody was validated against both recombinant and native H_4Rs using immunoblotting and immunohistochemistry as described for the anti-hH_3R antibodies (Chapter 3). In addition. immunoprecipitation was used to confirm the identity of the immunoreactive species as the H_4R. It was evident from immunoblots that higher molecular weight species were present both in recombinant and native tissue. Indeed, as with the H_3R, the monomer was often not detected in native tissue. Homo-oligomerisation was further investigated using both biochemical (cross-linking and nickel column affinity purification) and biophysical techniques (Bioluminescence Resonance Energy Transfer). The potential for hetero-dimerisation of the full length receptor with the newly identified splice variants was explored using

immunoprecipitation. Finally, since co-transfection of clonal cells with $hH_{4\,(390)}$ and either of the splice variants reduces the level of histamine binding it was relevant to ask whether the splice variants were affecting surface expression of the full length receptor. Surface expression of the different isoforms either individually or in combination, that is the full length with one of the shorter isoforms, was assessed. Following biotinylation of cell surface proteins, the surface fraction was separated from the intracellular fraction by streptavidin chromatography, and analysed by immunoblotting.

5.3 METHODS

The following methods were performed as described in Chapter 3.

Choice of peptide sequences

Peptide conjugation

The 3-maleimimdobenzoic acid N-hydroxysuccinimide ester (MBS) method for the coupling of peptides to carrier proteins

Immunisation of rabbits

Affinity purification

Coupling of peptides to sepharose beads via sulphydryl groups

Peptide affinity purification of antibodies

Transfection

Harvesting and membrane preparation

5.3.1 Production of human phytohaemagglutinin (PHA) blasts

Blast cells are immature, undifferentiated precursors of white blood cells. They are not found in normal peripheral blood, however they can be induced by stimulating mononuclear cells with the mitogen phytohaemagglutinin (PHA). PHA blasts were generated essentially as previously described (Bradford *et al*, 2005). Briefly, heparinized human whole blood was obtained from healthy volunteers (with Local ethical approval), and peripheral blood mononuclear cells (PBMCs) were separated using Lymphoprep (Axis-Shield Poc AS, Oslo, Norway) and centrifuged at 400 x g for 25 min. The PBMCs were isolated from the interfacial layer, washed twice in Roswell Park Memorial Institute medium (RPMI) without L-glutamine (Gibco™) and resuspended in RPMI complemented with 10% (v/v) Fetal Calf Serum, 1% (v/v) Penicillin, and Streptomycin, and 1% (v/v) L-Glutamine. Cell density was adjusted

accordingly to 1 x 10^6 cells/ml with RPMI. 100µl PHA ('Lectin', Sigma, UK) was added to the cells to make PHA Blasts. These were grown in culture for 24h, harvested and a cell homogenate prepared in the presence of protease inhibitors (Protease Inhibitor Cocktail III, Calbiochem, UK).

5.3.2 Immunoprecipitation to confirm H_4R selectivity of the antibody

HEK 293 cells were transfected with HA-H_4 receptor, and solubilized with 1% Triton X100/0.15M NaCl for 30 min at 4°C. Immunoprecipitation was performed essentially as previously described (Chazot *et al*, 1994). Solubilized HEK 293 cell extracts were incubated with 5 µg of rat anti-HA antibody (Roche Diagnostics, Germany) or rat non-immune Ig (ADI, USA) at 4°C for 1 hour. 50 µl of pre-chilled washed Protein G agarose (Sigma, UK) slurry was added and incubated for 1 hour at 4°C on a rocking platform. Precipitation pellets were collected by centrifugation at 10,000xg for 30 seconds at 4°C, washed with 3 x PBS, resuspended in sample buffer, vortex-mixed and heated to 90-100°C for 3 minutes. The sample was then re-centrifuged, and the supernatant subjected to immunoblotting. Control experiments were performed using untransfected HEK 293 cells.

5.3.3 Immunohistochemistry (IHC)

The immunohistochemistry method was a modified version of that described in Chapter 3. This method has recently been adopted in the laboratory. Following the 15 minute incubation in TBS, 0.2% (w/v) glycine and 0.2% (v/v) Tween-20 to mop up residual unreacted aldehyde groups from the fixative, four extra steps have been introduced to make the cell membranes more permeable and thus improve accessibility of cellular proteins (in this case the H_4R) to the antibody. Tissue sections were next

incubated in Triton-X-100 in TBS (20µl/10ml) for 15 minutes, then in 50mM sodium citrate pH 8.4 for 30 minutes at room temperature followed by a further 30 minutes also in 50mM sodium citrate pH 8.4 but this time in a waterbath at 80°C. Finally sections were incubated in Triton-X-100 in TBS (20µl/10ml) again for 15 minutes, before completing the procedure exactly as set out in Chapter 3.

5.3.4 Receptor immobilisation on a nickel column

This technique was used to provide evidence for H_4R homo-dimers. Membranes of COS-7 cells transiently co-expressing haemagluttinin-H_4R (HA-H_4R) and c-myc-H_4R-Histidine (His-H_4R) were homogenized, solubilized and subsequently immobilized on nickel columns: Ni-NTA (Invitrogen). Immobilized receptors were eluted using 250 mM imidazole. Samples were chloroform/methanol extracted and analysed by immunoblotting using an anti-HA antibody (gift from Richard van Rijn) as the probe. The His-H_4R can be immobilised via the Ni^{2+} ions on the column. HA-H_4R can only be immobilised indirectly if it dimerises with a His labelled H_4R (Fig 5.2). Therefore HA detected in the immobilised fraction eluted from the column confirms the presence of H_4R homo-dimers.

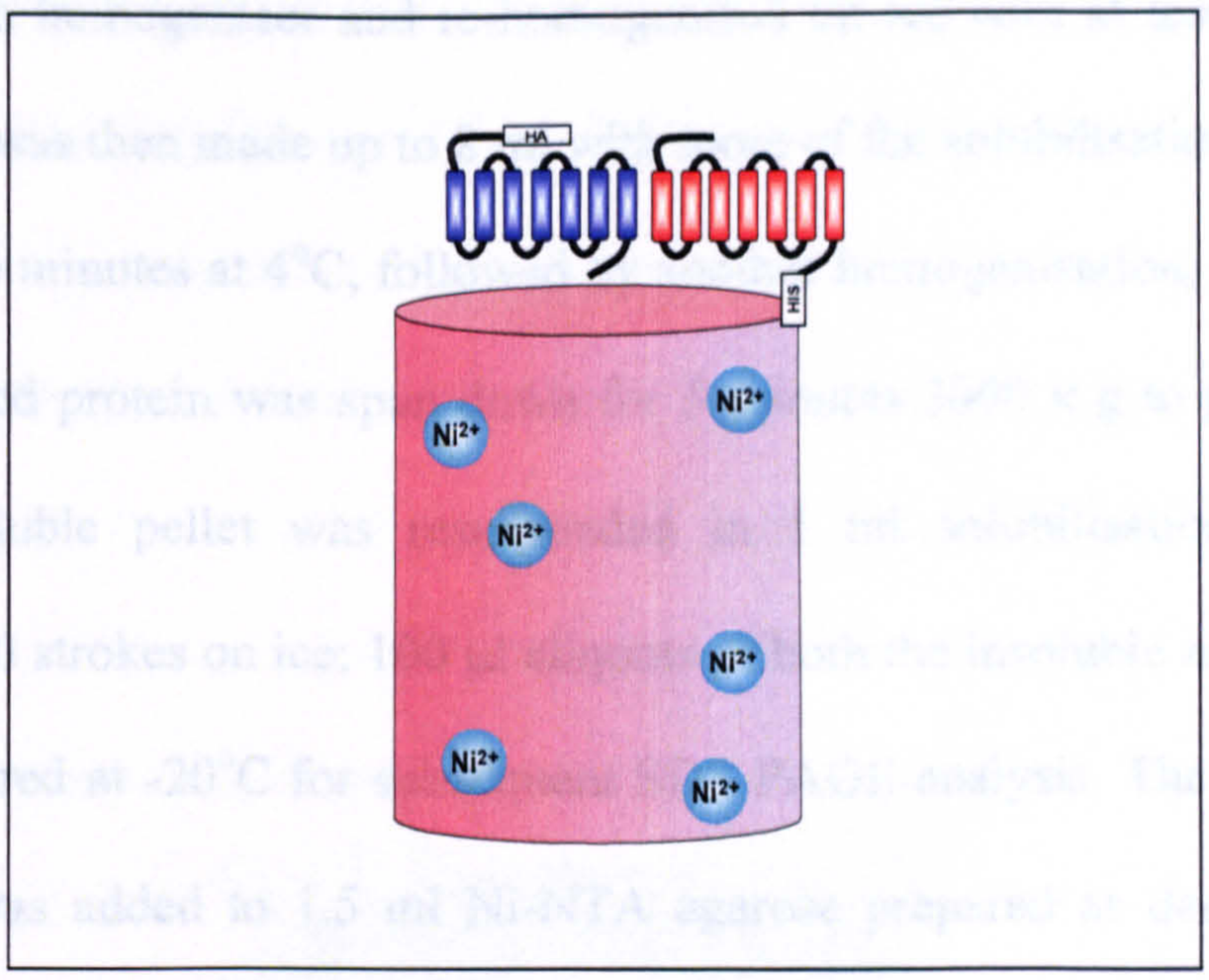

Fig 5.2 Schematic representation of nickel column purification

Haemagglutinin (HA) labelled receptors can only be immobilised on the nickel column via histidine (HIS) tagged receptors. Therefore HA detected in the eluted fraction confirms the existence of HIS-H_4R/HA-H_4R dimers.

The method was carried out as recommended in the Invitrogen instruction manual using native conditions, with only minor modifications. Native conditions were chosen in order to minimise the disruption of putative receptor dimers.

Native binding buffer

50 mM NaH_2PO_4, pH 8.0, 0.5 M Na Cl

Solubilisation buffer

Native binding buffer with 1% Triton-X-100/ Calbiochem protease inhibitors 1:100

Wash buffer

Native binding buffer with 20 mM imidazole, pH 8.0

Elution buffer

Native binding buffer with 250 mM imidazole, pH 8.0

Homogenised membranes of H_4R transfected COS-7 cells were pelleted and resuspended in approximately 1 ml solubilisation buffer. They were transferred to a

dounce glass-glass homogeniser and re-homogenised on ice with at least 30 strokes. The total volume was then made up to 8 ml with more of the solubilisation buffer. This was shaken for 30 minutes at 4°C, followed by another homogenisation, 30 strokes on ice. The solubilised protein was spun down for 5 minutes 3000 x g to pellet the cell debris. The insoluble pellet was resuspended in 1 ml solubilisation buffer and rehomogenised, 30 strokes on ice; 100 µl aliquots of both the insoluble and solubilised fractions were stored at -20°C for subsequent SDS PAGE analysis. The remainder of the supernatant was added to 1.5 ml Ni-NTA agarose prepared as described in the Invitrogen protocol. (Ni-NTA agarose preparation: 1.5 ml of the Ni-NTA agarose suspension was pipetted into a 10 ml purification column. The column was washed twice with 6 ml of sterile distilled water and twice with 6 ml of native binding buffer.) Binding was carried out with gentle mixing for 1 hour at 4°C. After binding the column was drained and 100 µl aliquots of the unbound fraction were stored as before for future immunoblotting. The column was washed with 4 x 8 ml of wash buffer. The immobilised protein was then eluted from the column by gently mixing the resin in 2 ml of the elution buffer for 10 minutes at 4°C, 100 µl aliquots of the eluate were retained as before. The column was washed several times with native binding buffer and then stored with 0.02% azide added to the same buffer as a preservative.

As a control the Ni-NTA purification experiment was carried out with a physical mixture of COS-7 cells individually expressing HA-H_4R and His-H_4R.

5.3.5 Bioluminescence Resonance Energy Transfer (BRET)

Fusion proteins

H_4Rs were C-terminally fused to either *Renilla* luciferase (H_4R-*R*luc) or a yellow fluorescent protein (H_4R-eYFP) (van Rijn *et al*, 2006).

The BRET assay is a biophysical technique used to demonstrate close association of two proteins within a cell membrane. The assay relies on the transfer of bioluminescence from a donor to an acceptor, excitation of the acceptor results in a detectable bioluminescent emission (see Fig 5.3). Transfer can only occur within a radius of 100Å.

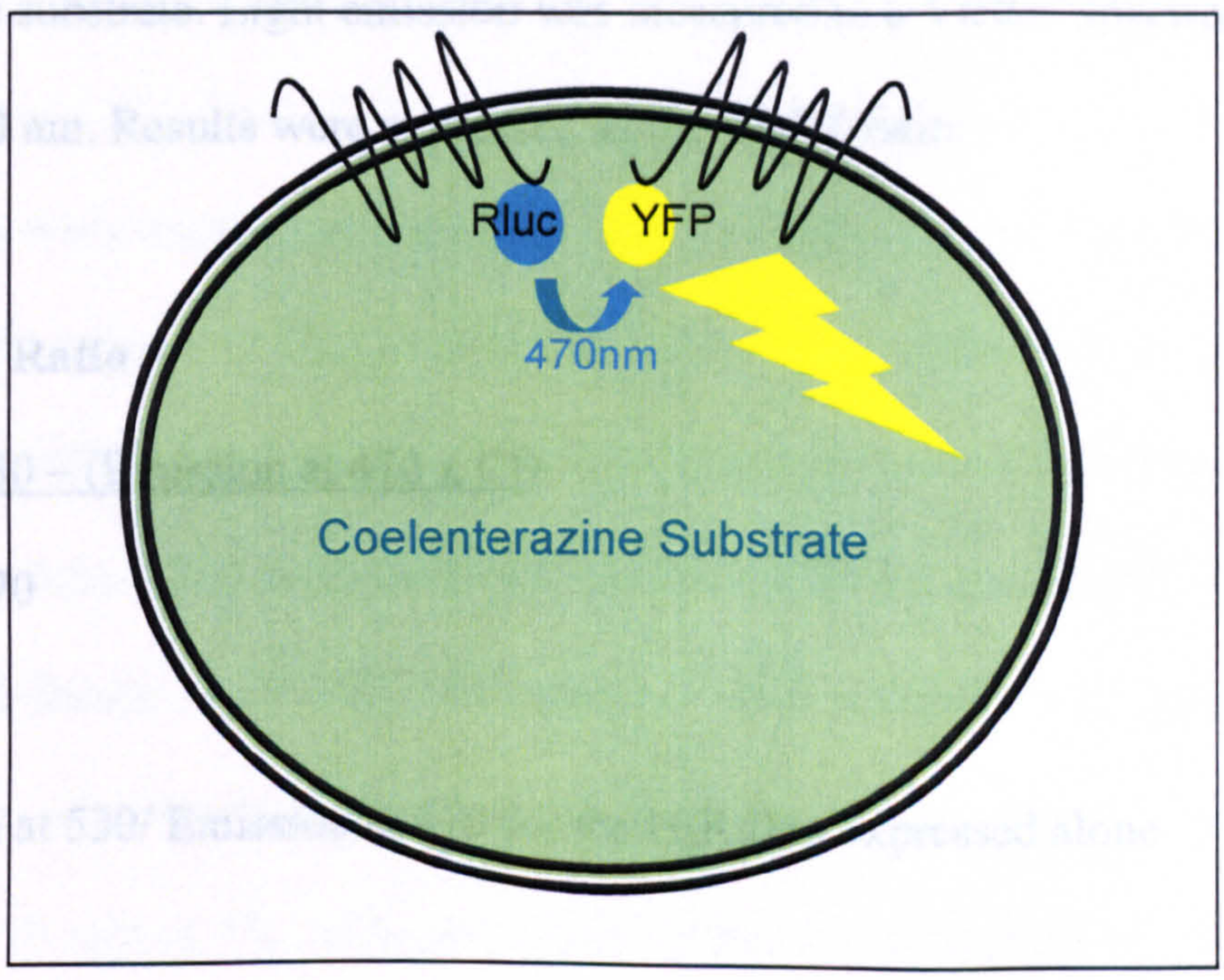

Fig 5.3 Schematic representation of the BRET assay

Here BRET was performed on COS-7 cells expressing either the H_4R-*R*luc construct alone or co-expressing the H_4R-*R*luc with the H_4R-eYFP. *Renilla* luciferase fused to the C-terminus of a receptor, catalyses the emission of light from the substrate coelenterazine at a wavelength of 470 nm. When in close proximity (< 100 Å) this can excite the eYFP fused to another H_4R to emit light at 530 nm.

Transfected COS-7 cells were harvested and washed twice with PBS. The cells were resuspended and counted and their numbers adjusted to give 5 x 10^5/ml either in PBS

or BRET buffer. BRET buffer was PBS supplemented with 1mM $CaCl_2$, 1mM $MgCl_2$ and 1% sucrose. The BRET buffer was a mini-trial since it had been recommended as an improvement over PBS in a recent paper (ref El-Asmar *et al*, 2005). 100 µl of cells (ie 50,000 cells) was transferred into a white 96 well plate, following this all work was carried out in the dark. 100µl of a 10µM coelenterazine solution in PBS was added to each well, thus exposing the cells to a final 5 µM concentration of the coelenterazine substrate. Light emission was measured in a Victor^2 spectrophotometer at 470 and 530 nm. Results were expressed as the BRET ratio:

5.3.5.1 BRET Ratio

$$\frac{\text{Emission at 530} - (\text{Emission at 470} \times \text{Cf})}{\text{Emission at 470}}$$

Cf = Emission at 530/ Emission at 470 for the H_4R*R*luc expressed alone

5.3.6 Immunoprecipitation (IP) to investigate hetero-dimerisation

HEK 293 cells were transfected with untagged $H_{4\,(390)}$ with or without FLAG $H_{4\,(302)}$ or FLAG $H_{4\,(67)}$. Cell samples were solubilised with 1% Triton X100 in Tris-HCl pH 7.4 (IP buffer) and incubated with 50 µl 50% (w/v) slurry of anti-FLAG sepharose beads (Sigma, UK) for 2hrs at 4°C. Following incubation, beads were centrifuged at 9000rpm at 4°C for 5 min. The supernatant was retained (unbound fraction). The beads were washed in IP buffer and the bound fraction eluted from them by incubation in SDS PAGE Sample buffer/50mM DTT at 50°C for 30 min. The supernatant following centrifugation at 9000 rpm (bound fraction) was retained for analysis.

5.3.7 Surface Biotinylation – H_4 isforms

PBS/sucrose

4% sucrose in PBS

Quenching buffer

50mM Tris-HCl pH 8.0 containing 192 mM glycine and 4% sucrose

Lysis buffer

50mM Tris-HCl pH 8.0 containing 2mM EDTA and protease inhibitor cocktail set III (1/100 dilution)

HEK 293 cells were transfected with individual H_4 isoforms or co-transfected with $H_{4\,(390)}$ with equal amounts of $H_{4\,(302)}$ or $_{(67)}$ isoforms. 24-40 hours post transfection, the medium was carefully removed and the cells washed with ice-cold PBS/sucrose (3 x1 ml per 35mm dish). The cells were then incubated for 30 min at 4°C with 1mg/ml Sulfo-NHS-SS-Biotin in ice-cold PBS/sucrose (0.5 ml/dish) with gentle shaking. Following this cells were washed with ice- cold PBS/sucrose once (1ml/dish), and incubated for 10 min at 4°C with quenching buffer (0.5 ml/dish). Cells were scraped into PBS/Sucrose and spun at 6000 rpm for 2 min. This wash procedure was repeated on a further occasion and the cells homogenised in lysis buffer/1% (w/v) SDS. The samples were diluted in lysis buffer /1% Triton-X100), and incubated with 40 µl 50% (w/v) slurry of streptavidin beads for 2 hrs at 4°C. Following incubation, the beads were centrifuged at 9000rpm at 4°C for 5 min. The supernatant (intracellular fraction) was retained and the beads washed in lysis buffer/1% Triton X100. The bound fraction was isolated by elution in SDS PAGE Sample buffer/50mM DTT at 50°C for 30 min. Supernatants following centrifugation at 9000 rpm (surface fraction) were retained for analysis.

5.4 RESULTS

5.4.1 Choice of peptide sequences

The following two sequences were chosen on the basis of their specificity to the hH_4R aa sequence and their potential immunogenicity:

hH_4R – CT (aa 374 – 390) Chazot 3 CIKKQPLPSQHSRSVSS

hH_4R (aa 251 – 266) Chazot 4 CERRRRKSSLMFSSRTK

The sequences are found at the C terminal end of the receptor (Chazot 3) and within the third intracellular loop (Chazot 4) (Fig 5.4). It should be noted that both sequences are also present in the hH_4 (302) isoform but **NOT** in the severely truncated hH_4 (67) isoform. Note: The sequences in RED are common between human, rat and mouse H_4 receptors.

Human sequence showing full length H_4 R

Third intracellular loop (i3) shown in red

Peptide sequence used to immunise rabbit blue and underlined (Chazot 3)

```
  1 mpdtnstinl slstrvtlaf fmslvafaim lgnalvilaf vvdknlrhrs syfflnlais
 61 dffvgvisip lyiphtlfew dfgkeicvfw lttdyllcta svynivlisy drylsvsnav
121 syrtqhtgvl kivtlmvvvw vlaflvngpm ilvseswkde gsecepgffs ewyilaitsf
181 lefvipvilv ayfnmniyws lwkrdrlsrc qshpgltavs snicghsfrg rlssrrslsa
241 stevpasfhs errrrksslm fssrtkmnsn tiaskmgsfs qsdsvalhqr ehvellrarr
301 lakslaillg vfavcwapys lftivlsfys satgpksvwy riafwlqwfn sfvnpllypl
361 chkrfqkafl kifcikkqpl psqhsrsvss
```

Human sequence showing full length H_4 R

Third intracellular loop (i3) shown in red

Peptide sequence used to immunise rabbit blue and underlined (Chazot 4)

```
  1 mpdtnstinl slstrvtlaf fmslvafaim lgnalvilaf vvdknlrhrs syfflnlais
 61 dffvgvisip lyiphtlfew dfgkeicvfw lttdyllcta svynivlisy drylsvsnav
121 syrtqhtgvl kivtlmvvvw vlaflvngpm ilvseswkde gsecepgffs ewyilaitsf
181 lefvipvilv ayfnmniyws lwkrdrlsrc qshpgltavs snicghsfrg rlssrrslsa
241 stevpasfhs errrrksslm fssrtkmnsn tiaskmgsfs qsdsvalhqr ehvellrarr
301 lakslaillg vfavcwapys lftivlsfys satgpksvwy riafwlqwfn sfvnpllypl
361 chkrfqkafl kifcikkqpl psqhsrsvss
```

Fig 5.4 Full length amino acid sequence of the hH_4R with the sequences of the immunising peptides highlighted

5.4.2 Antibody yields

Immune serum has been collected from both of the immunised rabbits, however to date only the anti-H_4(374-390) (H_4-3) has been purified. Affinity purification and the calculation of antibody yield were performed exactly as described in Chapter 3. Antibody yields were 442 and 489 μg per ml immune serum for bleeds 2 and 3, respectively.

5.4.3 The antibody was able to detect human H_4R expressed in HEK 293 cells

Evidence from immunoblots showed coincident bands where FLAG-hH_4R transfected cells were probed with anti-H_4 (374-390)R and anti-FLAG in parallel (n = 3). Immunoprecipitation experiments confirmed the H_4R reactivity of the anti-H_4 (374-390) antibody (Figs 5.5 and 5.6).

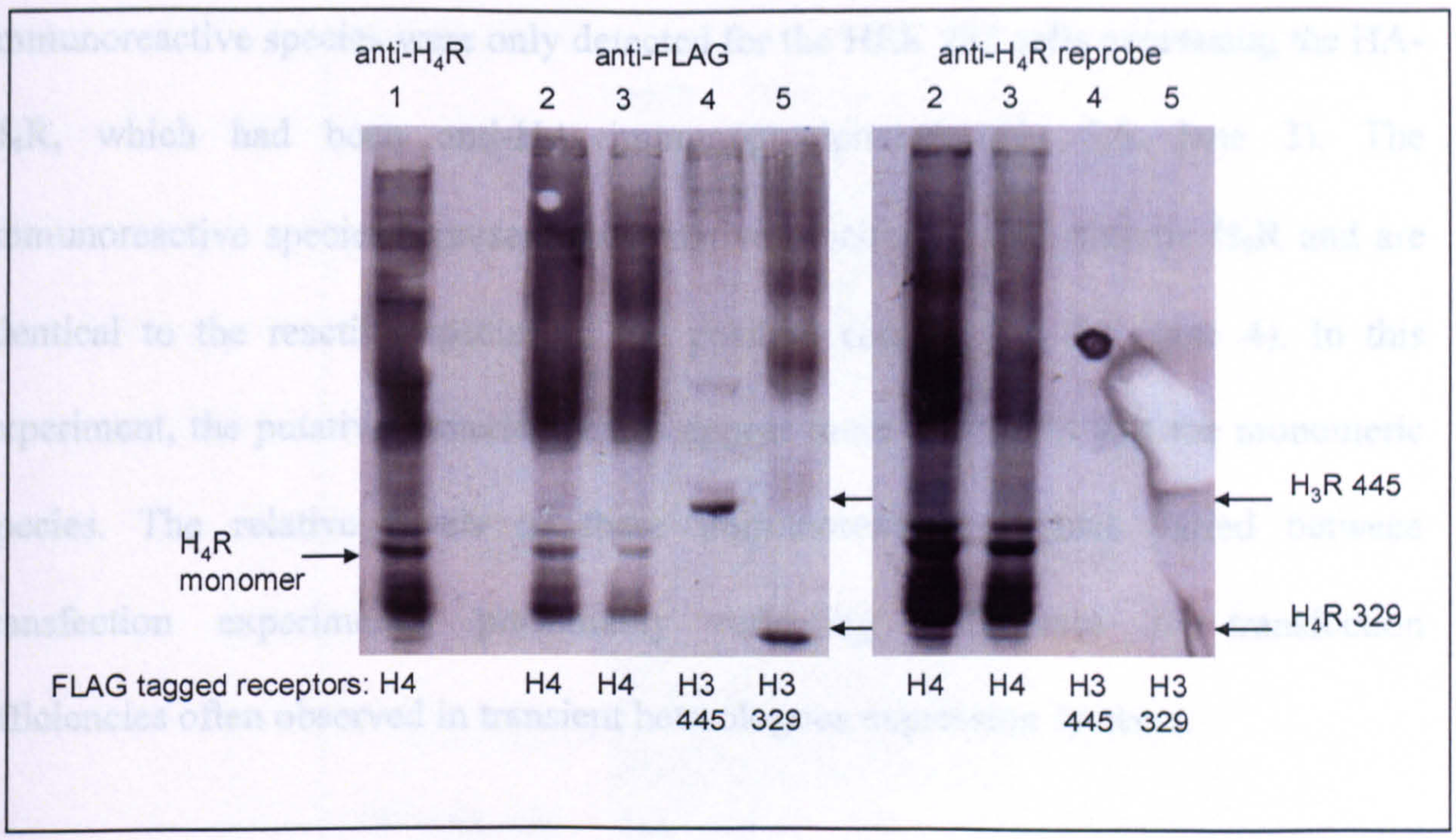

Fig 5.5 Anti-H_4 (374-390) and anti-FLAG immunoreactivity are coincident

Recombinant FLAG tagged human H_4 and H_3 receptors probed with anti-H_4 (374-390) (Lane 1, 2 μg/ml) and anti-FLAG (Lanes 2 -5 left hand blot,1:5,000). The right hand blot shows lanes 2-5 of the original blot following stripping of the first antibody by incubation of the nitrocellulose sheet in distilled water 15 mins, followed by 15 mins in 0.2M NaOH and a final 15 mins in water again. The sheet was then blocked in the usual way and reprobed with anti-H_4 (374-390), 2 μg/ml. The anti-H_4 (374-390) is a rabbit antibody whereas the anti-FLAG is a monoclonal mouse antibody, therefore the secondary antibodies are anti-rabbit and anti-mouse, respectively. The H_3R isoforms served as a negative control for the reprobe experiment. The immunoreactivity pattern was identical using the anti-FLAG and anti-H_4 (374-390) antibodies in all cases.

5.4.4 Immunoprecipitation of HA-H_4Rs transiently expressed in HEK 293 cells

To further characterize the selectivity of the H_4R antibody an immunoprecipitation assay was performed. HA-H_4Rs transiently expressed in HEK 293 cells (Fig 5.6, Lane 2 - 4) were immunoprecipitated using anti-HA antibodies (Fig 5.6, lane 3), or a non-immune Ig (Fig 5.6, lane 2). As negative control non transfected HEK 293 cells immunoprecipitated with anti-HA antibodies (Fig 5.6, lane 1) were used. As a positive control solubilized HEK 293 cells expressing HA-H_4Rs (Fig 5.6, lane 5) were used.

All samples were subjected to immunoblotting using the anti-H_4R antibodies. Immunoreactive species were only detected for the HEK 293 cells expressing the HA-H_4R, which had been anti-HA immunoprecipitated (Fig 5.6, lane 3). The immunoreactive species represent the putative monomeric and dimeric H_4R and are identical to the reactive species in the positive control (Fig 5.6, lane 4). In this experiment, the putative dimeric species appear more prominent that the monomeric species. The relative levels of these immunoreactive species varied between transfection experiments, presumably reflecting differences in transfection efficiencies often observed in transient heterologous expression systems.

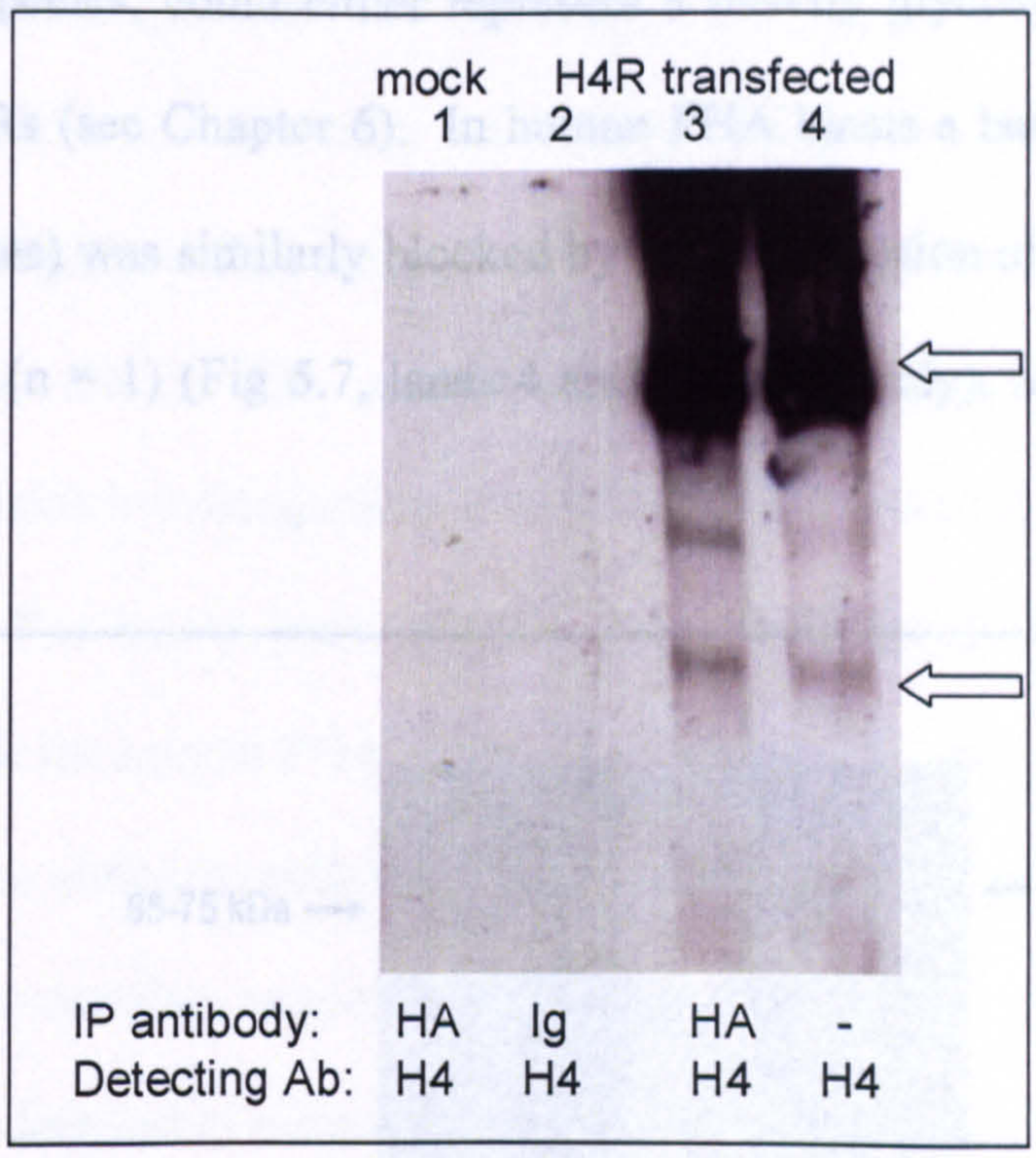

Fig 5.6 The anti-H_4R antibodies recognize anti-HA immunoprecipitated HA-H_4Rs

HEK 293 cells alone (lane 1-2) or transfected with cDNA encoding the HA-H_4R (lane 3-5) were subjected to immunoprecipitation with an anti-HA antibody (lane 2, 4) or a non-immune Ig (lane 3). The precipitates (lane 2-4) or solubilized cells (lane 1, 5) were immunoblotted using the anti-H_4R antibody. Putative dimeric and monomeric species indicated using arrows.

5.4.5 The antibody was specific for hH_4R expressed in HEK 293 cells

The selectivity of the anti-hH_4R antibody was confirmed by blockade with the C-terminal peptide of the H_4R (Fig 5.7, lane 3) (n = 3 replicates) and a lack of cross reactivity with the human H_3R (n = 3 replicates), the most related GPCR (de Esch *et al*, 2005) (Fig 5.7, lane 1). In transfected HEK 293 cells, the antibody detects two major reactive species at M_r 35,000 $\pm$ 1000 and 70,000 $\pm$ 5000 (Fig 5.7, lane 2). The lower bands appeared as a doublet (Mr 34,000 and 36,000) and most likely represent monomeric H_4Rs. Occasionally an additional band (Mr approx. 45,000) was detected which is likely to be a proteolytic fragment. The M_r 34,000 is probably the

unglycosylated product of the species at M_r 36,000 (see Chapter 6). The higher molecular weight species, could either represent a heavily glycosylated form of the H_4R or dimeric H_4Rs (see Chapter 6). In human PHA blasts a band at Mr 77,000 $\pm$ 3000 (n = 4 replicates) was similarly blocked by prior incubation of the antibody with the antigen peptide (n = 1) (Fig 5.7, lanes 4 and 5 respectively). Monomeric species were not detected.

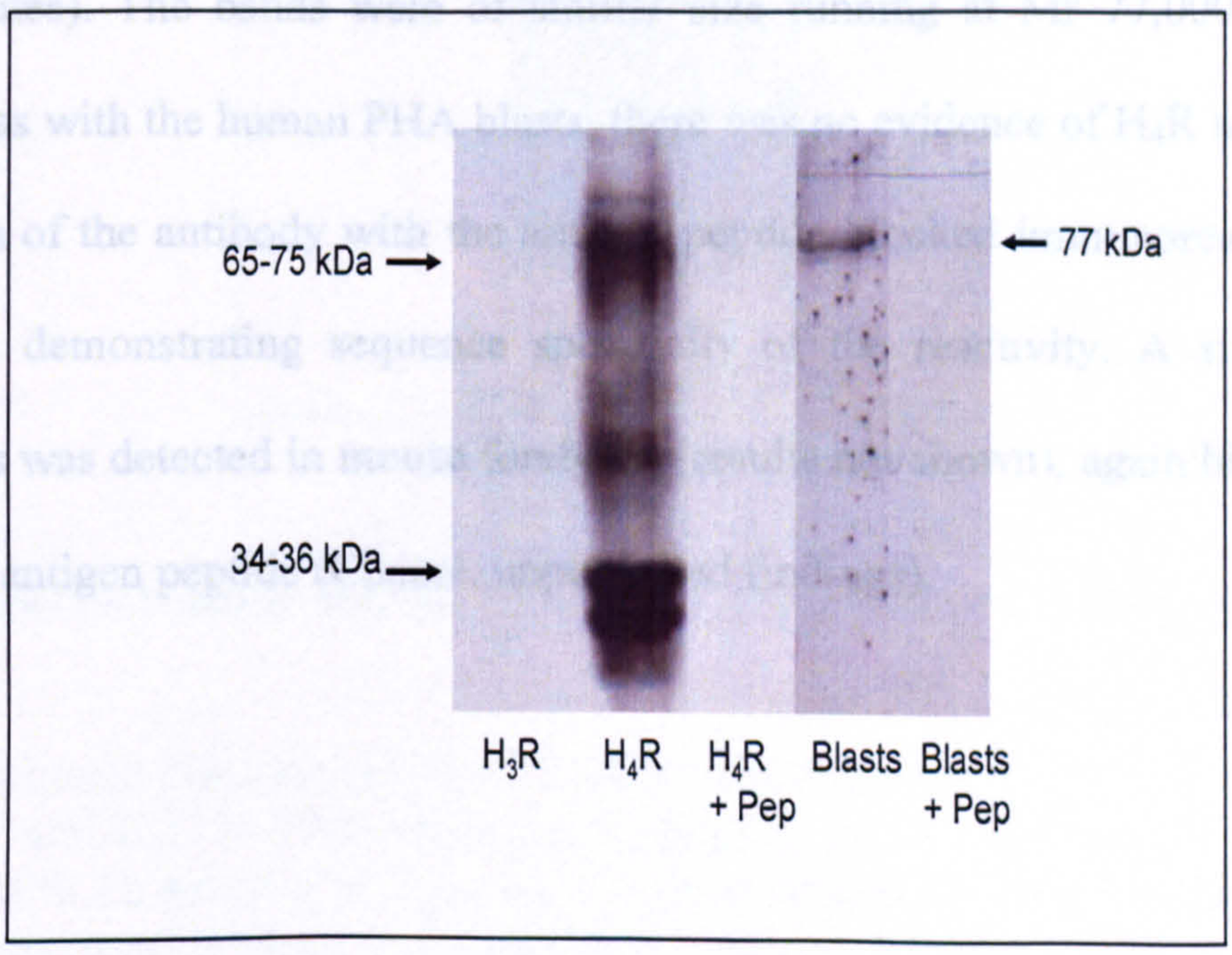

Fig 5.7 Characterization of specific polyclonal H_4R antibodies

HEK 293 cells expressing $hH_{3(445)}Rs$ or hH_4Rs, and human PHA blasts were probed by immunoblotting using the anti-H_4 (374-390) antibody (0.5 µg /ml) either alone or pre-incubated for 16h at 4°C with 500 µg /ml (374-390) peptide. The major immunoreactive species labeled in the HEK 293 hH_4R and the human PHA blasts were greatly suppressed by pre-incubation with the antigen peptide (lanes 3 and 5 respectively), demonstrating the sequence selectivity of the antibody. Furthermore, no significant labeling of the $hH_{3(445)}R$ (lane 1) or in untransfected HEK293 cells (not shown) was detected. (HEK 293 + $hH_{3(445)}$, n = 3; HEK 293 + hH_4R, n > 10 separate replicates; PHA blasts, n = 4 replicates; peptide block of H_4R transfected cells and PHA blasts, performed on n = 3 occasions with similar results.

5.4.6 The polyclonal H_4R antibodies are able to detect specific immunoreactivity in native tissue, including human and rat brain.

Although the H_4R is found primarily on immune cells there are some reports of mRNA expression in mammalian brain (Zhu *et al*, 2001; Lozada *et al*, abstract, EHRS 2004; Cogé *et al*, 2001). The anti-H_4 (374-390) antibody clearly identified immunoreactive species in homogenates of human putamen and rat forebrain (Fig 5.8) (n = 3 replicates). The bands were of similar size running at Mr 77,000 $\pm$ 3000. Interestingly, as with the human PHA blasts, there was no evidence of H_4R monomers. Pre-incubation of the antibody with the antigen peptide blocked immunoreactivity in both samples, demonstrating sequence specificity of the reactivity. A similar Mr 77,000 species was detected in mouse forebrain (results not shown), again blocked by the respective antigen peptide (Chazot, unpublished findings).

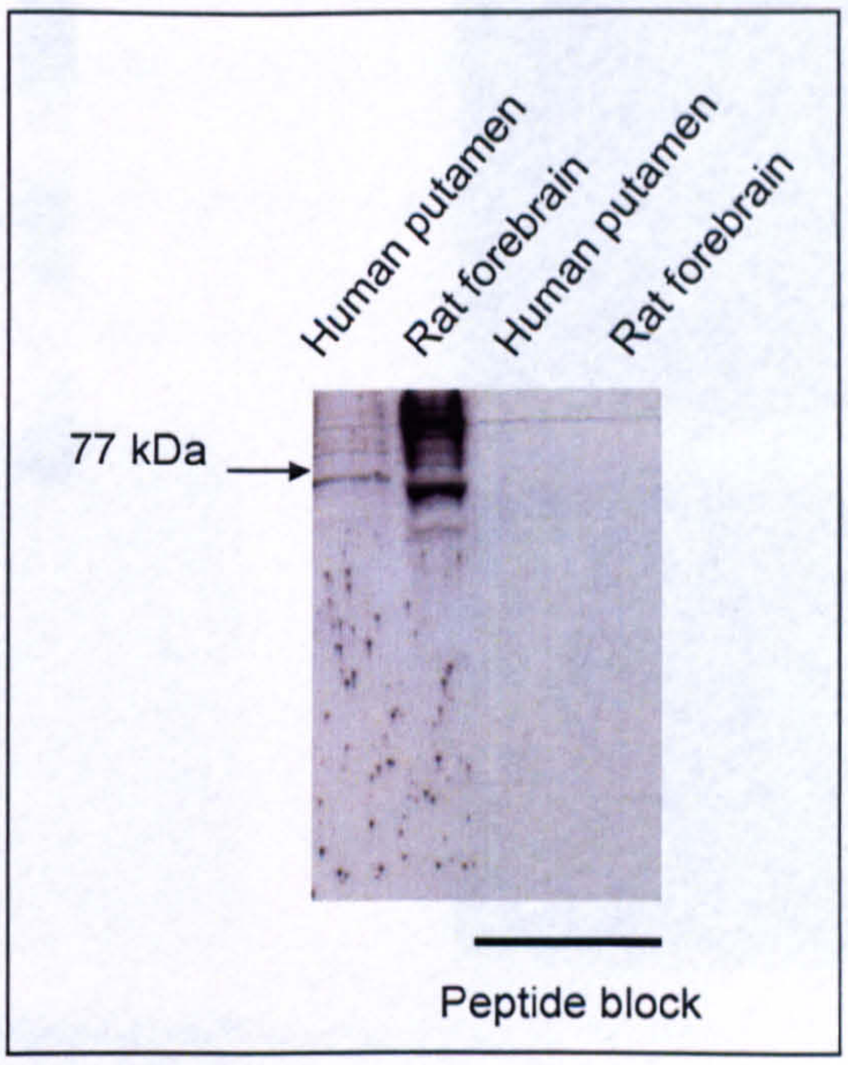

Fig 5.8 Immunoblot using anti-H_4 (374-390) receptor to probe human and rat brain.

Lane 1 and 3: Human Putamen and Lane 2 and 4: Rat forebrain
Lanes 1 and 2: anti-H_4(374-390) receptor at 1 μg/ml; Lanes 3 and 4: anti-H_4(374-390) preincubated with H_4 peptide, at 1 μg/ml. n = 3 replicates for both human putamen and rat forebrain; peptide block n = 2 specificity replicates for both preparations (and mouse forebrain (not shown).

5.4.7 The anti-H_4 (374-390) identified H_4R protein in human spleen lysates and tissue sections.

The H_4R is found predominantly on peripheral blood monocytes (PMBC) and in the tissues where these cells are found such as bone marrow and spleen. The anti-H_4 (374-390) identified H_4R protein in immunoblots of human spleen lysates (Fig 5.9 A) and in immunohistochemical staining of spleen tissue sections (Fig 5.9 B and C). In the immunoblot bands were detected at Mr 31,000 compatible with the monomer; and Mr 59 and 66,000; potentially glycosylated receptors and/or receptor dimers. Due to limited supply of human spleen material this experiment was only performed once.

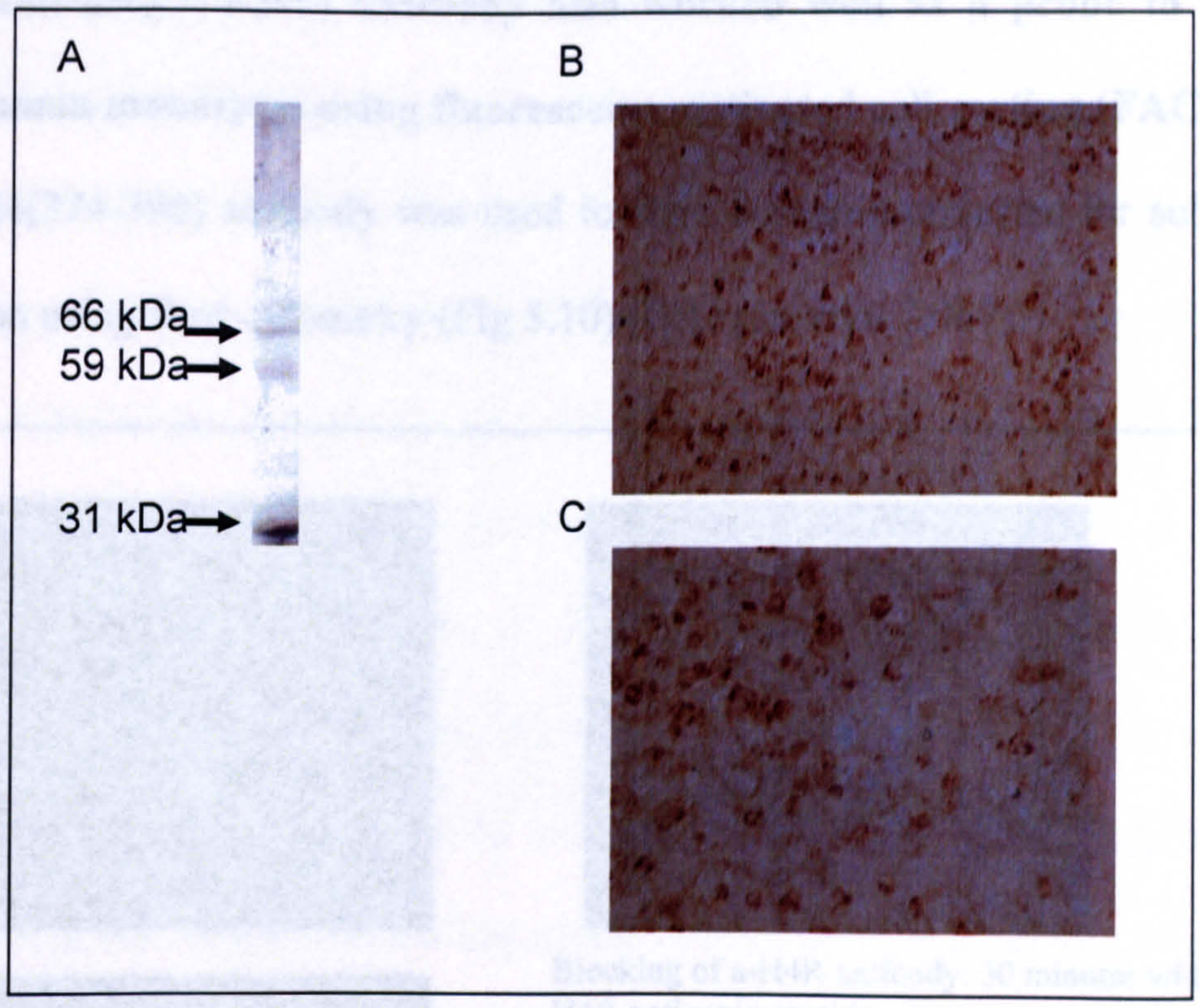

Fig 5.9 anti-H_4(374-390) reacts with human H_4R in spleen lysate and tissue sections

A: Immunoblot of human spleen lysate (10 µg). Anti-H_4 (374-390)R antibodies were used at 2 µg/ml and incubated overnight at 4°C. In addition to the monomer at Mr 31 kD, two higher molecular weight species were detected at 59 and 66 kD. B and C: Immunostaining of human spleen slice (x 200 and x 400 respectively), using anti-H_4(374-390) at 1 µg/ml. A single experiment was performed for both the immunoblotting and the IHC of human spleen.

5.4.8 The anti-hH_4(374-390) antibody also worked well as a probe to identify hH_4R on human monocytes using fluorescence-activated cell-sorting (FACS)

The anti-hH4(374-390) antibody was used to stain human monocytes for subsequent quantification using flow cytometry (Fig 5.10) (Dikkstra *et al*, 2007)

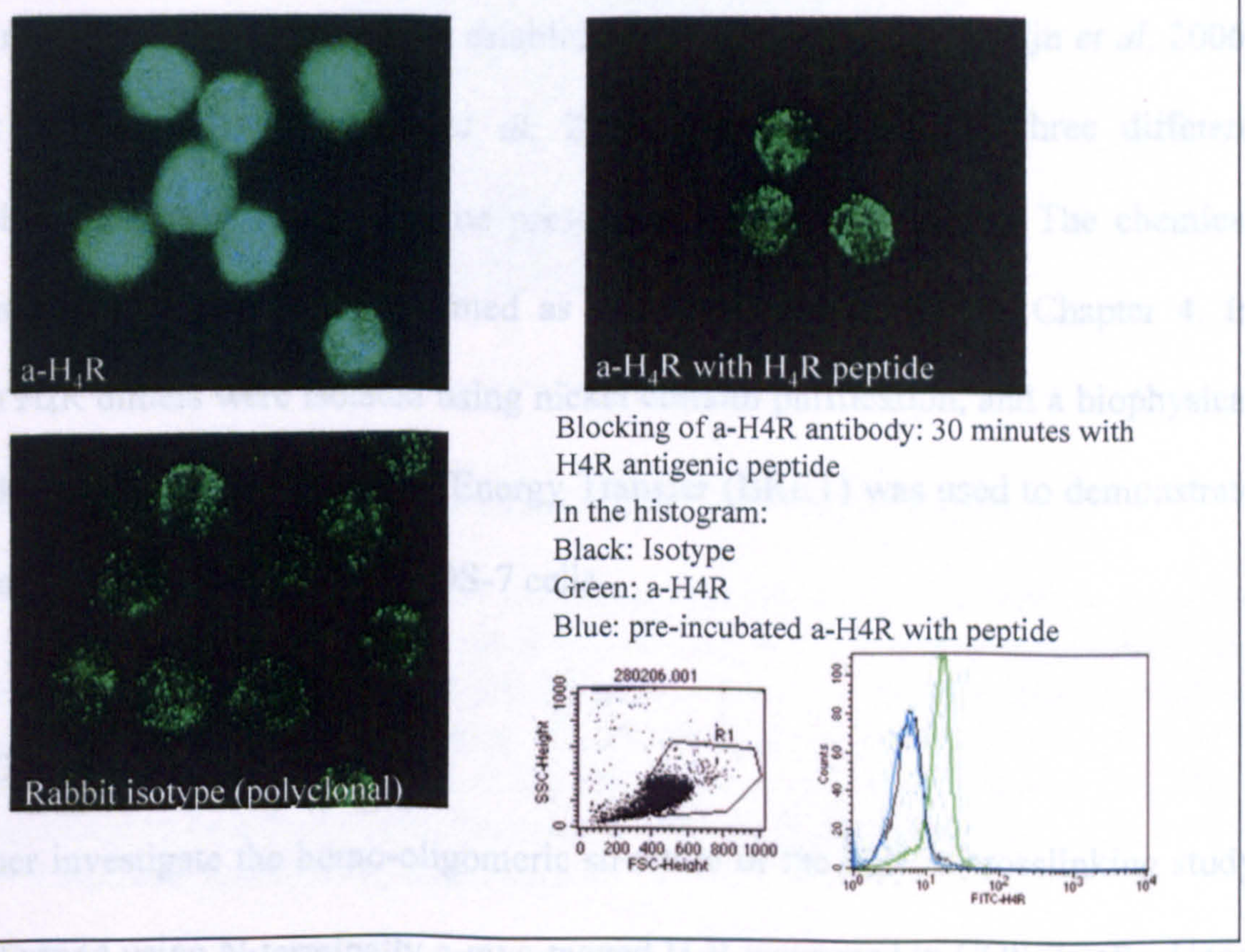

Reproduced with permission of Dorrit Dijkstra (Hannover University, Germany) (Dijkstra *et al*, 2007)

Fig 5.10 Staining of human monocytes with anti-H_4(374-390) R

Human monocytes labelled with anti-H_4(374-390) (a-H_4R); anti-H_4(374-390) pre-incubated with antigenic peptide (a-H_4R with H_4R peptide); or non-immune rabbit immunoglobulin (Rabbit isotype (polyclonal)) followed by biotin conjugated goat anti-rabbit and fluorescein isothiocyanate (FITC) coupled streptavidin. Labelled cell populations were quantified by flow cytometry (FACS Calibur, Becton Dickinson). Scatter plot shows granularity (side scatter: SSC-height) against cell size (forward scatter: FSC-height). The population R1 has characteristics typical of monocytes. The histogram shows cell numbers (counts) plotted against fluorescence intensity (FITC-H_4R).

5.4.9 The existence of heterogeneously expressed H_4R homo-dimers

Characterisation of the novel anti-human H_4R antibody provided evidence for higher molecular weight species in addition to the monomer. Dimeric versions of the receptor and/or post-translational modifications of the receptor, such as glycosylation, may account for these larger protein species. Dimerisation of the H_3R, the GPCR most closely related to the H_4R, has been established for both human (van Rijn *et al*, 2006; Chapter 4) and rodent (Bakker *et al*, 2006; Chapter 4) H_3Rs. Three different approaches were used to confirm the presence of H_4R homo-dimers. The chemical cross-linking technique was performed as described for the H_3R in Chapter 4. In addition H_4R dimers were isolated using nickel column purification, and a biophysical assay, Bioluminescence Resonance Energy Transfer (BRET) was used to demonstrate H_4R dimers in the membranes of COS-7 cells.

5.4.10 Cross-linking of H_4Rs

To further investigate the homo-oligomeric structure of the H_4R, a crosslinking study was performed using N-terminally c-myc-tagged H_4R expressed in COS-7 cells. Upon application of increasing concentrations of the cell impermeable crosslinker BS_3, a progressive reduction in the monomeric doublet species (M_r 34,000 and 36,000) was observed (Fig 5.11, representative blot from n = 3 replicates). The concomitant appearance of, initially, a diffuse species of M_r 77,000 (putative glycosylated and unglycosylated dimers) and, then, higher molecular weight species (M_r > 175,000) at 0.25mM and 2mM BS_3, respectively was noticed (Fig 5.11). These data are highly consistent with hH_4Rs expressed in HEK 293 cells (data not shown).

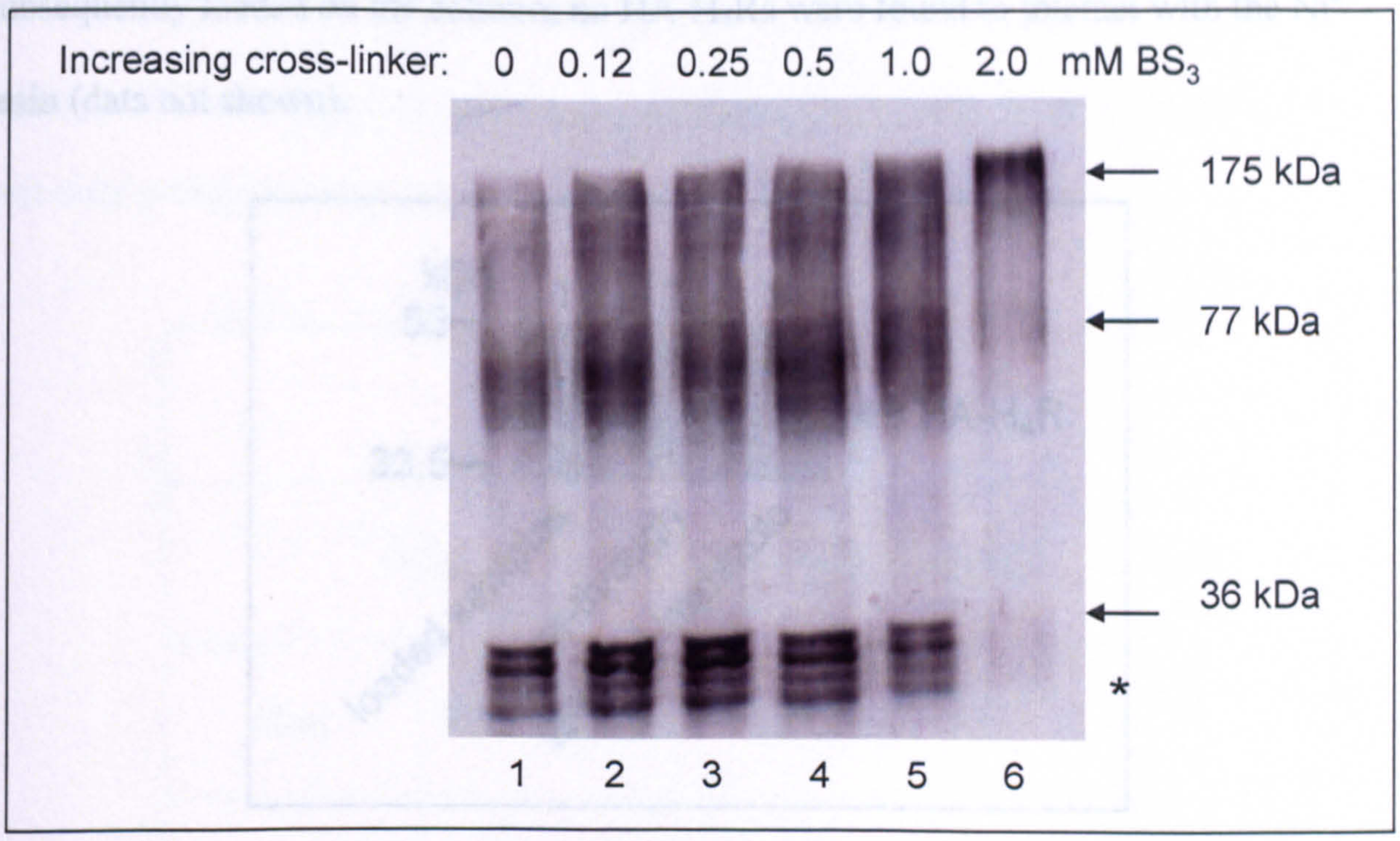

Fig 5.11 Cross-linking evidence for hH_4R dimers and higher oligomers

COS-7 cells transfected with cDNA encoding the hH_4R were subjected to cross-linking using increasing concentrations of BS_3 (0.12-2 mM). The resultant pellets were subjected to immunoblotting and probed with the anti-hH_4 (374-390) antibody (0.5 µg /ml). Lane 1, COS-7 cells expressing hH_4Rs as control; Lanes 2-5, COS-7 cells expressing hH_4Rs treated with 0.12, 0.25, 0.5, 1 and 2 mM BS_3, respectively. The * species is likely to be a proteolytic fragment of the hH_4R. Representative immunoblot from n = 3 replicate crosslinking experiments.

5.4.11 HA-H_4Rs associate with c-myc-H_4R-his_{10}

To further investigate whether the H_4Rs can associate with each other to form homo-oligomers, membranes of COS-7 cells co-expressing N-terminally c-myc and C-terminally his_{10} tagged hH_4Rs (c-myc-H_4R-his_{10}) and N-terminally HA-tagged hH_4Rs (HA-H_4R) were solubilized and loaded onto a Ni^{2+}-resin column. The HA-H_4Rs, when co-expressed with the c-myc-H_4R-his_{10}, were retained on the Ni^{2+}-column and could be eluted with 250 mM imidazole as detected with anti-HA antibodies (Figure 5.12, lane 3; representative blot from n = 3 replicates). When cells individually expressing c-myc-H_4R-his_{10} and HA-H_4Rs were mixed prior to solubilization, and

subsequently loaded on the column, no HA-H_4Rs were found to interact with the Ni^{2+}-resin (data not shown).

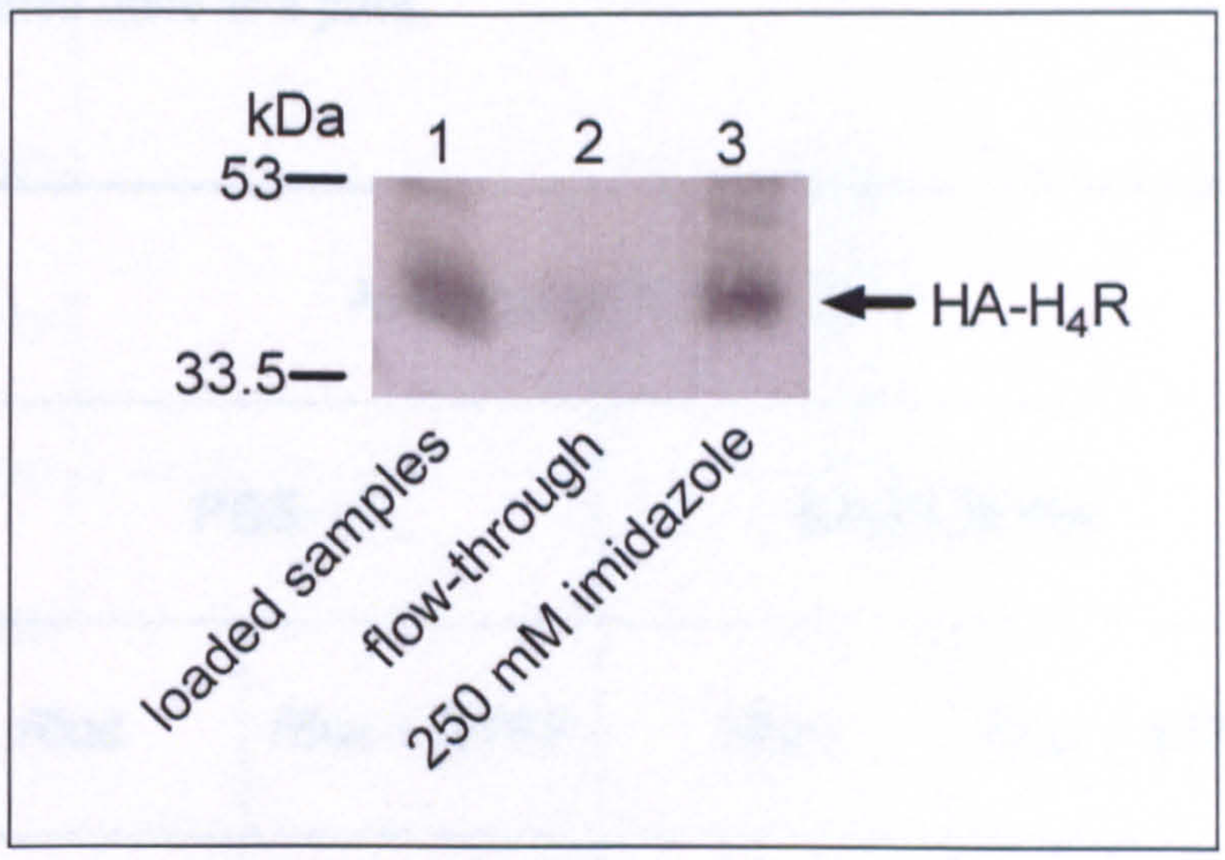

Fig 5.12 Nickel column purification of H_4R homo-oligomers

Cells co-expressing H_4Rs with an N-terminal c-myc- and C-terminal His_{10}-tag (c-myc-H_4R-his_{10}) and an N-terminal HA-tag H_4Rs (HA-H_4R) were solubilized and loaded onto a Ni^{2+}-NTA column. Samples were taken of the solubilized receptors before loading onto the column (lane 1), of the unbound fraction (lane 2) and of the bound fraction, that was eluted using 250 mM imidazole (lane 3). Samples were resolved by SDS-PAGE and then immunoblotted using anti-HA antibodies. Representative immunoblot from n = 3 purification replicate experiments.

5.4.12 BRET shows homo-oligomerization of hH_4Rs

The use of biophysical techniques has been of great value to the study of GPCR oligomerization. BRET was performed on COS-7 cells expressing either the H_4R-*R*luc or co-expressing the H_4R-*R*luc with the H_4R-eYFP. After addition of coelenterazine a robust BRET signal could be observed in the cells co-expressing the two H_4Rs (Table 5.1 and Fig 5.13, see section 5.3.5.1 for definition of BRET ratio). As a negative control, coelenterazine was also added to cells expressing H_4R-*R*luc alone. In this experiment a comparison was made between PBS and BRET buffer as the cell diluent. BRET buffer is PBS supplemented with 1mM $CaCl_2$, 1mM $MgCl_2$ and 1% glucose, it has been recommended as an improvement over PBS in a recent paper (El -Asmar *et*

al, 2005). The BRET signal was stronger using the BRET buffer, although further experiments are required to confirm the reproducibility of this result as the experiment was only performed once as a pilot.

Average BRET Ratio			
PBS		BRET Buffer	
*R*luc	*R*luc + eYFP	*R*luc	*R*luc + eYFP
1×10^{-5}	4037×10^{-5}	31×10^{-5}	5752×10^{-5}

Table 5.1 Average BRET ratios confirming the formation of H_4R homo-dimers in COS-7 cell membranes

Evaluation of homo-oligomerization of the H_4R by BRET using the co-expression of *Renilla* luciferase (*R*luc) and eYFP C-terminal receptor-fusion proteins. Cells expressing the indicated receptor-fusion proteins were exposed to 5 μM coelenterazine after which energy transfer was measured. Cells individually expressing H_4R-*R*luc were used as a control, (A single experiment performed in two different buffer systems with triplicate samples for each measurement).

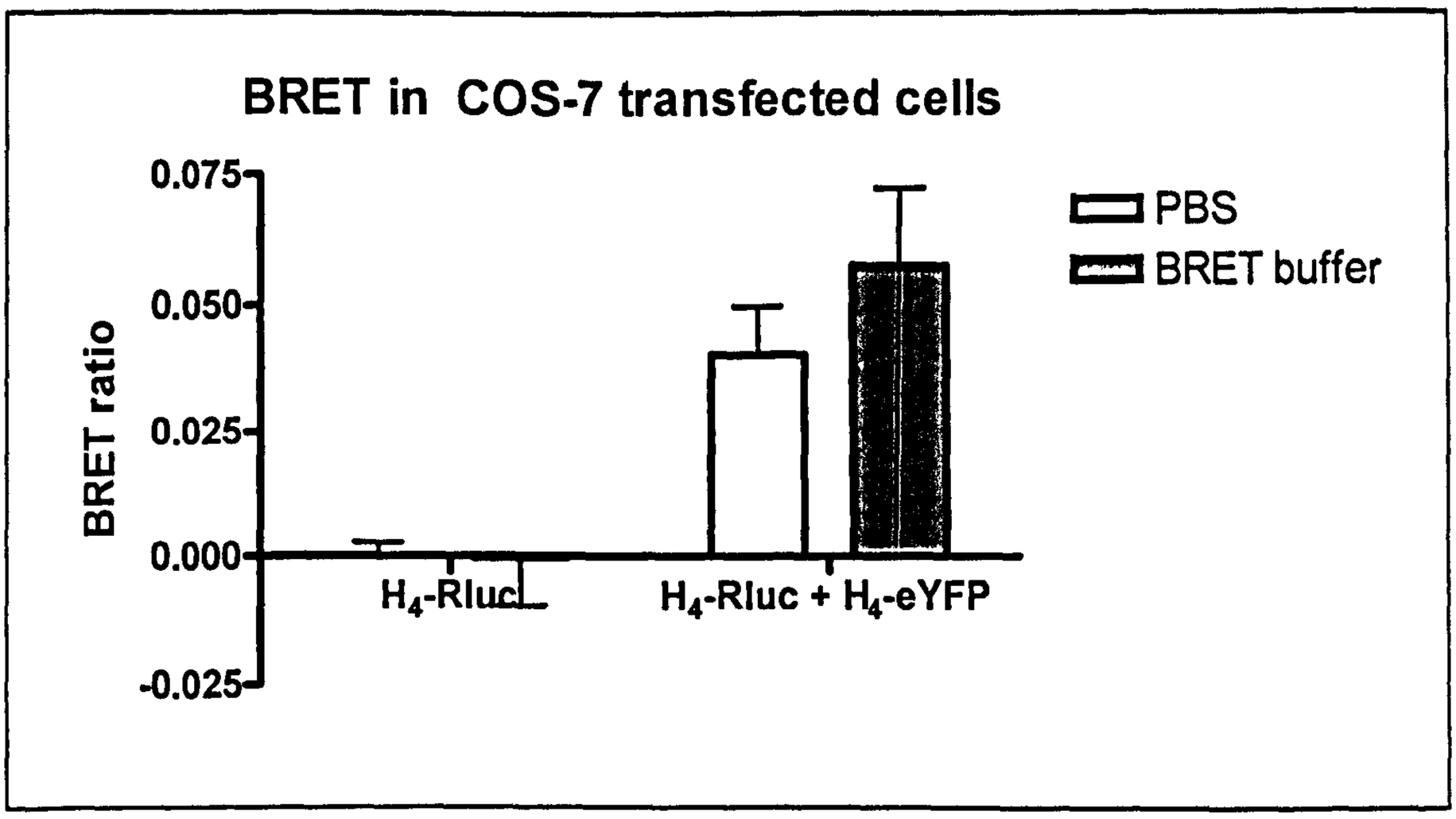

Fig 5.13 Average BRET ratios show the increase in signal from cells co-transfected with H_4-*R*luc and H_4-eYFP compared to cells expressing H_4-*R*luc alone

Data from Table 5.1 expressed as a bar chart. A robust BRET signal confirmed the formation of H_4R homo-dimers bringing the *R*luc C-terminal label close enough (within 100 Å) to the eYFP label to allow energy transfer on the addition of the *R*luc substrate coelenterazine, (A single experiment with two different buffer systems and triplicate samples for each measurement). Both systems showed a clear significant increase in BRET signal to similar ratio levels

5.4.13 Immunoprecipitation confirms the presence of hH_4R hetero-dimerisation

Solubilised proteins derived from HEK 293 cells co-transfected with equal amounts of untagged $hH_{4\,(390)}$ together with a FLAG tagged isoform: $hH_{4\,(390)}$ FLAG, $hH_{4\,(302)}$ FLAG or $hH_{4\,(67)}$ FLAG, were immunoprecipitated using anti-FLAG sepharose beads. The fractions isolated were analysed using immunoblotting with the novel anti-hH_4R as probe. Bands of a size compatible with the presence of $hH_4R_{\,(390)}$ were detected in all three of the precipitated fractions confirming association between the untagged $hH_{4\,(390)}$ and the FLAG labelled isoform (Fig 5.14, representative blot from n = 2 replicates). Both monomeric and dimeric species were evident in fractions from cells co-transfected with untagged hH_4 390 together with either $hH_{4\,(390)}$ FLAG or $hH_{4\,(302)}$

FLAG. By contrast only higher molecular weight species were seen with $hH_{4\ (390)}$ + $hH_{4\ (67)}$ FLAG transfected cells. The anti-hH_4R antibody would not be expected to react with the $hH_{4\ (67)}$ isoform, therefore immunoreactivity in this cell fraction is due to the presence of dimers which include $hH_{4\ (390)}$ as one of the partners. These results confirm FRET data (van Rijn *et al*, submitted) showing the presence of hH_4R hetero-dimers.

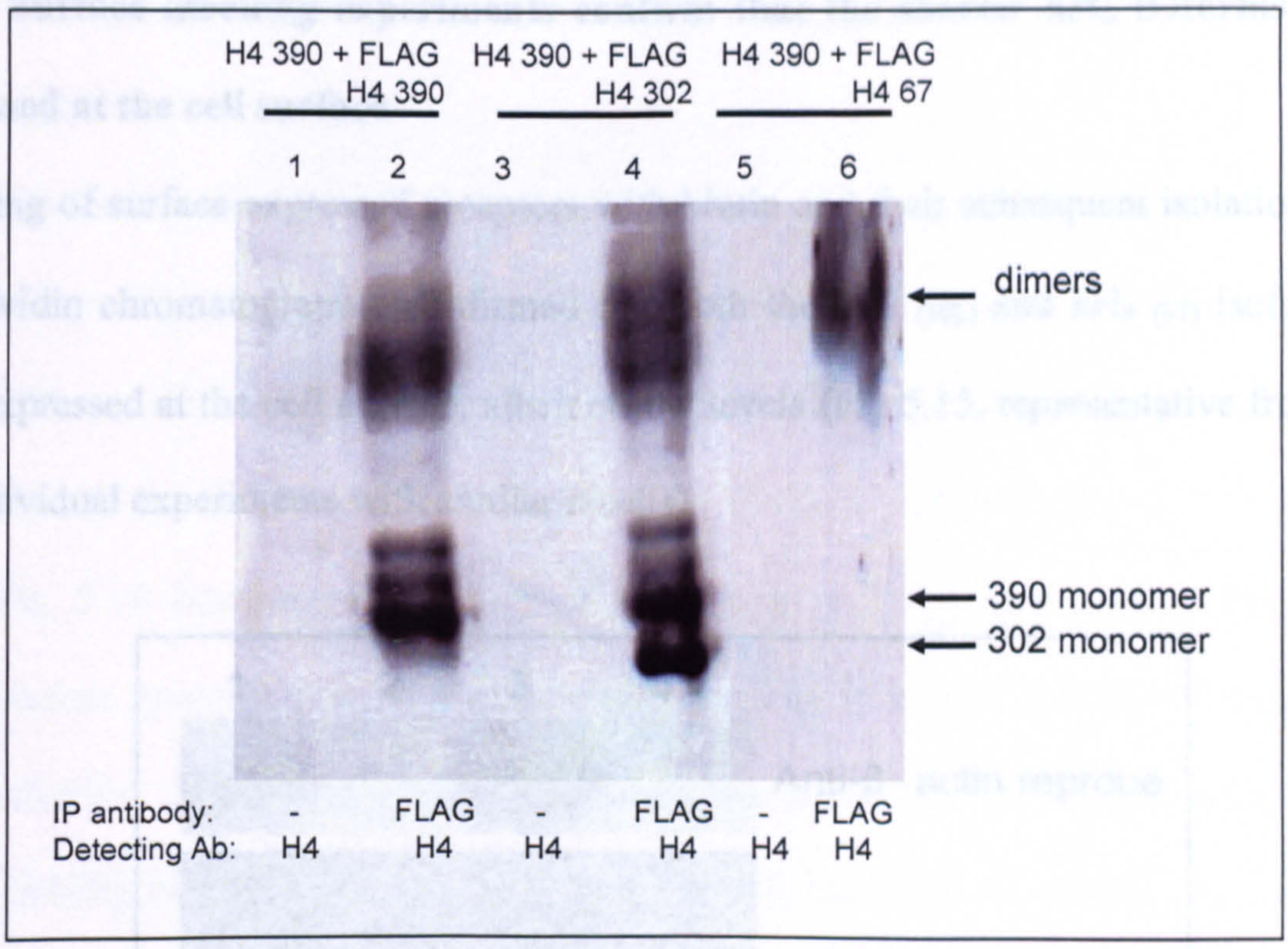

Fig 5.14 Immunoprecipitation evidence for $hH_{4\ (390)}$ receptor interaction with hH_4 receptor isoforms, $hH_{4\ (302)}$ and $hH_{4\ (67)}$

HEK 293 cells co-transfected with equal amounts of $hH_{4\ (390)}$ and a FLAG tagged isoform: $hH_{4\ (390)}$ FLAG (lanes 1,2), $hH_{4\ (302)}$ FLAG (lanes 3,4) or $hH_{4\ (67)}$ FLAG (lanes 5,6), harvested 48h post transfection, solubilised with 1% Triton X100 and subjected to immunoprecipitation with anti-FLAG sepharose or sepahrose control beads for 2h at 4°C. Following washing, bound material was collected using SDS-PAGE sample buffer and analysed by immunoblotting. Immunoblots were probed with anti-H_4 antibody, $hH_{4\ (67)}$ is not detected by this antibody. Lanes 1, 3 and 5 are control precipitations with sepahrose beads; lanes 2, 4, and 6 are precipitations with anti-FLAG sepharose. $hH_{4\ (390)}$ homo-dimers were detected (lane 2) as well as hetero-dimers between the $hH_{4\ (390)}$ isoform and the two shorter versions (lanes 4 and 6). Protein species consistent with monomeric $hH_{4(390)}$ and $hH_{4\ (302)}$ were seen in lanes 2 and 4, however no $hH_{4\ (390)}$ monomer was detected in lane 6. Representative blot from n = 2 replicate immunoprecipitation experiments from independent transfections.

5.4.14 Surface labelling experiments confirm that the shorter hH_4 isoforms are expressed at the cell surface

Labelling of surface expressed receptors with biotin and their subsequent isolation by streptavidin chromatography, confirmed that both the $hH_{4\ (302)}$ and $hH_{4\ (67)}$ isoforms were expressed at the cell surface, albeit at low levels (Fig 5.15, representative from n = 4 individual experiments with similar results).

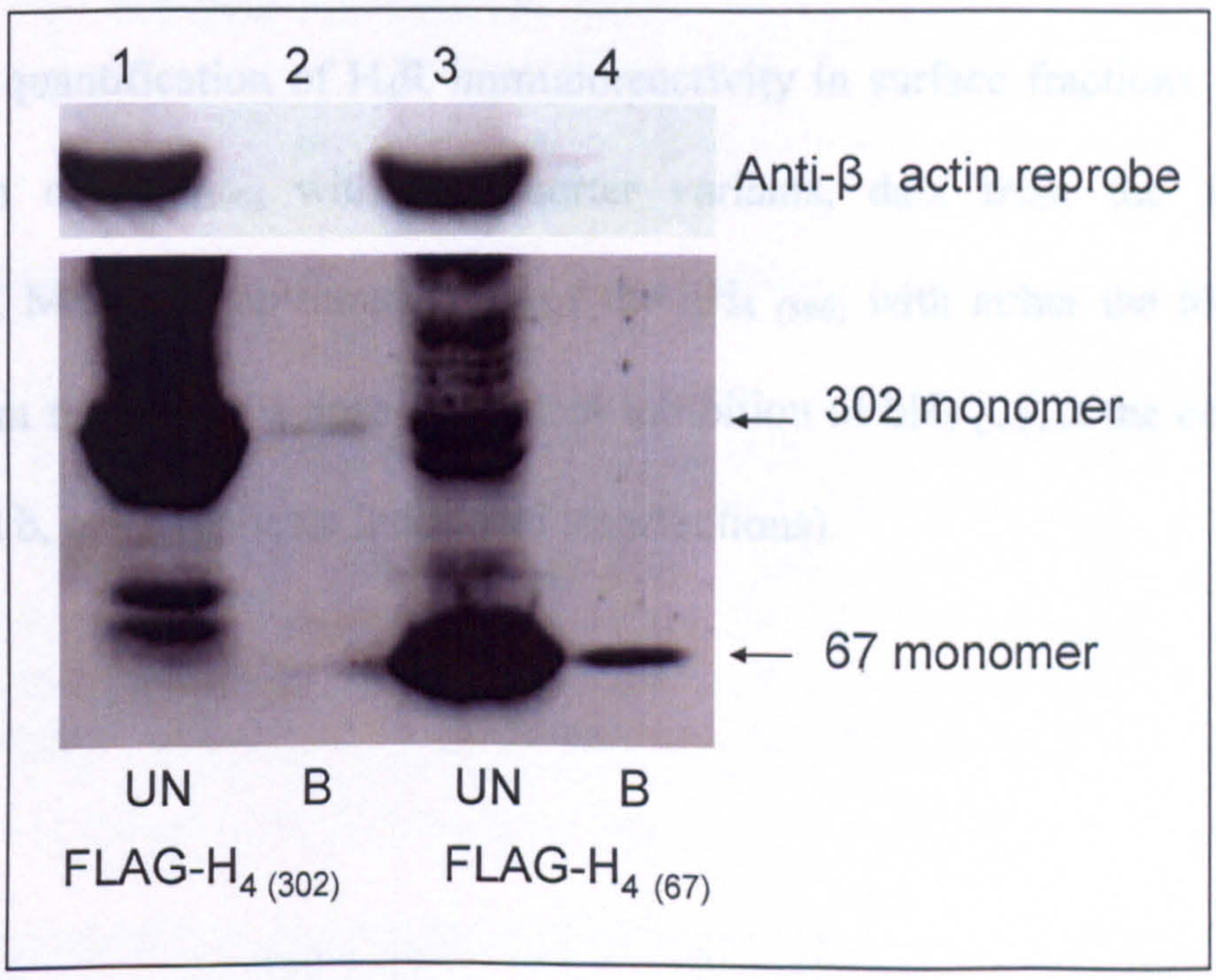

Fig 5.15 Surface labelling of hH_4 receptor isoforms

HEK 293 cells were transfected with either $hH_{4\ (302)}$ or $hH_{4\ (67)}$ receptor isoforms. Intact cells were biotinylated for 30 min at 4°C with 1mg/ml Sulfo-NHS-SS-Biotin, washed and homogenised. Biotinylated surface fraction was isolated by streptavidin chromatography, and analysed by immunoblotting. Lanes 1 and 3 UN: Unbound = Intracellular fraction; Lanes 2 and 4 B: Bound = Surface fractions, where Lanes 1 and 2 are $hH_{4\ (302)}$ FLAG samples, and Lanes 3 and 4 and $hH_{4\ (67)}$ FLAG samples. Probed with anti-FLAG (1:5000). The upper panel shows the same blot reprobed with anti-β actin antibody (1:800) as a control to confirm that intracellular proteins are not detected in the surface fraction (n = 4 experiments).

5.4.15 The shorter hH_4 isoforms reduce surface expression of the full length hH_4 $_{(390)}$ receptor

Using the same surface labelling technique surface expression of the full length hH_4 $_{(390)}$ was investigated following co-transfection with equal amounts of hH_4 $_{(390)}$, hH_4 $_{(302)}$ or hH_4 $_{(67)}$ cDNA. Co-transfection with a shorter isoform did not prevent surface expression of the full length receptor, however it was significantly reduced in each case (Fig 5.16 representative immunoblot from n = 2 replicates; and Table 5.2 densitometric quantification of H_4R immunoreactivity in surface fractions following co-transfection of H_4 $_{(390)}$ with the shorter variants, data from the same two immunoblots). Moreover co-transfection of the hH_4 $_{(390)}$ with either the hH_4 $_{(302)}$ or hH_4 $_{(67)}$ isoform resulted in a dose dependent inhibition of hH_4 $_{(390)}$ at the cell surface (Fig 5.17a and b, n = 2 replicate individual transfections).

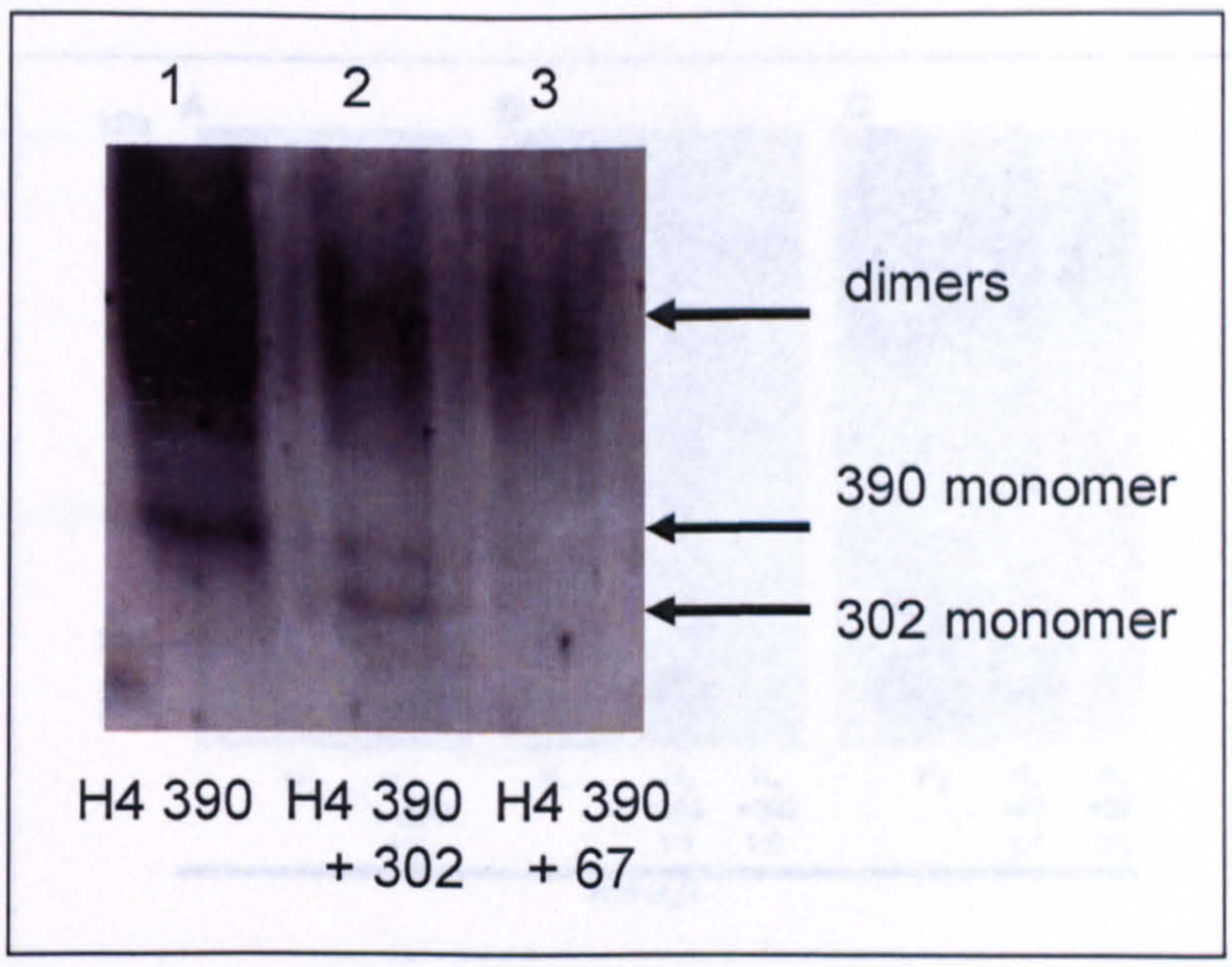

Fig 5.16 Surface Labelling of $hH_{4\ (390)}$: effect of isoforms

HEK 293 cells were transfected with $hH_{4\ (390)}$ alone, or co-transfected with $hH_{4\ (390)}$ together with either $hH_{4\ (302)}$ or $hH_{4\ (67)}$ receptor isoforms. Intact cells were biotinylated for 30 min at 4°C with 1mg/ml Sulfo-NHS-SS-Biotin, washed and homogenised. Biotinylated surface fractions was isolated by streptavidin chromatography, and analysed by immunoblotting. Surface fractions: Lane 1: $hH_{4\ (390)}$ alone; Lane 2: $hH_{4\ (390)}$ + $hH_{4\ (302)}$; Lane 3: $hH_{4\ (390)}$ + $hH_{4\ (67)}$. All Lanes were probed with anti-H_4 receptor antibody. The $hH_{4\ (67)}$ was not detected by this antibody.

H_4R Isoforms:	**390 + 390**	**390 + 302**	**390 + 67**
Dimer OD*:	1897	406 ± 29	388 ± 24
Monomer OD:	398	119 ± 18	63 ± 48

* OD = optical density

Table 5.2 Densitometric evaluation of surface expression of $hH_4R_{(390)}$ in the presence of the three different isoforms: 390 itself and the shortened splice variants 302 and 67.

Immunoblots were quantified by densitometry using NIH ImageJ in the linear range of the film. Optical density values were normalised to respective background as described previously (Chazot *et al*, 2002). Surface expression of the full length 390 isoform is significantly reduced on co-expression with either the 302 or the 67 isoform. Data are mean +/_ range values from the immunoblot shown in Fig 5.16 and another replicate blot.

Further experiments were performed to confirm these results, on this occasion increasing amounts of H_4 isoform cDNAs were utilised in order to assess the dose-dependency of the effect.

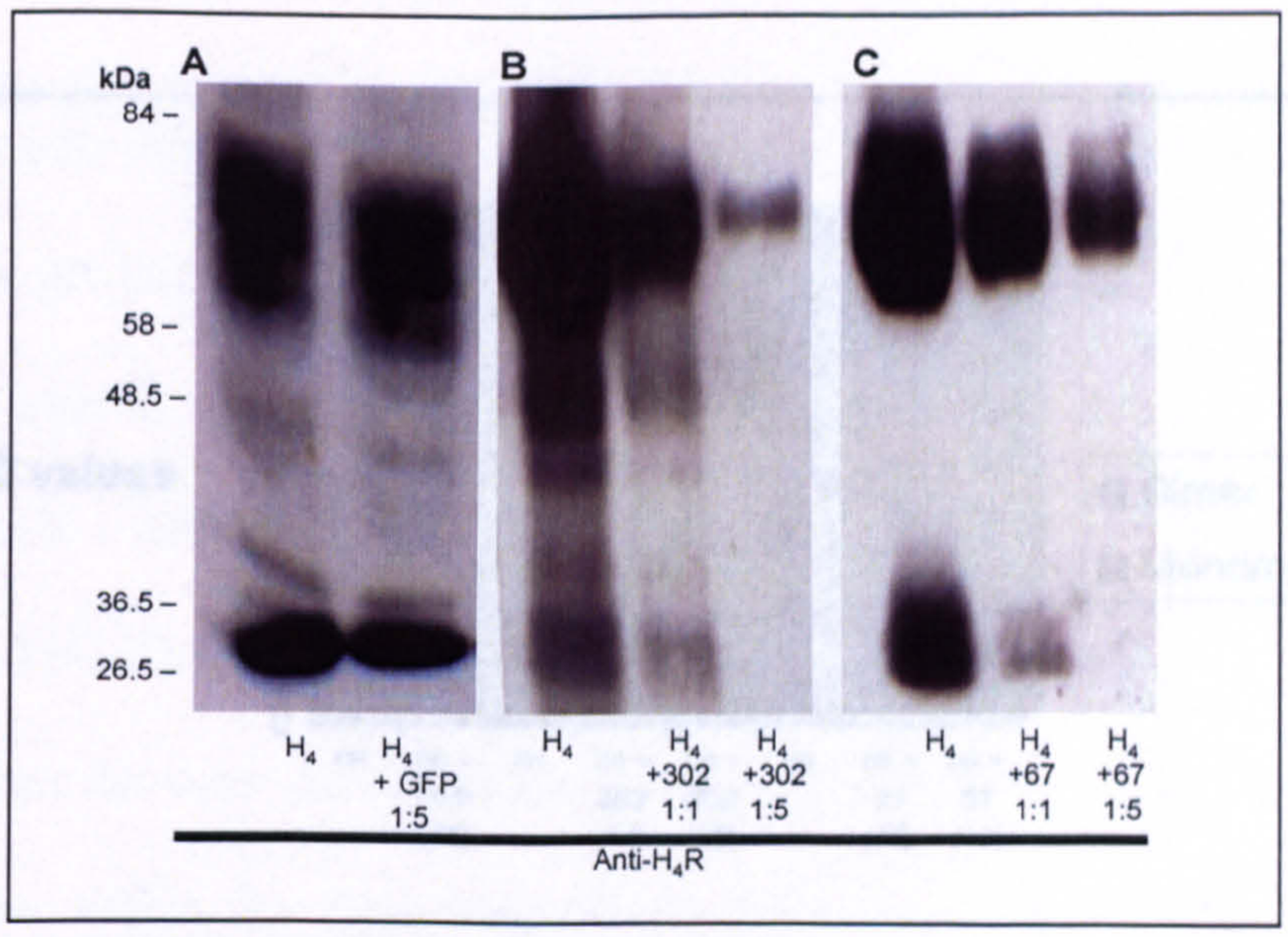

Fig 5.17 a) The two truncated H_4R isoforms dose dependently reduce surface expression of the full length $hH_{4\,(390)}$ isoform

Surface expression of hH_4 (390) was compared between cells transfected with hH_4 (390) cDna alone and cells co-transfected with hH_4 (390) plus Green Fluorescent Protein (GFP) (A); hH_4 (390) plus hH_4 (302) (B); and hH_4 (390) plus hH_4(67) (C). GFP was used as a negative control and transfected in the ratio 1:5 (hH_4 (390): GFP cDNA). For the truncated hH_4R isoforms co-transfections at 1:1, and 1:5 (hH_4 (390): hH_4 truncated isoform cDNA) were compared. Both the hH_4 (302) and hH_4 (67) isoforms dose dependently reduced the surface expression of the full length hH_4 (390). Representative immunoblot from two independent sets of transfections.

These data confirmed that both the H_4 302 and H_4 67 reduce the amounts of H_4 390 expressed at the cell surface.

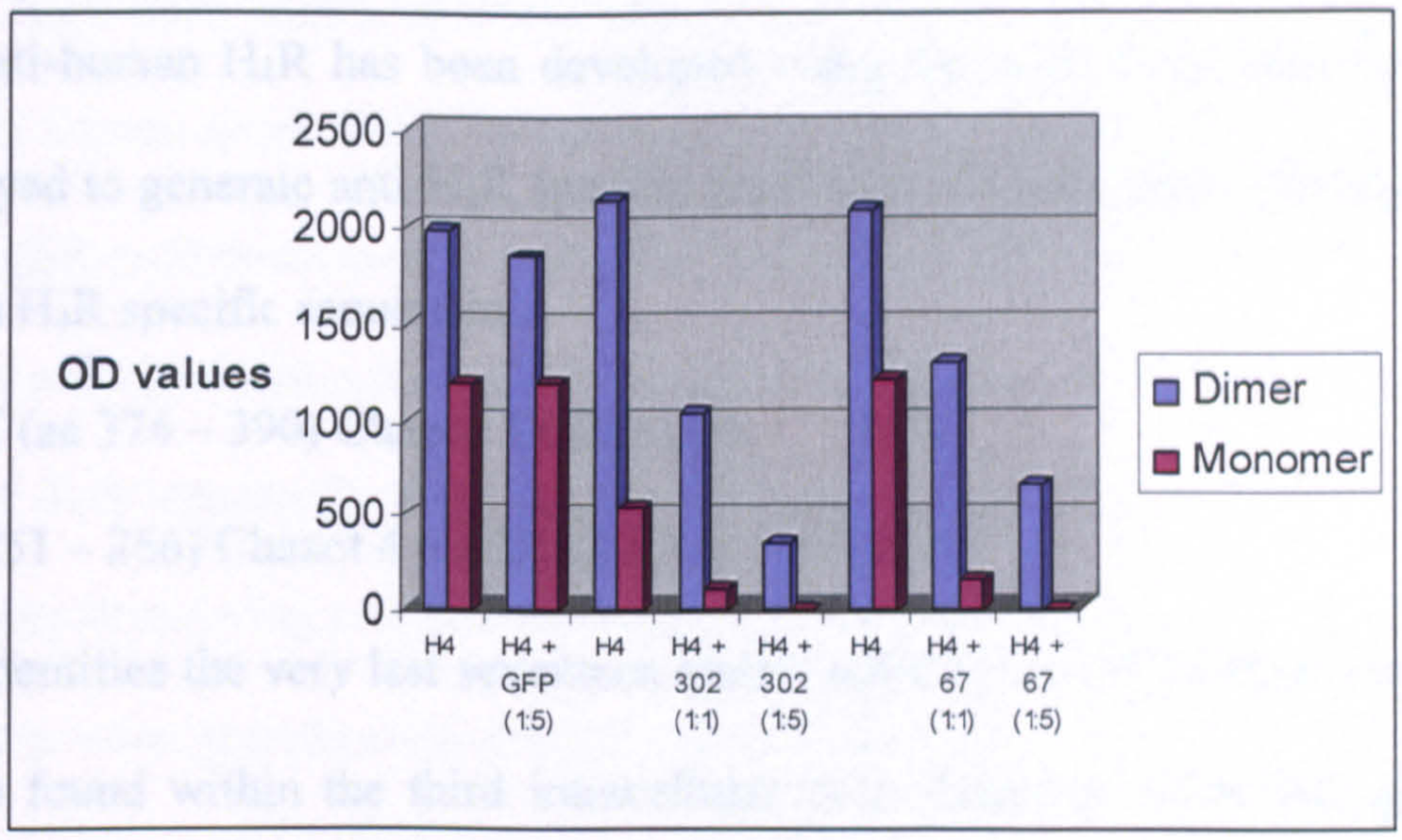

Fig 5.17 b) Densitometric quantification of surface expression of $hH_{4\ (390)}$ following co-expression with the shorter H_4 isoforms

Densitometric quantification of immunoblot shown in Fig 5.17 a. Representative experiment of two independent sets of transfections, replicated with similar results.

5.5 DISCUSSION

A novel anti-human H_4R has been developed using the same successful strategy as that employed to generate anti-H_3R specific antibodies. Rabbits were immunized with two human H_4R specific sequences:

hH_4R – CT (aa 374 – 390) Chazot 3 CIKKQPLPSQHSRSVSS

hH_4R (aa 251 – 266) Chazot 4 CERRRRKSSLMFSSRTK

Chazot 3 identifies the very last seventeen amino acids at the C-terminus, Chazot 4 is a sequence found within the third intracellular loop. Immune serum was generated from both these peptides, however only Chazot 3 (anti-hH_4(374-390) R) has been validated in this thesis. Note: The sequences in RED are common between human, rat and mouse H_4 receptors (see later for discussion of species cross-reactivities).

Anti-hH_4(374-390) identified FLAG-H_4R expressed in HEK 293 cells. The monomer migrated at Mr 34,000 – 36,000 usually as a doublet; and a higher molecular weight species, likely to correspond to the receptor dimer, was visualised at Mr 70,000 ± 5000. The anti-H_4R immunoreactivity was coincident with anti-FLAG immunoreactive bands, thus confirming their identity as H_4R. In addition, the antibody recognized the HA-H_4R which had been immunoprecipitated using an anti-HA antibody and then subjected to immunoblotting. Anti-hH_4(374-390) R immunoreactivity was greatly suppressed by prior incubation with the peptide antigen and no reactivity was seen against either HEK 293 negative cells or HEK 293 cells expressing the H_3R, the GPCR with the greatest homology to the H_4R (de Esch *et al*, 2005). Therefore the antibody was both specific to the immunising antigen and selective for the H_4R.

The new antibody also identified the H_4R in native tissue. High levels of H_4R mRNA expression have been shown in white blood cells, including T-lymphocytes (Hofstra *et al*, 2003; Morse *et al*, 2001; Nakamura *et al*, 2000; Oda *et al*, 2000; Zhu *et al*, 2001), but H_4R protein expression has so far not been shown. Western blot analysis of membranes of PHA blasts with our polyclonal anti-H_4R antibody, indeed revealed the presence of H_4R protein in PHA blasts. Interestingly, the endogenously expressed H_4R was only detected as a high molecular weight species, migrating at Mr 77,000 $\pm$ 3000. H_4R is also expressed in tissues containing white blood cells such as bone marrow and spleen. Our novel antibody identified three major bands in human spleen lysate and strong immunoreactivity was observed in spleen tissue sections using immunohistochemistry. Interestingly a low molecular weight species was clearly visible in the spleen lysate at Mr 31,000, likely to be the receptor monomer. Monomeric species were not evident in either the PHA blasts or in brain tissue (see later). Furthermore the two higher molecular weight bands at Mr 59,000 and 66,000 were smaller than the putative dimers/glycosylated versions of the receptors appearing in either in HEK 293-H_4R transfected cells or in other native tissue preparations. Several possibilities could account for these observations. The level of glycosylation could be tissue specific, the receptors might associate with different cellular proteins in different tissues or there may be, as yet unidentified, tissue specific isoforms of the H_4R. The possibility that the 59 and 66 kDa bands could be proteolytic fragments cannot be entirely dismissed since the spleen lysate was commercially supplied. However care was taken to avoid protein degradation during transit from the supplier and subsequent sample preparation.

The presence of H_4R mRNA in several human brain regions has been reported using RT-PCR (Cogé *et al*, 2001). (In the same study no signal was observed by Northern Blot in numerous brain regions or peripheral tissues.) The H_4R mRNA was predominantly expressed in the cerebellum and hippocampus, there was also expression in amygdala, caudate nucleus, substantia nigra, thalamus and hypothalamus; but none found in the cerebral cortex or raphe nucleus. Using *in situ* hybridisation analysis Zhu *et al* (2001) showed mouse H_4R mRNA to be selectively expressed in the hippocampus, particularly in the granular cell layer of the dentate gyrus and the pyramidal cell layer but not in the rest of the brain or other tissues such as skeletal muscle, fat, heart, liver, spleen, thymus, lymph node, adrenal gland, spinal cord or kidney. Given the findings of other studies it is surprising that no message was detected in spleen, thymus or lymph node. Liu *et al*, 2001 recorded high expression of H_4R mRNA in mouse bone marrow and spleen using RT-PCR; and investigations of the distribution of human H_4R message show it predominantly in immune cells. Using the novel anti-human H_4R, we have provided the first evidence for the presence of H_4R protein in human putamen and rat (and mouse) forebrain. The predominant band migrated with Mr 77, 000 $\pm$ 3000 in all three species; lower molecular weight species were very weak or undetected. The size of this band was consistent with a glycosylated dimer of the species identified in the human spleen. Alternatively it is reasonable to speculate that it may represent an H_4R variant. Pre-incubation of the antibody with the respective antigen peptide blocked immunoreactivity in both samples, demonstrating sequence specificity of the reactivity. Very recently, strong punctate decoration of putative neurons was observed by IHC using this antibody in both cortical and caudate nucleus regions of human brain; and thalamus, cortical layer

IV and CA3 hippocampus of mouse brain (Appendix, Chazot *et al*, EHRS, Florence, 2007).

Immunolocalisation of H_4R in the rat gastrointestinal (GI) tract has been reported by our group using this anti-H_4 antibody (Morini *et al*, Abstract for Digestive Disease Week Washington, 2006; EHRS, Florence, 2007). Immunoreactivity was detected in endocrine cells of the fundic mucosa and also in the myenteric plexus of all regions of the GI tract examined. This is the first report of the H_4R in the mammalian parasympathetic nervous system. No H_3R was detectable in the myenteric plexus. Furthermore, this study found evidence of H_3R and H_4R being present on mutually distinct subpopulations of GI endocrine cells.

The rat and mouse H_4Rs are significantly different from the human H_4R sequence at 69 and 68% homology, respectively (Liu *et al*, 2001). However, amino acids in the C-terminal sequence aa 374 – 390, while not identical to the human receptor, do share some sequence similarity to their human counterpart (Liu *et al*, 2001). It appears that the tertiary conformation and sequence overlap of the rat (and mouse) H_4R C-terminus is recognised by the anti-human H_4 (374-390) antibody highlighted in Results section, based on the results in this chapter and other studies from collaborators (Morini et al., 2007; Chazot et al., 2007).

In addition to its utility in immunoblotting and immunohistochemical techniques, the anti-H_4 (374-390) antibody also worked well as a probe to identify hH_4R on human monocytes using Fluorescence-Activated Cell-Sorting (FACS).

Higher molecular weight species were present on heterologous expression of H_4R in HEK-293 cells and in native tissue. Indeed in native tissue, the monomeric species was often not detected, in agreement with our observations with endogenous H_3 receptors (Chazot *et al*, 2001; Victoria Hann PhD thesis, 2004). In view of the strong reducing conditions under which the gels are run, the H_3 and H_4 dimers appear robust. Three different techniques were used to verify the presence of H_4R homo-dimers.

Chemical cross-linking of H_4Rs expressed in HEK 293 cells increased the intensity of putative dimeric species at Mr 77,000 and 175,000; with a simultaneous decrease in the strength of the monomer. The presence of homo-dimers was corroborated by immobilisation of His-H_4R/HA-H_4R dimers on a nickel column. The Ni^{2+} resin isolated the His-tagged receptor and the HA-tagged receptor was subsequently identified on immunoblotting using an anti-HA antibody. Similarly the biophysical technique, Bioluminescent Resonance Energy Transfer (BRET) demonstrated H_4R homo-dimers in COS-7 cell membranes.

As with the H_3R, H_4R dimers appear to be constitutively expressed even in the absence of ligand. A number of studies have investigated the effect of agonists on receptor oligomerization. However, at present the effects of ligand stimulation on GPCR oligomerization are not consistent. It has been found that agonists can promote or reduce GPCR oligomerization, or are without effect on GPCR oligomerization. (Angers *et al*, 2002; George *et al*, 2002; Pfleger & Eidne, 2005). In the case of the H_4R, our collaborators at the Vrije University, The Netherlands did not detect any significant difference in BRET signal when cells were treated with either the H_4R agonist histamine, the neutral H_4R antagonist iodophenpropit (Lim *et al*, 2005) or the

inverse H_4R agonist thioperamide (Lim *et al*, 2005; Morse *et al*, 2001), suggesting that H_4R ligands do not modulate H_4R homo-oligomerization. These findings were confirmed at physiological expression levels of the H_4R (van Rijn *et al*, 2006), since previously it has been reported that agonist induced oligomerization of somatostatin receptors was only detected at physiological expression levels, but not after over-expression (Patel *et al*, 2002). Similarly, no agonist or inverse agonist induced modulation of H_4R oligomerization was detected in the *tr*-FRET assay (van Rijn *et al*, 2006). Nevertheless, one should be aware that results concerning ligand effects on dimerization obtained with these biophysical assays can be difficult to interpret, since agonist induced changes in H_4R conformation could potentially influence the energy transfer between the energy acceptor and donor (Angers *et al*, 2000).

The anti-H_4R antibody was also used to investigate the expression and potential role of the newly described human H_4R isoforms: $hH_{4\ (302)}$ and $hH_{4\ (67)}$. Immunoprecipitation experiments in this chapter confirmed *tr*-FRET data (van Rijn *et al*, submitted) supporting the existence of hetero-oligomers between the full length receptor and the two shorter versions. Since mRNA coding for all three isoforms is found in several white blood cell types, hetero-oligomerisation may occur in native tissue. The two new isoforms are both non-functional as regards ligand binding and signalling. However they may play a regulatory role since they reduce histamine binding to the $H_{4\ (390)}$ receptor by 55% ($H_{4\ (302)}$) and 30% ($H_{4\ (67)}$). Biotinylation of intact cells was used to assess surface expression of the three isoforms. All three were expressed at the cell surface, although this is a minor population, presumably due to the high levels of expression possible with the lipofectamine transfection method. Furthermore co-expression of the $H_{4\ (390)}$ with either $H_{4\ (302)}$ or $H_{4\ (67)}$ resulted in

reduced surface expression of the full length receptor, as might be expected from their effect on ligand binding. These results provide further evidence to support the role of splice isoforms as dominant negative regulatory elements, which maybe a common theme in GPCR regulatory pathways.

Our novel anti-H_4R antibody clearly shows higher molecular weight species in immunoblots of both recombinant and native H_4Rs. Since the other three histamine GPCRs are all known to form homo-dimers (previous chapter), it is highly probable that the H_4R also dimerises. The presence of H_4R homo-dimers is supported here by results obtained from three different strategies: chemical cross-linking, nickel column isolation and BRET. Nevertheless, the observed sizes are not always completely consistent with H_4R dimers. There are several possible explanations for this, including novel H_4R isoforms and post-translational changes such as glycosylation and palmitoylation. In the cross-linking experiment (Fig 5.11), the monomer was resolved into four distinct bands which could represent different levels of monomer glycosylation. Also in the cross-linking studies (Fig 5.11), the higher molecular weight species are diffuse which may again be due to heterogeneous receptor glycosylation. Both the H_3R and the H_4R have potential glycosylation sites. Therefore the question of receptor glycosylation has been investigated further in Chapter 6.

CHAPTER 6

THE ROLE OF N-GLYCOSYLATION IN DIMERISATION AND PHARMACOLOGY OF H_3 AND H_4 RECEPTORS

6.1 OBJECTIVES

Demonstrate that H_3 and H_4 receptors are glycoproteins and to investigate the role of N-glycosylation in expression, dimerisation and pharmacology.

6.2 INTRODUCTION

As with many proteins expressed on the cell surface, GPCR's are glycosylated, and the N-terminal extra-cellular domain is the site of carbohydrate attachment. Both the H_3 and H_4Rs have potential sites for N-linked glycosylation: H_3R at N11, H_4R at N5 and N9 (Fig 6.1 putative glycosylation sites of H_3 and H_4 receptors). Relatively little is known about the effect of glycosylation on the function of GPCRs. N-glycosylation of the N-terminus of the human formyl peptide receptor (FPR) has been shown to be important for constitutive FPR activity (Seifert & Wenzel-Seifert, 2003). It does not appear to be essential for the production of a functional ligand binding pocket (Strader *et al*, 1994), but it has been shown to be important for appropriate processing and trafficking of many GPCRs to the membrane. Interestingly, glycosylation appears to have a differential role in H_1 and H_2 histamine receptor pharmacology (Mitsuhashi & Payan, 1989; Fukushima *et al*, 1995).

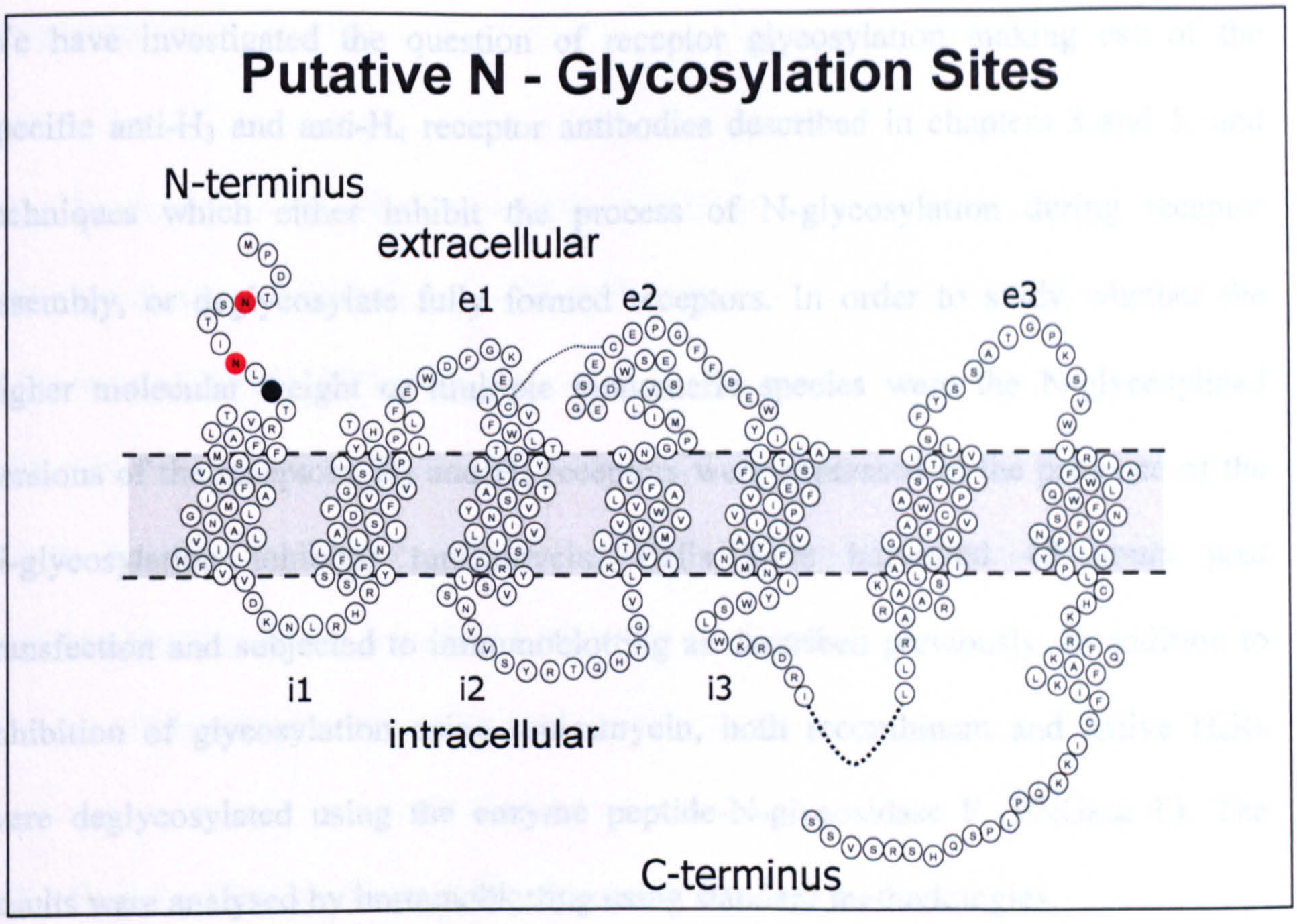

Fig 6.1 Putative sites of N-glycosylation

In the N-terminus of the the hH_3R Asn^{11} is a potential site for N-glycosylation (•), for the hH_4R there are two potential sites (•) at Asn^5 and Asn^9.

In the previous chapters, immunoblots of both recombinant and native hH_3 (Fig 3.5 recombinant; Figs 3.8 and 3.9 native) and hH_4 receptors (Fig 5.7) have clearly demonstrated the presence of higher molecular weight species. We have provided evidence for receptor dimers which can account for some of these immunoreactive species. However, receptor glycosylation is also likely to contribute to this heterogeniety. The larger protein bands often appear diffuse (Figs 3.5 and 5.7 for H_3R and H_4R respectively) which can be a characteristic of glycosylated receptors, and on some gels the monomers are resolved into multiple bands (Figs 4.4a and 4.5a for the H_3R; Fig 5.11 for the H_4R) which could correspond to different levels of monomer glycosylation.

We have investigated the question of receptor glycosylation making use of the specific anti-H_3 and anti-H_4 receptor antibodies described in chapters 3 and 5, and techniques which either inhibit the process of N-glycosylation during receptor assembly, or deglycosylate fully formed receptors. In order to study whether the higher molecular weight or multiple monomeric species were the N-glycosylated versions of the receptors, H_3 and H_4 receptors were expressed in the presence of the N-glycosylation inhibitor tunicamycin. Cells were harvested 48 hours post transfection and subjected to immunoblotting as described previously. In addition to inhibition of glycosylation using tunicamycin, both recombinant and native H_4Rs were deglycosylated using the enzyme peptide-N-glycosidase F (PNGase F). The results were analysed by immunoblotting using standard methodologies.

In order to determine whether N-glycosylation is important in ligand binding, cells expressing hH_3 (445) and grown in increasing concentrations of tunicamycin were harvested and assayed using the selective H_3R antagonist radioligand, [^{3}H]-clobenpropit.

6.3 METHODS

6.3.1 Tunicamycin experiments with recombinant H_3 and H_4 receptors

Glycosylation was inhibited using the antibiotic tunicamycin as described previously (Chazot *et al*, 1995). HEK 293 cells expressing histamine receptors were incubated with increasing concentrations of tunicamycin ranging from 0 - 8 μg/ml (stock dissolved in DMSO at 2 mg/ml) immediately after transfection and harvested 48 h post-transfection, homogenized and subjected to immunoblotting. Cells grown in the absence of tunicamycin were incubated with the respective volume of DMSO.

6.3.2 Deglycosylation of native H_4 receptor

Human PHA blast cell suspensions were resuspended in deglycosylation buffer (50μM sodium phosphate pH 6.0, containing 0.1% SDS, 0.1% β-mercaptoethanol and 20mM EDTA) and incubated with either water (control) or PNGase F enzyme (Sigma, UK) at a final enzyme concentration of 400iu/ml (test) for 16 hours at 37°C. The samples were then subjected to immunoblotting and probed with anti-H_4 374-390 antibody at a concentration of 2μg/ml. The NMDAR1 transfected into HEK 293 cells was used as a positive control essentially as described previously (Chazot *et al*, 1992).

6.3.3 Specific binding of [^{3}H]-clobenpropit to recombinant H_3 receptors

[^{3}H]-clobenpropit binding was performed essentially as described previously (Harper *et al*, 1999). We have evidence that clobenpropit acts as a neutral antagonist in this system (Victoria Hann PhD thesis, 2004). Briefly, HEK 293 cell homogenates expressing H_3 receptors (100-400 μg protein) were incubated, in triplicate for 3 hours at room temperature, with 50μl of metyrapone (3mM) and 50μl of [^{3}H] clobenpropit

(0.2nM) in 20mM HEPES buffer pH7.4, to a final volume of 500µl. Non-specific binding was defined using 50µl of R-alpha-methylhistamine (10^{-5}M). The assay was terminated by rapid filtration through Whatman GF/B filters pre-soaked in 0.3-1% polyethylenimine, which were washed (3x3ml) using ice cold 10mM sodium phosphate buffer pH 7.4, using a Brandell cell harvester. Filters were transferred into scintillation vials and 1ml of optiphase safe liquid scintillation cocktail was added. After 3 hours the bound radioactivity was determined by counting (3 minutes) in a Beckman liquid scintillation counter.

6.4 RESULTS

6.4.1 Human H_3 receptors are N-glycosylated and prevention of N-glycosylation does not have a major effect upon [^{3}H]-clobenpropit binding to the hH_3 445 receptor

The effect of increasing concentrations of tunicamycin was investigated using immunoblotting and radioligand binding assays with [^{3}H] clobenpropit. Cells transfected with the hH_3 445 receptor and grown in the absence of tunicamycin, yielded, upon immunoblotting, a closely spaced doublet immunoreactive species (M_r 47,000 and M_r 45,000), consistent with the presence of a glycosylated and non-glycosylated hH_3 receptor monomer, respectively. As previously reported, a range of higher molecular weight putative oligomers were also detected (Shenton *et al*, 2005), (Chapters 3 and 4).

Incubation of HEK cells transfected with the hH_3 445 with increasing concentrations of the N-glycosylation inhibitor, tunicamycin, dose-dependently reduced the molecular weight of the M_r 47,000 immunoreactive species to the M_r 45,000 immunoreactive species (Fig 6.2 A). This suggests that the hH_3 445 receptor is indeed modestly N-glycosylated, consistent with the predicted single putative glycosylation site. Inhibition of glycosylation did not appear to affect the size of the higher oligomers, however immunoreactivity was very strong in this region, therefore it is possible that modest reductions in size could have been masked on these particular immunoblots. As shown below, both inhibition of glycosylation using tunicamycin and deglycosylation with the enzyme PNGase do appear to affect the size of dimeric species in the case of the H_4R.

In parallel, cell samples were subjected to [^{3}H]-clobenpropit binding analysis, to assess whether N-glycosylation is absolutely required for ligand binding to the hH_3 445 receptor. Near complete prevention of N-glycosylation using 0.1 μg/ml tunicamycin resulted in no significant reduction in [^{3}H]-clobenpropit binding, while complete prevention, yielded only a modest 33% reduction in specific binding (Figure 6.2 B).

A

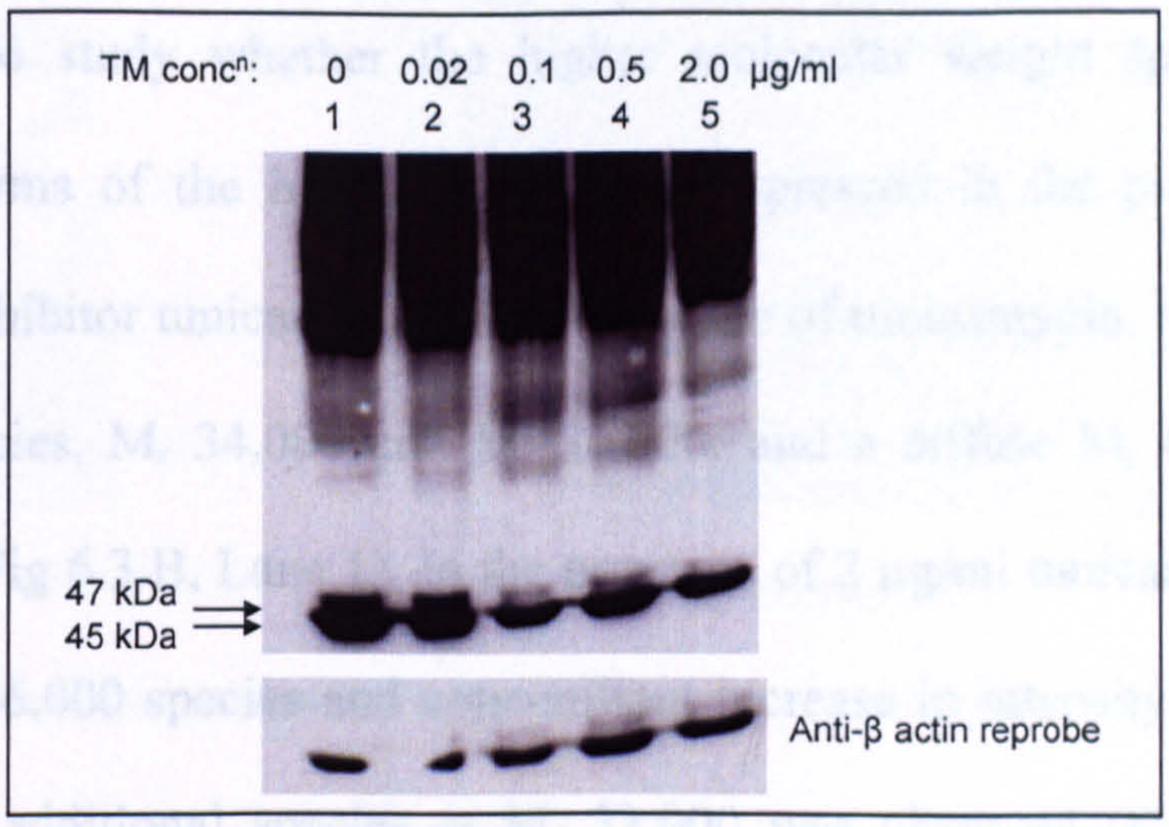

B

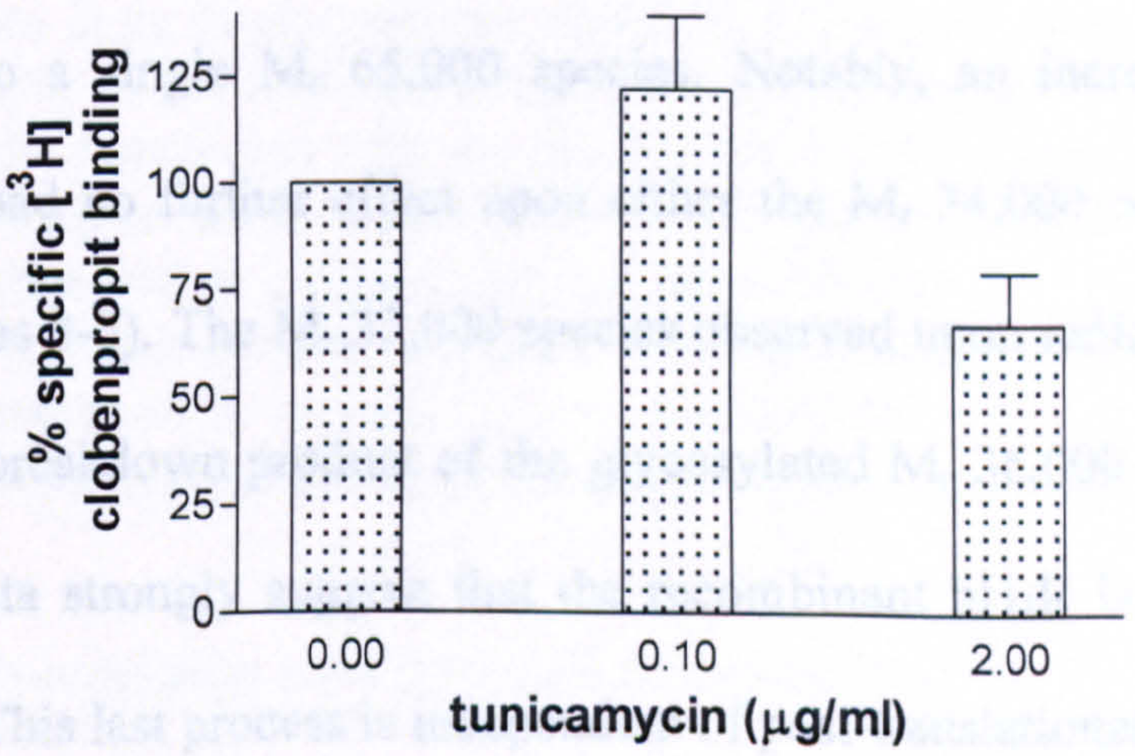

Fig 6.2 N-glycosylation inhibition of the human H_3 445 receptor

FLAG-tagged hH_3 445 receptors expressed in HEK 293 cells were incubated with increasing concentrations of tunicamycin (TM), harvested 48h post-transfection and subjected, in parallel to immunoblotting (A) and [^{3}H]-clobenpropit binding assays (B).

(A) Lane 1 FLAG-tagged hH_3 445 expressed in HEK 293 cells without tunicamycin; Lane 2-5 FLAG-tagged hH_3 445 expressed in HEK 293 cells grown in the presence of 0.02, 0.1, 0.5, and 2 µg/ml tunicamycin. The lower panel shows the same blot reprobed with anti-β actin antibody (1:800) as a control to confirm that total protein levels are very similar in each lane. Representative immunoblot, replicated twice more with similar results.

(B) FLAG-tagged hH_3 445 expressed in HEK 293 cells grown in the absence and presence of 0.02, 0.1, 0.5, and 2 µg/ml tunicamycin (mean ± SD for triplicate determinations from two independent transfections).

6.4.2 Biochemical evidence that the hH_4R is an N-glycosylated homo-dimer

In the N-terminus of the hH_4R Asn^5 and Asn^9 are potential sites for N-glycosylation (Fig 6.3 A). To study whether the higher molecular weight species are the N-glycosylated forms of the hH_4R, H_4Rs were expressed in the presence of the N-glycosylation inhibitor tunicamycin. In the absence of tunicamycin, two major putative monomeric species, M_r 34,000 and M_r 36,000; and a diffuse M_r 65-75,000 species were detected (Fig 6.3 B, Lane 1). In the presence of 2 μg/ml tunicamycin, a complete loss of the M_r 36,000 species and concomitant increase in intensity of the M_r 34,000 species and an additional species at M_r 32,000 was observed (Fig 6.3 B, lane 2). Furthermore, the diffuse M_r 65-75,000 species, detected in the absence of tunicamycin, was reduced to a single M_r 65,000 species. Notably, an increase in tunicamycin concentration had no further effect upon either the M_r 34,000 or M_r 65,000 species (Fig 6.3 B, lanes 3-5). The M_r 32,000 species observed upon tunicamycin treatment is likely to be a breakdown product of the glycosylated M_r 36,000 species in untreated cells. These data strongly suggest that the recombinant hH_4R is N-glycosylated and forms dimers. This last process is independent of post-translational N-glycosylation.

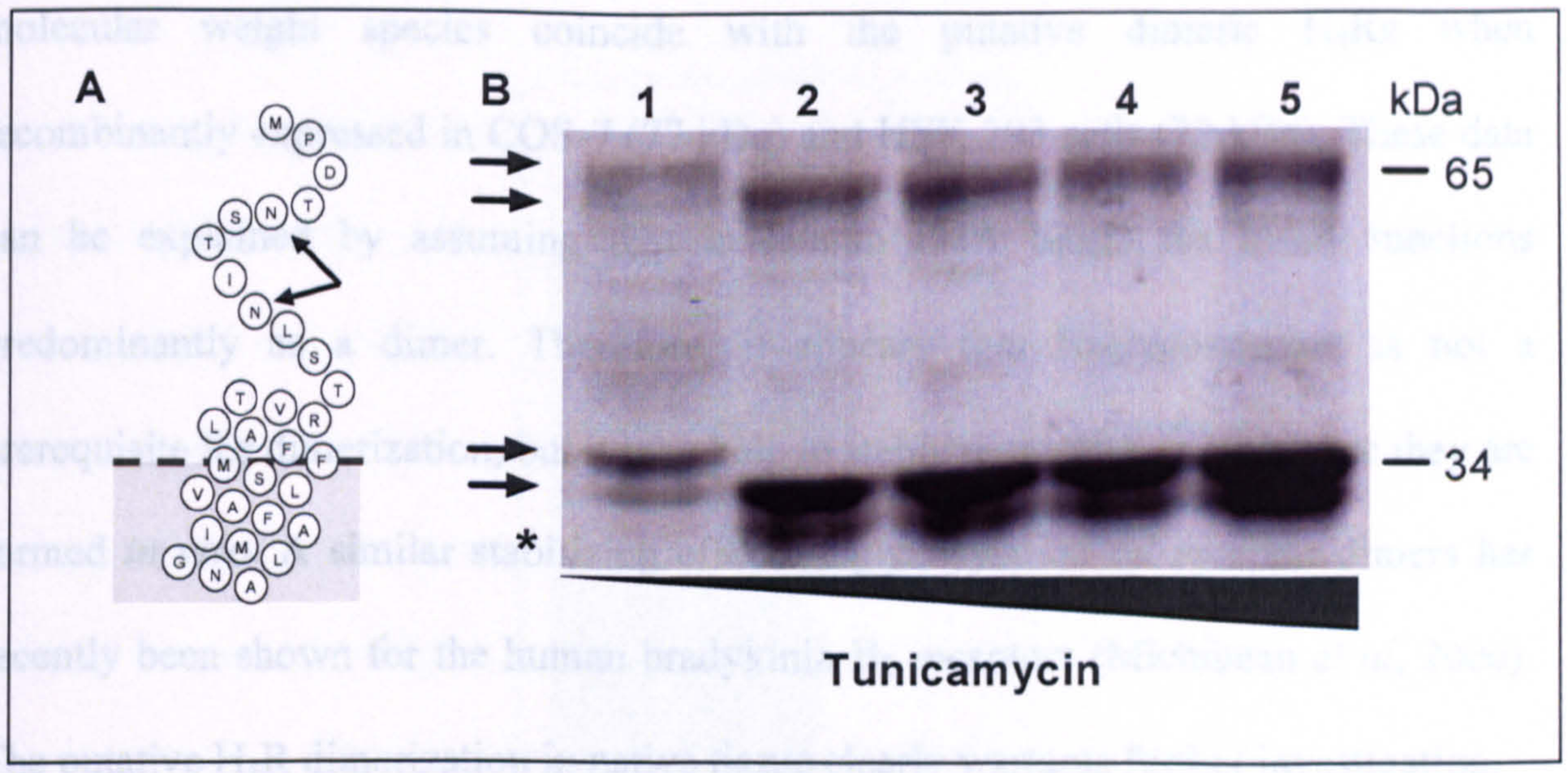

Fig 6.3 The effect of inhibition of glycosylation on the expression of human H_4R in HEK 293 cells.

The hH_4 receptor is an N-glycosylated dimer. *A* Snakeplot of the N-terminal tail and beginning of TM1 of the H_4R, arrows are directed to possible N-glycosylation sites. *B*, HEK 293 cells transfected with the hH_4R were grown in the absence and presence of 2, 4, 6 and 8 μg/ml tunicamycin for 48h. The cells were harvested, homogenates prepared and subjected to immunoblotting. Immunoblots were probed with the anti-hH_4 (374-390) receptor antibody. Lane 1, hH_4Rs in absence of tunicamycin; Lanes 2-5, hH_4Rs in presence of 2, 4, 6 and 8 μg/ml tunicamycin, respectively. Representative immunoblot from two sets of independent transfection experiments.

Enzymatic deglycosylation of human H_4R expressed in HEK 293 cells (Fig 6.4) gave a similar result to inhibition of glycosylation with tunicamycin (Fig 6.3 B). The monomeric species decreased from Mr 36,000 to the deglycosylated Mr 34,000 species, a putative breakdown product of the glycosylated monomer was again observed at Mr 32,000 (Fig 6.4, lane 2). Interestingly, the endogenously expressed H_4R in human PHA blasts was only detected as high molecular weight species (Fig 6.5, lane 1). Notably, upon enzymic N-deglycosylation of PHA blasts, the Mr 77,000 species was greatly reduced in intensity, and a new Mr 34,000 species was detected, consistent with the monomeric hH_4R (Fig 6.5, lane 2). These data do not directly exclude a heavily glycosylated (ca.33 kDa) H_4R protein. However the hH_4Rs in human HEK 293 cells are only moderately glycosylated (ca. 2 kDa) and the high

molecular weight species coincide with the putative dimeric H_4Rs when recombinantly expressed in COS-7 (77 kDa) and HEK 293 cells (72 kDa). These data can be explained by assuming that in human PHA blasts the hH_4R functions predominantly as a dimer. Therefore, it appears that N-glycosylation is not a prerequisite for dimerization, but it may help to stabilize the H_4R dimers once they are formed *in vivo*. A similar stabilizing effect of glycosylation on receptor dimers has recently been shown for the human bradykinin B_2 receptors (Michineau *et al*, 2006). The putative H_4R dimerization in native tissue clearly warrants further investigation.

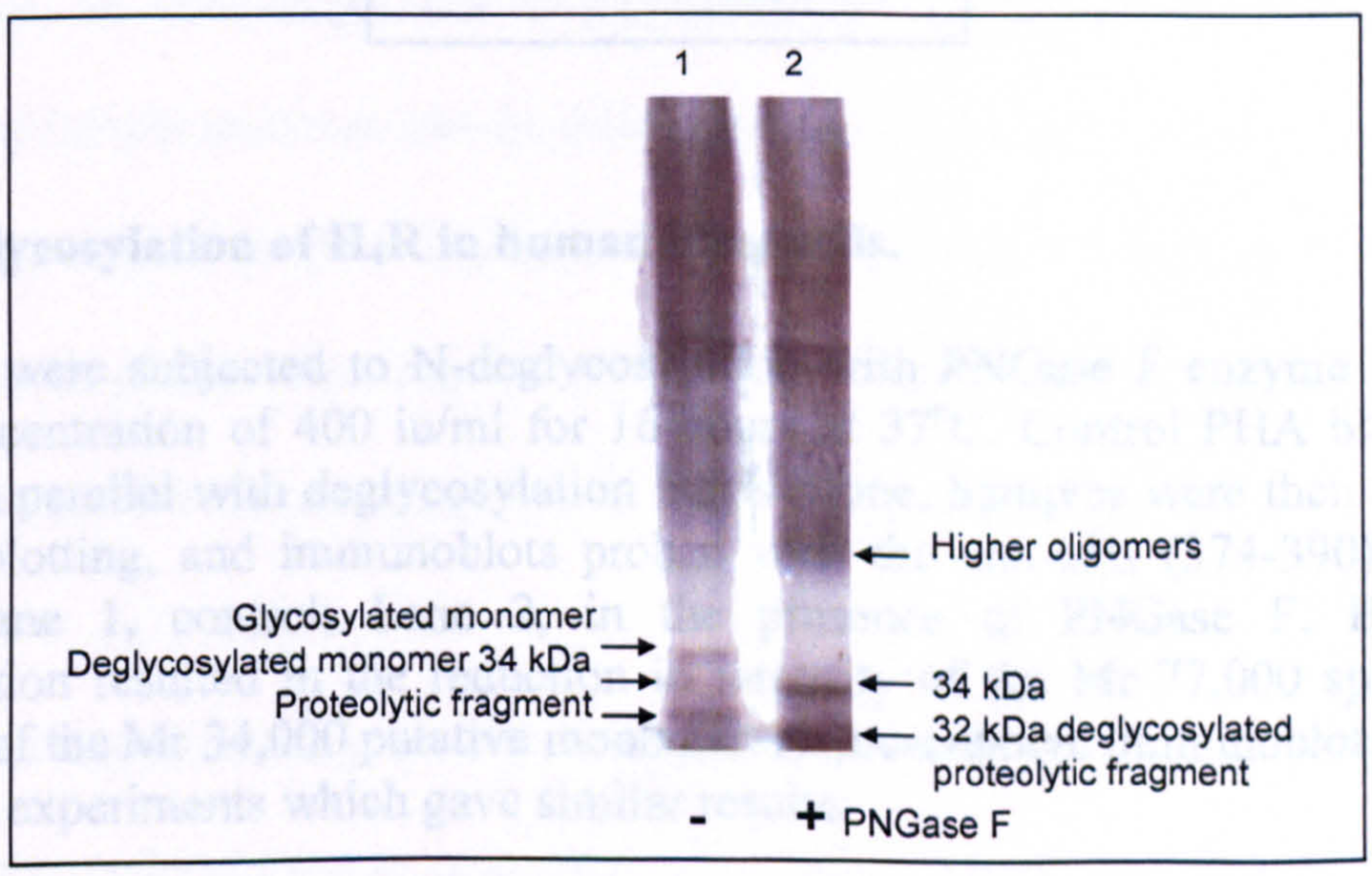

Fig 6.4 Deglycosylation of human H_4R expressed in HEK 293 cells.

Cell homogenates were subjected to N-deglycosylation with PNGase F enzyme at a final enzyme concentration of 400 iu/ml for 16 hours at 37°C. Control cells were incubated in parallel with deglycosylation buffer alone. Samples were then subjected to immunoblotting, and immunoblots probed with the anti-hH_4 (374-390) receptor antibody. Lane 1, control; Lane 2, in the presence of PNGase F. Enzymatic deglycosylation resulted in the reduction of monomeric species to Mr 34,000. The species apparent at approximately Mr 32,000 was presumed to be a breakdown product of the glycosylated monomer. There was also a decrease in the overall molecular size of the putative higher oligomers. This experiment was performed once but gave a result identical to inhibition of glycosylation with tunicamycin.

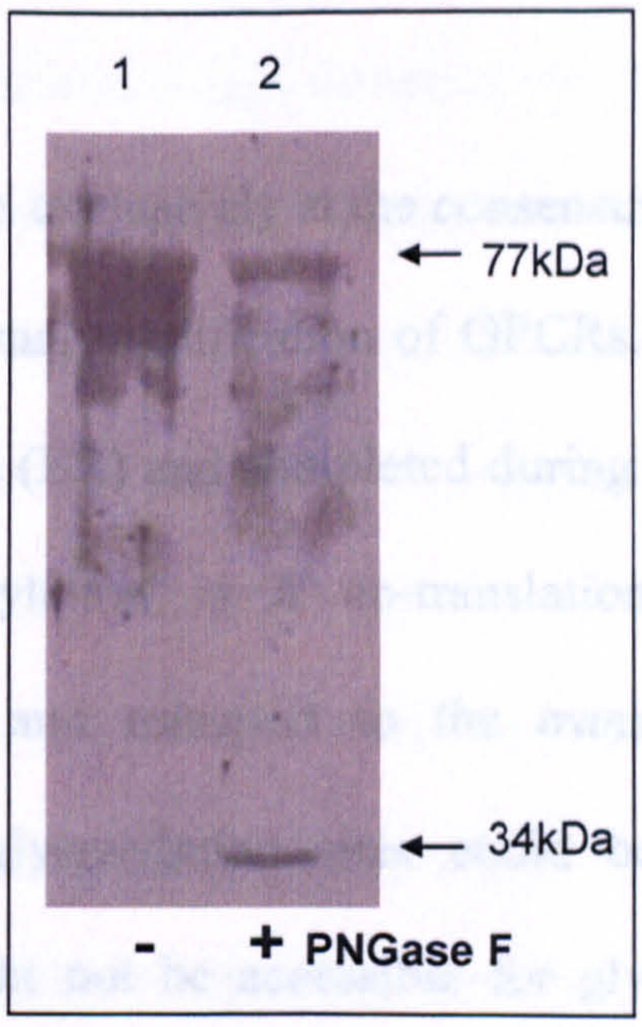

Fig 6.5 Deglycosylation of H_4R in human blast cells.

PHA blasts were subjected to N-deglycosylation with PNGase F enzyme at a final enzyme concentration of 400 iu/ml for 16 hours at 37°C. Control PHA blasts were incubated in parallel with deglycosylation buffer alone. Samples were then subjected to immunoblotting, and immunoblots probed with the anti-hH_4 (374-390) receptor antibody Lane 1, control; Lane 2, in the presence of PNGase F. Enzymatic deglycosylation resulted in the reduction in intensity of the Mr 77,000 species and appearance of the Mr 34,000 putative monomer. Representative immunoblot from two independent experiments which gave similar results.

6.5 DISCUSSION

N-linked glycosylation occurs exclusively at the consensus sequence NXS/T and is the most common post-translational modification of GPCRs. N-glycosylation is initiated in the endoplasmic reticulum (ER) and completed during transport through the Golgi. Strictly speaking N-glycosylation is a co-translational process and continues throughout protein folding and transport to the *trans*-Golgi. Differences in the glycosylation of potential glycosylation sites could be due to three-dimensional considerations, all sites might not be accessible for glycosylation. With increasing knowledge of GPCR structure and its relation to function there is now a great deal of interest in the role of co/post-translational changes, including N-glycosylation. The human histamine H_3 and H_4 receptors both have potential N-glycosylation sites within the extra-cellular N-terminus: H_3 at Asn^{11}; H_4 at Asn^5 and Asn^9.

In this chapter experiments have been undertaken to show whether the potential sites are indeed glycosylated, and to investigate the purpose of H_3 and H_4R glycosylation. Both receptors were expressed in HEK 293 cells in the presence of tunicamycin. The antibiotic tunicamycin blocks the transfer of GlcNAc-1-P from UDP-GlcNAc to dolichol phosphate, thereby blocking the synthesis of N-linked oligosaccharide chains on glycoproteins. Inhibition of glycosylation by tunicamycin clearly demonstrated that both histamine receptor subtypes are indeed glycosylated.

In the case of the H_3R tunicamycin dose-dependently reduced the molecular weight of the monomeric M_r 47,000 immunoreactive species to the M_r 45,000 immunoreactive species. There was no obvious effect on the amount or size of higher molecular weight

species. The fact that the amount of larger species was not altered suggests that glycosylation is not a prerequisite for H_3R dimerisation. In a study of AT1 receptor N-glycosylation (Lanctot *et al*, 2005) it was found that mutant mono-glycosylated and aglycosylated receptors had a greater tendency to aggregate as dimers and trimers, however we found no evidence of this with the deglycosylated H_3R. One might have expected the oligomeric species to be reduced in size at the same time as the monomer. Considering that the H_3R has only one potential glycosylation site, and glycosylation of the monomer suggests that it undergoes only moderate glycosylation (+2 kDa), any decrease in the molecular weight of the oligomeric species would probably result in only a minimal reduction in mobility on the gel.

With the H_4R expressed in HEK 293 cells in the absence of tunicamycin, two major putative monomeric species, M_r 34,000 and M_r 36,000, were observed and a diffuse M_r 65-75,000 species (Fig 6.3 B, lane 1). In the presence of 2 μg/ml tunicamycin the Mr 36,000 species was lost with a concomitant increase in intensity of the M_r 34,000 species together with the appearance of an additional species at M_r 32,000 (Fig 6.3 B, lane 2). Furthermore, the diffuse M_r 65-75,000 species, detected in the absence of tunicamycin, was reduced to a single M_r 65,000 species. Notably, an increase in tunicamycin concentration had no further effect upon either the M_r 34,000 or M_r 65,000 species (Fig 6.3 B, lanes 3-5). The M_r 32,000 species observed upon tunicamycin treatment could be a breakdown product of the glycosylated M_r 36,000 species in untreated cells. Alternatively the doublet could arise from some other post-translational change not affected by the presence of tunicamycin, both the 34,000 and 32,000 bands could be the deglycosylated versions of the monomeric species. These data strongly suggest that the recombinant hH_4R is N-glycosylated and forms dimers.

This last process is independent of post-translational N-glycosylation. It was not possible to determine whether both of the two potential glycosylation sites are actually glycosylated to any appreciable degree. In the canine histamine H_2R only two of the three potential sites for N-glycosylation, Asn^4 and Asn^{162} were primarily utilized (Fukushima *et al* 1995).

The enzyme peptide-N-glycosidase F (PNGase F) removes N-linked carbohydrates from both immature and mature glycoproteins modified with complex, fully processed carbohydrates. Enzymatic deglycosylation of human H_4R expressed in HEK 293 cells (Fig 6.4) gave a similar result to inhibition of glycosylation with tunicamycin (Fig 6.3 B). Three monomeric species were detected in the untreated cell homogenate: one at Mr 36,000 likely to be the glycosylated monomer, a much fainter band at Mr 34,000 probably the deglycosylated monomer and a band just below this thought to be a proteolytic fragment of the monomer (Fig 6.4, lane 1). The putative H_4R monomer was reduced from Mr 36,000 to 34,000 by the action of PNGase F, the size of the supposed proteolytic fragment decreased to Mr 32,000 indicating that it had also been deglycosylated (Fig 6.4, lane 2). There was simultaneously a decrease in the lowest extent of the diffuse band arising from putative higher H_4R oligomers.

Enzymatic deglycosylation of native H_4R was also undertaken in human PHA plasts. H_4 receptors were only detected as higher molecular weight oligomers in untreated cells (Fig 6.5, lane 1). Upon enzymic N-deglycosylation of PHA blasts, the Mr 77,000 species was greatly reduced in intensity, and a new Mr 34,000 species was detected, consistent with the monomeric hH_4R (Fig 6.5, lane 2). It is possible that the high molecular weight band at Mr 77,000 is a heavily glycosylated H_4R monomer rather

than a receptor dimer. However H_4R expressed in HEK 293 cells are only moderately glycosylated (ca. 2 kDa). In addition oligomeric forms of both the H_3R and H_4R appear to predominate in native tissue preparations (Figs in Chapters 3 and 5 respectively). Although data presented here suggest that glycosylation is not essential for receptor dimerisation, it may be that it helps to stabilize the H_4R dimers. Thus deglycosylation of the receptors with PNGase F results in some of the dimers breaking down into their constituent monomers. A similar stabilizing effect of glycosylation on receptor dimers has recently been shown for the human bradykinin B_2 receptors (Michineau *et al*, 2006). In this study a range of processes including sialylation of O-linked polysaccharide, N-glycosylation, disulphide bonding and processes as yet unknown, were found to be involved in B2 receptor dimerisation. This matter clearly warrants further investigation. Interestingly in immunoblots of human spleen lysate (Fig 5.9 A) bands were detected at Mr 31,000, compatible with the monomer; and Mr 59,000 and 66,000; potentially glycosylated receptors and/or receptor dimers. Comparing these sizes with those obtained for nonglycosylated receptors it appears that the H_4R in spleen cells may be predominantly the nonglycosylated versions. This could also account for the presence of the H_4R monomer in spleen lysate, because if glycosylation does indeed stabilize the dimers one might expect to find more of the monomer in tissues where the receptor is not glycosylated. It is known that the glycosylation state of transmembrane receptors can vary significantly in different tissue types (Heidenreich & Brandenburg, 1986; Muller *et al*, 2002). In addition the glycosylation state of the β_1AR in particular is known to be regulated via polymorphic variation between individuals (Rathz *et al*, 2002). Thus it appears that glycosylation can be regulated differentially between tissues and between individuals.

To assess whether N-glycosylation is absolutely required for ligand binding to the hH_3 445 receptor, cells expressing H_3R and grown in the presence of tunicamycin were subjected in parallel to [^{3}H]-clobenpropit binding analysis. Near complete prevention of N-glycosylation using 0.1 μg/ml tunicamycin resulted in no significant reduction in [^{3}H]-clobenpropit binding, while complete prevention, yielded only a modest 33% reduction in specific binding (Fig 6.2 B). This was perhaps not surprising since the putative glycosylation site on Asn^{11} is not within the ligand binding pocket, in addition it appears to be only moderately glycosylated and therefore unlikely to have a large steric effect on TM domains which are involved in agonist binding. N-glycosylation of the canine H_2R was not required for cell surface localization, ligand binding or functional coupling to G-proteins (Fukushima *et al*, 1995). Conversely for the histamine H_1R, the glycosylation inhibitors tunicamycin and swainsonine inhibited the expression of high affinity pyrilamine binding sites during differentiation of cultured smooth muscle cells, BC3H1 (Mitsuhashi & Payan, 1989). The molecular weight of high affinity [^{3}H]-pyrilamine binding sites on differentiated cells was approximately Mr 68,000, which after treatment with N-glycanase was shifted to Mr 40,000, a molecular weight similar to that of low affinity [^{3}H]-pyrilamine binding sites on undifferentiated cells. These data suggest that one element contributing to H_1 receptor heterogeneity is receptor N-glycosylation.

The majority of secreted and cell surface proteins that transit to the cell surface through the endoplasmic reticulum (ER) are N-glycosylated (95% of GPCRs) (Lanctot *et al*, 2005). In order for a GPCR to elicit intracellular signalling appropriately the right quantity of properly folded functional receptors must be available in the plasma membrane. It is equally essential that the signalling can be terminated at the proper

time and the receptors either recycled or permanently degraded. The regulatory mechanisms controlling export trafficking of GPCRs, including glycosylation, have recently been reviewed (Duvernay *et al*, 2005).

The role of post-translational changes to receptors is complex and an area where there is a great deal of interest. The functions of N-linked glycosylation are manifold and vary not only between different GPCRs but may also depend on the stage of differentiation of the cell (Mitsuhashi & Payan, 1989). Several studies have shown that glycosylation is involved in GPCR transport from the ER through the Golgi to the cell surface (reviewed in Duvernay *et al*, 2005). In this chapter it has been clearly demonstrated that both the H_3 and H_4 receptors are indeed N-glycosylated, although the immunoblot evidence suggests that they are not heavily glycosylated. **Receptor dimerisation does NOT appear to be dependent on glycosylation.** However, in the case of endogenous H_4R expressed in human PHA blasts, deglycosylation appears to destabilise the preformed dimeric species to individual monomers. It has been shown that human bradykinin B2 receptor dimers result from heterologous association of differently glycosylated mature receptors (Michineau *et al*, 2006). Importantly, receptor sialylation and N-glycosylation participate with disulphide bonding in the stabilisation of the cell surface B2R dimers. For growth factor receptors, such as the epidermal growth factor receptor, N-glycosylation strongly regulates receptor dimerisation and autophosphorylation (Fernandes *et al*, 2001). By contrast the involvement of N-glycosylation in GPCR dimerisation has not been widely reported though it has been described for β1-adrenergic homo-dimerisation (He *et al*, 2002) and for α2A- and β1-adrenergic receptor hetero-dimerisation (Xu *et al*, 2003), where it has been a positive and negative regulator respectively. Furthermore for the H_3R lack of

N-glycosylation did not appear to affect binding of the selective H_3R agonist [^{3}H]-clobenpropit. Clearly the location of glycosylated sites will determine their likely affect on receptor pharmacology. On the H_3R the Asn^{11} glycosylation site is not close to the regions thought to participate in agonist binding, in addition the site appears to be only moderately glycosylated. A study using artificial N-glycosylation sequons engineered into the human angiotensin II receptor subtype 1 (hAT1) (Lanctot *et al*, 2005) was used to explore the importance of N-glycosylation positioning for cell-surface expression, targeting, affinity and quality control of the hAT1 receptor. Glycosylation within e1 had a major influence on the pharmacological properties, while glycosylation within e2 did not affect the level of cell surface expression but the receptor was misfolded and therefore non-functional; glycosylation within e3 caused a significant decrease in membrane expression. Site-directed mutagenesis of the putative sites would confirm the location of the N-glycosylation sites, and functional studies would be useful to address the role of this post-translational modification on cell surface H_3 and H_4 histamine receptors.

CHAPTER 7

GENERAL DISCUSSION

During the course of this PhD project, new antibodies specific to the two most recent histamine receptors H_3R and H_4R have been generated and validated (Chapters 3 and 5). These novel immunological tools have been used to characterise the structural and molecular pharmacological properties of the rodent and human H_3R and H_4R receptors. A number of key hypotheses have been addressed:

1) Histamine H_3 and H_4 receptors are able to homo-oligomerise

Cross-linking experiments have confirmed the presence of homo-dimers for human and rodent H_3R and human H_4R. Furthermore these higher molecular weight species are evident both in recombinant expression systems and native tissue. There is an indication that some splice variants may have a greater potential to oligomerise than others. Results suggested that the $hH_{3\ (329)}$ formed homo-oligomers more readily than the $hH_{3\ (445)}$. In the case of rat H_3 receptors, $rH_{3\ (C)}$ dimers were not observed while $H_{3\ (A)}$ dimers were clearly evident. There was also evidence for interspecies differnces in receptor oligomerisation. In human putamen putative dimeric H_3R species were detected, similarly for endogenous hH_4R, oligomeric species were predominant. In contrast to this in rodent brain monomeric species were detected rather than receptor oligomers using the anti-rH_3 (268 – 277)/anti-$hH_{3\ (445)}$ antibody. The cross-linking evidence was corroborated by a range of biophysical and biochemical techniques for both the H_3 and H_4 receptors (Chapters 4 and 5).

2) Human H_3 and H_4 receptors are able to hetero-oligomerise with their respective splice variants

Both H_3 and H_4 receptors undergo alternative splicing, and many of these splice variants have overlapping expression profiles *in vivo.* This offers up the possibility that splicing may be a way of regulating the structure and function of these receptors. *Tr*-FRET experiments provided the first *in vitro* evidence for the existence of hH_3R hetero-oligomers, consisting of the full length receptor together with a shorter isoform. For the hH_4R immunoprecipitation was used to confirm the existence of hetero-oligomers *in vitro*.

Histamine H_3 and H_4 receptors are therefore able to form both homo- and hetero-oligomers. These appear to be robust, stable oligomers and histamine is not necessary for their formation.

3) Splice variants can act as dominant negative regulatory subunits

The human H_3 isoforms show differential tissue distribution, however in some brain regions several variants are expressed together. The 445 and 329 isoforms are co-expressed in key locations including the basal ganglia, a focus of this thesis (See Chapter 3). Ebenshade *et al*, 2006 reported that the 445 and 329 isoforms displayed a similar binding affinity for [^{3}H]-NAMH, however the total binding to the 329 was approximately five-fold less than to the 445. In the same study the 329 isoform was also incapable of activating calcium signalling responses to RAMH. We have limited preliminary data (not presented in this thesis) to suggest that while the 329 isoform does not itself bind the selective H_3 antagonist [^{3}H]-clobenpropit, it is able to dramatically reduce binding of this ligand to the 445 receptor. If confirmed these data

concur with the dominant negative nature of rat H_3 isoforms (Bakker *et al.*, 2006). This paper also provided the first evidence that isoform expression can be controlled by neuronal activity *in vivo*, which may have significant implications in situations of excessive excitatory transmission (eg. epilepsy).

mRNA encoding all three of the H_4R isoforms known to date is found in a number of different types of white blood cells (van Rijn *et al.*, manuscript submitted). Neither of the truncated H_4 isoforms can bind or transduce a signal. On co-expression with the full length $H_{4\ (390)}$ receptor the number of histamine binding sites is reduced by 55% (390 + 302) and 30% (390 + 67), which concurred with surface expression studies performed in this thesis (Chapter 5).

Therefore, splice variants may act as dominant negative regulatory subunits in many, if not all, GPCRs. This is analogous to the situation which is also apparent in the ligand-gated channel superfamily, e.g. the NR_3 subunits of the NMDA receptor act as a dominant negative subunit to reduce calcium permeability (function) of this key excitatory receptor. It would be interesting to assess whether histamine H_4R isoform expression is also controlled in an activity dependent manner.

4) N-glycosylation is a prerequisite for receptor dimerisation

Most, if not all GPCRs, are assumed to be N-linked glycoproteins, although this has not been formally proved. Histamine H_3 and H_4 receptors were expressed in HEK 293 cells in the presence of the N-glycosylation, inhibitor tunicamycin. Immunoblot analysis of cell homogenates confirmed that both receptors were indeed N-glycosylated. Interestingly, inhibition of N-glycosylation did **not** prevent the

formation of H_3 or H_4 homo-dimers. H_4R chemical deglycosylation of mature receptors using PNGase F enzyme was also undertaken. Deglycosylation reduced, but not completely, receptor dimers in both a recombinant expression system and in native tissue. Therefore, there was some indication that N-glycosylation may help to stabilise receptor dimers once they are formed as deglycosylation of H_4R in human PHA blasts reduced the amount of putative dimer with a concomitant appearance of the putative monomer. Interestingly, differential glycosylation was observed between different native preparations, as well as different *in vitro* expression systems (Chapters 3-6). The significance of this heterogeneity is still to be determined. For the H_3 receptor, near complete prevention of glycosylation had no significant effect on [^{3}H]-clobenpropit binding and complete inhibition saw only a modest reduction in binding. In conclusion, N-glycosylation is **NOT** a prerequisite for receptor dimerisation for either the H_3 or H_4 receptor, and plays a limited role in ligand binding for the H_3 receptor.

5) H_3 and H_4 histamine receptors are both expressed in brain and subserve distinct functions

The H_3 receptor is found almost exclusively within the brain. However there have been few reports of the latest H_4 receptor being detected in the CNS, and these describe mRNA distribution rather than H_4R protein itself. Using our novel anti-human H_4R, we have provided the first evidence for the presence of H_4R protein in human putamen and rat forebrain. In addition we have immunohistochemical data showing strong anti-H_4R immunoreactivity in human and rat brain slices. Interestingly the distribution pattern is different from that observed using our anti-H_3 antibodies, suggesting these two histamine receptors are likely to serve distinct functions within

the CNS. In addition the H_4R has been located in the rat gastrointestinal (GI) tract both in endocrine cells of the fundic mucosa and also in the myenteric plexus of all regions of the GI tract examined. This is the first report of the H_4R in the mammalian parasympathetic nervous system.

Understanding the biology of histamine and respective receptors is crucial to developing novel therapies targeting histamine receptors. Receptor heterogeneity has been a recurrent theme throughout this thesis because it is central to a complete understanding. Drugs which act at H_1 and H_2 receptors have been available for many years chiefly as treatments for allergies and gastric inflammation respectively. Expectations for similar successes with H_3 and H_4 specific compounds are high.

Cloning of the H_3 and H_4 receptors, and subsequent awareness of the potential for different receptor isoforms derived from splice variants, has opened up a number of possibilities for explaining the observed diversity. We have generated H_3 (Chapter 3) and H_4 (Chapter 5) specific antibodies with which to investigate this variety using a number of different techniques.

First and most importantly we, and our collaborators, have shown that different receptor isoforms are expressed in both rodent and human native tissue and are therefore not merely a laboratory artefact. The anti-H_3R described here was specific for the full length human $H_{3\,(445)}$ isoform and two of the rat isoforms namely the rat H_{3A} and H_{3C} isoforms. The distribution of the H_3R detected by this antibody in mouse brain slices was comparable to that found previously using a pan-H_3R antibody in rodent brain (Chazot *et al*, 2001; Victoria Hann, thesis, 2004).

Similarly mRNA encoding for all three of the human H_4R isoforms known to date is found at different levels in a number of white blood cell types. This requires confirmation with isoform-selective antibodies.

The purpose of the different isoforms is a topic of great interest. Previous studies have shown pharmacological differences between the different isoforms. We have preliminary evidence for the shorter human H_3R isoform affecting the pharmacology of the full length version of the receptor (consistent with the rat). These studies were performed in a recombinant system with the receptors artificially expressed in HEK 293 cells. However the $hH_{3\,(445)}$ and $hH_{3\,(329)}$ isoforms are known to be co-expressed in some important brain regions, thus providing the potential for such an interaction. In order to assess their functional significance, compounds capable of distinguishing between these isoforms alone or as hetero-oligomers are needed.

Receptor dimerisation and post-translational changes such as glycosylation, may also contribute to heterogeneity; both of which we were able to investigate using our specific antibodies. Homo-dimers and hetero-dimers were confirmed in recombinant systems using a variety of techniques. Our results suggest that some isoforms may dimerise more readily than others. For example, putative $hH_{3\,(329)}$ homo-dimers appeared stronger in immunoblots than bands compatible with $hH_{3\,(445)}$ homo-dimers. In agreement with this the FRET signal from homo-dimers was greater in $hH_{3\,(329)}R$ transfected cells compared with cells expressing $hH_{3\,(445)}$, although this did not reach statistical significance. Similarly using a cross-linking technique, homo-dimers were observed for the rH_{3A} isoform but not for the rH_{3C} isoform. Interestingly in native tissue both H_3 and H_4 were detected predominantly as higher molecular weight species

(with the exception of rodent brain using the anti-rH_3 (268 – 277)/anti-h$H_{3\ (445)}$ antibody) compatible with the existence of oligomeric versions of the receptors.

Glycosylation was demonstrated for both the human h$H_{3\ (445)}$R and the hH_4R. Neither are heavily glycosylated having only one (H_3R) or two (H_4R) potential glycosylation sites. Glycosylation did not appear to be necessary for ligand binding to the H_3R, however it may contribute to dimer stability in the case of the H_4R.

What is the purpose of this heterogeneity? In common with the other aminergic systems, histamine and the histaminergic system appears to have a modulatory role. It is important in homeostasis and helping the animal to respond appropriately to its' environment. It may be particularly important in stressful situations. Complex information has to be continually processed and integrated, flexibility in the system is crucial to its function. Heterogeneity may be the mechanism underlying this flexibility. Dimerisation has been discussed in chapters 4 (H_3R) and 5 (H_4R), glycosylation was covered in chapter 6. Both are likely to be involved in regulating receptor function. As described in the relevant chapters there are many points at which receptor function can be modulated: from synthesis and trafficking to the cell surface, ligand binding, signalling and eventual desensitisation, internalisation and recycling.

A number of areas for future research are clear from the results accrued in this thesis:

Antibodies to the other H_3 and H_4 receptor isoforms should be generated and used to map their distribution in detail. It would be interesting to find out whether expression levels and/or distribution patterns are influenced by environmental

factors such as day length, behavioural states or disease. In addition double labelling experiments to analyse their distribution in relation to other receptors may improve current understanding of the observed functional heterogeneity. We have preliminary data which suggests that the H_3 receptor is expressed on subsets of histaminergic and GABA-ergic neurons in the substantia nigra and tubomammilary nucleus, respectively which consequently control distinct output neurons (see Appendix), and therefore subserve distinct functions in the mammalian brain.

This thesis provides the first evidence that the H_4 receptor is expressed in the rodent and human CNS. We have preliminary evidence that the H_3 and H_4 receptors are expressed on distinct subsets of endocrine cells and most recently, that the H_4 receptor is expressed on ganglia in the myenteric complex within the GI tract. Therefore, both H_3 and H_4 receptors may have complimentary roles in the PNS and CNS. For effective therapeutic targeting of these two receptors this is a critical issue to follow up.

The putative regulatory role of splice variants and the mechanisms which underlie it require further investigation. Studies to investigate the role of post- and/or co-translational changes such as glycosylation and palmitoylation in relation to function should be undertaken. In addition the question as to whether receptors are differentially glycosylated (or otherwise changed) in different tissues should be addressed.

Research investigating receptor interactions with other cell components is in its infancy. Studies should include not only protein-protein interactions but relationship with lipids and other components of cell architecture. It has been proposed that neurotransmitter signalling might occur through a clustering of receptors and mediators of receptor-activated signalling in lipid rafts (Allen *et al*, 2007).

We have new evidence (not reported in this thesis) that the H_4 receptor can directly interact with a chemokine receptor. This has profound implications in both the brain and the periphery. Studies to probe the relationship between the H_4R and chemokine receptors may improve our current understanding of the relationship between CNS and immune system responses. This may be important for a number of neurodegenerative diseases where an inflammatory response is thought to contribute to the pathology.

While the histamine receptors clearly have potential as therapeutic targets, predicting the likely effect of any particular ligand is difficult in the face of the complexity found both within and across species. The work described in this thesis has furthered understanding of the two most recently described histamine receptors - where they are found and how they may be regulated. These are preliminary studies which will need to be extended to investigate the full range of receptor isoforms, their molecular characteristics and how they interact with other cell components. Advances in molecular biology are enabling scientists to unravel complex systems in minute detail, and the detail itself is intriguing. However, it is essential not to lose sight of the relevance of all this to the workings of the whole animal. In addition advances which

can transfer to the clinic will be the result of a combined effort from the fields of molecular biology, chemistry, pharmacology, animal behaviour and medicine.

REFERENCES

AbdAlla, S, Zaki, E, Lother, H and Quitterer, U (1999). Involvement of the amino terminus of the B-2 receptor in agonist-induced receptor dimerization. *Journal of Biological Chemistry* **274**(37): 26079-26084.

Adachi, N, Oishi, R, Itano, Y, Yamada, T, Hirakawa, M and Saeki, K (1993). Aggravation of Ischemic Neuronal Damage in the Rat Hippocampus by Impairment of Histaminergic Neurotransmission. *Brain Research* **602**(1): 165-168.

Airaksinen, M S and Panula, P (1988). The histaminergic system in the guinea-pig central nervous-system - an immunocytochemical mapping study using an antiserum against histamine. *Journal of Comparative Neurology* **273**(2): 163-186.

Akhtar, M, Devi, P U, Ali, A, Pillai, K K and Vohora, D (2006). Antipsychotic-like profile of thioperamide, a selective H-3-receptor antagonist in mice. *Fundamental & Clinical Pharmacology* **20**(4): 373-378.

Allen, J A, Halverson-Tamboli, R A and Rasenick, M M (2007). Lipid raft microdomains and neurotransmitter signalling. *Nature Reviews Neuroscience* **8**(2): 128-140.

Alphs, L D and Anand, R (1999). Clozapine: The commitment to patient safety. *Journal of Clinical Psychiatry* **60**: 39-42.

Alves-Rodrigues, A, Lemstra, S, Vollinga, R C, Menge, W, Timmerman, H and Leurs, R (2001). Pharmacological analysis of immepip and imetit homologues. Further evidence for histamine H-3 receptor heterogeneity? *Behavioural Brain Research* **124**(2): 121-127.

Alves-Rodrigues, A, Timmerman, H, Willems, E, Lemstra, S, Zuiderveld, O P and Leurs, R (1998). Pharmacological characterisation of the histamine H-3 receptor in the rat hippocampus. *Brain Research* **788**(1-2): 179-186.

Angers, S, Salahpour, A and Bouvier, M (2002). Dimerization: An emerging concept for G protein-coupled receptor ontogeny and function. *Annual Review of Pharmacology and Toxicology* **42**: 409-435.

Angers, S, Salahpour, A, Joly, E, Hilairet, S, Chelsky, D, Dennis, M and Bouvier, M (2000). Detection of beta(2)-adrenergic receptor dimerization in living cells using bioluminescence resonance energy transfer (BRET). *Proceedings of the National Academy of Sciences of the United States of America* **97**(7): 3684-3689.

Anichtchik, O V, Huotari, M, Peitsaro, N, Haycock, J W, Mannisto, P T and Panula, P (2000). Modulation of histamine H-3 receptors in the brain of 6-hydroxydopamine-lesioned rats. *European Journal of Neuroscience* **12**(11): 3823-3832.

Arrang, J M, Drutel, G and Schwartz, J C (1995). Characterization of Histamine H-3 Receptors Regulating Acetylcholine-Release in Rat Entorhinal Cortex. *British Journal of Pharmacology* **114**(7): 1518-1522.

Arrang, J M, Garbarg, M, Lancelot, J C, Lecomte, J M, Pollard, H, Robba, M, Schunack, W and Schwartz, J C (1987). Highly Potent and Selective Ligands for Histamine Receptors-H-3. *Nature* **327**(6118): 117-123.

Arrang, J M, Garbarg, M and Schwartz, J C (1983). Auto-Inhibition of Brain Histamine-Release Mediated by a Novel Class (H-3) of Histamine-Receptor. *Nature* **302**(5911): 832-837.

Arrang, J M, Roy, J, Morgat, J L, Schunack, W and Schwartz, J C (1990). Histamine H-3 Receptor-Binding Sites in Rat-Brain Membranes - Modulations by Guanine-Nucleotides and Divalent-Cations. *European Journal of Pharmacology-Molecular Pharmacology Section* **188**(4-5): 219-227.

Ashford, C A, Heller, H and Smart, G A (1949). The effect of anti-histamine substances on gastric secretion in man. *British Journal of Pharmacology and Chemotherapy* 4(2): 157-161.

Bacciottini, L, Passani, M B, Giovannelli, L, Cangioli, I, Mannaioni, P F, Schunack, W and Blandina, P (2002). Endogenous histamine in the medial septum-diagonal band complex increases the release of acetylcholine from the hippocampus: a dual-probe microdialysis study in the freely moving rat. *European Journal of Neuroscience* **15**(10): 1669-1680.

Bakker, R A, Dees, G, Carrillo, J J, Booth, R G, Lopez-Gimenez, J F, Milligan, G, Strange, P G and Leurs, R (2004). Domain swapping in the human histamine H-1 receptor. *Journal of Pharmacology and Experimental Therapeutics* **311**(1): 131-138.

Bakker, R A, Lozada, A F, van Marle, A, Shenton, F C, Drutel, G, Karlstedt, K, Hoffmann, M, Lintunen, M, Yamamoto, Y, van Rijn, R M, Chazot, P L, Panula, P and Leurs, R (2006). Discovery of naturally occurring splice variants of the rat histamine H-3 receptor that act as dominant-negative isoforms. *Molecular Pharmacology* **69**(4): 1194-1206.

Baneres, J L and Parello, J (2003). Structure-based analysis of GPCR function: Evidence for a novel pentameric assembly between the dimeric leukotriene B-4 receptor BLT1 and the G-protein. *Journal of Molecular Biology* **329**(4): 815-829.

Barrett, P, Ross, A W, Balik, A, Littlewood, P A, Mercer, J G, Moar, K M, Sallmen, T, Kaslin, J, Panula, P, Schuhler, S, Ebling, F J, Ubeaud, C and Morgan, P J (2005). Photoperiodic regulation of histamine H3 receptor and VGF messenger ribonucleic acid in the arcuate nucleus of the Siberian hamster. *Endocrinology* **146**(4): 1930-1939.

Baudry, M, Martres, M P and Schwartz, J C (1975). H1 and H2 Receptors in Histamine-Induced Accumulation of Cyclic-Amp in Guinea-Pig Brain-Slices. *Nature* **253**(5490): 362-364.

Bealer, S L (1993). Histamine Releases Norepinephrine in the Paraventricular Nucleus Anterior Hypothalamus of the Conscious Rat. *Journal of Pharmacology and Experimental Therapeutics* **264**(2): 734-738.

Bekkers, J M (1993). Enhancement by Histamine of Nmda-Mediated Synaptic Transmission in the Hippocampus. *Science* **261**(5117): 104-106.

Bennett, M J, Choe, S and Eisenberg, D (1994). Domain swapping - entangling alliances between proteins. *Proceedings of the National Academy of Sciences of the United States of America* **91**(8): 3127-3131.

Bermak, J C and Zhou, Q Y (2001). Accessory proteins in the biogenesis of GPCRs. *Molecular Interventions* **1**(5): 282- 287.

Bhattacharya, S K (1990). Central Histamine-Receptors in Learning and Memory in Rats. *European Journal of Pharmacology* **183**(3): 925-925.

Bhattacharya, S K and Parmar, S S (1985). Antinociceptive Effect of Intracerebroventricularly Administered Histamine in Rats. *Research Communications in Chemical Pathology and Pharmacology* **49**(1): 125-136.

Bjarnadottir, T K, Geirardsdottir, K, Ingemansson, M, Mirza, M A I, Fredriksson, R and Schioth, H B (2007). Identification of novel splice variants of Adhesion G protein-coupled receptors. *Gene* **387**(1-2): 38-48.

Black, J W, Parsons, E M, Durant, C J, Duncan, W A M and Ganellin, C R (1972). Definition and Antagonism of Histamine H2-Receptors. *Nature* **236**(5347): 385&.

Blandina, P, Giorgetti, M, Bartolini, L, Cecchi, M, Timmerman, H, Leurs, R, Pepeu, G and Giovannini, M G (1996). Inhibition of cortical acetylcholine release and cognitive performance by histamine H-3 receptor activation in rats. *British Journal of Pharmacology* **119**(8): 1656-1664.

Bongers, G, van Marle, A., Navis, M., Bakker, R.A., Leurs, R. (2006). New signalling pathways for the histamine H_3 receptor. *European Histamine Research Society XXXV Annual Meeting.* Delphi, Greece.

Bongers, G, Bakker, R A and Leurs, R (2007). Molecular aspects of the histamine H-3 receptor. *Biochemical Pharmacology* **73**(8): 1195-1204.

Bongers, G, Leurs, R, Robertson, J and Raber, J (2004). Role of H-3-receptor-mediated signaling in anxiety and cognition in wild-type and Apoe(-/-) mice. *Neuropsychopharmacology* **29**(3): 441-449.

Brady, A E and Limbird, L E (2002). G protein-coupled receptor interacting proteins: Emerging roles in localization and signal transduction. *Cellular Signalling* **14**(4): 297-309.

Brown, J D, Oshaughnessy, C T, Kilpatrick, G J, Scopes, D I C, Beswick, P, Clitherow, J W and Barnes, J C (1996). Characterisation of the specific binding of the histamine H-3 receptor antagonist radioligand H-3 GR168320. *European Journal of Pharmacology* **311**(2-3): 305-310.

Brown, R E, Haas H.L. (1999). Histamine actions on midbrain dopamine neurons of the rat in vitro. *Pflugers Arch.* **437**: P15.

Brown, R E, Fedorov, N B, Haas, H L and Reymann, K G (1995). Histaminergic Modulation of Synaptic Plasticity in Area Ca1 of Rat Hippocampal Slices. *Neuropharmacology* **34**(2): 181-190.

Brown, R E and Reymann, K G (1996). Histamine H-3 receptor-mediated depression of synaptic transmission in the dentate gyrus of the rat in vitro. *Journal of Physiology-London* **496**(1): 175-184.

Brown, R E, Stevens, D R and Haas, H L (2001). The physiology of brain histamine. *Progress in Neurobiology* **63**(6): 637-672.

Buckland, K F, Williams, T J and Conroy, D M (2003). Histamine induces cytoskeletal changes in human eosinophils via the H-4 receptor. *British Journal of Pharmacology* **140**(6): 1117-1127.

Bulenger, S, Marullo, S and Bouvier, M (2005). Emerging role of homo- and heterodimerization in G-protein-coupled receptor biosynthesis and maturation. *Trends in Pharmacological Sciences* **26**(3): 131-137.

Cannon, K E, Chazot, P L, Hann, V, Shenton, F, Hough, L B and Rice, F L (2007). Immunohistochemical localization of histamine H-3 receptors in rodent skin,

dorsal root ganglia, superior cervical ganglia, and spinal cord: Potential antinociceptive targets. *Pain* **129**(1-2): 76-92.

Cannon, K E and Hough, L B (2005). Inhibition of chemical and low-intensity mechanical nociception by activation of histamine H-3 receptors. *Journal of Pain* **6**(3): 193-200.

Carrillo, J J, Pediani, J and Milligan, G (2003). Dimers of class A G protein-coupled receptors function via agonist-mediated trans-activation of associated G proteins. *Journal of Biological Chemistry* **278**(43): 42578-42587.

Cecchi, M, Giorgetti, M, Bacciottini, L, Giovannini, M G and Blandina, P (1998). Increase of acetylcholine release from cortex of freely moving rats by administration of histamine into the nucleus basalis magnocellularis. *Inflammation Research* **47**: S32-S33.

Chalothorn, D, McCune, D F, Edelmann, S E, Garcia-Cazarin, M L, Tsujimoto, G and Piascik, M T (2002). Differences in the cellular localization and agonist-mediated internalization properties of the alpha(1)-adrenoceptor subtypes. *Molecular Pharmacology* **61**(5): 1008-1016.

Chand, N and Eyre, P (1994). Classification and biological distribution of histamine-receptor subtypes. *Agents and Actions* **43**(3-4): 97-116.

Chazot, P, Shenton, F, Schunack, W, Grandi, D and Morini, G (2007). Influence of (R)-alpha-Methylhistamine on the histamine H-3 receptor in the rat gastrointestinal tract. *Inflammation Research* **56**: S19-S20.

Chazot, P L, Shenton, F.C., Waldfogel, H., Grandi, D., Morini, G. (2007). The H_4 histamine receptor is expressed in both the human CNS and rodent PNS. *European Histamine Research Society XXXVI Annual Meeting*. Florence, Italy.

Chazot, P L, Cik, M and Stephenson, F A (1992). Immunological Detection of the Nmdar1 Glutamate Receptor Subunit Expressed in Human Embryonic Kidney-293 Cells and in Rat-Brain. *Journal of Neurochemistry* **59**(3): 1176-1178.

Chazot, P L, Cik, M and Stephenson, F A (1995). An investigation into the role of N-glycosylation in the functional expression of a recombinant heteromeric NMDA receptor. *Molecular Membrane Biology* **12**(4): 331-337.

Chazot, P L, Godukhin, O V, McDonald, A and Obrenovitch, T P (2002). Spreading depression-induced preconditioning in the mouse cortex: differential changes in the protein expression of ionotropic nicotinic acetylcholine and glutamate receptors. *Journal of Neurochemistry* **83**(5): 1235-1238.

Chazot, P L and Hann, V (2001). H3 histamine receptor isoforms: New therapeutic targets in the CNS. *Current Opinion in Investigational Drugs* **2**(10).

Chazot, P L, Hann, V, Wilson, C, Lees, G and Thompson, C L (2001). Immunological identification of the mammalian H-3 histamine receptor in the mouse brain. *Neuroreport* **12**(2): 259-262.

Chazot, P L and Shenton, F C (2004). H3 histamine receptors: the knockout data so far. *Curr Anaesth.Crit.Care* **15**: 23-28.

Chazot, P L, Wilson, C, Hann, V, Thompson, C L and Lees, G (2000). Immunological identification of the mammalian H3 histamine receptor expressed in mouse brain:

Evidence for receptor heterogenity? *European Journal of Neuroscience* **12**: 470-470.

Chen, J C, Liu, C L and Lovenberg, T W (2003). Molecular and pharmacological characterization of the. mouse histamine H-3 receptor. *European Journal of Pharmacology* **467**(1-3): 57-65.

Chen, K, Wang, J J, Yung, W H, Chan, Y S and Chow, B K C (2005). Excitatory effect of histamine on neuronal activity of rat globus pallidus by activation of H-2 receptors in vitro. *Neuroscience Research* **53**(3): 288-297.

Chen, K, Zhu, J N, Li, H Z and Wang, J J (2003). Histamine elicits neuronal excitatory response of red nucleus in the rat via H-2 receptors in vitro. *Neuroscience Letters* **351**(1): 25-28.

Chen, Z, Zhao, Q, Sugimoto, Y, Fujii, Y and Kamei, C (1999). Effects of histamine on MK-801-induced memory deficits in radial maze performance in rats. *Brain Research* **839**(1): 186-189.

Chung, Y H, Miyake, H, Kamei, C and Tasaka, K (1984). Analgesic Effect of Histamine Induced by Intracerebral Injection into Mice. *Agents and Actions* **15**(3-4): 137-142.

Cianchi, F, Cortesini, C, Schiavone, N, Perna, F, Magnelli, L, Fanti, E, Bani, D, Messerini, L, Fabbroni, V, Perigli, G, Capaccioli, S and Masini, E (2005). The role of cyclooxygenase-2 in mediating the effects of histamine on cell proliferation and vascular endothelial growth factor production in colorectal cancer. *Clinical Cancer Research* **11**(19): 6807-6815.

Clapham, J and Kilpatrick, G J (1992). Histamine H-3 Receptors Modulate the Release of H-3 Acetylcholine from Slices of Rat Entorhinal Cortex - Evidence for the Possible Existence of H-3 Receptor Subtypes. *British Journal of Pharmacology* **107**(4): 919-923.

Clark, E A and Hill, S J (1996). Sensitivity of histamine H-3 receptor agonist-stimulated S-35 GTP gamma S binding to pertussis toxin. *European Journal of Pharmacology* **296**(2): 223-225.

Coge, F, Guenin, S P, Audinot, V, Renouard-Try, A, Beauverger, P, Macia, C, Ouvry, C, Nagel, N, Rique, H, Boutin, J A and Galizzi, J P (2001). Genomic organization and characterization of splice variants of the human histamine H-3 receptor. *Biochemical Journal* **355**: 279-288.

Coge, F, Guenin, S P, Rique, H, Boutin, J A and Galizzi, J P (2001). Structure and expression of the human histamine H-4-receptor gene. *Biochemical and Biophysical Research Communications* **284**(2): 301-309.

Coruzzi, G, Adami, M., Guaita, E., de Esch, I.J.P., Leurs, R. (2007). Antiinflammatory, analgesic and gastric effects of the novel and selective histamine H_4 receptor antagonists VUF10214 and VUF10148. *European Histamine Research Society XXXVI Annual Meeting*. Florence, Italy.

Coruzzi, G, Adami, M, Guaita, E, de Esch, L J P and Leurs, R (2007). Antiinflammatory and antinociceptive effects of the selective histamine H_4-receptor antagonists JNJ7777120 and VUF6002 in a rat model of carrageenan-induced acute inflammation. *European Journal of Pharmacology* **563**(1-3): 240-244.

Coruzzi, G, Gambarelli, E, Bertaccini, G and Timmerman, H (1995). Cardiovascular effects of selective agonists and antagonists of histamine H-3 receptors in the anesthetized rat. *Naunyn-Schmiedebergs Archives of Pharmacology* **351**(6): 569-575.

Cumming, P, Laliberte, C and Gjedde, A (1994). Distribution of Histamine H-3 Binding in Forebrain of Mouse and Guinea-Pig. *Brain Research* **664**(1-2): 276-279.

Cvejic, S and Devi, L A (1997). Dimerization of the delta opioid receptor: Implication for a role in receptor internalization. *Journal of Biological Chemistry* **272**(43): 26959-26964.

Dai, H M, Kaneko, K, Kato, H, Fujii, S, Jing, Y H, Xu, A J, Sakurai, E, Kato, M, Okamura, N, Kuramasu, A and Yanai, K (2007). Selective cognitive dysfunction in mice lacking histamine H1 and H2 receptors. *Neuroscience Research* **57**(2): 306-313.

Darvas, Z, Boer, K., Pocza, P., Helinger, E., Helinger, A., Kisery, N., Szente, V., Fulus, A. (2007). Down regulation of histamine receptors in human colon cancer. *European Histamine Research Society XXXVI Annual Meeting*. Florence, Italy.

Daugherty, B L (2004). Histamine H-4 antagonism: a therapy for chronic allergy? *British Journal of Pharmacology* **142**(1): 5-7.

Daum, P R, Hill, S J and Young, J M (1982). Histamine H1-Agonist Potentiation of Adenosine-Stimulated Cyclic-Amp Accumulation in Slices of Guinea-Pig Cerebral-Cortex - Comparison of Response and Binding Parameters. *British Journal of Pharmacology* 77(2): 347-357.

De Esch, I J P and Belzar, K J (2004). Histamine H-3 receptor agonists. *Mini-Reviews in Medicinal Chemistry* 4(9): 955-963.

de Esch, I J P, Thurmond, R L, Jongejan, A and Leurs, R (2005). The histamine H-4 receptor as a new therapeutic target for inflammation. *Trends in Pharmacological Sciences* **26**(9): 462-469.

Deslauriers, B, Ponce, C, Lombard, C, Larguier, R, Bonnafous, J C and Marie, J (1999). N-glycosylation requirements for the AT(1a) angiotensin II receptor delivery to the plasma membrane. *Biochemical Journal* **339**: 397-405.

Dijkstra, D, Leurs, R., Chazot, P.L., Shenton, F.C., Stark, H., Werfel, T., Gutzmer, R. (2007). Histamine downregulates monocyte CCL2 production through the histamine H_4 receptor. *J Allergy Clin Immunol.*

Drutel, G, Peitsaro, N, Karlstedt, K, Wieland, K, Smit, M J, Timmerman, H, Panula, P and Leurs, R (2001). Identification of rat H-3 receptor isoforms with different brain expression and signaling properties. *Molecular Pharmacology* **59**(1): 1-8.

Duggan, M J, Pollard, S and Stephenson, F A (1991). Immunoaffinity Purification of Gaba-a Receptor Alpha-Subunit Iso-Oligomers - Demonstration of Receptor Populations Containing Alpha-1-Alpha-2, Alpha-1-Alpha-3, and Alpha-2-Alpha-3 Subunit Pairs. *Journal of Biological Chemistry* **266**(36): 24778-24784.

Dunford, P J, O'Donnell, N, Riley, J P, Williams, K N, Karlsson, L and Thurmond, R L (2006). The histamine H-4 receptor mediates allergic airway inflammation by regulating the activation of CD4(+) T cells. *Journal of Immunology* **176**(11): 7062-7070.

Duvernay, M T, Filipeanu, C M and Wu, G Y (2005). The regulatory mechanisms of export trafficking of G protein-coupled receptors. *Cellular Signalling* **17**(12): 1457-1465.

El-Asmar, L, Springael, J Y, Ballet, S, Andrieu, E U, Vassart, G and Parmentier, M (2005). Evidence for negative binding cooperativity within CCR5-CCR2b heterodimers. *Molecular Pharmacology* **67**(2): 460-469.

English, J D and Sweatt, J D (1996). Activation of p42 mitogen-activated protein kinase in hippocampal long term potentiation. *Journal of Biological Chemistry* **271**(40): 24329-24332.

Ennaceur, A, Michalikova, S and Chazot, P L (2006). Models of anxiety: Responses of rats to novelty in an open space and an enclosed space. *Behavioural Brain Research* **171**(1): 26-49.

Ericson, H, Blomqvist, A and Kohler, C (1989). Brain-stem afferents to the tuberomammillary nucleus in the rat-brain with special reference to monoaminergic innervation. *Journal of Comparative Neurology* **281**(2): 169-192.

Ericson, H, Blomqvist, A and Kohler, C (1991). Origin of neuronal inputs to the region of the tuberomammillary nucleus of the rat-brain. *Journal of Comparative Neurology* **311**(1): 45-64.

Eriksson, K S, Sergeeva, O, Brown, R E and Haas, H L (2001). Orexin/hypocretin excites the histaminergic neurons of the tuberomammillary nucleus. *Journal of Neuroscience* **21**(23): 9273-9279.

Esbenshade, T, Krueger, K M, Miller, T R, Branowski, J, Kang, C H, Yao, B B, Witte, D G, Pan, J B, Carr, T L, Fox, G B, Faghih, R, Black, L A, Bennani, Y L, Sullivan, J

P, Cowart, M D and Hancock, A A (2004). ABT-239, A novel, selective, and potent human histamine H-3 receptor antagonist with cognition enhancing properties. *Faseb Journal* **18**(4): A579-A579.

Esbenshade, T A, Krueger, K M, Miller, T R, Kang, C H, Denny, L I, Witte, D G, Yao, B B, Fox, G B, Faghih, R, Bennani, Y L, Williams, M and Hancock, A A (2003). Two novel and selective nonimidazole histamine H-3 receptor antagonists A-304121 and A-317920: I. In vitro pharmacological effects. *Journal of Pharmacology and Experimental Therapeutics* **305**(3): 887-896.

Esbenshade, T A, Strakhova, M I, Carr, T L, Sharma, R, Witte, D G, Yao, B B, Miller, T R and Hancock, A A (2006). Differential CNS expression and functional activity of multiple human H-3 receptor isoforms. *Inflammation Research* **55**: S38-S39.

Faghih, R, Dwight, W, Pan, J B, Fox, G B, Krueger, K M, Esbenshade, T A, McVey, J M, Marsh, K, Bennani, Y L and Hancock, A A (2003). Synthesis and SAR of aminoalkoxy-biaryl-4-carboxamides: Novel and selective histamine H-3 receptor antagonists. *Bioorganic & Medicinal Chemistry Letters* **13**(7): 1325-1328.

Ferguson, S S G (2001). Evolving concepts in G protein-coupled receptor endocytosis: The role in receptor desensitization and signaling. *Pharmacological Reviews* **53**(1): 1-24.

Ferguson, S S G, Barak, L S, Zhang, J and Caron, M G (1996). G-protein-coupled receptor regulation: Role of G-protein-coupled receptor kinases and arrestins. *Canadian Journal of Physiology and Pharmacology* **74**(10): 1095-1110.

Ferguson, S S G, Downey, W E, Colapietro, A M, Barak, L S, Menard, L and Caron, M G (1996). Role of beta-arrestin in mediating agonist-promoted G protein-coupled receptor internalization. *Science* **271**(5247): 363-366.

Fernandes, H, Cohen, S and Bishayee, S (2001). Glycosylation-induced conformational modification positively regulates receptor-receptor association - A study with an aberrant epidermal growth factor receptor (EGFRvIII/Delta EGFR) expressed in cancer cells. *Journal of Biological Chemistry* **276**(7): 5375-5383.

Filipeanu, C M, Zhou, F G, Claycomb, W C and Wu, G Y (2004). Regulation of the cell surface expression and function of angiotensin II type 1 receptor by Rab1-mediated endoplasmic reticulum-to-Golgi transport in cardiac myocytes. *Journal of Biological Chemistry* **279**(39): 41077-41084.

Fink, K, Schlicker, E, Neise, A and Gothert, M (1990). Involvement of Presynaptic H-3 Receptors in the Inhibitory Effect of Histamine on Serotonin Release in the Rat-Brain Cortex. *Naunyn-Schmiedebergs Archives of Pharmacology* **342**(5): 513-519.

Fleckenstein, A E, Lookingland, K J and Moore, K E (1993). Activation of Mesolimbic Dopaminergic-Neurons Following Central Administration of Histamine Is Mediated by H1 Receptors. *Naunyn-Schmiedebergs Archives of Pharmacology* **347**(1): 50-54.

Fleckenstein, A E, Lookingland, K J and Moore, K E (1994). Activation of Noradrenergic Neurons Projecting to the Diencephalon Following Central Administration of Histamine Is Mediated by H-1 Receptors. *Brain Research* **638**(1-2): 243-247.

Fleckenstein, A E, Lookingland, K J and Moore, K E (1994). Differential-Effects of Histamine on the Activity of Hypothalamic Dopaminergic-Neurons in the Rat. *Journal of Pharmacology and Experimental Therapeutics* **268**(1): 270-276.

Fleckenstein, A E, Lookingland, K J and Moore, K E (1994). Effects of Histamine on 5-Hydroxytryptaminergic Neuronal-Activity in the Rat Hypothalamus. *European Journal of Pharmacology* **254**(1-2): 35-42.

Fotiadis, D, Liang, Y, Filipek, S, Saperstein, D A, Engel, A and Palczewski, K (2003). Atomic-force microscopy: Rhodopsin dimers in native disc membranes. *Nature* **421**(6919): 127-128.

Fox, G B, Pan, J B, Lewis, A M, Browman, K E, Komater, V A, Buckley, M J, Curzon, P, Radek, R J, Faghih, R, Esbenshade, T A, Cowart, M D, Decker, M W and Hancock, A A (2004). Cognition enhancing effects of novel H-3 receptor (H3R) antagonists in several animal models. *Inflammation Research* **53**: S49-S50.

Frisch, C, Hasenohrl, R U, Krauth, J and Huston, J P (1998). Anxiolytic-like behavior after lesion of the tuberomammillary nucleus E2-region. *Experimental Brain Research* **119**(2): 260-264.

Fukushima, Y, Asano, T, Saitoh, T, Anai, M, Funaki, M, Ogihara, T, Katagiri, H, Matsuhashi, N, Yazaki, Y and Sugano, K (1997). Oligomer formation of histamine H2 receptors expressed in Sf9 and COS7 cells. *Febs Letters* **409**(2): 283-286.

Fukushima, Y, Oka, Y, Saitoh, T, Katagiri, H, Asano, T, Matsuhashi, N, Takata, K, Vanbreda, E, Yazaki, Y and Sugano, K (1995). Structural and Functional-

Analysis of the Canine Histamine-H2-Receptor by Site-Directed Mutagenesis - N-Glycosylation Is Not Vital for Its Action. *Biochemical Journal* **310**: 553-558.

Fundin, B T, Pfaller, K and Rice, F L (1997). Different distributions of the sensory and autonomic innervation among the microvasculature of the rat mystacial pad. *Journal of Comparative Neurology* **389**(4): 545-568.

Ganellin, C R, Leurquin, F, Piripitsi, A, Arrang, J M, Garbarg, M, Ligneau, X, Schunack, W and Schwartz, J C (1998). Synthesis of potent non-imidazole histamine H-3-receptor antagonists. *Archiv Der Pharmazie* **331**(12): 395-404.

Gantner, F, Sakai, K, Tusche, M W, Cruikshank, W W, Center, D M and Bacon, K B (2002). Histamine H-4 and H-2 receptors control histamine-induced interleukin-16 release from human CD8+ T cells. *Journal of Pharmacology and Experimental Therapeutics* **303**(1): 300-307.

Gantz, I, Schaffer, M, Delvalle, J, Logsdon, C, Campbell, V, Uhler, M and Yamada, T (1991). Molecular-Cloning of a Gene Encoding the Histamine-H2-Receptor. *Proceedings of the National Academy of Sciences of the United States of America* **88**(2): 429-433.

Garbarg, M, Barbin, G, Feger, J and Schwartz, J C (1974). Histaminergic Pathway in Rat-Brain Evidenced by Lesions of Medial Forebrain-Bundle. *Science* **186**(4166): 833-835.

Garcia, M, Floran, B, AriasMontano, J A, Young, J M and Aceves, J (1997). Histamine H-3 receptor activation selectively inhibits dopamine D-1 receptor-dependent H-3 GABA release from depolarization-stimulated slices of rat substantia nigra pars reticulata. *Neuroscience* **80**(1): 241-249.

Gbahou, F, Rouleau, A, Morisset, S, Parmentier, R, Crochet, S, Lin, J S, Ligneau, X, Tardivel-Lacombe, J, Stark, H, Schunack, W, Ganellin, C R, Schwartz, J C and Arrang, J M (2003). Protean agonism at histamine H-3 receptors in vitro and in vivo. *Proceedings of the National Academy of Sciences of the United States of America* **100**(19): 11086-11091.

George, S R, O'Dowd, B F and Lee, S R (2002). G-protein-coupled receptor oligomerization and its potential for drug discovery. *Nature Reviews Drug Discovery* **1**(10): 808-820.

Giovannini, M G, Bartolini, L, Bacciottini, L, Greco, L and Blandina, P (1999). Effects of histamine H-3 receptor agonists and antagonists on cognitive performance and scopolamine-induced amnesia. *Behavioural Brain Research* **104**(1-2): 147-155.

Glick, S D and Crane, L A (1978). Opiate-Like and Abstinence-Like Effects of Intra-Cerebral Histamine Administration in Rats. *Nature* **273**(5663): 547-549.

Gomez-Ramirez, J, Johnston, T H, Visanji, N P, Fox, S H and Brotchie, J M (2006). Histamine H3 receptor agonists reduce L-dopa-induced chorea, but not dystonia, in the MPTP-lesioned nonhuman primate model of Parkinson's disease. *Movement Disorders* **21**(6): 839-846.

Gomez-Ramirez, J, Ortiz, J and Blanco, I (2002). Presynaptic H-3 autoreceptors modulate histamine synthesis through cAMP pathway. *Molecular Pharmacology* **61**(1): 239-245.

Goodchild, R E, Court, J A, Hobson, I, Piggott, M A, Perry, R H, Ince, P, Jaros, E and Perry, E K (1999). Distribution of histamine H-3-receptor binding in the normal

human basal ganglia: comparison with Huntington's and Parkinson's disease cases. *European Journal of Neuroscience* **11**(2): 449-456.

Gorelova, N and Reiner, P B (1996). Histamine depolarizes cholinergic septal neurons. *Journal of Neurophysiology* **75**(2): 707-714.

Gouldson, P R, Higgs, C, Smith, R E, Dean, M K, Gkoutos, G V and Reynolds, C A (2000). Dimerization and domain swapping in g-protein-coupled receptors: A computational study. *Neuropsychopharmacology* **23**(4): S60-S77.

Green, J (1970). *Handbook of Neurochemistry*. New York, Plenum Press.

Greene, R W, Haas, H L and Reiner, P B (1990). 2 Transient Outward Currents in Histamine Neurons of the Rat Hypothalamus Invitro. *Journal of Physiology-London* **420**: 149-163.

Grosse, R, Schoneberg, T, Schultz, G and Gudermann, T (1997). Inhibition of gonadotropin-releasing hormone receptor signaling by expression of a splice variant of the human receptor. *Molecular Endocrinology* **11**(9): 1305-1318.

Gutzmer, R, Diestel, C, Mommert, S, Kother, B, Stark, H, Wittmann, M and Werfel, T (2005). Histamine H4 receptor stimulation suppresses IL-12p70 production and mediates chemotaxis in human monocyte-derived dendritic cells. *Journal of Immunology* **174**(9): 5224-5232.

Haas, H and Panula, P (2003). The role of histamine and the tuberomamillary nucleus in the nervous system. *Nature Reviews Neuroscience* **4**(2): 121-130.

Haas, H L (1984). Histamine Potentiates Neuronal Excitation by Blocking a Calcium-Dependent Potassium Conductance. *Agents and Actions* **14**(3-4): 534-537.

Hadac, E M, Ji, Z S, Pinon, D I, Henne, R M, Lybrand, T P and Miller, L J (1999). A peptide agonist acts by occupation of a monomeric G protein-coupled receptor: Dual sites of covalent attachment to domains near TM1 and TM7 of the same molecule make biologically significant domain-swapped dimerization unlikely. *Journal of Medicinal Chemistry* **42**(12): 2105-2111.

Hague, C, Uberti, M A, Chen, Z J, Bush, C F, Jones, S V, Ressler, K J, Hall, R A and Minneman, K P (2004). Olfactory receptor surface expression is driven by association with the beta(2)-adrenergic receptor. *Proceedings of the National Academy of Sciences of the United States of America* **101**(37): 13672-13676.

Hague, C, Uberti, M A, Chen, Z J, Hall, R A and Minneman, K P (2004). Cell surface expression of alpha(1D)-adrenergic receptors is controlled by heterodimerization with alpha(1B)-adrenergic receptors. *Journal of Biological Chemistry* **279**(15): 15541-15549.

Han, C, Esbenshade, T A and Minneman, K P (1992). Subtypes of alpha-1-adrenoceptors in DDT1 MF-2 and BC3H-1 clonal cell-lines. *European Journal of Pharmacology-Molecular Pharmacology Section* **226**(2): 141-148.

Hancock, A A (2006). The challenge of drug discovery of a GPCR target: Analysis of preclinical pharmacology of histamine H-3 antagonists/inverse agonists. *Biochemical Pharmacology* **71**(8): 1103-1113.

Hancock, A A, Bennani, Y L, Bush, E N, Esbenshade, T A, Faghih, R, Fox, G B, Jacobson, P, Knourek-Segel, V, Krueger, K M, Nuss, M E, Pan, J B, Shapiro, R, Witte, D G and Yao, B B (2004). Antiobesity effects of A-331440, a novel non-

imidazole histamine H-3 receptor antagonist. *European Journal of Pharmacology* **487**(1-3): 183-197.

Hancock, A A, Diehl, M S, Faghih, R, Bush, E N, Krueger, K M, Krishna, G, Miller, T R, Wilcox, D M, Nguyen, P, Pratt, J K, Cowart, M D, Esbenshade, T A and Jacobson, P B (2004). In vitro optimization of structure activity relationships of analogues of A-331440 combining radioligand receptor binding assays and micronucleus assays of potential antiobesity histamine H-3 receptor antagonists. *Basic & Clinical Pharmacology & Toxicology* **95**(3): 144-152.

Hancock, A A, Esbenshade, T A, Krueger, K M and Yao, B B (2003). Genetic and pharmacological aspects of histamine H-3 receptor heterogeneity. *Life Sciences* **73**(24): 3043-3072.

Hann, V, Shenton, F C and Chazot, P L (2004). GTP-insensitive agonist binding to native and recombinant H-3 receptors. *Inflammation Research* **53**: S67-S68.

Harper, E A, Lovenberg, T W, Shankley, N P and Black, J W (2001). Comparison of ligand affinity values at the recombinant human H-3 receptor and at H-3 receptor(s) of human cingulate cortex. *Inflammation Research* **50**: S106-S107.

Harper, E A, Shankley, N P and Black, J W (1999). Characterization of the binding of [H-3]-clobenpropit to histamine H-3-receptors in guinea-pig cerebral cortex membranes. *British Journal of Pharmacology* **128**(4): 881-890.

Harper, E A, Shankley, N P and Black, J W (1999). Evidence that histamine homologues discriminate between H-3-receptors in guinea-pig cerebral cortex and ileum longitudinal muscle myenteric plexus. *British Journal of Pharmacology* **128**(3): 751-759.

Hashimoto, T, Harusawa, S, Araki, L, Zuiderveld, O P, Smit, M J, Imazu, T, Takashima, S, Yamamoto, Y, Sakamoto, Y, Kurihara, T, Leurs, R, Bakker, R A and Yamatodani, A (2003). A selective human H-4-receptor agonist: (-)-2-cyano-1-methyl-3-{(2R,5R)-5- 1H-imidazol-4(5)-yl tetrahydrofuran-2 -yl}methylguanidine. *Journal of Medicinal Chemistry* **46**(14): 3162-3165.

Haugeto, O, Ullensvang, K, Levy, L M, Chaudhry, F A, Honore, T, Nielsen, M, Lehre, K P and Danbolt, N C (1996). Brain glutamate transporter proteins form homomultimers. *Journal of Biological Chemistry* **271**(44): 27715-27722.

Hawtin, S R, Tobin, A B, Patel, S and Wheatley, M (2001). Palmitoylation of the vasopressin V-1a receptor reveals different conformational requirements for signaling, agonist-induced receptor phosphorylation, and sequestration. *Journal of Biological Chemistry* **276**(41): 38139-38146.

He, J Q, Xu, J G, Castleberry, A M, Lau, A G and Hall, R A (2002). Glycosylation of beta(1)-adrenergic receptors regulates receptor surface expression and dimerization. *Biochemical and Biophysical Research Communications* **297**(3): 565-572.

Hegstrand, L R, Kanof, P D and Greengard, P (1976). Histamine-Sensitive Adenylate-Cyclase in Mammalian Brain. *Nature* **260**(5547): 163-165.

Heidenreich, K A and Brandenburg, D (1986). Oligosaccharide Heterogeneity of Insulin-Receptors - Comparison of N-Linked Glycosylation of Insulin-Receptors in Adipocytes and Brain. *Endocrinology* **118**(5): 1835-1842.

Herbert, T E, Moffett, S and Bouvier, M (1996). beta(2)-Adrenergic receptor dimerization is important for receptor activation. *Faseb Journal* **10**(3): 1722-1722.

Heron, A, Rouleau, A, Cochois, V, Pillot, C, Schwartz, J C and Arrang, J M (2001). Expression analysis of the histamine H-3 receptor in developing rat tissues. *Mechanisms of Development* **105**(1-2): 167-173.

Hey, J A, Delprado, M, Egan, R W, Kreutner, W and Chapman, R W (1992). Inhibition of Sympathetic Hypertensive Responses in the Guinea-Pig by Prejunctional Histamine H3-Receptors. *British Journal of Pharmacology* **107**(2): 347-351.

Hey, J A, Delprado, M, Egan, R W, Kreutner, W and Chapman, R W (1992). (R)-alpha-methylhistamine augments neural, cholinergic bronchospasm in guinea-pigs by histamine-H1 receptor activation. *European Journal of Pharmacology* **211**(3): 421-426.

Hill, S J (1990). DISTRIBUTION, PROPERTIES, AND FUNCTIONAL-CHARACTERISTICS OF 3 CLASSES OF HISTAMINE-RECEPTOR. *Pharmacological Reviews* **42**(1): 45-83.

Hill, S J (2006). G-protein-coupled receptors: past, present and future. *British Journal of Pharmacology* **147**: S27-S37.

Hill, S J, Emson, P C and Young, J M (1978). Binding of [H-3] mepyramine to histamine H-1 receptors in guinea-pig brain. *Journal of Neurochemistry* **31**(4): 997-1004.

Hill, S J, Ganellin, C R, Timmerman, H, Schwartz, J C, Shankley, N P, Young, J M, Schunack, W, Levi, R and Haas, H L (1997). International union of pharmacology

.13. Classification of histamine receptors. *Pharmacological Reviews* **49**(3): 253-278.

Hofstra, C L, Desai, P J, Thurmond, R L and Fung-Leung, W P (2003). Histamine H-4 receptor mediates chemotaxis and calcium mobilization of mast cells. *Journal of Pharmacology and Experimental Therapeutics* **305**(3): 1212-1221.

Honrubia, M A, Vilaro, M T, Palacios, J M and Mengod, G (2000). Distribution of the histamine H-2 receptor in monkey brain and its mRNA localization in monkey and human brain. *Synapse* **38**(3): 343-354.

Horr, B, Borck, H, Diel, J, Wackes, C, Nierich, K, Thurmond, R L and Diel, F (2006). The role of the histamine H-4 receptor in signal transduction of atopic and non-atopic human lymphocytes ex vivo. *Inflammation Research* **55**: S53-S54.

Hough, L B (1988). Cellular-Localization and Possible Functions for Brain Histamine - Recent Progress. *Progress in Neurobiology* **30**(6): 469-505.

Hough, L B (2001). Genomics meets histamine receptors: New subtypes, new receptors. *Molecular Pharmacology* **59**(3): 415-419.

Hough, L B and Nalwalk, J W (1992). Modulation of Morphine Antinociception by Antagonism of H2-Receptors in the Periaqueductal Gray. *Brain Research* **588**(1): 58-66.

Huang, Y W, Hu, W W, Chen, Z, Zhang, L S, Shen, H Q, Timmerman, H, Leurs, R and Yanai, K (2004). Effect of the histamine H-3-antagonist clobenpropit on spatial memory deficits induced by MK-801 as evaluated by radial maze in Sprague-Dawley rats. *Behavioural Brain Research* **151**(1-2): 287-293.

Ikawa, Y, Suzuki, M, Shiono, S, Ohki, E, Moriya, H, Negishi, E and Ueno, K (2005). Histamine H4 receptor expression in human synovial cells obtained from patients suffering from rheumatoid arthritis. *Biological & Pharmaceutical Bulletin* **28**(10): 2016-2018.

Imaizumi, M and Onodera, K (1993). The Behavioral and Biochemical Effects of Thioperamide, a Histamine H3-Receptor Antagonist, in a Light/Dark Test Measuring Anxiety in Mice. *Life Sciences* **53**(22): 1675-1683.

Inagaki, N, Yamatodani, A, Andoyamamoto, M, Tohyama, M, Watanabe, T and Wada, H (1988). Organization of histaminergic fibers in the rat-brain. *Journal of Comparative Neurology* **273**(3): 283-300.

Ireland-Denny, L, Parihar, A S, Miller, T R, Kang, C H, Krueger, K M, Esbenshade, T A and Hancock, A A (2001). Species-related pharmacological heterogeneity of histamine H-3 receptors. *European Journal of Pharmacology* **433**(2-3): 141-150.

Ishizuka, T, Sakamoto, Y, Sakurai, T and Yamatodani, A (2003). Modafinil increases histamine release in the anterior hypothalamus of rats. *Neuroscience Letters* **339**(2): 143-146.

Jablonowski, J A, Grice, C A, Chai, W Y, Dvorak, C A, Venable, J D, Kwok, A K, Ly, K S, Wei, J M, Baker, S M, Dsesai, P J, Jiang, W, Wilson, S J, Thurmond, R L, Karlsson, L, Edwards, J P, Lovenberg, T W and Carruthers, N I (2003). The first potent and selective non-imidazole human histamine H-4 receptor antagonists. *Journal of Medicinal Chemistry* **46**(19): 3957-3960.

Jansen, F P, Wu, T S, Voss, H P, Steinbusch, H W M, Vollinga, R C, Rademaker, B, Bast, A and Timmerman, H (1994). Characterization of the Binding of the First

Selective Radiolabeled Histamine H-3 Receptor Antagonist, I-125 Iodophenpropit, to Rat-Brain. *British Journal of Pharmacology* **113**(2): 355-362.

Jelinek, I, Laszlo, V., Pallinger, E., Hegyesi, H., Thurmond, R.L., Falus, A. (2005). H4R is implicated in various effects exerted by histamine on mouse dendritic cells. *European Histamine Research Society XXXIV Annual Meeting*. Bled, Slovenia.

Jin, C Y and Panula, P (2005). The laminar histamine receptor system in human prefrontal cortex suggests multiple levels of histaminergic regulation. *Neuroscience* **132**(1): 137-149.

Jones, K A, Borowsky, B, Tamm, J A, Craig, D A, Durkin, M M, Dai, M, Yao, W J, Johnson, M, Gunwaldsen, C, Huang, L Y, Tang, C, Shen, Q R, Salon, J A, Morse, K, Laz, T, Smith, K E, Nagarathnam, D, Noble, S A, Branchek, T A and Gerald, C (1998). GABA(B) receptors function as a heteromeric assembly of the subunits GABA(B)R1 and GABA(B)R2. *Nature* **396**(6712): 674-679.

Jordan, B A and Devi, L A (1999). G-protein-coupled receptor heterodimerization modulates receptor function. *Nature* **399**(6737): 697-700.

Kakinoki, H, Ishizawa, K, Fukunaga, M, Fujii, Y and Kamei, C (1998). The effects of histamine H-3-receptor antagonists on amygdaloid kindled seizures in rats. *Brain Research Bulletin* **46**(5): 461-465.

Karlstedt, K, Ahman, M J, Anichtchik, O V, Soinila, S and Panula, P (2003). Expression of the H-3 receptor in the developing CNS and brown fat suggests novel roles for histamine. *Molecular and Cellular Neuroscience* **24**(3): 614-622.

Kirkby, D L, Jones, D N C, Barnes, J C and Higgins, G A (1996). Effects of anticholinesterase drugs tacrine and E2020, the 5-HT3 antagonist ondansetron,

and the H-3 antagonist thioperamide, in models of cognition and cholinergic function. *Behavioural Pharmacology* 7(6): 513-525.

Kitbunnadaj, R, Hashimoto, T, Poli, E, Zuiderveld, O P, Menozzi, A, Hidaka, R, de Esch, I J P, Bakker, R A, Menge, W, Yamatodani, A, Coruzzi, G, Timmerman, H and Leurs, R (2005). N-substituted piperidinyl alkyl imidazoles: Discovery of methimepip as a potent and selective histamine H-3 receptor agonist. *Journal of Medicinal Chemistry* **48**(6): 2100-2107.

Kitbunnadaj, R, Zuiderveld, O P, Christophe, B, Hulscher, S, Menge, W, Gelens, E, Snip, E, Bakker, R A, Celanire, S, Gillard, M, Talaga, P, Timmerman, H and Leurs, R (2004). Identification of 4-(1H-imidazol-4(5)-ylmethyl)pyridine (immethridine) as a novel, potent, and highly selective histamine H-3 receptor agonist. *Journal of Medicinal Chemistry* **47**(10): 2414-2417.

Kjaer, A, Knigge, U, Rouleau, A, Garbarg, M and Warberg, J (1994). Dehydration-Induced Release of Vasopressin Involves Activation of Hypothalamic Histaminergic Neurons. *Endocrinology* **135**(2): 675-681.

Knoche, A, Yokoyama, H, Ponomarenko, A, Frisch, C, Huston, J and Haas, H L (2003). High-frequency oscillation in the hippocampus of the behaving rat and its modulation by the histaminergic system. *Hippocampus* **13**(2): 273-280.

Kobilka, B (1992). Adrenergic-Receptors as Models for G Protein-Coupled Receptors. *Annual Review of Neuroscience* **15**: 87-114.

Korotkova, T M, Haas, H L and Brown, R E (2002). Histamine excites GABAergic cells in the rat substantia nigra and ventral tegmental area in vitro. *Neuroscience Letters* **320**(3): 133-136.

Krause, M, Rouleau, A, Stark, H, Luger, P, Lipp, R, Garbarg, M, Schwartz, J C and Schunack, W (1995). Synthesis, X-Ray Crystallography, and Pharmacokinetics of Novel Azomethine Prodrugs of (R)-Alpha-Methylhistamine - Highly Potent and Selective Histamine H-3 Receptor Agonists. *Journal of Medicinal Chemistry* **38**(20): 4070-4079.

Krupp, P and Barnes, P (1992). Clozapine-associated agranulocytosis - risk and etiology. *British Journal of Psychiatry* **160**: 38-40.

Laitinen, J T and Jokinen, M (1998). Guanosine 5 '-(gamma- S-35 thio)triphosphate autoradiography allows selective detection of histamine H-3 receptor-dependent G protein activation in rat brain tissue sections. *Journal of Neurochemistry* **71**(2): 808-816.

Lamberti, C, Bartolini, A, Ghelardini, C and MalmbergAiello, P (1996). Investigation into the role of histamine receptors in rodent antinociception. *Pharmacology Biochemistry and Behavior* **53**(3): 567-574.

Lambright, D G, Sondek, J, Bohm, A, Skiba, N P, Hamm, H E and Sigler, P B (1996). The 2.0 angstrom crystal structure of a heterotrimeric G protein. *Nature* **379**(6563): 311-319.

Lanctot, P M, Leclerc, P C, Clement, M, Auger-Messier, M, Escher, E, Leduc, R and Guillemette, G (2005). Importance of N-glycosylation positioning for cell-surface expression, targeting, affinity and quality control of the human AT(1) receptor. *Biochemical Journal* **390**: 367-376.

Laroche, G, Lepine, M C, Theriault, C, Giguere, P, Giguere, V, Gallant, M A, de Brum-Fernandes, A and Parent, J L (2005). Oligomerization of the alpha and isoforms

of the thromboxane A(2) receptor: Relevance to receptor signaling and endocytosis. *Cellular Signalling* **17**(11): 1373-1383.

Larsson, M C, Domingos, A I, Jones, W D, Chiappe, M E, Amrein, H and Vosshall, L B (2004). Or83b encodes a broadly expressed odorant receptor essential for Drosophila olfaction. *Neuron* **43**(5): 703-714.

Leconiat, M, Traiffort, E, Ruat, M, Arrang, J M and Berger, R (1994). Chromosomal Localization of the Human Histamine H-1-Receptor Gene. *Human Genetics* **94**(2): 186-188.

Lefkowitz, R J (1993). G-protein-coupled receptor kinases. *Cell* **74**(3): 409-412.

Lefkowitz, R J (2004). Historical review: A brief history and personal retrospective of seven-transmembrane receptors. *Trends in Pharmacological Sciences* **25**(8): 413-422.

Lefkowitz, R J, Cotecchia, S, Samama, P and Costa, T (1993). Constitutive Activity of Receptors Coupled to Guanine-Nucleotide Regulatory Proteins. *Trends in Pharmacological Sciences* **14**(8): 303-307.

Leurs, R, Bakker, R A, Timmerman, H and de Esch, I J P (2005). The histamine H-3 receptor: From gene cloning to H-3 receptor drugs. *Nature Reviews Drug Discovery* **4**(2): 107-U18.

Leurs, R, Hoffmann, M, Wieland, K and Timmerman, H (2000). H-3 receptor gene is cloned at last. *Trends in Pharmacological Sciences* **21**(1): 11-12.

Leurs, R, Kathmann, M, Vollinga, R C, Menge, W, Schlicker, E and Timmerman, H (1996). Histamine homologues discriminating between two functional H-3

receptor assays. Evidence for H-3 receptor heterogeneity? *Journal of Pharmacology and Experimental Therapeutics* **276**(3): 1009-1015.

Leurs, R, Smit, M J and Timmerman, H (1995). Molecular pharmacological aspects of histamine-receptors. *Pharmacology & Therapeutics* **66**(3): 413-463.

Leurs, R, Traiffort, E, Arrang, J M, Tardivellacombe, J, Ruat, M and Schwartz, J C (1994). Guinea-Pig Histamine H-1 Receptor .2. Stable Expression in Chinese-Hamster Ovary Cells Reveals the Interaction with 3 Major Signal-Transduction Pathways. *Journal of Neurochemistry* **62**(2): 519-527.

Leurs, R, Watanabe, T and Timmerman, H (2001). Histamine receptors are finally `coming out'. *Trends in Pharmacological Sciences* **22**(7): 337-339.

Levi, R and Smith, N C E (2000). Histamine H-3-receptors: A new frontier in myocardial ischemia. *Journal of Pharmacology and Experimental Therapeutics* **292**(3): 825-830.

Ligneau, X, Lin, J S, Vanni-Mercier, G, Jouvet, M, Muir, J L, Ganellin, C R, Stark, H, Elz, S, Schunack, W and Schwartz, J C (1998). Neurochemical and behavioral effects of ciproxifan, a potent histamine H-3-receptor antagonist. *Journal of Pharmacology and Experimental Therapeutics* **287**(2): 658-666.

Ligneau, X, Morisset, S, Tardivel-Lacombe, J, Gbahou, F, Ganellin, C R, Stark, H, Schunack, W, Schwartz, J C and Arrang, J M (2000). Distinct pharmacology of rat and human histamine H-3 receptors: role of two amino acids in the third transmembrane domain. *British Journal of Pharmacology* **131**(7): 1247-1250.

Lim, H D, Sadek, P., Jongejan, A., Haaksma, E., de Esch, I., Leurs, R. (2007). Histamine H_4 receptor species variants and the molecular basis for their pharmalogical

differences. *European Histamine Research Society XXXVI Annual Meeting*. Florence, Italy.

Lim, H D, Bakker, R A, Thurmond, R L and Leurs, R (2006). Screening of histaminergic ligands for histamine H-4 receptor activity: discovery of a potent and selective H4R agonist. *Naunyn-Schmiedebergs Archives of Pharmacology* **373**(1): 94-94.

Lim, H D, Smits, R A, Leurs, R and De Esch, I J P (2006). The emerging role of the histamine H-4 receptor in anti-inflammatory therapy. *Current Topics in Medicinal Chemistry* **6**(13): 1365-1373.

Lim, H D, van Rijn, R M, Ling, P, Bakker, R A, Thurmond, R L and Leurs, R (2005). Evaluation of histamine H-1-, H-2-, and H-3-receptor ligands at the human histamine H-4 receptor: Identification of 4-methylhistamine as the first potent and selective H-4 receptor agonist. *Journal of Pharmacology and Experimental Therapeutics* **314**(3): 1310-1321.

Lin, J S, Hou, Y P, Sakai, K and Jouvet, M (1996). Histaminergic descending inputs to the mesopontine tegmentum and their role in the control of cortical activation and wakefulness in the cat. *Journal of Neuroscience* **16**(4): 1523-1537.

Lin, J S, Sakai, K, Vannimercier, G and Jouvet, M (1989). A critical role of the posterior hypothalamus in the mechanisms of wakefulness determined by microinjection of muscimol in freely moving cats. *Brain Research* **479**(2): 225-240.

Ling, P, Ngo, K, Nguyen, S, Thurmond, R L, Edwards, J P, Karlsson, L and Fung-Leung, W P (2004). Histamine H-4 receptor mediates eosinophil chemotaxis with cell shape change and adhesion molecule upregulation. *British Journal of Pharmacology* **142**(1): 161-171.

Linney, I D, Buck, I M, Harper, E A, Kalindjian, S B, Pether, M J, Shankley, N P, Watt, G F and Wright, P T (2000). Design, synthesis, and structure-activity relationships of novel non-imidazole histamine H-3 receptor antagonists. *Journal of Medicinal Chemistry* **43**(12): 2362-2370.

Liou, S Y, Shibata, S, Yamakawa, K and Ueki, S (1983). Inhibitory and Excitatory Effects of Histamine on Suprachiasmatic Neurons in Rat Hypothalamic Slice Preparation. *Neuroscience Letters* **41**(1-2): 109-113.

Lipp, R, Stark, H, Arrang, J M, Garbarg, M, Schwartz, J C and Schunack, W (1995). Synthesis and histamine H-3 receptor agonist activity of mono-substituted and dialkyl-substituted histamine derivatives. *European Journal of Medicinal Chemistry* **30**(3): 219-225.

Lippert, U, Artuc, M, Grutzkau, A, Babina, M, Guhl, S, Haase, I, Blaschke, V, Zachmann, K, Knosalla, M, Middel, P, Kruger-Krasagakis, S and Henz, B M (2004). Human skin mast cells express H2 and H4, but not H3 receptors. *Journal of Investigative Dermatology* **123**(1): 116-123.

Liu, C L, Ma, X J and Lovenberg, T W (2000). Alternative splicing of the histamine H-3 receptor mRNA at the third cytoplasmic loop is not detectable in humans. *Molecular Brain Research* **83**(1-2): 145-150.

Liu, C L, Wilson, S J, Kuei, C and Lovenberg, T W (2001). Comparison of human, mouse, rat, and guinea pig histamine H-4 receptors reveals substantial pharmacological species variation. *Journal of Pharmacology and Experimental Therapeutics* **299**(1): 121-130.

Liu, F, Wan, Q, Pristupa, Z B, Yu, X M, Wang, Y T and Niznik, H B (2000). Direct protein-protein coupling enables cross-talk between dopamine D5 and gamma-aminobutyric acid A receptors. *Nature* **403**(6767): 274-280.

Lovenberg, T W, Pyati, J, Chang, H, Wilson, S J and Erlander, M G (2000). Cloning of rat histamine H-3 receptor reveals distinct species pharmacological profiles. *Journal of Pharmacology and Experimental Therapeutics* **293**(3): 771-778.

Lovenberg, T W, Roland, B L, Wilson, S J, Jiang, X X, Pyati, J, Huvar, A, Jackson, M R and Erlander, M G (1999). Cloning and functional expression of the human histamine H-3 receptor. *Molecular Pharmacology* **55**(6): 1101-1107.

Lozada, A, Michelsen, KA, Karlstedt, K, Yamamoto, Y, Panula, P (2004). Expression of the histamine H_4 receptor during rat development. *European Histamine Research Society XXXIII Annual Meeting*. Dusseldorf/Koln, Germany.

Maggio, R, Barbier, P, Fornai, F and Corsini, G U (1996). Functional role of the third cytoplasmic loop in muscarinic receptor dimerization. *Journal of Biological Chemistry* **271**(49): 31055-31060.

Maggio, R, Vogel, Z and Wess, J (1993). Coexpression Studies with Mutant Muscarinic Adrenergic-Receptors Provide Evidence for Intermolecular Cross-Talk between G-Protein-Linked Receptors. *Proceedings of the National Academy of Sciences of the United States of America* 90(7): 3103-3107.

Maggio, R, Vogel, Z and Wess, J (1993). Reconstitution of functional muscarinic receptors by coexpression of amino-terminal and carboxyl-terminal receptor fragments. *Febs Letters* **319**(1-2): 195-200.

Malmbergaiello, P, Lamberti, C, Ghelardini, C, Giotti, A and Bartolini, A (1994). Role of Histamine in Rodent Antinociception. *British Journal of Pharmacology* **111**(4): 1269-1279.

Malmlof, K, Hastrup, S, Wulff, B S, Hansen, B C, Peschke, B, Jeppesen, C B, Hohlweg, R and Rimvall, K (2007). Antagonistic targeting of the histamine H-3 receptor decreases caloric intake in higher mammalian species. *Biochemical Pharmacology* **73**(8): 1237-1242.

Mariottini, C, Chiarugi, A., Fossati, S., Blandina, P., Passani, B. (2006). H_3 receptor activation phosphorylates Akt in rat cortical neurons. *European Histamine Research Society XXXV Annual Meeting*. Delphi, Greece.

Marshall, F H, Jones, K A, Kaupmann, K and Bettler, B (1999). GABA(B) receptors - the first 7TM heterodimers. *Trends in Pharmacological Sciences* **20**(10): 396-399.

Martin, G A, Cricco, G.P., Mohamad, N.A., Sambuco, L.A., Genre, F., Croci, M., Guttierez, A.S., Medina, V.A., Bergoc, R.M., Rivera, E.S. (2007). Histamine regulates pancreatic carcinoma cell growth through H_1, H_2, H_3 and H_4 receptors. *European Histamine Research Society XXXVI Annual Meeting*. Florence, Italy.

Martinez Mir MI, P H, Moreau J, Arrang JM, Ruat M, Traiffort E, Schwartz JC, Palacios JM (1990). Three histamine receptors (H1, H2 and H3) visualised in the brain of human and non-human primates. *Brain Research* **526**: 322 - 327.

Martinez-Mir MI, P H, Moreau J, Traiffort E, Ruat M, Schwartz JC, Palacios JM (1993). Loss of striatal histamine H2 receptors in Huntington's chorea but not in Parkinson's disease: comparison with animal models. *Synapse* **15**: 209-220.

Maslinska, D, Laure-Kamionowska, M, Maslinski, K T, Deregowski, K, Szewczyk, G and Maslinski, S (2006). Histamine H-4 receptors on mammary epithelial cells of the human breast with different types of carcinoma. *Inflammation Research* **55**: S77-S78.

Matsubara, T, Moskowitz, M A and Huang, Z H (1992). Uk-14,304, R(-)-Alpha-Methyl-Histamine and Sms-201-995 Block Plasma-Protein Leakage within Dura-Mater by Prejunctional Mechanisms. *European Journal of Pharmacology* **224**(2-3): 145-150.

McCormick, D A (1992). Neurotransmitter Actions in the Thalamus and Cerebral-Cortex and Their Role in Neuromodulation of Thalamocortical Activity. *Progress in Neurobiology* **39**(4): 337-388.

McCormick, D A and Williamson, A (1989). Convergence and Divergence of Neurotransmitter Action in Human Cerebral-Cortex. *Proceedings of the National Academy of Sciences of the United States of America* **86**(20): 8098-8102.

McLatchie, L M, Fraser, N J, Main, M J, Wise, A, Brown, J, Thompson, N, Solari, R, Lee, M G and Foord, S M (1998). RAMPs regulate the transport and ligand specificity of the calcitonin-receptor-like receptor. *Nature* **393**(6683): 333-339.

McLeod, R L, Aslanian, R, Del Prado, M, Duffy, R, Egan, R W, Kreutner, W, McQuade, R and Hey, J A (1998). Sch 50971, an orally active histamine H-3 receptor agonist, inhibits central neurogenic vascular inflammation and produces sedation in the guinea pig. *Journal of Pharmacology and Experimental Therapeutics* **287**(1): 43-50.

McLeod, R L, Mingo, G G, Herczku, C, DeGennaro-Culver, F, Kreutner, W, Egan, R W and Hey, J A (1999). Combined histamine H-1 and H-3 receptor blockade produces nasal decongestion in an experimental model of nasal congestion. *American Journal of Rhinology* **13**(5): 391-399.

McVey, M, Ramsay, D, Kellett, E, Rees, S, Wilson, S, Pope, A J and Milligan, G (2001). Monitoring receptor oligomerization using time-resolved fluorescence resonance energy transfer and bioluminescence resonance energy transfer - The human delta-opioid receptor displays constitutive oligomerization at the cell surface, which is not regulated by receptor occupancy. *Journal of Biological Chemistry* **276**(17): 14092-14099.

Medhurst, A D, Atkins, A R, Beresford, I J, Brackenborough, K, Briggs, M A, Calver, A R, Cilia, J, Cluderay, J E, Crook, B, Davis, J B, Davis, R K, Davis, R P, Dawson, L A, Foley, A G, Gartlon, J, Gonzalez, M I, Heslop, T, Hirst, W D, Jennings, C, Jones, D N C, Lacroix, L P, Martyn, A, Ociepka, S, Ray, A, Regan, C M, Roberts, J C, Schogger, J, Southam, E, Stean, T O, Trail, B K, Upton, N, Wadsworth, G, Wald, J A, White, T, Witherington, J, Woolley, M L, Worby, A and Wilson, D M (2007). GSK189254, a novel H-3 receptor antagonist that binds to histamine H-3 receptors in Alzheimer's disease brain and improves cognitive performance in preclinical models. *Journal of Pharmacology and Experimental Therapeutics* **321**(3): 1032-1045.

Medina, V, Cricco, G, Nunez, M, Martin, G, Mohamad, N, Correa-Fiz, F, Sanchez-Jimenez, F, Bergoc, R and Rivera, E S (2006). Histamine-mediated signaling

processes in human malignant mammary cells. *Cancer Biology & Therapy* **5**(11): 1462-1471.

Meyer, J L, Hall, A C and Harrington, M E (1998). Histamine phase shifts the hamster circadian pacemaker via an NMDA dependent mechanism. *Journal of Biological Rhythms* **13**(4): 288-295.

Michel, I, Borck, H., Diel, F. (2007). Histamine receptor H_4R-selective ligands influence the STAT6 Transcription Activation Domain (TAD) and the DNA-binding. *European Histamine Research Society XXXVI Annual Meeting*. Florence, Italy.

Michel, I, Klarwitter, B and Diel, F (2007). The DNA-binding of STAT6 and transcription activation domaine (TAD) are regulated via histamine receptor H4R in human lymphocytes ex vivo. *Allergy* **62**: 471-472.

Michineau, S, Alhenc-Gelas, F and Rajerison, R M (2006). Human bradykinin B2 receptor sialylation and N-glycosylation participate with disulfide bonding in surface receptor dimerization. *Biochemistry* **45**(8): 2699-2707.

Millan-Guerrero, R O, Pineda-Lucatero, A G, Hernandez-Benjamin, T, Tene, C E and Pacheco, M F (2003). N-alpha-methylhistamine safety and efficacy in migraine prophylaxis: Phase I and phase II studies. *Headache* **43**(4): 389-394.

Milligan, G (2001). Oligomerisation of G-protein-coupled receptors. *Journal of Cell Science* **114**(7): 1265-1271.

Milligan, G, Lopez-Gimenez, J, Wilson, S and Carrillo, J J (2004). Selectivity in the oligomerisation of G protein-coupled receptors. *Seminars in Cell & Developmental Biology* **15**(3): 263-268.

Minneman, K P (2007). Heterodimerization and surface localization of G protein coupled receptors. *Biochemical Pharmacology* **73**(8): 1043-1050.

Mitsuhashi, M and Payan, D G (1989). Receptor Glycosylation Regulates the Affinity of Histamine H1-Receptors During Smooth-Muscle Cell-Differentiation. *Molecular Pharmacology* **35**(3): 311-318.

Miyazaki, S, Imaizumi, M and Onodera, K (1995). Effects of Thioperamide, a Histamine H-3 Receptor Antagonist, on a Scopolamine-Induced Learning Deficit Using an Elevated Plus-Maze Test in Mice. *Life Sciences* **57**(23): 2137-2144.

Miyazaki, S, Onodera, K, Imaizumi, M and Timmerman, H (1997). Effects of clobenpropit (VUF-9153), a histamine H-3-receptor antagonist, on learning and memory, and on cholinergic and monoaminergic systems in mice. *Life Sciences* **61**(4): 355-361.

Mobarakeh, J I, Sakurada, S, Katsuyama, S, Kutsuwa, M, Kuramasu, A, Lin, Z Y, Watanabe, T, Hashimoto, Y, Watanabe, T and Yanai, K (2000). Of histamine H-1 receptor in pain perception: a study of the receptor gene knockout mice. *European Journal of Pharmacology* **391**(1-2): 81-89.

Mobarakeh, J I, Takahashi, K, Sakurada, S, Kuramasu, A and Yanai, K (2006). Enhanced antinociceptive effects of morphine in histamine H2 receptor gene knockout mice. *Neuropharmacology* **51**(3): 612-622.

Mochizuki, T, Okakuramochizuki, K, Horii, A, Yamamoto, Y and Yamatodani, A (1994). Histaminergic Modulation of Hippocampal Acetylcholine-Release in-Vivo. *Journal of Neurochemistry* **62**(6): 2275-2282.

Moench, S J, Moreland, J, Stewart, D H and Dewey, T G (1994). Fluorescence studies of the location and membrane accessibility of the palmitoylation sites of rhodopsin. *Biochemistry* **33**(19): 5791-5796.

Molina-Hernandez, A, Nunez, A and Arias-Montano, J A (2000). Histamine H-3-receptor activation inhibits dopamine synthesis in rat striatum. *Neuroreport* **11**(1): 163-166.

Molinengo, L, Di Carlo, G and Ghi, P (1999). Combined action of thioperamide plus scopolamine, diphenhydramine, or methysergide on memory in mice. *Pharmacology Biochemistry and Behavior* **63**(2): 221-227.

Monnot, C, Bihoreau, C, Conchon, S, Curnow, K M, Corvol, P and Clauser, E (1996). Polar residues in the transmembrane domains of the type 1 angiotensin II receptor are required for binding and coupling - Reconstitution of the binding site by co-expression of two deficient mutants. *Journal of Biological Chemistry* **271**(3): 1507-1513.

Morgan, P J, Ross, A W, Mercer, J G and Barrett, P (2006). What can we learn from seasonal animals about the regulation of energy balance? *Hypothalamic Integration of Energy Metabolism*. **153:** 325-337.

Morini, G, Grandi, D., Becchi, G., Shenton, F.C., Chazot, P.L. (2007). Histamine H_3 and H_4 receptors are expressed on distinct endocrine cell types in the rat fundic mucosa. *European Histamine Research Society XXXVI Annual Meeting*. Florence, Italy.

Morisset, S, Rouleau, A, Ligneau, X, Gbahou, F, Tardivel-Lacombe, J, Stark, H, Schunack, W, Ganellin, C R, Schwartz, J C and Arrang, J M (2000). High

constitutive activity of native H-3 receptors regulates histamine neurons in brain. *Nature* **408**(6814): 860-864.

Morisset, S, Sasse, A, Gbahou, F, Heron, A, Ligneau, X, Tardivel-Lacombe, J, Schwartz, J C and Arrang, J M (2001). The rat H-3 receptor: Gene organization and multiple isoforms. *Biochemical and Biophysical Research Communications* **280**(1): 75-80.

Morse, K L, Behan, J, Laz, T M, West, R E, Greenfeder, S A, Anthes, J C, Umland, S, Wan, Y T, Hipkin, R W, Gonsiorek, W, Shin, N, Gustafson, E L, Qiao, X D, Wang, S K, Hedrick, J A, Greene, J, Bayne, M and Monsma, F J (2001). Cloning and characterization of a novel human histamine receptor. *Journal of Pharmacology and Experimental Therapeutics* **296**(3): 1058-1066.

Muller, D, Middendorff, R, Olcese, J and Mukhopadhyay, A K (2002). Central nervous system-specific glycosylation of the type A natriuretic peptide receptor. *Endocrinology* **143**(1): 23-29.

Nakamura, T, Itadani, H, Hidaka, Y, Ohta, M and Tanaka, K (2000). Molecular cloning and characterization of a new human histamine receptor, HH4R. *Biochemical and Biophysical Research Communications* **279**(2): 615-620.

Nakaya, M, Takeuchi, N and Kondo, K (2004). Immunohistochemical localization of histamine receptor subtypes in human inferior turbinates. *Annals of Otology Rhinology and Laryngology* **113**(7): 552-557.

Nakayama, T, Kato, Y, Hieshima, K, Nagakubo, D, Kunori, Y, Fujisawa, T and Yoshie, O (2004). Liver-expressed chemokine/CC chemokine ligand 16 attracts eosinophils by interacting with histamine H4 receptor. *Journal of Immunology* **173**(3): 2078-2083.

Nelson, G, Hoon, M A, Chandrashekar, J, Zhang, Y F, Ryba, N J P and Zuker, C S (2001). Mammalian sweet taste receptors. *Cell* **106**(3): 381-390.

Ng, G Y K, Odowd, B F, Lee, S P, Chung, H T, Brann, M R, Seeman, P and George, S R (1996). Dopamine D2 receptor dimers and receptor-blocking peptides. *Biochemical and Biophysical Research Communications* **227**(1): 200-204.

Nguyen, T, Shapiro, D A, George, S R, Setola, V, Lee, D K, Cheng, R, Rauser, L, Lee, S P, Lynch, K R, Roth, B L and O'Dowd, B F (2001). Discovery of a novel member of the histamine receptor family. *Molecular Pharmacology* **59**(3): 427-433.

Oda, T, Matsumoto, S, Masuho, Y, Takasaki, J, Matsumoto, M, Kamohara, M, Saito, T, Ohishi, T, Soga, T, Hiyama, H, Matsushime, H and Furuichi, K (2002). cDNA cloning and characterization of porcine histamine H4 receptor. *Biochimica Et Biophysica Acta-Gene Structure and Expression* **1575**(1-3): 135-138.

Oda, T, Matsumoto, S I, Matsumoto, M, Takasaki, J, Kamohara, M, Soga, T, Hiyama, H, Kobori, M and Katoh, M (2005). Molecular cloning of monkey histamine H-4 receptor. *Journal of Pharmacological Sciences* **98**(3): 319-322.

Oda, T, Morikawa, N, Saito, Y, Masuho, Y and Matsumoto, S (2000). Molecular cloning and characterization of a novel type of histamine receptor preferentially expressed in leukocytes. *Journal of Biological Chemistry* **275**(47): 36781-36786.

Okamoto, Y, Ninomiya, H, Tanioka, M, Sakamoto, A, Miwa, S and Masaki, T (1997). Palmitoylation of human endothelin(B) - Its critical role in G protein coupling and a differential requirement for the cytoplasmic tail by G protein subtypes. *Journal of Biological Chemistry* **272**(34): 21589-21596.

Onodera, K, Miyazaki, S, Imaizumi, M, Stark, H and Schunack, W (1998). Improvement by FUB 181, a novel histamine H-3-receptor antagonist, of learning and memory in the elevated plus-maze test in mice. *Naunyn-Schmiedebergs Archives of Pharmacology* **357**(5): 508-513.

Onodera, K, Tuomisto, L, Tacke, U and Airaksinen, M (1992). Strain Differences in Regional Brain Histamine Levels between Genetically Epilepsy-Prone and Resistant Rats. *Methods and Findings in Experimental and Clinical Pharmacology* **14**(1): 13-16.

O'Reilly, M, Alpert, R, Jenkinson, S, Gladue, R P, Foo, S, Trim, S, Peter, B, Trevethick, M and Fidock, M (2002). Identification of a histamine H-4 receptor on human eosinophils - Role in eosinophil chemotaxis. *Journal of Receptor and Signal Transduction Research* **22**(1-4): 431-448.

Orsetti, M, Ferretti, C, Gamalero, S R and Ghi, P (2002). Histamine H-3-receptor blockade in the rat nucleus basalis magnocellularis improves place recognition memory. *Psychopharmacology* **159**(2): 133-137.

Overton, M C, Chinault, S L and Blumer, K J (2003). Oligomerization, biogenesis, and signaling is promoted by a glycophorin A-like dimerization motif in transmembrane domain 1 of a yeast G protein-coupled receptor. *Journal of Biological Chemistry* **278**(49): 49369-49377.

Owen, S M, Sturman, G and Freeman, P (1994). Modulation of Morphine-Induced Antinociception in Mice by Histamine H-3 Receptor Ligands. *Agents and Actions* **41**: C62-C63.

Palczewski, K, Kumasaka, T, Hori, T, Behnke, C A, Motoshima, H, Fox, B A, Le Trong, I, Teller, D C, Okada, T, Stenkamp, R E, Yamamoto, M and Miyano, M (2000). Crystal structure of rhodopsin: A G protein-coupled receptor. *Science* **289**(5480): 739-745.

Pallinger, E, Horvath, Z., Buzas, E., Hegyesi, H., Jelinek, I., Thurmond, R.L., Falus, A. (2005). Is there any influence of the absence of H4 receptor on T cell development: comparison of T cell precursors and thymic stroma cells involvrd in thymic selection of H4 receptor knockout (H4R-KO) and wild type (WT) mice. *European Histamine Research Society XXXIV Annual Meeting*. Bled, Slovenia.

Panula, P, Pirvola, U, Auvinen, S and Airaksinen, M S (1989). Histamine-Immunoreactive Nerve-Fibers in the Rat-Brain. *Neuroscience* **28**(3): 585-610.

Panula, P, Rinne, J, Kuokkanen, K, Eriksson, K, Sallmen, T, Kalimo, H and Relja, M (1998). Neuronal histamine deficit in Alzheimer's disease. *Neuroscience* **82**(4): 993-997.

Panula, P, Yang, H Y T and Costa, E (1984). Histamine-containing neurons in the rat hypothalamus. *Proceedings of the National Academy of Sciences of the United States of America-Biological Sciences* **81**(8): 2572-2576.

Pape, H C and McCormick, D A (1995). Electrophysiological and Pharmacological Properties of Interneurons in the Cat Dorsal Lateral Geniculate-Nucleus. *Neuroscience* **68**(4): 1105-1125.

Parmentier, R, Ohtsu, H, Djebbara-Hannas, Z, Valatx, J L, Watanabe, T and Lin, J S (2002). Anatomical, physiological, and pharmacological characteristics of histidine decarboxylase knock-out mice: Evidence for the role of brain histamine

in behavioral and sleep-wake control. *Journal of Neuroscience* **22**(17): 7695-7711.

Parsons, M E and Ganellin, C R (2006). Histamine and its receptors. *Br J Pharmacol* **147**(S1): S127-S135.

Passani, M B, Bacciottini, L, Mannaioni, P F and Blandina, P (2000). Central histaminergic system and cognition. *Neuroscience and Biobehavioral Reviews* **24**(1): 107-113.

Payne, G W and Neuman, R S (1997). Effects of hypomagnesia on histamine H-1 receptor-mediated facilitation of NMDA responses. *British Journal of Pharmacology* **121**(2): 199-204.

Petroianu, G, Arafat, K, Sasse, B C and Stark, H (2006). Multiple enzyme inhibitions by histamine H-3 receptor antagonists as potential procognitive agents. *Pharmazie* **61**(3): 179-182.

Pfleger, K D G and Eidne, K A (2005). Monitoring the formation of dynamic G-protein-coupled receptor-protein complexes in living cells. *Biochemical Journal* **385**: 625-637.

Philippu, A, Bald, M, Kraus, A and Dietl, H (1984). Invivo Release by Histamine Agonists and Antagonists of Endogenous Catecholamines in the Cat Hypothalamus. *Naunyn-Schmiedebergs Archives of Pharmacology* **326**(2): 116-123.

Pillot, C, Heron, A, Cochois, V, Tardivel-Lacombe, J, Ligneau, X, Schwartz, J C and Arrang, J M (2002). A detailed mapping of the histamine H-3 receptor and its gene transcripts in rat brain. *Neuroscience* **114**(1): 173-193.

Pollard, H, Moreau, J, Arrang, J M and Schwartz, J C (1993). A Detailed Autoradiographic Mapping of Histamine-H-3 Receptors in Rat-Brain Areas. *Neuroscience* **52**(1): 169-189.

Prast, H, Argyriou, A and Philippu, A (1996). Histaminergic neurons facilitate social memory in rats. *Brain Research* **734**(1-2): 316-318.

Prast, H, Fischer, H and Philippu, A (1994). Release of Acetylcholine in the Ventral Striatum Is Influenced by Histamine-Receptors. *Agents and Actions* **41**: C85-C86.

Prast, H, Tran, M H, Fischer, H, Kraus, M, Lamberti, C, Grass, K and Philippu, A (1999). Histaminergic neurons modulate acetylcholine release in the ventral striatum: role of H-3 histamine receptors. *Naunyn-Schmiedebergs Archives of Pharmacology* **360**(5): 558-564.

Prell, G D, Khandelwal, J K, Burns, R S, Lewitt, P A and Green, J P (1991). Influence of Age and Gender on the Levels of Histamine Metabolites and Pros-Methylimidazoleacetic Acid in Human Cerebrospinal-Fluid. *Archives of Gerontology and Geriatrics* **12**(1): 1-12.

Privou, C, Knoche, A, Hasenohrl, R U and Huston, J P (1998). The H-1- and H-2-histamine blockers chlorpheniramine and ranitidine applied to the nucleus basalis magnocellularis region modulate anxiety and reinforcement related processes. *Neuropharmacology* **37**(8): 1019-1032.

Qanbar, R and Bouvier, M (2003). Role of palmitoylation/depalmitoylation reactions in G-protein-coupled receptor function. *Pharmacology & Therapeutics* 97(1): 1-33.

Rands, E, Candelore, M R, Cheung, A H, Hill, W S, Strader, C D and Dixon, R A F (1990). Mutational analysis of beta-adrenergic-receptor glycosylation. *Journal of Biological Chemistry* **265**(18): 10759-10764.

Rathz, D A, Brown, K M, Kramer, L A and Liggett, S B (2002). Amino acid 49 polymorphisms of the human beta(1)-adrenergic receptor affect agonist-promoted trafficking. *Journal of Cardiovascular Pharmacology* **39**(2): 155-160.

Reggio, P H (2006). Computational methods in drug design: Modeling G protein-coupled receptor monomers, dimers, and oligomers. *Aaps Journal* **8**(2): E322-E336.

Richelson, E (1978). Histamine H-1 Receptor-Mediated Guanosine 3',5'-Monophosphate Formation by Cultured Mouse Neuroblastoma-Cells. *Science* **201**(4350): 69-71.

Rizk, A, Curley, J, Robertson, J and Raber, J (2004). Anxiety and cognition in histamine H-3 receptor(-/-) mice. *European Journal of Neuroscience* **19**(7): 1992-1996.

Rouleau, A, Heron, A, Cochois, V, Pillot, C, Schwartz, J C and Arrang, J M (2004). Cloning and expression of the mouse histamine H-3 receptor: evidence for multiple isoforms. *Journal of Neurochemistry* **90**(6): 1331-1338.

Rouleau, A, Stark, H, Schunack, W and Schwartz, J C (2000). Anti-inflammatory and antinociceptive properties of BP 2-94, a histamine H-3-receptor agonist prodrug. *Journal of Pharmacology and Experimental Therapeutics* **295**(1): 219-225.

Ryu, J H, Yanai, K, Iwata, R, Ido, T and Watanabe, T (1994). Heterogeneous Distributions of Histamine H3, Dopamine D1 and D2 Receptors in Rat-Brain. *Neuroreport* **5**(5): 621-624.

Ryu, J H, Yanai, K and Watanabe, T (1994). Marked Increase in Histamine H-3 Receptors in the Striatum and Substantia-Nigra Alter 6-Hydroxydopamine-

Induced Denervation of Dopaminergic-Neurons - an Autoradiographic Study. *Neuroscience Letters* **178**(1): 19-22.

Sadeghi, H M, Innamorati, G, Dagarag, M and Birnbaumer, M (1997). Palmitoylation of the V-2 vasopressin receptor. *Molecular Pharmacology* **52**(1): 21-29.

Sakai, K, M. El Mansari, J.S. Lin, Z.G. Zhang, G. Vanni-Mercier (1990). *The Diencephalon and Sleep*. New York, Raven Press.

Schild, H O (1947). Pa, a New Scale for the Measurement of Drug Antagonism. *British Journal of Pharmacology and Chemotherapy* **2**(3): 189-206.

Schlicker, E, Behling, A, Lummen, G and Gothert, M (1992). Histamine-H3a Receptor-Mediated Inhibition of Noradrenaline Release in the Mouse-Brain Cortex. *Naunyn-Schmiedebergs Archives of Pharmacology* **345**(4): 489-493.

Schlicker, E, Betz, R and Gothert, M (1988). Histamine H-3 Receptor-Mediated Inhibition of Serotonin Release in the Rat-Brain Cortex. *Naunyn-Schmiedebergs Archives of Pharmacology* **337**(5): 588-590.

Schlicker, E, Fink, K, Detzner, M and Gothert, M (1993). Histamine Inhibits Dopamine Release in the Mouse Striatum Via Presynaptic-H3 Receptors. *Journal of Neural Transmission-General Section* **93**(1): 1-10.

Schlicker, E, Fink, K, Hinterthaner, M and Gothert, M (1989). Inhibition of Noradrenaline Release in the Rat-Brain Cortex Via Presynaptic H-3 Receptors. *Naunyn-Schmiedebergs Archives of Pharmacology* **340**(6): 633-638.

Schlicker, E, Kathmann, M, Bitschnau, H, Marr, I, Reidemeister, S, Stark, H and Schunack, W (1996). Potencies of antagonists chemically related to iodoproxyfan at histamine H-3 receptors in mouse brain cortex and guinea-pig ileum: Evidence

for H-3 receptor heterogeneity? *Naunyn-Schmiedebergs Archives of Pharmacology* **353**(5): 482-488.

Schwartz, J C, Morisset, S, Rouleau, A, Tardivel-Lacombe, J, Gbahou, F, Ligneau, X, Heron, A, Sasse, A, Stark, H, Schunack, W, Ganellin, R C and Arrang, J M (2001). Application of genomics to drug design: the example of the histamine H-3 receptor. *European Neuropsychopharmacology* **11**(6): 441-448.

Segal, M (1981). Histamine Modulates Reactivity of Hippocampal Ca3 Neurons to Afferent Stimulation Invitro. *Brain Research* **213**(2): 443-448.

Seifert, R and Wenzel-Seifert, K (2003). The human formyl peptide receptor as model system for constitutively active G-protein-coupled receptors. *Life Sciences* **73**(18): 2263-2280.

Selbach, O, Brown, R E and Haas, H L (1997). Long-term increase of hippocampal excitability by histamine and cyclic AMP. *Neuropharmacology* **36**(11-12): 1539-1548.

Self, T J, Oakley, S M and Hill, S J (2005). Clathrin-independent internalization of the human histamine H-1-receptor in CHO-K1 cells. *British Journal of Pharmacology* **146**(4): 612-624.

Senba, E, Kaneko, T, Mizuno, N and Tohyama, M (1991). Somato-motor, branchio-motor and viscero-motor neurons contain glutaminase-like immunoreactivity. *Brain Research Bulletin* **26**(1): 85-97.

Shah, C, McAtee, L, Breitenbucher, J G, Rudolph, D, Li, X B, Lovenberg, T W, Mazur, C, Wilson, S J and Carruthers, N I (2002). Novel human histamine H-3 receptor antagonists. *Bioorganic & Medicinal Chemistry Letters* **12**(22): 3309-3312.

Shenton, F C and Chazot, P L (2006). Probing the importance of N-glycosylation for [H-3] clobenpropit binding to human H-3 receptors expressed in HEK 293 cells. *Inflammation Research* **55**: S40-S41.

Shenton, F C, Hann, V and Chazot, P L (2005). Evidence for native and cloned H-3 histamine receptor higher oligomers. *Inflammation Research* **54**: S48-S49.

Shi, L and Javitch, J A (2002). The binding site of aminergic G protein-coupled receptors: The transmembrane segments and second extracellular loop. *Annual Review of Pharmacology and Toxicology* **42**: 437-467.

Shin, N, Coates, E, Murgolo, N J, Morse, K L, Bayne, M, Strader, C D and Monsma, F J (2002). Molecular Modeling and site-specific mutagenesis of the histamine-binding site of the histamine H-4 receptor. *Molecular Pharmacology* **62**(1): 38-47.

Silver, R B, Mackins, C J, Smith, N C E, Koritchneva, I L, Lefkowitz, K, Lovenberg, T W and Levi, R (2001). Coupling of histamine H-3 receptors to neuronal Na+/H+ exchange: A novel protective mechanism in myocardial ischemia. *Proceedings of the National Academy of Sciences of the United States of America* 98(5): 2855-2859.

Smith, C P S, Hunter, A J and Bennett, G W (1994). Effects of (R)-Alpha-Methylhistamine and Scopolamine on Spatial-Learning in the Rat Assessed Using a Water Maze. *Psychopharmacology* **114**(4): 651-656.

Sogawa, N, Sogawa, C, Pohjanvirta, R, Tuomisto, J, Tuomisto, L, Onodera, K and Kitayama, S (2004). mRNA expression for histamine H3 receptor isoforms in rat brain. *Journal of Pharmacological Sciences* **94**: 234P-234P.

Sondek, J, Bohm, A, Lambright, D G, Hamm, H E and Sigler, P B (1996). Crystal structure of a G(A) protein beta gamma dimer at 2.1 angstrom resolution. *Nature* **379**(6563): 369-374.

Soyer, O S, Dimmic, M W, Neubig, R R and Goldstein, R A (2003). Dimerization in aminergic G-protein-coupled receptors: Application of a hidden-site class model of evolution. *Biochemistry* **42**(49): 14522-14531.

Staines, W A, Yamamoto, T, Daddona, P E and Nagy, J I (1986). Neuronal colocalization of adenosine-deaminase, monoamine-oxidase, galanin and 5-hydroxytryptophan uptake in the tuberomammillary nucleus of the rat. *Brain Research Bulletin* **17**(3): 351-365.

Stark, H, Ligneau, X, Arrang, J M, Schwartz, J C and Schunack, W (1998). General construction pattern of histamine H-3-receptor antagonists: Change of a paradigm. *Bioorganic & Medicinal Chemistry Letters* **8**(15): 2011-2016.

Stehle, J (1991). Effects of Histamine on Spontaneous Electrical-Activity of Neurons in Rat Suprachiasmatic Nucleus. *Neuroscience Letters* **130**(2): 217-220.

Strader, C D, Fong, T M, Tota, M R, Underwood, D and Dixon, R A F (1994). Structure and Function of G-Protein-Coupled Receptors. *Annual Review of Biochemistry* **63**: 101-132.

Suh, H W, Chung, K M, Kim, Y H, Huh, S O and Song, D K (1999). Effects of histamine receptor antagonists injected intrathecally on antinociception induced by opioids administered intracerebroventricularly in the mouse. *Neuropeptides* **33**(2): 121-129.

Szewczyk, G, Maslinska, D, Szukiewicz, D, Smiertka, W, Klimkiewicz, J and Pyzlak, M (2007). Histamine H-4 receptors in human placenta in diabetes-complicated pregnancy. *Inflammation Research* **56**: S31-S32.

Takahashi, K, Suwa, H, Ishikawa, T and Kotani, H (2002). Targeted disruption of H3 receptors results in changes in brain histamine tone leading to an obese phenotype. *Journal of Clinical Investigation* **110**(12): 1791-1799.

Takeshita, K, Bacon, K B and Gantner, F (2004). Critical role of L-selectin and histamine H4 receptor in zymosan-induced neutrophil recruitment from the bone marrow: Comparison with carrageenan. *Journal of Pharmacology and Experimental Therapeutics* **310**(1): 272-280.

Takeshita, K, Sakai, K, Bacon, K B and Gantner, F (2003). Critical role of histamine H-4 receptor in leukotriene B-4 production and mast cell-dependent neutrophil recruitment induced by zymosan in vivo. *Journal of Pharmacology and Experimental Therapeutics* **307**(3): 1072-1078.

Takeshita, Y, Watanabe, T, Sakata, T, Munakata, M, Ishibashi, H and Akaike, N (1998). Histamine modulates high-voltage-activated calcium channels in neurons dissociated from the rat tuberomammillary nucleus. *Neuroscience* **87**(4): 797-805.

Tang, B, Zhang, J, Li, H Z, Zhu, J N and Wang, J J (2007). Excitatory effect of histamine on neuronal activity of rat cerebellar fastigial nucleus in vitro. *Chinese Science Bulletin* **52**(4): 497-503.

Tardivel-Lacombe, J, Morisset, S, Gbahou, F, Schwartz, J C and Arrang, J M (2001). Chromosomal mapping and organization of the human histamine H-3 receptor gene. *Neuroreport* **12**(2): 321-324.

Tardivel-Lacombe, J, Rouleau, A, Heron, A, Morisset, S, Pillot, C, Cochois, V, Schwartz, J C and Arrang, J M (2000). Cloning and cerebral expression of the guinea pig histamine H-3 receptor: evidence for two isoforms. *Neuroreport* **11**(4): 755-759.

Terzioglu, N, van Rijn, R M, Bakker, R A, De Esch, I J P and Leurs, R (2004). Snythesis and structure-activity relationships of indole and benzimidazole piperazines as histamine H-4 receptor antagonists. *Bioorganic & Medicinal Chemistry Letters* **14**(21): 5251-5256.

Thoburn, K K, Hough, L B, Nalwalk, J W and Mischler, S A (1994). Histamine-Induced Modulation of Nociceptive Responses. *Pain* **58**(1): 29-37.

Thompson, C L, Bodewitz, G, Stephenson, F A and Turner, J D (1992). Mapping of Gaba-a Receptor Alpha-5 and Alpha-6 Subunit-Like Immunoreactivity in Rat-Brain. *Neuroscience Letters* **144**(1-2): 53-56.

Thurmond, R L, Desai, P J, Dunford, P J, Fung-Leung, W P, Hofstra, C L, Jiang, W, Nguyen, S, Riley, J P, Sun, S Q, Williams, K N, Edwards, J P and Karlsson, L (2004). A potent and selective histamine H-4 receptor antagonist with anti-inflammatory properties. *Journal of Pharmacology and Experimental Therapeutics* **309**(1): 404-413.

Toyota, H, Dugovic, C, Koehl, M, Laposky, A D, Weber, C, Ngo, K, Wu, Y, Lee, D H, Yanai, K, Sakurai, E, Watanabe, T, Liu, C L, Chen, J C, Barbier, A J, Turek, F W, Fung-Leung, W P and Lovenberg, T W (2002). Behavioral characterization of mice lacking histamine H-3 receptors. *Molecular Pharmacology* **62**(2): 389-397.

Traiffort, E, Pollard, H, Moreau, J, Ruat, M, Schwartz, J C, Martinezmir, M I and Palacios, J M (1992). Pharmacological characterization and autoradiographic

localization of histamine H-2 receptors in human brain identified with [I-125] iodoaminopotentidine. *Journal of Neurochemistry* **59**(1): 290-299.

Traiffort, E, Vizuete, M L, Tardivellacombe, J, Souil, E, Schwartz, J C and Ruat, M (1995). The Guinea-Pig Histamine H-2-Receptor - Gene Cloning, Tissue Expression and Chromosomal Localization of Its Human Counterpart. *Biochemical and Biophysical Research Communications* **211**(2): 570-577.

Traynelis, S F, Hartley, M and Heinemann, S F (1995). Control of Proton Sensitivity of the Nmda Receptor by Rna Splicing and Polyamines. *Science* **268**(5212): 873-876.

Tucker, T A, Varga, K, Bebok, Z, Zsembery, A, McCarty, N A, Collawn, J F, Schwiebert, E M and Schwiebert, L M (2003). Transient transfection of polarized epithelial monolayers with CFTR and reporter genes using efficacious lipids. *American Journal of Physiology-Cell Physiology* **284**(3): C791-C804.

Tuomisto, L and Tacke, U (1986). Is Histamine an Anticonvulsive Inhibitory Transmitter. *Neuropharmacology* **25**(8): 955-958.

Uveges, A J, Kowal, D, Zhang, Y X, Spangler, T B, Dunlop, J, Semus, S and Jones, P G (2002). The role of transmembrane helix 5 in agonist binding to the human H3 receptor. *Journal of Pharmacology and Experimental Therapeutics* **301**(2): 451-458.

Valentine, A F, Rizzo, C A, Rivelli, M A and Hey, J A (1999). Pharmacological characterization of histamine H-3 receptors in human saphenous vein and guinea pig ileum. *European Journal of Pharmacology* **366**(1): 73-78.

van Rijn, R M, Chazot, P L, Shenton, F C, Sansuk, K, Bakker, R A and Leurs, R (2006). Oligomerization of recombinant and endogenously expressed human histamine H-4 receptors. *Molecular Pharmacology* **70**(2): 604-615.

Varty, L M, Gustafson, E, Laverty, M and Hey, J A (2004). Activation of histamine H-3 receptors in human nasal mucosa inhibits sympathetic vasoconstriction. *European Journal of Pharmacology* **484**(1): 83-89.

Vauquelin, G and Van Liefde, I (2005). G protein-coupled receptors: a count of 1001 conformations. *Fundamental & Clinical Pharmacology* **19**(1): 45-56.

Villemagne, V L, Dannals, R F, Sanchezroa, P M, Ravert, H T, Vazquez, S, Wilson, A A, Natarajan, T K, Wong, D F, Yanai, K and Wagner, H N (1991). Imaging histamine H1 receptors in the living human brain with carbon-11-pyrilamine. *Journal of Nuclear Medicine* **32**(2): 308-311.

Vizuete, M L, Traiffort, E, Bouthenet, M L, Ruat, M, Souil, E, TardivelLacombe, J and Schwartz, J C (1997). Detailed mapping of the histamine H-2 receptor and its gene transcripts in guinea-pig brain. *Neuroscience* **80**(2): 321-343.

Vohora, D, Pal, S N and Pillai, K K (2000). Thioperamide, a selective histamine H-3 receptor antagonist, protects against PTZ-induced seizures in mice. *Life Sciences* **66**(22): PL297-PL301.

Vorobjev, V S, Sharonova, I N, Walsh, I B and Haas, H L (1993). Histamine Potentiates N-Methyl-D-Aspartate Responses in Acutely Isolated Hippocampal-Neurons. *Neuron* **11**(5): 837-844.

Waldhoer, M, Fong, J, Jones, R M, Lunzer, M M, Sharma, S K, Kostenis, E, Whistler, J L and Portoghese, P S (2005). A heterodimer-selective agonist shows in vivo

relevance of G protein-coupled receptor dimers. *Proceedings of the National Academy of Sciences of the United States of America* **102**(25): 9050-9055.

Watanabe, T, Taguchi, Y, Shiosaka, S, Tanaka, J, Kubota, H, Terano, Y, Tohyama, M and Wada, H (1984). Distribution of the histaminergic neuron system in the central nervous-system of rats - a fluorescent immunohistochemical analysis with histidine-decarboxylase as a marker. *Brain Research* **295**(1): 13-25.

Wellendorph, P, Goodman, M W, Burstein, E S, Nash, N R, Brann, M R and Weiner, D M (2002). Molecular cloning and pharmacology of functionally distinct isoforms of the human histamine H-3 receptor. *Neuropharmacology* **42**(7): 929-940.

West, R E, Wu, R L, Billah, M M, Egan, R W and Anthes, J C (1999). The profiles of human and primate H-3 N-alpha-methylhistamine binding differ from that of rodents. *European Journal of Pharmacology* **377**(2-3): 233-239.

West, R E, Zweig, A, Granzow, R T, Siegel, M I and Egan, R W (1990). Biexponential Kinetics of (R)-Alpha- H-3 Methylhistamine Binding to the Rat-Brain H3 Histamine-Receptor. *Journal of Neurochemistry* **55**(5): 1612-1616.

West, R E, Zweig, A, Shih, N Y, Siegel, M I, Egan, R W and Clark, M A (1990). Identification of 2-H-3-Histamine Receptor Subtypes. *Molecular Pharmacology* **38**(5): 610-613.

Wiedemann, P, Bonisch, H, Oerters, F and Bruss, M (2002). Structure of the human histamine H-3 receptor gene (HRH3) and identification of naturally occurring variations. *Journal of Neural Transmission* **109**(4): 443-453.

Wieland, K, Bongers, G, Yamamoto, Y, Hashimoto, T, Yamatodani, A, Menge, W, Timmerman, H, Lovenberg, T W and Leurs, R (2001). Constitutive activity of

histamine H-3 receptors stably expressed in SK-N-MC cells: Display of agonism and inverse agonism by H-3 antagonists. *Journal of Pharmacology and Experimental Therapeutics* **299**(3): 908-914.

Williams, K (1994). Subunit-Specific Potentiation of Recombinant N-Methyl-D-Aspartate Receptors by Histamine. *Molecular Pharmacology* **46**(3): 531-541.

Witkin, J M and Nelson, D L (2004). Selective histamine H-3 receptor antagonists for treatment of cognitive deficiencies and other disorders of the central nervous system. *Pharmacology & Therapeutics* **103**(1): 1-20.

Wu, G Y, Zhao, G Q and He, Y (2003). Distinct pathways for the trafficking of angiotensin II and adrenergic receptors from the endoplasmic reticulum to the cell surface - Rab1-independent transport of a G protein-coupled receptor. *Journal of Biological Chemistry* **278**(47): 47062-47069.

Xu, J G, He, J Q, Castleberry, A M, Balasubramanian, S, Lau, A G and Hall, R A (2003). Heterodimerization of alpha(2A)- and beta(1)-adrenergic receptors. *Journal of Biological Chemistry* **278**(12): 10770-10777.

Yabe, T, Dewaele, C, Serafin, M, Vibert, N, Arrang, J M, Muhlethaler, M and Vidal, P P (1993). Medial Vestibular Nucleus in the Guinea-Pig - Histaminergic Receptors .2. an Invivo Study. *Experimental Brain Research* **93**(2): 249-258.

Yamashita, M, Fukui, H, Sugama, K, Horio, Y, Ito, S, Mizuguchi, H and Wada, H (1991). Expression Cloning of a Cdna-Encoding the Bovine Histamine-H1 Receptor. *Proceedings of the National Academy of Sciences of the United States of America* **88**(24): 11515-11519.

Yanai, K, Son, L Z, Endou, M, Sakurai, E, Nakagawasai, O, Tadano, T, Kisara, K, Inoue, I, Watanabe, T and Watanabe, T (1998). Behavioural characterization and amounts of brain monoamines and their metabolites in mice lacking histamine H1 receptors. *Neuroscience* **87**(2): 479-487.

Yanai, K, Watanabe, T, Yokoyama, H, Hatazawa, J, Iwata, R, Ishiwata, K, Meguro, K, Itoh, M, Takahashi, T, Ido, T and Matsuzawa, T (1992). Mapping of histamine H1 receptors in the human brain using [C-11] pyrilamine and positron emission tomography. *Journal of Neurochemistry* **59**(1): 128-136.

Yanovsky, Y and Haas, H L (1998). Histamine increases the bursting activity of pyramidal cells in the CA3 region of mouse hippocampus. *Neuroscience Letters* **240**(2): 110-112.

Yao, B B, Hutchins, C W, Carr, T L, Cassar, S, Masters, J N, Bennani, Y L, Esbenshade, T A and Hancock, A A (2003). Molecular modeling and pharmacological analysis of species-related histamine H-3 receptor heterogeneity. *Neuropharmacology* **44**(6): 773-786.

Yao, B B, Sharma, R, Cassar, S, Esbenshade, T A and Hancock, A A (2003). Cloning and pharmacological characterization of the monkey histamine H-3 receptor. *European Journal of Pharmacology* **482**(1-3): 49-60.

Yokoyama, H, Onodera, K, Iinuma, K and Watanabe, T (1993). Effect of Thioperamide, a Histamine-H(3) Receptor Antagonist, on Electrically Induced Convulsions in Mice. *European Journal of Pharmacology* **234**(1): 129-133.

Yoshida, M, Noguchi, E and Tsuru, N (2000). Lack of substantial effect of the H-3-antagonist thioperamide and of the non-selective mixed H-3-antagonist/H-1-

agonist betahistine on amygdaloid kindled seizures. *Epilepsy Research* 40(2-3): 141-145.

Zhao, G Q, Zhang, Y F, Hoon, M A, Chandrashekar, J, Erlenbach, I, Ryba, N J P and Zuker, C S (2003). The receptors for mammalian sweet and umami taste. *Cell* **115**(3): 255-266.

Zhu, X and Wess, J (1998). N-terminal V2 vasopressin receptor fragments inhibit wild type receptor function via heterodimer formation. *Faseb Journal* **12**(8): A1457-A1457.

Zhu, X Y and Wess, J (1998). Truncated V2 vasopressin receptors as negative regulators of wild-type V2 receptor function. *Biochemistry* **37**(45): 15773-15784.

Zhu, Y, Michalovich, D, Wu, H L, Tan, K B, Dytko, G M, Mannan, I J, Boyce, R, Alston, J, Tierney, L A, Li, X T, Herrity, N C, Vawter, L, Sarau, H M, Ames, R S, Davenport, B M, Hieble, J P, Wilson, S, Bergsma, D J and Fitzgerald, L R (2001). Cloning, expression, and pharmacological characterization of a novel human histamine receptor. *Molecular Pharmacology* **59**(3): 434-441.

Zuckerman, R, Buzdygon, B, Philp, N, Liebman, P and Sitaramayya, A (1985). Arrestin - an ATP ADP exchange protein that regulates CGMP phosphodiesterase activity in retinal rod disk membranes (RDM). *Biophysical Journal* **47**(2): A37-A37.

APPENDIX

HETEROGENIETY OF H_3 RECEPTORS IN THE RODENT BRAIN: THE TUBEROMAMMILARY NUCLEUS (TMN)

FIGURE 1: The H_3 receptor is expressed on subpopulations of GABA-ergic neurons in the rat TMN

Double labeling immunoflurorescence experiments were performed using pan anti-H_3 (green) and anti-GAD67 (red) antibodies in the tuberomammilary nucleus (TMN). Images were captured using a confocal microscope. A. Low magnification merged image; B. Region of high GAD-positive staining and low H_3-postive staining; C. Region of low GAD-staining and high H_3-positive staining; D. Region of GAD/H_3 double labeling; E and F. examples of H_3 +ve/GAD –ve and a H_3 +ve/GAD +ve cells. (S Trelfel[1], S Cragge[1], FC Shenton and PL Chazot, unpublished) [1] *Department of Pharmacology, Oxford University*

A.

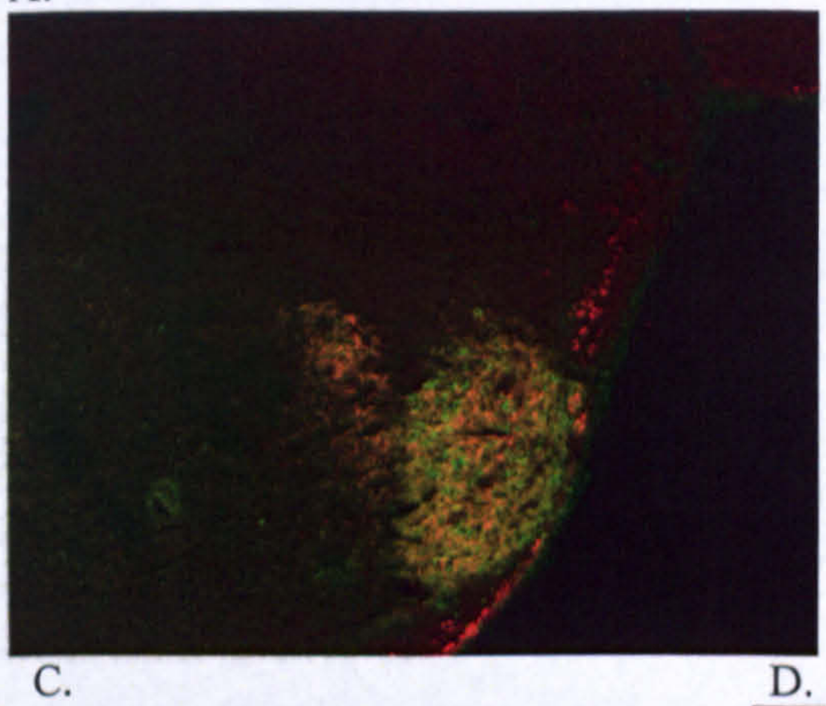

B.

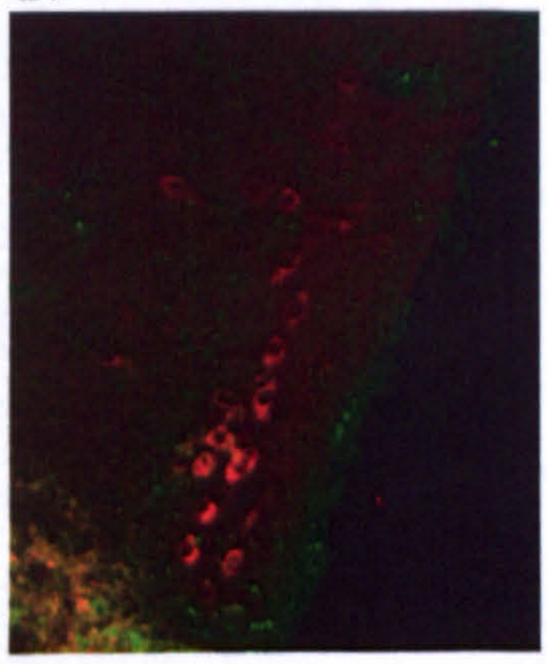

C.

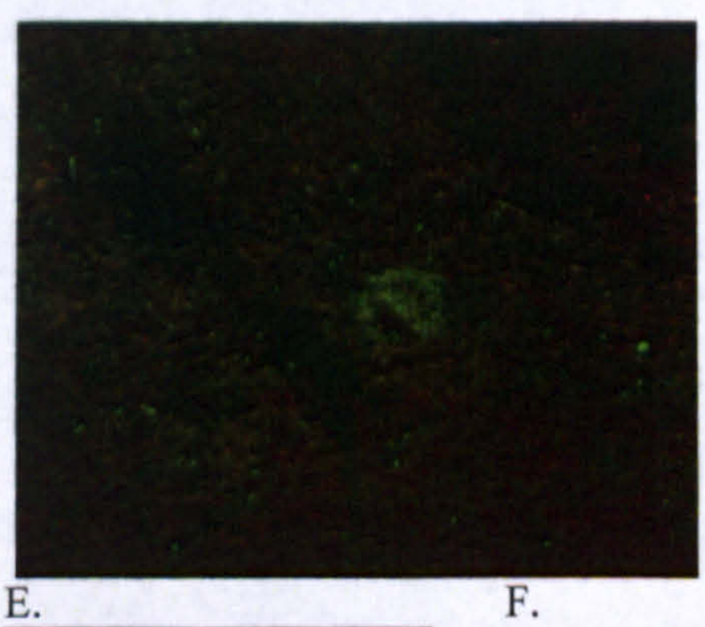

D.

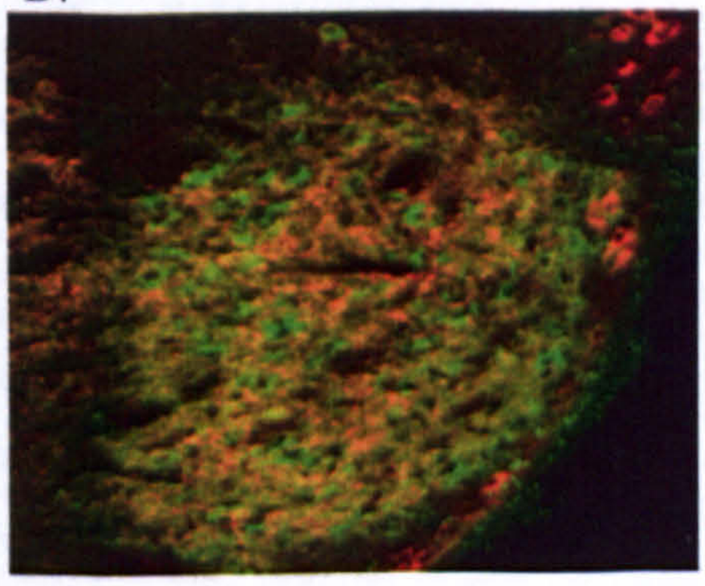

E.

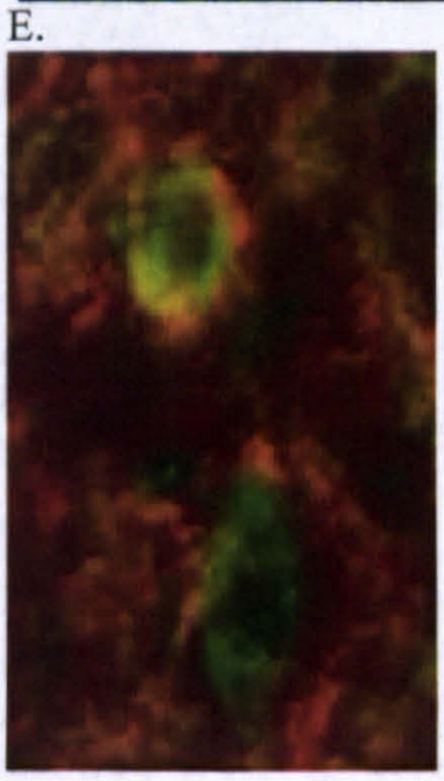

F.

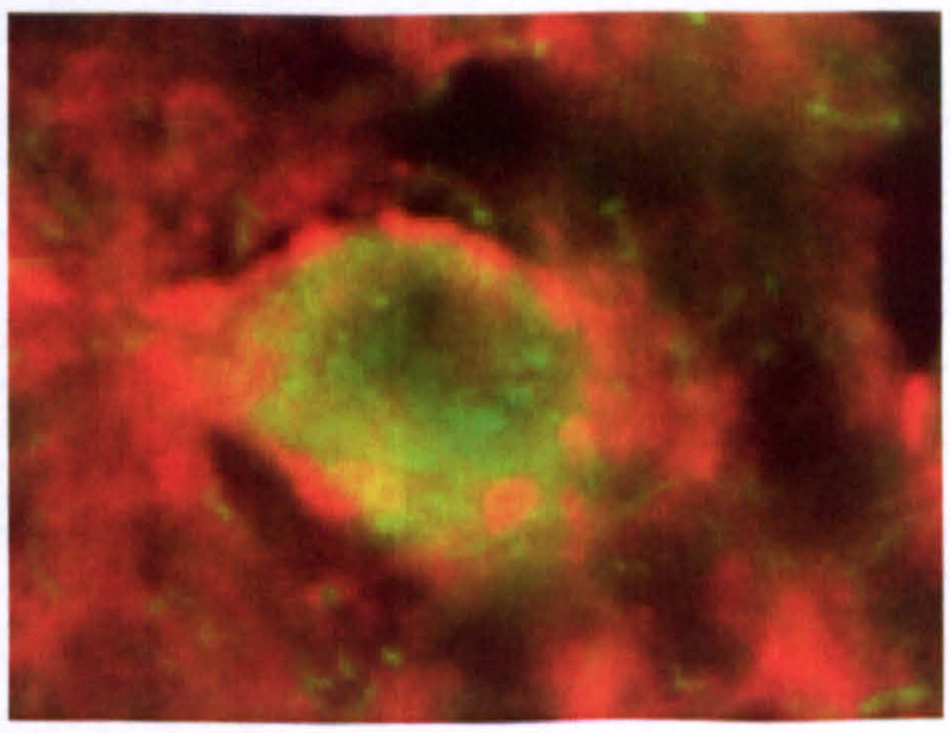

FIGURE 2: The H_3 receptor is expressed on subpopulations of histaminergic neurons in the rat TMN

Double labeling immunoflurorescence experiments were performed using pan anti-H_3 (red) and anti-HDC (green) antibodies in the tuberomammilary nucleus (TMN). Images were captured using a confocal microscope (B Passani[1], P Blandina[1], FC Shenton and PL Chazot, unpublished) [1] *Department of Preclinical and Clinical Pharmacology, University of Florence, Italy*

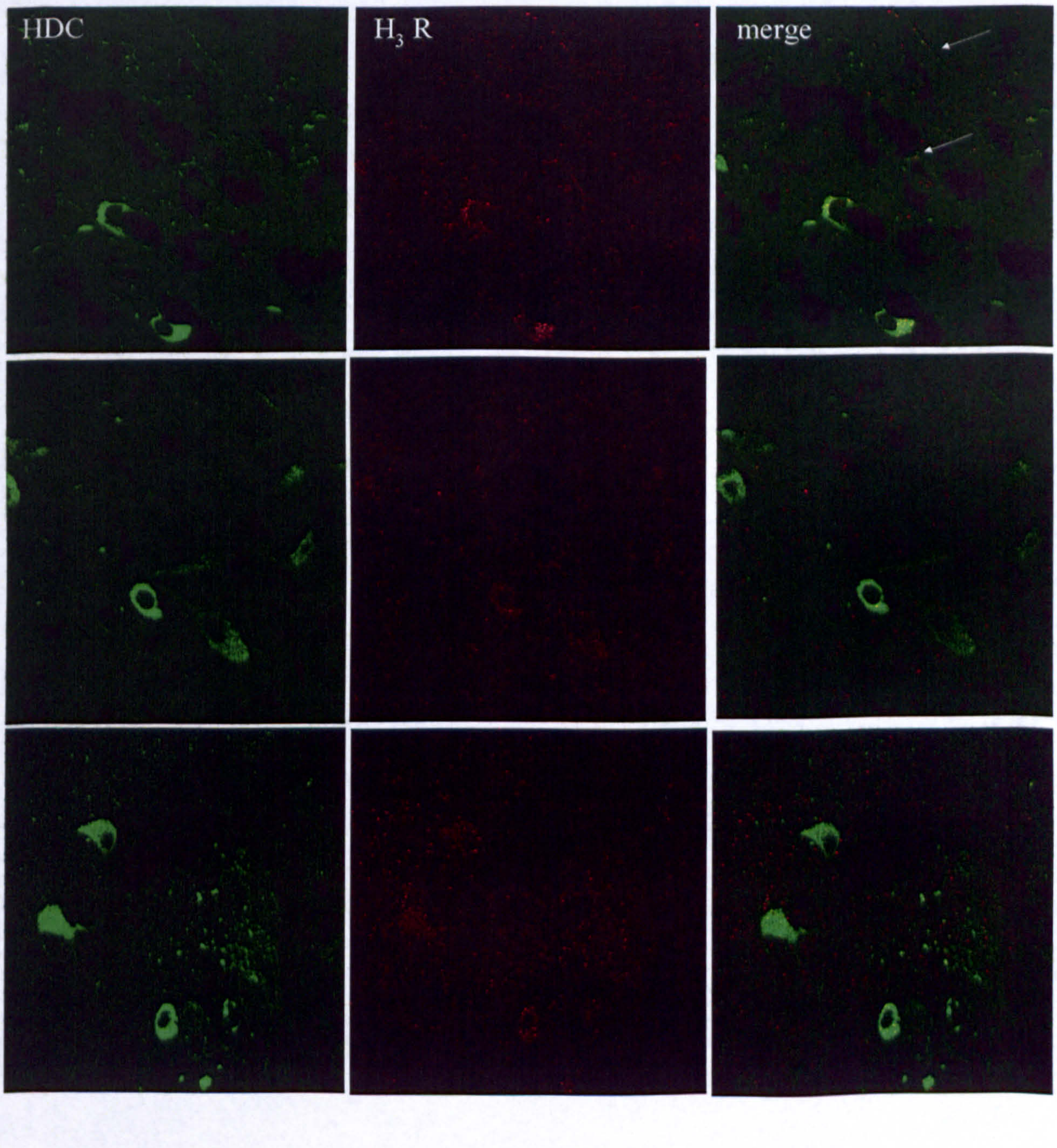

H_4 RECEPTOR EXPRESSION IN THE RODENT AND HUMAN CENTRAL AND PERIPHERAL NERVOUS SYSTEM

FIGURE 3: The expression of histamine H_4R in the mouse brain (A) and rat gastrointestinal tract (B), respectively, using our anti-hH_4R (374-390).

A). High levels of H_4-IR were evident in the thalamus, layer IV of the cerebral cortex, entorhinal cortex and CA3 of the hippocampus (FC Shenton and PL Chazot, unpublished). B). H_4-IR was present in the myenteric plexus of all regions of the gastrointestinal tract examined (Colon shown as an example). Staining for H_4R was particularly strong in ganglion soma and present, although to a lesser degree, on neuronal fibres. By contrast, the submucosal plexus was immunonegative for H_4R (PL Chazot, FC Shenton, D Grandy[1] and G Morini[1], 2007) [1]*Department of Human Anatomy, Pharmacology and Forensic Medicine, University of Parma, 43100 Parma, Italy*

A.

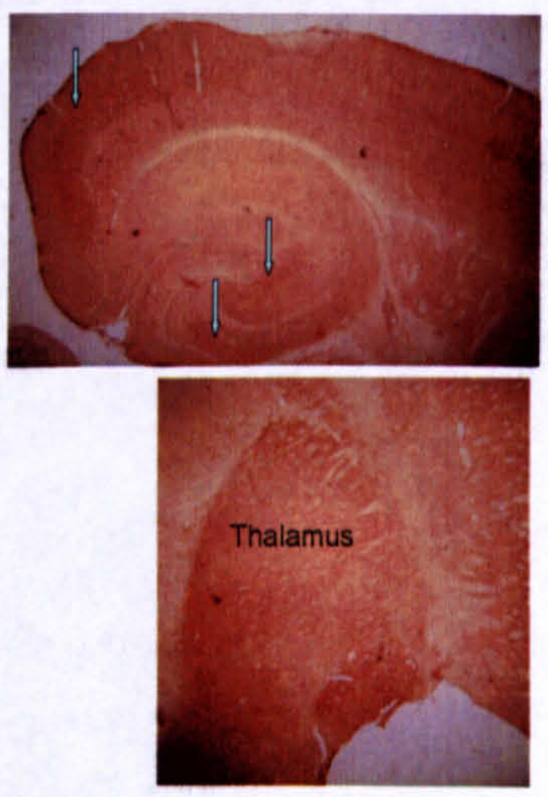

H_4 major expression in mouse brain
Thalamus +++++
Striatum +
Entorhinal cortex +++
Layer IV cortex ++++
CA3 +++
CA1 (-)

B.

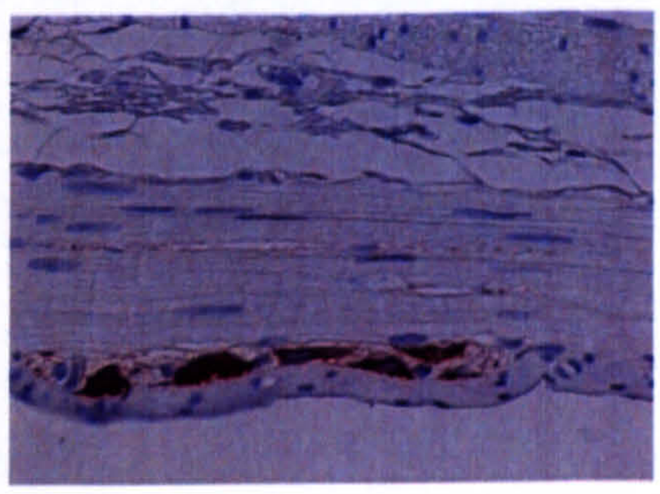

FIGURE 4: Expression of the H_4 receptor in the human brain.

A). Strong H_4R-IR punctuate decoration of putative neurons was observed in cortical and caudate regions of human brain slices by IHC (H Waldvogel[1], FC Shenton and PL Chazot, unpublished, [1] *Medical and Health Sciences, University of Auckland, NZ.* B).We have identified the first human H_4 receptor isoforms which act as dominant negative subunits *in vitro*. Both isoforms reduce the numbers of full length dimeric hH_4 receptors determined pharmacologically (Chapter 5, van Rijn *et al.*, 2007).

A. Cortex

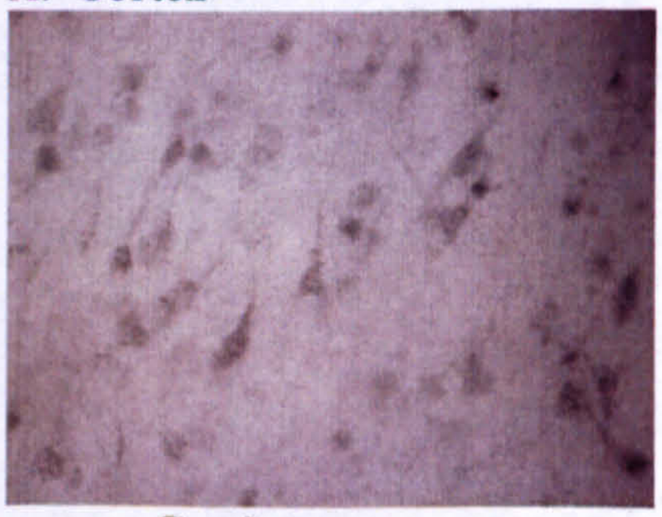

Caudate

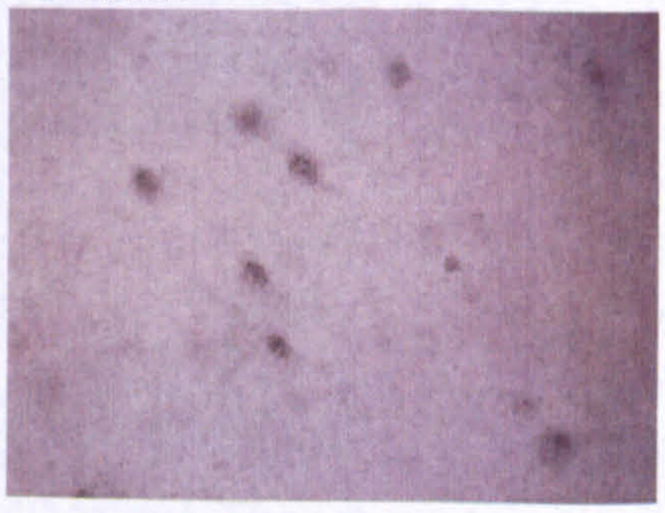

B.

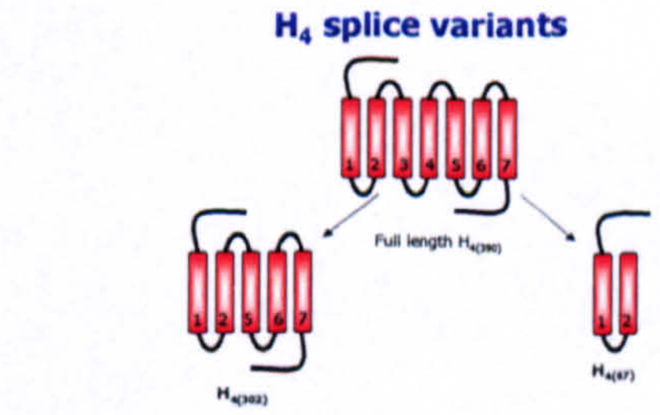

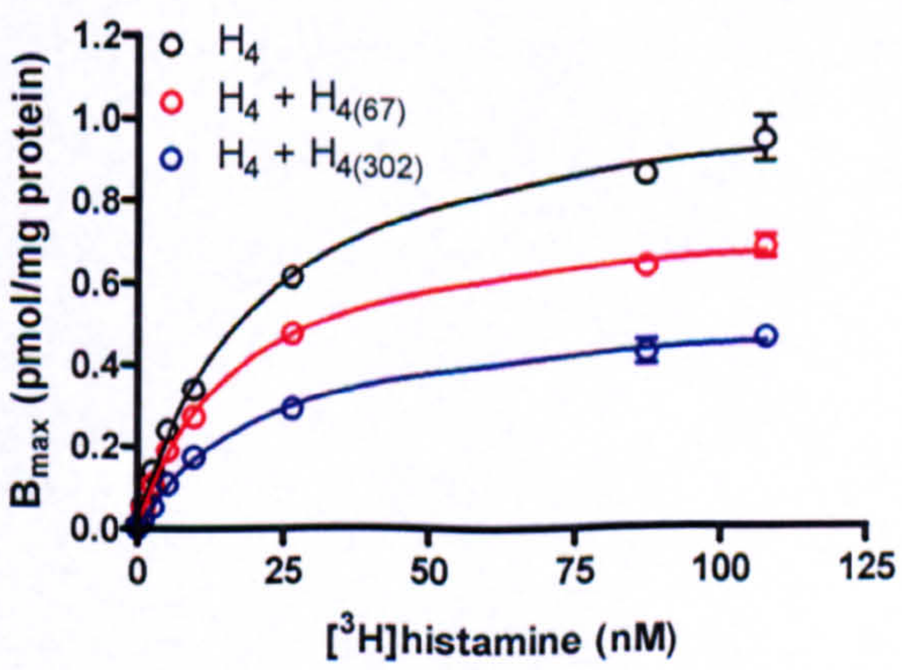

PUBLICATIONS

Hann, V, Shenton, F C and Chazot, P L (2004). "GTP-insensitive agonist binding to native and recombinant H_3 receptors." *Inflammation Res.* **53**: 67-68.

Chazot, P L and Shenton, F C (2004). "H_3 histamine receptors: the knockout data so far." *Curr Anaesth.Crit.Care* **15**: 23-28.

Shenton, F C, Hann, V and Chazot, P L (2005). "Evidence for native and cloned H_3 histamine receptor higher oligomers." *Inflammation Res.* **54**: 48-49.

Chazot, P L and Shenton, F C (2005). European Histamine Research Society Conference, Conference review. *ID weekly highlights*.

Shenton, F C (2005). British Neuroscience Meeting Report: Post Graduate and Early Career Symposium and Workshop on Communicating Science. *BNA Newsletter*.

Chazot, P L and Shenton, F C (2006). European Histamine Research Society Conference, Conference review. *ID weekly highlights*.

Shenton, F C and Chazot, P L (2006). "Probing the importance of N-glycosylation for [^{3}H] clobenpropit binding to human H_3 receptors expressed in HEK 293 cells." *Inflammation Res.* **55**: 40-41.

Bakker, R A, Lozada, A F, Van Marle, A, Shenton, F C, Van Rijn, R M, Karlstedt, K, Hoffmann, M, Lintunen, M, Yamamoto, Y, Drutel, G, Chazot, P L, Panula, P and Leurs, R(2006). "Discovery of naturally occurring splice variants of the rat histamine H_3 receptor that act as dominant negative." *Mol Pharmacol.* **69**: 1194-1206.

Cannon, K E, Chazot, P L, Hann, V, Shenton, F C, Hough, L B and Rice, F (2007). "Spinal Histamine H_3 receptor-mediated antinociception and localization on Sensory neurons." *Pain* **129** (Issue 1-2): 76-92.

Van Rijn, R M, Chazot, P L, Shenton, F C, Sansuk, K, Bakker, R A and Leurs, R (2006). "Oligomerisation of recombinant and endogenously expressed human histamine H_4 receptors." *Mol. Pharmacol.* **70** No. 2: 604-615.

Dijkstra, D, Leurs, R, Chazot, P L, Shenton, F C, Stark, H, Werfel, T and Gutzmer, R (2007). "Histamine down-regulates monocyte CCL2 production through the histamine H_4 receptor." *J. Allergy Clin. Immunol.* (in press).

Chazot, P L, Shenton, F C, Schunack, W, Grandi, D and Morini, G (2007). "Influence of (R)-α-Methylhistamine on the histamine H_3 receptor in the rat gastrointestinal tract." *Inflammation Res.* **56**: S19-S20.

Abstracts

Hann, V, Shenton, F C and Chazot, P L (2003). "Probing G-protein coupling to the H_3 receptor expressed in the adult mouse striatum." *XXII Annual European Histamine Research Society meeting, Holland.*

Hann, V, Shenton, F C and Chazot, P L (2003). "Probing G-protein coupling to the cloned human H_{3A} receptor expressed in HEK 293 cells." *XXII Annual European Histamine Research Society meeting, Holland.*

Shenton, F C, Hann, V, Ahmed, F and Chazot, P L (2003). "Human and rodent H_3 histamine receptor isoforms form homooligomers." *Neuroscience North East.*

Shenton, F C and Chazot, P L (2004). "Human and rodent H_3 histamine receptor isoforms form higher oligomers." *Br. J. Pharmacol. (Suppl.) Bath Meeting.*

Shenton, F C and Chazot, P L (2004). "Evidence for homo- and hetero-oligomeric H_3 histamine receptors: a biochemical study." *Biochem Soc Trans.*

Shenton, F C, Hann, V, Ahmed, F and Chazot, P L (2004). "The H_3 histamine receptor is a homooligomer." *XXIII Annual European Histamine Research Society meeting, Germany.*

Shenton, F C, van Rijn, R M, Leurs, R, Bakke, R and Chazot, P L (2005). "Human H_3 and H_4 histamine receptors are N-glycosylated homo-oligomers." *BNA conference, Durham.*

van Rijn, R M, Shenton, F C, Chazot, P L, Bakker, R A, Leurs, R (2005). "Oligomerization of the human histamine H_4 receptor." *Noordwijkerhout Camarino conference.*

Shenton, F C, van Rijn, R M, Bakker, R A, Leurs, R and Chazot, P L (2005). "Further evidence for rat and human H_3 receptor dimers: a cross-linking study." *XXXIV Annual European Histamine Research Society meeting, Slovenia.*

Chazot, P L, Cannon, K E, Hann, V, Shenton, F C, Hough, L B and Rice, F L (2005). "Immunohistochemical Localization of Histamine H_3 Receptors in Rodent Skin and Spinal Cord: Identification of potential anti-nociceptive Targets" *BNA conference*

van Rijn, R M, Shenton, F C, Chazot, P L, Bakker, R A and Leurs, R (2006). "Oligomerization of the human histamine H_4 receptor." *XXXV Annual European Histamine Research Society meeting, Greece.*

Chazot, P L, Shenton, F C, Schunack, W, Grandi, D, Morini, G (2006). "Immunolocalisation of histamine H_3 receptor in the rat gastrointestinal tract." *XXXV Annual European Histamine Research Society meeting, Greece.*

Grandi, D, Chazot, P L, Shenton, F C and Morini, G (2007). "Immunolocalisation of the histamine H_4 receptor in the rat gastrointestinal tract: first evidence for H_4 expression in the mammalian parasympathetic nervous system." *Digestive Disease Week conference, USA.*

Shenton, F C, van Rijn, R, Bakker, R, Leurs, R and Chazot, P L (2007). "Histamine H_4 receptor isoform hetero-oligomerisation and cell surface expression *in vitro*." *XXXVI Annual European Histamine Research Society meeting, Italy.*

Chazot, P L, Shenton, F C, Grandi, D, and Morini, G (2007). "Histamine H_3 and H_4 receptors are expressed on distinct endocrine cell types in the rat fundic mucosa." *XXXVI Annual European Histamine Research Society meeting, Italy.*

Chazot, P L, Shenton, F C, Waldvogel, H, Grandi, D and Morini, G (2007). "The H_4 histamine receptor is expressed in both the human CNS and rodent PNS." *XXXVI Annual European Histamine Research Society meeting, Italy.*

Giannoni, P, Passani, M B, Nosi, D, Medhurst, A D, Chazot, P L, Shenton, F C, Blandina, P (2007). "Detection of functional heterogeneity of histaminergic neurons in response to GSK189254, a novel H_3 receptor antagonist." *XXXVI Annual European Histamine Research Society meeting, Italy.*

In Preparation

Grandi, G, Shenton, F C, Chazot, P L and Morini G (2006). "Expression and distribution of histamine H_3 receptors in the rat gastrointestinal tract assessed by immunohistochemistry." Cell and Tissue Research (submitted).

Chazot, P L and Shenton, F C (2007). "Histamine H_3 receptors" Therapeutic effects in the CNS. (invited book chapter) Taylor & Francis Publishers (in preparation).

Hann, V, Shenton, F C and Chazot, P L (2003). "Evidence for coupling of $G_{\alpha}i3$ with rodent striatal H_3-histamine receptors."

Hann, V, Shenton, F C and Chazot, P L (2003). "Characterisation of human H_3 445 receptor transiently expressed in HEK 293 cells: immunological identification and G-protein coupling properties."

Inflamm. res. 53, *Supplement 1* (2004) S67–S68
1023-3830/04/01S67-02
DOI 10.1007/s00011-003-0332-3

Inflammation Research

GTP-insensitive agonist binding to native and recombinant H_3 receptors

V. Hann, F. C. Shenton and P. L Chazot

Sunderland Pharmacy School, University of Sunderland, Wharncliffe Street, Sunderland, Tyne and Wear, SR2 3SD, UK, Fax: ++ 44 191 515 3405, e-mail: paul.chazot@sunderland.ac.uk

Introduction

Molecular cloning has confirmed that the H_3 receptor is a G-protein coupled receptor (GPCR), subject to alternative splicing [1], which yields multiple potential receptor isoforms in rat, guinea pig and man [2]. The full-length gene product H_3 445 appears to be consistently expressed in all species studied to date and has been the most intensively studied isoform. R-α-Methylhistamine (RαMH) is considered the prototypical H_3 receptor full agonist and has been used widely as a selective pharmacological tool [3]. Many GPCR studies have identified guanine nucleotide-insensitive agonist binding, a feature which has been commonly attributed to a 'tight coupling mode constitutively active' state of the particular GPCR. There is growing compelling evidence that the H_3 receptor is endowed with a high level of constitutive activity, being most evident in the rodent striatum [4]. Here, we report that both native rodent and cloned human H_3 receptors display GTP-insensitive agonist binding, and the degree of insensitivity was comparable in both preparations, indicating a similar level of constitutive activity.

Materials and methods

HEK 293 cells were cultured and transfected with pCI-neo hH_3 445 (20 µg) or pCISNMDAR1 (10 µg) (mock) using the calcium phosphate precipitation method [5]. Transfected cells were harvested 48 h post-transfection, cell homogenates were prepared and subjected to immunoblotting [6] and [^{3}H]-clobenpropit binding assays [7].

Sodium dodecyl sulphate polyacrylamide gel electrophoresis (SDS-PAGE) was carried out using 7.5% polyacrylamide slab gels under reducing conditions. Immunoblots were probed with our previously described polyclonal anti-$hH_3$445 (349–358) antibody [6], used at a final protein concentration of 2 µg/ml.

[^{3}H] clobenpropit binding was performed essentially as described in [7]. Briefly, HEK 293 cell homogenates were incubated for 3 h at room temperature in 20 mM HEPES-NaOH buffer, in the presence of 3 mM metyrapone. Specific binding was defined using 10^{-5}M thioperamide. High affinity [^{3}H] R-α-Methylhistamine (RαMH) (2 nM) binding assays were performed on well-washed rat striatal P_2 membranes, essentially as described by Harper et al. [8]. Adult rat (Wistar strain) striatal membranes (400 µg protein) were incubated, in triplicate for 3 h at 22 °C, with [^{3}H] RαMH (2 nM) in 20 mM HEPES buffer pH 7.4. Non-specific binding was defined using unlabelled RαMH or thioperamide (both at 10^{-5}M). The assays were terminated by rapid filtration through Whatman GF/B filters pre-soaked in 0.1% polyethyleneimine, which were washed (3 × 3 ml) with ice-cold 10 mM sodium phosphate buffer (pH 7.4), using a 12-place Brandell cell harvester. Bound radioactivity was determined by liquid scintillation counting. The data were analysed using GraphPad Prism and all values cited are mean ± SD for at least 3 independent determinations.

Correspondence to: P. L. Chazot

Results and discussion

HEK 293 rNR1 (control) and HEK 293 hH_3 445 receptor cell homogenates were probed in parallel by immunoblotting, with our anti-H_3 445 (349–358) antibody. Selective expression was observed of a major polypeptide species of approx. M_r 45,000, corresponding to the predicted size of the *monomeric* H_3 445 receptor [1].

In pharmacological competition studies with HEK 293 $hH_3$445 receptor cell homogenates, using [^{3}H] clobenpropit (B_{max} < 500 fmol specific [^{3}H]-clobenpropit binding sites/mg protein), RαMH behaved as a classical agonist, displaying a complex binding curve, best fit to a two-site binding model, with a high affinity (apparent IC_{50} = 1.10 ± 0.06nM) and a low affinity (apparent IC_{50} = 89.13 ± 3.29 nM) binding component in the ratio 40:60 (high:low %, SD = 3), respectively. The presence of the non-hydrolysable GTP analogue, 5-guanylylimidodiphosphate (GppNHp) (0.1 mM) elicited a rightward shift in the RαMH competition curve. Interestingly, in the presence of GppNHp, RαMH can still discriminate between two binding sites, (apparent IC_{50} = 1.62 ± 0.09 nM and 60.26 ± 0.92 nM, respectively), but in the ratio 22:78 (high:low %, SD = 9). Notably the apparent IC_{50} values are very similar in the presence or absence of GppNHp.

In a parallel study, we investigated the GppNHp-sensitivity of [^{3}H] RαMH binding to native H_3 receptors expressed in the rat striatum. Both GppNHp (100 µM) and NaCL (1 M) promoted dissociation of the G-protein, eliciting a 68 ± 8% and 94 ± 18% reduction in specific [^{3}H] RαMH binding, respectively.

The molecular nature of this high-affinity guanine nucleotide-insensitive agonist binding to the H_3 receptor remains to be fully established. Some insight may be provid-

ed by the allosteric ternary complex model, which was developed to account for the phenomenon of constitutive activity. The H_3 receptor has recently been shown to be constitutively active in vivo, and the striatum reported to display the highest constitutive activity due to the high density of receptors in this region [4]. The GppNHp-insensitive RαMH component of [^{3}H] clobenpropit binding to the cloned hH_3 445 receptor (22 ± 9%) compares well with the GppNHp-insensitive component of [^{3}H] RαMH binding to native rat striatal H_3 receptors (32 ± 8%). This is consistent with a recent proposal that constitutive activity is observed at physiological densities of both human and rat H_3 receptors (with expression levels < 500 fmol/mg protein) [4]. This study provides evidence that we have a useful model system to study the pharmacology of a major human H_3 receptor isoform.

Acknowledgements: The authors wish to thank the Wellcome Trust and The European Social Fund for financial support, and Drs Tim Lovenberg and Elaine Harper for pCIneoH_3 445 and [^{3}H]-clobenpropit, respectively.

References

[1] Lovenberg TW, Roland BL, Wilson SJ, Jiang X, Pyati J, Huvar A et al. Cloning and Functional expression of the Human Histamine H_3 receptor. Mol. Pharmacol. 1999; 55: 1101–7

[2] Chazot PL, Hann V. Central H_3 histamine receptors: potential novel therapeutic targets. Current Opinion in Investigational Drugs. 2001; 2: 1428–31.

[3] Kilpatrick GJ, Michel AD. Characterisation of the binding of the histamine H_3 receptor agonist [^{3}H] R-α-methylhistamine to homogenates of rat and guinea-pig cortex. Agents Actions 1987; 33: 69–75.

[4] Rouleau A, Ligneau X, Tardivel-Lacombe J, Morisset S, Gbahou F, Schwartz JC et al. Histamine H_3 receptor-mediated [^{35}S] GTPγS binding: evidence for constitutive activity of the recombinant and native rat and human H_3 receptors. Br. J. Pharmacol 2002; 135: 383–92.

[5] Chazot PL, Coleman SK, Cik M, Stephenson FA. Molecular characterisation of NMDA receptors expressed in mammalian cells yields evidence for the coexistence of three subunit types within a discrete receptor molecule. J Biol Chem 1994; 269: 24403–9.

[6] Chazot PL, Wilson C, Hann V, Thompson CL, Lees G. Immunological identification of the mammalian H_3 histamine receptor in the adult mouse. NeuroReport 2001; 12: 259–62.

[7] Harper EA, Shankley NP, Black JW. Characterisation of the binding of [^{3}H] clobenpropit to histamine H_3 receptors in guinea-pig cerebral cortex membranes. Br J Pharmacol 1999; 128: 881–90.

[8] Harper EA, Shankley NP, Black JW. Evidence that histamine homologues discriminate between H_3-receptors in guinea-pig cerebral cortex and ileum longitudinal muscle myenteric plexus. Br J Pharmacol 1999; 128: 751–9.

Current Anaesthesia & Critical Care (2004) 15, 23–28

Current
ANAESTHESIA &
CRITICAL CARE

www.elsevier.com/locate/cacc

FOCUS ON: HUMAN GENOME

H_3 Histamine receptors: the gene knockout data so far

P.L. Chazot*, F.C. Shenton

Sunderland Pharmacy School, University of Sunderland, Sunderland, Tyne and Wear SR2 3SD, UK

KEYWORDS
Histamine receptors;
Histamine H3 central nervous system;
Mice;
Knockout;
Phenotype

Summary The Histamine H_3 receptor was identified over 20 years ago, but it was only recently cloned in 1999. This achievement has led to major strides in our understanding of the receptor, and a growing appreciation of the H_3 receptor as a novel therapeutic candidate particularly in the CNS. A number of recent gene-deletion 'knockout' studies have been reported which strengthen this optimism, particularly in areas of obesity, movement disorders, pain, dementias and anxiety.

Introduction

The neurotransmitter histamine is synthesized in the cell bodies of histaminergic neurons exclusively localized in the tuberomammillary nuclei of the hypothalamus. These neurons project widely in the CNS, lending credence to the idea that the histaminergic system may act as a major regulatory centre for the mammalian brain. Histamine elicits its major actions by binding to four distinct Histamine receptors, termed H_1–H_4, based on amino acid sequence identity. Schwartz and colleagues first demonstrated the presence of a novel pre-synaptic Histamine autoreceptor, termed H_3, in 1983.[1] Pharmacological confirmation of this receptor followed swiftly in 1985,[2] but it has taken 14 further years to finally identify the receptor itself, with the seminal work of Lovenberg and colleagues in the US.[3]

Structural features

Consistent with previous predictions, the H_3 receptor deduced protein sequence possesses all the primary structural characteristics of a G-protein coupled receptor (GPCR). Since the initial cloning of the human H_3 receptor, both the guinea pig and rat H_3 receptor orthologues have been successfully cloned.[4–7] Subsequently, the number has grown with the identification of multiple H_3 receptor splice isoforms in guinea pig, rat and, importantly, man.[4,6,8] This expansion now offers the possibility of new therapeutic targets and more selective drug design.

The human H_3 receptor splice isoforms display either a deletion in the second transmembrane (TM) domain (14 amino acids), a variable deletion in the third intracellular (IL) loop (30, 80, 116 amino acids) or a deletion in the fifth TM and the third IL (119 amino acids).[9] A consistent splice site identified for all three mammalian species occurs in the third IL, which implies that the different isoforms could couple to different G-proteins or to the same G-protein with different efficiencies, with resultant differential signalling consequences

*Corresponding author: Tel.: +44-191-515-3077; fax: +44-191-515-3405.
E-mail address: paul.chazot@sunderland.ac.uk (P.L. Chazot).

0953-7112/$ • see front matter © 2004 Elsevier Ltd. All rights reserved.
doi:10.1016/j.cacc.2004.01.006

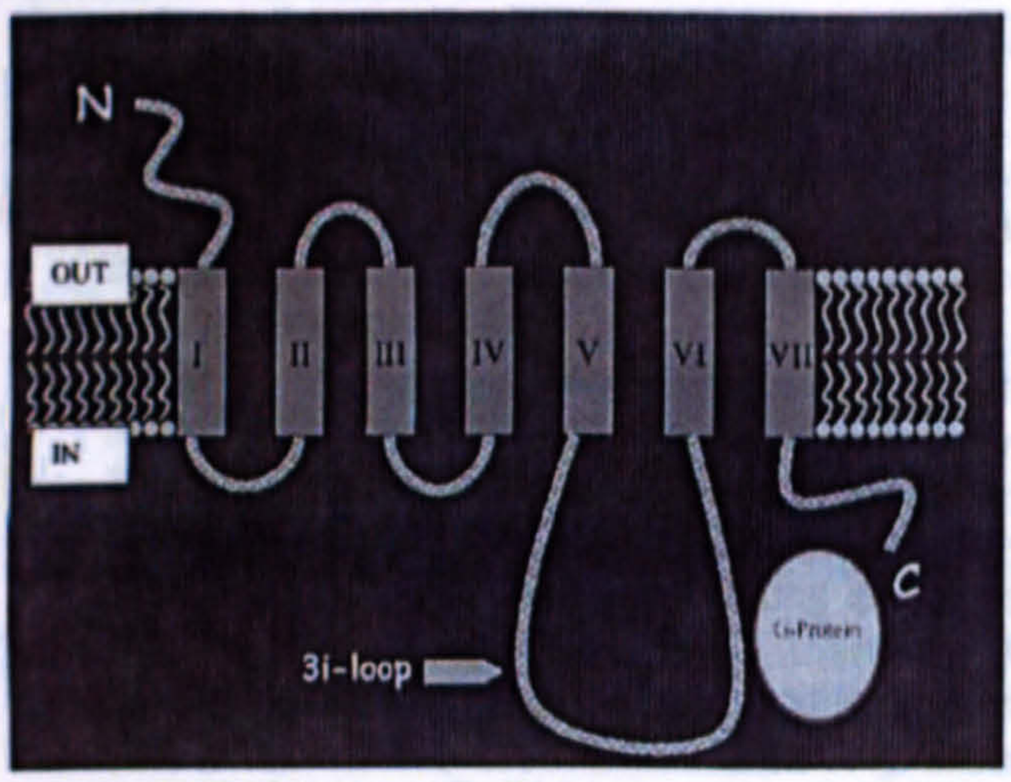

Figure 1 Schematic diagram of the H_3 histamine receptor.

(Fig. 1). It still remains unclear whether the H_3 receptor isoforms exist in vivo.[10]

Anatomical framework

The H_3 receptor polypeptide(s) has a widespread and abundant neuronal expression throughout the mammalian brain. High levels of H_3 receptor *protein* expression were detected in the deep layers of the cerebral cortex, the CA3 field and the dentate gyrus of the hippocampal formation, cerebellar purkinje cells, thalamus and striatum. Modest levels of H_3 receptor expression were also observed in many other areas of the brain.[11] In situ hybridization studies of human[3] and guinea pig,[4] the full length (445 amino acids) H_{3A} receptor isoform revealed no significant gross species differences in distribution patterns. However, interestingly two studies have shown that the rat and human H_3 receptor splice isoforms display differential expression patterns in the brain.[6,8,9] In the rat, the H_{3C} mRNA is the most strongly expressed isoform in many therapeutically relevant tissues, including the striatum, deep cortical layers, pyramidal layers of hippocampal fields CA1 and CA2 and locus ceruleus. H_{3A} expression is the most prominent isoform in the dorsal part of the dentate gyrus and CA1 field in the ventral hippocampus. The H_{3B} isoform displays the weakest expression generally and appears not to be expressed in the dentate gyrus. In man, interestingly, two of the short H_3 isoforms, with deletions in the third IL {H_3 (Δi3, 329 a.a.); H_3 (Δi3, 365 a.a.)}, are preferentially expressed in the hippocampus and the amygdala (implications for learning and memory). An important issue, yet to be addressed is whether the isoforms show any differential protein expression at the synaptic level. This awaits appropriate immunological tools.[11]

The knockout story so far

The histamine H_3 receptor subtype was originally discovered on histamine-containing neurons as a pre-synaptic receptor regulating the release and synthesis of histamine.[1] However, modulation of a number of other neurotransmitter systems throughout the brain via pre- and post-synaptic H_3 heteroreceptors has been clearly demonstrated.[12–20] The widespread distribution of H_3 receptors in the mammalian (rodent and human) CNS indicates strongly the multifaceted physiological role of this receptor family and hence the therapeutic potential as novel drug targets.

An important advance made possible by the cloning of the H_3 receptor has been the generation of H_3R knockout mice (H_3 –/–). The first description of an H_3 receptor-deficient mouse was by Toyota and colleagues.[21] Knockout mice were created from mouse embryonic stem cells in which the H_3 receptor gene had been disrupted. Histamine receptors play a complex role in the regulation of several important neurotransmitters in the brain. Therefore, the brain levels of a number of neurotransmitters and their metabolites were measured. The only change was a clear decrease in histamine levels in the cortex of H_3 (–/–) mice. This decrease was attributed to removal of the stimulatory effect of the H_3 receptor on the synthesis of histamine. There was no change in the levels of the other neurotransmitters, *including* dopamine, homovanillic acid, 3,4-dihydroxyphenylacetic acid, noradrenaline, serotonin and 5-hydroxyidolacetic acid.

Arousal and locomotion

The pre-synaptic autoregulatory H_3 receptor inhibits the release of neuronal histamine, which in turn leads to decrease of post-synaptic H_1 receptor function.[22] The role of the central H_1 receptor in arousal is well known and is the reason for the sedative effects of many H_1 receptor antagonists. The absence of the H_3 receptor might be expected to increase arousal via an increase in histaminergic transmission, but interestingly, this was not the case. H_3 (–/–) mice showed a decreased level of motor activity at night (normally their active period) and decreased wheel-running behaviour.

Several possible explanations were put forward to explain this anomaly:

(1) H_1 receptors may be downregulated to compensate for increased levels of histamine at the synapse. But H_1R binding experiments disproved this possibility.
(2) Removal of H_3 receptors may have lead to perturbations in the homeostasis of neurotransmitter levels borne out perhaps by lower levels of histamine in the H_3 (–/–) mice. The hypothesis being that although the braking effect of the H_3 receptor is removed, there is a compensatory decrease in the availability of histamine in the nerve terminals leading to an overall decrease in histaminergic neurotransmission.
(3) Histaminergic neurons may have diminished histamine content, due to the lack of inhibition by the H_3R throughout development.
(4) The influence of the histaminergic system on locomotor activity is complex e.g. the unexpected effects of H_1 receptor (–/–) on locomotion in light/dark, H1 –/– mice actually displayed an increase in locomotor activity during the light phase.[23]
(5) Finally the continuous absence of H_3 receptor throughout development could be compensated by changes in expression of other genes.

Although H_3 (–/–) mice showed decreased overall locomotion, wheel running behaviour, and body temperature during the dark phase, they maintained normal circadian rhythms. H_3 (–/–) mice were insensitive to the wake-promoting effects of the H_3 antagonist thioperamide, confirming the role of the H_3 receptor as a mediator of wakefulness.

The pre-synaptic H_3 receptor regulates the release of histamine and other neurotransmitters such as dopamine and acetylcholine.[13–17] Therefore, the effects of disruption of the H_3 receptor on these transmitter systems were investigated. Dopaminergic transmission is affected by methamphetamine which increases locomotor activity and stereotypic behaviour, by increasing dopamine release. Methamphetamine had less effect on H_3 (–/–) mice than controls, the increase in locomotor activity was less, and H_3 (–/–) mice scored lower on a stereotypy scale in response to methamphetamine. These data suggest that H_3 (–/–) mice may have decreased dopaminergic activity. This could play a part in the decrease in total activity and wheel running behaviour seen in these mice. However, it should also be noted that methamphetamine has effects on other pathways including serotonergic transmission.

Cognition and anxiety

The H_3 receptor appears to play a role in memory in some experimental models. It was found, using the passive avoidance model, that H_3 (–/–) mice learned as normal, but were insensitive to the amnesia-inducing effects of the muscarinic antagonist scopolamine. This is in agreement with studies where H_3 receptor antagonists have been shown to have the same effect on scopolamine-induced memory deficits.[24] Interestingly the H_3 (–/–) mice were not insensitive to scopolamine in the open field habituation test, which measures memory as the habituation of exploratory activity in a new environment. The fact that H_3 (–/–) mice were only insensitive to the effects of scopolamine in an aversion model may point to a specific role for the H_3 receptor in memory formation associated with painful stimuli.

In another study, H_3 (–/–) mice were used to probe the role of the H_3 receptor in anxiety and cognition. H_3 (–/–) mice displayed an age-dependent enhanced acquisition of spatially encoded information, using the water-maze model. Furthermore, the H_3 (–/–) mice displayed age-independent reduced measures of anxiety in the elevated plus maze and elevated zero maze models.[25] These findings point to the H_3 receptor as a potential new target for treating dementias and anxiety, respectively.

Obesity

Takahashi and colleagues generated a further H_3 (–/–) mouse[26] and probed the issue of obesity. They found that changes in the brain histamine tone lead to an obese phenotype. H_3 (–/–) mice manifest a mild obese phenotypes characterized by increased body weight, increased food intake and adiposity and decreased energy expenditure. As with the Toyota H_3 (–/–) mouse, body temperature and locomotor activity were found to be reduced (in this case both total and dark-phase locomotor activity were affected), while circadian rhythmicity was unaffected. Consistent with this obese phenotype, H3 –/– mice have insulin and leptin resistance; increased levels of plasma insulin and leptin, and increased expression of UCP1 and UCP3 in brown adipose tissue, while expression in white adipose tissue and skeletal muscle is decreased. Increase in adipose weight is known to increase leptin and insulin secretion in rodents. UCP1 and UCP3 are amongst a number of genes associated with food consumption and energy expenditure.

Changes in UCP expression may be caused by impaired leptin signalling in the hypothalamus of H_3 (–/–) mice, since leptin not only regulates appetite but also UCP expression in some peripheral tissues. Furthermore, injection of fluoromethylhistidine, which inhibits histamine synthesis, before leptin administration, blocked the anorexigenic effect of leptin,[27] and leptin receptor-deficient mice and Zucker fatty rats have decreased levels of hypothalamic histamine.[28] It is suggested that a possible underlying mechanism to these observations is impaired regulation of histaminergic neurons. The increased levels of the histamine metabolite, *tele*-methylhistamine, found in all brain areas of the H_3 (–/–) mice would support this. The lack of inhibitory H_3 autoreceptors could result in continuous release of histamine from presynaptic neurons. This could in turn lead to overload of the histamine synthesis machinery and a chronic shortage of histamine in the nerve terminals. Total histamine levels were lower in the hypothalamic/thalamic region of H_3 (–/–) mouse brains, although total brain histamine was not significantly altered. Since several H_3 antagonists have been shown to increase histamine release within the CNS and decrease food intake, increases in the concentration of *tele*-methylhistamine in the hypothalamic region together with increased food intake was unexpected. One explanation offered here is the desensitization of H_1 receptors. H_1 receptors could be downregulated to compensate for constitutive histamine exposure. In support of this, H_1 receptors were slightly reduced in the hypothalamic region of H_3 (–/–) mice compared with controls. More studies are needed to investigate the role of H_1 receptors in regulation of appetite. The anorexigenic effect of thioperamide following the administration of the hyperphagia-inducing peptide neuropeptide Y (NPY), was not observed in H_3 (–/–) mice, confirming the role of H_3 receptors in this system.

Pain

Earlier studies have indicated a possible pain-modulatory role for H_3 histamine receptors, but the loci and nature of this modulation has been poorly understood. The H_3 receptor agonist, Immepip produced robust antinociception in the rat mechanical (tail pinch) test, but not the thermal (tail flick) test, indicating a differential role of H_3 receptors. Intrathecal administration of thioperamide reversed the antinociceptive responses induced by systemically administered immepip, indicating a spinal site of action. Significantly, intrathecally administered immepip produced a maximal antinoceptive response on the tail pinch test in wild type, but not in H_3 (–/–) mice.[29] Recently, we have demonstrated immunologically, that the H_3 receptor is specifically located on deep dermal vascular innervation. Although more studies are underway, the present work reveals a group of H_3 receptor-containing fibres that may mediate some forms of mechanical nociception and could be a target for analgesic drugs that activate H_3 receptors.[30]

Table 1 Summary of H_3 receptor gene knockout data.

Therapeutic issues	H_3 (–/–) phenotype	Reference
Arousal	Insensitive to thioperamide-induced arousal	21
Locomotion	Decreased locomotor activity in active period	21
Cognition	• Insensitive to scopolamine-induced memory deficit in aversion model (painful memories)	25
	• Increased age-dependent spatial memory in water-maze model	
Anxiety	Reduced anxiety in elevated plus maze models	25
Obesity	• Impaired leptin signalling	26
	• Absent anorexigenic effect of thioperamide	
Pain	• Agonist-induced antinociceptive response in tail-pinch test absent	29,30
	• Deep dermal H_3 receptors absent	
Arrythmias	• Increased severity of reperfusion-induced cardiac arrythmias	31,32
	• Noradrenalin release increased in ischaemic heart	

Cardiac arrythmias

H_3 receptors are present in cardiac sympathetic nerve in man, where they attenuate norepinephrine release under normal physiological conditions, and in hyperadrenerigc states, e.g. myocardial ischaemia. Using H_3 (-/-) mice, it has been recently demonstrated that in the absence of H_3 receptors, norepinephrine release from an ischaemic heart is greatly increased, which may underlie the major cause of arrhythmic cardiac dysfunction. Indeed, follow-up work has shown that H_3 (-/-) mice display a markedly increased severity of reperfusion cardiac arrhythmias. These data reveal a significant cardioprotective role for H_3 receptors on cardiac sympathetic nerve endings.[31,32]

Concluding remarks

The H_3 receptor is a highly topical and growing area of research, notably in the pharmaceutical industry, and it is easy to predict that our knowledge and understanding will grow rapidly in the next couple of years. These gene knockout publications have provided further compelling evidence that the H_3 receptor is a strong candidate for therapeutic targetting in many important clinical arenas (Table 1).

Acknowledgements

Our work on the H_3 histamine receptor is currently funded by The Wellcome Trust. The author would like to acknowledge the ongoing collaboration with Professor LB Hough (Albany, NY, USA) and colleagues.

References

1. Arrang JM, Garbarg M, Schwartz JC. Auto-inhibition of brain histamine release mediated by a novel class (H3) of histamine receptor. *Nature* 1983;302(5911):832–7.
2. Arrang JM, Schwartz JC, Schunack W. Stereoselectivity of the histamine H3-presynaptic autoreceptor. *Eur J Pharmacol* 1985;117(1):109–14.
3. Lovenberg TW, Roland BL, Wilson SJ, et al. Cloning and functional expression of the human histamine H3 receptor. *Mol Pharmacol* 1999;55(6):1101–7.
4. Tardivel-Lacombe J, Rouleau A, Heron A, et al. Cloning and cerebral expression of the guinea pig histamine H3 receptor: evidence for two isoforms. *Neuroreport* 2000;11(4):755–9.
5. Lovenberg TW, Pyati J, Chang H, Wilson SJ, Erlander MG. Cloning of rat histamine H(3) receptor reveals distinct species pharmacological profiles. *J Pharmacol Exp Ther* 2000;293(3):771–8.
6. Drutel G, Peitsaro N, Karlstedt K, et al. Identification of rat H3 receptor isoforms with different brain expression and signaling properties. *Mol Pharmacol* 2001;59(1):1–8.
7. Morisset S, Sasse A, Gbahou F, et al. The rat H3 receptor: gene organization and multiple isoforms. *Biochem Biophys Res Commun* 2001;280(1):75–80.
8. Coge F, Guenin SP, Audinot V, et al. Genomic organization and characterization of splice variants of the human histamine H3 receptor. *Biochem J* 2001;355(Part 2):279–88.
9. Leurs R, Watanabe T, Timmermann H. Histamine receptors are finally "coming out". *TIPS* 2001;22:337–339.
10. Usiello A, Baik JH, Rouge-Pont F, et al. Distinct functions of the two isoforms of dopamine D2 receptors. *Nature* 2000; 408(6809):199–203.
11. Chazot PL, Hann V, Wilson C, Lees G, Thompson CL. Immunological identification of the mammalian H3 histamine receptor in the mouse brain. *Neuroreport* 2001;12(2): 259–62.
12. Clapham J, Kilpatrick GJ. Histamine H3 receptors modulate the release of [3H]-acetylcholine from slices of rat entorhinal cortex: evidence for the possible existence of H3 receptor subtypes. *Br J Pharmacol* 1992;107(4):919–23.
13. Blandina P, Giorgetti M, Bartolini L, et al. Inhibition of cortical acetylcholine release and cognitive performance by histamine H3 receptor activation in rats. *Br J Pharmacol* 1996;119(8):1656–64.
14. Giorgetti M, Bacciottini L, Bianchi L, Giovannini MG, Cecchi M, Blandina P. GABAergic mechanism in histamine H3 receptor inhibition of K(+)-evoked release of acetylcholine from rat cortex in vivo. *Inflamm Res* 1997;46(Suppl 1): S33–4.
15. Prast H, Tran MH, Fischer H, et al. Histaminergic neurons modulate acetylcholine release in the ventral striatum: role of H3 histamine receptors. *Naunyn Schmiedebergs Arch Pharmacol* 1999;360(5):558–64.
16. Schlicker E, Fink K, Detzner M, Gothert M. Histamine inhibits dopamine release in the mouse striatum via presynaptic H3 receptors. *J Neural Transm Gen Sect* 1993;93(1):1–10.
17. Molina-Hernandez A, Nunez A, Arias-Montano JA. Histamine H3-receptor activation inhibits dopamine synthesis in rat striatum. *Neuroreport* 2000;11(1):163–6.
18. Schlicker E, Werthwein S, Zentner J. Histamine H3 receptor-mediated inhibition of noradrenaline release in the human brain. *Fundam Clin Pharmacol* 1999;13(1):120–2.
19. Brown RE, Reymann KG. Histamine H3 receptor-mediated depression of synaptic transmission in the dentate gyrus of the rat in vitro. *J Physiol* 1996;496(Part 1):175–84.
20. Doreulee N, Yanovsky Y, Flagmeyer I, Stevens DR, Haas HL, Brown RE. Histamine H(3) receptors depress synaptic transmission in the corticostriatal pathway. *Neuropharmacology* 2001;40(1):106–13.
21. Toyota H, Dugovic C, Koehl M et al. Behavioral characterization of mice lacking histamine H(3) receptors. *Mol Pharmacol* 2002;62(2):389–397; *Erratum in: Mol Pharmacol* 2002;62(3):763.
22. Brown RE, Stevens DR, Haas HL. The physiology of brain histamine. *Prog Neurobiol* 2001;63(6):637–672.
23. Inoue I, Yanai K, Kitamura D, et al. Impaired locomotor activity and exploratory behavior in mice lacking histamine H1 receptors. *Proc Natl Acad Sci U S A* 1996;93(23):13316–20.
24. Giovannini MG, Bartolini L, Bacciottini L, Greco L, Blandina P. Effects of histamine H3 receptor agonists and antagonists on cognitive performance and scopolamine-induced amnesia. *Behav Brain Res* 1999;104(1–2):147–55.
25. Bongers G, Leurs R, Robertson J, Raber J. Role of H3 receptor—mediated signalling in anxiety and cognition in

wild type and Apoe (-/-) mice. *Neuropsychopharmacology* 2004;29:441–9.
26. Takahashi K, Suwa H, Ishikawa T, Kotani H. Targeted disruption of H3 receptors results in changes in brain histamine tone leading to an obese phenotype. *J Clin Invest* 2002;110(12):1791–9.
27. Itateyama E, Chiba S, Sakata T, Yoshimatsu H. Hypothalamic neuronal histamine in genetically obese animals: its implication of leptin action in the brain. *Exp Biol Med (Maywood)* 2003;228(10):1132–7.
28. Yoshimatsu H, Itateyama E, Kondou S, et al. Hypothalamic neuronal histamine as a target of leptin in feeding behavior. *Diabetes* 1999;48(12):2286–91.
29. Cannon KE, Nalwalk JW, Stadel R, et al. Activation of spinal histamine H3 receptors inhibits mechanical nociception. *Eur J Pharmacol* 2003;470(3):139–47.
30. Cannon KE, Nalwark JW, Stadel R, et al. Immunochemical localisation of H3 receptors on sensory neurons in wild type and H3 receptor knockout mice. *Soc Neurosci* 2003; 693–18.
31. Koyama M, Seyedi N, Fung-Leung WP, Lovenberg TW, Levi R. Norepinephrine release from the ischemic heart is greatly enhanced in mice lacking histamine H3 receptors. *Mol Pharmacol* 2003;63(2):378–82.
32. Koyama M, Heerdt PM, Levi R. Increased severity of reperfusion arrhythmias in mouse hearts lacking histamine H3-receptors. *Biochem Biophys Res Commun* 2003;306(3):792–6.

Inflamm. res. 54, *Supplement 1* (2005) S48–S49
1023-3830/05/01S48-02
DOI 10.1007/s00011-004-0422-x

Inflammation Research

Evidence for native and cloned H_3 Histamine receptor higher oligomers

F. C. Shenton, V. Hann and P. L. Chazot

School of Biological and Biomedical Sciences, University of Durham, South Road, DH1 3LE, Durham., UK, e-mail: paul.chazot@durham.ac.uk

Introduction

The H_3 histamine receptor subtype is a classic G-protein coupled receptor (GPCR) expressed almost exclusively in the CNS. Pharmacological heterogeneity in H_3 receptors within and across species has long been recognised, which may be explained by the presence of different isoforms and/or receptor oligomerisation reviewed in [1, 2]. There is evidence for the existence of higher molecular weight (MW) oligomers of many GPCRs, including the H_1 [3] and H_4 [4] histamine receptors. We have developed the first panel of specific anti-H_3 receptor antibodies, which have identified two specific immunoreactive species in adult rat and mouse brain homogenates analysed under reducing conditions, compatible with the presence of robust dimeric H_3 receptor isoforms (M_r 68,000 and 93,000) [5]. Here, we provide evidence using cross-linking strategies for the existence of native and recombinant H_3 receptor higher oligomers.

Materials and methods

Chemical cross-linking experiments were carried out on homogenates of rat forebrain membranes or HEK 293 cells expressing the hH_3 445 isoform, using both the reversible cross-linker dithiobis (succinimidyl propionate) (DSP) and the irreversible cross-linker bis (sulfosuccinimidyl) suberate (BS_3). Cross-linking using DSP was carried out essentially as described by Brose et al. [6].

HEK 293 cells were transfected with cDNA encoding the FLAG-tagged hH_3 445 receptor isoform, essentially using the Lipofectamine-Plus method described by Tucker et al. [7]. Cells were harvested 48 h post-transfection.

Chemical cross-linking using BS_3 was performed as described by Haugeto et al. [8]. Briefly, adult rat (Wistar strain) forebrain membranes or HEK 293 (hH_3 445) cell homogenates were incubated at a final concentration of 0.5 mg protein/ml buffer (150 mM sodium chloride, 100 mM HEPES, pH 7.5, containing 5 mM EDTA and 5 mM DTT), with BS_3 (0.01–3 mM) freshly prepared in 20 mM hydrochloric acid, for 12 min at room temperature, and the reaction terminated in 200 mM Tris-HCl pH 9.0.

Proteins were extracted using the chloroform/methanol precipitation method, and the precipitate subjected to SDS-PAGE under reducing conditions, using 6–7.5% (v/v) acrylamide slab gels. Proteins were transferred onto nitrocellulose and probed with the anti-hH_3 349–358 antibody [5] for the native experiments or the mouse anti-FLAG (Sigma Aldrich, UK) antibody for recombinant experiments, antibodies used at a final concentration of 1 µg/ml and dilution of 1/5,000, respectively. Immunological detection was achieved as described in [5].

Correspondence to: P. L. Chazot

Results and discussion

A series of chemical cross-linking experiments were performed on adult forebrain membranes and HEK 293 cell homogenates expressing the hH_3 445 isoform. In the absence of either cross-linker, the anti-H_3 349–358 antibody labelled two prominent immunoreactive species, M_r 68,000 and M_r 93000 in adult rat forebrain membranes, as previously reported [5] (Fig. 1). These protein sizes are consistent with the presence of dimeric rH_3 receptor isoforms. Low levels of putative monomers were also evident. By contrast, the recombinant hH_3 receptor expressed in HEK 293 cells migrated as both prominent monomers (M_r 47,000) and

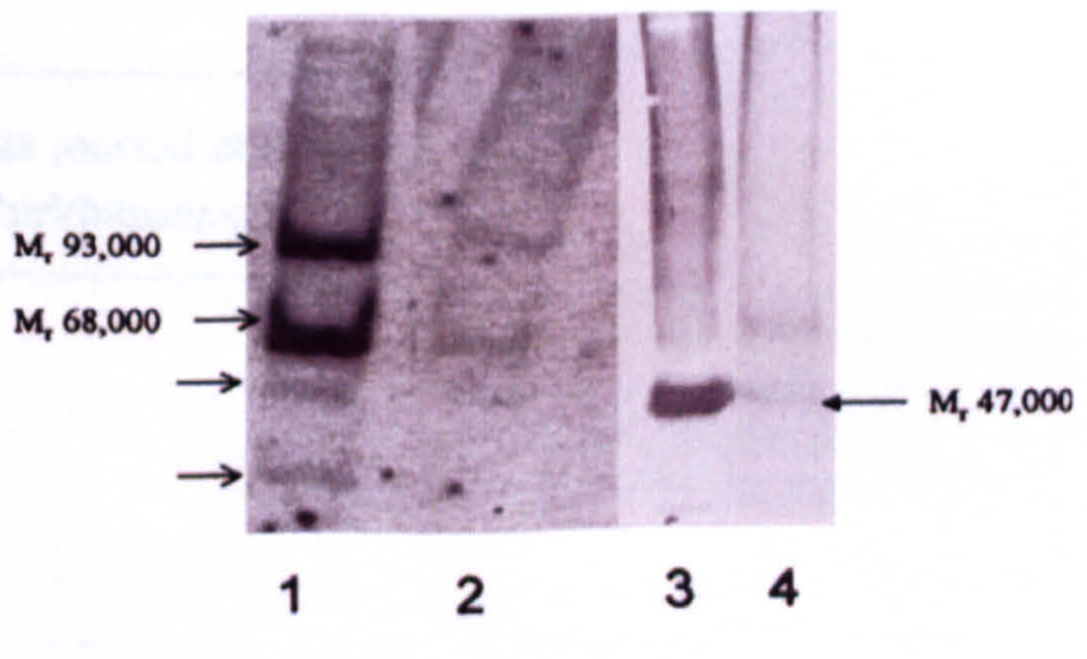

Fig. 1. Cross-linking of rat forebrain and recombinant FLAG-tagged hH_3 445 receptors. Adult rat forebrain membranes and FLAG-tagged hH_3 445 receptors expressed in HEK 293 cells were subjected to cross-linking with the irreversible crosslinker BS_3 (1 mM). The resultant preparations were then assessed by immunoblotting using anti-H_3 (349–358) and anti-FLAG antibodies for native (Lanes 1 and 2) and recombinant samples (Lanes 3 and 4), respectively. Lane 1, rat forebrain without cross-linker. Lane 2, rat forebrain in the presence of 1 mM BS_3. Lane 3, FLAG-tagged hH_3 445 expressed in HEK 293 cells without cross-linker. Lane 4, FLAG-tagged hH_3 445 expressed in HEK 293 cells in the presence of 1 mM BS_3.

dimers (M_r 93,000) (Fig. 1). The variation in dimer: monomer protein ratios between the native and recombinant preparations are likely to be due to the higher levels of overall H_3 receptor protein expression in the clonal cell line. Results with both the reversible and irreversible cross-linking agents (DSP and BS_3, respectively) were essentially identical. For the native tissue, in the presence of 0.1–3 mM DSP, little immunoreactivity was detected in the resolving gel. Notably, a concentration-dependent increase in hH_3 445 receptor dimers was observed up to 1 mM BS_3 (results not shown). Again, anti-H_3 receptor immunoreactivity was largely absent from the resolving gel in both preparations using concentrations of BS_3 in excess of 1 mM (Fig. 1).

The disappearance of detectable immunoreactivity in the resolving gel in the presence of the cross-linkers is most likely explained by the stabilisation of higher MW species (> M_r 200,000), too large to enter the resolving gel. The higher molecular weight oligomers contain disulphide bridges as they are disrupted by reduction with 20 mM DTT (Fig. 1, lane 1), to yield putative H_3 receptor dimers. The putative dimers in the untreated native tissue are robust non-disulphide linked oligomers since they are not disrupted by strong reducing (up to 200 mM DTT)/denaturing gel conditions adopted (results not shown). These findings suggest, for the first time, that native H_3 receptors exist as dimers and/or higher oligomers, which has important implications for understanding of the structure and function of H_3 receptors.

Acknowledgements. The authors wish to thank the Wellcome Trust for financial support and Dr Coge (Servier, France) for the hH_3445 clone.

References

[1] Chazot PL, Hann V. Central H_3 histamine receptors: potential novel therapeutic targets. Current Opinion in Investigational Drugs 2001; 2: 1428–31.
[2] Chazot PL, Shenton FC. H_3 Histamine receptors: the gene knockout data so far. Current Anaesthesia & Critical Care 2004; 15: 23–8.
[3] Bakker RA, Dees G, Carrillo JJ, Booth RG, Lopez-Gimenez JF, Milligan G et al. Domain swapping in the human histamine H_1 receptor. J Pharmacol Exp Ther 2004; in press.
[4] Van Rijn RM, Bakker RA, Leurs R. Homo-oligomerisation of the human histamine H_4 receptor. Proceedings of the Annual Meeting of the European Histamine Research Society 2004; p23.
[5] Chazot PL, Wilson C, Hann V, Thompson CL, Lees G. Immunological identification of the mammalian H_3 histamine receptor in the adult mouse. Neuroreport 2001; 12: 259–62.
[6] Brose N, Gasic GP, Vetter DE, Sullivan JM, Heineman SF. Protein chemical characterisation and immunocytochemical localisation of the NMDA receptor subunit NMDA R1. J Biol Chem 1993; 263: 22663–71.
[7] Tucker TA, Varga K, Bebok Z, Zsembery A, McCarty NA, Collawin JF et al. Transient transfection of polarised epithelial monolayers with CFTR and reporter genes using efficacious lipids. Am J Physiol Cell Physiol 2003; 284: C791–804.
[8] Haugeto O, Ullensvang K, Levt LM, Chaudry FA, Honore T, Nielsen M et al. Brain glutamate transporter proteins form homomultimers. J Biol Chem 1996; 271(44): 27715–22.

Inflamm. res. 55, *Supplement 1* (2006) S40–S41
1023-3830/06/01S40-02
DOI 10.1007/s00011-005-0033-1

Inflammation Research

3. Molecular and chemical aspects of the histamine receptors

Probing the importance of N-glycosylation for [^{3}H] clobenpropit binding to human H_3 receptors expressed in HEK 293 cells

F.C. Shenton and P.L. Chazot

School of Biological and Biomedical Sciences, University of Durham, South Road, DH1 3LE, Durham, UK, e-mail: paul.chazot@durham.ac.uk

Published Online First 20 March 2006

Introduction

The H_3 histamine receptor subtype is a classic G-protein coupled receptor (GPCR) expressed almost exclusively in the CNS. Pharmacological heterogeneity in H_3 receptors within and across species has long been recognised, which may be explained by the presence of different isoforms, receptor oligomerisation and/or glycosylation variance reviewed in [1] and [2]. The H_3 receptor possesses one putative N-glycosylation site, although the utility of this site has not been formally confirmed. Glycosylation has been previously shown to be important for appropriate processing and trafficking of many GPCRs to the membrane. Interestingly, glycosylation appears to have a differential role in H_1 and H_2 histamine receptor pharmacology [3, 4]. Tunicamycin is an N-glycosylation inhibitor, which has been previously used in our laboratory to probe the importance of post-translational N-glycosylation of the ionotropic NMDA receptor [5]. In this paper, we provide the first evidence that the human histamine hH_3 445 receptor is indeed N-glycosylated and this post-translational modification is not absolutely required for antagonist binding to the H_3 histamine receptor subtype.

Materials and methods

HEK 293 cells were transfected with cDNA encoding the FLAG epitope-tagged hH_3 445 receptor isoform, essentially using the LipofectaminePlus method described previously [6]. Cells were incubated with increasing concentrations of tunicamycin (0–2 μg/ml) in the media and harvested 48 h post-transfection.

Proteins were precipitated and subjected to SDS-PAGE under reducing conditions, using 6–7.5 % (v/v) acrylamide slab gels. Proteins were transferred onto nitrocellulose and probed with mouse anti-FLAG (Sigma Aldrich, UK), antibodies used at a final dilution of 1/5,000. Immunological detection was achieved as described in [7].

Correspondence to: P.L. Chazot

[^{3}H] clobenpropit binding was performed as described in [6]. We have evidence that clobenpropit acts as a neutral antagonist in this system (not shown). Specific binding was defined using thioperamide or R-alpha-Methylhistamine (10 μM).

Results and discussion

The effect of increasing concentrations of tunicamycin was investigated using immunoblotting and radioligand binding assays with [^{3}H] clobenpropit. Cells transfected with the hH_3 445 receptor and grown in the absence of tunicamycin, yielded, upon immunoblotting, a closely spaced doublet immunoreactive species (M_r 47,000 and M_r 45,000), consistent with the presence of a glycosylated and non-glycosylated hH_3 receptor monomer, respectively. As previously reported, a range of higher molecular putative oligomers were also detected (not shown) [8]. Incubation of HEK cells transfected with the hH_3 445 with increasing concentrations of the N-glycosylation inhibitor, tunicamycin, dose-dependently reduced the molecular weight of the M_r 47,000 immunoreactive species to the M_r 45,000 immunoreactive species (Fig. 1). This suggests that the hH_3 445 receptor is indeed modestly N-glycosylated, consistent with the predicted single putative glycosylation site.

In parallel, cell samples were subjected to [^{3}H] clobenpropit binding analysis, to assess whether N-glycosylation is absolutely required for ligand binding to the hH_3 445 receptor. Partial inhibition of N-glycosylation using 0.1 μg/ml tunicamycin resulted in no significant reduction in [^{3}H] clobenpropit binding, while near complete inhibition yielded only a modest 33 % reduction in specific binding (Fig. 1).

In conclusion, these findings demonstrate, for the first time, that human H_3 receptors are N-glycosylated and prevention of N-glycosylation does not appear to have a major effect upon [^{3}H] clobenpropit binding to the hH_3 445 receptor. This suggests that N-glycosylation is not absolutely required for antagonist binding to H_3 receptors.

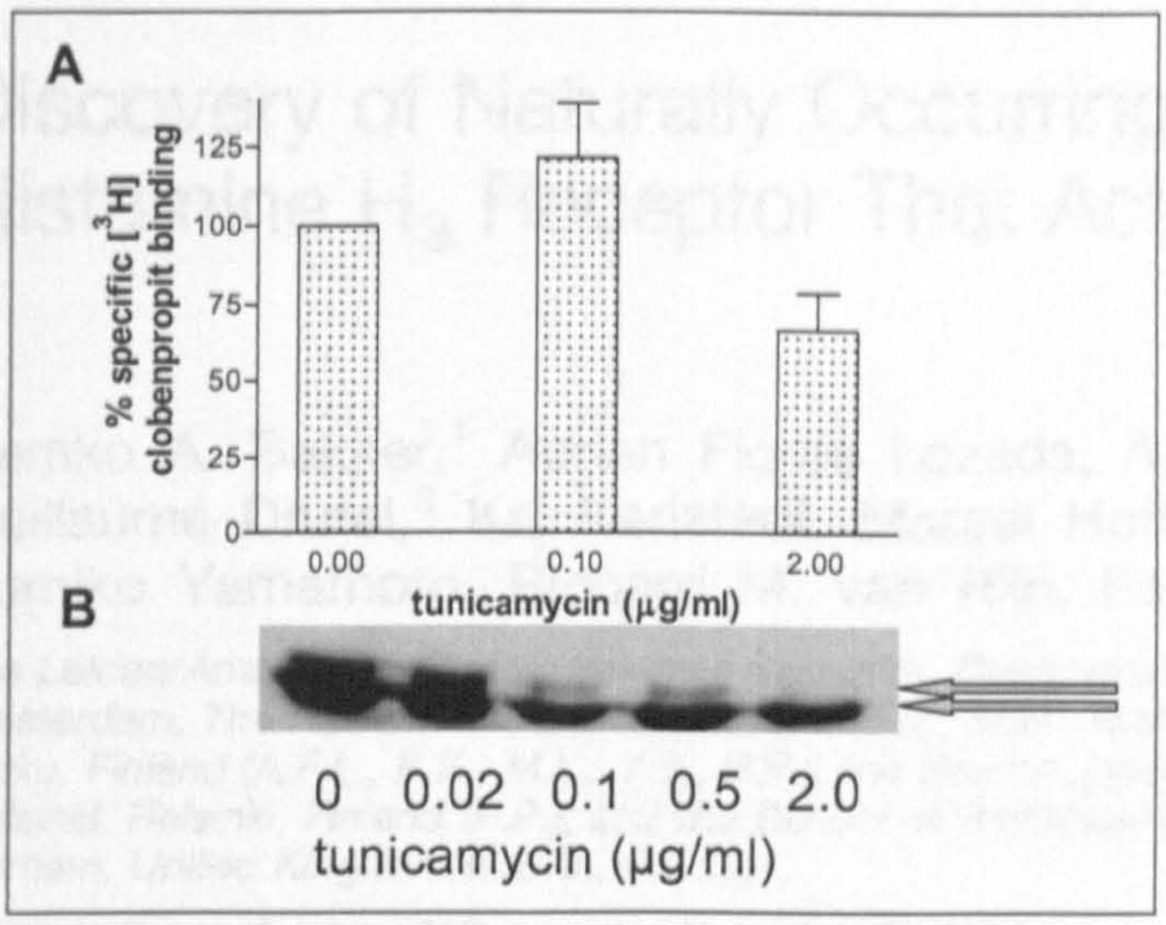

Fig. 1. N-glycosylation inhibition of the human H_3 445 receptor. FLAG-tagged hH_3 445 receptors expressed in HEK 293 cells were incubated with increasing concentrations of tunicamycin, harvested 48 h post-transfection and subjected, in parallel, to (A) [^{3}H] clobenpropit binding assays (B) immunoblotting. A: FLAG-tagged hH_3 445 expressed in HEK 293 cells grown in the absence and presence of 0.1 and 2 µg/ml tunicamycin (mean +/– SD for triplicate determinations from two independent transfections). B: Lane 1 FLAG-tagged hH_3 445 expressed in HEK 293 cells without tunicamycin; Lane 2–6 FLAG-tagged hH_3 445 expressed in HEK 293 cells grown in the presence of 0.1, 0.2, 0.5, 1 and 2 µg/ml tunicamycin. Representative immunoblot, replicated with similar results.

Acknowledgements. The authors wish to thank the Wellcome Trust and Parkinson's Disease Society for financial support, and Dr Harper (James Black Foundation, UK) and Dr Coge (Servier, France) for the [^{3}H] clobenpropit and the $hH_3$445 clone, respectively.

References

[1] Chazot PL, Hann V. Central H_3 histamine receptors: potential novel therapeutic targets. Curr Opin Investig Drugs 2001; 2: 1428–31.
[2] Chazot PL, Shenton FC. H_3 Histamine receptors: the gene knockout data so far. Curr Anaes Critical Care 2004; 15: 23–8.
[3] Mitsuhashi M, Payan DG. Receptor glycosylation regulates the affinity of histamine H_1 receptors during smooth muscle cell differentiation. Mol Pharmacol 1989; 35: 311–8.
[4] Fukushima Y, Asano T, Saitoh T, Anai M, Funaki M, Ogihara T, Katagiri H, Matsuhashi N, Yazaki Y, Sugano K. Structural and functional analysis of the canine histamine H_2 receptor by site-directed mutagenesis: N-glycosylation is not vital for its action. Biochem J 1995; 310: 553–8.
[5] Chazot PL, Cik M, Stephenson FA. An investigation into the role of N-glycosylation in the functional expression of a recombinant heteromeric NMDA receptor. Mol Membr Biol 1995; 12: 331–7.
[6] Hann V, Shenton FC, Chazot PL. GTP-insensitive agonist binding to native and recombinant H_3 receptors. Inflamm res 2004; 53: 67–8.
[7] Chazot PL, Wilson C, Hann V, Thompson CL, Lees G. Immunological identification of the mammalian H_3 histamine receptor in the adult mouse. Neuroreport 2001; 12: 259–62.
[8] Shenton FC, Hann V, Chazot PL. Evidence for native and cloned H_3 histamine receptor higher oligomers. Inflamm res 2005; 54: 48–9.

0026-895X/06/6904-1194–1206$20.00
MOLECULAR PHARMACOLOGY
Copyright © 2006 The American Society for Pharmacology and Experimental Therapeutics
Mol Pharmacol 69:1194–1206, 2006

Vol. 69, No. 4
19299/3099070
Printed in U.S.A.

Discovery of Naturally Occurring Splice Variants of the Rat Histamine H_3 Receptor That Act as Dominant-Negative Isoforms

Remko A. Bakker,[1] Adrian Flores Lozada, André van Marle, Fiona C. Shenton, Guillaume Drutel,[2] Kaj Karlstedt, Marcel Hoffmann,[3] Minnamaija Lintunen, Yumiko Yamamoto, Richard M. van Rijn, Paul L. Chazot, Pertti Panula, and Rob Leurs

The Leiden/Amsterdam Center for Drug Research, Department of Medicinal Chemistry, Vrije Universiteit Amsterdam, Amsterdam, The Netherlands (R.A.B., A.v.M., G.D., M.H., R.M.v.R., R.L.); the Department of Biology, Åbo Akademi University, Turku, Finland (A.F.L., K.K., M.L., Y.Y., P.P.); the Neuroscience Center and Institute of Biomedicine/Anatomy, University of Helsinki, Helsinki, Finland (P.P.); and the School of Biological and Biomedical Sciences, University of Durham, Durham, United Kingdom (F.C.S., P.L.C.)

Received September 26, 2005; accepted December 21, 2005

ABSTRACT

We described previously the cDNA cloning of three functional rat histamine H_3 receptor (rH_3R) isoforms as well as the differential brain expression patterns of their corresponding mRNAs and signaling properties of the resulting rH_{3A}, rH_{3B}, and rH_{3C} receptor isoforms (*Mol Pharmacol* **59:**1–8). In the current report, we describe the cDNA cloning, mRNA localization in the rat central nervous system, and pharmacological characterization of three additional rH_3R splice variants (rH_{3D}, rH_{3E}, and rH_{3F}) that differ from the previously published isoforms in that they result from an additional alternative-splicing event. These new H_3R isoforms lack the seventh transmembrane (TM) helix and contain an alternative, putatively extracellular, C terminus (6TM-rH_3 isoforms). After heterologous expression in COS-7 cells, radioligand binding or functional responses upon the application of various H_3R ligands could not be detected for the 6TM-rH_3 isoforms. In contrast to the rH_{3A} receptor ($rH_{3A}R$), detection of the rH_{3D} isoform using hemagglutinin antibodies revealed that the rH_{3D} isoform remains mainly intracellular. The expression of the rH_{3D-F} splice variants, however, modulates the cell surface expression-levels and subsequent functional responses of the 7TM H_3R isoforms. Coexpression of the $rH_{3A}R$ and the rH_{3D} isoforms resulted in the intracellular retention of the $rH_{3A}R$ and reduced $rH_{3A}R$ functionality. Finally, we show that in rat brain, the H_3R mRNA expression levels are modulated upon treatment with the convulsant pentylenetetrazole, suggesting that the rH_3R isoforms described herein thus represent a novel physiological mechanism for controlling the activity of the histaminergic system.

Histamine receptors are members of the superfamily of seven transmembrane domain (7TM) G-protein-coupled receptors (GPCRs). The histamine H_3 receptor (H_3R) was pharmacologically identified in 1983 and holds great promise as a target for the development of therapeutics for numerous disorders, including obesity, epilepsy, and such cognitive diseases as attention deficit hyperactivity disorder and Alzheimer's disease (see Bakker, 2004; Leurs et al., 2005 for reviews). The cloning of the H_3R cDNA allowed for the subsequent cloning of related sequences, including a variety of H_3R isoforms from different species (for review, see Bakker, 2004; Leurs et al., 2005).

Alternative splicing of pre-mRNA represents a widespread mechanism for increasing the variability of eukaryotic gene expression by generating structurally distinct isoforms from a single gene. Alterations in the expression of GPCR isoforms could be associated with disease (Schmauss et al., 1993). Although α_1-AR adrenoceptors and dopamine receptors are prime examples of alternatively spliced GPCRs (Cogé et al.,

R.L. is the recipient of a PIONIER award of the Technologiestichting Stichting Technische Wetenschappen of the Nederlandse Organisatie voor Wetenschappelijk Onderzoek. Supported by the Academy of Finland (P.P.), and the Finnish Foundation for Alcohol Studies (P.P., M.L., and A.F.L.).

[1] Current affiliation: Department of Metabolic Diseases, Boehringer Ingelheim Pharma GmbH, Biberach, Germany.
[2] Current affiliation: Institut François Magendie, Bordeaux, France.
[3] Current affiliation: Galapagos Genomics BV, Leiden, The Netherlands.

Article, publication date, and citation information can be found at http://molpharm.aspetjournals.org.
doi:10.1124/mol.105.019299.

ABBREVIATIONS: 7TM, seven transmembrane domain; GPCR, G-protein-coupled receptor; H_3R, histamine H_3 receptor; PTZ, pentylenetetrazole; HA, hemagglutinin; HEK, human embryonic kidney; GTPγS, guanosine 5′-*O*-(3-thio)triphosphate; APT, aminopotentidine; ^{125}IPP, [^{125}I]iodophenpropit; ELISA, enzyme-linked immunosorbent assay; FRET, fluorescence resonance energy transfer; BS3, bis(sulfosuccinimidyl)suberate; PCR, polymerase chain reaction; CREB, cAMP-responsive element-binding protein; *tr*-FRET, time-resolved fluorescence resonance energy transfer; ER, endoplasmic reticulum; 7TM-rH_3R isoforms, the rH_{3A}, rH_{3B}, and rH_{3C} receptors; 6TM-rH_3R isoforms, the rH_{3D}, rH_{3E}, and rH_{3F} isoforms.

1999; Kilpatrick et al., 1999; Hawrylyshyn et al., 2004), more and more GPCR splice variants are identified for other members of the GPCR superfamily. A variety of H_3R isoforms from several species has been reported (for review, see Bakker, 2004; Leurs et al., 2005). In addition to the 445 amino acids containing $rH_{3A}R$, two presumably nonfunctional truncated isoforms (reported as rH_{3T} or $rH_{3(nf1)}$ and $rH_{3(nf2)}$) (Drutel et al., 2001; Morisset et al., 2001) and three functional rH_3R isoforms have been detected: rH_{3B}, rH_{3C}, and the $rH_{3(410)}$ receptor, generated by deletions in the third intracellular loop of the rH_3R of 32, 48, and 35 amino acids, respectively. Because several H_3R isoforms have been shown to possess specific pharmacological characteristics in terms of ligand-binding and initiation of signal-transductions events (Drutel et al., 2001), the H_3R mRNA splicing can significantly affect cellular responses to histamine. A detailed understanding of the spectrum of H_3R splice variants in different species is of importance not only for the understanding of histaminergic system, but also for future drug development efforts.

In the present study, we describe the identification of three additional 6TM-rH_3 isoforms after an RT-PCR approach using rat brain cDNA. Although the mRNA for these 6TM-rH_3 isoforms is detected in the rat brain, in attempting their characterization, we failed to detect radioligand binding using H_3R specific radioligands as well as functional effects upon heterologous expression in COS-7 cells. Coexpression of 7TM-rH_3Rs with the 6TM-rH_3 isoforms, however, revealed that the 6TM-rH_3 isoforms inhibit the cell surface trafficking and subsequent functional activity of the 7TM-rH_3Rs. The regulation of the expression of the 6TM-rH_3 isoforms may therefore represent a novel mechanism for the regulation of H_3R functionality. To study possible in vivo functional relationships between 7TM-rH_3R and 6TM-rH_3 isoforms, relative expression levels were analyzed in a model of generalized tonic-clonic seizures induced by pentylenetetrazole (PTZ). Data from a study on kainic acid-induced status epilepticus indicates that systemic kainic acid induces a direct or indirect selective increase in H_3R isoforms with a full third intracellular loop in areas that suffer rapid neuronal damage (Lintunen et al., 2005). No data are currently available regarding whether 7TM-rH_3R and 6TM-rH_3 isoforms are similarly regulated under pathophysiological conditions in the rat brain. The PTZ seizure model used in this study allows us to determine whether an H_3R isoform-specific response occurs in a pathological setting. Our findings therefore uncover a new mechanism that may control the regulation of H_3R activity in the brain.

Materials and Methods

Materials. Immepip, clobenpropit, and thioperamide were synthesized at the department of Medicinal Chemistry at the Vrije Univeristeit Amsterdam. Gifts of $pcDEF_3$ (Dr. J. Langer, Robert Wood Johnson Medical School, Piscataway, NJ), pTLN21CRE-Luc (Dr. W. Born, National Jewish Medical and Research Center, Denver, CO), and of the cDNAs encoding the PTX-insensitive mutant rat $G\alpha_{i/o}$ proteins $G\alpha_{i1}C^{351}I$, $G\alpha_{i2}C^{352}I$, $G\alpha_{i3}C^{351}I$, and $G\alpha_oC^{351}I$ (Dr. G. Milligan, University of Glasgow, Glasgow, UK), the cDNA encoding the FLAG-tagged $rH_{3A}R$ (Dr. F. Cogé, Institut de Recherches Servier, Croissy sur Seine, France), the cDNA encoding the human histamine H_1 receptor (Dr. H. Fukui, University of Tokushima, Tokushima, Japan), the cDNA encoding the KSHV-GPCR ORF74 (Dr. T. Schwartz, University of Copenhagen, Copenhagen, Denmark), mianserin hydrochloride (Organon NV, The Netherlands), and the HA antibody and rhodamine-labeled secondary antibody (Dr. J. van Minnen, Vrije Universiteit, Amsterdam, The Netherlands), are greatly acknowledged. All other materials were from commercial suppliers.

Constructs. The reverse transcription and PCR amplification for cloning of the rH_{3D-F} (6TM-rH_3) isoform cDNAs were performed as described previously (Drutel et al., 2001). The full-length cDNAs were isolated with primers overlapping the rat H_3R cDNA sequence. The forward sequence included a Kozak sequence (underlined) (5′-CCG CCA CCA TGG AGC GCG CGC CGC CCG ACG GGC TG-3′). The reverse sequence was based on cDNA for rat orphan GPCR (Genbank accession number AB015646) (5′-CTC TAC CCC ATA ACC ACC CAC C-3′). The use of these primers resulted in the amplification of at least three different products. After cloning in pCRII-TOPO, the cDNAs were sequenced on both DNA strands and subcloned in $pcDNA_3$. The sequence of the identified rH_{3F} isoform is identical to one of the sequences found in the GenBank database (accession number AB015646; GI: 6681587), the sequences of the rH_{3D} and rH_{3E} isoforms have been deposited in the GenBank database (accession numbers DQ112342 and DQ112343, respectively). The hydropathic profile of the H_{3D-F} isoforms was analyzed using the TMHMM Server at the Center for Biological Sequence Analysis, Technical University of Denmark, DTU, Lyngby, Denmark (http://www.cbs.dtu.dk/services/TMHMM/).

Construction of rH_3R-Gα Protein Fusion Constructs. Fusion proteins between the rat H_3R and PTX-insensitive mutant rat Gα-proteins of the $G_{i/o}$ class were created by PCR using Turbo Pfu to remove the translation initiation codon from the Gα-protein cDNA sequence and the stop codon from the $rH_{3A}R$ cDNA sequence.

HA-Tagging of the rH_3R Isoforms. N-Terminal hemagglutinin (HA)-tagged expression constructs of the $rH_{3A}R$ and rH_{3D} isoform were generated by PCR (5′-GCC ACC ATG GGC TAC CCA TAC GAC GTC CCA GAC TAC GCC GCG GAG CGC GCG CCG C-3′) and cloned into pcDNA 3.1 (Invitrogen, Leek, The Netherlands). Construct integrity was verified by sequence analysis.

Animals. The study was conducted in accordance with the European Convention (1986) guidelines and approved by the local committee for Animal Experiments and the Provincial State Office of Western Finland and the Animal Ethics Committee of Abo Akademi University. Male Sprague-Dawley rats (260–280 g) were given PTZ (50 mg/kg, i.p.). Animals were stunned with CO_2 and killed by decapitation 6 h (PTZ, $n = 3$), 24 h (PTZ, $n = 3$), and 48 h (PTZ, $n = 3$; saline control, $n = 3$) after injection.

In Situ Hybridization Histochemistry. Probes were labeled with deoxy-[α-^{33}P]ATP (PerkinElmer Life and Analytical Sciences, Boston, MA) at their 3′ ends using terminal deoxynucleotide transferase (Promega, Madison, WI), and subsequent in situ hybridization histochemistry was performed essentially as described previously (Drutel et al., 2001). The following oligo-probe sequence was used for detecting H_{3DEF} isoform mRNAs: 5′-AAG TTT CCC GAG GCG CTC GAC ACA GTA ATC GGG GAT GCA GCG GCC-3′.

Image Analysis and Data Interpretation. Autoradiographic films were quantified by digitizing the film images using the MCID 5+ image analysis system (Imaging Research, St. Catherines, ON, Canada) and by measuring gray scale pixel values. The relative optic density was converted to integrated optic density based on a curve derived from ^{14}C standards exposed to films. Gray scale values were determined by using a total of four sections for each animal.

Cell Culture and Transfection. African green monkey kidney COS-7 cells were maintained and transfected as described previously (Drutel et al., 2001; Bakker et al., 2004a). HEK 293 cells were cultures under similar conditions and transfected with cDNA encoding the $rH_{3A}R$ using the LipofectaminePlus method according to the manufacturer's protocols.

Reporter-Gene Assay. H_3R isoform-mediated modulation of cAMP mediated gene transcription activity was measured using the

luciferase reporter-gene plasmid pTLNC121–3 (2.5 μg/10^6 cells) containing 21 cAMP-responsive elements. Luminescence was assayed 48 h after incubation of transfected cells with ligands as described previously (Bakker et al., 2004b).

[^{35}S]GTPγS Binding Assays. Transfected COS-7 cells were resuspended in 4°C binding buffer (20 mM HEPES, 3 μM GDP, 10 mM $MgCl_2$, and 150 mM NaOH, pH 7.4). For measurement of agonist-stimulated GTPγS binding, 6 μg of the crude cell extract was incubated in binding buffer with ligands for 15 min at 30°C after which 0.1 to 0.2 nM [^{35}S]GTPγS (1250 Ci/mmol; PerkinElmer Life and Analytical Sciences) was added to make a final total volume of 100 μl. Bound radioactivity was separated by filtration after 15 min through Whatman GF/C filters on a Brandel cell harvester using 4°C wash buffer (20 mM HEPES and 5 mM $MgCl_2$, pH 7.4). Radioactivity retained on the filters was measured by liquid scintillation counting.

Receptor Binding Studies. Radioligand binding studies for the H_1R, H_2R, and H_3R using [^{3}H]mepyramine, [^{125}I]aminopotentidine, and [N^α-methyl-^{3}H]histamine, respectively, were performed as described previously (Bakker et al., 2004b). The H_3R radioligand binding studies using [^{125}I]iodophenpropit (^{125}IPP) were carried out under the same experimental conditions as for [N^α-methyl-^{3}H]histamine. CXCL8 was labeled with ^{125}I using the Iodogen method (Pierce, Rockford, IL) and subsequently used in ORF74 radioligand binding studies as described previously (Smit et al., 2002).

Detection of Tagged rH$_3$Rs. In the enzyme-linked immunosorbent assays (ELISA), a mouse anti-HA monoclonal primary antibody was used as primary antibody, and a goat anti-mouse–horseradish peroxidase conjugate as secondary antibody for the detection of tagged rH$_3$Rs in transfected cells. The 3,3′-, 5,5′-tetramethylbenzidine liquid substrate system for ELISA was used as substrate and the optical density was measured at 450 nm using a Victor^2 Wallac multilabel counter (PerkinElmer Life and Analytical Sciences). The same primary antibody was used for immunocytochemistry in conjunction with a secondary rhodamine labeled goat-anti-mouse antibody. Permeabilization of cells was achieved by an optional incubation of the cells for 5 min with 0.5% Nonidet P-40 in TBS before antibody application. For imaging, coverslips were mounted in 90% glycerol containing 0.02 M Tris-HCl, pH 8.0, 0.002% NaN_3, and 2% 1,4-diazabicyclo-(2,2,2)-octane (Merck, Darmstadt, Germany).

Time-Resolved FRET. The time-resolved fluorescence resonance energy transfer (FRET) experiments were conducted essentially as described previously (Bakker et al., 2004a). Energy transfer was measured by exciting the Eu^{3+} at 320 nm and monitoring the allophycocyanin emission for 1 ms at 665 nm using a Novostar (BMG LABTECH GmbH, Offenburg, Germany) configured for time-resolved fluorescence after a 50-μs delay.

Cross-Linking and Immunoblotting of rH$_{3A}$ Receptors. Cells were harvested by centrifugation, and the resulting pellet was resuspended in 150 μl of cross-linking buffer (150 mM NaCl, 100 mM Na-HEPES, 5 mM EDTA, pH 7.5, and 5 mM DTT) to give a final protein concentration of approximately 0.5 mg/ml. The samples were incubated at room temperature with continual mixing for 12 min with either a 0.12 mM or a 0.25 mM concentration of the cell permeable cross-linker bis(sulfosuccinimidyl)suberate (BS3), after which the cross-linking mixture was removed by centrifugation and the resultant pellet was used for immunoblotting as described previously (Chazot et al., 2001). Immunoblots were probed either with anti-H_{3C} 188–197Cys antibody (Shenton et al., 2005) at a 0.2 μg/ml, or with an anti-H_3 329–358 antibody used at a final protein concentration of 1.5 μg/ml (Chazot et al., 2001).

Analytical Methods. All data shown are expressed as mean ± S.E.M. Data from radioligand binding assays and functional assays data were evaluated by a nonlinear, least-squares curve-fitting procedure using Prism (GraphPad Software, Inc., San Diego, CA).

Results

Cloning of cDNAs Encoding Additional Rat H_3R Isoforms

The existence of additional H_3R isoforms was investigated by RT-PCR analysis of rat whole-brain total RNA using specific primers 1 and 2 (see *Materials and Methods*), and revealed the existence of three previously uncharacterized full-length cDNAs with putative corresponding proteins of 497 (rH_{3D}), 465 (rH_{3E}), and 449 (rH_{3F}) amino acids. The amino acid sequence of the rH_{3F} isoform corresponds to one of the sequences found in the GenBank database (accession number AB015646; GI: 6681587). These three new rH_3 isoforms correspond in a large part to the sequences of rat histamine H_3R isoforms A, B, and C (rH_{3A}R, rH_{3B}R, and rH_{3C}R, respectively) and exhibit exactly the same differences in length for the third intracellular loop (Fig. 1A). This insertion in the third intracellular loop in the rH_{3D}, rH_{3E}, and rH_{3F} isoforms seems to be created by a retention/deletion system already described for the third intracellular loop (Cogé et al., 2001; Drutel et al., 2001; Morisset et al., 2001). However, the rH_{3D}, rH_{3E}, and rH_{3F} isoforms differ from the rH_{3A}R, rH_{3B}R, and rH_{3C}R in their C-terminal region, in which the last C-terminal 53 amino acids, which correspond to the seventh transmembrane-domain and carboxyl terminus of the rH_{3A}R, rH_{3B}R, and rH_{3C}R proteins, are replaced by a sequence of 105 amino acids that do not share any homology with the last 53 C-terminal amino acids of the rH_{3A}R, rH_{3B}R, and rH_{3C}R. Sequence analysis of the rH_3R gene indicates that the alternative C-terminal domain that is found in the $rH_{3D\text{-}F}$ isoforms is due to a change in the open reading frame upon alternative splicing using previously unidentified exon/intron junctions present within the rH_3R gene (see Fig. 1B). Analysis of the hydropathic profile of the rH_{3D}, rH_{3E}, and rH_{3F} isoforms does not reveal a clear putative seven transmembrane domain (Fig. 2, A and B). Therefore, the rH_{3D}, rH_{3E}, and rH_{3F} isoforms are predicted to possess only six transmembrane domains 6TM-rH_3 isoforms) and an extracellular C-teriminal domain (Fig. 2, C and D).

Heterologous Expression of Epitope-Tagged rH$_3$R Isoforms. We have successfully characterized the rH_{3A}R, rH_{3B}R, and rH_{3C}R using COS-7 cells heterologously expressing these receptors (Drutel et al., 2001). We therefore used the same approach in this study to characterize the three additional 6TM-rH_3 isoforms described herein. To evaluate the cell surface expression of the 6TM-rH_3 isoforms, we generated the cDNAs coding for the N-terminally HA-tagged rH_{3A}R (HA-rH_{3A}R) and the N-terminally HA-tagged rH_{3D} (HA-rH_{3D}) isoform by PCR. Although we detected clear immunological evidence for the cell surface expression of the HA-rH_{3A}R with the use of an ELISA assay using anti HA-antibodies on intact cells, we can hardly detect the HA-rH_{3D} isoforms on the cell surface on intact cells (Fig. 2E). We observe, however, a clear immunofluorescent signal upon permeabilization of cells expressing the HA-rH_{3D} isoform (Fig. 2E), indicating successful synthesis of the HA-tagged rH_{3D} isoform protein and retention of the HA-tagged rH_{3D} isoform inside the cell. There is an apparent difference in detection of the HA-rH_{3D} isoform versus the HA-rH_{3A}R, which might indicate differences in, for example, the rate of synthesis, the inherent stability, or the rate of degradation of the H_3 isoforms, but we have not pursued this issue further. To evaluate the plasma membrane localization of the HA-rH_{3A}R and the HA-rH_{3D} isoform, we subsequently performed immunocy-

A

```
                1         10        20        30                  40  TM1  50          60
rH3A            MERAPPDGLMNASGTLAGEAAAAGGARGFSAAWTAVLAALMALLIVATVLGNALVMLAFV
rH3B            MERAPPDGLMNASGTLAGEAAAAGGARGFSAAWTAVLAALMALLIVATVLGNALVMLAFV
rH3C            MERAPPDGLMNASGTLAGEAAAAGGARGFSAAWTAVLAALMALLIVATVLGNALVMLAFV
rH3D            MERAPPDGLMNASGTLAGEAAAAGGARGFSAAWTAVLAALMALLIVATVLGNALVMLAFV
rH3E            MERAPPDGLMNASGTLAGEAAAAGGARGFSAAWTAVLAALMALLIVATVLGNALVMLAFV
rH3F            MERAPPDGLMNASGTLAGEAAAAGGARGFSAAWTAVLAALMALLIVATVLGNALVMLAFV

                61        70        80  TM2   90        100       110       120
rH3A            ADSSLRTQNNFFLLNLAISDFLVGAFCIPLYVPYVLTGRWTFGRGLCKLWLVVDYLLCAS
rH3B            ADSSLRTQNNFFLLNLAISDFLVGAFCIPLYVPYVLTGRWTFGRGLCKLWLVVDYLLCAS
rH3C            ADSSLRTQNNFFLLNLAISDFLVGAFCIPLYVPYVLTGRWTFGRGLCKLWLVVDYLLCAS
rH3D            ADSSLRTQNNFFLLNLAISDFLVGAFCIPLYVPYVLTGRWTFGRGLCKLWLVVDYLLCAS
rH3E            ADSSLRTQNNFFLLNLAISDFLVGAFCIPLYVPYVLTGRWTFGRGLCKLWLVVDYLLCAS
rH3F            ADSSLRTQNNFFLLNLAISDFLVGAFCIPLYVPYVLTGRWTFGRGLCKLWLVVDYLLCAS

                121 TM3 130       140       150       160  TM4  170       180
rH3A            SVFNIVLISYDRFLSVTRAVSYRAQQGDTRRAVRKMALVWVLAFLLYGPAILSWEYLSGG
rH3B            SVFNIVLISYDRFLSVTRAVSYRAQQGDTRRAVRKMALVWVLAFLLYGPAILSWEYLSGG
rH3C            SVFNIVLISYDRFLSVTRAVSYRAQQGDTRRAVRKMALVWVLAFLLYGPAILSWEYLSGG
rH3D            SVFNIVLISYDRFLSVTRAVSYRAQQGDTRRAVRKMALVWVLAFLLYGPAILSWEYLSGG
rH3E            SVFNIVLISYDRFLSVTRAVSYRAQQGDTRRAVRKMALVWVLAFLLYGPAILSWEYLSGG
rH3F            SVFNIVLISYDRFLSVTRAVSYRAQQGDTRRAVRKMALVWVLAFLLYGPAILSWEYLSGG

                181       190       200       210  TM5  220       230       240
rH3A            SSIPEGHCYAEFFYNWYFLITASTLEFFTPFLSVTFFNLSIYLNIQRRTRLRLDGGREAG
rH3B            SSIPEGHCYAEFFYNWYFLITASTLEFFTPFLSVTFFNLSIYLNIQRRTRLRLDGGREAG
rH3C            SSIPEGHCYAEFFYNWYFLITASTLEFFTPFLSVTFFNLSIYLNIQRRTRLRLDGGREAG
rH3D            SSIPEGHCYAEFFYNWYFLITASTLEFFTPFLSVTFFNLSIYLNIQRRTRLRLDGGREAG
rH3E            SSIPEGHCYAEFFYNWYFLITASTLEFFTPFLSVTFFNLSIYLNIQRRTRLRLDGGREAG
rH3F            SSIPEGHCYAEFFYNWYFLITASTLEFFTPFLSVTFFNLSIYLNIQRRTRLRLDGGREAG

                241       250       260       270       280       290       300
rH3A            PEPPPDAQPSPPPAPPSCWGCWPKGHGEAMPLHRYGVGEAGPGVEAGEAALGGGSGGGAA
rH3B            PEPPPDAQPSPPPAPPSCWGCWPKGHGEAMPLH----------------------------
rH3C            PEPPPDAQPSPPPAPPSCWGCWPKGHGEAMPLH----------------------------
rH3D            PEPPPDAQPSPPPAPPSCWGCWPKGHGEAMPLHRYGVGEAGPGVEAGEAALGGGSGGGAA
rH3E            PEPPPDAQPSPPPAPPSCWGCWPKGHGEAMPLH----------------------------
rH3F            PEPPPDAQPSPPPAPPSCWGCWPKGHGEAMPLH----------------------------

                301       310       320       330       340       350       360
rH3A            ASPTSSSGSSSRGTERPRSLKRGSKPSASSASLEKRMKMVSQSITQRFRLSRDKKVAKSL
rH3B            -----SSGSSSRGTERPRSLKRGSKPSASSASLEKRMKMVSQSITQRFRLSRDKKVAKSL
rH3C            ----------------------RGSKPSASSASLEKRMKMVSQSITQRFRLSRDKKVAKSL
rH3D            ASPTSSSGSSSRGTERPRSLKRGSKPSASSASLEKRMKMVSQSITQRFRLSRDKKVAKSL
rH3E            -----SSGSSSRGTERPRSLKRGSKPSASSASLEKRMKMVSQSITQRFRLSRDKKVAKSL
rH3F            ----------------------RGSKPSASSASLEKRMKMVSQSITQRFRLSRDKKVAKSL

                361       370  TM6  380       390       400  TM7  410       420
rH3A            AIIVSIFGLCWAPYTLLMIIRAACHGRCIPDYWYETSFWLLWANSAVNPVLYPLCHYSFR
rH3B            AIIVSIFGLCWAPYTLLMIIRAACHGRCIPDYWYETSFWLLWANSAVNPVLYPLCHYSFR
rH3C            AIIVSIFGLCWAPYTLLMIIRAACHGRCIPDYWYETSFWLLWANSAVNPVLYPLCHYSFR
rH3D            AIIVSIFGLCWAPYTLLMIIRAACHGRCIPDYCVERLGKLEASLLLPLWMFSGRWRRRKH
rH3E            AIIVSIFGLCWAPYTLLMIIRAACHGRCIPDYCVERLGKLEASLLLPLWMFSGRWRRRKH
rH3F            AIIVSIFGLCWAPYTLLMIIRAACHGRCIPDYCVERLGKLEASLLLPLWMFSGRWRRRKH

                421       430       440  445  450       460       470       480
rH3A            RAFTKLLCPQKLKVQPHGSLEQCWK
rH3B            RAFTKLLCPQKLKVQPHGSLEQCWK
rH3C            RAFTKLLCPQKLKVQPHGSLEQCWK
rH3D            VCELDVPWMFNQERQNCRGARGWIGRCGLPRPPPSVLQLPAEPRQLLLPAPPPGLGRWPC
rH3E            VCELDVPWMFNQERQNCRGARGWIGRCGLPRPPPSVLQLPAEPRQLLLPAPPPGLGRWPC
rH3F            VCELDVPWMFNQERQNCRGARGWIGRCGLPRPPPSVLQLPAEPRQLLLPAPPPGLGRWPC

                481       490   497
rH3D            PACPVCTIRIWGWVVMG
rH3E            PACPVCTIRIWGWVVMG
rH3F            PACPVCTIRIWGWVVMG
```

B

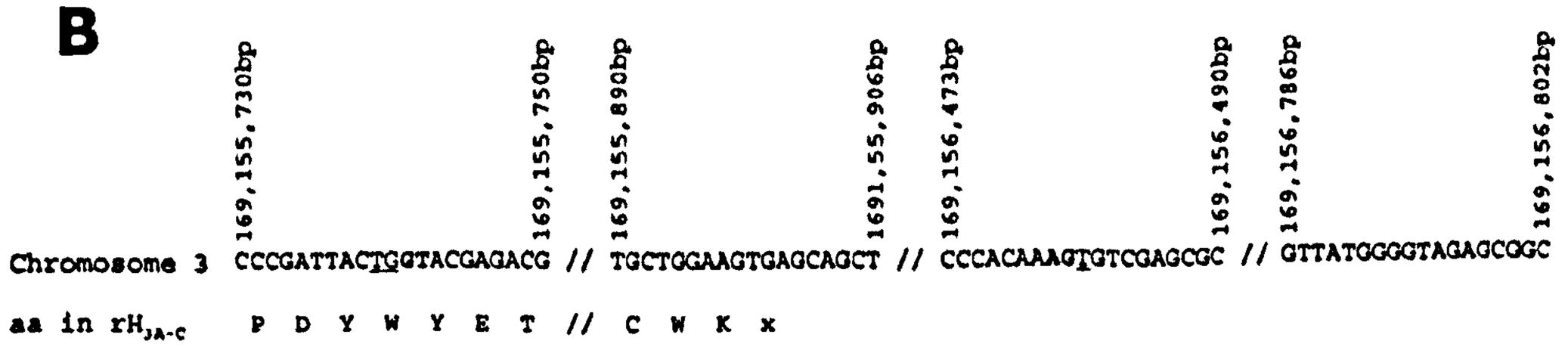

Fig. 1. Sequence alignment of rH_3R isoforms and genomic organization of the rH_3R gene. A, amino acid sequence alignment of various rH_3R isoforms. The $rH_{3B}R$ and $rH_{3C}R$ isoforms exhibit amino acid deletions in the third intracellular loop of the rH_3R protein compared with the full-length $rH_{3A}R$. The rH_{3D}, rH_{3E}, and rH_{3F} isoforms differ from the $rH_{3A}R$, $rH_{3B}R$, and $rH_{3C}R$ isoforms, respectively, in an alternative C-terminal domain as a result of an additional splicing event. Indicated above the amino acids are the seven transmembrane domains as they are found for the $rH_{3A}R$, $rH_{3B}R$, and $rH_{3C}R$ isoforms (TM1 through TM7). B, diagram of the exon/intron structure of the rat H_3R gene on chromosome 3 (Genbank accession number NM_053506.1; GI:16758263) and the resulting amino acid (aa) sequences found in rH_{3A-C} receptors and rH_{3D-E} isoforms generated by retention/deletion of the pseudointrons. The exon/intron junctions within the rH_3R gene are indicated in bold (GT and AG), whereas the codon that corresponds to the cysteine (C) found in the rH_{3D-F} isoforms (formed by TG and T) is underlined. For simplicity, only part of the exon/intron structure of the rat H_{3R} gene and of the rH_3R gene sequence is shown (indicated by //). See Morisset et al. (2001) for an overview of the exon/intron structure of the rH_3R gene corresponding to the two presumably nonfunctional H_3R isoforms, $H_{3(nf1)}$ and $H_{3(nf2)}$, and the four previously described functional shorter isoforms, rH_{3B} ($rH_{3(413)}$), $rH_{3(410)}$, and rH_{3C} ($rH_{3(397)}$).

tochemistry studies using rhodamine labeled anti-HA antibodies. Plasma membrane localization of the rhodamine-derived fluorescence was easily detected using cells expressing HA-rH_{3A}Rs in intact cells (Fig. 2F, top left) and only a limited intracellular fluorescence was observed in Nonidet P40-permeabilized cells (Fig. 2F, top right). In contrast, corroborating the findings obtained by the ELISA studies, using cells transfected with cDNA encoding the HA-rH_{3D} isoform, appreciable rhodamine-derived fluorescence is detected only in permeabilized cells (Fig. 2F, bottom right) and not on intact cells (Fig. 2F, bottom left). Moreover, no plasma membrane localization of the rhodamine-derived fluorescence was detected using permeabilized HA-rH_{3D} isoform-expressing cells. These data indicate an intracellular localization for the HA-rH_{3D} isoform.

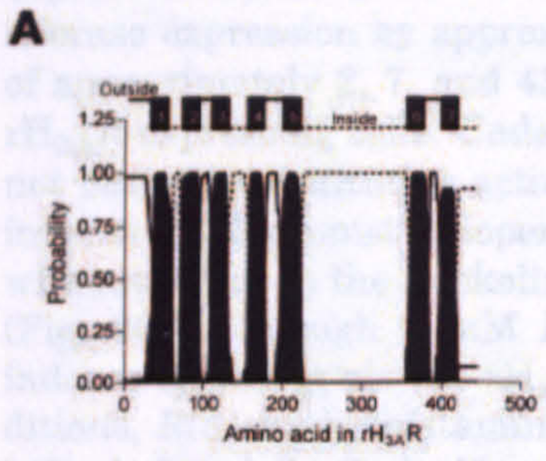

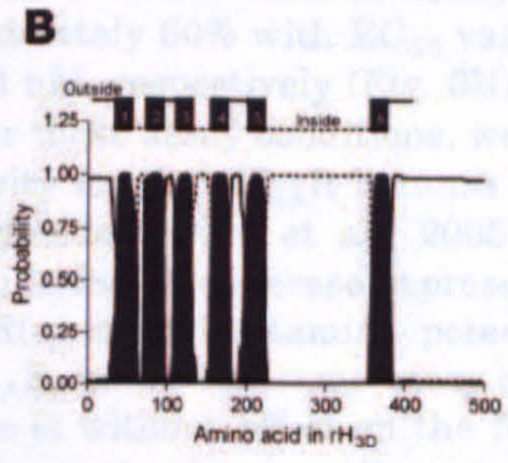

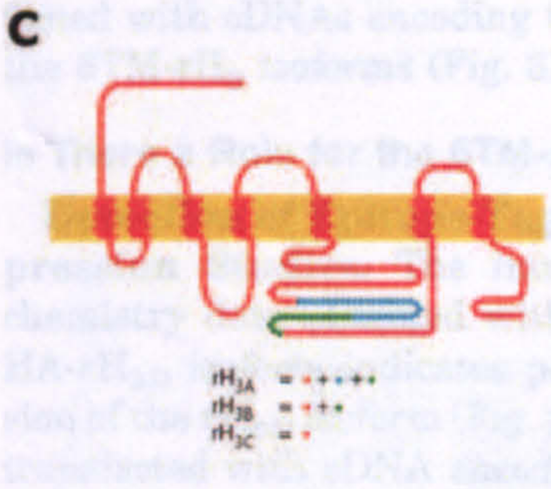

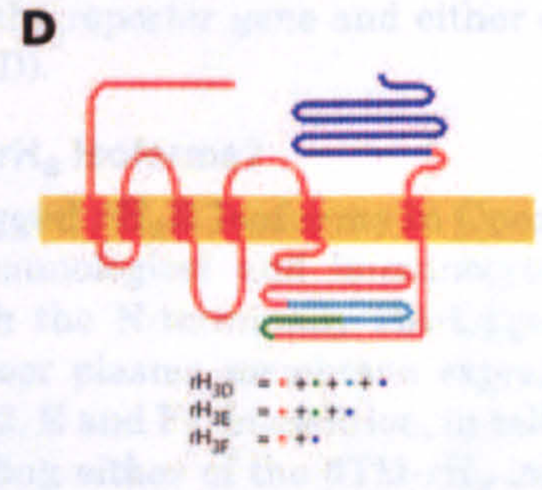

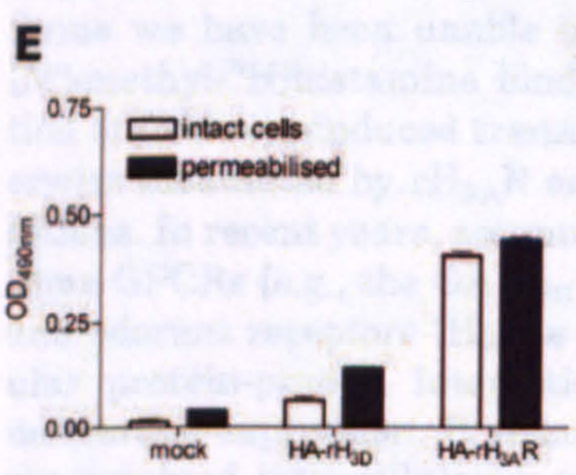

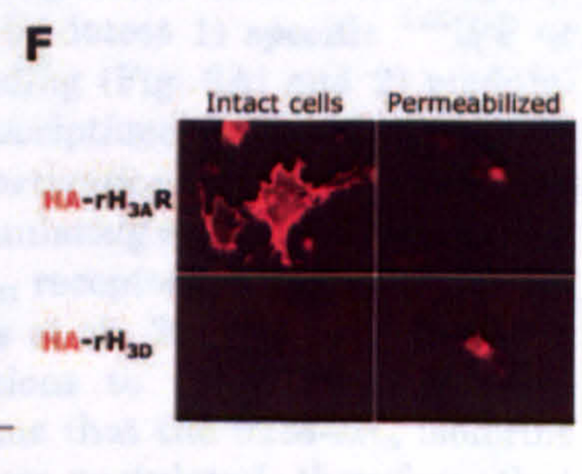

Fig. 2. Topology of the rH_3R isoforms. Prediction of the topology of the $rH_{3A}R$ (A) versus the $rH_{3D}R$ (B), as predicted by the TMHMM Server at the Center for Biological Sequence Analysis, Technical University of Denmark, DTU (http://www.cbs.dtu.dk/services/TMHMM/). Indicated by the solid line are the probabilities for localization on the extracellular side (outside); the probabilities of localization on the intracellular side (inside) are indicated by the dotted lines. The probability for transmembrane (TM) domains are indicated by the filled areas. From these two plots, it can be deduced that seven TM domains are predicted for the $rH_{3A}R$, whereas for the $rH_{3D}R$, only six TM domains are predicted, as indicated above the graphs. C, graphical representation of the topology of the rH_{3A}, rH_{3B}, and rH_{3C} receptors, versus the rH_{3D}, rH_{3E}, and rH_{3F} isoforms (D). In contrast to the rH_{3A}, rH_{3B}, and rH_{3C} receptors, the rH_{3D}, rH_{3E}, and rH_{3F} isoforms are predicted to possess an extracellular C-terminal domain. Also indicated in C and D are the variations in the third intracellular loop between the isoforms. E and F, immunological detection of N-terminally HA-tagged rH_{3A}Rs (HA-rH_{3A}) and the N-terminally HA-tagged rH_{3D} isoform (HA-rH_{3D}) on transfected COS-7 cells. E, Detection of HA-rH_{3A}Rs and the HA-rH_{3D} isoform in intact cells versus cells that have been permeabilized using 0.5% Nonidet P-40 in an ELISA assay. F, immunocytochemical detection of HA-tagged rH_3R isoforms using a rhodamine conjugated antibody directed against the HA-tag. Detection of HA-rH_{3A}Rs on intact COS-7 cells (top left) and in permeabilized cells (top right). Detection of the HA-rH_{3D} isoform on intact cells (bottom left) and in permeabilized cells (bottom right).

Are the 6TM-rH_3 Isoforms Functional H_3Rs?

Radioligand Binding Studies. To evaluate whether the identified mRNA species for the 6TM-rH_3 isoforms code for functional H_3Rs, we transfected COS-7 cells with the cDNA encoding either the $rH_{3A}R$ or one of the 6TM-rH_3 isoforms and evaluated corresponding membrane preparations for their ability to bind either the inverse H_3R agonist radioligand ^{125}IPP or the H_3R agonist radioligand [N^{α}-methyl-^{3}H]histamine. Cell homogenates derived from cells expressing the $rH_{3A}R$ bind ^{125}IPP with high affinity (K_D = 2.1 nM, B_{max} = 2.5 pmol/mg of protein) and exhibits the expected affinities for IPP, immepip, and thioperamide (pK_b for ^{125}IPP, 8.2 ± 0.1; pK_i values for immepip and thioperamide, 6.5 ± 0.2 and 7.7 ± 0.1, respectively). In contrast, we failed to detect specific ^{125}IPP-binding to cells transfected with cDNAs coding for any of the 6TM-rH_3 isoforms (Fig. 3A). Likewise, we did not detect [N^{α}-methyl-^{3}H]histamine binding to membranes of cells transfected with cDNAs encoding the 6TM-rH_3 isoforms (data not shown).

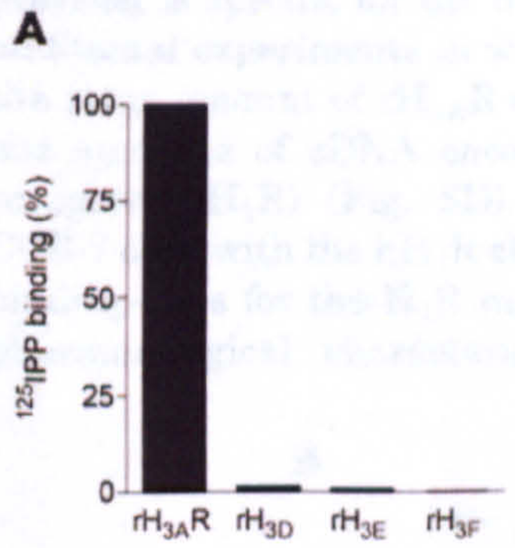

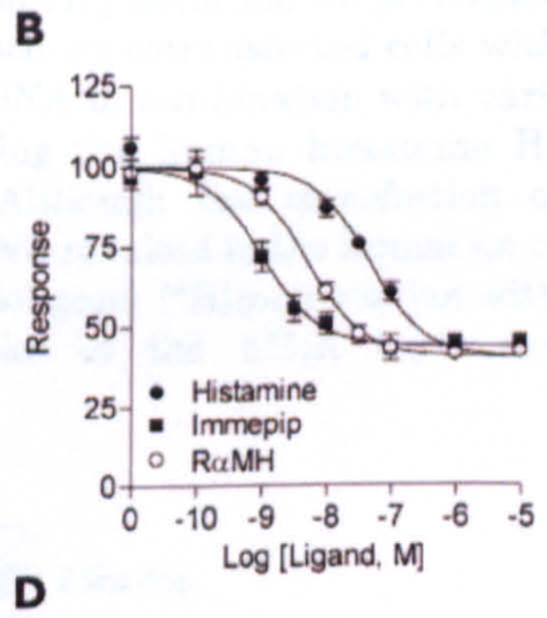

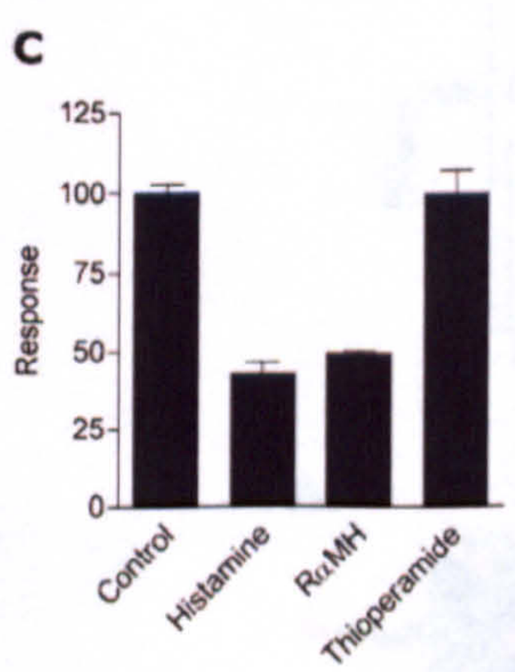

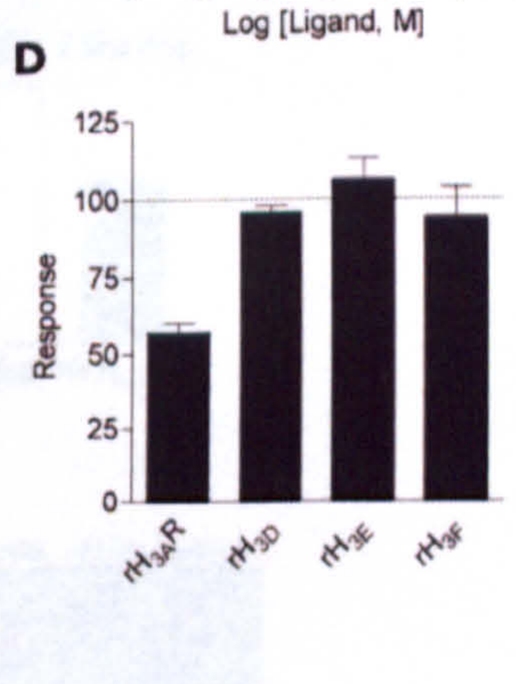

Fig. 3. Functional analysis of the $rH_{3A}R$ and the rH_{3D} isoform upon transient transfection of their corresponding cDNAs in COS-7 cells. A, transfection of cells with $rH_{3A}R$ coding cDNA (pcDEF$_3$$rH_{3A}R$; 5 mg/$10^6$ cells) resulted in the expression of ^{125}IPP binding sites, whereas no specific ^{125}IPP binding was detected to membrane fractions of cells transfected with an equal amount of cDNA coding for either the rH_{3D}, rH_{3E}, or rH_{3F} isoform. B, dose-dependent modulation of 10 mM forskolin induced responses by histamine, immepip, and $R(\alpha)$-methylhistamine using COS-7 cells cotransfected with 5 mg/10^6 cells of both pcDEF$_3$$rH_{3A}R$ and a CREB-responsive firefly-luciferase reporter gene (pTLNC121CRE). C, modulation of forskolin (10 mM) induced responses by 10 mM histamine, $R(\alpha)$-methylhistamine (RaMH), and thioperamide using cells transfected with both pcDEF$_3$$rH_{3A}R$ and pTLNC121CRE. The forskolin-induced responses are set to 100% as indicated by "control". D, effects of 10 mM $R(\alpha)$-methylhistamine on forskolin (10 mM) induced responses using cells cotransfected with either pcDEF$_3$$rH_{3A}R$, pcDEF$_3$$rH_{3D}$, pcDEF$_3$$rH_{3E}$, or pcDEF$_3$$rH_{3F}$, and pTLN121CRE. The forskolin induced responses are set to 100% as indicated by the dashed line.

Functional Assays. The H_3R couples to members of the $G_{i/o}$ family of G-proteins to inhibit adenylyl cyclase activity and subsequently inhibits the formation of intracellular cAMP (Leurs et al., 2005). Cotransfection of COS-7 cells with the $rH_{3A}R$ encoding cDNA together with pTLN121CRE, a cAMP-responsive element-binding protein (CREB)-responsive firefly-luciferase reporter gene, allowed us to monitor H_3R-induced modulation of forskolin-induced reporter-gene expression. In concert with the $G_{i/o}$-coupled nature of the H_3R (see Leurs et al., 2005), treatment of cotransfected cells with varying concentrations of the H_3R agonists immepip, $R(\alpha)$-methylhistamine, and histamine results in the dose-dependent inhibition of 10 mM forskolin-induced firefly-luciferase expression by approximately 60% with EC_{50} values of approximately 2, 7, and 43 nM, respectively (Fig. 3B), in $rH_{3A}R$-expressing cells. Under these assay conditions, we do not observe constitutive activity for the $rH_{3A}R$ because the inverse H_3R agonist thioperamide (Leurs et al., 2005) is without effect on the forskolin-induced luciferase expression (Fig. 3C). Although 1 mM $R(\alpha)$-methylhistamine potently induces signaling via the $rH_{3A}R$, under the same assay conditions, $R(\alpha)$-methylhistamine is without effect on the forskolin-induced firefly-luciferase expression in cells cotransfected with cDNAs encoding the reporter gene and either of the 6TM-rH_3 isoforms (Fig. 3D).

Is There a Role for the 6TM-rH_3 Isoforms?

Detection of Epitope-Tagged rH_3R Isoforms in Coexpression Studies. The immunological and immunocytochemistry data obtained with the N-terminally HA-tagged HA-rH_{3D} isoform indicates poor plasma membrane expression of the rH_{3D} isoform (Fig. 2, E and F). In addition, in cells transfected with cDNA encoding either of the 6TM-rH_3 isoforms we have been unable to detect 1) specific ^{125}IPP or [N^{α}-methyl-^{3}H]histamine binding (Fig. 3A) and 2) modulation of forskolin-induced transcriptional events that are otherwise modulated by $rH_{3A}R$ activation under the same conditions. In recent years, accumulating evidence suggests that some GPCRs [e.g., the $GABA_B$ receptors (White et al., 1998) and odorant receptors (Hague et al., 2004a)] require particular protein-protein interactions to allow proper plasma membrane expression. It seems that the 6TM-rH_3 isoforms are retained intracellularly; we postulated, therefore, that the additional expression of GPCRs might aid the cell surface expression of the 6TM-rH_3 isoforms. Conversely, the 6TM-rH_3 isoforms may possibly retain the coexpressed GPCRs intracellularly by acting as dominant-negative isoforms.

Do the 6TM-rH_3 Isoforms Interfere with Cell Surface Expression of 7TM-rH_3Rs? We cotransfected COS-7 cells with the cDNAs coding for the HA-$rH_{3A}R$ and the rH_{3D} isoform. Similar to the effects of coexpression of alternative splice variants of human α_{1A}-adrenoceptors (Cogé et al., 1999), we found that the coexpression of the rH_{3D} isoform reduced the expression of the HA-$rH_{3A}R$ at the plasma membrane. This phenomenon is observed using either an ELISA assay on intact cells or by applying immunocytochemistry techniques using a rhodamine labeled anti-HA antibody (Fig. 4, A and B, respectively).

Evaluation of Ligand-Binding Sites upon Coexpression of 7TM-H_3R and 6TM-rH_3 Isoforms. To evaluate whether the loss of HA-$rH_{3A}R$-derived immunofluorescence at the cell surface upon coexpression of the rH_{3D} isoform also results in a loss of ligand binding sites for H_3R ligands we performed radioligand binding assays. As shown in Fig. 3A, ^{125}IPP binding sites are detected upon the expression of 7TM-rH_3Rs (Drutel et al., 2001), such as the $rH_{3A}R$, whereas expression of the 6TM-rH_3 isoforms does not result in the formation of ^{125}IPP binding sites.

The transfection of 0.25 mg/10^6 cells of cDNA coding for the $rH_{3A}R$ resulted in the expression of 2.5 pmol/mg of protein ^{125}IPP binding sites. Coexpression of the $rH_{3A}R$ together with the rH_{3D} isoform, however, resulted in an rH_{3D}-isoform gene-dosage–dependent reduction of $rH_{3A}R$-derived ^{125}IPP binding sites (Fig. 5A); the remaining ^{125}IPP binding sites exhibit a pharmacological indistinguishable from that of the $rH_{3A}R$ (pK_b for ^{125}IPP, 8.1 ± 0.1; pK_i values for immepip and thioperamide, 6.9 ± 0.2 and 7.6 ± 0.1, respectively). The coexpression of the rH_{3E} or rH_{3F} isoform together with the $rH_{3A}R$ resulted in a similar reduction of ^{125}IPP binding sites (Fig. 5, B and C, respectively), indicating that the 6TM-rH_3 isoforms interfere with the expression of the $rH_{3A}R$. The maximal inhibition of ^{125}IPP binding sites (as evaluated by a transfection of cells with an $rH_{3A}R$/6TM-rH_3 isoform cDNA ratio of 1:10) is ~50 to 75% (Fig. 5, A–C). To evaluate whether the observed inhibition of ^{125}IPP binding-site expression is specific for the 6TM-rH_3 isoforms, we performed additional experiments in which we cotransfected cells with the same amount of $rH_{3A}R$ cDNA in combination with various amounts of cDNA encoding the human histamine H_1 receptor (hH_1R) (Fig. 5D). Although the transfection of COS-7 cells with the hH_1R cDNA resulted in the formation of binding-sites for the H_1R radioligand [^{3}H]mepyramine with pharmacological characteristics of the hH_1R (data not

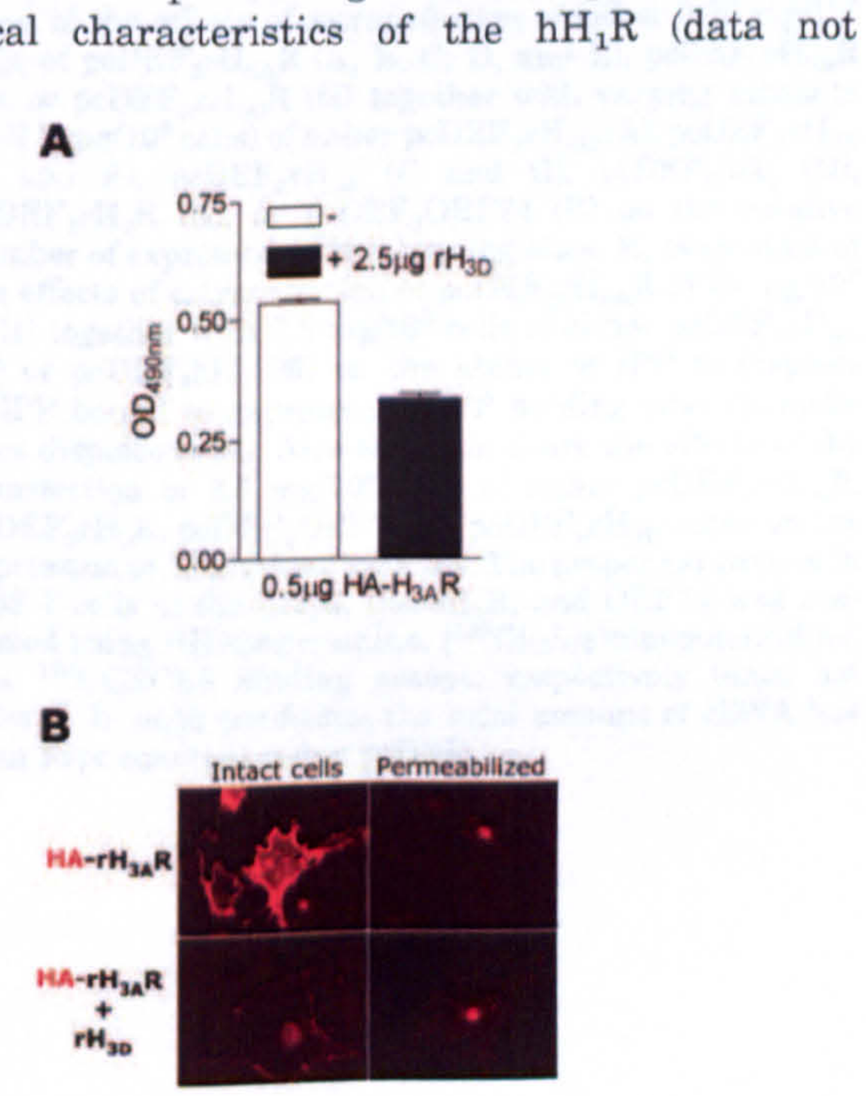

Fig. 4. Immunological detection of N-terminally HA-tagged rH_{3A}Rs (HA-rH_{3A}) on COS-7 cells cotransfected with cDNA coding for HA-rH_{3A} receptors and the N-terminally HA-tagged rH_{3D} isoform (HA-rH_{3D}). A, effects of the cotransfection of pcDEF$_3$$rH_{3D}$ on the detection of HA-rH_{3A}Rs on intact cells using an ELISA assay. B, immunocytochemical detection of HA-rH_{3A}Rs using a rhodamine conjugated antibody directed against the HA-tag. Detection of HA-rH_{3A}Rs on intact COS-7 cells (top left) and in permeabilized cells (top right), and effects of cotransfection cells with both pcDEF$_3$.HA-rH_{3A} and pcDEF$_3$$rH_{3D}$ on the detection of the HA-rH_{3A}Rs on intact cells (bottom left) and in permeabilized cells (bottom right). Control slides of cells transfected with N-terminally HA-epitope tagged H_3 isoforms that did not receive the primary antibody or of untransfected cells showed no appreciable staining.

shown), no specific ^{125}IPP binding was detected in hH_1R-expressing cells (Fig. 5D). Cotransfection of cells with cDNAs encoding both the $rH_{3A}R$ and the hH_1R, however, did not influence the formation of ^{125}IPP binding sites.

Similar to the findings with the hH_1R, expression of the rat H_2R (rH_2R) or the viral chemokine receptor from Karposi's sarcoma herpes virus KSHV-GPCR (also known as ORF74) in COS-7 cells resulted in the formation of binding sites for the H_2R radioligand ^{125}IAPT and ^{125}I-CXCL8, a radioligand for ORF74, respectively, but not in the formation of ^{125}IPP binding sites. Coexpression of the $rH_{3A}R$ with either the rH_2R or ORF74, however, did not affect the formation of $rH_{3A}R$-derived ^{125}IPP binding sites (Fig. 5E).

We also evaluated the effects of the coexpression of the $rH_{3B}R$ and $rH_{3C}R$ with the rH_E and rH_F isoforms, respectively, on the formation of ^{125}IPP binding sites. Similar to the expression of the $rH_{3A}R$, expression of the $rH_{3B}R$ or $rH_{3C}R$ in COS-7 cells results in the formation of ^{125}IPP binding sites (Drutel et al., 2001). Coexpression of the $rH_{3B}R$ or $rH_{3C}R$ together with either the rH_{3E} or rH_{3F} isoform resulted in an

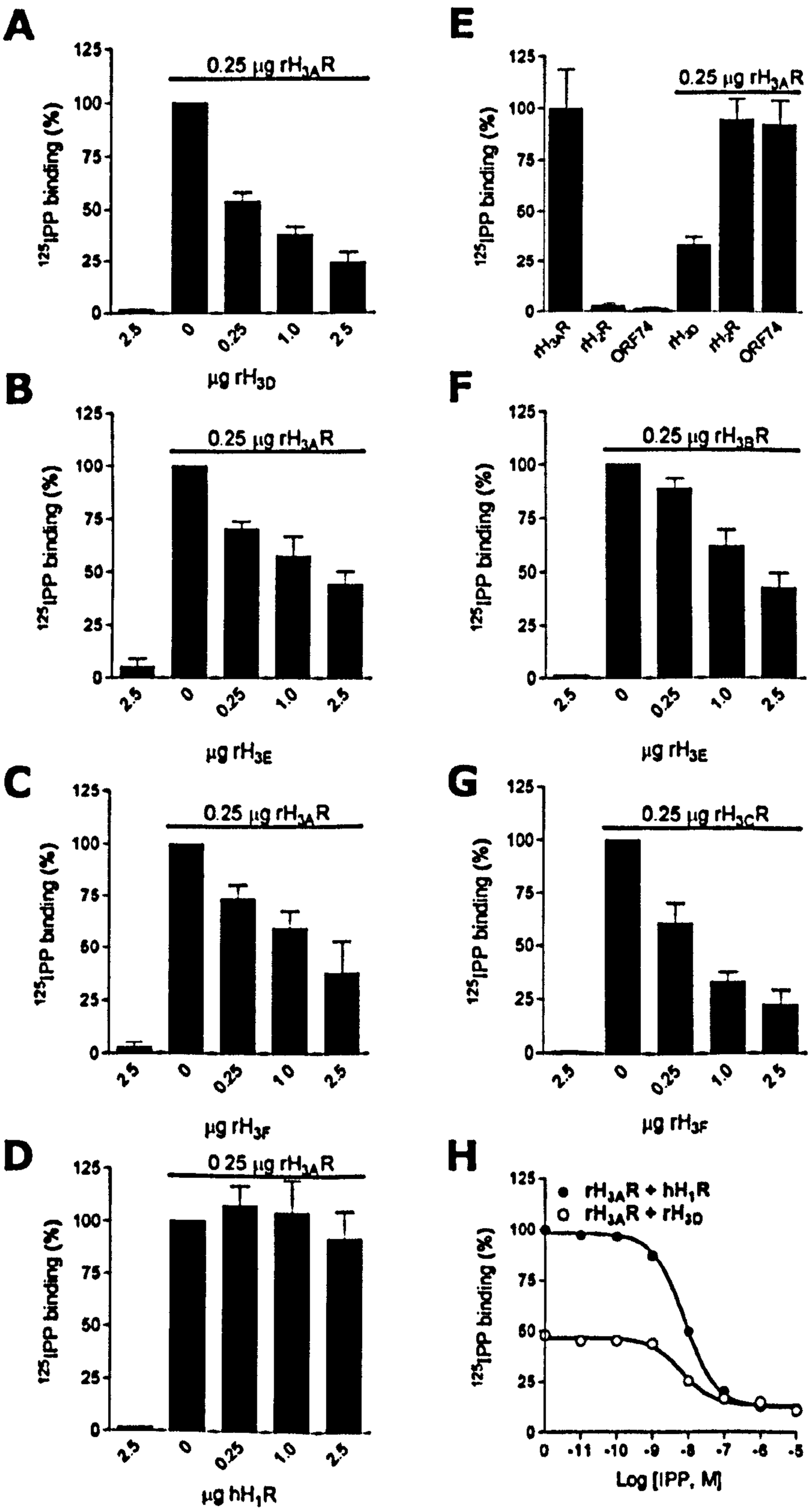

Fig. 5. Effects of cotransfection of cDNA coding for rH_3R isoforms on the expression of ^{125}IPP binding sites. Evaluation of the effects of cotransfection of either 0.25 mg/10^6 cells of $pcDEF_3rH_{3A}R$ (A, B, C, D, and E), $pcDEF_3rH_{3B}R$ (F), or $pcDEF_3rH_{3C}R$ (G) together with varying amounts (0–2.5 mg/10^6 cells) of either $pcDEF_3rH_{3D}$ (A), $pcDEF_3rH_{3E}$ (B and F), $pcDEF_3rH_{3F}$ (C and G), $pcDEF_3hH_1$ (D), $pcDEF_3rH_2R$ (E), or $pcDEF_3$ORF74 (E) on the relative number of expressed ^{125}IPP binding sites. H, evaluation of the effects of cotransfection of $pcDEF_3rH_{3A}R$ (0.25 mg/10^6 cells) together with 2.5 mg/10^6 cells of either $pcDEF_3rH_{3D}$ (○) or $pcDEF_3hH_1$ (●) on the ability of IPP to displace ^{125}IPP bound to expressed ^{125}IPP binding sites (homologous displacement). Also shown in E are the effects of the transfection of 2.5 mg/10^6 cells of either $pcDEF_3rH_{3A}R$, $pcDEF_3rH_2R$, $pcDEF_3$ORF74, or $pcDEF_3rH_{3D}$ alone on the expression of ^{125}IPP binding sites. The proper expression in COS-7 cells of the hH_1R, the rH_2R, and ORF74 was confirmed using [^{3}H]mepyramine, [^{125}I]iodoaminopotentidine, and ^{125}I-CXCL8 binding assays, respectively (data not shown). In each condition, the total amount of cDNA has been kept constant using $pcDEF_3$.

rH_{3E} isoform and rH_{3F} isoform gene-dosage dependent reduction of $rH_{3B}R$-derived (Fig. 5F) and $rH_{3C}R$-derived (Fig. 5G) ^{125}IPP binding sites, respectively. The maximal inhibition of ^{125}IPP binding sites, as evaluated by a transfection of cells with an $rH_{3B}R$ or $rH_{3C}R$-to-6TM-rH_3 isoform cDNA ratio of 1:10 is ~50 to 75% (Fig. 5, F and G), similar to our findings on the coexpression of the $rH_{3A}R$ with the 6TM-rH_3 isoforms (Fig. 5, A–C).

Although the coexpression of the $rH_{3A}R$ with the rH_{3D} isoform inhibits the formation of ^{125}IPP binding sites, the remaining ^{125}IPP binding sites exhibit unchanged pharmacological characteristics of the $rH_{3A}R$, as evidenced by its unchanged affinity for IPP (Fig. 5H). Taken together, these radioligand-binding data clearly demonstrate that the expression of the 6TM-rH_3 isoforms selectively interferes with the expression of the 7TM-rH_3Rs.

Evaluation of H_3R Ligand-Induced [^{35}S]GTPγS Binding upon Coexpression of 7TM-H_3R and 6TM-rH_3 Isoforms

Creation of $rH_{3A}R$ Gα Fusion Proteins. Because we failed to detect H_3R-agonist mediated [^{35}S]GTPγS binding to activated Gα proteins in cell membranes derived from 6TM-rH_3 isoform expressing cells (data not shown), we chose to evaluate H_3R-agonist induced [^{35}S]GTPγS binding to assess the effects of the coexpression of 6TM-rH_3 isoforms on the functionality of 7TM-rH_3Rs. To assess the effects of the coexpression of 6TM-rH_3 isoforms on the functionality of 7TM-rH_3Rs, we chose to evaluate H_3R-agonist induced [^{35}S]GTPγS binding to activated Gα proteins. To increase the sensitivity of this assay (Milligan, 2000), we created fusion proteins consisting of the $rH_{3A}R$ fused to one of the PTX-insensitive mutant rat $G\alpha_{i/o}$ proteins: $G\alpha_{i1}C^{351}I$, $G\alpha_{i2}C^{352}I$, $G\alpha_{i3}C^{351}I$, or $G\alpha_oC^{351}I$ (creating $rH_{3A}R$-$G\alpha_{o1}C^{351}I$, $rH_{3A}R$-$G\alpha_{i1}C^{351}I$, $rH_{3A}R$-$G\alpha_{i2}C^{352}I$, and $rH_{3A}R$-$G\alpha_{i3}C^{351}I$, respectively) by PCR according to *Materials and Methods*.

Characterization of $rH_{3A}R$. Gα fusion proteins—the four different $rH_{3A}R$ fusion proteins $rH_{3A}R$-$G\alpha_{o1}C^{351}I$, $rH_{3A}R$-$G\alpha_{i1}C^{351}I$, $rH_{3A}R$-$G\alpha_{i2}C^{352}I$, and $rH_{3A}R$-$G\alpha_{i3}C^{351}I$—were subsequently characterized by ^{125}IPP binding assays upon their heterologous expression in COS-7 cells. Based on these studies (data not shown), we decided to continue our experiments using the $rH_{3A}R$-$G\alpha_{o1}C^{351}I$ fusion protein as this fusion protein exhibited a pK_b value for ^{125}IPP of 8.4 ± 0.2 that corresponds to the obtained pK_b value of ^{125}IPP for the wild-type $rH_{3A}R$ of 8.2 ± 0.1. In addition, the affinities of the wild-type $rH_{3A}R$ and the $rH_{3A}R$-$G\alpha_{o1}C^{351}I$ fusion protein for the H_3R agonist immepip and the inverse H_3R agonist thioperamide are similar (6.5 ± 0.2 and 7.7 ± 0.1 versus 6.9 ± 0.1 and 7.9 ± 0.1, respectively).

Subsequently, we compared the capability of the $rH_{3A}R$-$G\alpha_{o1}C^{351}I$ fusion protein to mediate the inhibition of 10 mM forskolin-induced activation of cAMP response element-mediated gene transcription in COS-7 cells. We found the $rH_{3A}R$-$G\alpha_{o1}C^{351}I$ fusion protein to potently inhibit the forskolin-induced response upon activation with H_3R agonists. In concert with our findings on the wild-type $rH_{3A}R$, treatment of cells cotransfected with cDNAs encoding the $rH_{3A}R$-$G\alpha_{o1}C^{351}I$ fusion protein and the cAMP response element-reporter gene with varying concentrations of the H_3R agonists immepip, *R*(α)-methylhistamine, and histamine results in the dose-dependent inhibition of 10 mM forskolin-induced firefly luciferase expression by approximately 40% with EC_{50} values of approximately 4, 30, and 76 nM, respectively (Fig. 6A). These data indicate that the $rH_{3A}R$-$G\alpha_{o1}C^{351}I$ fusion protein is fully functional and shows an $rH_{3A}R$ pharmacology.

Coexpression of $rH_{3A}R$-$G\alpha_{o1}C^{351}I$ Fusion Proteins and the rH_{3D} Isoform. Consistent with our findings on the coexpression of 7TM-rH_{3A}Rs with the 6TM-rH_3 isoforms (see Fig. 5), coexpression of the $rH_{3A}R$-$G\alpha_{o1}C^{351}I$ fusion protein together with the rH_{3D} isoform, results in an rH_{3D}-isoform gene-dosage dependent reduction of $rH_{3A}R$-$G\alpha_{o1}C^{351}I$ fusion protein-derived ^{125}IPP binding sites (Fig. 6B), and the remaining ^{125}IPP binding sites exhibit an $rH_{3A}R$-$G\alpha_{o1}C^{351}I$-like pharmacological profile (pK_b for ^{125}IPP, 8.5 ± 0.1; pK_i values for immepip and thioperamide, 7.0 ± 0.2 and 7.6 ± 0.1, respectively). The maximal inhibition of $rH_{3A}R$-$G\alpha_{o1}C^{351}I$-derived ^{125}IPP binding sites, as evaluated by a transfection of cells with an $rH_{3A}R$-$G\alpha_{o1}$/rH_{3D} isoform cDNA ratio of 1:10 is ~65% (Fig. 6B).

We subsequently assessed the influence of coexpression of the rH_{3D} isoform on the [^{35}S]GTPγS binding induced by

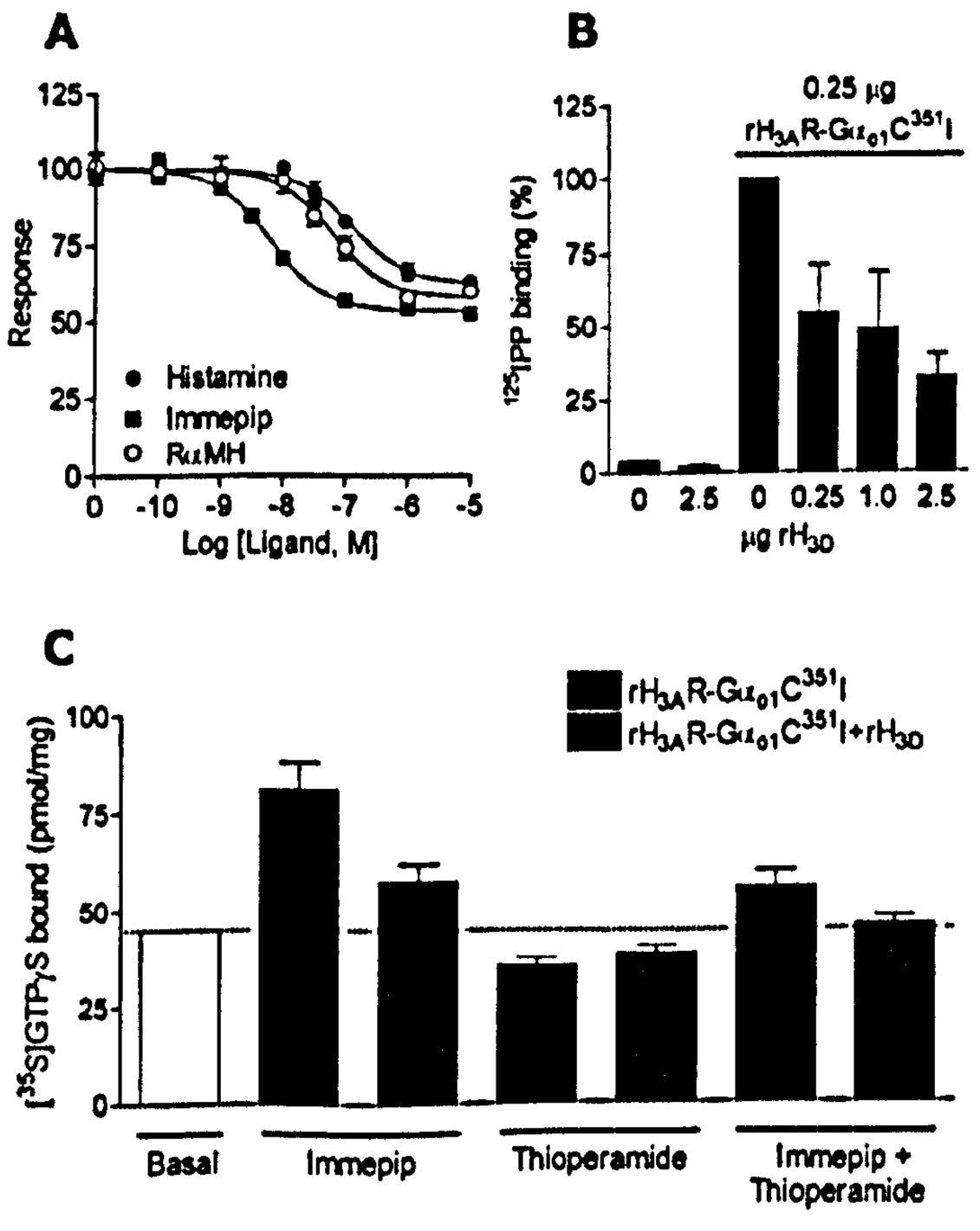

Fig. 6. Effects of cotransfection of the rH_{3D} isoform on the function of the $rH_{3A}R$. A, dose-dependent modulation of 10 mM forskolin induced responses by histamine, immepip, and *R*(α)-methylhistamine using PTX-treated (100 ng/ml) COS-7 cells cotransfected with 5 mg/10^6 cells of both $pcDEF_3rH_{3A}R$-$G\alpha_{o1}C^{351}I$ and a CREB-responsive firefly-luciferase reporter gene (pTLNC121CRE). B, evaluation of the effects of cotransfection of 0.25 mg/10^6 cells of $pcDEF_3rH_{3A}R$-$G\alpha_{o1}C^{351}I$ together with varying amounts of $pcDEF_3rH_{3D}$ (0–2.5 mg/10^6 cells) on the relative number of expressed ^{125}IPP binding sites. C, effects of the cotransfection of 0.25 mg/10^6 cells $pcDEF_3rH_{3A}R$ and 2.5 mg/10^6 cells $pcDEF_3rH_{3D}$ on [^{35}S]GTPγS binding to the PTX-insensitive mutant $G\alpha_{o1}C^{351}I$ protein fused to the C-terminal domain of the $rH_{3A}R$ ($rH_{3A}R$-$G\alpha_{o1}C^{351}I$ fusion protein). Shown are the effects of cotransfection of $pcDEF_3rH_{3D}$ on the H_3R agonist immepip (1 mM)-induced [^{35}S]GTPγS binding to the $rH_{3A}R$-$G\alpha_{o1}C^{351}I$ fusion protein in PTX-treated cells (100 ng/ml), and the effects of the inverse H_3R agonist thioperamide (1 mM) on the 1 mM immepip-induced [^{35}S]GTPγS binding. Shown are the averages of three independent experiments.

agonist-mediated activation of coexpressed $rH_{3A}R$-$G\alpha_{o1}C^{351}I$ fusion proteins. The H_3R agonist immepip (1 mM) resulted in a robust stimulation of [^{35}S]GTPγS binding in $rH_{3A}R$-$G\alpha_{o1}C^{351}I$ expressing cells that was inhibited by coincubation with a 1 mM concentration of the inverse H_3R agonist thioperamide (Fig. 6C). Under the assay conditions used, we could not detect significant thioperamide-mediated inhibition of basal $rH_{3A}R$-$G\alpha_{o1}C^{351}I$ mediated [^{35}S]GTPγS binding, indicating that we could not detect constitutive $rH_{3A}R$-$G\alpha_{o1}C^{351}I$ activity. The 1 mM immepip-induced [^{35}S]GTPγS binding was inhibited by 70% by coexpression of the $rH_{3A}R$-$G\alpha_{o1}C^{351}I$ fusion protein with the rH_{3D} isoform (Fig. 6C). The 6TM-rH_3 isoforms themselves did not mediate changes in [^{35}S]GTPγS binding upon incubation with H_3R ligands (data not shown).

Can rH_3Rs Form Homo-Oligomers? In view of the emerging concept of GPCR dimerization that is now well documented in literature (for review, see, for example, Pfleger and Eidne, 2005), we speculated that the 6TM-rH_3 isoforms might interfere with the cell surface expression of 7TM-rH_3 receptors through dimerization.

We have described the generation of anti-rH_{3C} 268–277Cys antibodies (Shenton et al., 2005), which, based on immunoblotting, selectively recognize both the $rH_{3A}R$ and $rH_{3C}R$ isoform, but not the $rH_{3B}R$ isoform expressed in HEK 293 cells. Wild-type $rH_{3A}R$-expressing cells were collected and subjected to cross-linking with varying amounts of the cell permeable cross-linker bis(sulfosuccinimidyl)suberate (BS3) before resolving the samples using SDS-PAGE. Immunoblotting with anti-H_{3C} 268–277Cys antibody yielded three major protein species (M_r 90,000, 135,000, and ~200,000, respectively), corresponding well to putative dimeric, trimeric and tetrameric $rH_{3A}R$ oligomers, respectively (Fig. 7, lanes 1–3). Performing similar experiments using native rat brain tissue, the major species observed is a coincident M_r 90,000 species (Fig. 7, lane 4). It is noteworthy that a recombinant putative monomeric M_r 47,000 species was clearly observed, which was barely detectable in the native forebrain preparation. Higher cross-linker concentrations yielded >200,000 species for both recombinant and native H_3R preparations (Shenton et al., 2005).

We have successfully used the time-resolved FRET (*tr*-FRET) fluorescence (665-nm emission after excitation at 320 nm) for the detection of hH_1R dimerization using epitope-tagged hH_1Rs and fluorescently labeled antibodies recognizing the N-terminally epitope-tagged receptors (Bakker et al., 2004a). We have used this approach to confirm the formation of oligomerization of rH_3Rs.

tr-FRET fluorescence results obtained with the different samples are shown in Fig. 7B. A clear specific *tr*-FRET signal is observed using live cells expressing the HA-$rH_{3A}Rs$. The data are presented as the *tr*-FRET that is observed using HA-$rH_{3A}R$-expressing cells that have been incubated with both anti-HA-Eu^{3+} and anti-HA-allophycocyanin antibodies versus the *tr*-FRET that is observed using a mix of two populations of HA-$rH_{3A}R$-expressing cells that before mixing were independently incubated with either of the two antibodies. The increased *tr*-FRET signal can only be explained by the resonance energy transfer from anti-HA-Eu^{3+} antibodies bound to HA-$rH_{3A}Rs$ to anti-HA-allophycocyanin antibodies bound to HA-$rH_{3A}Rs$, indicative of the formation of $rH_{3A}R$ multimers in living cells.

Modulation of rH_{3AD} and rH_{3DEF} Isoform-Specific mRNAs in Rat Brain after Delivery of a Systemic Convulsant. We have successfully used specific oligonucleotide probes to characterize the 7TM-rH_3R mRNA expression in the rat brain (Drutel et al., 2001). To evaluate the CNS expression of the 6TM-rH_3 isoforms, we have designed domain specific probes. We have used one probe specific for the C terminus present in the 6TM-rH_3 isoforms, and, for comparison, we have also performed studies using a oligonucleotide probe specific for the (full-length) third intracellular loop of the $rH_{3A}R$, which is also present in the rH_{3D} isoform

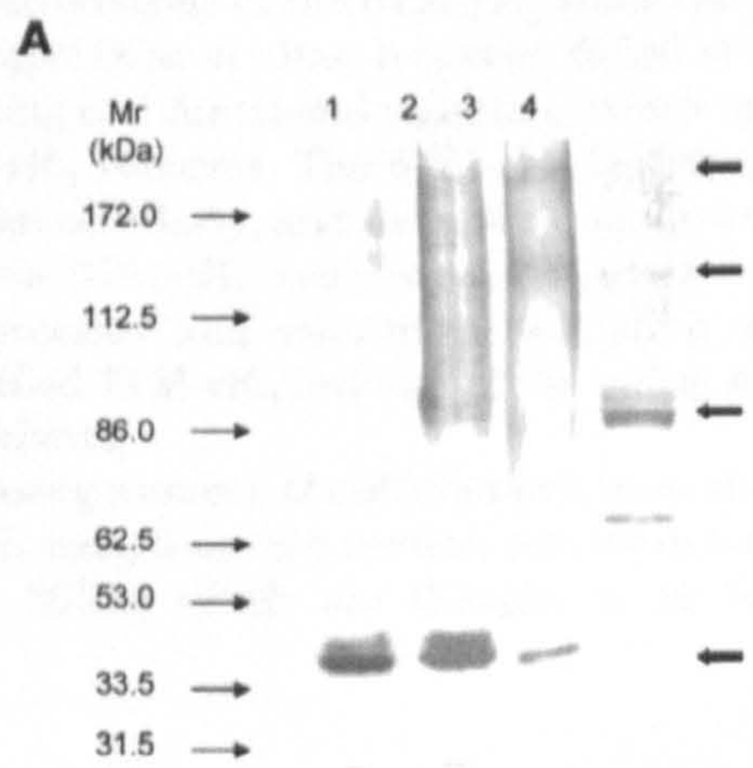

Fig. 7. Detection of oligomerization of heterologous and native $rH_{3A}Rs$. A, biochemical evidence for $rH_{3A}R$ oligomers. Membranes derived from either cells heterologously expressing $rH_{3A}Rs$ or from native rat forebrain membranes were analyzed by immunoblotting (lanes 1–3 and 4, respectively) as described under *Materials and Methods*. In addition, samples of membranes expressing $rH_{3A}Rs$ were subjected to chemical cross-linking with either 0.12 mM or 0.25 mM BS3 (lanes 2 and 3, respectively) before immunoblotting. Lanes 1 to 3 were subsequently probed with rabbit anti-H_{3C} 268–277Cys antibody (0.2 μg/ml), and lane 4 was probed with rabbit anti-H_3 349–358 antibody (1.5 μg/ml). The immunoblot is representative of at least three separate experiments. The molecular mass standards are displayed on the left and are indicated in kilodaltons. B, detection of dimeric $rH_{3A}Rs$ by *tr*-FRET. Upon measuring fluorescence emission at 665 nm, after excitation at 337 nm, *tr*-FRET signals are seen using live cells expressing HA-$rH_{3A}Rs$, because of the resonance energy transfer of specific HA-$rH_{3A}Rs$ bound to anti-HA-Eu^{3+} antibody to the specific HA-$rH_{3A}Rs$ bound to anti-HA-allophycocyanin antibody. *tr*-FRET signals were seen only using membranes of HA-$rH_{3A}R$ expressing cells that were coincubated with both the anti-HA-Eu^{3+} (Eu^{3+}) antibody and the anti-HA-allophycocyanin (XL665) antibody (Eu^{3+} + XL665). Mixing of two populations of cells expressing HA-$rH_{3A}Rs$ independently incubated with either anti-HA-Eu^{3+} or anti-HA-allophycocyanin antibodies resulted in a reduced *tr*-FRET signal. Data are plotted as the *tr*-FRET that is observed using HA-$rH_{3A}R$ expressing cells that have been incubated with both anti-HA-Eu^{3+} and anti-HA-allophycocyanin antibodies versus the *tr*-FRET that is observed using a mix of two populations of HA-$rH_{3A}R$ expressing cells that before mixing were independently incubated with either of the two antibodies.

(but not any of the other rH_3 isoforms identified to date; Fig. 8A).

Significant increases in mRNA expression levels of H_3R isoforms with full-length third intracellular loop (detected using probe H_{3AD}) were observed in layers II-VIb of cortex (48 h after injection), caudate putamen (48 h after injection), piriform cortex (48 h after injection), and CA1 region of the hippocampus (24 h after injection) (Fig. 8B) after PTZ. Figure 8C illustrates mRNA expression levels and differences for H_{3A} and H_{3D} isoforms in representative sections from control and 48 h after injection animals.

In contrast, decreases in mRNA expression pattern of 6TM-rH_3 isoforms (detected using probe H_{3DEF}) were observed in layers II-VIb of cortex (6 h after injection), piriform cortex (6, 24, and 48 after injection), CA1 region of the hippocampus (24 h after injection), and CA3 region of the hippocampus (24 h after injection) (Fig. 8D). Figure 8E shows mRNA expression patterns and differences for 6TM-rH_3 isoforms in representative sections from control animals and animals 24 h after injection.

Discussion

Our search for additional alternative splice variants of the rH_3R resulted in the identification of three mRNAs coding for heretofore uncharacterized rH_3 isoforms. In contrast to the known functional H_3Rs, sequence analysis of these newly identified isoforms reveals that an additional splicing event occurs within a region corresponding to TM6, resulting in isoforms with an alternative C-terminal domain and isoforms that are predicted to possess only 6 TMs. The mRNAs encoding these 6TM-rH_3 isoforms are expressed in the rat brain with a distribution pattern that is similar to the previously identified functional 7TM-rH_3Rs (Drutel et al., 2001). Although there may be differences in the rate of synthesis, the inherent stability, and the rate of degradation of the various H_3 isoforms, resulting in differences in their expression levels, extensive analysis of the 6TM-rH_3 isoforms through heterologous expression studies, however, failed to identify any ligand-binding and functional signaling events modulated by these 6TM-rH_3 isoforms. The 6TM-rH_3 isoforms seem to be localized intracellularly, and succeeding studies revealed the ability of the 6TM-rH_3 isoforms to interfere with the cell surface expression and subsequent signaling of the previously identified 7TM-rH_3 isoforms, thus acting as dominant-negative isoforms.

An increasing number of GPCRs have been shown to exist as oligomeric complexes (for review, see, for example, Pfleger and Eidne, 2005), which are thought to be formed early

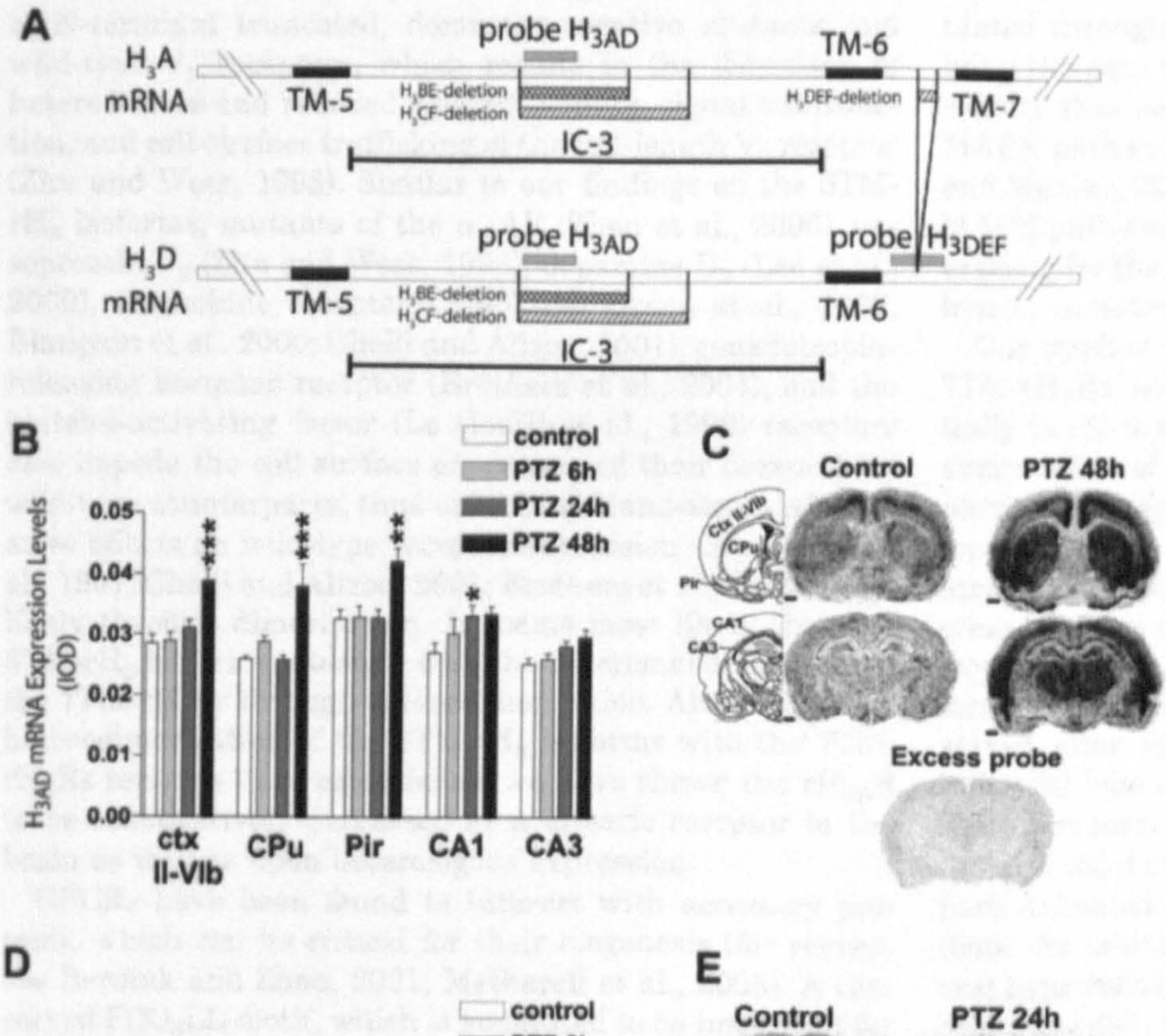

Fig. 8. Detection of rH_3 isoform mRNA in rat brain. A, diagrammatic representation of mRNA sequences recognized by probes H_{3AD} and H_{3DEF}. B, mRNA levels of isoforms detected with probe H_{3AD}. C, images of representative sections from control animals and animals 48 h after PTZ injection. D, expression mRNA levels of isoforms detected with probe H_{3DEF}. E, images of representative sections from control animals and animals 24 h after injection. Data are presented as integrated optic density ± S.E.M.; levels of significance are as follows: *, $p < 0.05$; **, $p < 0.01$; ***, $p < 0.001$. ctx II-VIb, cortex layers II to VIb; CPu, caudate putamen; Pir, piriform cortex; CA1, CA1 region of the hippocampus; CA3, CA3 region of the hippocampus.

during biosynthesis (Terrillon et al., 2003). In this study, we show also that the $rH_{3A}R$ is present as dimers or higher order oligomeric complexes in both transfected cells and rat brain. The oligomerization of GPCRs during biosynthesis and maturation seems crucial for proper exportation of receptors to the plasma membrane (for review, see Bulenger et al., 2005). The coexpression and formation of heterodimeric β_2-ARs (Hague et al., 2004a) aids, for instance, the cell surface trafficking of olfactory GPCRs that are otherwise retained and degraded in the ER (Lu et al., 2003, 2004), as well as of the α_{1D}-AR that normally is trafficked poorly to the cell surface (Uberti et al., 2005). The coexpression of differentially spliced GPCR variants may also aid the cell-surface expression, as shown for instance by the coexpression of the α_{1D}-AR with α_{1B}-ARs (Hague et al., 2004b). In contrast, certain alternatively spliced variants of, for instance, the α_{1A}-AR (Cogé et al., 1999), the calcitonin receptor (Seck et al., 2003), and the dopamine D_3 receptor (Karpa et al., 2000) seem to dimerize with their cognate full-length receptors and impede their cell surface expression because of mislocalization to an intracellular compartment. The coexpression of the 6TM-rH_3 isoforms described herein not only reduced cell surface expression of the 7TM-rH_3Rs but also consequently resulted in a reduced 7TM-rH_3R-mediated signaling. Our data are therefore consistent with the reported findings on the coexpression of N-terminal truncated, dominant-negative mutants and wild-type V_2 receptors, which results in the formation of heterodimers and reduced agonist binding, signal transduction, and cell-surface trafficking of the full-length V_2 receptor (Zhu and Wess, 1998). Similar to our findings on the 6TM-rH_3 isoforms, mutants of the α_2-AR (Zhou et al., 2006), vasopressin V_2 (Zhu and Wess, 1998), dopamine D_2 (Lee et al., 2000), chemokine receptor CCR5 (Benkirane et al., 1997; Blanpain et al., 2000; Chelli and Alizon, 2001), gonadotropin-releasing hormone receptor (Brothers et al., 2004), and the platelet-activating factor (Le Gouill et al., 1999) receptors also impede the cell surface expression of their coexpressed wild-type counterparts, thus exhibiting trans-dominant-negative effects on wild-type receptor expression (Benkirane et al., 1997; Chelli and Alizon, 2001; Brothers et al., 2004), most likely through dimerization. It seems most likely that the 6TM-rH_3 isoforms interfere with the functional expression of the 7TM-rH_3Rs through heterodimerization. Although direct heterodimerization of the 6TM-rH_3 isoforms with the 7TM-rH_3Rs remains to be established, we have shown the $rH_{3A}R$ to be constitutively expressed as a dimeric receptor in the brain as well as upon heterologous expression.

GPCRs have been found to interact with accessory proteins, which can be critical for their biogenesis (for review, see Bermak and Zhou, 2001; Metherell et al., 2005). A conserved $F(X)_6LL$ motif, which is suggested to be important for the proper GPCR folding and subsequent export from the ER (Duvernay et al., 2004), is also present in the C-terminal domain of the 7TM-rH_3Rs but is lacking in the 6TM-rH_3 isoforms. Mutations in regions overlapping the $F(X)_6LL$ motif in the dopamine D_1 receptor resulted in ER retention of the mutant receptor and loss of cell surface expression, and subsequent studies revealed that this region is important for a interactions with a specific ER-membrane-associated protein that regulates transport of GPCRs (Bermak et al., 2001). It is noteworthy that, instead of the $F(X)_6LL$ motif, the 6TM-rH_3 isoforms possess an RXR ER retention signal. Taken together, these data suggest that the 6TM-rH_3 isoforms lack protein-protein interactions with specific accessory proteins in the ER that are required for cell-surface expression. Although the localization of the 6TM-rH_3 isoforms within the ER seems likely, this needs to be verified by future experiments. Nonetheless, the findings on GPR30 as an intracellular GPCR (Revankar et al., 2005) points out that the 6TM-rH_3 isoforms may well have yet undiscovered intracellular functions in addition to their capability to retain the 7TM-rH_3Rs intracellularly.

On the one hand, the 6TM-rH_3 splice variants may act as "antichaperones" inhibiting specific chaperones' activities or preventing their access to the 7TM-rH_3Rs. On the other hand, the association of the 6TM-rH_3 isoforms with the 7TM-rH_3R isoforms in the ER may actively unfold or result in the misfolding of the protein complex. Because we find that the rH_{3D} isoform does not interfere with the cell surface expression of unrelated GPCRs, it seems unlikely the 6TM-rH_3 isoforms act through blocking either the ER or Golgi, or to promote ER-associated protein degradation. The precise mechanism underlying the action of the newly identified isoforms, however, remains unknown. Our data suggest that the regulation of the alternative rH_3R mRNA splicing is a new and effective means for the regulation of H_3R signaling. Functional (including constitutive) H_3R activity may be regulated through the regulation of the splicing events underlying the occurrence of the various H_3R isoforms. It is noteworthy that several cell signaling pathways, including the MAPK pathway, regulate mRNA splicing (reviewed in Shin and Manley, 2004). It is intriguing that the H_3R activates the MAPK pathway (Drutel et al., 2001; Giovannini et al., 2003), arguing for the possibility of activation of splicing factors and hence, an autoregulation of the H_3R activity.

Our studies also show that the expression pattern of the 7TM-rH_3Rs and the 6TM-rH_3 isoforms overlaps substantially in rat brain. Moreover, PTZ-induced seizures result in suppression of 6TM-rH_3 (probe H_{3DEF}) isoform mRNAs in particular brain regions, whereas mRNA levels of the isoforms with the full third intracellular loop (probe H_{3AD}) are increased. A characteristic transient and short-living increase in the mRNA for the full-length third intracellular loop (probe H_{3AD}), hippocampal CA_{3c} area, followed by piriform cortex, amygdala, and hippocampal CA_1 area is observed after systemic injection of kainic acid, a model of temporal lobe epilepsy (Lintunen et al., 2005), indicating a spatiotemporal correlation to progressing neuronal damage in this model of temporal epilepsy. Previous studies on PTZ have indicated damaged neurons in the rostral limbic cortex (both the orbital, agranular insular, and prelimbic), the lateral hypothalamus (in the vicinity of the rostral medial forebrain bundle), the bed nucleus of the stria terminalis, the claustrum, the hippocampal formation (CA3 and entorhinal cortex), and lateral thalamic nuclei 50 min after injection (Ben-Ari et al., 1981). The increases in H_3R mRNA with full third intracellular loop as observed in this study after PTZ were observed significantly later than the reported damage begins (Ben-Ari et al., 1981), in agreement with the concept that the mechanisms of neuronal damage after kainic acid and PTZ are different. Although the piriform cortex has not been reported to suffer significant damage after PTZ (Ben-Ari et al., 1981), it seems not to be only a primary sensory area but because of its neuronal organization and associative

fiber system may also be involved in the pathological mechanisms leading to seizures (Löscher and Ebert, 1996). Of the areas studied here, the piriform cortex showed a sustained decline in 6TM-rH_3 mRNA expression. We observed a significant transient increase in H_3R radioligand binding in piriform cortex at 6 h after PTZ concomitantly with the decline of H_{3DEF} isoform mRNAs (data not shown). However, a similar strong correlation was not found in all areas where smaller changes were seen, suggesting that other factors in addition to mRNA ratios may affect receptor binding. The high susceptibility for induction of seizures by chemical or electrical stimulation and various studies addressing its role in seizure generation suggest that the piriform cortex can also function as an amplifier region to increase and propagate seizure activity induced in other limbic regions (Löscher and Ebert, 1996). Increased H_3R activity (e.g., expression and translation) in this region could result in decreased glutamate release (Brown and Haas, 1999; Molina-Hernandez et al., 2001), because glutamatergic neurons exist in the piriform cortex (Riba-Bosch and Perez-Clausell, 2004), for control of overall neuronal activity in the region.

The abundance of mRNA coding for the 6TM-rH_3 isoforms suggest that its production may have important biological implications. For example, in addition to its ability to interfere with cell surface expression of functional rH_3Rs, which may arise from modification of the stability of the mRNA encoding functional 7TM-rH_3Rs, the 6TM-rH_3 isoform mRNAs might encode proteins with yet unidentified functions. Further analysis of the alternatively spliced products of the H_3R gene is required to elucidate their biological significance.

In conclusion, we have identified three additional splice variants of the rH_3R. The mRNAs of these isoforms are abundantly expressed in the brain and the expression pattern largely overlaps with that of the known rH_{3A-C}R isoforms. Analysis of the sequence of these rH_{3D}, rH_{3E}, and rH_{3F} isoforms reveals these isoforms to consist of 6TM domains. The 6TM-rH_3 isoforms are retained intracellularly upon heterologous expression, and in subsequent pharmacological analysis studies we could detect no ligand binding or functional activity for these 6TM-rH_3 isoforms. The 6TM-rH_3 isoforms, however, selectively impede cell surface expression of the functional 7TM-rH_3Rs. Moreover, the mRNA levels of the rH_3 isoforms in rat brain are modulated by treatment with the convulsant PTZ. Although the functional significance and possible roles of these 6TM-rH_3 isoforms in (patho)physiology remain to be established, these findings provide novel insight in the regulation of the histaminergic system in the brain.

Acknowledgments

This article is dedicated to Dr. Art A. Hancock, who passed away on November 11, 2005. Dr. Hancock was a great scientist with a warm and generous personality. Under his inspired leadership, Abbott Laboratories made many seminal contributions to the field of H_3 receptors.

We thank Sarina M. Meusburger, Franca di Summa, Kim Retra, and José Antonio Arias-Montaño for expert assistance.

References

Bakker RA (2004) Histamine H_3-receptor isoforms. *Inflamm Res* 53:509–516.
Bakker RA, Dees G, Carrillo JJ, Booth RG, López-Gimenez JF, Milligan G, Strange PG, and Leurs R (2004a) Domain swapping in the human histamine H_1 receptor. *J Pharmacol Exp Ther* 311:131–138.
Bakker RA, Weiner DM, ter Laak T, Beuming T, Zuiderveld OP, Edelbroek M, Hacksell U, Timmerman H, Brann MR, and Leurs R (2004b) 8R-Lisuride is a potent stereospecific histamine H_1-receptor partial agonist. *Mol Pharmacol* 65: 538–549.
Ben-Ari Y, Tremblay E, Riche D, Ghilini G, and Naquet R (1981) Electrographic, clinical and pathological alterations following systemic administration of kainic acid, bicuculline or pentetrazole: metabolic mapping using the deoxyglucose method with special reference to the pathology of epilepsy. *Neuroscience* 6:1361–1391.
Benkirane M, Jin DY, Chun RF, Koup RA, and Jeang KT (1997) Mechanism of transdominant inhibition of CCR5-mediated HIV-1 infection by ccr5D32. *J Biol Chem* 272:30603–30606.
Bermak JC, Li M, Bullock C, and Zhou QY (2001) Regulation of transport of the dopamine D1 receptor by a new membrane-associated ER protein. *Nat Cell Biol* 3:492–498.
Bermak JC and Zhou QY (2001) Accessory proteins in the biogenesis of G protein-coupled receptors. *Mol Intervent* 1:282–287.
Blanpain C, Lee B, Tackoen M, Puffer B, Boom A, Libert F, Sharron M, Wittamer V, Vassart G, Doms RW, et al. (2000) Multiple nonfunctional alleles of CCR5 are frequent in various human populations. *Blood* 96:1638–1645.
Brothers SP, Cornea A, Janovick JA, and Conn PM (2004) Human loss-of-function gonadotropin-releasing hormone receptor mutants retain wild-type receptors in the endoplasmic reticulum: molecular basis of the dominant-negative effect. *Mol Endocrinol* 18:1787–1797.
Brown RE and Haas HL (1999) On the mechanism of histaminergic inhibition of glutamate release in the rat dentate gyrus. *J Physiol* 515 (Pt 3):777–786.
Bulenger S, Marullo S, and Bouvier M (2005) Emerging role of homo- and heterodimerization in G-protein-coupled receptor biosynthesis and maturation. *Trends in Pharmacological Sciences* 26:131–137.
Chazot PL, Hann V, Wilson C, Lees G, and Thompson CL (2001) Immunological identification of the mammalian H_3 histamine receptor in the mouse brain. *Neuroreport* 12:259–262.
Chelli M and Alizon M (2001) Determinants of the *trans*-dominant negative effect of truncated forms of the CCR5 chemokine receptor. *J Biol Chem* 276:46975–46982.
Cogé F, Guénin SP, Audinot V, Renouard-Try A, Beauverger P, Macia C, Ouvry C, Nagel N, Rique H, Boutin JA, et al. (2001) Genomic organization and characterization of splice variants of the human histamine H_3 receptor. *Biochem J* 355: 279–288.
Cogé F, Guenin SP, Renouard-Try A, Rique H, Ouvry C, Fabry N, Beauverger P, Nicolas JP, Galizzi JP, Boutin JA, et al. (1999) Truncated isoforms inhibit [^{3}H]prazosin binding and cellular trafficking of native human a_{1A}-adrenoceptors. *Biochem J* 343:231–239.
Drutel G, Peitsaro N, Karlstedt K, Wieland K, Smit MJ, Timmerman H, Panula P, and Leurs R (2001) Identification of rat H_3 receptor isoforms with different brain expression and signaling properties. *Mol Pharmacol* 59:1–8.
Duvernay MT, Zhou F, and Wu G (2004) A conserved motif for the transport of G protein-coupled receptors from the endoplasmic reticulum to the cell surface. *J Biol Chem* 279:30741–30750.
Giovannini MG, Efoudebe M, Passani MB, Baldi E, Bucherelli C, Giachi F, Corradetti R, and Blandina P (2003) Improvement in fear memory by histamine-elicited ERK2 activation in hippocampal CA3 cells. *J Neurosci* 23:9016–9023.
Hague C, Uberti MA, Chen Z, Bush CF, Jones SV, Ressler KJ, Hall RA, and Minneman KP (2004a) Olfactory receptor surface expression is driven by association with the β_2-adrenergic receptor. *Proc Natl Acad Sci USA* 101:13672–13676.
Hague C, Uberti MA, Chen Z, Hall RA, and Minneman KP (2004b) Cell surface expression of α_{1D}-adrenergic receptors is controlled by heterodimerization with α_{1B}-adrenergic receptors. *J Biol Chem* 279:15541–15549.
Hawrylyshyn KA, Michelotti GA, Coge F, Guenin SP, and Schwinn DA (2004) Update on human alpha1-adrenoceptor subtype signaling and genomic organization. *Trends Pharmacol Sci* 25:449–455.
Karpa KD, Lin R, Kabbani N, and Levenson R (2000) The dopamine D3 receptor interacts with itself and the truncated D3 splice variant d3nf: D3–D3nf interaction causes mislocalization of D3 receptors. *Mol Pharmacol* 58:677–683.
Kilpatrick GJ, Dautzenberg FM, Martin GR, and Eglen RM (1999) 7TM receptors: the splicing on the cake. *Trends Pharmacol Sci* 20:294–301.
Lee SP, O'Dowd BF, Ng GY, Varghese G, Akil H, Mansour A, Nguyen T, and George SR (2000) Inhibition of cell surface expression by mutant receptors demonstrates that D2 dopamine receptors exist as oligomers in the cell. *Mol Pharmacol* 58:120–128.
Le Gouill C, Parent JL, Caron CA, Gaudreau R, Volkov L, Rola-Pleszczynski M, and Stankova J (1999) Selective modulation of wild type receptor functions by mutants of G-protein-coupled receptors. *J Biol Chem* 274:12548–12554.
Leurs R, Bakker RA, Timmerman H, and de Esch IJ (2005) The histamine H_3 receptor: from gene cloning to H_3 receptor drugs. *Nat Rev Drug Discov* 4:107–120.
Lintunen M, Sallmen T, Karlstedt K, and Panula P (2005) Transient changes in the limbic histaminergic system after systemic kainic acid-induced seizures. *Neurobiol Dis* 20:155–169.
Löscher W and Ebert U (1996) The role of the piriform cortex in kindling. *Prog Neurobiol* 50 (5–6):427–481.
Lu M, Echeverri F, and Moyer BD (2003) Endoplasmic reticulum retention, degradation and aggregation of olfactory G-protein coupled receptors. *Traffic* 4:416–433.
Lu M, Staszewski L, Echeverri F, Xu H, and Moyer BD (2004) Endoplasmic reticulum degradation impedes olfactory G-protein coupled receptor functional expression. *BMC Cell Biol* 5:34.
Metherell LA, Chapple JP, Cooray S, David A, Becker C, Ruschendorf F, Naville D, Begeot M, Khoo B, Nurnberg P, et al. (2005) Mutations in MRAP, encoding a new

interacting partner of the ACTH receptor, cause familial glucocorticoid deficiency type 2. *Nat Genet* 37:166–170.
Milligan G (2000) Insights into ligand pharmacology using receptor-G-protein fusion proteins. *Trends Pharmacol Sci* 21:24–28.
Molina-Hernandez A, Nunez A, Sierra JJ, and Arias-Montano JA (2001) Histamine H_3 receptor activation inhibits glutamate release from rat striatal synaptosomes. *Neuropharmacology* 41:928–934.
Morisset S, Sasse A, Gbahou F, Héron A, Ligneau X, Tardivel-Lacombe J, Schwartz JC, and Arrang JM (2001) The rat H_3 receptor: gene organization and multiple isoforms. *Biochem Biophys Res Commun* 280:75–80.
Pfleger KD and Eidne KA (2005) Monitoring the formation of dynamic G-protein-coupled receptor-protein complexes in living cells. *Biochem J* 385:625–637.
Revankar CM, Cimino DF, Sklar LA, Arterburn JB, and Prossnitz ER (2005) A transmembrane intracellular estrogen receptor mediates rapid cell signaling. *Science (Wash DC)* 307:1625–1630.
Riba-Bosch A and Perez-Clausell J (2004) Response to kainic acid injections: changes in staining for zinc, FOS, cell death and glial response in the rat forebrain. *Neuroscience* 125:803–818.
Schmauss C, Haroutunian V, Davis KL, and Davidson M (1993) Selective loss of dopamine D_3-type receptor mRNA expression in parietal and motor cortices of patients with chronic schizophrenia. *Proc Natl Acad Sci USA* 90:8942–8946.
Seck T, Baron R, and Horne WC (2003) The alternatively spliced De13 transcript of the rabbit calcitonin receptor dimerizes with the C1a isoform and inhibits its surface expression. *J Biol Chem* 278:23085–23093.
Shenton FC, Hann V, and Chazot PL (2005) Evidence for native and cloned H_3 histamine receptor higher oligomers. *Inflammation Res* 54:S48–S49.
Shin C and Manley JL (2004) Cell signalling and the control of pre-mRNA splicing. *Nat Rev Mol Cell Biol* 5:727–738.
Smit MJ, Verzijl D, Casarosa P, Navis M, Timmerman H, and Leurs R (2002) Kaposi's sarcoma-associated herpesvirus-encoded G protein-coupled receptor ORF74 constitutively activates p44/p42 MAPK and Akt via G_i and phospholipase C-dependent signaling pathways. *J Virol* 76:1744–1752.
Terrillon S, Durroux T, Mouillac B, Breit A, Ayoub MA, Taulan M, Jockers R, Barberis C, and Bouvier M (2003) Oxytocin and vasopressin V1a and V2 receptors form constitutive homo- and heterodimers during biosynthesis. *Mol Endocrinol* 17:677–691.
Uberti MA, Hague C, Oller H, Minneman KP, and Hall RA (2005) Heterodimerization with b_2-adrenergic receptors promotes surface expression and functional activity of a_{1D}-adrenergic receptors. *J Pharmacol Exp Ther* 313:16–23.
White JH, Wise A, Main MJ, Green A, Fraser NJ, Disney GH, Barnes AA, Emson P, Foord SM, and Marshall FH (1998) Heterodimerization is required for the formation of a functional $GABA_B$ receptor. *Nature (Lond)* 396:679–682.
Zhou F, Filipeanu CM, Duvernay MT, and Wu G (2006) Cell-surface targeting of α_2-adrenergic receptors—inhibition by a transport deficient mutant through dimerization. *Cell Signal* 18:318–327.
Zhu X and Wess J (1998) Truncated V_2 vasopressin receptors as negative regulators of wild-type V_2 receptor function. *Biochemistry* 37:15773–15784.

Address correspondence to: Prof. Dr. R. Leurs, The Leiden/Amsterdam Center for Drug Research, Department of Medicinal Chemistry, Vrije Universiteit Amsterdam, De Boelelaan 1083, 1081HV Amsterdam, The Netherlands. E-mail: r.leurs@few.vu.nl

Pain 129 (2007) 76–92

PAIN

www.elsevier.com/locate/pain

Immunohistochemical localization of histamine H_3 receptors in rodent skin, dorsal root ganglia, superior cervical ganglia, and spinal cord: Potential antinociceptive targets

Keri E. Cannon [a], Paul L. Chazot [b], Victoria Hann [b], Fiona Shenton [b], Lindsay B. Hough [a], Frank L. Rice [a,*]

[a] *Center for Neuropharmacology and Neuroscience, Albany Medical College MC-136, Albany, NY 12208, USA*
[b] *School of Biological and Biomedical Sciences, University of Durham, Durham, UK*

Received 12 May 2006; received in revised form 4 August 2006; accepted 28 September 2006

Abstract

Activation of histamine H_3 receptors (H_3Rs) reduces inflammation and nociception, but the existence of H_3Rs on peripheral innervation has never been demonstrated. Here we use antibodies to locate H_3Rs in whisker pads, hairy and glabrous hind paw skin, dorsal root ganglia (DRGs), and spinal cords of rats, wild type mice, and H_3R knockout (H_3KO) mice. Although H_3Rs have been hypothesized to be on C and sympathetic fibers, H_3R-like immunoreactivity (H_3R-LI) was only detected on presumptive periarterial Aδ fibers and on Aβ fibers that terminated in Meissner's corpuscles and as lanceolate endings around hair follicles. The H_3R-positive periarterial fibers were thin-caliber and coexpressed immunoreactivity for calcitonin gene-related peptide (CGRP), substance P, acid sensing ion channel 3, and 200 kDa neurofilament protein (NF). H_3R-LI was also detected on epidermal keratinocytes and Merkel cells, but not on Merkel endings, C fibers, any other Aδ fibers, or sympathetic fibers. In DRGs, H_3R-LI was preponderantly on medium to large neurons coexpressing NF-LI and mostly CGRP-LI. In dorsal horn, CGRP-positive fibers with and without H_3R-LI ramified extensively in lamina II; many of the former formed a plexus in lamina V. Low levels of H_3R-LI were also present on Aβ fibers penetrating superficial and into deeper laminae. The distribution of H_3R-LI was similar in rats and wild type mice, but was eliminated or strongly reduced in Aδ fibers and Aβ fibers, respectively, in H_3KO mice. Taken with recently published behavioral results, the present findings suggest that periarterial, peptidergic, H_3R-containing Aδ fibers may be sources of high threshold mechanical nociception.

Keywords: Histamine; H_3 receptors; Arterial innervation; Aδ fibers; Aβ fibers; Calcitonin gene-related peptide; Substance P; Sensory innervation

1. Introduction

Histamine is a chemical messenger that is released by neuronal and non-neuronal sources (Hough and Leurs, 2006). Histamine can act at four known types of histamine receptors, including H_3 receptors (Hough, 2001). Although H_3 receptors (H_3Rs) were originally reported to exist in the CNS as presynaptic inhibitory autoreceptors (Arrang et al., 1983; Arrang et al., 1987), lesion studies have revealed that a large fraction of brain H_3Rs exist as postsynaptic inhibitory heteroreceptors (Pollard et al., 1993). Subsequently, pre- and postsynaptic expression of H_3Rs has been detected throughout the CNS. Detailed H_3R radioligand binding in rat brains revealed high densities of binding sites in the cerebral cortex, striatum, and olfactory tubercles (Pollard et al., 1993). In agreement with this distribution, *in situ* hybridization studies showed strong H_3R mRNA signals in the

* Corresponding author. Tel.: +1 518 262 5384; fax: +1 518 262 5799.
E-mail address: ricef@mail.amc.edu (F.L. Rice).

0304-3959/$32.00
doi:10.1016/j.pain.2006.09.039

cerebral cortex, thalamus, and striatum of the rat (Lovenberg et al., 1999; Drutel et al., 2001). Although the majority of H_3Rs are located in the brain, H_3R mRNA is also found in various non-brain tissues, including skin, dorsal root ganglia, stomach, intestines, and brown adipose tissue (Heron et al., 2001; Karlstedt et al., 2003).

Administration of H_3R agonists has been shown to inhibit neuropeptide release from sensory fibers in the heart, lung, and skin, leading to the hypothesis that H_3Rs are located on peptidergic C fibers (Dimitriadou et al., 1994; Delaunois et al., 1995; Ohkubo et al., 1995; Imamura et al., 1996; Dimitriadou et al., 1997; Nemmar et al., 1999). Consistent with this hypothesis, recent studies revealed that H_3R agonists have anti-inflammatory as well as some antinociceptive properties (Rouleau et al., 1997; Rouleau et al., 2000; Cannon et al., 2003; Cannon and Hough, 2005). Other studies suggest that H_3Rs are located on sympathetic efferents (Ishikawa and Sperelakis, 1987; Molderings et al., 1992; Koss, 1994; Godlewski et al., 1997a,b). However, no immunohistochemical studies have been performed to determine the precise localization H_3Rs on either sensory or sympathetic fibers. Thus, the present study has performed the first investigation of the distribution of H_3R immunofluorescence on nerve cells and fibers in skin, dorsal root ganglia, and spinal cords of rats and mice.

2. Materials and methods

2.1. Specimens

The subjects were 6 rats, 6 wild type mice, and 6 H_3KO mice. Animal housing and procedures were approved by the Institutional Animal Care and Use Committee of Albany Medical College. Male Sprague–Dawley rats (300–350 g, Taconic Farms, Germantown, NY), housed in groups of two or three per cage, and female wild type or H_3KO mice (10–14 weeks old, 20–30 g), housed up to seven per cage, were maintained on a 12 h light/dark cycle (lights on from 7:00 to 19:00 h). Food and water were provided *ad libitum*.

H_3KO mice, kindly provided by Millennium Pharmaceuticals, Inc. (Cambridge, MA), were generated by targeted deletion of exon 3 of the mouse H_3R gene (Cannon et al., 2003). H_3KO mice showed no detectable histamine H_3R mRNA in the brain or the spinal cord by *in situ* hybridization (Cannon et al., 2003). Brains from these subjects also had no detectable histamine H_3R binding (Mobarakeh et al., 2003). Following an overdose of sodium pentobarbital, the animals were transcardially perfused with 0.9% saline, followed by 4% paraformaldehyde in 0.1 M phosphate-buffered saline (PBS, pH 7.4, 4 °C). Immediately after perfusion, the tissues were dissected and post-fixed at 4 °C in perfusion fixative for 4 h. Following post-fixation, the tissues were rinsed several times in PBS and stored in 0.1% sodium azide PBS. The following tissues were taken from each animal: (1) lumbar spinal cord, (2) lumbar dorsal root ganglia (DRG), (3) superior cervical ganglia (SCG), (4) glabrous and hairy skin from hind paws, and (5) whisker pads. The forebrains were removed from some rats, wild type mice and H_3KO mice for control purposes.

For cryostat sectioning, tissues were cryoprotected by overnight immersion in PBS containing 30% sucrose at 4 °C. Serial sections (14 μm-thick) were cut on a cryostat and thawed in sequential order onto and rotating across 5–15 gelatinized slides. The slides were air dried overnight and processed for single or double immunolabeling.

2.2. Production and characterization of H_3R antibodies

Our study used two different rabbit polyclonal antibodies for H_3R: one produced by Chazot et al. (2001) and the other obtained commercially (AB5660P, Chemicon, see Table 1). The Chazot antibody was directed against residues 349–358 of the human and rat H_3R, which is identical in the mouse sequence (Chen et al., 2003). Western blots on P2 membranes taken from wild type and H_3KO forebrains were performed with this antibody as previously described (Chazot et al., 2001). Proteins (30 μg) were extracted using the chloroform/methanol precipitation method, and the precipitate subjected to SDS–PAGE under reducing conditions, using 7.5% (v/v) acrylamide slab gels. Proteins were transferred onto nitrocellulose, probed with the H_3R antibody (2 μg/ml), and detected using an ECL PLUS system (Amersham, UK). The Chemicon antibody was targeted against an 18 amino acid sequence in the C-terminus region of rat H_3R. This sequence is 100% identical in mouse, 88% conserved in guinea pig, and 82% in human H_3R.

Table 1
List of antibodies used for immunofluorescence studies

Antigen	Antibody (dilution)	Source
Protein gene product 9.5 (PGP)	Rabbit polyclonal (1:800)	UltraClone Ltd. (Wellow, Isle of Wight, UK)
Calcitonin gene-related peptide (CGRP)	Guinea pig polyclonal (1:400)	Peninsula Laboratories Inc. (San Carlos, CA)
Neurofilament 200 kDa (NF)	Rabbit polyclonal (1:800)	Chemicon International Inc. (Temecula, CA)
Substance P (SP)	Guinea pig polyclonal (1:400)	Research Diagnostics Inc. (Flanders NJ)
Neuropeptide Y (NPY)	Sheep polyclonal (1:800)	Chemicon International Inc.
Acid-sensing ion channel 3 (ASIC3)	Guinea Pig (1:500)	Neuromics Antibodies (Northfield, MN)
Histamine H_3 receptor (H_3R)		
(1) Intracellular loop 3[a] (rat and human)	Rabbit polyclonal (1:50–500)	Chazot et al., 2001
(2) C-terminus[b] (rat)	Rabbit polyclonal (1:50–500)	Chemicon International Inc.

[a] This antibody was raised against a 10 amino acid peptide sequence found in intracellular loop 3 of the rat and human H_3R protein.
[b] This commercial antibody was raised against the C-terminus of rat H_3R.

2.3. Immunofluorescence preparation and observation

As previously described (Rice et al., 1997; Paré et al., 2002), serial 14 μm sections were prepared for single or double labeling with the antibodies listed in Table 1. Antibodies were diluted in a PBS solution containing 1% bovine serum albumin (BSA) and 0.3% Triton X-100. Appropriate species of secondary antibodies were raised in donkey or goat and conjugated with either Cy3 (1:250; Jackson ImmunoResearch Laboratories, Inc.), Cy2 (1:500; Jackson ImmunoResearch Laboratories, Inc.), or Alexa 488 (1:500; Molecular Probes, Inc.).

Slides were first preincubated in PBS containing 1% BSA and 0.3% Triton X-100 for 30 min, then incubated overnight at 4 °C in primary antibody under high humidity. Following a 30 min rinse in PBS, slides were incubated under the appropriate secondary antibody for 2 h at room temperature then rinsed for 30 min in PBS. For double labeling, the sequence was repeated with the desired additional primary antibody and its appropriate secondary antibody. After the final rinse, slides were coverslipped with 90% glycerin/10% PBS solution. If the two primary antibodies were raised in different species, then the double labeling revealed by Cy3 and Cy2 (or Alexa 488) was clearly separate. In some cases, double labeling combinations were desired where only two rabbit primary antibodies (A and B) were available or optimal. After verifying that separate single labeled preparations with each antibody labeled similar innervation in a specific anatomical location, some slides were incubated first with antibody A followed by anti-rabbit Cy3, then incubated with antibody B followed by anti-rabbit Cy2 or Alexa 488. Other slides with alternating tissue sections were processed with the sequence of primary antibodies reversed (i.e., first B, then A). The validity and limitations of this double labeling method have been discussed in detail (Rice et al., 1997). For example, if fibers and endings labeled with A are a subset of those labeled with B, then the first sequence will have some fibers and endings that will be double labeled both with Cy3 and Cy2, whereas additional fibers and endings will only be labeled with Cy2. In the reverse sequence, all fibers and endings will be double labeled, and none will be only labeled with Cy2.

2.4. Immunochemical specificity and fiber classification

As shown in previous studies, protein gene product 9.5 (PGP) is a pan-neuronal cytoplasmic enzyme (Rice et al., 1997). As such, anti-PGP labels all types of normal cutaneous innervation in rats and mice including sympathetic fibers and various types of sensory fibers (i.e. Aβ, Aδ, and C fibers), as well as their terminations (Rice et al., 1997; Fundin et al., 1997a,b; Rice et al., 1998; Fünfschilling et al., 2004; Zylka et al., 2005). Other antibodies directed against 200 kDa neurofilament (NF), CGRP, substance P (SP), and neuropeptide Y (NPY) discriminate between specific types of innervation. The previous studies on rat skin cited above demonstrated that NF-LI was present on all thick-caliber and many thin-caliber sensory fibers. The anti-NF labeling in the rat was consistently coexpressed with myelin basic protein (MBP) LI indicating that these thick and thin fibers are Aβ and Aδ fibers, respectively. NF-positive fibers with thick and thin calibers that have similar distributions and types of endings are also present in mouse skin. Based upon their morphologically distinct endings, the thick caliber fibers are the clear equivalent of the Aβ fibers in the rat. The thin NF-positive caliber fibers in the mouse are presumably the equivalent Aδ fibers, although in attempting to directly confirm this presumption we have not found an antibody that effectively reveals myelin basic protein in sections of mouse skin. CGRP-LI and SP-LI are vasodilatory neuropeptides commonly coexpressed in subsets of Aδ and C "peptidergic" fibers in mouse and rat skin. Likewise, in mouse and rat skin, NPY is a neuropeptide normally expressed mostly in adrenergic sympathetic fibers that also are immunoreactive for tyrosine hydroxylase and are implicated in vasoconstriction.

Three experiments were performed to control for nonspecific labeling. First, incubations were conducted without the primary antibody to observe immunofluorescence provided by the secondary antibody alone. Second, slides were incubated under primary antibodies that had been preincubated with their specific blocking peptide to observe any nonspecific interactions of the primary antibody. Blocking peptide was added to the H_3R antibody at 1000-fold molar excess and was allowed to sit at room temperature for one hour prior to application to tissue sections. Third, immunolabeling was assessed in H_3KO mice. To recognize the possibility that an antibody made against a particular antigen might label a different, albeit antigenically similar molecule, all detectable immunofluorescence will be referred to as a particular antigen-like immunoreactivity (LI), for example H_3R-LI. For simplicity, structures having LI for a particular antigen will also be referred to as positive for that antigen, for example H_3R-positive.

Sections were analyzed with an Olympus Provis AX70 microscope equipped with conventional fluorescence: (1) Cy3 filters (528–553 nm excitation, 590–650 nm emission), and (2) Cy2 filters (460–500 nm excitation, 510–560 nm emission). Fluorescence images were captured with a high resolution (1280 × 1024 pixels) three chip color CCD camera (Sony, DKC-ST5) interfaced with Northern Eclipse software (Empix Imaging, Inc., Mississauga, ON).

Since the intensity of immunolabeling for the numerous antibodies used in the present study is attributed to many variables that cannot be individually quantified, this study does not attempt to quantify the relative amounts of labeled antigens. These variables include: (1) true differences in the presence and quantity of the antigen, (2) whether the antibody is monoclonal or polyclonal, (3), background labeling, (4) antibody concentration, (5) efficacy of the antibody, and (6) location of the antigen (i.e. membrane or cytosol). Because the labeling intensities differed between the various types of antibodies, the photomicrographs compiled for illustrative purposes were adjusted using Northern Eclipse, Adobe Photoshop (San Jose, CA), and Microsoft Powerpoint (Redmond, WA) software so that the maximum labeling contrast and intensity were similar for each antibody.

2.5. Dorsal root ganglia quantifications

Analyses of the double labeling combinations in DRGs and SCGs were performed with Neurolucida software (MicroBrightField, Inc., Willston, VT). Analyses were conducted for sections spaced at least 100 μm apart from three L4 or L5 DRGs double-labeled with antibodies for (1) H_3R and calcitonin gene-related peptide (CGRP), (2) H_3R and

substance P (SP), and (3) for H_3R and 200 kDa neurofilament protein (NF). The H_3R and CGRP antibodies were raised in rabbit and guinea pig (respectively), allowing for distinct detection of single or double labeling. The H_3R and NF antibodies were both made in rabbit. Single labeling with anti-H_3R or anti-NF revealed that many neurons expressed H_3R-LI and/or NF-LI. Sequential incubations first with anti-H_3R followed by anti-rabbit Cy3, then in anti-NF followed by anti-rabbit Cy2 revealed that many neurons had NF-LI without H_3R-LI. Sequential incubations first with anti-NF followed by anti-rabbit Cy3, then anti-H_3R followed by anti-rabbit Cy2 revealed that virtually all the anti-H_3R labeled neurons coexpress NF-LI. Interestingly, since anti-H_3R labeling was much less robust than anti-NF labeling, when H_3R antibodies were used first in the double labeling sequence the subsequent binding of the first anti-rabbit secondary antibody effectively blocked any erroneous cross labeling by the anti-rabbit secondary antibody used in the second round of incubations.

In order to standardize assessment of labeling, digital images of double labeled ganglion sections were captured separately for the red (Cy3) and green (Cy2 or Alexa 488) fluorescent channels, using camera settings that produced a comparable range of low fluorescence intensities in each channel. The lowest fluorescence intensities captured for each antibody were set to levels comparable to the fluorescence captured from sections processed only with the secondary antibodies. Next, the range of fluorescence intensities in each channel was adjusted linearly so that many cells remained barely evident, and the most brightly fluorescing cells had a comparable intensity in both channels. The resultant images in the red and green channels were merged by Boolean addition and the double labeled images were stored. A copy of each double labeled image was purposefully extremely enhanced so that contours of even the most faint cell profiles in the background could be delineated. Using these extremely enhanced images, the contours of all visible cells were circumscribed to calculate the area of each cell for as many cells as possible. The contour outlines obtained in the enhance images were then superimposed onto separate copies of the unenhanced red and green images. In each channel, the labeling of the cell underlying each contour was subjectively rated as: (1) blank, (2) very weak, (3) weak, (4) moderate, or (5) strong. The independent results from each channel were then combined to conclude which cells had labeling for either or both antibodies. Only those cells regarded as weak, moderate, or strong in each channel were regarded as "labeled" for the antibody corresponding to the particular channel. The **Abercrombie (1946)** correction was used to compensate for the progressive under representation of cells that occurs in proportion to decreasing diameter.

3. Results

3.1. Characterization of the H_3R antibody

In order to more fully characterize the H_3R antibody first developed by **Chazot et al. (2001)**, this antibody was used to detect H_3R-LI in coronal brain sections of rats, wild type mice and H_3KO mice. In rats and wild type mice, pronounced H_3R-LI was observed in several brain regions known to contain moderate to high levels of H_3R mRNA in rats (**Pollard et al., 1993; Heron et al., 2001; Pillot et al., 2002**). For example, in both species we found robust H_3R-LI in the striatum (**Fig. 1A**), consistent with the previous detection in rats of H_3R mRNA in the striatum and H_3R-LI on striatal, medium spiny neurons of rats. H_3R-LI was also observed in the cingulate cortex, substantia nigra pars reticulata, and cerebral cortex of rats and wild type mice (data not shown). In contrast, the medial septal regions and hippocampal pyramidal layers of rats and wild type mice contained little to no H_3R-LI (data not shown), consistent with the published paucity of H_3R mRNAs in these locations (**Pollard et al., 1993; Heron et al., 2001; Pillot et al., 2002**). Analysis of brain sections taken from H_3KO mice revealed a virtually complete absence of H_3R-LI in most brain regions examined, including the striatum (**Fig. 1C**). However, a weak residual H_3R-LI remained in the cerebral cortex and cingulate cortex of H_3KO mice (data not shown).

In Western blots performed on membrane extracts from the forebrains of wild type mice (**Fig. 1D**), two major H_3R-related species were detected (M_r 93,000 and M_r 68,000), as previously seen in the rat (**Chazot et al., 2001**). These immunoreactive species were

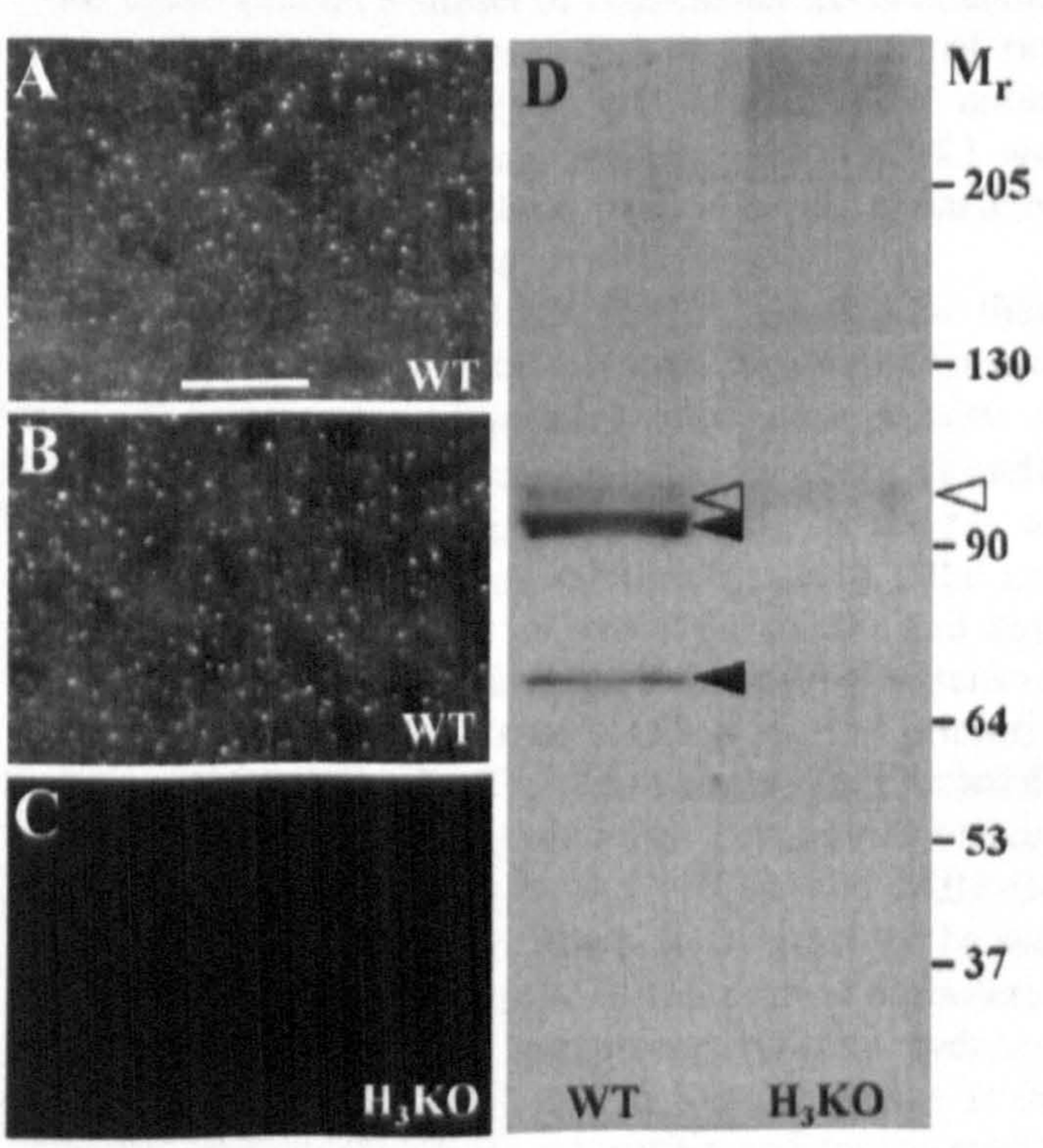

Fig. 1. Characterization of anti H_3R labeling. (A–C) Digital images of punctate anti-H_3R labeling among the neurons in the striatum as seen in coronal sections from wild type (A and B) and H_3KO mice (C). Scale bar, 25 μm. Comparable labeling was obtained with anti-H_3R antibodies produced independently by **Chazot et al. (2001)** (A) and Chemicon (B). Virtually all labeling is absent in the striatum of H_3KO mice prepared with the Chazot antibody (C). (D) A Western blot with the Chazot antibody reveals two dense bands (solid arrowheads) in the wild type mice that are eliminated in H_3KO mice, and a faint band (open arrowheads) that is reduced but still persists in the H_3KO mice.

eliminated in H_3KO forebrain extracts (Fig. 1D). The two species are likely to represent dimeric mouse H_3R isoforms as has been suggested using cross-linking strategies (Shenton et al., 2005). A third, previously unknown species (M_r 95,000) was faintly labeled in wild type extracts and persisted at lower levels in H_3KO extracts (Fig. 1D), which might account for weak residual immunolabeling in H_3KO tissues. The residual labeling may be due to an H_3R-like protein or protein fragment, or to a protein completely unrelated to H_3Rs. However, a GenBank BLASTp search of the H_3R antibody peptide sequence revealed no similarities to any other known vertebrate protein. Although several H_3R isoforms have been proposed to exist (Tardivel-Lacombe et al., 2000; Coge et al., 2001; Drutel et al., 2001; Wellendorph et al., 2002; Rouleau et al., 2004), the H_3KO gene construct eliminated the sequences encoding the epitopes used to make both of the H_3R antibodies.

In other control experiments, brain sections as well as hind paw and whisker pad skin sections from rats, wild type mice, and H_3KO mice were examined after incubation with H_3R antibody serum that had undergone preabsorption with the specific blocking peptide. The preabsorbed serum failed to label any components in all three types of animals (e.g. Fig. 2J–L). Finally, immunofluorescence studies of brain, skin, and spinal cord were repeated in rats, wild type mice, and H_3KO mice using a commercially available H_3R antibody (see Table 1) that targeted a different portion (C-terminus) of the H_3R protein sequence. In all cases, results with the commercially available H_3R antibody yielded comparable H_3R-LI patterns in rat, wild type mouse and H_3KO mouse tissues similar to the labeling patterns observed with the Chazot anti-H_3R (e.g. Figs. 1B and 4A–C). However, the Chazot antibody produced consistently more robust labeling and was used for most of the double labeling analyses (e.g. compare Figs. 3A–C and 4A–C).

3.2. Anti-H_3R labeling in skin

In order to determine specifically which types of cutaneous innervation express H_3Rs, sections of glabrous and hairy hind paw skin and of whisker pad skin from rats, wild type mice and H_3KO mice were processed for immunofluorescence with the two H_3R antibodies in combinations with antibodies for several other neuronal antigens (Table 1). As expected, anti-PGP labeled all types of previously known sensory and sympathetic innervation in our skin specimens, including all the types labeled with the other antibodies. The anti-PGP-labeled innervation consisted of numerous thin-caliber fibers that ramify and terminate as free nerve endings (FNEs) in the epidermis and superficial dermis (Fig. 2). Virtually all of the thin-caliber epidermal and superficial dermal innervation lacked H_3R-LI in rats and wild type mice (Fig. 2A–F). This included all combinations of CGRP, SP, and NF-positive and negative fibers indicative of peptidergic and nonpeptidergic Aδ and C fibers. Surprisingly, H_3R-LI was detected on thick-caliber Aβ fibers that terminated as lanceolate endings around hair and whisker follicles and as endings in Meissner corpuscles located in the dermal papillae of glabrous skin (Fig. 2A–F; D–F inset). Likewise, the H_3R antibodies labeled the more proximal portions of these Aβ fibers passing through large nerves in the deep dermis (Figs. 3 and 4). As has been published previously, all of the Aβ fibers labeled with anti-NF (not shown). H_3R-LI was also detected on Merkel cells located in lamina basalis of the glabrous epidermis and in the outer root sheath of whisker follicles (Fig. 2D–F), but H_3R-LI was not definitively evident on the Aβ fibers that innervate the Merkel cells. Finally, H_3R-LI was detected on keratinocytes of the epidermis, with the strongest expression in the stratum granulosum and stratum spinosum (Fig. 2A–F). Anti-H_3R labeling in H_3KO mice was severely reduced but faint labeling persisted on the Aβ fibers, Merkel cells and keratinocytes (Fig. 2G–I).

Although the H_3R antibodies failed to label thin-caliber fibers of the epidermis and upper dermis, H_3R-LI was detectable on a subset of thin-caliber fibers affiliated with arteries and arterioles deep in the dermis of rats (Fig. 3A–C) and mice (Fig. 3D–F). However, unlike the faint residual labeling on Aβ fibers, H_3R-LI was completely absent on these deep dermal, periarterial fibers of H_3KO mice (Fig. 3G–I).

Next we sought to determine the identity of these fibers. Previous studies in rats and mice demonstrated that the cutaneous periarterial innervation consists of thin-caliber sensory and sympathetic fibers (Fundin et al., 1997b; Fünfschilling et al., 2004). In the rat, all of the sensory innervation labels with anti-CGRP and anti-SP. Some of it also labels with anti-NF, and anti-MBF, and is presumptively classified as Aδ. The sensory innervation is relatively sparse and is located primarily in the tunica adventitia (Fundin et al., 1997b; Fünfschilling et al., 2004). Other peptidergic periarterial sensory fibers in mouse and rat lacked NF-IR and MBP-IR, indicating that they are C fibers. In contrast to the sensory innervation, virtually all of the normal periarterial sympathetic innervation coexpresses tyrosine hydroxylase and NPY, and distributes as a dense plexus at the border between the tunica adventitia and tunica media. Thus, both the anatomical localization of the innervation, and the immunochemical characteristics of the periarterial innervation permit a clear classification of these fibers as either Aδ, C, or sympathetic.

As seen in our anti-PGP double labeled preparations, virtually all of the anti-H_3R labeled periarterial fibers were located in the tunica adventitia on a subset of fibers within the small vascular nerves and on some of the

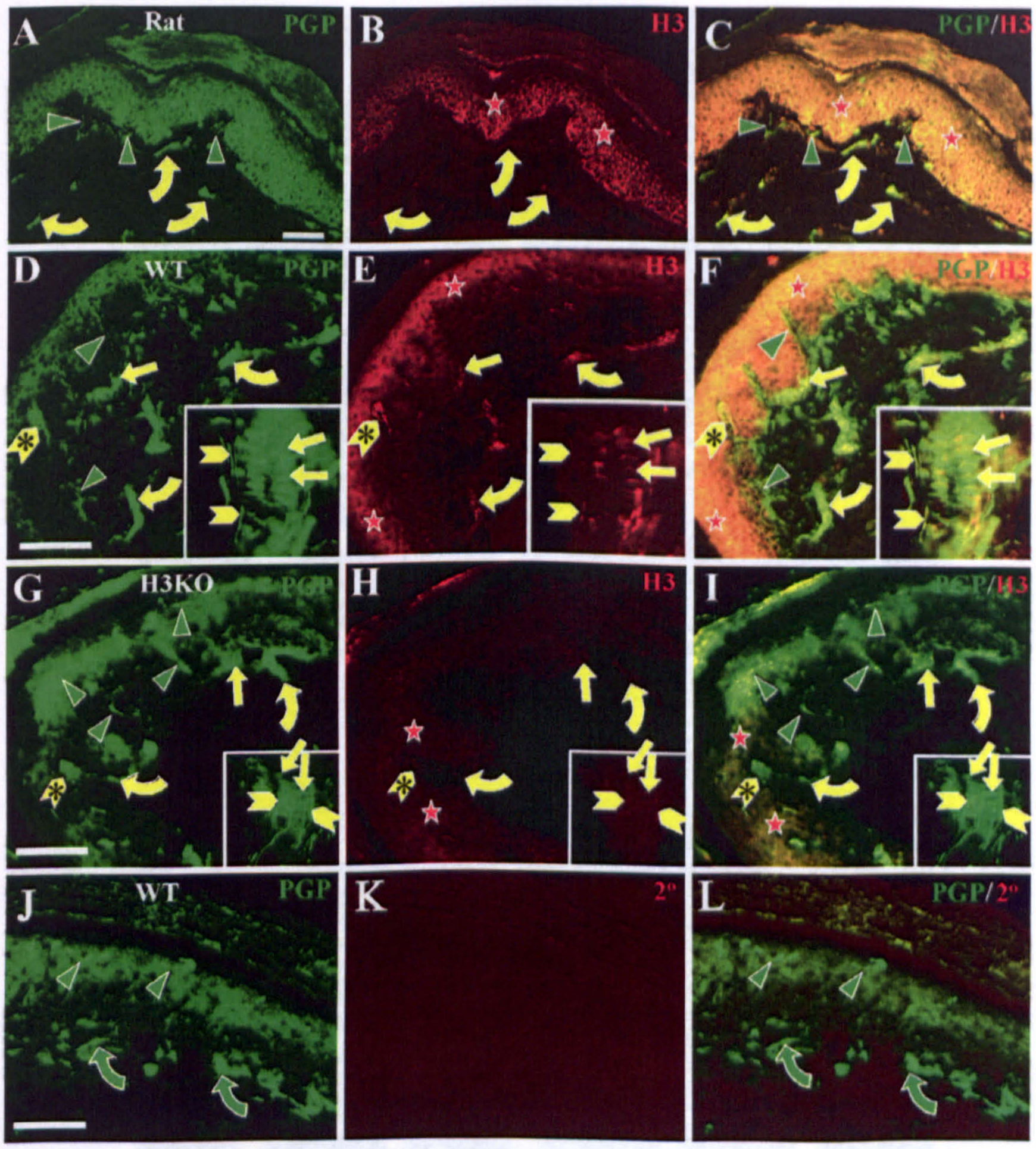

Fig. 2. H_3R-LI is absent on thin caliber innervation to the epidermis and upper dermis, but is present on some Aβ fiber innervation, Merkel cells and keratinocytes. Digital images of glabrous hind paw sections from rats (A–C), wild type mice (D–F and J–L), and H_3KO (G–I) mice double labeled with anti-PGP (left panels) and anti-H_3R (middle panels). Merged double labeled images are shown in the right panels. Insets in (D–I) show labeling in whisker follicles from mystacial pads. Scale bars = 25 μm (50 μm for insets). In this and subsequent figures, green (Cy2 or Alexa 488) and red (Cy3) symbols indicate single labeled structures; yellow symbols indicate double labeled structures. (A–F) As seen in rat and wild type mouse skin, thin caliber innervation labeled with anti-PGP (green arrowheads) in the epidermis or upper dermis is not labeled with anti-H_3R. This includes all C-fiber and Aδ-fiber innervation. Anti-PGP and anti-H_3R double labeling was present on some large caliber Aβ fibers (yellow curved arrows), and on Aβ-fiber endings in Meissner corpuscles (yellow chevrons with asterisks) and Aβ-fiber endings on whisker follicles (yellow chevrons) and hair follicles (not shown). H_3R-LI is also present on keratinocytes in the epidermis (red stars) as well as on anti-PGP labeled Merkel cells (yellow straight arrows) in lamina basalis of the epidermis and the outer root sheath of whisker follicles. H_3R-LI was not evident on the Aβ fibers that innervate the Merkel cells. (G–I) In H_3KO mice, H_3R-LI is drastically reduced but faint residual Cy3 labeling was detected on keratinocytes in the epidermis (red stars), some Aβ fibers (yellow curved arrows), Meissner corpuscles (yellow chevrons with arrowheads), lanceolate endings (yellow chevrons), and Merkel cells (yellow straight arrows). All thin caliber innervation was Cy3 negative (green arrowheads). (J–L) Images of wild type glabrous mouse skin double labeled with anti-PGP and peptide preabsorbed anti-H_3R. None of the innervation (green arrowheads and curved arrows) nor cells in the epidermis were labeled with the preabsorbed anti-H_3R.

individual fibers (**Fig. 3**A–F). Moreover, the anti-H_3R labeled fibers consistently colabeled with anti-CGRP (**Fig. 4**D–F), anti-SP (**Fig. 4**G–I), and anti-NF (**Fig. 4**J–L) indicating that the H_3R-LI was primarily if not exclusively on the presumptive Aδ fiber innervation. The remaining CGRP/SP-positive fibers, which lack NF-LI, were virtually all H_3R-negative indicating that most if not all of the C fibers were H_3R-negative. Although some C fibers could potentially be H_3R-positive, H_3R-LI was never detectable unless some

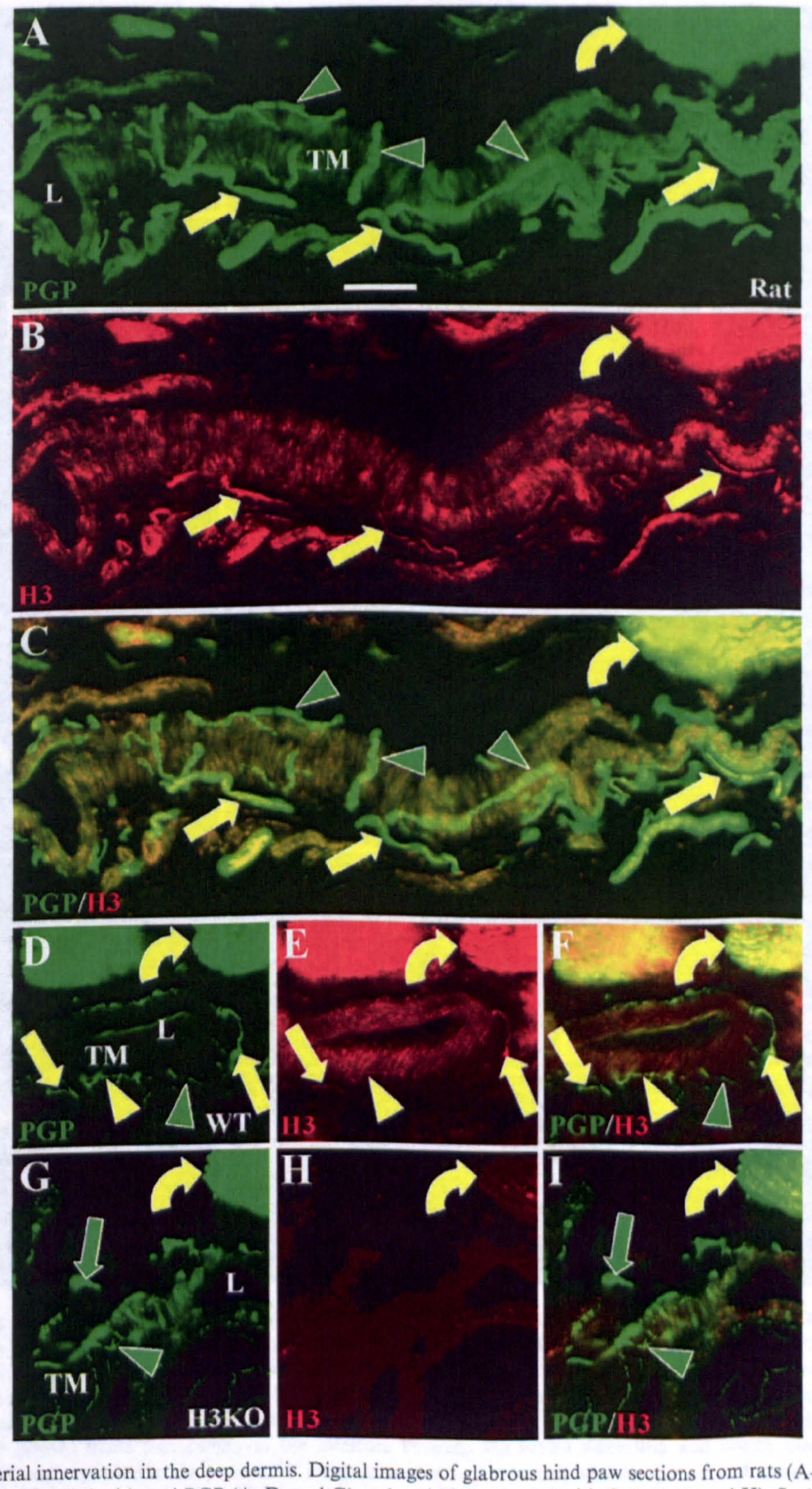

Fig. 3. H_3R-LI on periarterial innervation in the deep dermis. Digital images of glabrous hind paw sections from rats (A–C), wild type mice (D–F), and H_3KO mice (G–I) double labeled with anti-PGP (A, D, and G) and anti H_3R revealed with Cy3 (B, E, and H). Scale bars, 25 μm. L = arterial lumens, TM = tunica media. (A–F) Double labeling is present among individual axons and bundles of axons (yellow straight arrows) which are located in the tunica adventitia (which surrounds the tunica media) and have previously been shown to be mostly CGRP-positive presumptive C fibers and Aδ fibers (see also **Fig. 4**). Thin-caliber fibers that ramify at the interface between the tunica adventitia and tunica media have previously been shown to be NPY and TH-positive and are presumptive sympathetic innervation. They were entirely labeled only with anti-PGP (green arrowheads) in the rat, but some double labeled with anti-H_3R in the mouse (yellow arrowheads). Many Aβ fibers in large deep dermal nerves were double labeled (yellow curved arrows). (G–I) No H_3R-LI was present among sensory (green arrows) and sympathetic (green arrowheads) periarterial fibers in H_3KO mice, but faint residual labeling was detected on Aβ fibers (yellow curved arrows).

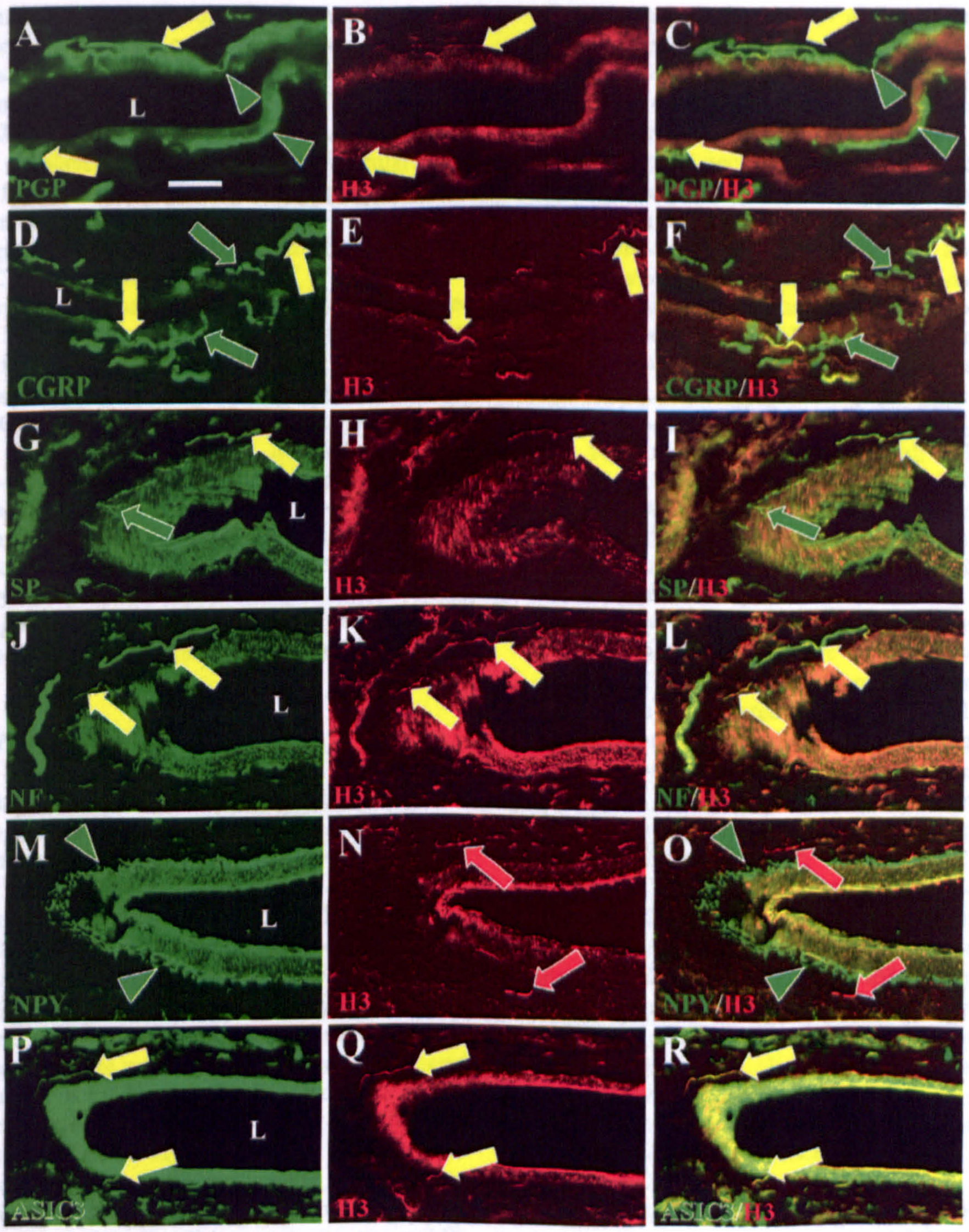

Fig. 4. Co-localization of H_3 receptors with CGRP, SP, NF, and ASIC3, but not NPY on deep dermal, peptidergic, arterial innervation. Digital images of glabrous hind paw sections from rats double labeled with antibodies against H_3R (middle panels) and against several other neuronal antigens (left panels). Merged images are in the right panels. The Chemicon anti-H_3R used in B (yellow arrows) did not label innervation as intensely as the Chazot antibody used in all the other middle panels (red and yellow arrows). Scale bar, 25 μm. L = lumen of arteries. (A–C) H_3R-LI was expressed almost entirely among the anti-PGP individual fibers and bundles of fibers (yellow arrows) located in the tunica adventitia which surrounds the tunica media. Anti-PGP labeled fibers that ramify at the interface between the tunica adventitia and tunica media lack H_3R-LI (green arrowheads). (D–F) CGRP-LI was expressed in the periarterial innervation that is presumably sensory (yellow and green arrows). A subset of this innervation co-expresses H_3R-LI (yellow arrows). (G–I) SP-LI was also expressed in periarterial fibers that are presumably sensory (yellow and green arrows). H_3R-LI was expressed on a subset of this innervation (yellow arrows). (J–L) H_3R-LI was expressed on periarterial fibers that co-labeled with anti-NF. Previous studies showed that the NF-positive fibers are a subset of those that label with anti-CGRP. (M–O) H_3R-LI was only expressed on fibers (red arrows) that were distinct from those that label with anti-NPY (green arrowheads). (P–R) H_3R-positive fibers also labeled with anti-ASIC3 (yellow arrows).

NF-LI was also present. Unfortunately, the H_3R-LI was not sufficiently intense for capture by confocal microscopy at a resolution that was any better than that achieved by epifluorescence, especially since the sections were only 14 μM thick. In a study of vascular innervation in muscle (Molliver et al., 2005), the Aδ vascular fibers were also found to label with antibodies against the acid sensing ion channel 3 (ASIC3). Likewise, we found that the H_3R-positive periarterial fibers also colabeled with anti-ASIC3 in the skin (Fig. 4P–R).

Our double label assessments with anti-PGP revealed very little H_3R-LI among the dense plexus of fibers that ramify at the tunica media and adventitia border. H_3R-LI was especially absent in this location in the rat (Fig. 3A–C), but barely detectable H_3R-LI was present on some fibers in this location in wild type mice (Fig. 3D–F). Double labeling assessments with anti-NPY revealed no co-labeling with H_3R-LI (Fig. 4M–O), thereby supporting the observations indicating that the detectable anti-H_3R labeling was restricted to the Aδ sensory innervation. H_3R-LI was also absent among the sweat glands of the glabrous skin that are the site of dense cholinergic sympathetic terminations (data not shown).

3.3. Anti-H_3R labeling in DRG cell bodies

Our immunochemical localization of H_3Rs on some cutaneous innervation was consistent with previously detected moderate levels of H_3R mRNA in DRGs (Heron et al., 2001). However, as noted above, our assessments of cutaneous innervation indicated that H_3R-LI was definitively detectable only on Aβ fibers that terminated as lanceolate endings and Meissner's corpuscles, and on CGRP/SP-positive Aδ fibers that innervate arteries and arterioles. Therefore, our next objective was to assess the size and immunochemical characteristics of neurons in rat lumbar DRGs. Consistent with a general relationship between DRG neuronal diameter and fiber caliber (McCarthy and Lawson, 1990), virtually all neurons less than 25 μm in diameter were NF-negative, about 20–30% of neurons from 25 to 35 μm were NF-positive, and virtually all larger neurons were NF-positive (Fig. 6A). Although there are known to be exceptions to this correlation, smaller neurons are typically the source of C fibers and larger neurons the source of Aβ fibers (McCarthy and Lawson, 1990). Aδ fibers presumably arise mostly from medium sized neurons.

Depending upon whether anti-H_3R treated DRG sections were double labeled with anti-NF or anti-CGRP, a considerable discrepancy was evident between the percentage of total neurons that were initially judged as H_3R-positive: i.e. 33% in section double labeled with anti-NF vs. 55% with anti-CGRP. Presumably the percentage of H_3R-LI neurons should be the same in both types of preparations. An assessment of the overall distribution of all labeled and unlabeled cells revealed that the discrepancy was among the cells less than 25 μm in diameter, where a much greater total number of cells regarded as unlabeled were detected in anti-H_3R/anti-NF treated sections than in anti-H_3R/CGRP treated sections. Thus, unlabeled cells were over-represented in the former and/or under represented in the latter. This may have been due to the potential additive effect of background levels of cross labeling among the primary and secondary antibodies raised in the same species. Based on prior assessments of the proportion of CGRP-positive and negative small cells and of NF-positive and negative small cells in DRGs (e.g. Zylka et al., 2005), it was evident that the discrepancy in small cell counts was primarily due to a lack of overall unlabeled small cell detection in our anti-CGRP labeled specimens. Therefore the graphs in Fig. 6B were normalized to the small cell counts in Fig. 6A. Independent of the small cell discrepancy, it must be emphasized that H_3R-LI in the DRG was detected primarily on medium to large cells equal to or greater than 25 μm in diameter. Among cells of this size, 33–55% are H_3R positive.

In DRG sections taken from H_3KO mice, H_3R-LI was virtually eliminated on the small and medium size neurons, but some weak residual labeling persisted on large neurons (Fig. 5B). Consistent with our peripheral innervation double labeling results, about two-thirds of the neurons with H_3R-LI also coexpressed anti-CGRP labeling (Figs. 5C, D and 6B, C), and nearly all H_3R-LI cells (97%) co-labeled with anti-NF (Fig. 5G, H and 6D, E). In comparison to CGRP/H_3R co-localization, about half as many small, medium and large H_3R-positive neurons also coexpressed SP-LI (Fig. 5E and F). This is consistent with previous observations that SP is present in about half of the neurons that contain CGRP (Ju et al., 1987; Lawson, 1995), although SP has previously been shown to have nearly complete co-localization with CGRP in cutaneous fibers (Fundin et al., 1997a,b; Rice et al., 1997). At least some of the medium-sized neurons that are positive for CGRP, SP, NF, and H_3R (approximately 25–35 μm) may be the source of the vascular Aδ fibers that express the same immunolabeling characteristics. Likewise, the larger-sized neurons (greater than 35 μm) with H_3R-LI may be the source of the H_3R-positive Aβ fibers seen in the skin that supply lanceolate or Meissner endings (Fig. 2D–F). Interestingly, many if not most of the large neurons with H_3R-LI also expressed CGRP and SP-LI. This is consistent with previous observations of low levels of CGRP and SP-LI in lanceolate and Meissner endings, even though the peptide immunoreactivity was usually below detectable levels in their Aβ source axons (Fundin et al., 1997a; Rice et al., 1997; Paré et al., 2001).

A bimodal distribution was observed among H_3R-negative/NF-positive, medium- and large-sized neurons

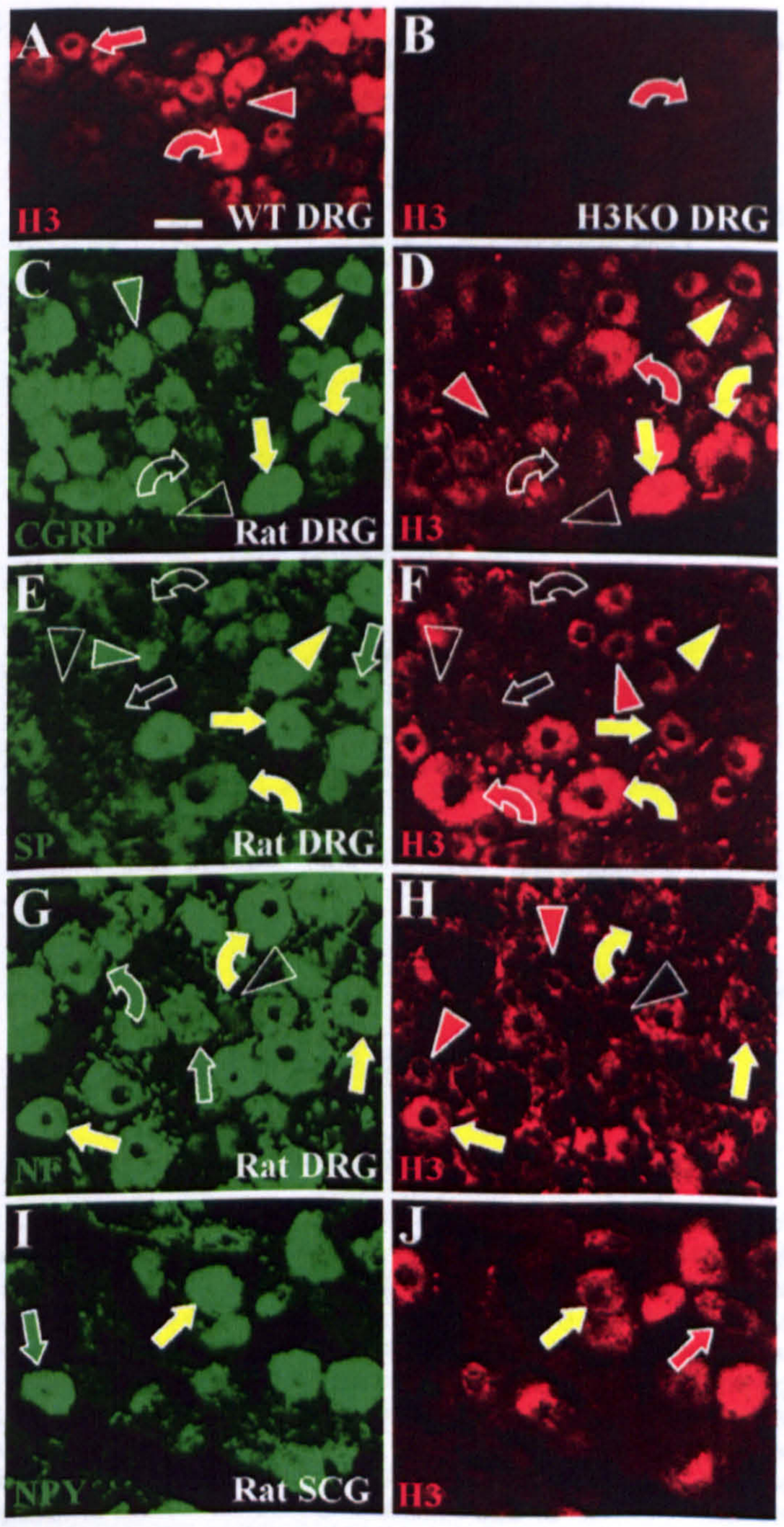

Fig. 5. Immunochemical characterization of H_3R expressing neurons in lumbar dorsal root ganglia (DRG) and superior cervical ganglia (SCG). Sections of ganglia were all labeled with anti-H_3R (red) and some sections were double labeled with other antibodies (green). Small size neurons are indicated by arrowheads, medium size neurons by straight arrows and large size neurons by curved arrows. Red indicators show neurons only labeled with anti-H_3R, green indicators only neurons labeled with other antibodies, and yellow indicators neurons that are double labeled. Empty indicators show neurons that were regarded as having only background fluorescence. Scale bar = 25 μm. (A and B) Images from mouse DRG sections. Anti-H_3R labeled many of the small (red arrowhead), medium (red arrow), and large (red curved arrow) DRG neurons from a wild type mouse (A). Anti-H_3R is virtually eliminated in DRG neurons from a H_3KO mouse (B) except for very low residual leveling on some relatively large neurons (red curved arrow). (C–H) Images from rat lumbar DRG sections. (C and D) Small neurons double labeled with anti-CGRP and anti-H_3R (yellow arrowheads), only labeled with anti-CGRP (green arrowhead), or only labeled with anti-H_3R (red arrowhead). Some small neurons were not labeled with either antibody (unfilled arrowheads). Most medium size neurons expressed both CGRP-IR and H_3R-IR (yellow straight arrows). Large neurons were typically immunolabeled for both CGRP and H_3R (yellow curved arrows) or were negative for both (unfilled curved arrows). (E and F) Overall, fewer neurons label with anti-SP than with anti-CGRP. Some small neurons were double labeled with anti-SP and anti-H_3R (yellow arrowheads), only labeled with anti-SP (green arrowhead), or only labeled with anti-H_3R (red arrowhead). Some small neurons were not labeled with either antibody (unfilled arrowheads). Most medium size neurons were immunolabeled for both SP and H_3R (yellow arrows) or negative for both (unfilled arrow). The green straight arrow indicates a relatively rare medium size neuron that only expressed SP-IR. Some large neurons were double labeled with anti-SP and anti-H_3R (yellow curved arrows), some were labeled only with anti-H_3R (red curved arrow), and others were not labeled with either antibody (unfilled curved arrows). (G and H) Virtually all small neurons were NF-negative, whereas virtually all medium and large neurons were NF-positive. Small neurons were H_3R-positive (red arrowheads) or negative (unfilled arrowheads). Medium and large neurons were H_3R-positive (yellow straight arrows and curved arrows) or H_3R -negative (green straight arrows and curved arrows). (I and J) Double labeling of rat superior cervical ganglia revealed neurons that coexpressed anti-NPY-IR and anti-H_3-IR (yellow arrows) or that are positive only for NPY (green arrow) or H_3R (red arrow).

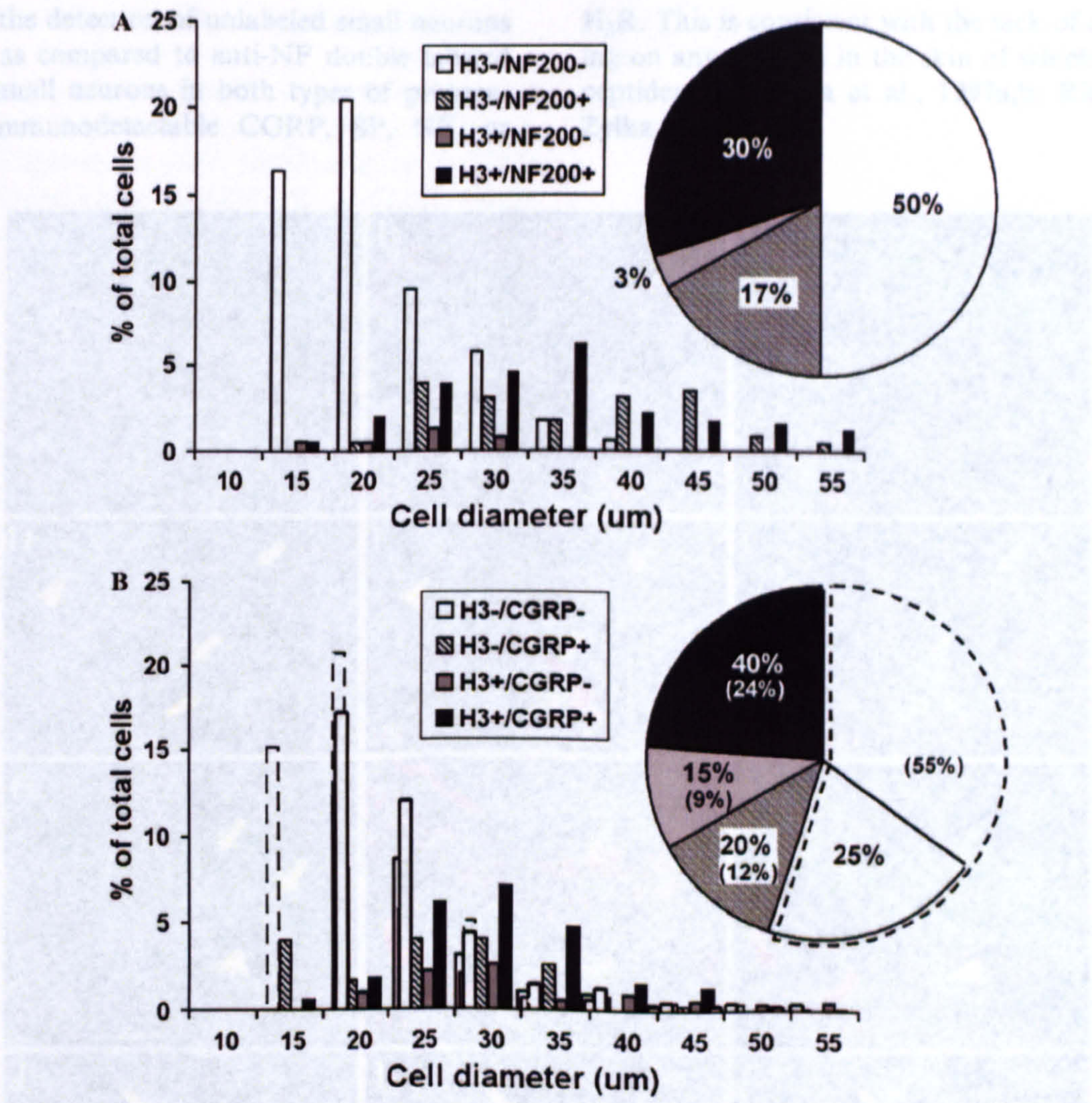

Fig. 6. Quantification of anti-H_3R labeling in rat dorsal root ganglia. Distribution of cell sizes and labeling characteristics in rat lumbar DRG neurons as assessed in sections double labeled with anti-H_3R and anti-NF (A) or with anti-H_3R and anti-CGRP (B). Data were normalized from measurements of 758 cells in three L4 and L5 rat DRGs and the proportions were corrected for cell size. (A) After double labeling with anti-H_3R and anti-NF, 33% of all presumptive neurons had H_3R-LI. Most of these H_3R-LI neurons were NF-positive (30% vs. 3%) and had medium to large diameters. 17% of all detected neurons were NF-positive and H_3R-negative and had a bimodal distribution among medium and large cells. 50% of presumptive neurons were negative for both H_3R-LI and NF-LI, and most had relatively small diameters. (B) After double labeling with anti-H_3R and anti-CGRP, the actual detected proportions of H_3R-positive and negative neurons are shown in the solid line enclosed bars and pie chart sectors. The actual percentages of double-labeled, single-labeled, and unlabeled neurons are shown by the numbers without brackets in the pie chart sectors. The proportion of anti-H_3R labeled neurons in (B) was much higher (55%) than in (A) (33%), but presumably should be the same. This was most likely due to a failure to detect many unlabeled cells in the anti-H_3R and anti-CGRP labeled sections (see Sections **2 and 3**). To correct for this likely lack of detection, the total % of H_3R-LI neurons observed in the anti-H_3R and anti-CGRP (B) was normalized to 33% by adjusting the proportion of H_3R-negative/CGRP-negative cells to reflect the level of H_3R-negative neurons observed in the anti-H_3R and anti-NF labeled sections (A). The adjusted increase is indicated by broken line bars and pie sectors, and the adjusted percentages are the numbers shown in brackets in (B). With or without this adjustment, neurons with H_3R-LI had predominantly medium to large diameters, with a 3:1 ratio of CGRP-positive to CGRP-negative neurons (24% vs 9% in adjusted percentages). Based on adjusted percentages, 12% of the neurons were H_3R-negative and CGRP-positive and had a bimodal distribution among small and medium diameters. Even without an adjustment, the neurons that lacked both H_3R-LI and CGRP-LI were skewed towards smaller diameters (white bars and white pie sector within solid lines).

(**Fig. 6**A). The larger of these neurons may give rise to Aβ fibers that innervate Merkel endings. As noted above, the Merkel cells in the epidermis of the glabrous skin and outer root sheath of whisker follicles expressed H_3R-LI, but this labeling was not definitively evident on the Aβ fibers that form endings on the Merkel cells. The more medium-sized H_3R-negative/NF-positive neurons may be the source of Aδ fibers that have been shown to innervate the epidermis, upper dermis and hair follicles where no anti-H_3R labeling was detected among thin-caliber fibers (**Fundin et al., 1997a; Rice et al., 1997; Fünfschilling et al., 2004**). Likewise, about one-third of the small- to medium-sized anti-CGRP labeled neurons lacked H_3R-LI (**Fig. 6B**). These cells may be sources of peptidergic C fibers (some of which terminate on arteries) and non-arterial peptidergic Aδ fibers that also lacked immunodetectable H_3R in the skin (**Fundin et al., 1997a,b; Rice et al., 1997**). Regardless of some

discrepancy in the detection of unlabeled small neurons in anti-CGRP as compared to anti-NF double labeled section, most small neurons in both types of preparations lacked immunodetectable CGRP, SP, NF, or H_3R. This is consistent with the lack of anti-H_3R labeling on any C fibers in the skin of which most are non-peptidergic (**Fundin et al., 1997a,b; Rice et al., 1997; Zylka et al., 2005**).

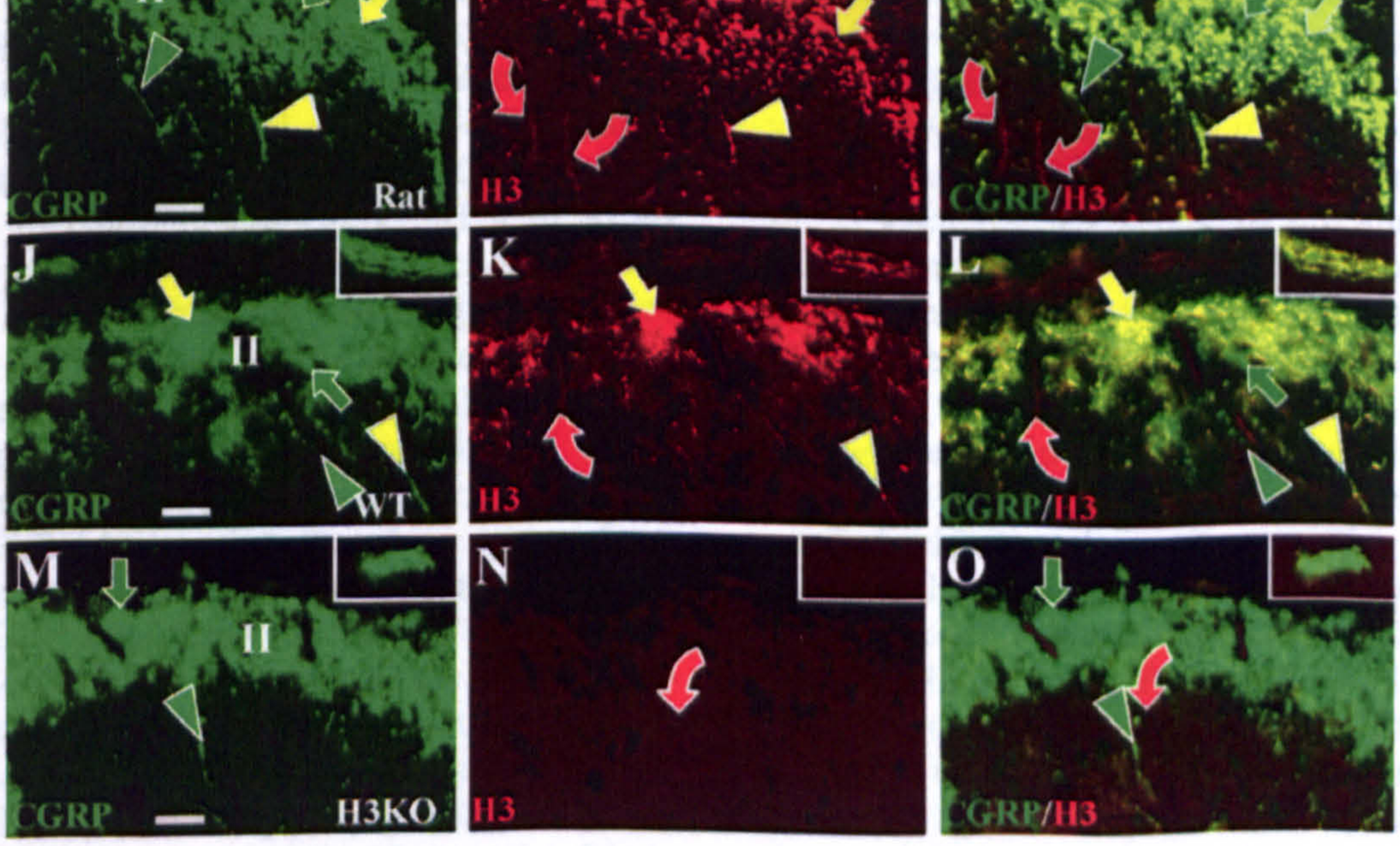

Fig. 7. Anti-H_3R labeling in the dorsal horn of rats, wild type mice, and H_3KO mice. Digital cross sectional images of lumbar spinal cords from rats (A–I), wild type mice (J–L), and H_3KO (M–O) mice. The sections are double labeled with anti-CGRP revealed by Cy2 or Alexa 488 conjugated secondary antibodies (left panels) and with the Chazot anti-H_3R revealed by Cy3 conjugated antibodies (middle panels). Merged images are shown in the right panels. Fibers definitively labeled with only anti-CGRP are denoted by green indicators; with only anti-H_3R by red indicators, and with both antibodies by yellow indicators. Scale bars, 25 μm. Anti-CGRP and anti-H_3R labeling is shown at low magnification in the rat dorsal horn (A–C). Areas in (A–C) that include lamina V (white broken line boxes) and laminae I–III (white solid line boxes) are shown at higher magnification in (D–F) and (G–I), respectively. Comparable high magnification images of the superficial dorsal horn are shown for WT (J–L) and H_3KO (M–O) mice. High magnification images from lamina V of mice are shown in insets in (J–O). As shown in (D–F) and in the insets in (J–L), most of the CGRP-positive fibers that ramify in lamina V coexpress H_3LI (yellow arrows), whereas few fibers only express CGRP-LI (green arrowheads). As shown in the inset in E, some dorsal horn neurons deep to lamina II have faint levels of H_3R-LI detectable primarily over the cell body. As shown in (G–L), anti-CGRP labeled fibers ramify extensively in superficial lamina and include fibers that express H_3R-LI (yellow arrows) and those that lack H_3R-LI (green arrows). Some individual CGRP-positive fibers express H_3R-LI (yellow arrowheads) and others lack H_3R-LI (green arrowheads). Some thick-caliber Aβ fibers passing through the superficial laminae have low levels of H_3R-LI (red curved arrows). As seen in (M–O), H_3R-LI is absent on the CGRP-positive innervation in H_3KO mice (green arrows and arrowheads), but very faint residual labeling persists on some Aβ fibers (red curved arrows).

3.4. Anti-H_3R labeling in superior cervical ganglia

Although many previous functional studies suggested that the H_3R may be located on sympathetic innervation (Ishikawa and Sperelakis, 1987; Molderings et al., 1992; Koss, 1994; Godlewski et al., 1997a,b), we rarely detected H_3R-LI on any NPY-positive fibers or on fibers in sites where sympathetic fibers are known to terminate on arteries. Therefore, we assessed anti-H_3R labeling in superior cervical ganglia of rats in double label combination with an antibody against NPY which is widely expressed among adrenergic sympathetic neurons. These results revealed a heterogeneous mix with some neurons coexpressing NPY-LI and H_3R-LI and others expressing only NPY-LI or H_3R-LI (Fig. 5I and J).

3.5. Anti-H_3R labeling in dorsal horn

Consistent with the characteristics of H_3R-positive cutaneous fibers, our immunofluorescence assessments of rat and wild type mouse spinal cords revealed H_3R-LI on several thick and thin-caliber axons entering the superficial dorsal horn via dorsal roots (Fig. 7A–L). The thick-caliber, H_3R-LI axons passed through laminae I and II and penetrated at least as far as lamina III in both species (Fig. 7G–I and J–L). Although a few cases were found in which thick-caliber, H_3R-LI axons were also faintly labeled with anti-CGRP, most of the thick-caliber, H_3R-LI axons were CGRP-negative (Fig. 2G–L). In contrast, thin-caliber, H_3R-LI axons consistently co-expressed anti-CGRP labeling (Fig. 7D–L). Many of these thin-caliber fibers ramified extensively in lamina II, and some extended to and ramified in lamina V (Fig. 7D–F and J–L). These observations suggest that the thin-caliber, H_3R-LI fibers synapse on neurons in both locations. Interestingly, CGRP and H_3R-LI was coexpressed on most of the fibers ramifying in lamina V, whereas lamina II also had many CGRP fiber ramifications that lacked H_3R-LI. In general, CGRP-positive fibers that lacked H_3R-LI were thinner than those that expressed H_3R-LI. Superficial (i.e. laminae I–III) dorsal horn neurons appeared to lack H_3R-LI. Sparsely scattered neurons in the deep dorsal horn and ventral horn were faintly labeled with anti H_3R (inset, Fig. 7E) and lacked CGRP-IR making it unlikely that they were the source of any H_3R/CGRP-positive fibers in the dorsal horn. Moreover, the sparsely scattered locations of these neurons did not correlate with the concentrated sites of H_3R-LI fibers in the dorsal horn. In spinal sections from H_3KO mice, H_3R-LI was completely absent on thin-caliber axons in the superficial and deep dorsal horn (Fig. 7M–O). Although the labeling intensity was drastically reduced, faint detectable H_3R-LI was observed in H_3KO mice on thick-caliber afferents found in the lumbar dorsal roots as well as thick-caliber fibers that passed through laminae I-II and entered into laminae III–V (Fig. 7M–O).

4. Discussion

Functional studies have suggested that H_3Rs exist on sensory peptidergic C-fibers and on sympathetic efferents, but no previous immunochemical experiments have been reported. The present work has not confirmed these suggestions. Results with various combinations of double labeling found that H_3R-LI was detectable only on (1) peptidergic presumptive Aδ fibers that innervate cutaneous arteries and on (2) Aβ fibers that terminate in Meissner corpuscles in glabrous skin and as lanceolate endings in hairy skin. H_3R-LI was also present on epidermal keratinocytes, which contain H_3R mRNA (Heron et al., 2001), as well as on Merkel cells in lamina basalis of the epidermis and the outer root sheath of whisker follicles. All of these H_3R-positive structures contain CGRP-LI. Low levels of this labeling in keratinocytes were seen previously but disregarded as nonspecific (Rice et al., 1997; Rice and Rasmusson, 2000; Paré et al., 2001; Khodorova et al., 2003; Fünfschilling et al., 2004). H_3R-LI was not definitively evident on (1) peptidergic C fibers, non-peptidergic C fibers, or Aδ fibers that innervate the epidermis or hair follicles; (2) peptidergic C fibers or any sympathetic fibers that innervate vasculature; or (3) Aβ-fibers that innervate Merkel cells. Our use of two antibodies from the same species, and the absence of confocal microscopy for double-labeling leave open the possibility that false positive colocalizations were observed. However, the use of two different H_3R antibodies, and the extensive control procedures employed minimize this possibility.

The present findings strongly support the hypothesis that the H_3R-LI labels the H_3R. All present results were verified with two different antibodies targeted against different domains of the H_3R. Both antibodies labeled CNS regions known to express this receptor (e.g. striatum, cerebral cortex, Pollard et al., 1993). All of the H_3R-LI was eliminated or severely attenuated in H_3R knockout skin, DRGs and CNS. We previously showed that the H_3KO mice used presently lack H_3R radioligand binding, and lack responses to H_3R agonists (Cannon et al., 2003). Although H_3R isoforms may exist (Tardivel-Lacombe et al., 2000; Coge et al., 2001; Drutel et al., 2001; Wellendorph et al., 2002; Rouleau et al., 2004), the H_3KO gene construct eliminated the coding for both antigenic epitopes used presently.

In situ hybridization studies found moderate levels of H_3R mRNA in rat DRGs (Heron et al., 2001), but the characteristics of the positive neurons were not elucidated. Although our methods cannot determine which DRG neurons are the source of particular sensory fibers and endings, the size and immunochemical characteristics of the H_3R-positive neurons are consistent with

the caliber and immunochemical characteristics of the H_3R-positive cutaneous innervation. These neurons were primarily medium to large DRG cells that coexpressed NF and CGRP-LI, consistent with our observation that H_3R-LI was expressed on particular types of peptidergic Aδ and Aβ fibers. In contrast, the large neurons that lacked H_3R-LI as well as CGRP-LI are consistent with the characteristics of Aβ fibers that are the source of Merkel endings. Many of the medium size neurons with and without CGRP-LI were also NF-positive, but lacked H_3R-LI. This is consistent with the presence of peptidergic and nonpeptidergic Aδ fibers in the upper dermis that innervate hair follicles and the epidermis (Fundin et al., 1997a; Rice et al., 1997; Fünfschilling et al., 2004). Importantly, most of the small DRG neurons lacked H_3R-LI. These include CGRP-positive and negative neurons that are the source of peptidergic and nonpeptidergic C fibers. Cumulatively, our data indicate that, at least for cutaneous innervation, H_3R functions previously attributed to sensory peptidergic C fibers are most likely to be mediated through peptidergic periarterial Aδ-fiber endings and perhaps Aβ-fiber lanceolate and Meissner endings.

Although functional studies suggest that H_3Rs exist on sympathetic innervation, H_3R-LI was not detected on cutaneous sympathetic NPY-expressing fibers in the rat, and only a few double labeled fibers were seen in the mouse. Some NPY-positive/H_3R-negative neurons were observed in the SCG which could be a source for the sympathetic cutaneous arterial innervation. However, most of the SCG neurons co-expressed H_3R-LI and NPY-LI, implying an H_3R localization on sympathetic neurons. Apparent mismatches between ganglion cell and axon immunochemistry have been noted previously (Fundin et al., 1997a; Rice et al., 1997). The lack of detectable H_3R-LI on the arterial sympathetic fibers may be due to a diffuse distribution among their extensive terminal arborizations. Alternatively, the SCG may contain H_3R-positive sympathetic neurons that innervate structures other than the skin.

4.1. Functional roles for the H_3R

H_3R agonists are known to inhibit neuropeptide release from presumed sensory fibers in the heart, lung, and skin. Consistent with this, H_3R agonists have some anti-inflammatory and antinociceptive properties (Rouleau et al., 1997, 2000; Cannon et al., 2003, Cannon and Hough, 2005). The present results show that periarterial Aδ fibers possess the H_3R and are likely to be a site of H_3 agonist action. However, some Aβ fibers, as well as keratinocytes, also have both H_3R-LI and CGRP immunoreactivity, and therefore may also have functional significance.

H_3R antagonists have been reported to produce pruritus-like effects in mice, possibly mediated by C fibers (Schmelz et al., 1997; Hossen et al., 2003; Sugimoto et al., 2004). Because H_3R-LI is present on keratinocytes but not on epidermal endings, the former may participate in these effects of H_3R antagonists (also see Fitzsimons et al., 2001). Recently, keratinocytes have been shown to be critical mediators following the activation of endothelin B (Khodorova et al., 2003) and cannabinoid CB_2 receptors (Ibrahim et al., 2005).

Although the lanceolate and Meissner endings that are supplied by H_3R positive Aβ-fibers are thought to be rapidly adapting low threshold mechanoreceptors, the Meissner endings express a wide range of immunochemical properties associated with nociception (Paré et al., 2001). Both types of endings are also intimately affiliated with several types of C fibers (Fundin et al., 1997a; Paré et al., 2001). The functional importance of these chemical characteristics and potential interactions with the affiliated C fibers in the skin has not been investigated. However, modulation of Aβ fiber activity is known to affect pain sensations that have typically been attributed to C fiber and/or Aδ fiber activity. Peripheral, as well as central, mechanisms could account for these observations.

We recently reported that pharmacological activation of spinal H_3Rs inhibits mechanical nociceptive responses to tail pinch in wild type, but not, H_3KO mice (Cannon et al., 2003). This effect is both modality- and intensity-specific (Cannon et al., 2003; Cannon and Hough, 2005). For example, noxious thermal responses are unaffected. The intensity of the mechanical stimulus needed to elicit these responses suggests that the relevant fibers are high threshold mechanoreceptors (HTM) (Burgess and Perl, 1967; Beck et al., 1974; Szolcsanyi et al., 1988; Yeomans and Proudfit, 1996; Ringkamp et al., 2001). Consistent with the spinal H_3R inhibition of mechanical nociception, we detected H_3R-LI on small-caliber CGRP-positive fibers ramifying in the superficial laminae of the dorsal horn, as well as in lamina V, which are known sites of HTM termination (Light and Perl, 1979). We hypothesize that these HTMs are the periarterial Aδ fibers. Consistent with this, Aδ HTMs in the deep dermis of guinea pigs were shown to be CGRP-immunoreactive (Lawson et al., 2002). We also found that these periarterial Aδ fibers coexpressed immunoreactivity for ASIC3, a channel which has been implicated in mechanical nociceptive transmission (Price et al., 2001). Conceivably, the high intensity mechanical stimulus needed to activate HTMs and the lack of thermal responsiveness may not be an inherent property of the fiber, but may be due to their relatively deep disposition in the skin. The close proximity of these fibers to blood vessels and their probable mechanosensitivity suggest the possibility that vasodilation could provide local mechanical forces to activate these fibers.

The H_3R-mediated inhibition of neuropeptide release in skin may be an important mechanism to control the extent of inflammation that occurs during or following

injury. CGRP and SP, released during tissue damage, produce vasodilation and plasma extravasation (Lembeck and Holzer, 1979; Brain and Williams, 1989; Saria, 1984; Brain et al., 1992), which, in turn, allow the infiltration of additional inflammatory mediators (Bar-Shavit et al., 1980; Payan et al., 1984; Helme and Andrews, 1985; Hartung et al., 1986; Saito et al., 1986). Peptide release also activates mast cells to release histamine (Johnson and Erdos, 1973; Owen et al., 1980; Owen and Woodward, 1980). Subsequent activation of H_1 receptors on nociceptive fibers results in sensitization and increased pain (Owen and Woodward, 1980; Owen et al., 1980; Mobarakeh et al., 2000), but activation of H_3Rs can inhibit further peptide release from such endings as the periarterial Aδ fibers, thereby limiting subsequent inflammatory events (Dimitriadou et al., 1994; Ohkubo et al., 1995; Delaunois et al., 1995; Imamura et al., 1996; Dimitriadou et al., 1997; Nemmar et al., 1999). Consistent with this, several studies have demonstrated that systemic administration of the H_3R agonist immepip significantly attenuates formalin-induced paw swelling (Imamura et al., 1996; Cannon et al., unpublished). Thus, the injury-induced release of histamine may play a pro-nociceptive, pro-inflammatory role through H_1 receptors, and/or an anti-inflammatory, antinociceptive role via H_3Rs (Imamura et al., 1996).

Acknowledgements

This work was supported by grants from the National Institute on Drug Abuse (DA-03816, DA-015915, and DA-07307) and the Wellcome Trust (UK). We thank Dr. I. Silos-Santiago formerly of Millennium Pharmaceuticals, Inc. (Cambridge, MA) for providing H_3KO mice.

References

Abercrombie M. Estimation of nuclear population from microtome sections. Anat Rec 1946;94:239–47.

Arrang JM, Garbarg M, Schwart JC. Auto-inhibition of brain histamine release mediated by a novel class (H_3) of histamine receptors. Nature 1983;302:832–7.

Arrang JM, Garbarg M, Lancelot J, Lecomte JM, Pollard H, Robba M, Schunack W, Schwart JC. Highly potent and selective ligands for histamine H_3-receptors. Nature 1987;327:117–23.

Bar-Shavit Z, Goldman R, Stabinsky Y, Gottlieb P, Fridkin M, Teichberg VI, Blumberg S. Enhancement of phagocytosis – a newly found activity of Substance P residing in its N-terminal tetrapeptide. Biochem Biophys Res Commun 1980;94:1445–51.

Beck PW, Handwerker HO, Zimmermann M. Nervous outflow from the cat's foot during noxious radiant heat stimulation. Brain Res 1974;67:373–86.

Brain SD, Williams TJ. Interactions between tachykinins and calcitonin gene-related peptide lead to the modulation of oedema formation and blood flow in rat skin. Br J Pharmacol 1989;97:77–82.

Brain SD, Cambridge H, Hughes SR, Wilsoncroft P. Evidence that calcitonin gene-related peptide contributes to inflammation in skin and joint. Ann NY Acad Sci 1992;657:412–9.

Burgess PR, Perl ER. Myelinated afferent fibres responding specifically to noxious stimulation of the skin. J Physiol 1967;190:541–62.

Cannon KE, Hough LB. Inhibition of chemical and low-intensity mechanical nociception by activation of histamine H_3 receptors. J Pain 2005;6:193–200.

Cannon KE, Nalwalk JW, Stadel R, Ge P, Lawson D, Silos-Santiago I, Hough LB. Activation of spinal histamine H_3 receptors inhibits mechanical nociception. Eur J Pharmacol 2003;470:139–47.

Chazot PL, Hann V, Wilson C, Lees G, Thompson CL. Immunological identification of the mammalian H_3 histamine receptor in the mouse brain. Neuroreport 2001;12:259–62.

Chen J, Liu C, Lovenberg TW. Molecular and pharmacological characterization of the mouse histamine H(3) receptor. Eur J Pharmacol 2003;467:57–65.

Coge F, Guenin SP, Audinot V, Renouard-Try A, Beauverger P, Macia C, Ouvry C, Nagel N, Rique H, Boutin JA, Galizzi JP. Genomic organization and characterization of splice variants of the human histamine H_3 receptor. Biochem J 2001;355:279–88.

Delaunois A, Gustin P, Garbarg M, Ansay M. Modulation of acetylcholine, capsaicin and substance P effects by histamine H3 receptors in isolated perfused rabbit lungs. Eur J Pharmacol 1995;277:243–50.

Dimitriadou V, Rouleau A, Dam Trung TM, Newlands GJ, Miller HR, Luffau G, Schwartz JC, Garbarg M. Functional relationship between mast cells and C-sensitive nerve fibres evidenced by histamine H3-receptor modulation in rat lung and spleen. Clin Sci (Lond) 1994;87:151–63.

Dimitriadou V, Rouleau A, Trung T, Newlands GJ, Miller HR, Luffau G, Schwartz JC, Garbarg M. Functional relationships between sensory nerve fibers and mast cells of dura mater in normal and inflammatory conditions. Neuroscience 1997;77:829–39.

Drutel G, Peitsaro N, Karlstedt K, Wieland K, Smit MJ, Timmerman H, Panula P, Leurs R. Identification of rat H_3 receptor isoforms with different brain expression and signaling properties. Mol Pharmacol 2001;59:1–8.

Fitzsimons C, Engel N, Duran H, Policastro L, Cricco G, Martin G, Molinari B, Rivera E. Histamine production in mouse epidermal keratinocytes is regulated during cellular differentiation. Inflamm Res 2001;50:S100–1.

Fundin BT, Arvidsson J, Aldskogius H, Johansson O, Rice SN, Rice FL. Comprehensive immunofluorescence and lectin binding analysis of intervibrissal fur innervation in the mystacial pad of the rat. J Comp Neurol 1997a;385:185–206.

Fundin BT, Pfaller K, Rice FL. Different distribution of the sensory and autonomic innervation among the microvasculature of the rat mystacial pad. J Comp Neurol 1997b;389:545–68.

Fünfschilling U, Ng Y-G, Zang K, Miyazaki JK, Reichardt LF, Rice FL. TrkC kinase expression in distinct subsets of cutaneous trigeminal innervation and non-neuronal cells. J Comp Neurol 2004;480:392–414.

Godlewski G, Malinowska B, Buczko W, Schlicker E. Inhibitory H3 receptors on sympathetic nerves of the pithed rat: activation by endogenous histamine and operation in spontaneously hypertensive rats. Naunyn Schmiedebergs Arch Pharmacol 1997a;355:261–6.

Godlewski G, Malinowska B, Schlicker E, Bucher B. Identification of histamine H3 receptors in the tail artery from normotensive and spontaneously hypertensive rats. J Cardiovasc Pharmacol 1997b;29:801–7.

Hartung H-P, Wolters K, Tokya KV. Substance P binding properties and studies on cellular responses in guinea-pig macrophages. J Immunol 1986;136:3856–63.

Helme RD, Andrews PV. The effect of nerve lesions on the inflammatory response to injury. J Neurosci Res 1985;13:453–9.

Heron A, Rouleau A, Cochois V, Pillot C, Schwartz JC, Arrang JM. Expression analysis of the histamine H(3) receptor in developing rat tissues. Mech Dev 2001;105:167–73.

Hossen MA, Sugimoto Y, Kayasuga R, Kamei C. Involvement of histamine H3 receptors in scratching behaviour in mast cell-deficient mice. Br J Dermatol 2003;149:17–22.

Hough LB. Genomics meets histamine receptors: new subtypes, new receptors. Mol Pharmacol 2001;59:1–5.

Hough LB, Leurs R. Histamine. In: Siegel G, Agranoff B, Albers R, Fisher S, Uhler M, editors. Basic neurochemistry. 7nd ed. Lippincott: Williams and Wilkins; 2006. p. 249–66.

Ibrahim MM, Porreca F, Lai J, Albrecht PJ, Rice FL, Khodorova A, Davar G, Makriyannis A, Vanderah TW, Mata HP, Malan Jr TP. CB_2 cannabinoid receptor activation produces antinociception by stimulating peripheral release of endogenous opioids. Proc Natl Acad Sci USA 2005;102:3093–8.

Imamura M, Smith NC, Garbarg M, Levi R. Histamine H_3-receptor-mediated inhibition of calcitonin gene-related peptide release from cardiac C fibers. A regulatory negative-feedback loop. Circ Res 1996;78:863–9.

Ishikawa S, Sperelakis N. A novel class (H3) of histamine receptors on perivascular nerve terminals. Nature 1987;327:158–60.

Johnson AR, Erdos EG. Release of histamine from mast cells by vasoactive peptides. Proc Soc Exp Biol Med 1973;142:1252–6.

Ju G, Hokfelt T, Brodin E, Fahrenkrug J, Fischer JA, Frey P, Elde RP, Brown JC. Primary sensory neurons of the rat showing calcitonin gene-related peptide immunoreactivity and their relation to substance P-, somatostatin-, galanin-, vasoactive intestinal polypeptide- and cholecystokinin-immunoreactive ganglion cells. Cell Tissue Res 1987;247:417–31.

Karlstedt K, Ahman MJ, Anichtchik OV, Soinila S, Panula P. Expression of the H_3 receptor in the developing CNS and brown fat suggests novel roles for histamine. Mol Cell Neurosci 2003;24:614–22.

Khodorova A, Navarro B, Jouaville LS, Murphy JE, Rice FL, Mazurkiewicz JE, Long-Woodward D, Stoffel M, Strichartz GR, Yukhananov R, Davar G. Endothelin-B receptor activation triggers an endogenous analgesic cascade at sites of peripheral injury. Nat Med 2003;9:1055–61.

Koss MC. Histamine H_3 receptor activation inhibits sympathetic-cholinergic responses in cats. Eur J Pharmacol 1994;257:109–15.

Lawson SN. Neuropeptides in morphologically and functionally identified primary afferent neurons in dorsal root ganglia: substance P, CGRP and somatostatin. Prog Brain Res 1995;104:161–73.

Lawson SN, Crepps B, Perl ER. Calcitonin gene-related peptide immunoreactivity and afferent receptive properties of dorsal root ganglion neurones in guinea-pigs. J Physiol 2002;540:989–1002.

Lembeck F, Holzer P. Substance P as neurogenic mediator of antidromic vasodilation and neurogenic plasma extravasation. Naunyn Schmiedebergs Arch Pharmacol 1979;352:201–5.

Light AR, Perl ER. Spinal termination of functionally identified primary afferent neurons with slowly conducting myelinated fibers. J Comp Neurol 1979;186:133–50.

Lovenberg TW, Roland BL, Wilson SJ, Jiang X, Pyati J, Huvar A, Jackson MR, Erlander MG. Cloning and functional expression of the human histamine H_3 receptor. Mol Pharmacol 1999;55:1101–7.

McCarthy PW, Lawson SN. Cell type and conduction velocity of rat primary sensory neurons with calcitonin gene-related peptide-like immunoreactivity. Neuroscience 1990;34:623–32.

Mobarakeh JI, Sakurada S, Katsuyama S, Kutsuwa M, Kuramasu A, Lin ZY, Watanabe T, Hashimoto Y, Yanai K. Role of histamine H(1) receptor in pain perception: a study of the receptor gene knockout mice. Eur J Pharmacol 2000;391:81–9.

Mobarakeh JI, Nalwalk JW, Watanabe T, Sakurada S, Hoffmann M, Leurs R, Timmerman H, Silos-Santiago I, Yanai K, Hough LB. Improgan antinociception does not require neuronal histamine or histamine receptors. Brain Res 2003;974:146–52.

Molderings GJ, Weissenborn G, Schlicker E, Likungu J, Gothert M. Inhibition of noradrenaline release from the sympathetic nerves of the human saphenous vein by presynaptic histamine H3 receptors. Naunyn Schmiedebergs Arch Pharmacol 1992;346:46–50.

Molliver DC, Immke DC, Fierro L, Paré M, Rice FL, McCleskey EW. ASIC3, an acid-sensing ion channel, is expressed in metaboreceptive sensory neurons. Mol Pain 2004;1:35.

Nemmar A, Delaunois A, Beckers JF, Sulon J, Bloden S, Gustin P. Modulatory effect of imetit, a histamine H3 receptor agonist, on C-fibers, cholinergic fibers and mast cells in rabbit lungs *in vitro*. Eur J Pharmacol 1999;371:23–30.

Ohkubo T, Shibata M, Inoue M, Kaya H, Takahashi H. Regulation of substance P release mediated via prejunctional histamine H_3 receptors. Eur J Pharmacol 1995;273:83–8.

Owen DA, Woodward DF. Histamine and histamine H_1- and H_2-receptor antagonists in acute inflammation. Biochem Soc Trans 1980;8:150–5.

Owen DA, Poy E, Woodward DF, Daniel D. Evaluation of the role of histamine H_1- and H_2- receptors in cutaneous inflammation in the guinea-pig produced by histamine and mast cell degranulation. Br J Pharmacol 1980;69:615–23.

Paré M, Elde R, Mazurkiewicz JE, Smith AM, Rice FL. The Meissner corpuscle revised: a multiafferented mechanoreceptor with nociceptor immunochemical properties. J Neurosci 2001;21:7236–46.

Paré M, Smith AM, Rice FL. Distribution and terminal arborizations of cutaneous mechanoreceptors in the glabrous finger pads of the monkey. J Comp Neurol 2002;445:347–59.

Payan DG, Levine JD, Goetzl EJ. Modulation of immunity and hypersensitivity by sensory neuropeptides. J Immunol 1984;132:1601–4.

Pillot C, Heron A, Cochois V, Tardivel-Lacombe J, Ligneau X, Schwartz JC, Arrang JM. A detailed mapping of the histamine H(3) receptor and its gene transcripts in rat brain. Neuroscience 2002;114:173–93.

Pollard H, Moreau J, Arrang JM, Schwartz JC. A detailed autoradiographic mapping of histamine H_3 receptors in rat brain areas. Neuroscience 1993;52:169–89.

Price MP, McIlwrath SL, Xie J, Cheng C, Qiao J, Tarr DE, Sluka KA, Brennan TJ, Lewin GR, Welsh MJ. The DRASIC cation channel contributes to the detection of cutaneous touch and acid stimuli in mice. Neuron 2001;32:1071–83.

Rice FL, Rasmusson DD. Innervation of the digit on the forepaw of the raccoon. J Comp Neurol 2000;417:467–90.

Rice FL, Fundin BT, Arvidsson J, Aldskogius H, Johansson O. Comprehensive immunofluorescence and lectin binding analysis of vibrissal follicle sinus complex innervation in the mystacial pad of the rat. J Comp Neurol 1997;385:149–84.

Rice FL, Albers KM, Davis BM, Silos-Santiago I, Wilkinson GA, LeMaster AM, Ernfors PJ, Smeyne RJ, Aldskogius H, Phillips HS, Barbacid M, DeChiara TM, Yancopoulos GD, Dunne CE, Fundin BT. Differential effects of various neurotrophin and trk receptor deletions on the unmyelinated innervation of the epidermis in the whisker pad of the mouse. Develop Biol 1998;198:57–81.

Ringkamp M, Peng YB, Wu G, Hartke TV, Campbell JN, Meyer RA. Capsaicin responses in heat-sensitive and heat-insensitive A-fiber nociceptors. J Neurosci 2001;21:4460–8.

Rouleau A, Garbarg M, Ligneau X, Mantion C, Lavie P, Advenier C, Lecomte JM, Krause M, Stark H, Schunack W, Schwartz JC. Bioavailability, antinociceptive and antiinflammatory properties of BP 2-94, a histamine H_3 receptor agonist prodrug. J Pharmacol Exp Ther 1997;281:1085–94.

Rouleau A, Stark H, Schunack W, Schwartz JC. Anti-inflammatory and antinociceptive properties of BP 2-94, a histamine H(3)-receptor agonist prodrug. J Pharmacol Exp Ther 2000;295:219–25.

Rouleau A, Heron A, Cochois V, Pillot C, Schwartz JC, Arrang JM. Cloning and expression of the mouse histamine H_3 receptor: evidence for multiple isoforms. J Neurochem 2004;90:1331–8.

Saito A, Kimura S, Goto K. Calcitonin gene-related peptide as potential neurotransmitter in guinea-pig right atrium. Am J Physiol 1986;250:H693–8.

Saria A. Substance P in sensory nerve fibers contributes to the development of oedema in the rat hindpaw after thermal injury. Br J Pharmacol 1984;323:341–2.

Schmelz M, Schmidt R, Bickel A, Handwerker HO, Torebjork HE. Specific C-receptors for itch in human skin. J Neurosci 1997;17:8003–8.

Shenton FC, Hann V, Chazot PL. Evidence for native and cloned H3 histamine receptor higher oligomers. Inflammation Res 2005;54(Suppl. 1):548–9.

Sugimoto Y, Iba Y, Nakamura Y, Kayasuga R, Kamei C. Pruritus-associated response mediated by cutaneous histamine H3 receptors. Clin Exp Allergy 2004;34:456–9.

Szolcsanyi J, Anton F, Reeh PW, Handwerker HO. Selective excitation by capsaicin of mechano-heat sensitive nociceptors in rat skin. Brain Res 1988;446:262–8.

Tardivel-Lacombe J, Rouleau A, Heron A, Morisset S, Pillot C, Cochois V, Schwartz JC, Arrang JM. Cloning and cerebral expression of the guinea pig histamine H3 receptor: evidence for two isoforms. Neuroreport 2000;11:755–9.

Wellendorph P, Goodman MW, Burstein ES, Nash NR, Brann MR, Weiner DM. Molecular cloning and pharmacology of functionally distinct isoforms of the human histamine H(3) receptor. Neuropharmacology 2002;42:929–40.

Yeomans DC, Proudfit HK. Nociceptive responses to high and low rates of noxious cutaneous heating are mediated by different nociceptors in the rat: electrophysiological evidence. Pain 1996;68:141–50.

Zylka MJ, Rice FL, Anderson DJ. Axonal tracers targeted to Mrgprd define a nociceptive circuit with exclusive peripheral projections to the epidermis. Neuron 2005;45:17–25.

0026-895X/06/7002-604–615$20.00
MOLECULAR PHARMACOLOGY
Copyright © 2006 The American Society for Pharmacology and Experimental Therapeutics
Mol Pharmacol 70:604–615, 2006

Vol. 70, No. 2
20818/3124822
Printed in U.S.A.

Oligomerization of Recombinant and Endogenously Expressed Human Histamine H_4 Receptors

Richard M. van Rijn, Paul L. Chazot, Fiona C. Shenton, Kamonchanok Sansuk, Remko A. Bakker,[1] and Rob Leurs

Leiden/Amsterdam Center for Drug Research, Department of Medicinal Chemistry, Vrije Universiteit Amsterdam, Amsterdam, The Netherlands (R.M.V.R., K.S., R.A.B., R.L.).; and School of Biological & Biomedical Sciences, Durham University, Durham, United Kingdom (F.C.S., P.L.C.)

Received November 15, 2005; accepted April 27, 2006

ABSTRACT

In this study, we report the homo- and hetero-oligomerization of the human histamine H_4R by both biochemical (Western blot and immobilized metal affinity chromatography) and biophysical [bioluminescence resonance energy transfer and time-resolved fluorescence resonance energy transfer (*tr*-FRET)] techniques. The H_4R receptor is the most recently discovered member of the histamine family of G-protein-coupled receptors. Using specific polyclonal antibodies raised against the C-terminal tail of the H_4R, we demonstrate the presence of H_4R oligomers in human embryonic kidney 293 and COS-7 cells heterologously overexpressing H_4Rs and putative native H_4R oligomers in human phytohaemagglutinin blasts endogenously expressing H_4Rs. Moreover, we show that H_4R homo-oligomers are formed constitutively, are formed at low receptor densities (300 fmol/mg of protein), and are present at the cell surface, as detected by *tr*-FRET. The formation of these oligomers is independent of *N*-glycosylation and is not modulated by H_4R ligands, covering the full spectrum of agonists, neutral antagonists, and inverse agonists. Although we show H_4R homo-oligomer formation at physiological expression levels, the detection of H_1R-H_4R hetero-oligomers was achieved only at higher H_1R expression levels and are most likely not physiologically relevant.

The human histamine H_4 receptor (hH_4R), a prototypical member of the superfamily of G-protein-coupled receptors (GPCRs), has been identified recently through the use of bioinformatics by several groups simultaneously (Oda et al., 2000; Liu et al., 2001; Morse et al., 2001; Nguyen et al., 2001; Zhu et al., 2001). The H_4R couples to members of the $G_{i/o}$ family of heterotrimeric G-proteins to mediate the inhibition of adenylyl cyclase. In addition, the receptor may activate phospholipase C and induce calcium mobilization (de Esch et al., 2005). The H_4R expression is almost exclusively restricted to hematopoietic cells and is suggested to mediate functions of the immune system. As such, the H_4R is a target for the development of anti-inflammatory drugs (Hofstra et al., 2003; Thurmond et al., 2004; de Esch et al., 2005).

The use of various biochemical and biophysical approaches has revealed recently that members of the GPCR family may exist as homo- and hetero-oligomers at the cell surface. When considering the heterotrimeric G protein, which is approximately twice the size of the GPCR (Lambright et al., 1996), it seems reasonable that GPCRs need to oligomerize to interact with the G protein, as suggested for the leukotriene B_4 receptor (Baneres and Parello, 2003). Hetero-oligomerization has been shown to be pivotal for the $GABA_BR1$, which needs to associate with $GABA_BR2$ receptors to be transported to the cell membrane (Jones et al., 1998), and for the T1R taste receptors, which require hetero-oligomerization to form receptors that can recognize sweets (Nelson et al., 2001) or amino acids (Nelson et al., 2002). In other cases, hetero-oligomerization may change the ligand binding characteristics, potentially giving rise to a new dimension in GPCR drug

Financial support was received from Nederlandse Organisatie voor Wetenschappelijk Onderzoek-Stichting Technische Wetenschappen (to R.L.) and Wellcome Trust and Parkinson's Disease Society (United Kingdom) (P.L.C. and F.C.S.).

R.M.v.R. and P.L.C. contributed equally to this work.

[1] Current affiliation: Department of Metabolic Diseases, Boehringer Ingelheim Pharma GmbH and Co. KG, Biberach, Germany.

Article, publication date, and citation information can be found at http://molpharm.aspetjournals.org.
doi:10.1124/mol.105.020818.

ABBREVIATIONS: hH_4R, human histamine H_4 receptor; GPCR, G-protein-coupled receptor; BRET, bioluminescence resonance energy transfer; *tr*-FRET, time-resolved fluorescence resonance energy transfer; HA, hemagglutinin; HEK, human embryonic kidney; eYFP, enhanced yellow fluorescent protein; *R*luc, *Renilla reniformis* luciferase; PCR, polymerase chain reaction; APC, allophycocyanin; PHA, phytohemagglutinin; PBMC, peripheral blood mononuclear cell; PBS, phosphate-buffered saline; Ni^{2+}-NTA, nickel-nitrilotriacetic acid; JNJ 7777120, 1-[(5-chloro-1*H*-indol-2-yl)carbonyl]-4-methylpiperazine.

discovery (Devi, 2001; Terrillon and Bouvier, 2004; Waldhoer et al., 2005).

We have reported previously the detection of homo-oligomers of the human histamine H_1 receptor (H_1R) by applying biochemical and *tr*-FRET experiments and by the formation of H_1R radioligand binding sites upon the coexpression of two ligand binding-deficient mutant H_1Rs (Bakker et al., 2004). The H_1R is a well-known target for the treatment of seasonal allergies but has also been shown to mediate inflammatory responses in keratinocytes (Giustizieri et al., 2004; Matsubara et al., 2005). The H_1R is ubiquitously expressed and is coexpressed together with the H_4R in leukocytes, including monocytes and T lymphocytes (Cameron et al., 1986; Morse et al., 2001), suggesting that on these cells, histamine may modulate inflammatory actions through the action on both H_1Rs and H_4Rs. We therefore investigated the potential homo-oligomerization of the H_4R and the hetero-oligomerization of the H_1R with the H_4R using heterologous expression systems.

Herein, we report on the generation of specific antibodies raised against the H_4R, the detection of homo-oligomers of the H_4R, and the potential formation of H_1R-H_4R hetero-oligomers by using biochemical and BRET and *tr*-FRET approaches. Using these methodologies, we show the human H_4R to constitutively form homo-oligomers at the cell surface and that the oligomerization is independent of ligand stimulation of the receptors. Furthermore, *N*-glycosylation of the H_4R receptor is not a prerequisite for oligomer formation. Although we can detect H_4R homo-oligomers at physiologically relevant H_4R expression levels and in endogenously H_4R expressing PHA blast cells, the detection of H_1R-H_4R hetero-oligomers requires higher receptor expression levels.

Materials and Methods

Materials. Reagents for *tr*-FRET were from Cis Bio International (Bagnols-sur-Cèze Cedex, France). Coelenterazine was purchased from Chemicon International (Temecula, CA). Sheep anti-mouse IgG horseradish peroxidase was from GE Healthcare (Little Chalfont, Buckinghamshire, UK). Bovine serum albumin, chloroquine diphosphate, DEAE-dextran (chloride form), histamine (2-[4-imidazolyl]-ethylamine hydrochloride), mepyramine (pyrilamine maleate), monoclonal mouse anti-FLAG (DYKDDDDK), and polyethyleneimine were purchased from Sigma (St. Louis, MO). Calf serum (Integro BV, Dieren, The Netherlands). Cell culture media, penicillin, and streptomycin were obtained from Invitrogen (Merelbeke, Belgium). Cell culture plastics were from Greiner Bio-one (Wemmel, Belgium). Tris was from AppliChem (Darmstadt, Germany). [^{3}H]Histamine (12.40 and 18.10 Ci/mmol) and [^{3}H]mepyramine (23.00 Ci/mmol) were purchased from PerkinElmer Life Science (Boston, MA). Oligonucleotides were purchased from Isogen Biocience (Maarsen, The Netherlands). *Pfu* Turbo DNA polymerase was purchased from Stratagene (La Jolla, CA). Restriction enzymes were from MBI Fermentas (St. Leon-Rot, Germany). Thioperamide, iodophenpropit, clobenpropit, and JNJ 7777120 were synthesized at the Department of Medicinal Chemistry, Vrije Universiteit Amsterdam (Amsterdam, The Netherlands). Gifts of mouse anti-hemagglutinin (anti-HA) antibody (Dr. J. van Minnen), pcDNA3.1-eYFP vector (Dr. T. Schmidt), pRL-CMV vector (Dr. G. Milligan), pCR3.1-HA-H_1R and pcDEF$_3$-c-myc-H_1R (Dr. S Hill), expression vector pcDEF$_3$ (Dr. J. Langer) (Goldman et al., 1996), and mianserin (Organon NV, Oss, The Netherlands) are greatly acknowledged.

Wild-type human H_4R in pcDNA3.1 was purchased from Guthrie cDNA resource center (Sayre, PA). The vector was subcloned into the pcDEF$_3$ using BamHI/XbaI sites.

Construction of Epitope-Tagged Proteins for *tr*-FRET. An N-terminally FLAG (DYKDDDDK) epitope-tagged H_4R was created by PCR. The coding sequence of the hH_4 gene was amplified using the sense oligonucleotide primer 5′-GGGAAGCTTGCCACCATGGACTACAAGGACGACGATGACAAGGATCCAGATACTAATAGCAC-3′ and the antisense primer 5′-GGAAGG CACGGGGGAGGGC-3′. The amplified gene was first cloned into the pCRII-Topo vector by TOPO TA cloning (Invitrogen BV, Breda, The Netherlands) and subsequently subcloned into the pcDEF$_3$ expression vector using EcoRV/XbaI sites.

An N-terminally HA (YPYDVPDYA) epitope-tagged H_4R was created by PCR in two steps. The H_4R gene was amplified by PCR with a 5′ SacII site and without start codon using the sense primer 5′-ACCGCGGCCCCAGATACTA ATAGCACAATC-3′and the antisense primer 5′-GGAAGGCACGGGGAGGGC-3′. The fragment was directly cloned to the pCRII-Topo vector. The gene was subsequently subcloned using SacII/XbaI sites into the pcDNA3.1-HA-rH_{3A}R vector (Bakker et al., 2006). The HA-H_4 gene was finally subcloned using BamHI/XbaI sites to pcDEF$_3$. The HA-H_1R gene was subcloned from the pCR3.1-HA-H_1R into the pcDEF$_3$ using Bsp1407I/SpeI restriction sites.

Construction of Fusion Proteins for BRET. For the BRET assay, H_4Rs were C-terminally fused to either a *Renilla reniformis* luciferase (H_4R-*R*luc) or a yellow fluorescent protein (H_4R-eYFP) in two steps. The coding sequence of the hH_4R gene was amplified without its stop codon using the sense primer 5′-TCGGATCCACCATGCCAGATACTAATAGC-3′ and the antisense primer 5′-CCGCGGC CGCACTAGTAGAAGATACTGACCGAC-3′, harboring unique BamHI and NotI restriction sites, respectively. The gene was cloned directly into the pCRII-Topo vector and subsequently subcloned to a pcDEF$_3$ vector using BamHI/NotI sites [pcDEF$_3$-H_4R (Del stop)].

The coding sequence for the *R*luc gene was amplified from the p*R*L-CMV vector lacking a start codon and harboring a NotI restriction site using the sense primer 5′-AGCGGCCGCGACTTCGAAAGTTTATGATCC-3′ and the antisense primer 5′-TCTAGAATTATTGTTCATTTTTGAG-3′. The gene was directly cloned to the pCRII-Topo vector and subsequently subcloned in frame using NotI/XbaI sites into the pcDEF$_3$-H_4R (Del stop) vector.

The coding sequence for the eYFP gene was amplified from the pcDNA3.1-eYFP vector lacking a start codon and harboring a NotI restriction site using the sense primer 5′-CGCGGCCGCGGTGAGCAAGGGCGAGGAG-3′ and the antisense primer 5′-GTCTAGATTACTTGTACAGCTCGTCCATG-3′. The gene was directly cloned to the pCRII-Topo vector and subsequently subcloned in frame using NotI/XbaI sites into the pcDEF$_3$-H_4R (Del stop) vector.

An hH_1R-eYFP fusion was generated by PCR using the sense primer 5′-AAGAGAATTCTGCATATTCGCTCCATGGTGAGCAAGGGCG-3′ and the antisense primer 5′-TTCTCTAGATTACTTGTACAGCTCGTCC-3′, harboring unique EcoRI and XbaI restriction sites, using pcDNA3.1eYFP as template. The PCR fragment was digested using EcoRI and XbaI, and the purified fragment was subsequently ligated together with the fragment that was obtained by digestion of the pcDEF$_3$-hH_1R plasmid using EcoRI/XbaI sites.

An hH_1R-*R*luc fusion was generated by PCR using the sense primer 5′-AAGAGAATTCTGCATATTCGCTCCATGACTTCGAAAGTTTATGATCC-3′ and the antisense primer 5′-CGCTCTAGAATTATTGTTCATTTTTGAGAACTCGC-3′, harboring unique EcoRI and XbaI restriction sites. The PCR fragment was digested using EcoRI and XbaI and the purified fragment was subsequently ligated together with the fragment that was obtained by digestion of the pcDEF$_3$-hH_1R plasmid using EcoRI/XbaI sites. Each construct was fully sequenced before its expression and analysis.

Construction of His_{10}-Tagged Proteins for Immobilization. An N-terminally c-myc (EQKLISEEDL) and C-terminally His_{10}-epitope-tagged H_4R was created as follows. First, a c-myc epitope-tagged H_4R was created by PCR in two steps. The c-myc tag was amplified by PCR using a pcDEF$_3$-c-myc-H_1R vector as template

with a 3′-NheI site using the sense primer 5′-GGGTGGAGAC TGAAGTTAGGCC-3′and the antisense primer 5′-GTGCTAGCAG-GTCCTCCTCGGAG-3′. The fragment was directly cloned to the pCRII-Topo vector (pCRII-topo-myc). The H_4R gene was amplified without start codon and contained a 5′-NheI restriction site using the following sense 5′-CCGCTAGCCAGATACTAATAGCAC-3′ and the antisense primer 5′- TCTTTAAGAAGATACTGACC-3′. The gene was directly cloned to the pcDNA3.1/V5-His-Topo vector. The H_4R gene was subsequently subcloned in frame using NheI/NotI into the pCRII-topo-c-myc vector (pCRII-topo-c-myc-H_4R). The c-myc-H_4R gene was subsequently subcloned into the pcDEF$_3$ expression vector using the BamHI/XbaI sites.

Second, the gene of the wild-type H_4R was amplified by PCR without a start and stop codon with a 5′-BamHI site and a 3′-SpeI site using the sense primer 5′-CCGG ATCCCCAGATACTAATAG-CACAATCAA-3′ and the antisense primer 5′-CCGCGGCCG CAC-TAGTAGAAGATACTGACCGAC-3′ and directly cloned into the pC-RII-Topo vector. The H_4R gene was then subcloned in frame from the pCRII-topo-vector using BamHI/SpeI sites in the pSFV2genB vector. An N-terminally tagged FLAG and C-terminally tagged H_4R-His$_{10}$ gene was subcloned from the pSFV2genB-FLAG-H_4R-His$_{10}$ behind the p10 promoter of the pFastbac_DUAL vector using NcoI/NheI restriction sites.

The H_4R-His$_{10}$ gene was amplified by PCR from the pFastbac_DUAL-FLAG-H_4R-His$_{10}$ vector without start codon and a 3′-XbaI site using the sense primer 5′-CATCTAGATTAATTACCCACT-GGGCCC-3′and the antisense primer 5′-GAGGATCCGCCAGATAC-TAATAGCACAATC-3′ and directly cloned into the pcDNA3.1/V5-His-Topo vector by TOPO TA cloning and subsequently subcloned into the pcDEF$_3$-c-myc-H_4R vector using BoxI/XbaI restriction sites. Each construct was fully sequenced before its expression and analysis.

Cell Culture and Transfection of COS-7 Cells. COS-7 African green monkey kidney cells were maintained at 37°C humidified in 5% CO_2/95% air atmosphere in Dulbecco's modified Eagle's medium supplemented with 5% (v/v) fetal calf serum, 50 IU/ml penicillin and 50 μg/ml streptomycin and grown in 100-mm dishes. Cells were transiently transfected using the DEAE-dextran method as described previously (Bakker et al., 2001). The total amount of DNA transfected was maintained constant by the addition of pcDEF$_3$.

Cell Culture and Transfection of HEK 293 Cells. HEK 293 cells were maintained at 37°C humidified in 5% CO_2/95% air atmosphere in Dulbecco's modified Eagle's medium/F-12 (Cambrex, Nottingham, UK) supplemented with 10% (v/v) fetal calf serum, 50 IU/ml penicillin, and 50 μg/ml streptomycin and grown in 100-mm dishes. HEK 293 cells were transfected with pcDEF$_3$-H_4R receptor essentially using the Lipofectamine Plus method described by Shenton et al. (2005). In brief, for each cDNA, two microtubes were prepared: tube 1 contained 2 μg of cDNA, 6 μl of Lipofectamine Plus reagent (Invitrogen), and 150 μl of Opti-MEM I media (Invitrogen); tube 2 contained 5 μl of Lipofectamine reagent (Invitrogen) and 150 μl of Opti-MEM I media. The mixtures were incubated at room temperature for 15 min, after which the contents of tube 2 were added to tube 1, followed by a further 15-min incubation. In the meantime, the HEK 293 cells at 50 to 80% confluence in 2-ml Petri dishes were washed three times with Opti-MEM I media. At the end of the second incubation period, the contents of tube 1 were increased to 1.5 ml with Optimem-I media and added to the washed HEK 293 cells. The cells were incubated at 37°C for 6 h. The transfection mixture was then removed and replaced with growth media. The cells were harvested 48 h after transfection, and cell homogenates were prepared for immunoblotting.

[^{3}H]Histamine Binding Studies. Cells used for radioligand binding studies were harvested 48 h after transfection and homogenized in ice-cold H_4R binding buffer (50 mM Tris, pH 7.4). For saturation isotherms, cell membrane homogenates were incubated at 37°C for 60 min with 0 to 125 nM [^{3}H]histamine in a total assay volume of 200 μl. Nonspecific binding was determined by incubation in the presence of 10 μM JNJ 7777120. For competition binding assays, the cell homogenates were incubated at 37°C for 60 min with 0.1 to 10,000 nM ligand in the presence of ~15 nM [^{3}H]histamine in a total volume of 200 μl. The incubations were stopped by rapid dilution with ice-cold H_4R binding buffer. The bound radioactivity was separated by filtration through GF/C filter plates (Whatman, Maidstone, UK) that had been treated with 0.3% polyethyleneimine. Filters were washed four times with H_4R binding buffer, and radioactivity retained on the filters was measured by liquid scintillation counting.

[^{3}H]Mepyramine Binding Studies. Cells used for radioligand binding studies were harvested 48 h after transfection and homogenized in ice-cold H_1R binding buffer (50 mM Na^{2+}/potassium phosphate buffer, pH 7.4). For saturation isotherms, cell membrane homogenates were incubated at room temperature for 30 min with 0 to 25 nM [^{3}H]mepyramine in a total assay volume of 200 μl. Nonspecific binding was determined by incubation in the presence of 1 μM mianserin. For competition binding assays, the cell homogenates were incubated at room temperature for 30 min with 0.1 to 10,000 nM in the presence of ~1.5 nM [^{3}H]mepyramine in a total volume of 200 μl. The incubations were stopped by rapid dilution with ice-cold H_1R binding buffer. The bound radioactivity was separated by filtration through Whatman GF/C filter plates that had been treated with 0.3% polyethyleneimine. Filters were washed four times with H_1R binding buffer, and radioactivity retained on the filters was measured by liquid scintillation counting.

Anti-H_4R Antibody Generation. The unique peptide corresponding to the amino acids CIKKQPLPSQHSRSVSS of the human H_4R subtype was conjugated to thyroglobulin by the cysteine-coupling method (Chazot et al., 1998). The resultant conjugate was used to generate polyclonal antibodies in rabbits. Antibody production and affinity purification was performed as described previously (Chazot et al., 2001).

Production of Human PHA Blasts. Human peripheral blood mononuclear cells (PBMCs) stimulated with phytohemagglutinin (PHA blasts) were generated essentially as described previously (Bradford et al., 2005). In brief, heparinized human whole blood was obtained from healthy volunteers (with local ethical approval), and PBMCs were separated using Lymphoprep (Axis-Shield Poc AS, Oslo, Norway) and centrifuged at 400*g* for 25 min. The PBMCs were isolated from the interfacial layer, washed twice in RPMI 1640 medium without L-glutamine (Invitrogen), and resuspended in RPMI 1640 medium complemented with 10% (v/v) fetal calf serum, 1% (v/v) penicillin and streptomycin, and 1% (v/v) l-glutamine. Cell density was adjusted accordingly to 1×10^6 cells/ml with RPMI 1640 medium. Next, 100 μl of PHA (Lectin; Sigma, Poole, Dorset, UK) was added to the cells to make PHA blasts. These were grown in culture for 24 h, harvested, and a cell homogenate was prepared in the presence of protease inhibitors (Protease Inhibitor Cocktail III; Calbiochem, Beeston, Nottingham, UK).

Immunoblotting. SDS-polyacrylamide gel electrophoresis was carried out using 6 or 7.5% polyacrylamide slab gels under reducing conditions. Samples of HEK 293 cells, COS-7 cells, and PHA blasts (20–50 μg of protein) were prepared using a chloroform/methanol method of protein precipitation, and immunoblotting was performed as described previously (Chazot et al., 2001; Bakker et al., 2006). Immunoblots were probed with anti-H_4 374–390 antibody at a concentration of 0.5 μg/ml.

Blots containing FLAG or c-myc-tagged receptors were probed with primary antibodies, mouse anti-FLAG (1.5 μg/ml), or mouse anti-c-myc (1 μg/ml), respectively. Horseradish peroxidase-conjugated goat anti-mouse antibodies (1:2000–5000) were used as secondary antibodies.

Immunoprecipitation. HEK 293 cells were transfected with HA-H_4 receptor and solubilized with 1% Triton X-100/0.15 M NaCl for 30 min at 4°C. Immunoprecipitation was performed essentially as described previously (Chazot et al., 1994). Solubilized HEK 293 cell extracts were incubated with 5 μg of rat anti-HA antibody (Roche

Diagnostics, Mannheim, Germany) or rat nonimmune Ig (ADI, San Antonio, TX) at 4°C for 1 h. Prechilled, washed Protein G agarose slurry (50 μl; Sigma) was added and incubated for 1 h at 4°C on a rocking platform. Precipitation pellets were collected by centrifugation at 10,000*g* for 30 s at 4°C, washed with 3× PBS, resuspended in sample buffer, vortex-mixed, and heated to 90 to 100°C for 3 min. The sample was then recentrifuged, and the supernatant was subjected to immunoblotting. Control experiments were performed using untransfected HEK 293 cells.

Cross-Linking Experiments. The cross-linking method used was essentially as described by Shenton et al. (2005; Bakker et al., 2006). In brief, aliquots of COS-7 cells expressing c-myc-H_4Rs were pelleted, and the suspension buffer was removed and replaced with 150 μl of cross-linking buffer (150 mM NaCl, 100 mM sodium HEPES, 5 mM EDTA, pH 7.5, and 5 mM dithiothreitol) to give a final protein concentration of approximately 0.5 mg/ml. The cross-linker [bis(sulfosuccinimidyl) suberate sodium salt] was dissolved in 20 mM HCl to give a 100 mM stock solution. The tubes were incubated at room temperature with continual mixing for 12 min with 0.25, 0.5, 1.0, and 2 mM cross-linker, centrifuged at 10,000 rpm for 5 min, the cross-linking mixture was removed, and the resultant pellet was prepared for immunoblotting.

Tunicamycin Experiments. HEK 293 cells expressing H_4Rs were incubated with 2, 4, 6, and 8 μg/ml tunicamycin (stock dissolved in dimethyl sulfoxide at 2 mg/ml) immediately after transfection and were harvested 48 h after transfection, homogenized, and subjected to immunoblotting (Chazot et al., 1995). Cells grown in the absence of tunicamycin were incubated with the respective volume of dimethyl sulfoxide.

Deglycosylation of Native H_4 Receptor. Human PHA blast cell suspensions were resuspended in deglycosylation buffer (50 μM sodium phosphate, pH 6.0, containing 0.1% SDS, 0.1% β-mercaptoethanol, and 20 mM EDTA) and incubated with either water (control) or PNGase F enzyme (Sigma) at a final enzyme concentration of 400 IU/ml (test) for 16 h at 37°C. The samples were then subjected to immunoblotting and probed with anti-H_4 374–390 antibody at a concentration of 2 μg/ml. The NMDAR1 transfected into HEK 293 cells was used as a positive control essentially as described by Chazot et al. (1992).

Receptor Immobilization. Membranes of COS-7 cells transiently expressing c-myc-H_4R-His and FLAG-H_4R or HA-H_1R-His and FLAG-H_4R receptors were homogenized, solubilized, and subsequently immobilized on Ni^{2+}-NTA columns (Invitrogen) as described previously (Bakker et al., 2006). Immobilized receptors were eluted using 250 mM imidazole. Samples were prepared for immunoblotting and were subjected to chloroform/methanol extraction loaded on a 7.5% SDS page gel and subsequently blotted on nitrocellulose paper (GE Healthcare).

BRET Assay. Forty-eight hours after transfection, cells were detached with trypsin and washed twice with PBS. Approximately 50,000 cells per well were distributed in white-bottomed 96-well microplates (Corning BV, Schiphol-Rijk, The Netherlands). Coelenterazine was added to a final concentration of 5 μM, and readings were collected immediately after this addition using a Victor$_2$ allowing signal detection at 460 and 530 nm.

tr-FRET Assay. *tr*-FRET assays were performed using Europium (Eu^{3+})-labeled and allophyocyanin anti-FLAG and anti-HA antibodies as described by Bakker et al. (2006). In brief, *tr*-FRET was assessed in 1×10^6 whole COS-7 cells transiently expressing the appropriate HA- and FLAG-tagged receptors. Cells were incubated in PBS containing 50% fetal calf serum (v/v), 0.8 nM Eu^{3+}-labeled antibody, and 8 nM allophycocyanin-labeled antibody for 2 h at room temperature on a rotating wheel, after which the membranes were washed twice with PBS. The final pellet was resuspended in 50 μl of PBS and transferred to a 384-microtiter plate. Energy transfer was measured by exciting the Eu^{3+} at 320 nm and monitoring the XL-665 allophycocyanin emission for 500 μs at 665 nm using a Novostar (BMG LabTechnologies, Offenburg, Germany) configured for time-resolved fluorescence after a 100-μs delay.

Analytical Methods. Binding data were evaluated by a nonlinear least-squares curve-fitting program using Prism software (GraphPad Software Inc., San Diego, CA). Protein concentrations were determined according to Bradford's method (1976) using bovine serum albumin as standard. All data are represented as mean ± S.E.M. from at least three independent experiments performed in triplicate. Statistical significance was determined by a Student's unpaired *t* test ($p < 0.05$ was considered statistically significant).

Results

Pharmacological Characterization of the hH_4R and hH_1R Expressed in COS-7 Cells. We have used COS-7 cells previously successfully for the heterologous expression of the hH_1R and for the identification of H_1R oligomers (Bakker et al., 2004). To investigate the potential oligomerization of the hH_4R, we therefore expressed the hH_4R heterologously in COS-7 cells. Transfection of these cells with cDNA coding for the hH_4R resulted in the expression of a high-affinity [^{3}H]histamine binding site (Table 1). Subsequent displacement studies using [^{3}H]histamine as a radioligand revealed these binding sites to display a characteristic H_4R pharmacological profile (Table 1). The H_1R and H_4R constructs used in the *tr*-FRET, BRET, and immobilization assays were also characterized by radioligand binding (saturation and displacement) assays. COS-7 cells were transiently transfected with cDNA encoding the HA-H_4R, FLAG-H_4R, H_4R-*R*luc, H_4R-eYFP, c-myc-H_4R-His, HA-H_1R, H_1R-*R*luc, or the H_1R-eYFP. [^{3}H]Histamine bound to the H_4Rs according to a one-site saturable model with Hill slopes of approximately 1 and dissociation constants (K_d) similar to those of the wild-type hH_4R, although the B_{max} value is affected by fusion of the *R. reniformis* luciferase enzyme (Table 1). Bound [^{3}H]histamine

TABLE 1

Characterization of epitope-tagged and H_4R fusion constructs

The pK_i values of histamine and thioperamide for the H_4R constructs used in the experiments were determined by [^{3}H]histamine saturation and displacement binding assays. The pEC_{50} values of histamine and thioperamide were determined using a CRE-luciferase reporter gene assay. The values are expressed as mean ± S.E.M. of at least three separate experiments performed in triplicate.

Receptor	[^{3}H]Histamine		pK_i		pEC_{50}	
	K_d	B_{max}	Histamine	Thioperamide	Histamine	Thioperamide
	nM	*pmol/mg protein*				
Wild-type H_4R	19.9 ± 1.4	1.0 ± 1.4	7.6 ± 0.1	7.3 ± 0.1	8.8 ± 0.2	6.4 ± 0.3
HA-H_4R	23.2 ± 0.6	2.0 ± 0.5	7.4 ± 0.1	7.0 ± 0.1	8.9 ± 0.2	6.4 ± 0.2
FLAG-H_4R	26.3 ± 5.5	1.3 ± 0.3	7.6 ± 0.1	7.4 ± 0.1	9.0 ± 0.1	6.5 ± 0.4
H_4R-*R*luc	30.8 ± 2.3	0.1 ± 0.02	7.6 ± 0.1	7.4 ± 0.1	9.0 ± 0.1	6.0 ± 0.3
H_4R-eYFP	57.4 ± 3.6	1.1 ± 0.3	7.2 ± 0.1	7.3 ± 0.2	8.6 ± 0.3	5.7 ± 0.1
c-myc-H_4R-His_{10}	33.3 ± 2.0	2.6 ± 0.5	7.3 ± 0.1	7.6 ± 0.1	9.0 ± 0.1	6.3 ± 0.3

could be displaced from all of the N- and/or C-terminally tagged H_4Rs by the agonist histamine and the inverse agonist thioperamide with affinity values (pK_i) comparable with the wild-type (Table 1). Likewise, the H_1R radioligand [^{3}H]mepyramine bound the various hH_1R constructs according to a one-site saturable binding model with K_d values similar to those of the wild-type hH_1R (data not shown). The agonist histamine and H_1R inverse agonist mepyramine were able to displace the radioligand with affinities equal to those of the wild-type H_1R (data not shown). The aforementioned H_4R constructs were functionally characterized using a cAMP response element-luciferase-luciferase reporter gene assay. In these assays, histamine behaved as a full H_4R agonist and thioperamide as a full inverse H_4R agonist for each H_4R construct, with pEC_{50} values comparable with those obtained for the wild-type H_4R (Table 1).

Generation of hH_4R-Specific Antibodies. To enable our biochemical approaches and to study H_4R function in native tissue, we raised a rabbit polyclonal anti-hH_4 (374–390) receptor antibody, which represents the first published selective immunological probe for the hH_4R. The antibody was generated against the last 17 amino acids of the C-terminal tail of the H_4R (Fig. 1A). The selectivity of the anti-hH_4R antibody was confirmed by blockade with the C-terminal peptide of the H_4R (Fig. 1B, lane 3) and a lack of cross reactivity with the human H_3R, the most related GPCR (de Esch et al., 2005) (Fig. 1B, lane 1). In transfected HEK 293 cells, the antibody detects two major reactive species at 34 to 36 and 65 to 72 kDa (Fig. 1B, lane 2). The lower bands most likely represent monomeric H_4Rs. An additional band (approximately 45 kDa) was occasionally detected; such bands are likely to represent a proteolytic fragment. We suspect the 34-kDa species to be the unglycosylated product of the species at 36 kDa. The higher molecular mass species could either represent a heavily glycosylated form of the H_4R or dimeric H_4Rs.

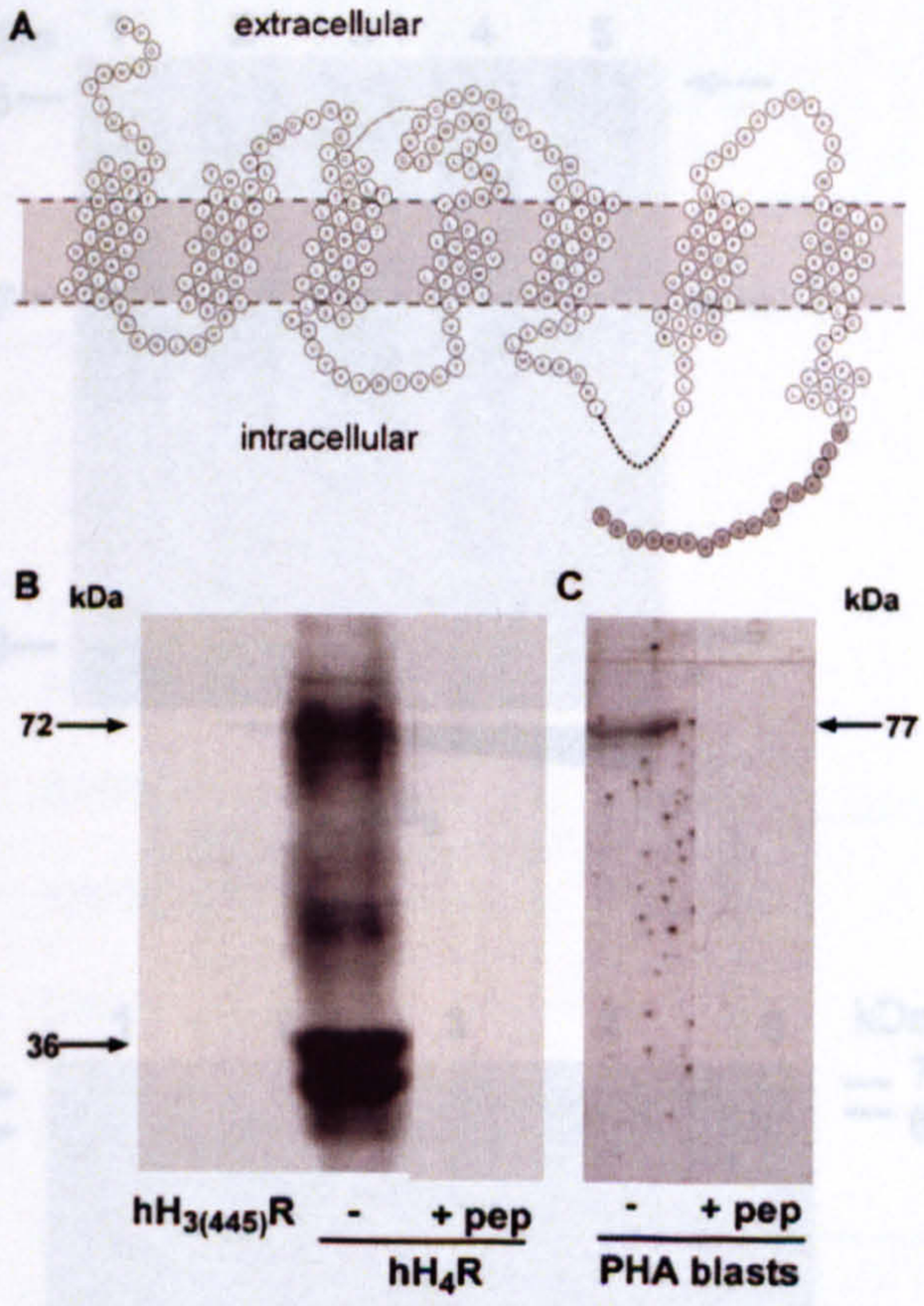

Fig. 1. Characterization of specific polyclonal H_4R antibodies. A, snake plot of the hH_4R; the region of the C-terminal tail (374–390) against which the antibody was raised is marked in gray. HEK 293 cells expressing $hH_{3(445)}$Rs or hH_4Rs (B), and human PHA blasts (C) were probed by immunoblotting using the anti-H_4 (374–390) antibody (0.5 μg/ml) either alone or preincubated for 16 h at 4°C with 500 μg/ml (374–390) peptide. The major immunoreactive species labeled in the HEK 293 hH_4R and the human PHA blasts were greatly suppressed by preincubation with the antigen peptide (B, lane 3; and C, lane 2, respectively), demonstrating the sequence selectivity of the antibody. Furthermore, no significant labeling of the $hH_{3(445)}$R (B, lane 1) or in untransfected HEK 293 cells (data not shown) was detected.

Evidence that Native H_4R Are Robust Dimers. The H_4R clearly plays a role as an immune modulator, with mRNA expression shown in human mast cells, neutrophils, eosinophils, and T lymphocytes (Nakamura et al., 2000; Oda et al., 2000; Morse et al., 2001; Zhu et al., 2001; Gantner et al., 2002; Hofstra et al., 2003). A single major diffuse immunoreactive species (approximately 77 kDa) coincident with the putative recombinant dimeric hH_4R species expressed in COS-7 cells was detected in human PHA blasts (Fig. 1C, lane 1). This species was abolished by preincubation with the 374–390 peptide, again demonstrating the peptide selectivity of the antibody. Little or no protein monomers were detected in the native preparation, consistent with our previous data with the H_3R (Chazot et al., 2001; Bakker et al., 2006). It is noteworthy that these experiments were performed under reducing conditions, indicating the robust nature of the dimeric species in native tissue. An identical labeling pattern was detected with the anti-hH_4 374–390 antibody probing human spleen lysates (data not shown). The putative dimeric recombinant hH_4R species expressed in HEK 293 cells was consistently smaller (approximately 72 kDa), which may reflect differential glycosylation in the two cell lines (Fig. 3). Coincident protein species were detected by the anti-hH_4 374–390 and the anti-epitope-tagged antibodies in the respective cell lines, further confirming that the hH_4 receptor is being labeled by the anti-hH4 374–390 antibody (data not shown). No signal was detected in either COS-7 or HEK 293 cell lines, further supporting the selectivity of the anti-hH_4 374–390 antibody. These data identify for the first time the H_4R protein in human T lymphocytes.

Immunoprecipitation of Recombinantly Expressed HA-H_4Rs from HEK 293 Cells. To further characterize the selectivity of the H_4R antibody, an immunoprecipitation assay was performed. HA-H_4Rs expressed transiently in HEK 293 cells (Fig. 2, lanes 3–5) were immunoprecipitated using anti-HA antibodies (Fig. 2, lane 4) or a nonimmune Ig (Fig. 2, lane 3). As negative controls, nontransfected HEK 293 cells (Fig. 2, lane 1) and nontransfected HEK 293 cells immunoprecipitated with anti-HA antibodies (Fig. 2, lane 2) were used. As positive control, solubilized HEK 293 cells expressing HA-H_4Rs (Fig. 2, lane 5) was used. All samples were subjected to immunoblotting using the anti-H_4R antibodies. Immunoreactive species were only detected for the HEK 293 cells expressing the HA-H_4R, which had been anti-HA-immunoprecipitated (Fig. 2, lane 4). The immunoreactive species represent the putative monomeric and dimeric H_4R and are identical with the reactive species in the positive control (Fig. 2, lane 5).

Cross-Linking of H_4Rs. To further investigate the homo-oligomeric structure of the H_4R, a cross-linking study was performed using N-terminally c-myc-tagged H_4R expressed

in COS-7 cells. Upon application of increasing concentrations of the cell-impermeable cross-linker BS_3, a progressive reduction in the monomeric doublet species (34 and 36 kDa) was observed (Fig. 3A). Concomitant the appearance of, initially, a diffuse species of 77 kDa (putative glycosylated and unglycosylated dimers) and then higher molecular mass species (>175 kDa) at 0.25 mM and 2 mM BS_3, respectively, was noticed (Fig. 3A). These data are highly consistent with hH_4Rs expressed in HEK 293 cells (data not shown).

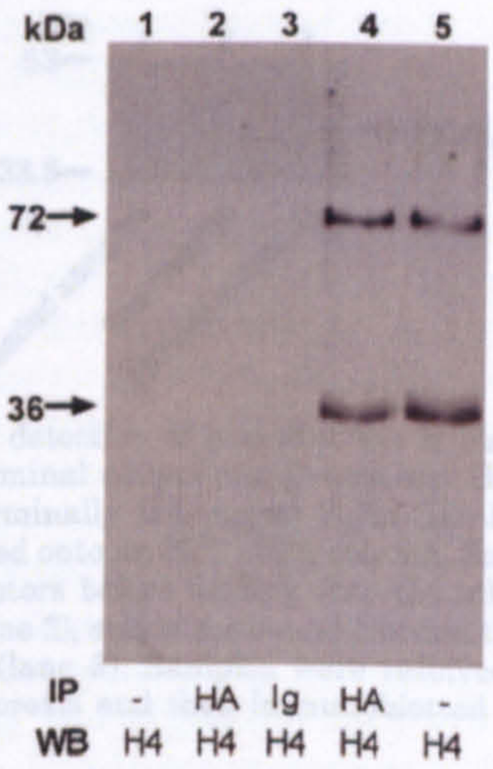

Fig. 2. The anti-H_4R antibodies recognize anti-HA immunoprecipitated (IP) HA-H_4Rs. HEK 293 cells alone (lanes 1 and 2) or transfected with cDNA encoding the HA-H_4R (lanes 3–5) were subjected to immunoprecipitation with an anti-HA antibody (lanes 2 and 4) or a nonimmune Ig (lane 3). The precipitates (lanes 2–4) or solubilized cells (lanes 1 and 5) were immunoblotted using the anti-H_4R antibody.

Biochemical Evidence that the hH_4Rs Is an *N*-Glycosylated Homodimer. In the N terminus of the hH_4R, Asn^5 and Asn^9 are potential sites for *N*-glycosylation (Fig. 3B). To study whether the higher molecular mass species are the *N*-glycosylated forms of the hH_4R, we expressed H_4Rs in the presence of the *N*-glycosylation inhibitor tunicamycin. In the absence of tunicamycin, two major putative monomeric species, 34 and 36 kDa, and a diffuse 65- to 72-kDa species were detected as in Fig. 1 (also see Fig. 3C, lane 1). In the presence of 2 μg/ml tunicamycin, a complete loss of the 36-kDa species and concomitant increase in intensity of the 34-kDa species and an additional species at 32 kDa were observed (Fig. 3C, lane 2). Furthermore, the diffuse 65- to 72-kDa species, detected in the absence of tunicamycin, was reduced to a single 65-kDa species. It is noteworthy that an increase in tunicamycin concentration had no further effect on either the 34- or 65-kDa species (Fig. 3C, lanes 3–5). The 32-kDa species observed upon tunicamycin treatment is probably a breakdown

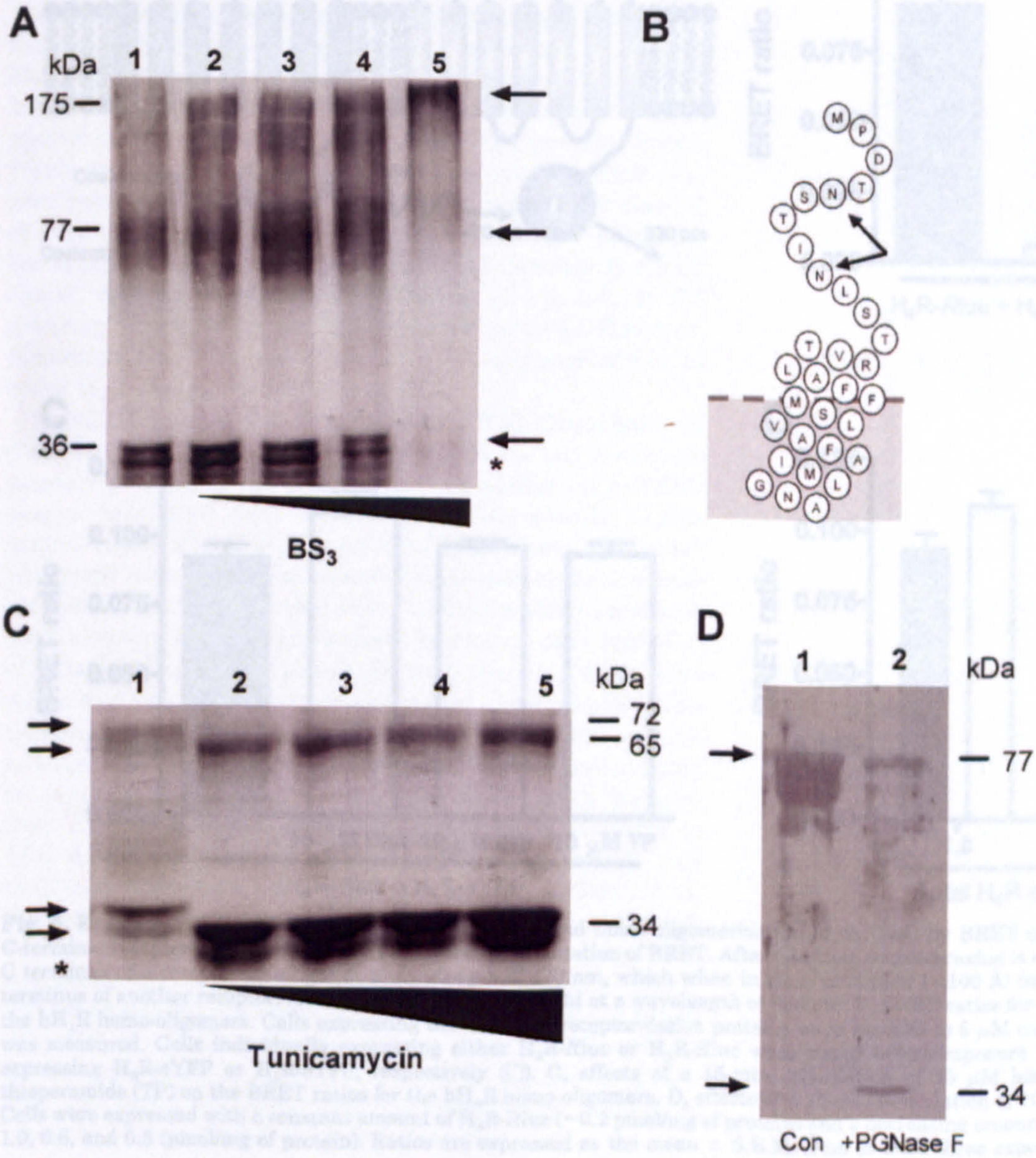

Fig. 3. Evidence for hH_4R dimers and higher oligomers and glycosylation of the hH_4R dimers. A, COS-7 cells transfected with cDNA encoding the hH_4R were subjected to cross-linking using increasing concentrations of BS_3 (0.12–2 mM). The resultant pellets were subjected to immunoblotting and probed with the anti-hH_4 (374–390) antibody (0.5 μg/ml). Lane 1, COS-7 cells expressing hH_4Rs as control; lanes 2 to 5, COS-7 cells expressing hH_4Rs treated with 0.12, 0.5, 1, and 2 mM BS_3, respectively. *, a species that is likely to be a proteolytic fragment of the hH_4R (observed in both host cells). B, snake plot of the N-terminal tail and beginning of transmembrane 1 of the H_4R; arrows indicate possible *N*-glycosylation sites. C, HEK 293 cells transfected with the hH_4R were grown in the absence and presence of 2, 4, 6, and 8 μg/ml tunicamycin for 48 h. The cells were harvested, and homogenates were prepared and subjected to immunoblotting. Immunoblots were probed with the anti-hH_4 (374–390) receptor antibody. Lane 1, hH_4Rs in absence of tunicamycin; lanes 2 to 5, hH_4Rs in presence of 2, 4, 6, and 8 μg/ml tunicamycin, respectively. D, PHA blasts were subjected to *N*-deglycosylation with PNGase F enzyme at a final enzyme concentration of 400 IU/ml for 16 h at 37°C. Control PHA blasts were incubated in parallel with deglycosylation buffer alone. Samples were then subjected to immunoblotting, and immunoblots were probed with the anti-hH_4 (374–390) receptor antibody. Lane 1, control; lane 2, in the presence of PNGase F. Enzymatic deglycosylation resulted in the reduction in intensity of the 77-kDa species and appearance of the 34-kDa putative monomer.

product of the glycosylated 36-kDa species in untreated cells. These data strongly suggest that the recombinant hH_4R is *N*-glycosylated and forms dimers. This last process is independent of post-translational *N*-glycosylation. It is noteworthy that upon enzymic *N*-deglycosylation of PHA blasts, the 77-kDa species was greatly reduced in intensity, and a new 34-kDa species was detected, consistent with the monomeric hH_4R (Fig. 3D, lane 2).

Fig. 4. Biochemical detection of homodimeric H_4Rs. Cells coexpressing H_4Rs with an N-terminal c-myc- and C-terminal His_{10}-tag (c-myc-H_4R-His_{10}) and an N-terminally HA-tagged H_4Rs (HA-H_4R) receptors were solubilized and loaded onto an Ni^{2+}-NTA column. Samples were taken of the solubilized receptors before loading onto the column (lane 1), of the unbound fraction (lane 2), and of the bound fraction that was eluted using 250 mM imidazole (lane 3). Samples were resolved by SDS-polyacrylamide gel electrophoresis and then immunoblotted using anti-HA antibodies.

HA-H_4Rs Associate with c-myc-H_4R-His_{10}. To further investigate whether the H_4Rs can associate with each other to form homo-oligomers, membranes of COS-7 cells coexpressing N-terminally c-myc and C-terminally His_{10}-tagged hH_4Rs (c-myc-H_4R-His_{10}) and N-terminally HA-tagged hH_4Rs (HA-H_4R) were solubilized and loaded on an Ni^{2+}-resin column. The HA-H_4Rs, when coexpressed with the c-myc-H_4R-His_{10}, were retained on the Ni^{2+}-column and could be eluted with 250 mM imidazole, as detected with anti-HA antibodies (Fig. 4, lane 3). When cells individually expressing c-myc-H_4R-His_{10} and HA-H_4Rs were mixed before solubilization and subsequently loaded on the column, no HA-H_4Rs were found to interact with the Ni^{2+} resin (data not shown).

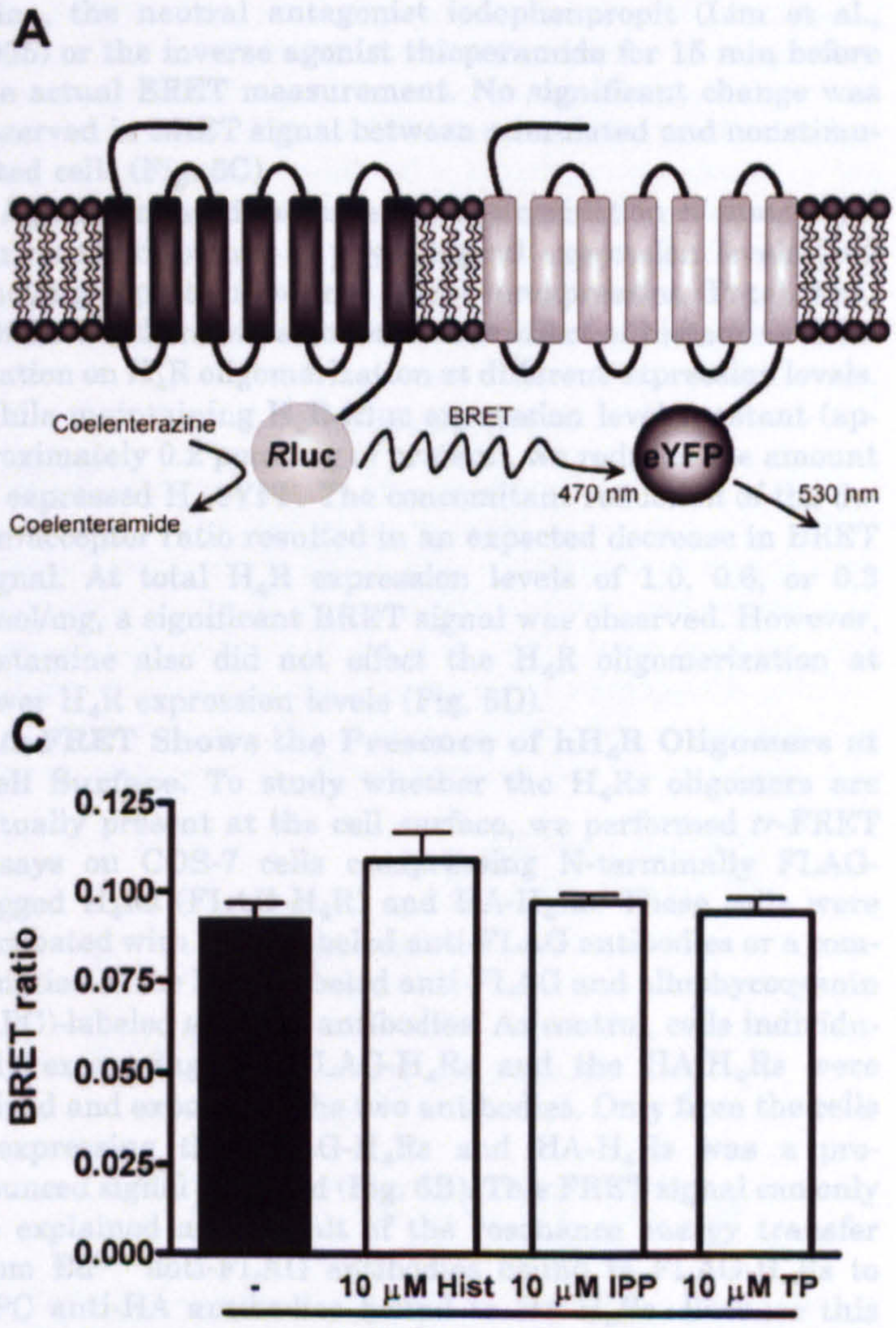

Fig. 5. Evaluation of homo-oligomerization of the H_4R and homo-oligomerization of the H_1R by BRET using the coexpression of *R*luc and eYFP C-terminal receptor-fusion proteins. A, schematic representation of BRET. After addition, coelenterazine is converted by the *R*luc enzyme fused to the C terminus of a receptor into light of a wavelength of 470 nm, which when in close proximity (<100 Å) can excite the eYFP protein fused to the C terminus of another receptor, leading to the emission of light at a wavelength of 530 nm. B, BRET ratios for the hH_4R homo-oligomers compared with the hH_1R homo-oligomers. Cells expressing the indicated receptor-fusion proteins were exposed to 5 μM coelenterazine, after which energy transfer was measured. Cells individually expressing either H_4R-*R*luc or H_1R-*R*luc were mixed before exposure to coelenterazine with cells individually expressing H_4R-eYFP or H_1R-eYFP, respectively (□). C, effects of a 15-min stimulation of 10 μM histamine (Hist), iodophenpropit (IPP), or thioperamide (TP) on the BRET ratios for the hH_4R homo-oligomers. D, effects of a 15-min stimulation of 10 μM histamine on H_4Rs homo-oligomers. Cells were expressed with a constant amount of H_4R-*R*luc (~0.2 pmol/mg of protein) and a decreasing amount of H_4R-eYFP. Total H_4R expression was 1.0, 0.6, and 0.3 (pmol/mg of protein). Ratios are expressed as the mean ± S.E.M. from at least three experiments performed in triplicate.

BRET Shows Constitutive Ligand-Independent Homo-Oligomerization of hH_4Rs. The use of biophysical techniques has been of great value to the study of GPCR oligomerization. We have used BRET to study in further detail the homo-oligomerization of the H_4R. BRET was performed on COS-7 cells expressing either the H_4R-*R*luc or coexpressing the H_4R-*R*luc with the H_4R-eYFP. After the addition of coelenterazine, a robust BRET signal could be observed in the cells coexpressing the two H_4Rs (Fig. 5B). As a negative control, cells individually expressing either of the H_4R constructs were mixed before adding coelenterazine (Fig. 5B). Previous studies have reported the ability of H_1Rs to oligomerize (Carrillo et al., 2003; Bakker et al., 2004) Therefore, cells in which the H_1R-*R*luc and the H_1R-eYFP were coexpressed were taken as a positive control. In these cells, a BRET signal was detected that was approximately 2-fold lower than that observed for the H_4Rs (Fig. 5B).

To investigate the effect of ligands on H_4R oligomerization, cells coexpressing the H_4R-*R*luc with the H_4R-eYFP were incubated with a 10 μM concentration of the agonist histamine, the neutral antagonist iodophenpropit (Lim et al., 2005) or the inverse agonist thioperamide for 15 min before the actual BRET measurement. No significant change was observed in BRET signal between stimulated and nonstimulated cells (Fig. 5C).

Agonist-induced increase in oligomerization of somatostatin receptors occurs at physiological expression levels (160 fmol/mg of protein) but not after overexpression (Patel et al., 2002). We therefore also tested the effect of histamine stimulation on H_4R oligomerization at different expression levels. While maintaining H_4R-*R*luc expression level constant (approximately 0.2 pmol/mg of protein), we reduced the amount of expressed H_4-eYFP. The concomitant reduction of the donor/acceptor ratio resulted in an expected decrease in BRET signal. At total H_4R expression levels of 1.0, 0.6, or 0.3 pmol/mg, a significant BRET signal was observed. However, histamine also did not effect the H_4R oligomerization at lower H_4R expression levels (Fig. 5D).

***tr*-FRET Shows the Presence of hH_4R Oligomers at Cell Surface.** To study whether the H_4Rs oligomers are actually present at the cell surface, we performed *tr*-FRET assays on COS-7 cells coexpressing N-terminally FLAG-tagged H_4Rs (FLAG-H_4R) and HA-H_4Rs. These cells were incubated with Eu^{3+}-labeled anti-FLAG antibodies or a combination of the Eu^{3+}-labeled anti-FLAG and allophycocyanin (APC)-labeled anti-HA antibodies. As control, cells individually expressing the FLAG-H_4Rs and the HA-H_4Rs were mixed and exposed to the two antibodies. Only from the cells coexpressing the FLAG-H_4Rs and HA-H_4Rs was a pronounced signal observed (Fig. 6B). This FRET signal can only be explained as a result of the resonance energy transfer from Eu^{3+} anti-FLAG antibodies bound to FLAG-H_4Rs to APC anti-HA antibodies bound to HA-H_4Rs. Because this resonance energy transfer can only take place within 100 Å, the data indicate the formation of H_4R oligomers at the cell surface of living cells. Stimulation of the COS-7 cells with 10 μM histamine or 10 μM thioperamide preceding *tr*-FRET measurement did not result in a significant change in signal (Fig. 6B). The used antibodies did not have an influence on the ligand binding to the H_4Rs because no significant difference was found in [^{3}H]histamine binding in the absence or presence of the antibodies (data not shown).

Lack of Hetero-Oligomerization between H_4R and H_1Rs. We have subsequently used *tr*-FRET to investigate whether hetero-oligomerization occurs between H_4Rs and H_1Rs. *tr*-FRET was performed on COS-7 cells coexpressing the FLAG-H_4Rs and N-terminally HA-tagged histamine H_1Rs (HA-H_1Rs). As a control, cells individually expressing the FLAG-H_4Rs and the HA-H_1Rs were mixed and exposed to the two antibodies. No significantly increased *tr*-FRET signal could be observed compared with the signal obtained from cells individually expressing the two receptors that were mixed before incubation with the antibodies (Fig. 6C). The ratio and total amount of antibodies was maintained equal between experiments with H_1R-H_4Rs and H_4R-H_4Rs to ensure proper comparison.

Comparable results were obtained using Eu^{3+} anti-HA antibodies and APC anti-FLAG antibodies (data not shown).

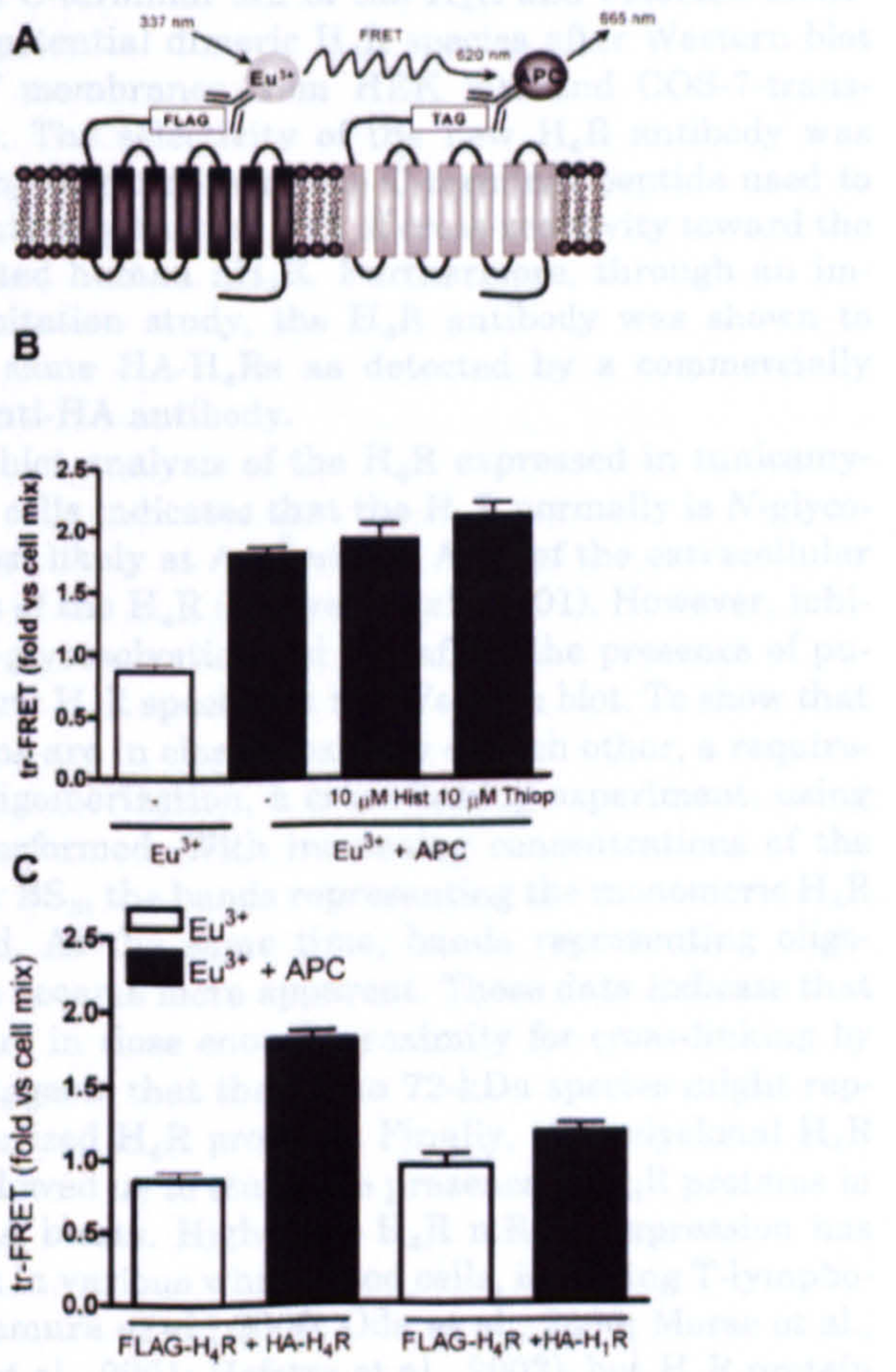

Fig. 6. Evaluation of homo-oligomerization of the H_4R and hetero-oligomerization of the H_4R with the H_1R by *tr*-FRET using coexpression of differentially epitope-tagged receptors. A, schematic representation of *tr*-FRET. Excitation at 337 nm of anti-FLAG Eu^{3+} antibody bound to the FLAG-epitope-tagged receptor leads to the emission of light at a wavelength of 620 nm, which, when in close proximity (<100 Å), can excite the anti-FLAG APC antibody bound to another FLAG-epitope-tagged receptor, leading to the emission of light at a wavelength of 665 nm. B, *tr*-FRET using cells coexpressing FLAG- and HA-tagged H_4Rs. Cells were incubated for 2 h with the Eu^{3+}-labeled anti-FLAG antibodies (□, Eu^{3+}) or with both Eu^{3+}-labeled anti-FLAG and APC-labeled anti-HA antibodies (■, APC) in the presence or absence of 10 μM histamine (Hist) or 10 μM thioperamide (Thiop). C, *tr*-FRET using cells coexpressing FLAG-tagged H_4Rs (FLAG-H_4R) and either HA-tagged H_4Rs (HA-H_4R) or HA-tagged H_1Rs (HA-H_1R). Cells were incubated for 2 h with the Eu^{3+}-labeled anti-FLAG antibodies (□, Eu^{3+}), or with both Eu^{3+}-labeled anti-FLAG and APC-labeled anti-HA antibodies (■, APC). Data are normalized for the *tr*-FRET signal obtained from a mixture of cells that was obtained by mixing of cells that have been incubated with Eu^{3+}-labeled anti-FLAG antibodies with cells that have been incubated with APC-labeled anti-FLAG antibodies. Data shown are from a representative experiment.

Stimulation of cotransfected cells with 10 μM histamine did not lead to a change in FRET signal (data not shown).

Homo-Oligomerization of H_4Rs versus Hetero-Oligomerization between H_4Rs and H_1Rs. To further investigate hetero-oligomerization between H_4Rs and H_1Rs, BRET saturation curves were produced for both the H_4R homo-oligomer and the H_1R-H_4R hetero-oligomer. Experiments were performed in which COS-7 cells were transfected with a fixed amount of H_4-*R*luc and increasing amounts of either H_4R-eYFP or H_1R-eYFP cDNA. Expression levels were determined by radioligand binding. Expression of the H_4R-*R*luc was maintained at approximately 0.2 pmol/mg of protein. Expression levels of H_4R-*R*luc were correlated with luminescence and expression levels for the eYFP fused H_1R and H_4R were correlated with fluorescence. A linear correlation was obtained for all three constructs. Expression for the H_4*R*-eYFP ranged from 0.3 to 2.5 pmol/mg of protein, whereas expression levels of the H_1R-eYFP ranged from 0.5 to 16 pmol/mg of protein. For the H_4R homo-oligomers, a steep increase in BRET signal is observed, showing detectable BRET when total H_4R expression is 0.3 pmol/mg of protein. For the H_1R-H_4R hetero-oligomers, a more gradual increase in BRET signal is observed upon increased expression of the H_1R-eYFP. A BRET signal is observed for the first time at expression levels of 1 pmol/mg of protein of the H_1R-eYFP. The H_4R-H_4R homo-oligomer showed a 2-fold lower $BRET_{50}$ value (0.77 versus 1.6) and a 2.5-fold higher B_{max} (0.1 versus 0.04) than the H_1R-H_4R hetero-oligomer as determined from the BRET saturation curve (Fig. 7).

Discussion

GPCR oligomerization has become a generally accepted phenomenon and has been reported to occur in all GPCR classes (George et al., 2002). Data obtained from atomic force microscopy (Fotiadis et al., 2003), electron microscopy, and Western blot analysis (Suda et al., 2004) have provided compelling evidence that the light-sensitive rhodopsin is predominantly present as a dimer in the retinal disc membrane. For histamine receptors, oligomerization has been shown convincingly for the hH_1Rs (Carrillo et al., 2003; Bakker et al., 2004), the hH_2Rs (Fukushima et al., 1997), and H_3Rs (Shenton et al., 2005; Bakker et al., 2006). In view of the emerging role of GPCR oligomerization in GPCR function and our interest in the H_4R as a new target for inflammatory conditions (de Esch et al., 2005), we investigated oligomerization of the human H_4R by various means. Combining biophysical measurements like *tr*-FRET and BRET (Angers et al., 2002; Boute et al., 2002) with biochemical approaches, like Western blot analysis and histidine-tag-based affinity chromatography, we provide compelling evidence for homo- and hetero-oligomer formation of hH_4Rs.

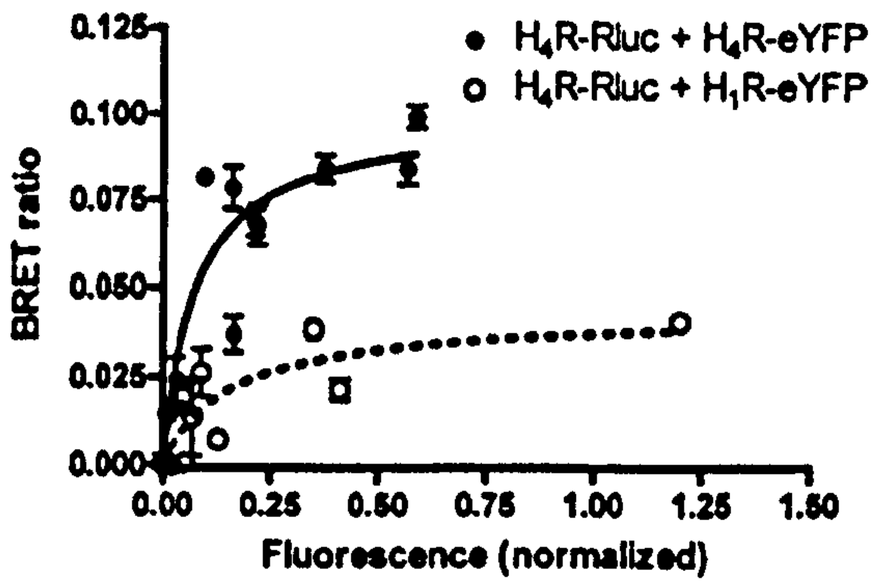

Fig. 7. Evaluation of receptor-expression dependence of the detection of H_4R homo-oligomers and H_1R-H_4R hetero-oligomers using BRET. BRET saturation curves for the hH_4R homo-oligomers (H_4R-*R*luc + H_4*R*-eYFP, solid line) compared with H_1R-H_4R hetero-oligomers (H_4R-*R*luc + H_1R-eYFP, broken line) at increasing expression levels of the eYFP-tagged receptor. COS-7 cells were transfected with a fixed amount DNA encoding for the H_4R-*R*luc and increasing amounts of DNA encoding for the H_4*R*-eYFP or the H_1R-eYFP. Plotted on the *x*-axis is the fluorescence obtained from the eYFP, which has been correlated to the expression of H_4*R*-eYFP (●) and H_1R-eYFP (○). Expression level of the H_4R-*R*luc was maintained at approximately 200 fmol/mg of protein, as determined from the luminescence, which has been correlated to the expression of the H_4R-*R*luc.

To enable our biochemical approaches and to study H_4R function in native tissues, we report in this study on the first polyclonal H_4R antibody that can successfully be used for Western blot analysis. This new molecular tool is directed against the C-terminal tail of the H_4R and detected monomeric and potential dimeric H_4R species after Western blot analysis of membranes from HEK 293 and COS-7-transfected cells. The selectivity of the new H_4R antibody was confirmed by blockade with the C-terminal peptide used to raise the antibody and the lack of cross-reactivity toward the highly related human hH_3R. Furthermore, through an immunoprecipitation study, the H_4R antibody was shown to detect the same HA-H_4Rs as detected by a commercially available anti-HA antibody.

Western blot analysis of the H_4R expressed in tunicamycin-treated cells indicates that the H_4R normally is *N*-glycosylated, most likely at Asn^5 and/or Asn^9 of the extracellular N terminus of the H_4R (Nguyen et al., 2001). However, inhibition of *N*-glycosolyation did not affect the presence of putative dimeric H_4R species on the Western blot. To show that H_4R proteins are in close proximity of each other, a requirement for oligomerization, a cross-linking experiment, using BS_3 was performed. With increasing concentrations of the cross-linker BS_3, the bands representing the monomeric H_4R disappeared. At the same time, bands representing oligomeric H_4Rs became more apparent. These data indicate that the H_4Rs are in close enough proximity for cross-linking by BS_3 and suggests that the 65- to 72-kDa species might represent dimerized H_4R proteins. Finally, the polyclonal H_4R antibody allowed us to study the presence of H_4R proteins in human PHA blasts. High-level H_4R mRNA expression has been shown in various white blood cells, including T-lymphocytes (Nakamura et al., 2000; Oda et al., 2000; Morse et al., 2001; Zhu et al., 2001; Hofstra et al., 2003), but H_4R protein expression so far has not been shown. Western blot analysis of membranes of PHA blasts with our polyclonal anti-H_4R antibody indeed revealed the presence of H_4R protein in PHA blasts. It is interesting to note that the endogenously expressed H_4R was only detected as a high molecular mass species. Enzymatic deglycosylation of the native H_4R protein resulted in a partial reduction of the high molecular mass species (77 kDa) to monomeric H_4Rs (34 kDa). These data in themselves do not directly exclude a heavily glycosylated (approximately 33 kDa) H_4R protein. However, the hH_4Rs in human HEK 293 cells is only moderately glycosylated (approximately 2 kDa), and the high molecular mass species coincide with the putative dimeric H_4Rs when recombinantly expressed in COS-7 (77 kDa) and HEK 293 cells (72 kDa). These data can be explained by assuming that in human PHA blasts, the hH_4R functions predominantly as a dimer.

We hypothesize that *N*-glycosylation is not a prerequisite for dimerization, but it helps to stabilize the H_4R dimers. A similar stabilizing effect of glycosylation on receptor dimers has recently been shown for the human bradykinin B_2 receptors (Michineau et al., 2006). The putative H_4R dimerization in native tissue clearly warrants further investigation.

As an alternative biochemical method, we used an immobilized metal (Ni^{2+}) affinity chromatography approach with a histidine-tagged H_4R protein. To this end, we coexpressed c-myc-H_4R-His_{10} and HA-H_4Rs receptors to study oligomer formation via affinity column chromatography. In contrast to c-myc-H_4R-His_{10} receptors, HA-H_4Rs are not robustly retained onto an Ni^{2+}-NTA resin when expressed alone. Yet c-myc-H_4R-His_{10} receptors immobilized onto Ni^{2+}-NTA resin were shown also to retain coexpressed HA-H_4Rs on the Ni^{2+}-NTA column, as determined by HA-immunoreactivity detected after elution of histidine-tagged proteins with high imidazole concentrations. These findings indicate that c-myc-H_4R-His_{10} receptors physically interact with the coexpressed HA-H_4Rs to form oligomers that can be retained on the Ni^{2+}-NTA resin through the C-terminal His_{10} tag.

We continued our investigation of the oligomerization of the H_4Rs in living cells using BRET and *tr*-FRET assays. Using the BRET assay, a clear signal could be detected when coexpressing H_4R-*R*luc with H_4R-eYFP in nonstimulated cells, suggesting constitutive homo-oligomerization of H_4Rs. Because the oligomers detected in the immobilization and BRET assays do not necessarily have to be present at the cell surface, we also studied H_4R oligomerization on the cell membrane of living cells by *tr*-FRET. The *tr*-FRET approach uses antibodies that do not permeate the cell membrane and detects cell surface H_4R oligomers present at the cell surface. Similar to the BRET assay, we detected a robust signal, indicating the constitutive presence of H_4R homo-oligomers at the cell surface.

A number of studies have investigated the effect of agonists on receptor oligomerization. However, at present, the effects of ligand stimulation on GPCR oligomerization are not consistent. It has been found that agonists can promote or reduce GPCR oligomerization or are without effect on GPCR oligomerization (Angers et al., 2002; George et al., 2002; Pfleger and Eidne, 2005). In the case of the H_4R, we did not detect any significant difference in BRET signal if cells were treated with either the H_4R agonist histamine, the neutral H_4R antagonist iodophenpropit (Lim et al., 2005), or the inverse H_4R agonist thioperamide (Morse et al., 2001; Lim et al., 2005), suggesting that H_4R ligands do not modulate H_4R homo-oligomerization. Likewise, no agonist- or inverse agonist-induced modulation of H_4R oligomerization was detected in the *tr*-FRET assay. Patel et al. (2002) reported that agonist-induced oligomerization of somatostatin receptors was only detected at physiological expression levels but not after overexpression. We therefore performed BRET experiments at various H_4R expression levels. First, it is noteworthy that already at an H_4R expression level of approximately 300 fmol/mg of protein, significant BRET signals can be observed. These data indicate that at physiological expression levels, the H_4R can indeed homo-oligomerize and corroborate our findings of H_4R dimers, detected on PHA blasts with our anti-H_4R antibody. Second, from the BRET experiments, we also conclude that also at low expression levels of the H_4Rs, homo-oligomerization is not affected by agonist stimulation. Nevertheless, one should be aware that results concerning ligand effects on dimerization obtained with these biophysical assays can be difficult to interpret, because agonist-induced changes in H_4R conformation could potentially influence the energy transfer between the energy acceptor and donor (Angers et al., 2000).

The H_4R has been linked to play a role in inflammation based on its expression pattern and recent findings, showing that the H_4R induces chemotaxis of eosinophils (O'Reilly et al., 2002; Buckland et al., 2003) and mast cells (Hofstra et al., 2003) and stimulates the release of interleukin-16 from $CD8^+$ T cells (Gantner et al., 2002) and the release of leukotriene B_4 in zymosan-challenged mice (Takeshita et al., 2003). The H_1R is colocalized with the H_4R in several white blood cells (Cameron et al., 1986; Morse et al., 2001) and plays a prominent role in inflammatory conditions (Giustizieri et al., 2004; Matsubara et al., 2005). Because both the H_1Rs (Carrillo et al., 2003; Bakker et al., 2004) and the H_4R (this study) are able to form homo-oligomers, we were prompted to study whether the H_4Rs can form hetero-oligomers with the H_1Rs. In fact, previous work with hetero-oligomeric opioid receptors has revealed that GPCR hetero-oligomerization brings an additional layer of complexity to the class of GPCR proteins (Bouvier, 2001; Devi, 2001; Franco et al., 2003; Waldhoer et al., 2005) but also offers opportunities to develop hetero-oligomeric-selective ligands (Waldhoer et al., 2005). Yet using *tr*-FRET assays, we were unable to detect H_1R-H_4R hetero-oligomers, suggesting that such GPCR hetero-oligomers are not present at the cell surface. In contrast to the *tr*-FRET experiments, we were able to detect an expression level-dependent formation of H_1R-H_4R hetero-oligomers using BRET. Distinct from the detection of H_4R homo-oligomers, H_1R-H_4R hetero-oligomers were only detected at high-expression levels, and we failed to detect hetero-oligomers at physiologically relevant conditions. Results from BRET saturation studies demonstrate a higher propensity for the formation of H_4R-H_4R homo-oligomers over H_1R-H_4R hetero-oligomers. We presume that the signal observed with BRET at high expression levels possibly originates from intracellular H_1R-H_4R hetero-oligomers. Whereas some receptors, such as the 5-hydroxytryptamine-1A receptor seem to readily form heteromeric receptors (Salim et al., 2002), our present H_4R data corroborate the idea that GPCR hetero-oligomerization is highly selective, as reported for the adrenergic receptors (Stanasila et al., 2003; Uberti et al., 2005) and the thyrotropin-releasing hormone receptors (Kroeger et al., 2001). Although hetero-oligomerization has been shown to occur even between receptors from different classes (Ferre et al., 2002), the relatively low homology (23%) between H_1R and H_4R (Oda et al., 2000) is apparently too low to readily form hetero-oligomers.

In conclusion, we have developed specific antibodies against the C terminus of the H_4R which allowed the detection of endogenously expressed H_4R proteins. This anti-hH_4R antibody is an important new molecular tool for studying the localization and function of the H_4R. Moreover, we determined by various methods that the H_4R constitutively forms cell surface homo-oligomers. Homodimeric H_4Rs are not only found using heterologous ex-

pression systems but are also present in PHA blasts and spleen lysates endogenously expressing H_4Rs. The formation of H_4R oligomers is not dependent on *N*-glycosylation or affected by ligand stimulation but is possibly destabilized by deglycosylation. Although H_1R-H_4R hetero-oligomers could be detected using BRET upon receptor overexpression, these hetero-oligomers are probably not present at the cell surface. Moreover, H_1R-H_4R hetero-oligomers were not found at physiologically relevant expression levels. Future studies will have to reveal whether the H_4R can form hetero-oligomers with other GPCR family members or if it preferentially exists as homo-oligomer.

References

Angers S, Salahpour A, and Bouvier M (2002) Dimerization: an emerging concept for G protein-coupled receptor ontogeny and function. *Annu Rev Pharmacol Toxicol* 42:409–435.

Angers S, Salahpour A, Joly E, Hilairet S, Chelsky D, Dennis M, and Bouvier M (2000) Detection of β_2-adrenergic receptor dimerization in living cells using bioluminescence resonance energy transfer (BRET). *Proc Natl Acad Sci USA* 97:3684–3689.

Bakker RA, Dees G, Carrillo JJ, Booth RG, Lopez-Gimenez JF, Milligan G, Strange PG, and Leurs R (2004) Domain swapping in the human histamine H_1 receptor. *J Pharmacol Exp Ther* 311:131–138.

Bakker RA, Lozada AF, van Marle A, Shenton FC, Drutel G, Karlstedt K, Hoffmann M, Lintunen M, Yamamoto Y, van Rijn RM, et al. (2006) Discovery of naturally occurring splice variants of the rat histamine h3 receptor that act as dominant-negative isoforms. *Mol Pharmacol* 69:1194–1206.

Bakker RA, Schoonus SB, Smit MJ, Timmerman H, and Leurs R (2001) Histamine H_1-receptor activation of nuclear factor-κB: roles for $G_{\beta\gamma}$- and $G_{\alpha q/11}$-subunits in constitutive and agonist-mediated signaling. *Mol Pharmacol* 60:1133–1142.

Baneres JL and Parello J (2003) Structure-based analysis of GPCR function: evidence for a novel pentameric assembly between the dimeric leukotriene B_4 receptor BLT1 and the G-protein. *J Mol Biol* 329:815–829.

Boute N, Jockers R, and Issad T (2002) The use of resonance energy transfer in high-throughput screening: BRET versus FRET. *Trends Pharmacol Sci* 23:351–354.

Bouvier M (2001) Oligomerization of G-protein-coupled transmitter receptors. *Nat Rev Neurosci* 2:274–286.

Bradford A, Barlow A, and Chazot PL (2005) Probing the differential effects of infrared light sources IR1072 and IR880 on human lymphocytes: evidence of selective cytoprotection by IR1072. *J Photochem Photobiol B* 81:9–14.

Bradford MM (1976) A rapid and sensitive method for the quantitation of microgram quantities of protein utilizing the principle of protein-dye binding. *Anal Biochem* 72:248–254.

Buckland KF, Williams TJ, and Conroy DM (2003) Histamine induces cytoskeletal changes in human eosinophils via the H_4 receptor. *Br J Pharmacol* 140:1117–1127.

Cameron W, Doyle K, and Rocklin RE (1986) Histamine type I (H_1) receptor radioligand binding studies on normal T cell subsets, B cells and monocytes. *J Immunol* 136:2116–2120.

Carrillo JJ, Pediani J, and Milligan G (2003) Dimers of class A G protein-coupled receptors function via agonist-mediated trans-activation of associated G proteins. *J Biol Chem* 278:42578–42587.

Chazot PL, Cik M, and Stephenson FA (1992) Immunological detection of the NMDAR1 glutamate receptor subunit expressed in embryonic kidney 293 cells and in rat brain. *J Neurochem* 59:1176–1178.

Chazot PL, Cik M, and Stephenson FA (1995) An investigation into the role of N-glycosylation in the functional expression of a recombinant heteromeric NMDA receptor. *Mol Membr Biol* 12:331–337.

Chazot PL, Coleman SK, Cik M, and Stephenson FA (1994) Molecular characterization of *N*-methyl-D-aspartate receptors expressed in mammalian cells yields evidence for the coexistence of three subunit types within a discrete receptor molecule. *J Biol Chem* 269:24403–24409.

Chazot PL, Hann V, Wilson C, Lees G, and Thompson CL (2001) Immunological identification of the mammalian H_3 histamine receptor in the mouse brain. *Neuroreport* 12:259–262.

Chazot PL, Pollard S, and Stephenson FA (1998) immunoprecipitation of receptors, in *General Neurochemical Techniques: Techniques in Vitro, Molecular* (Boulton A, Baker G, and Bateson A eds) pp 257–286, Humana Press Inc, Totowa.

de Esch IJ, Thurmond RL, Jongejan A, and Leurs R (2005) The histamine H_4 receptor as a new therapeutic target for inflammation. *Trends Pharmacol Sci* 26:462–469.

Devi LA (2001) Heterodimerization of G-protein-coupled receptors: pharmacology, signaling and trafficking. *Trends Pharmacol Sci* 22:532–537.

Ferre S, Karcz-Kubicha M, Hope BT, Popoli P, Burgueno J, Gutierrez MA, Casado V, Fuxe K, Goldberg SR, Lluis C, et al. (2002) Synergistic interaction between adenosine A_{2A} and glutamate $mGlu_5$ receptors: implications for striatal neuronal function. *Proc Natl Acad Sci USA* 99:11940–11945.

Fotiadis D, Liang Y, Filipek S, Saperstein DA, Engel A, and Palczewski K (2003) Atomic-force microscopy: rhodopsin dimers in native disc membranes. *Nature (Lond)* 421:127–128.

Franco R, Canals M, Marcellino D, Ferre S, Agnati L, Mallol J, Casado V, Ciruela F, Fuxe K, Lluis C, et al. (2003) Regulation of heptaspanning-membrane-receptor function by dimerization and clustering. *Trends Biochem Sci* 28:238–243.

Fukushima Y, Asano T, Saitoh T, Anai M, Funaki M, Ogihara T, Katagiri H, Matsuhashi N, Yazaki Y, and Sugano K (1997) Oligomer formation of histamine H_2 receptors expressed in Sf9 and COS7 cells. *FEBS Lett* 409:283–286.

Gantner F, Sakai K, Tusche MW, Cruikshank WW, Center DM, and Bacon KB (2002) Histamine H_4 and H_2 receptors control histamine-induced interleukin-16 release from human $CD8^+$ T cells. *J Pharmacol Exp Ther* 303:300–307.

George SR, O'Dowd BF, and Lee SP (2002) G-protein-coupled receptor oligomerization and its potential for drug discovery. *Nat Rev Drug Discov* 1:808–820.

Giustizieri ML, Albanesi C, Fluhr J, Gisondi P, Norgauer J, and Girolomoni G (2004) H_1 histamine receptor mediates inflammatory responses in human keratinocytes. *J Allergy Clin Immunol* 114:1176–1182.

Goldman LA, Cutrone EC, Kotenko SV, Krause CD, and Langer JA (1996) Modifications of vectors pEF-BOS, $pcDNA_1$ and $pcDNA_3$ result in improved convenience and expression. *Biotechniques* 21:1013–1015.

Hofstra CL, Desai PJ, Thurmond RL, and Fung-Leung WP (2003) Histamine H_4 receptor mediates chemotaxis and calcium mobilization of mast cells. *J Pharmacol Exp Ther* 305:1212–1221.

Jones KA, Borowsky B, Tamm JA, Craig DA, Durkin MM, Dai M, Yao WJ, Johnson M, Gunwaldsen C, Huang LY, et al. (1998) $GABA_B$ receptors function as a heteromeric assembly of the subunits $GABA_BR1$ and $GABA_BR2$. *Nature (Lond)* 396:674–679.

Kroeger KM, Hanyaloglu AC, Seeber RM, Miles LE, and Eidne KA (2001) Constitutive and agonist-dependent homo-oligomerization of the thyrotropin-releasing hormone receptor. Detection in living cells using bioluminescence resonance energy transfer. *J Biol Chem* 276:12736–12743.

Lambright DG, Sondek J, Bohm A, Skiba NP, Hamm HE, and Sigler PB (1996) The 2.0 Å crystal structure of a heterotrimeric G protein. *Nature (Lond)* 379:311–319.

Lim HD, van Rijn RM, Ling P, Bakker RA, Thurmond RL, and Leurs R (2005) Evaluation of histamine H_1-, H_2- and H_3-receptor ligands at the human histamine H_4 receptor: identification of 4-methylhistamine as the first potent and selective H_4 receptor agonist. *J Pharmacol Exp Ther* 314:1310–1321.

Liu C, Ma X, Jiang X, Wilson SJ, Hofstra CL, Blevitt J, Pyati J, Li X, Chai W, Carruthers N, et al. (2001) Cloning and pharmacological characterization of a fourth histamine receptor (H_4) expressed in bone marrow. *Mol Pharmacol* 59:420–426.

Matsubara M, Tamura T, Ohmori K, and Hasegawa K (2005) Histamine H_1 receptor antagonist blocks histamine-induced proinflammatory cytokine production through inhibition of Ca^{2+}-dependent protein kinase C, Raf/MEK/ERK and IKK/I κB/NF-κB signal cascades. *Biochem Pharmacol* 69:433–449.

Michineau S, Alhenc-Gelas F, and Rajerison RM (2006) Human bradykinin B2 receptor sialylation and N-glycosylation participate with disulfide bonding in surface receptor dimerization. *Biochemistry* 45:2699–2707.

Morse KL, Behan J, Laz TM, West RE Jr, Greenfeder SA, Anthes JC, Umland S, Wan Y, Hipkin RW, Gonsiorek W, et al. (2001) Cloning and characterization of a novel human histamine receptor. *J Pharmacol Exp Ther* 296:1058–1066.

Nakamura T, Itadani H, Hidaka Y, Ohta M, and Tanaka K (2000) Molecular cloning and characterization of a new human histamine receptor, HH4R. *Biochem Biophys Res Commun* 279:615–620.

Nelson G, Chandrashekar J, Hoon MA, Feng L, Zhao G, Ryba NJ, and Zuker CS (2002) An amino-acid taste receptor. *Nature (Lond)* 416:199–202.

Nelson G, Hoon MA, Chandrashekar J, Zhang Y, Ryba NJ, and Zuker CS (2001) Mammalian sweet taste receptors. *Cell* 106:381–390.

Nguyen T, Shapiro DA, George SR, Setola V, Lee DK, Cheng R, Rauser L, Lee SP, Lynch KR, Roth BL, et al. (2001) Discovery of a novel member of the histamine receptor family. *Mol Pharmacol* 59:427–433.

Oda T, Morikawa N, Saito Y, Masuho Y, and Matsumoto S (2000) Molecular cloning and characterization of a novel type of histamine receptor preferentially expressed in leukocytes. *J Biol Chem* 275:36781–36786.

O'Reilly M, Alpert R, Jenkinson S, Gladue RP, Foo S, Trim S, Peter B, Trevethick M, and Fidock M (2002) Identification of a histamine H_4 receptor on human eosinophils–role in eosinophil chemotaxis. *J Recept Signal Transduct Res* 22:431–448.

Patel RC, Lange DC, and Patel YC (2002) Photobleaching fluorescence resonance energy transfer reveals ligand-induced oligomer formation of human somatostatin receptor subtypes. *Methods* 27:340–348.

Pfleger KD and Eidne KA (2005) Monitoring the formation of dynamic G-protein-coupled receptor-protein complexes in living cells. *Biochem J* 385:625–637.

Salim K, Fenton T, Bacha J, Urien-Rodriguez H, Bonnert T, Skynner HA, Watts E, Kerby J, Heald A, Beer M, et al. (2002) Oligomerization of G-protein-coupled receptors shown by selective co-immunoprecipitation. *J Biol Chem* 277:15482–15485.

Shenton FC, Hann V, and Chazot PL (2005) Evidence for native and cloned H_3 histamine receptor higher oligomers. *Inflamm Res* 54 (Suppl 1):S48–S49.

Stanasila L, Perez JB, Vogel H, and Cotecchia S (2003) Oligomerization of the α1a- and α1b-adrenergic receptor subtypes. Potential implications in receptor internalization. *J Biol Chem* 278:40239–40251.

Suda K, Filipek S, Palczewski K, Engel A, and Fotiadis D (2004) The supramolecular structure of the GPCR rhodopsin in solution and native disc membranes. *Mol Membr Biol* 21:435–446.

Takeshita K, Sakai K, Bacon KB, and Gantner F (2003) Critical role of histamine H_4 receptor in leukotriene B_4 production and mast cell-dependent neutrophil recruitment induced by zymosan in vivo. *J Pharmacol Exp Ther* 307:1072–1078.

Terrillon S and Bouvier M (2004) Roles of G-protein-coupled receptor dimerization. *EMBO (Eur Mol Biol Organ) Rep* 5:30–34.

Thurmond RL, Desai PJ, Dunford PJ, Fung-Leung WP, Hofstra CL, Jiang W, Nguyen S, Riley JP, Sun S, Williams KN, et al. (2004) A potent and selective histamine H_4 receptor antagonist with anti-inflammatory properties. *J Pharmacol Exp Ther* 309:404–413.

Uberti MA, Hague C, Oller H, Minneman KP, and Hall RA (2005) Heterodimerization with beta2-adrenergic receptors promotes surface expression and functional activity of α1D-adrenergic receptors. *J Pharmacol Exp Ther* 313:16–23.

Waldhoer M, Fong J, Jones RM, Lunzer MM, Sharma SK, Kostenis E, Portoghese PS, and Whistler JL (2005) From the cover: a heterodimer-selective agonist shows in vivo relevance of G protein-coupled receptor dimers. *Proc Natl Acad Sci USA* 102:9050–9055.

Zhu Y, Michalovich D, Wu H, Tan KB, Dytko GM, Mannan IJ, Boyce R, Alston J, Tierney LA, Li X, et al. (2001) Cloning, expression and pharmacological characterization of a novel human histamine receptor. *Mol Pharmacol* 59:434–441.

Address correspondence to: Dr. R. Leurs, Leiden/Amsterdam Center for Drug Research, Department of Medicinal Chemistry, Vrije Universiteit Amsterdam, De Boelelaan 1083, 1081 HV Amsterdam, The Netherlands. E-mail: r.leurs@few.vu.nl

Original article

Histamine downregulates monocyte CCL2 production through the histamine H_4 receptor

Dorothea Dijkstra, MSc,[a] Rob Leurs, PhD,[b] Paul Chazot, PhD,[c] Fiona C. Shenton, MSc,[c] Holger Stark, PhD,[d] Thomas Werfel, MD,[a] and Ralf Gutzmer, MD[a] *Hannover and Frankfurt/Main, Germany, Amsterdam, The Netherlands, and Durham, United Kingdom*

Background: The expression of the recently cloned histamine H_4 receptor (H_4R) by leukocytes suggests a role in immunomodulation.
Objective: The expression and function of the H_4R on human monocytes obtained from peripheral blood was investigated.
Methods: H_4R expression was studied by using flow cytometry. Effects of H_4R stimulation on Ca^{2+} mobilization was determined fluorometrically, CCL2 production was determined by means of ELISA, intracellular CCL2 staining was measured with flow cytometry, and CCL2 mRNA was measured by using real-time quantitative LightCycler PCR. The relevance of CCL2 production was determined in chemotaxis transmigration assays.
Results: H_4R protein was expressed by monocytes and upregulated by IFN-γ. H_4R agonists (clobenpropit and 4-methylhistamine) induce a Ca^{2+} mobilization in monocytes, which could be blocked with the selective H_4R antagonist JNJ7777120. Furthermore, H_4R agonists downregulated CCL2 protein production. This effect could also be blocked by JNJ7777120. Supernatants of H_4R agonist–stimulated monocytes attracted less monocytes in transmigration assays. The downregulation of CCL2 production was regulated at different levels. First, the synthesis of CCL2 mRNA was significantly decreased. Second, intracellular staining suggested an inhibition of CCL2 secretion after stimulation with H_4R agonists.
Conclusion: Human monocytes express the H_4R, and its stimulation leads to a Ca^{2+} influx and an inhibition of CCL2 production, resulting in a reduction of monocyte recruitment.
Clinical implications: The H_4R could represent an important anti-inflammatory receptor on monocytes and could be an interesting target for drug development. (J Allergy Clin Immunol ■■■■;■■■:■■■-■■■.)

Key words: Histamine, monocytes, H_4 receptor, CCL2

Histamine is an important mediator of allergic reactions. In the periphery it is released mainly by mast cells[1] and basophils.[2] The effects of histamine are diverse and mediated through 4 known G-protein–coupled receptors, the histamine H_1, H_2, H_3, and H_4 receptors (H_4Rs). The recently discovered and cloned histamine H_4R[3-8] is expressed by leukocytes and is thought to have an immunomodulatory function. Several functions of the histamine H_4R expressed by different cell types have been found. In particular directly on chemotaxis of mast cells[9] and eosinophils[10,11] and indirectly, through leukotriene B_4 produced by mast cells, on neutrophil mobilization from the bone marrow.[12] Recently, we showed that monocyte-derived dendritic cells (DCs) are chemoattracted through the histamine H_4R, and stimulation of the H_4R led to suppression of IL-12p70 production.[13] Furthermore, effects on T lymphocytes have also been observed. Agonist stimulation of the H_4R upregulates IL-16 release by $CD8^+$ T lymphocytes.[14] The importance of the H_4R in modulation of $CD4^+$ T-lymphocyte activation and T_H2 responses in a murine model of asthma has been shown.[15] These results indicate that the H_4R is an important modulator during DC–T-lymphocyte interactions. Because the monocyte ($CD14^+$) fraction of PBMCs contain the direct precursors of DC- and skin-associated macrophages, we investigated the expression and function of the H_4R on monocytes. We demonstrate that the H_4R is expressed and upregulated by IFN-γ. In microarray experiments the mRNA expression of several cytokines and chemokines after incubation with the most specific H_4R agonist, 4-methylhistamine,[16] was investigated (results not shown). The results indicated an inhibition of CCL2 mRNA and prompted us to investigate the effect of histamine on the expression of this chemokine in more detail because it plays an important role in allergic inflammation. In mice lacking CCL2, macrophage attraction to sites of inflammation was disturbed, and antigen-specific T_H1 cells were producing less IFN-γ.[17] In mice lacking CCR2 (the receptor for CCL2), an enhanced airway T_H2 response was found (eg, eosinophilia, Ig subclass switching, and IL-5 production).[18] In human subjects CCL2 production of keratinocytes was enhanced by the

From [a]the Department of Dermatology and Allergology, Hannover Medical University; [b]Leiden/Amsterdam Center for Drug Research, Department of Medicinal Chemistry, Vrije Universiteit Amsterdam; [c]Durham University, Centre for Integrative Neuroscience, School of Biological and Biomedical Sciences; and [d]Institute for Pharmaceutical Chemistry, ZAFES, Johann Wolfgang Goethe-University, Frankfurt/Main.

Supported by grants from the Deutsche Forschungsgemeinschaft (DFG Gu434/5-1) and SFB 566A6 and Wellcome Trust (United Kingdom).
Disclosure of potential conflict of interest: The authors have declared that they have no conflict of interest.
Received for publication December 22, 2006; revised February 26, 2007; accepted for publication March 22, 2007.

Reprint requests: Dorothea Dijkstra, MSc, Department of Dermatology and Allergology, Hannover Medical University, Ricklinger Str. 5, D-30449, Hannover, Germany. E-mail: dijkstra.dorothea@mh-hannover.de.

0091-6749/$32.00

doi:10.1016/j.jaci.2007.03.024

Abbreviations used
DC: Dendritic cell
GAPDH: Reduced glyceraldehyde-phosphate dehydrogenase
H_4R: Histamine H_4 receptor
MMP: Matrix metalloproteinase

T_H2 cytokine IL-13, which is found, for example, in lesions of atopic dermatitis.[19] Furthermore, a polymorphism (−2518G) in the gene regulatory region of CCL2, which resulted in a higher expression of CCL2, was found associated to a more severe asthma phenotype in children.[20] Thus CCL2 is induced by and contributes to a T_H2 environment in allergic inflammation and leads to migration of cells found in allergic inflammation, such as monocytes, activated T lymphocytes, and natural killer cells, which express CCR2.[21] Here we show that histamine H_4R stimulation results in the downregulation of spontaneous CCL2 production in monocytes. This could represent a negative feedback mechanism to avoid an overwhelming T_H2 environment in case of a persistent histamine release at sites of allergic inflammation and could contribute to the shift from T_H2 to T_H1 observed in the transition from acute to chronic allergic inflammation (eg, in atopic dermatitis).[22]

METHODS

Monocyte enrichment and isolation

Buffy coats from anonymous healthy blood donors obtained from the local blood bank were used. The buffy coats were disposed of by the blood bank after thrombocyte preparation. Total IgE levels, as well as levels IgE against common aeroallergens (sx-1 screening test), were measured (CAP System; Pharmacia, Freiburg, Germany) and were less than the normal limits of 100 kU/L and 0.35 kU/L, respectively. In case of increased IgE levels, the patient was excluded from the study. Human PBMCs were separated from the buffy coats by means of density gradient centrifugation on Lymphoprep (Fresenius Kabi Norge AS, Oslo, Norway).

PBMCs were then cultured in supplemented Iscove medium on flat-bottom plates (6-well plate: 1×10^7 cells per well for chemotaxis-supernatants; 24-well plate: 1×10^6 cells per well for ELISA or intracellular CCL2 measurements) for 1 hour (37°C, 5% CO_2, humidified atmosphere). Then the nonadherent cells were removed by washing with PBS. The adherent cells (enriched monocytes, purity ≥85%) were further cultured (and stimulated with H_4R agonists or other substances used in the H_4R regulation studies) in supplemented RPMI 1640 medium (6-well plate: 2 mL; 24-well plate: 400 μL; 96-well plate: 250 μL). Adherent cells were counted after detaching them with trypsin-EDTA (Pan Biotech GmbH, Aidenbach, Germany). The number of adherent cells was generally around 2.5×10^5 cells per well in a 24-well plate. The purity of the adherent monocytes was 85% minimum. This was controlled by using flow cytometry to determine $CD14^+$ cells in each experiment. Contaminating cells were evaluated in selected experiments by means of flow cytometry and included minimal numbers of T lymphocytes ($CD3^+$ cells, <0.5%), B lymphocytes (CD19, <0.5%), and natural killer cells (CD56, <3.0%), whereas granulocytes (CD16) were absent. Macrophages (CD206) and DCs (CD1a) represented around 10% of the nonmonocyte fraction. The viability of trypsinated cells (used for the intracellular CCL2 staining and staining controls only) was tested in each experiment by staining with trypan blue and was greater than 95%. In experiments for quantitative PCR, we isolated monocytes by means of magnetic cell sorting (MACS; Monocyte isolation kit II; Miltenyi Biotec Inc, Bergisch Gladbach, Germany; monocyte purity ≥95%), adhered the cells (2×10^5 cells per well on a 96-well flat-bottom plate) for 1 hour (37°C, 5% CO_2, humidified atmosphere) in supplemented Iscove medium, and cultured them in supplemented RPMI medium.

Media

For the adherence of monocytes, Iscove medium supplemented with AB serum (5% vol/vol), nonessential salts (1% wt/vol), L-glutamine (1% wt/vol), penicillin/streptomycin (1% wt/vol), and gentamicin (0.5% wt/vol) was used. For culturing monocytes after adherence, we used RPMI 1640 medium supplemented with FCS (5% vol/vol), 12 mmol/L Hepes, L-glutamine (1% wt/vol), and penicillin/streptomycin (1% wt/vol; all media and supplements were from Biochrom AG, Berlin, Germany).

Chemicals

Clobenpropit was obtained from Sigma-Aldrich (Deisenhofen, Germany). 4-Methylhistamine was kindly provided by R. Leurs and synthesized in the Department of Pharmacochemistry of the Vrije Universiteit Amsterdam in The Netherlands, as described previously.[16] JNJ7777120 was synthesized by H. Stark from the Johann Wolfgang Goethe University in Frankfurt/Main, Germany, as described previously.[23] GM6001[24] was obtained from Chemikon (Hampshire, United Kingdom).

The polyclonal rabbit anti-human H_4R antibody and its antigenic peptide were prepared by F. C. Shenton and P. Chazot from Durham University, United Kingdom, and was described previously.[25] The antibody recognizes the amino acid sequence (374-390) that is positioned in the C-terminal tail of the H_4R. Neutralizing anti-CCL2 was obtained from R&D Systems (Wiesbaden, Germany). CCL2 was obtained from TebuBio (Offenbach, Germany).

H_4R (amino acid 374-390) staining

Cells were stained according to the protocol and with the reagents provided by BD Biosciences (Heidelberg, Germany) for intracellular epitope-directed antibodies. In brief, cells were fixed and permeabilized. Subsequently, the cells were labeled with (1) H_4R antibody, (2) polyclonal rabbit isotype antibody, or (3) H_4R antibody preincubated with a 10-fold higher concentration of antigenic oligopeptide used to generate the antibody. This was followed by labeling with goat anti-rabbit antibody conjugated with biotin (Jackson ImmunoResearch Laboratories, Suffolk, England). Subsequently, staining was performed with fluorescein isothiocyanate–coupled streptavidin, and the H_4R positivity of the cells was quantified by means of flow cytometry (FACS Calibur; Becton Dickinson, Heidelberg, Germany).

Calcium mobilization assay

Monocytes were plated after isolation by means of magnetic cell sorting (Miltenyi Biotec, Inc) and adhered on flat-bottom 96-well plates (2.5×10^5 cells per well). Then they were labeled with FLUO-4 according to the manufacturer's description (Invitrogen GmbH, Karlsruhe, Germany). Calcium mobilization was measured in a FluoStar plate reader (BMG Lab Technologies GmbH, Jena, Germany). Fluorescence (excitation, 485 nm; emission, 520 nm) was measured per second for 50 seconds, and at a time of 5 seconds, the H_4R ligands histamine, clobenpropit, and 4-methylhistamine (10^{-5} mol/L) were added to the cells. A calcium ionophore (20 nmol/L A23187, Sigma) was used as a positive control. JNJ7777120 (10^{-5} mol/L) was added to respective wells 30 minutes before the measurements.

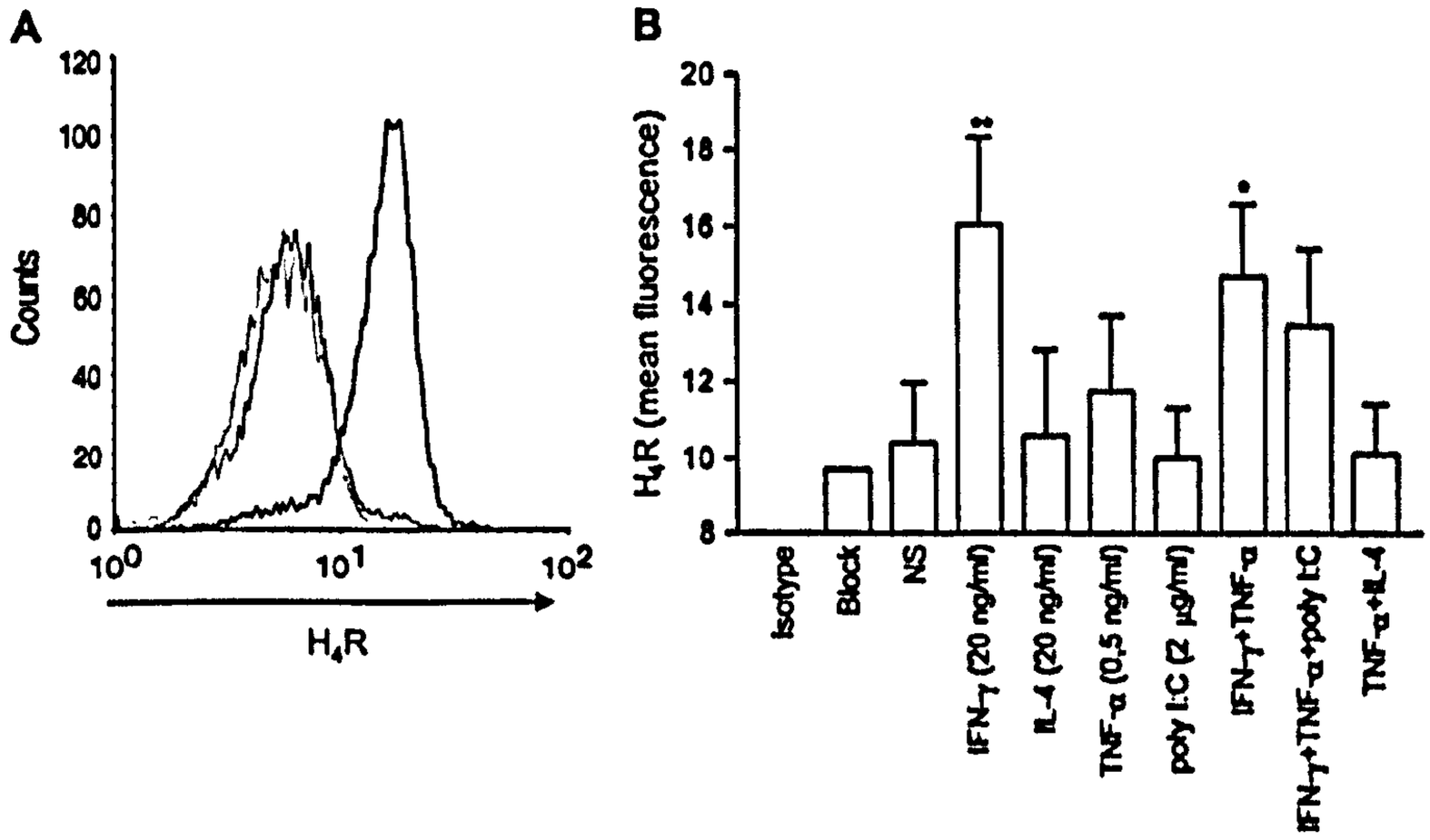

FIG 1. The H_4R is expressed by monocytes and upregulated by IFN-γ. A, Staining of monocytes with H_4R *(solid, thick line)*, isotype *(dotted line)*, and blocked H_4R antibody *(solid, thin line)*. B, H_4R protein expression after 48 hours' incubation with different ligands. Averages and SDs of 3 experiments are shown (statistical test: ANOVA). *NS*, Nonstimulated cells.

CCL2 ELISA

CCL2 levels were investigated by using a CCL2 sandwich ELISA with a lower detection limit of 8 pg/mL and a highest detection limit of 3000 pg/mL. For the CCL2 ELISA (TebuBio), PBMCs were plated in supplemented Iscove medium on a 24-well plate (1×10^6 cells per well/250 μL). Monocytes were allowed to adhere for 1 hour, as previously described, and subsequently washed vigorously with PBS. Adherent cells were incubated in RPMI with ligands at the indicated concentrations for 4, 24, and 48 hours; supernatants were taken; and CCL2 was determined according to the manufacturer's instructions. The plate was read at a wavelength of 405 nm on a FluoStar plate reader (BMG Lab Technologies, GmbH).

CCL2 intracellular staining

Adherent cells (from 1×10^6 PBMCs per well) were stimulated with 10^{-5} M H_4R ligands for 4 or 48 hours to measure amounts of intracellular CCL2. Cells were detached with trypsin-EDTA at 37°C, and the reactions were stopped with an equal volume of heat-inactivated FCS after 10 minutes. Then the cells were washed twice with PBS, and intracellular CCL2 was stained according to the protocol provided by BD Biosciences for intracellular staining. In brief, cells were fixed and permeabilized and then stained with the allophycocyanin-labeled anti-CCL2 antibody (50 ng/mL, IgG2B, clone 23002) or an allophycocyanin-labeled isotype control antibody (IgG2B) for 30 minutes at 4°C. The cells were washed, and CCL2 positivity was quantified by means of flow cytometry.

CCL2 quantitative PCR

Monocytes were isolated by means of magnetic cell sorting (Miltenyi Biotec, Inc) and then adhered on flat-bottom 96-well plates (2×10^5 cells/200 μL), as previously described. After transfer to supplemented RPMI, monocytes were stimulated with ligands for 4 hours. Total RNA was isolated, according to the manufacturer's instructions, with the High Pure mRNA Isolation kit (Roche Molecular Biochemicals, Mannheim, Germany). The cDNA was synthesized by means of reverse transcription (Quantitect reverse transcription kit; Qiagen, Hilden, Germany). Real-time quantitative PCR was performed with Quantitect primer assays for CCL2 (QT00212730) and reduced glyceraldehyde-phosphate dehydrogenase (GAPDH; QT00079247) by using SYBR Green, according to the manufacturer's instructions (Qiagen). A genomic DNA digestion was included in this kit.

The following settings in the LightCycler PCR were used. An initial activation step of 15 minutes at 95°C and a ramp of 20°C/s was followed by 3-step cycling (42 cycles): denaturation; 15 seconds at 94°C, annealing; 20 seconds at 55°C, extension; and 20 seconds at 72°C (all 3 with a ramp of 2°C/s). A melting curve was recorded by cooling the samples down to 60°C and then increasing the temperature to 95°C (ramp, 2°C/s). The amounts of CCL2 relative to the amount of the reference GAPDH in the same sample was calculated by using the relative quantification approach with the software provided by the manufacturer (Roche). Mathematically, the result for each sample is expressed as the ratio of CCL2 and GAPDH derived from the crossing points, which are obtained in the Lightcycler software (version 1.0, Roche). In addition, because the basal levels of CCL2 were different per patient, the data were normalized to the CCL2 level in the nonstimulated sample (100%). The values obtained for H_4R agonist-stimulated monocytes were then expressed as the percentage of the nonstimulated monocytes.

Chemotaxis assay

Chemotaxis of monocytes was measured over polycarbonate membranes with a 5-μm pore diameter (Corning, Inc/Costar, NY). A 600-μL supernatant from cultured adhered monocytes (with 10^{-5} mol/L stimuli and neutralizing anti-CCL2 antibody, as indicated in the text) was used as a chemoattractant in the lower chamber. The upper chamber with the membrane was filled with 250 μL of medium with 10^6 isolated monocytes. Chemotaxis was allowed for 1.5 hours, and the number of transmigrated cells was counted after staining with trypan blue (Sigma-Aldrich) in a Burker-Türk counting chamber. Controls were conducted as described in the text and figures.

Statistics

Paired *t* tests and ANOVA (the Bonferonni multiple comparisons test) were used, and a *P* value of less than .05 was regarded as significant ($P < .05$ was labeled with an asterisk, and $P < .005$ was labeled with a double

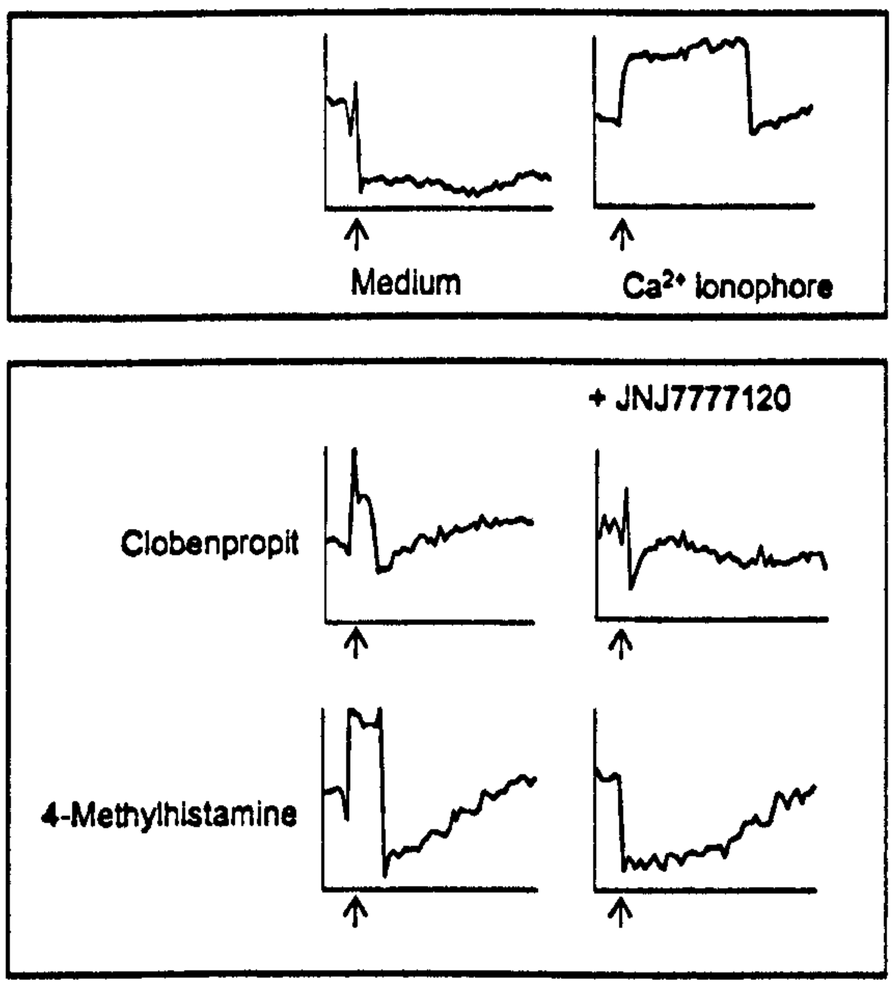

FIG 2. Histamine, 10^{-5} mol/L, induces calcium mobilization in monocytes through the H_4R. JNJ7777120 at 10^{-5} mol/L blocks this effect. Injection of the ligands was at a time of 5 seconds *(arrows)*, and FLUO-4 fluorescence was measured for 40 seconds. A representative of 3 experiments is shown.

asterisk). For the statistical analyses, the program GraphPad Prism, version 3.02 (GraphPad Software, Inc, San Diego, Calif), was used.

RESULTS

Expression of the H_4R in monocytes

Monocytes have been shown to express the H_4R at the mRNA level, as described by us[13] and others.[6] Here we showed H_4R protein expression on monocytes by means of flow cytometry after staining with a selective H_4R antibody directed against the C-terminal tail.[25] The specificity of the immunoreactivity was controlled by blocking the staining of the H_4R antibody with the respective peptide used to generate the antibody (Fig 1, *A*).

Upregulation of H_4R expression by IFN-γ

The regulation of H_4R protein expression was investigated after incubation with various ligands, such as IFN-γ (20 ng/mL), IL-4 (20 ng/mL), TNF-α (0.5 ng/mL), and the Toll-like receptor 3 ligand poly I:C (2 μg/mL), as well as combinations of these. The H_4R expression was measured by means of antibody staining, followed by flow cytometry. We found that IFN-γ upregulated the H_4R significantly at the protein level (Fig 1, *B*). In contrast, IL-4, TNF-α, and poly I:C or combinations of these did not regulate H_4R protein expression.

Calcium influx

The H_4R agonists histamine, clobenpropit, and 4-methylhistamine[16] were all able to stimulate calcium mobilization in monocytes. The effects caused by 10^{-5} mol/L clobenpropit and 4-methylhistamine were blocked by 10^{-5} mol/L JNJ7777120,[26] the specific H_4R blocker (Fig 2).

H_4R agonists inhibit monocyte CCL2 production dose dependently

Monocytes synthesize CCL2 spontaneously.[27] Histamine, 4-methylhistamine, and clobenpropit as H_4R agonists dose-dependently and effectively inhibited CCL2 production with different inhibitory concentration of 50% values (4-methylhistamine > histamine > clobenpropit; Fig 3, *A*). The inhibition of CCL2 production by histamine and the H_4R agonists clobenpropit and 4-methylhistamine was already seen after 4 hours of incubation and was consistent after 24 and 48 hours of incubation (Fig 3, *B*). This effect was inhibited by the specific H_4R antagonist JNJ7777120 at 10^{-5} mol/L. The amount of CCL2 produced by nonstimulated monocytes was increasing with time (Fig 3, *C*). In some experiments, also TNF-α was measured (results not shown). The cells did not spontaneously produce this inflammatory cytokine, demonstrating that the adherent cells were not activated during this isolation method.

Histamine inhibits CCL2 synthesis and secretion

We investigated the mechanism of CCL2 downregulation by the H_4R agonists. First, it was found that the mRNA synthesis for CCL2 was downregulated in monocytes incubated with H_4R agonists for 4 hours at 10^{-5} mol/L (Fig 4). Furthermore, when monocytes were incubated with the most selective H_4R ligand, 4-methylhistamine, for 4 hours at 10^{-5} mol/L, the intracellular level of CCL2, as determined by means of intracellular staining and flow cytometry, was higher than in nonstimulated cells (Fig 5). Second, after 48 hours of incubation, 10^{-5} mol/L of 4-methylhistamine inhibited intracellular CCL2 content compared with that seen in nonstimulated cells. The melting point of the amplified CCL2 was 74.7°C (see Fig E1 in the Online Repository at www.jacionline.org).

Matrix metalloproteinases (MMPs) 1, 3, or 8 are not responsible for the decrease of CCL2 levels

MMP1, MMP3, and MMP8 are known to degrade CCL2.[28] To test whether MMPs were responsible for the histamine-induced CCL2 decrease, we applied an appropriate inhibitor, GM6001.[24] This potent broad-spectrum MMP inhibitor was coincubated with the H_4R agonists. No change in the effect induced by H_4R agonists was seen (see Fig E2 in the Online Repository at www.jacionline.org) at GM6001 concentrations of 1 or 10 μM. This indicates that the lower CCL2 level was not caused by a higher MMP secretion by the monocytes.

Monocyte chemotaxis is lower toward supernatants of H_4R-stimulated monocytes

The medium from H_4R-stimulated monocytes (48 hours) attracted less monocytes than medium from nonstimulated monocytes (Fig 6). This effect was caused by CCL2 in the supernatants because chemotaxis toward nonstimulated monocyte medium was inhibited by a

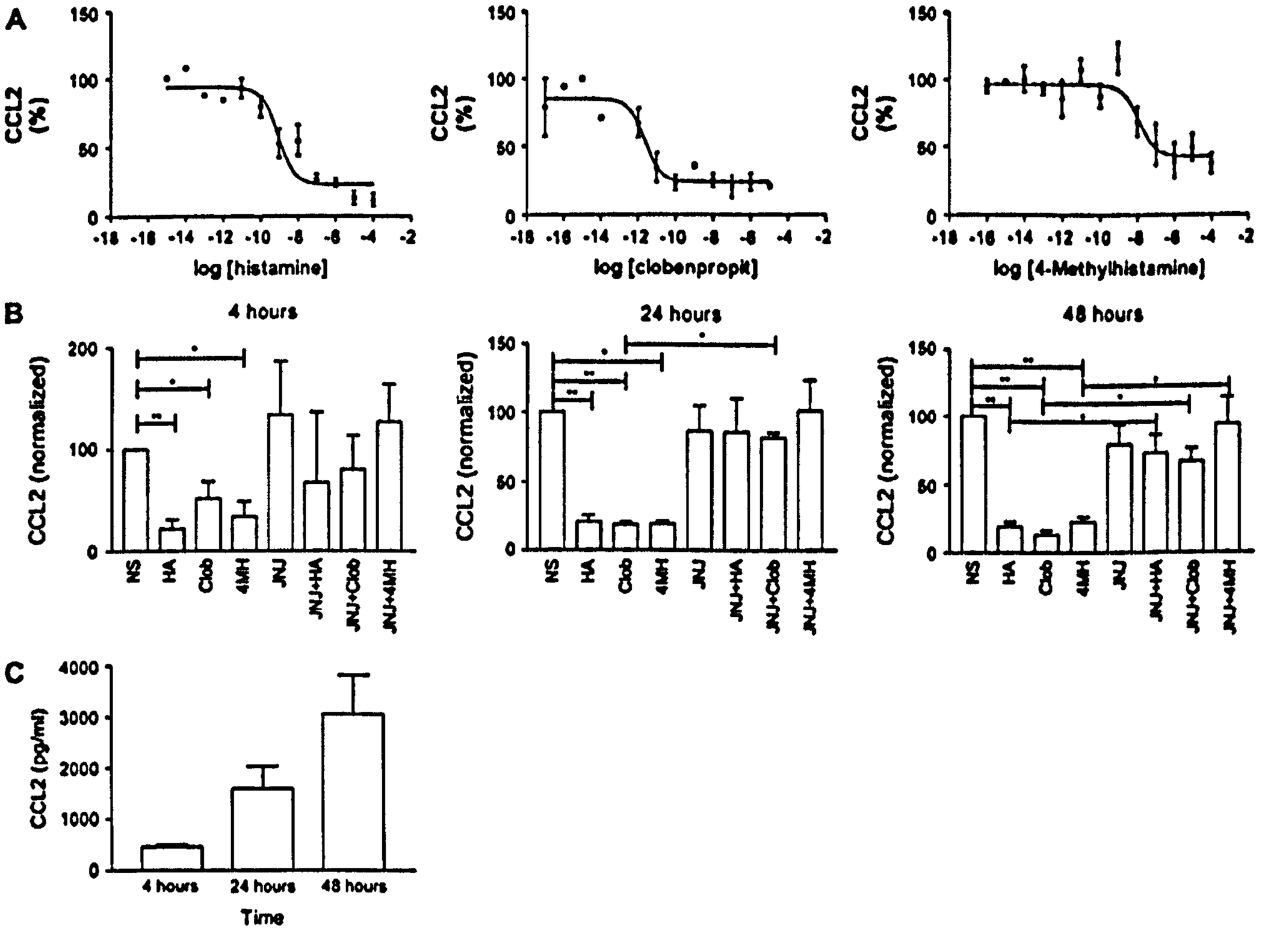

FIG 3. A, Dose dependency of CCL2 downregulation by histamine *(HA)*, clobenpropit *(Clob)*, and 4-methylhistamine *(4-MH)*. B, Inhibition of CCL2 production is blocked by JNJ7777120. C, Absolute CCL2 production at different incubation times. Data are normalized to nonstimulated *(NS)* values in Fig 3, *A* and *B*. Averages and SEMs (Fig 3, *A*), SDs (Fig 3, *B*), and SEMs (Fig 3, *C*) of at least 3 experiments are shown (statistical test: ANOVA).

neutralizing CCL2 antibody. Furthermore, addition of human recombinant CCL2 to the H_4R agonist–stimulated monocyte media could reinduce chemotaxis. As a control, fresh medium with histamine, clobenpropit, or 4-methylhistamine did not induce chemotaxis of monocytes.

DISCUSSION

Previously, it has been shown that the H_4R has important immunomodulatory effects on human T lymphocytes[14,29] and human DCs[13] *in vitro*. In a recent investigation using a murine model of allergic airway inflammation, an immunomodulatory role for the H_4R was also shown *in vivo*. H_4R knockout mice and mice treated with the H_4R inhibitor JNJ7777120 had decreased T-lymphocyte function, which was attributed to a decreased cytokine and chemokine production by DCs.[15] The monocyte cell fraction that contains the precursor cells for DCs and skin-associated macrophages has not been investigated thus far and was addressed in this study.

Here we show for the first time that human monocytes express the H_4R at the protein level, taking advantage of

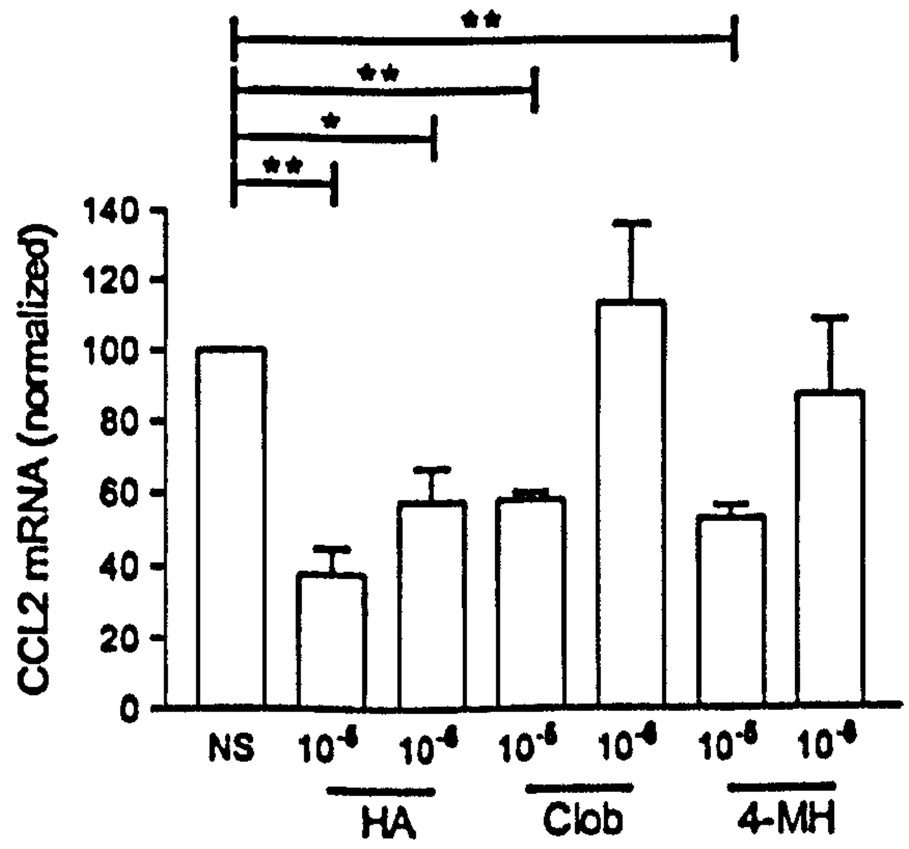

FIG 4. CCL2 mRNA synthesis is downregulated through histamine *(HA)* and the H_4R agonists clobenpropit *(Clob)* and 4-methylhistamine *(4-MH)*. Averages and SEMs of 6 experiments are shown (statistical test: ANOVA).

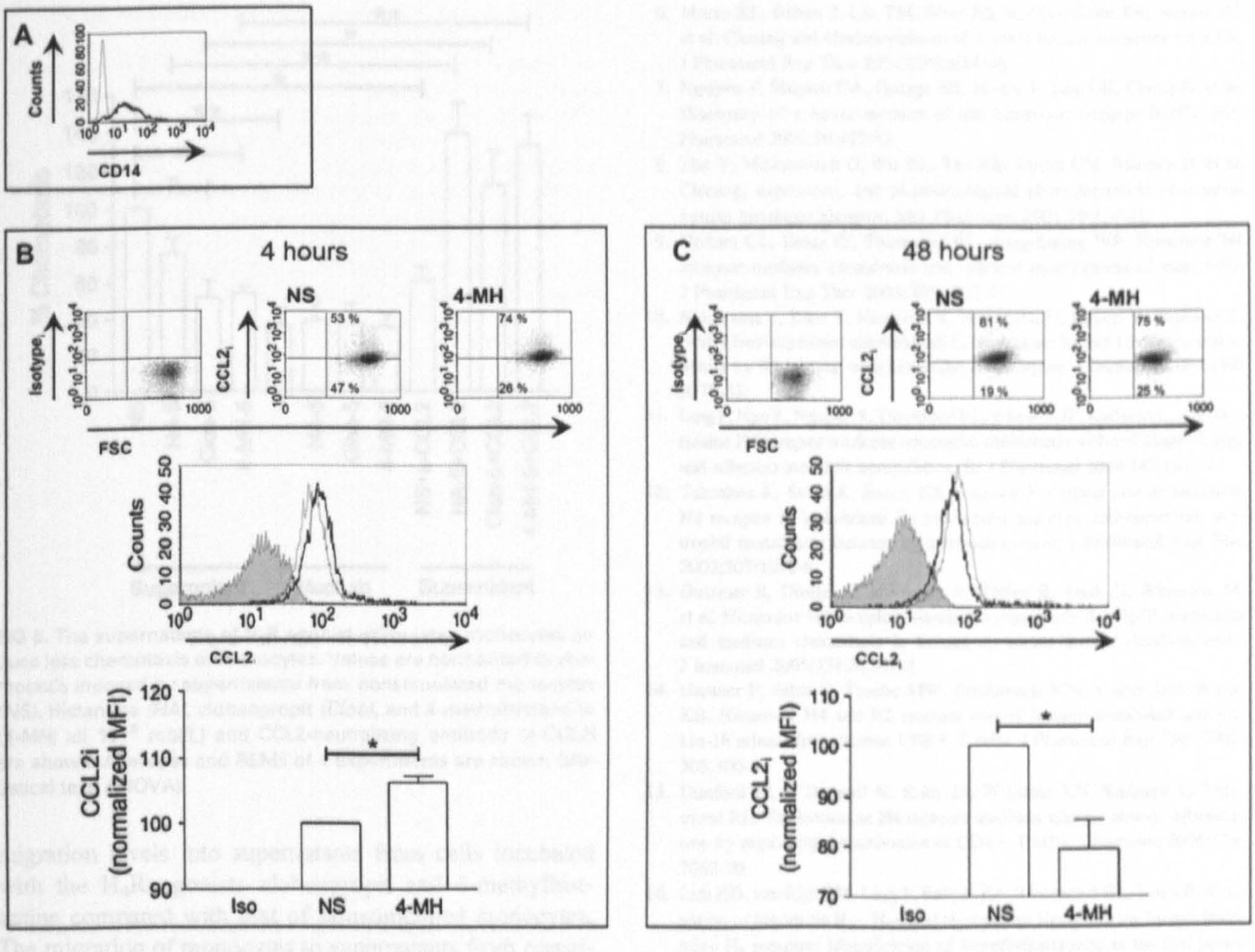

FIG 5. CD14 staining to determine the monocyte fraction within adherent cells **(A)**. Effect of 4-methylhistamine (*4-MH, thick solid line*) on intracellular CCL2 after 4 hours **(B)** and 48 hours **(C)** of incubation. *Thin solid line,* Nonstimulated cells *(NS); filled section,* isotype. A representative experiment and averages of normalized mean intracellular CCL2 fluorescence values and SEMs of 5 experiments are shown (statistical test: paired *t* test).

the newly developed anti-human H_4R antibody.[25] The expression of H_4R mRNA by monocytes has already been shown by our group[13] and another group,[6] but thus far, no function for the H_4R expressed by monocytes has been reported. Here we show that monocytes express H_4R protein and that IFN-γ upregulates the receptor. It has been shown previously that stimulation of the H_4R leads to a calcium mobilization in cells.[4,6,8,9] Also, in human monocytes H_4R agonists induced calcium mobilization, which was inhibited when the cells were coincubated with the H_4R-specific antagonist JNJ7777120.[23] Furthermore, we show that monocytes, on stimulation with the H_4R-specific agonists clobenpropit and 4-methylhistamine and the H_4R-nonspecific agonist histamine, downregulate CCL2 production dose dependently. JNJ7777120 was able to fully block this downregulation.

We found 2 possible mechanisms to explain the H_4R-mediated decrease in CCL2 levels produced by monocytes. First, an inhibition of synthesis was demonstrated by decreased CCL2 mRNA levels (4 hours of incubation), leading to decreased intracellular CCL2 levels (48 hours of incubation) when cells were incubated with H_4R agonist compared with levels seen in nonstimulated cells. Second, intracellular CCL2 protein levels were increased after 4 hours of incubation with 4-methylhistamine compared with levels in the nonstimulated control cells, demonstrating an inhibition of CCL2 secretion after H_4R agonist binding. In contrast, no evidence was found for CCL2 degradation by MMPs, which were previously shown to potently degrade CCL2.[21]

Histamine has not been shown previously to modulate the secretion of soluble mediators, although it is able to inhibit the production of IL-12p70 by monocytes and monocyte-derived DCs through the H_2R and H_4R,[13,30] as well as of TNF-α by macrophages and mast cells through the H_2R and H_3R.[31,32] The possible downregulation of secretion of these mediators, however, has not been investigated, and the decreased cytokine levels were explained by a downregulation of synthesis. In this study we provide evidence that CCL2 synthesis and secretion is indeed downregulated.

The supernatants of monocytes stimulated with H_4R agonists were used as chemoattractants in Boyden chamber assays. We observed significantly lower monocyte

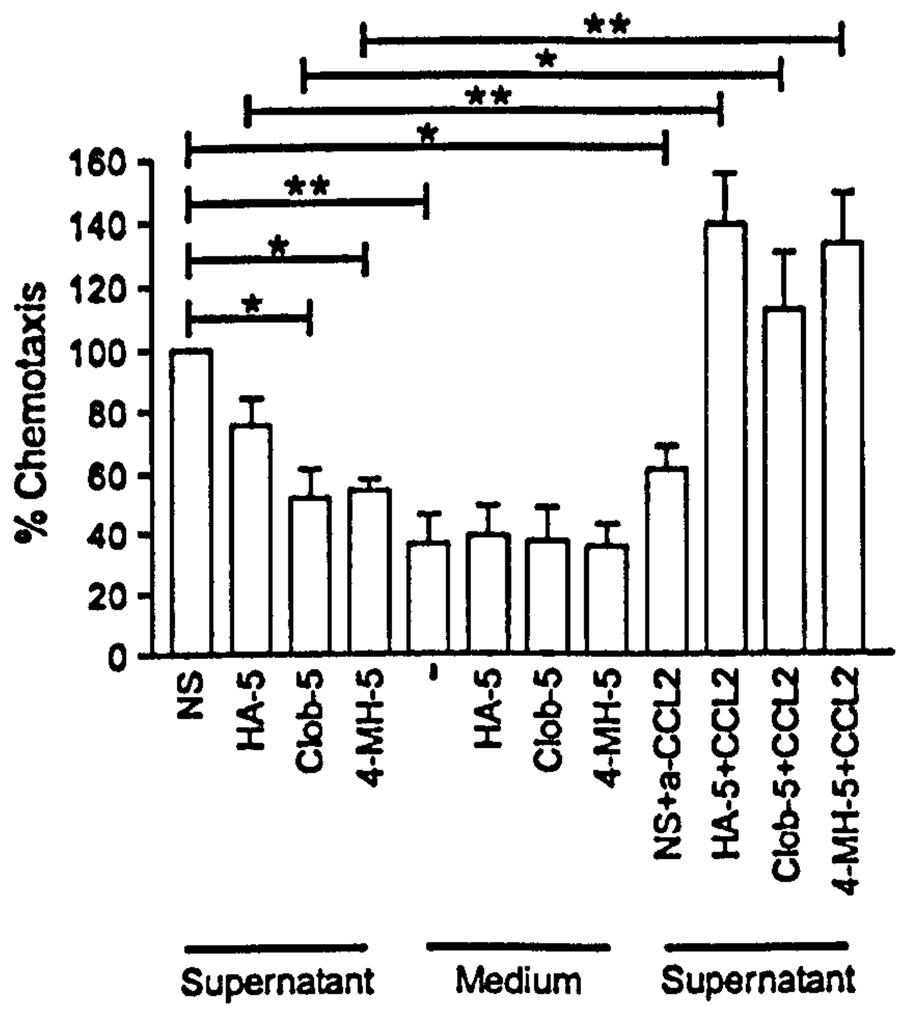

FIG 6. The supernatants of H_4R agonist–stimulated monocytes induce less chemotaxis of monocytes. Values are normalized to chemotaxis induced by supernatants from nonstimulated monocytes *(NS)*. Histamine *(HA)*, clobenpropit *(Clob)*, and 4-methylhistamine (*4-MH*; all 10^{-5} mol/L) and CCL2-neutralizing antibody *(a-CCL2)* are shown. Averages and SEMs of 4 experiments are shown (statistical test: ANOVA).

migration levels into supernatants from cells incubated with the H_4R agonists clobenpropit and 4-methylhistamine compared with that of nonstimulated monocytes. The migration of monocytes to supernatants from nonstimulated monocytes could be blocked close to media control levels by a CCL2-neutralizing antibody, which demonstrated the importance of CCL2 as a monocyte chemoattractant. The ligands themselves did not stimulate chemotaxis of freshly isolated monocytes, as was previously shown for monocyte-derived DCs,[13] eosinophils,[10,11] and mast cells.[9]

In summary, we showed, for the first time, that the H_4R protein is expressed by monocytes and that the H_4R is functional. This is demonstrated by the induction of a Ca^{2+} influx and the downregulation of CCL2. This extends our understanding of the immunologic role of the H_4R and the therapeutic potential of H_4R antagonists in inflammatory disorders.

REFERENCES

1. Riley JF, West GB. Histamine in tissue mast cells. J Physiol 1952;117: 72P-3P.
2. Dvorak AM, Morgan ES, Lichtenstein LM, MacGlashan DW Jr. Activated human basophils contain histamine in cytoplasmic vesicles. Int Arch Allergy Immunol 1994;105:8-11.
3. Nakamura T, Itadani H, Hidaka Y, Ohta M, Tanaka K. Molecular cloning and characterization of a new human histamine receptor, HH4R. Biochem Biophys Res Commun 2000;279:615-20.
4. Oda T, Morikawa N, Saito Y, Masuho Y, Matsumoto S-I. Molecular cloning and characterization of a novel type of histamine receptor preferentially expressed in leukocytes. J Biol Chem 2000;275:36781-6.
5. Liu C, Ma X-J, Jiang X, Wilson SJ, Hofstra CL, Blevitt J, et al. Cloning and pharmacological characterization of a fourth histamine receptor (H4) expressed in bone marrow. Mol Pharmacol 2001;59:420-6.
6. Morse KL, Behan J, Laz TM, West RE Jr, Greenfeder SA, Anthes JC, et al. Cloning and characterization of a novel human histamine receptor. J Pharmacol Exp Ther 2001;296:1058-66.
7. Nguyen T, Shapiro DA, George SR, Setola V, Lee DK, Cheng R, et al. Discovery of a novel member of the histamine receptor family. Mol Pharmacol 2001;59:427-33.
8. Zhu Y, Michalovich D, Wu HL, Tan KB, Dytko GM, Mannan IJ, et al. Cloning, expression, and pharmacological characterization of a novel human histamine receptor. Mol Pharmacol 2001;59:434-41.
9. Hofstra CL, Desai PJ, Thurmond RL, Fung-Leung WP. Histamine H4 receptor mediates chemotaxis and calcium mobilization of mast cells. J Pharmacol Exp Ther 2003;305:1212-21.
10. Nakayama T, Kato Y, Hieshima K, Nagakubo D, Kunori Y, Fujisawa T, et al. Liver-expressed chemokine/CC chemokine ligand 16 attracts eosinophils by interacting with histamine H4 receptor. J Immunol 2004;173: 2078-83.
11. Ling P, Ngo K, Nguyen S, Thurmond RL, Edwards JP, Karlsson L, et al. Histamine H4 receptor mediates eosinophil chemotaxis with cell shape change and adhesion molecule upregulation. Br J Pharmacol 2004;142:161-71.
12. Takeshita K, Sakai K, Bacon KB, Gantner F. Critical role of histamine H4 receptor in leukotriene B4 production and mast cell-dependent neutrophil recruitment induced by zymosan in vivo. J Pharmacol Exp Ther 2003;307:1072-8.
13. Gutzmer R, Diestel C, Mommert S, Köther B, Stark H, Wittmann M, et al. Histamine H4 receptor stimulation suppresses IL-12p70 production and mediates chemotaxis in human monocyte-derived dendritic cells. J Immunol 2005;174:5224-32.
14. Gantner F, Sakai K, Tusche MW, Cruikshank WW, Center DM, Bacon KB. Histamine H4 and H2 receptor control histamine-induced interleukin-16 release from human CD8+ T cells. J Pharmacol Exp Ther 2002; 303:300-7.
15. Dunford PJ, O'Donnell N, Riley JP, Williams KN, Karlsson L, Thurmond RL. The histamine H4 receptor mediates allergic airway inflammation by regulating the activation of CD4+ T cells. J Immunol 2006;176: 7062-70.
16. Lim HD, van Rijn RM, Ling P, Bakker RA, Thurmond RL, Leurs R. Evaluation of histamine H_1-, H_2-, and H_3-receptor ligands at the human histamine H_4 receptor: Identification of 4-methylhistamine as the first potent and selective H4 receptor agonist. J Pharmacol Exp Ther 2005;314: 1310-27.
17. Huang BD, Wang J, Kivisakk P, Rollins BJ, Ransohoff RM. Absence of monocyte chemoattractant protein 1 in mice leads to decreased local macrophage recruitment and antigen-specific T helper cell type 1 immune response in experimental autoimmune encephalomyelitis. J Exp Med 2001;193:713-25.
18. Kim Y, Sung SJ, Kuziel WA, Feldman S, Fu SM, Rose CE Jr. Enhanced airway Th2 response after allergen challenge in mice deficient in CC chemokine receptor-2 (CCR2). J Immunol 2001;166:5183-92.
19. Purwar R, Werfel T, Wittmann M. IL-13 stimulated keratinocytes preferentially attract CD4+CCR4+ T cells: possible role in atopic dermatitis. J Invest Dermatol 2005;126:1043-51.
20. Szalai C, Kozma GT, Nagy A, Bojszko A, Krikovszky D, Szabo T, et al. Polymorphism in the gene regulatory region of MCP-1 is associated with asthma susceptibility and severity. J Allergy Clin Immunol 2001;108: 375-81.
21. Sozzani S, Locati M, Zhou D, Rieppi M, Luini W, Lamorte G, et al. Receptors, signal transduction, and spectrum of action of monocyte chemotactic protein-1 and related chemokines. J Leukoc Biol 1995;57: 788-94.
22. Leung DYM, Boguniewicz M, Howell MD, Nomura I, Hamid QA. New insights into atopic dermatitis. J Clin Invest 2004;113:651-7.
23. Jablonowski JA, Grice CA, Chai W, Dvorak CA, Venable JD, Kwok AK, et al. The first potent and selective non-imidazole human histamine H4 receptor antagonists. J Med Chem 2003;46:3957-60.
24. Galardy RE, Cassabonne ME, Giese C, Gilbert JH, Lapierre F, Lopez H, et al. Low molecular weight inhibitors in corneal ulceration. Ann N Y Acad Sci 1994;732:315-23.
25. Van Rijn RM, Chazot PL, Shenton FC, Sansuk K, Bakker RA, Leurs R. Oligomerization of recombinant and endogenously expressed human histamine H4 receptors. Mol Pharmacol 2006;70:604-15.
26. Thurmond RL, Desai PJ, Dunford PJ, Fung-Leung WP, Hofstra CL, Jiang W, et al. A potent and selective histamine H4 receptor antagonist

with anti-inflammatory properties. J Pharmacol Exp Ther 2004;309: 404-13.
27. Vestergaard C, Gesser B, Lohse N, Jensen SL, Sindet-Pedersen S, Thestrup-Pedersen K, et al. Monocyte chemotactic and activating factor (MCAF/MCP-1) has an autoinductive effect in monocytes, a process regulated by IL-10. J Dermatol Sci 1997;15:14-22.
28. McQuibban GA, Gong JH, Wong JP, Wallace JL, Clark-Lewis I, Overall CM. Matrix metalloproteinase processing of monocyte chemoattractant proteins generates CC chemokine receptor antagonists with anti-inflammatory properties in vivo. Blood 2002;100:1160-7.
29. Horr B, Borck H, Diel J, Wackes C, Nierich K, Thurmond RL, et al. The role of the histamine H4 receptor in signal transduction of atopic and non-atopic human lymphocytes ex vivo. Inflamm Res 2006; 55(suppl 1):S53-4.
30. Van der Pouw-Kraan TC, Snijders A, Boeije LC, de Groot ER, Alewijnse AE, Leurs R, et al. Histamine inhibits the production of interleukin-12 through interaction with H_2 receptors. J Clin Invest 1998;102:1866-73.
31. Azuma Y, Shinohara M, Wang PL, Hidaka A, Ohura K. Histamine inhibits chemotaxis, phagocytosis, superoxide anion production, and the production of TNF alpha and IL-12 by macrophages via H_2 receptors. Int Immunopharmacol 2001;1:1867-75.
32. Bissonnette EY. Histamine inhibits tumor necrosis factor alpha release by mast cells through H_2 and H_3 receptors. Am J Respir Cell Mol Biol 1996;14:620-6.

Inflamm. res. 56, *Supplement 1* (2007) S19–S20
1023-3830/07/01S19-02
DOI 10.1007/s00011-006-0509-7

Inflammation Research

2. Histamine in gastrointestinal and cardiovascular systems

Influence of (R)-α-Methylhistamine on the histamine H_3 receptor in the rat gastrointestinal tract

P. Chazot[1], F. Shenton[1], W. Schunack[2], D. Grandi[3] and G. Morini[3]

[1] Center for Integrative Neurosciences (CINS), School of Biological and Biomedical Sciences, Durham University, Durham, DH15NQ, UK
[2] Institut für Pharmazie, Freie Universität Berlin, 14195 Berlin, Germany
[3] Department of Human Anatomy, Pharmacology and Forensic Medicine, University of Parma, 43100 Parma, Italy, Fax: ++39 0521 903852, e-mail: giuseppina.morini@unipr.it

Published Online First 14 March 2007

Introduction

The histamine H_3 receptor (H_3R) is a presynaptic receptor, reported to be abundantly expressed in the central nervous system of different animal species [1]. Recent studies have also suggested that the H_3R plays various roles in the periphery [2, 3]. Ligands for histamine H_3 receptors are reported to regulate gastric acid secretion, maintenance of gastric mucosal integrity as well as gastric and intestinal epithelial cell proliferation [4, 5]. In the present study, we have determined the anatomical distribution of the H_3R in the gastrointestinal tract, and probed the influence of activation by the selective histamine H_3-receptor agonist (R)-α-methylhistamine [(R)α-MeHA] upon the levels of H_3Rs in fed and fasted rats.

Materials and methods

Adult male Wistar rats (180–200 g, Harlan, Italy), were treated with (R)α-MeHA,100 mg/kg, or saline, intragastrically in a 5 ml/kg volume, 1 and 48 h before sacrifice. Half the rats in each group were fed *ad libitum* or fasted with free access to water for 24 h before the sacrifice. Four to five rats were employed for each treatment subgroup. Tissue samples were taken from stomach, distal ileum and distal colon, fixed in 10 % (v/v) formalin, prepared for immunohistochemistry and probed with our anti-H_3 349–358 antibody previously generated in rabbits [6] and validated using H_3R knockout mice [Cannon et al., submitted]. The positive cells were visualized by diaminobenzidine and counterstained with hematoxylin. The number of positive cells was counted in at least 3 different sections for a total of 40 glands or crypts per rat and the results were expressed as number of positive cells per unit. (R)α-MeHA was synthesized by W.S.

Results are expressed as mean ±SEM. Comparisons between the mean values of control and treated groups were performed with one-way ANOVA followed by Newman-Keuls test. A P value <0.05 was considered statistically significant.

All experiments were approved by the Italian Animal Care and Use Committee.

Results and discussion

Anti-H_3 receptor (anti-H_3R) immunoreactivity was differentially distributed in the various regions of the rat gastrointes-

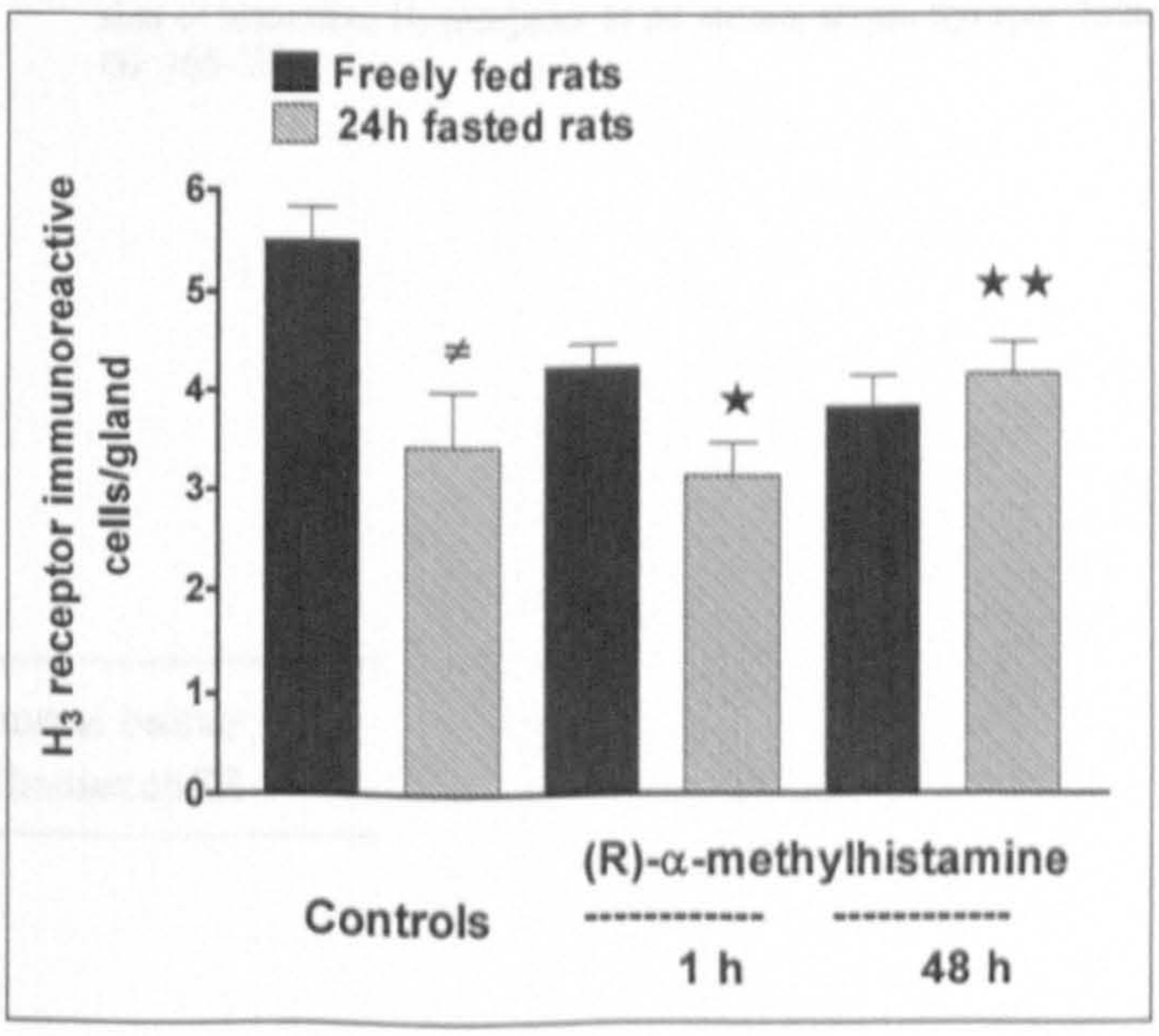

Fig. 1. Effect of (R)-α-methylhistamine on density of anti-H_3 receptor positive cells in the fundic mucosa of the rat stomach. Positive cells are decreased by 24 h fasting in control group. At 1 h and 48 h after the administration of a single dose, (R)-α-methylhistamine, 100 mg/kg intragastrically, reduces the number of positive cells in freely fed rats only, while it is ineffective in fasted rats. Mean ±SEM; n = 4–5. #P < 0.01 between freely fed and fasted control rats; *P < 0.05 and **P < 0.01 between corresponding control and (R)-α-methylhistamine-treated rats.

Correspondence to: G. Morini

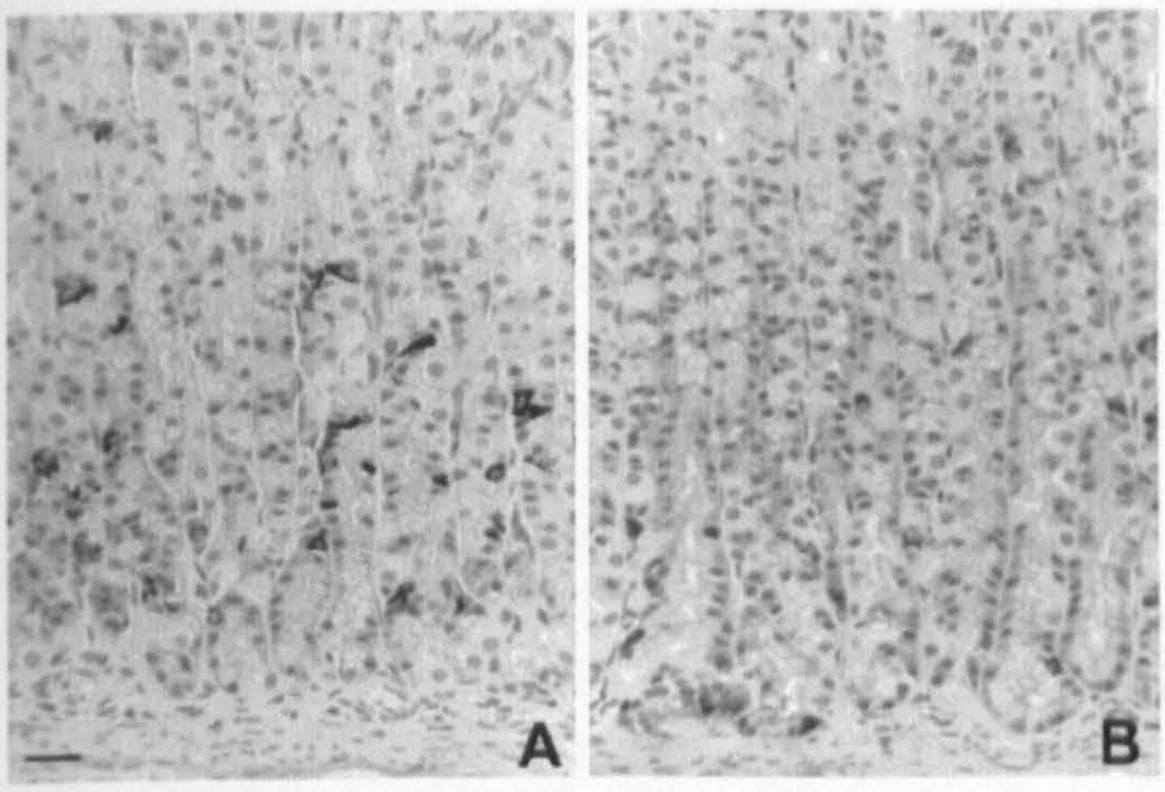

Fig. 2. Representative sections of the fundic mucosa of the stomach in freely fed rats. (A) Control rat and (B) rat sacrificed 48 h after the single administration of (R)-α-methylhistamine, 100 mg/kg intragastrically. Prior treatment with (R)-α-methylhistamine decreases the density of anti-H_3 receptor positive cells with no change in their position along the gland. Scale bar = 28 μm.

tinal tract. The immunoreactive cells were most frequently detected in the gastric fundus, where they occurred in the basal half of the mucosa. Their density sharply decreased in the antrum, with a further gradual decrease towards the distal ileum and distal colon. In the fundic mucosa 24 h fasting significantly lowered anti-H_3R immunoreactivity, the number of positive cells per gland being 5.31 ± 0.53 and 3.44 ± 1.59 in freely fed and fasted rats respectively (Fig. 1). In freely fed rats administration of (R)α-MeHA 100 mg/kg promptly decreased the density of anti-H_3R immunoreactive cells. The number of immunoreactive cells/gland was 4.24 ± 0.33 and 3.83 ±0.31 at 1 h and 48 h respectively after dosing. Compared with controls, the decrease was 20 % ($P < 0.05$) and 28 % ($P < 0.01$) in 1 h- and 48 h-treated groups respectively (Figs. 1, 2). By contrast in fasted rats the density of immunoreactive cells was unaffected by prior treatment with (R)α-MeHA. Interestingly the number of immunoreactive cells was similar in fasted and (R)α-MeHA treated rats. Food deprivation or (R)α-MeHA did not influence positive cell density in the regions of the gastrointestinal tract other than gastric fundus.

These data are of interest to compare to recent studies which showed agonist-dependent down-regulation of H_3R, resulting in a significant loss of function in the rat striatum [7]. These results suggest homologous desensitisation maybe a common regulatory mechanism for both the central and peripheral H_3R.

References

[1] Hancock AA, Esbenshade TA, Krueger KM, Yao BB. Genetic and pharmacological aspects of histamine H_3 receptor heterogeneity. Life Sci 2001; 12: 259–62.

[2] Hill SJ. Distribution, properties, and functional characteristics of three classes of histamine receptors. Pharmacol Rev 1990; 42: 45–82.

[3] Parsons ME, Ganellin CR. Histamine and its receptors. Br J Pharmacol 2006; 147: S127–35.

[4] Coruzzi G, Poli E, Morini G, Bertaccini G. The Histamine H_3 receptor. Pharmacotherapy Targets in Gastrointestinal Disorders. In: Gaginella TS, Guglietta A (eds). Drug Development: Molecular Targets for GI Diseases. Humana Press Inc, Totowa, 1999: 239–67.

[5] Morini G, Grandi D, Schunack W. Ligands for histamine H_3 receptors modulate cell proliferation and migration in rat oxyntic mucosa. Br J Pharmacol 2002; 137: 237–44.

[6] Chazot PL, Hann V, Wilson C, Lees G, Thompson CL. Immunological identification of the mammalian H_3 histamine receptor in the mouse brain. Neuroreport 2001; 12: 259–62.

[7] Garduno-Torres B, Arias-Montano JA. Homologous down-regulation of histamine H_3 receptors in rat striatal slices. Synapse 2006; 60: 165–71.

LAY SUMMARY

"..... the Hitch Hiker's Guide *has already supplanted the great* Encyclopaedia Galactica *as the standard repository of all knowledge and wisdom.....it scores over the older, more pedestrian work in two important respects.*

First, it is slightly cheaper; and secondly it has the words DON'T PANIC *inscribed in large friendly letters on its cover."*

The Hitch Hikers Guide to the Galaxy, Douglas Adams

Background

Many people have heard of histamine and may know that it is important in allergies, inflammation and excess gastric acid secretion. Although it is involved in conditions that can be harmful, it is also an important chemical messenger in the body. Histamine is found almost everywhere, but is present in highest concentrations in the lungs, skin and particularly the gut. It is also found in the brain. Outside the brain it is found mainly in special white blood cells: mast cells and basophils; inside the brain it is also found in nerve cells (neurons). Most of the early studies describing the biological action of histamine were carried out by Sir Henry Dale and colleagues in the 1930s. Following these studies, anti-histamines were developed as successful therapies for many allergic and inflammatory conditions. It was recognized that anti-histamines had a sedative action and were therefore affecting the brain. Further studies demonstrated that histamine is one of the many different chemical messengers found in the brain. These are called neurotransmitters and they are released from neurons when they are electrically stimulated by a nerve impulse (Fig 1). The neurotransmitter is released into the tiny gap between the neuron and its target. In the brain this is usually another neuron. The histamine then binds to special receptors on the next neuron which either stimulates or inhibits the activity of the receiving neuron.

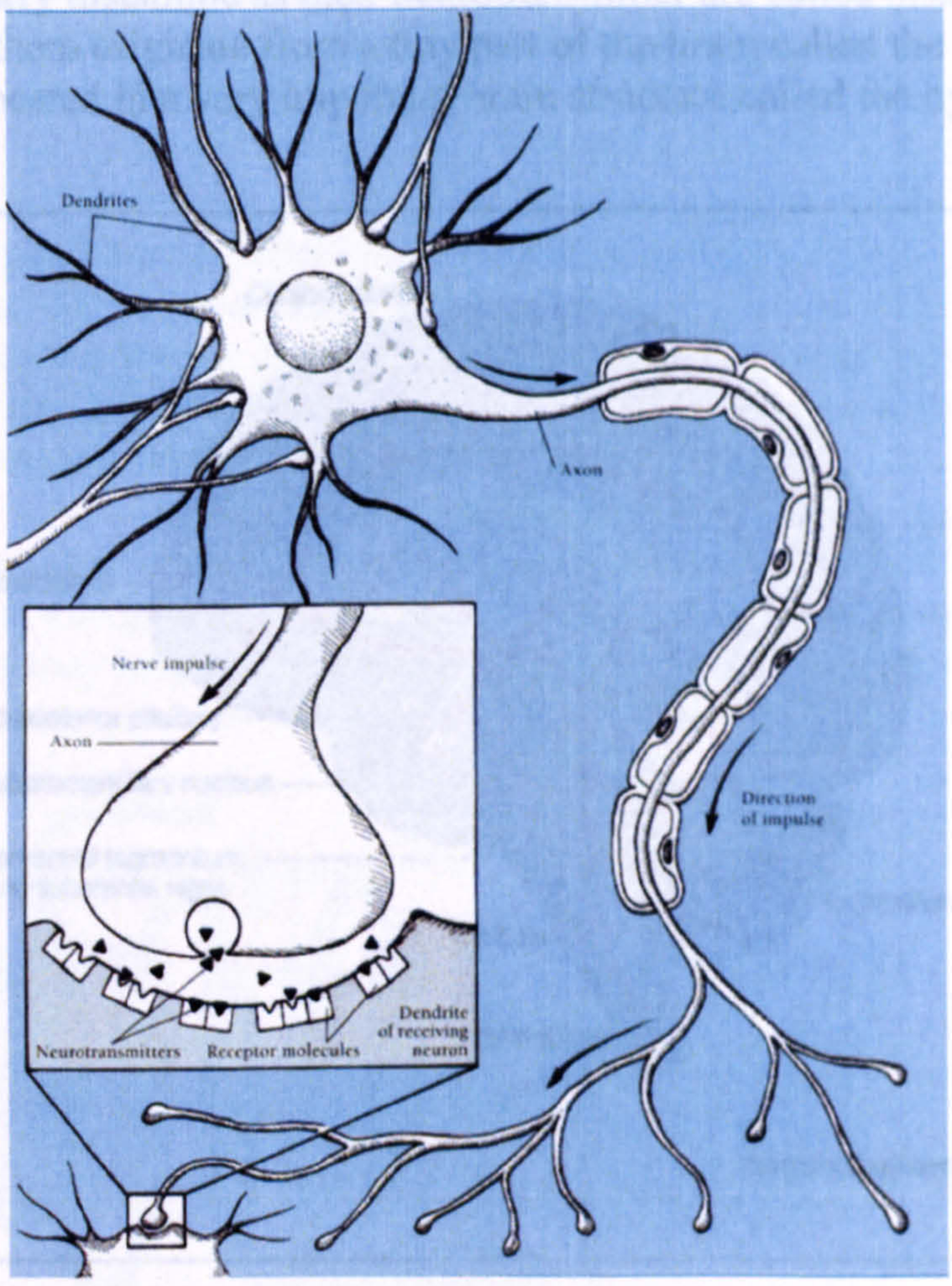

Fig 1 Release of neurotransmitter from a neuron.

Neurons which carry histamine as their neurotransmitter are called histaminergic neurons and almost all of them originate from a tiny part of the brain called the tuberomammillary nucleus (Fig 2), located in a very important brain structure called the hypothalamus.

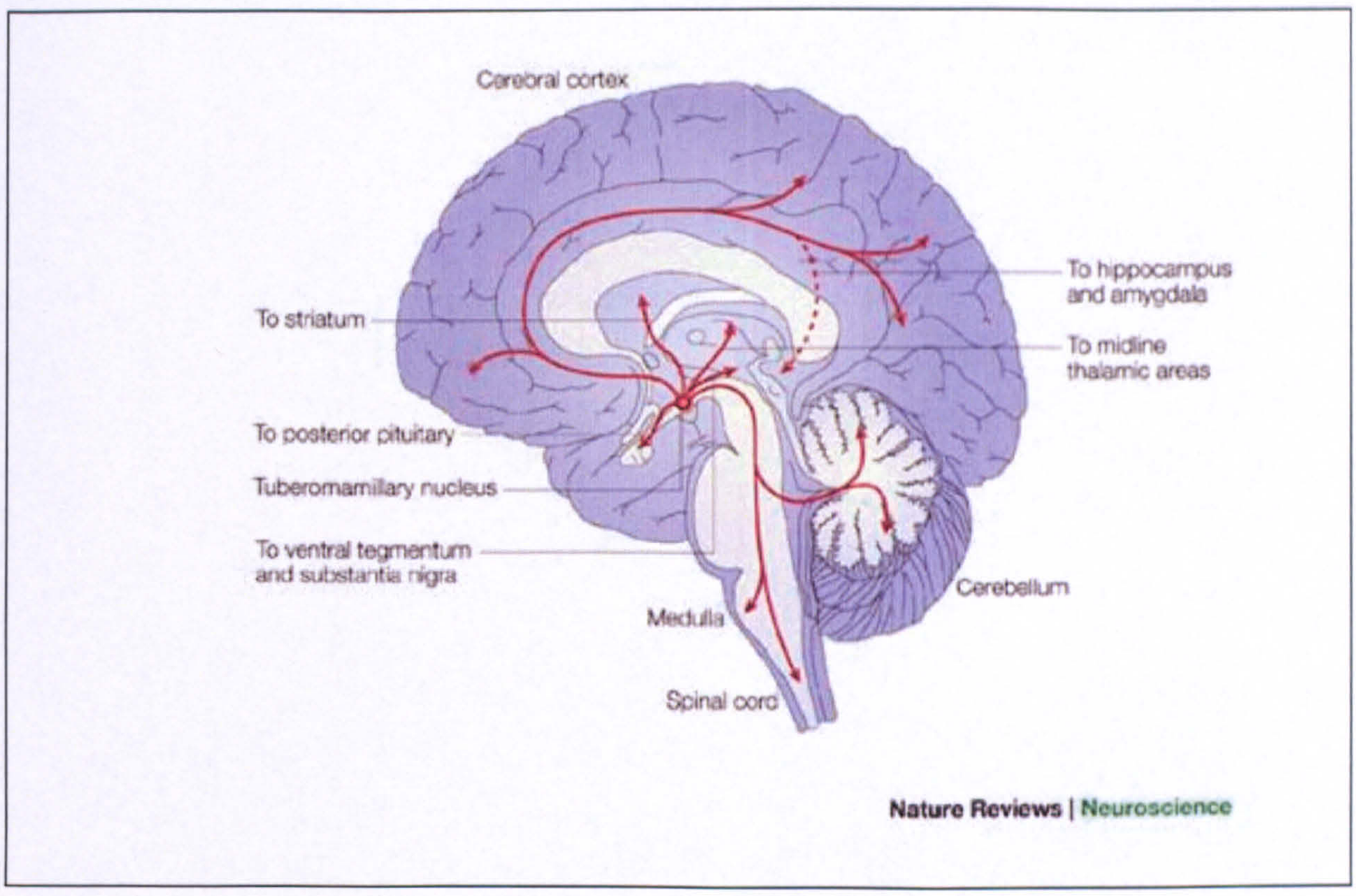

Fig 2 Histaminergic system in the brain

Histaminergic neurons branch to many different areas of the brain and down into the spinal cord. They occur in many key regions, including those important in learning and memory, voluntary movement and responses to stress. This is perhaps not surprising since the hypothalamus is an important control centre essential for the survival of an organism and reproduction. The hypothalamus sends out messages along pathways that use both nerve impulses and hormones, and it also responds to messages which come back from the systems that it regulates. In this way the hypothalamus can orchestrate the complex and diverse behaviours that underlie the way in which the body's internal environment is maintained, reproduction and motivated action.

So far four different histamine receptors have been identified. These bind histamine to cells, tissues and organs and mediate the effects of histamine on various targets. The H_1 and H_2 receptors mostly excite neurons or potentiate excitatory inputs whereas H_3 is an inhibitory receptor. The H_4 receptor is the most recently described, and not much is known about it yet. The H_1 histamine receptor is found on smooth muscle and it is also important in the brain. It causes dilation of blood vessels, bronchoconstriction and smooth muscle activation. It is involved in hayfever, pain and itching due to insect stings,

and travel sickness. The H_2 histamine receptor is located on special cells in the gut which primarily regulate gastric acid secretion. Again it is also important in the brain. H_3 histamine receptors are found almost exclusively in the brain, although it has also been reported at low levels in the spinal cord, gut, skin and some blood vessels. It usually inhibits neurotransmitter release. It can inhibit the release of histamine itself and a number of other important neurotransmitters including acetylcholine, noradrenaline and serotonin. H_4 histamine receptors have been located primarily on white blood cells in the thymus, small intestine, spleen, and colon. They are likely to have a role in immune function. There are however a number of laboratories, including our own, reporting H_4 histamine receptors in rodent and human brain.

All four histamine receptors come from a family of receptors called G-protein coupled receptors (GPCRs). GPCRs are also known as seven transmembrane receptors (7TM receptors) because they loop back and forth across the outer membrane of the cell seven times (Fig 3).

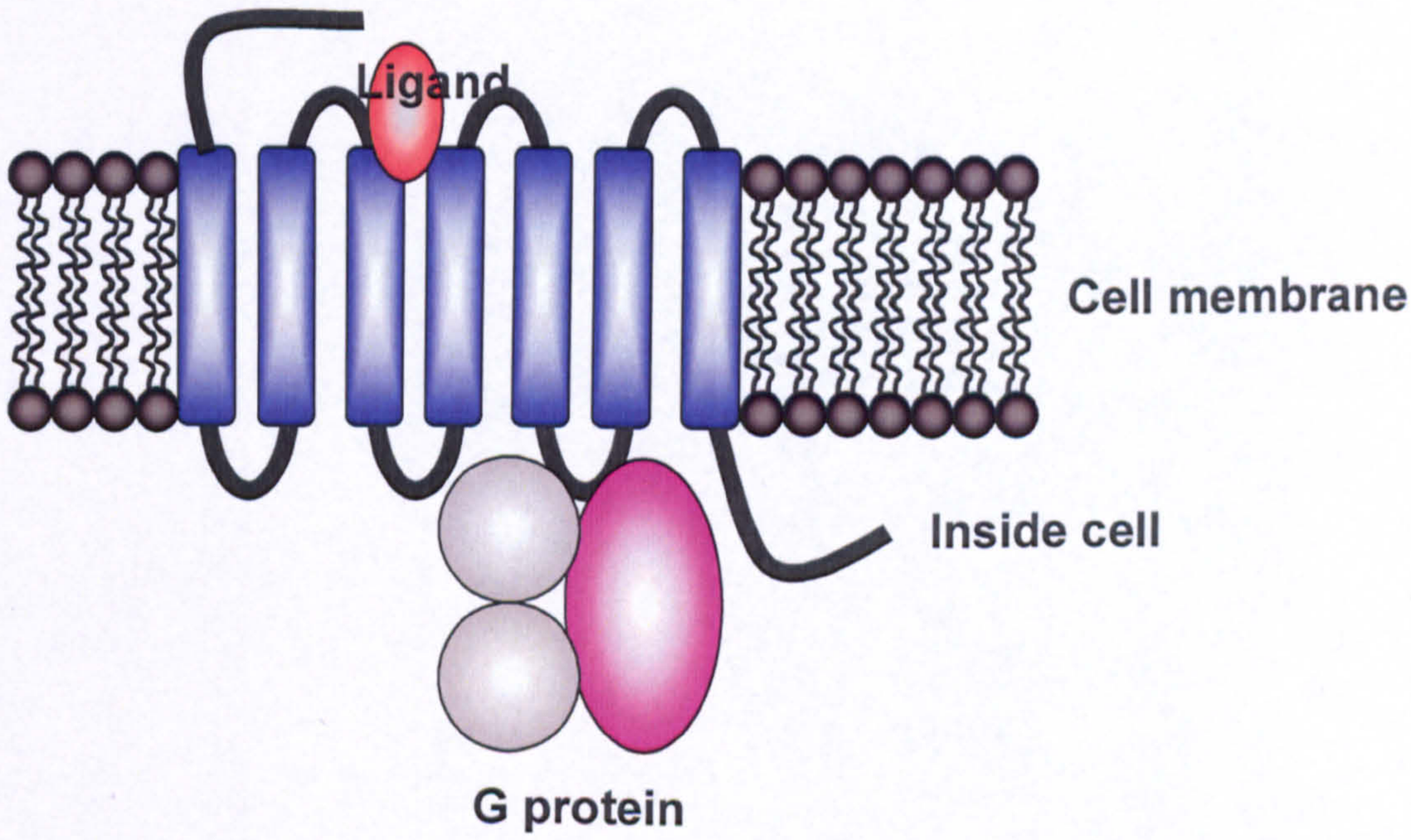

Fig 3 GPCR Cartoon

They convert or transduce signals from outside the cell into an intracellular signal via activation of a G-protein. The GPCRs are the largest protein family known with over 1000 identified to date. They are involved in all types of stimulus-response pathways and regulate all known physiological pathways in higher vertebrates. As GPCRs are involved at some stage in all normal biological processes it is not surprising that they are the target for 40 to 50% of modern medicinal drugs. The diversity of functions is matched by the wide range of ligands (a ligand is anything that can bind and activate a receptor) recognized by members of the family, from photons, as is the case for rhodopsin receptors in the eye, to small molecules, like histamine, and proteins, for example, hormones. The role of GPCRs is often regulatory and the manner in which they function is ideally suited to this. They work relatively slowly compared with other receptors taking

seconds rather than milliseconds. In addition the signalling pathways involve many steps so there are multiple points at which the signal can be manipulated and fine tuned. This is extremely important so that the organism is able to continually adapt to a changing environment. GPCR signalling is enormously complex and new layers of complexity are uncovered almost daily. However the broad principle remains the same. When a ligand binds a GPCR it alters the shape of the receptor in such a way that it is able to couple to a G-protein on the inside of the cell. This has the effect of activating the G-protein which in turn activates other intracellular events or signalling cascades. These intracellular signals eventually trigger an effector within the cell to bring about some change or action (Fig 4).

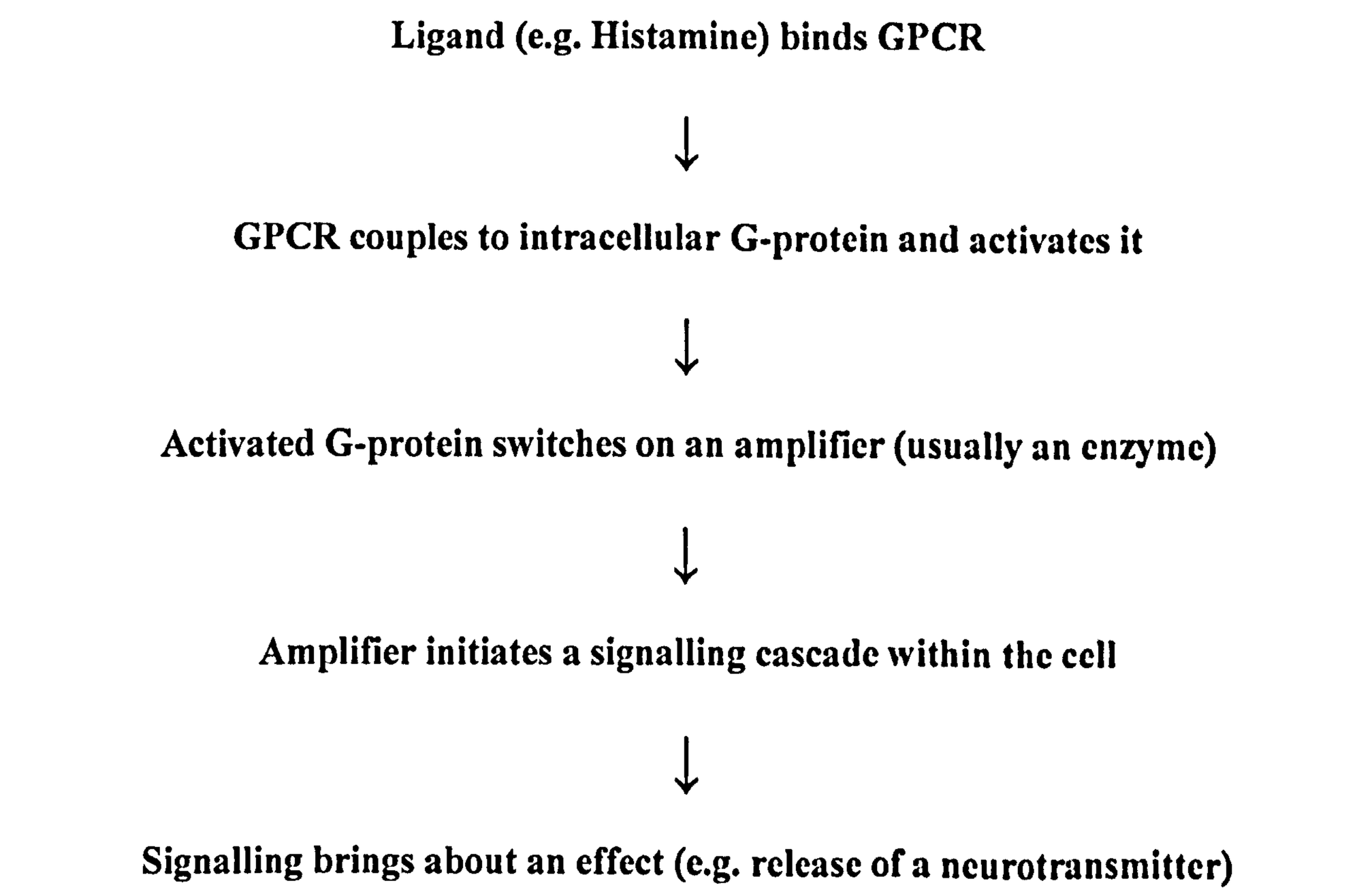

Fig 4 GPCR signalling

In the case of histamine acting as a neurotransmitter in the brain, if it binds to either an H_1 or H_2 histamine receptor the end result is likely to be the release of more histamine from a histaminergic neuron. However if it binds to a histamine H_3 receptor it usually inhibits neurotransmitter release. The H_4 receptor is also likely to be inhibitory.

We are trying to establish the function of H_3 and H_4 receptors in the brain. The H_3 receptor is widespread in many important brain areas. In contrast, the H_4 appears to be at rather low levels in the brains of rodents and humans. In some species we do not know yet whether the H_4 receptor is in the brain at all. Histamine in the brain helps to co-ordinate bodily functions and behaviours in response to changing needs. In particular it

plays a part in circadian rhythms (responding appropriately to the normal 24 hour daily cycle), eating and drinking, maintaining body temperature, paying attention and learning. Knowing more about all the histamine receptors in the brain and how they work will help our understanding of how the brain functions. Histamine receptors may provide the key to future therapies. Drugs which can activate the receptors in a similar way to histamine could be used to intervene where the equilibrium has been lost through disease or physical damage. Histamine receptors H_1 and H_2 are already the targets of some very effective modern drugs outside the brain and there are high hopes that the most recently discovered receptors, H_3 and H_4, may prove just as useful. With its widespread distribution in the brain and its effects on other important neurotransmitters besides histamine there are a number of neurological disorders and diseases where manipulation of the H_3 receptor could have potential. These include Attention Deficit Hyperactivity Disorder (ADHD), Alzheimers Disease, Parkinsons Disease and Schizophrenia. Also, due to the role of histamine in eating and drinking, drugs which affect the H_3 histamine receptor might have a use in combating obesity. The H_4 receptor is found on many types of immune cells and has been shown to influence the production of some of the chemical messengers which these cells manufacture. Drugs which target the H_4 receptor may be useful in controlling inflammatory diseases such as rheumatoid arthritis. In addition it has some effects on cell growth and development so anti-cancer therapies are also a possibility.

The purpose of my research was to delve deeper into the details of the structure of the H_3 and H_4 receptors and the way in which they work. So far no drugs targeting the H_3 receptor have made it into the clinic, although it was first described over 20 years ago. This is mainly because there is a great deal of variation in the pharmacology (ie how the receptors respond to H_3 directed drugs) which has not yet been explained. This variation or heterogeneity is seen both when comparing H_3 pharmacology between different animal species, and even within the same animal species when comparing H_3 receptors from different brain regions or tissues. In my research I have sought to find explanations for this variation. Even less is known about the H_4 histamine receptor. However, since the gene which codes for it is very similar to the H_3 receptor gene, it is likely that both receptors have many characteristics in common. Before I can explain the work I carried out for my PhD it is necessary to explain more about GPCRs in general and histamine receptors H_3 and H_4 in particular.

1) The H_3 and H_4 receptors can exist as different isoforms (slightly different types)

Due to the way the message from the genes coding these two receptors is translated into protein slightly different types (isoforms) can be generated. It seems likely that these isoforms are part of the explanation for the observed variations in pharmacology. For the H_3 receptor the isoforms are often the result of deletions within the third intracellular loop of the full length receptor (Fig 5).

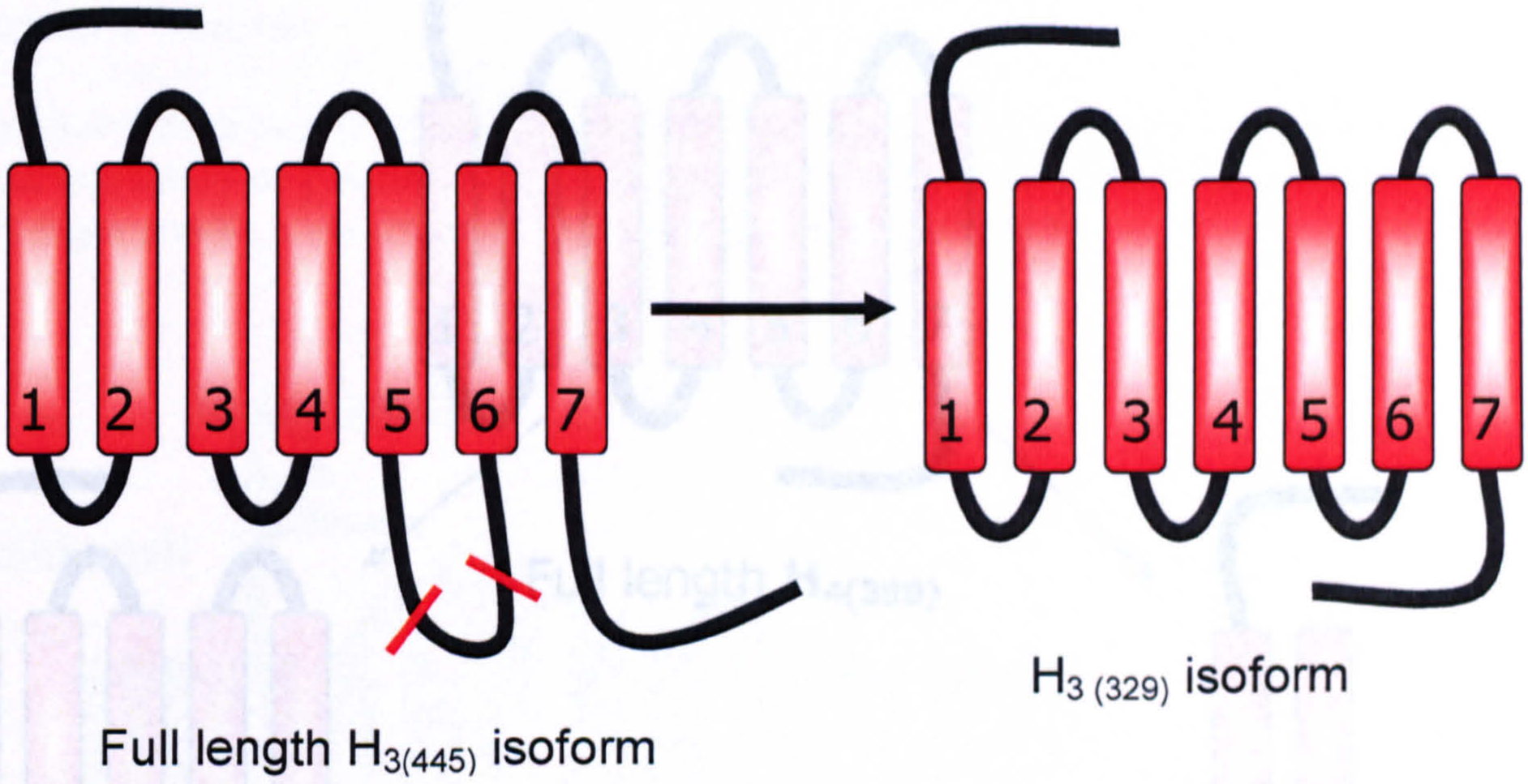

Fig 5 H_3R isoforms

For the H_3 receptor over twenty different isoforms may exist. There is evidence that the pharmacology of some of the different isoforms differs from that of the full length receptor. In addition the distribution of the various isoforms throughout the brain differs. I concentrated on the full length receptor which is 445 amino acids long H_3 (445) and a shorter isoform which is 329 amino acids long H_3 (329), because they are both found in a region of the brain which is crucial to the control of voluntary movement

At present only two isoforms of the H_4 receptor have been identified by our collaborators at the Vrije University in Amsterdam, however there are likely to be more. These are drastically truncated versions of the full length receptor, lacking two or more of the transmembrane domains (Fig 6).

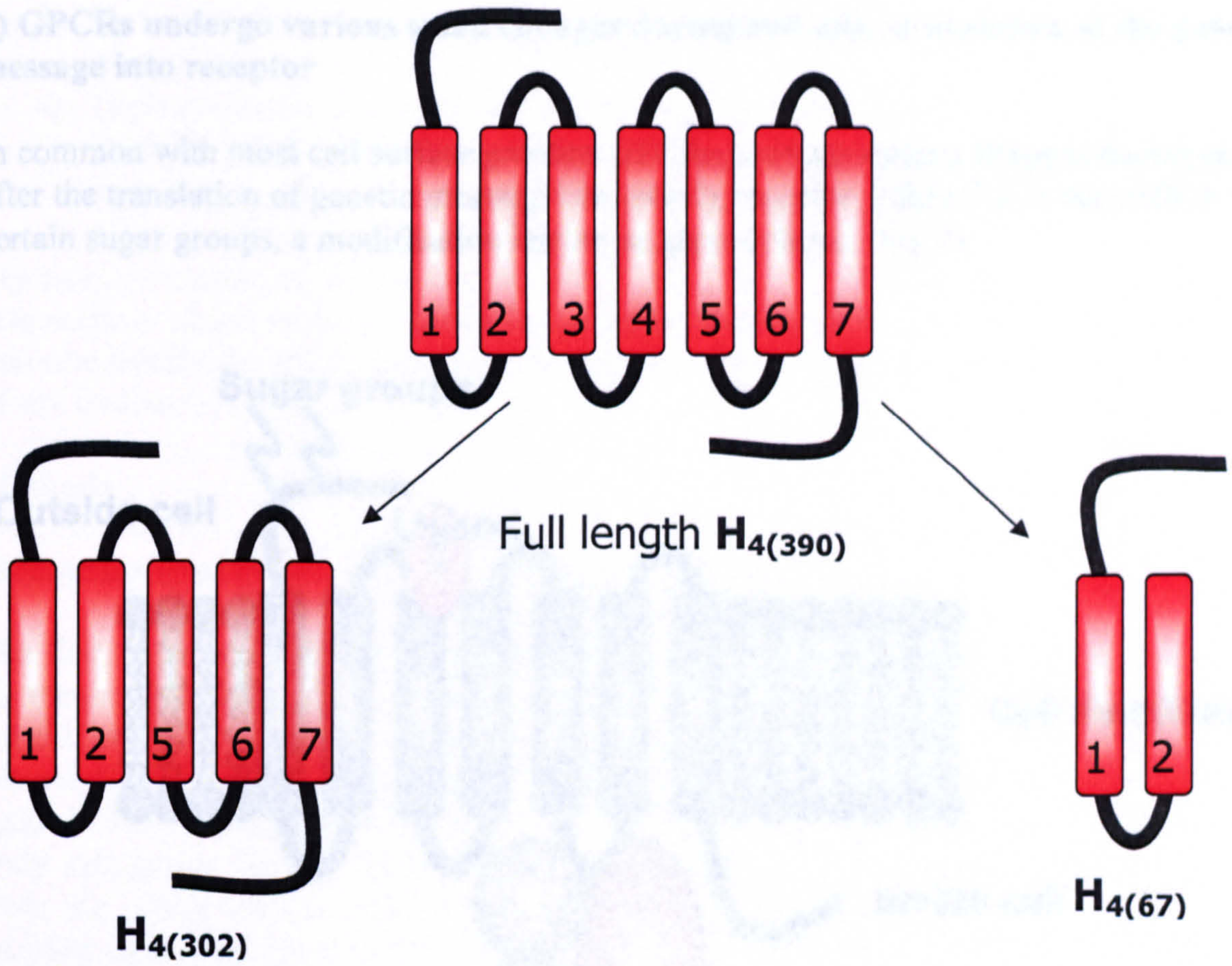

Fig 6 H_4R isoforms

Many of the H_3 isoforms and both the H_4 isoforms appear to be non-functional because they neither bind histamine nor signal. However it is very unlikely that they have no purpose at all. My work has shed light on a possible role for these apparently non-functional isoforms.

2) Two or more GPCRs are likely to join together in order to signal

Although in Fig 4 one GPCR is shown interacting with one G-protein the current thinking is that GPCRs operate as dimers (two together) or higher oligomers (two or more together), a process called oligomerisation. I wanted to investigate whether this is true of H_3 and H_4 receptors; not only for the full length receptors: homo-oligomers (like with like) but can hetero-oligomers exist (full length with a different isoform). In addition if hetero-oligomers can exist does the shorter isoform affect the functioning of the full length receptor in any way?

3) GPCRs undergo various small changes *during* and after translation of the genetic message into receptor

In common with most cell surface proteins GPCRs undergo various changes during and after the translation of genetic message into protein receptor. Often this is the addition of certain sugar groups, a modification known as glycosylation (Fig 7).

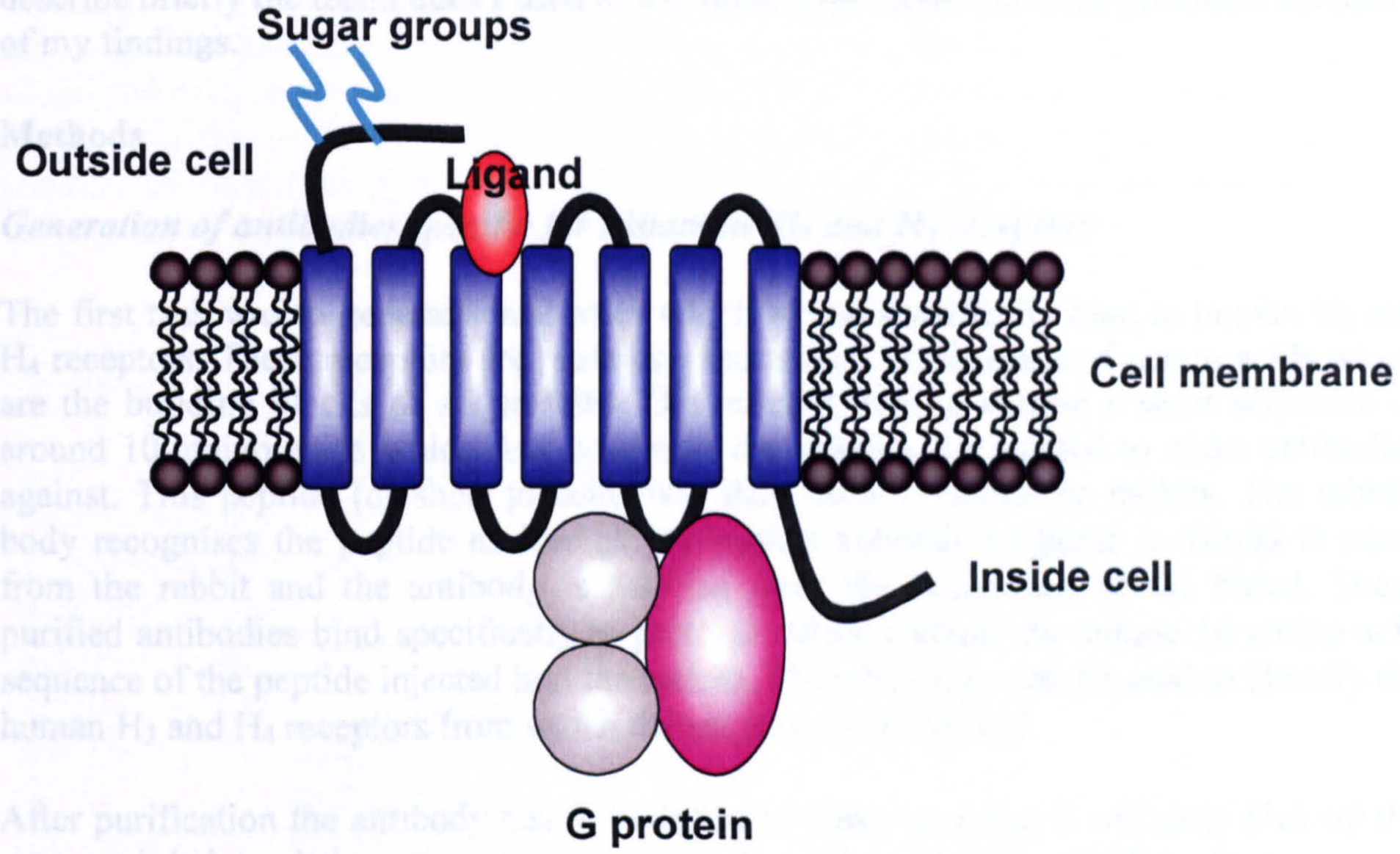

Fig 7 Glycosylation of GPCRs

The reason for this glycosylation is not fully understood, current research suggests a number of possible functions which may not be the same for all receptor types. For example, for some GPCRs these additional sugar groups appear to be necessary for the trafficking of the receptor to the cell membrane, in others they may help with drug binding. Glycosylation might also be involved in the formation of GPCR oligomers. I carried out experiments to find out whether H_3 and H_4 receptors are glycosylated since differences in glycosylation might affect the way in which receptors work and could underlie some of the variation seen in receptor pharmacology.

There were five main hypotheses I set out to address –

1) Human H_3 and H_4 receptors are able to homo-oligomerise
2) Human H_3 and H_4 receptors are able to hetero-oligomerise with their respective isoforms

3) Shorter isoforms can influence how the full length human H_3 and H_4 receptors work
4) N-glycosylation is a prerequisite for receptor oligomerisation
5) Both H_3 and H_4 receptors are present in human brain where they serve distinct functions

My work concentrated on **human** receptors because of the longer term goal of providing information which may be useful in designing therapies for use in people. I will next describe briefly the techniques I used to test these hypotheses and then provide a summary of my findings.

Methods

Generation of antibodies specific for histamine H_3 and H_4 receptors

The first task was to generate antibodies which would specifically bind to human H_3 and H_4 receptors. These receptors are proteins, constructed from chains of amino acids which are the building blocks of all proteins. Our strategy was to choose a short sequence of around 10 amino acids which was unique to the receptor we wanted to make antibodies against. This peptide (or short protein) was then used to immunise rabbits. The rabbits body recognises the peptide as foreign and makes antibodies against it. Blood is taken from the rabbit and the antibody is purified from the liquid part of the blood. These purified antibodies bind specifically to proteins which contain the unique 10 amino acid sequence of the peptide injected into the rabbits. Therefore they can be used to identify the human H_3 and H_4 receptors from which the sequence was derived.

After purification the antibody has to be tested to make sure that it will only pick up the receptor it is intended to recognise. The antibody can be tested in a number of ways.

Immunoblotting

This technique was used to visualise histamine receptors from two different sources:

1) The gene coding for a receptor can be temporarily introduced (transfected) into cultured mammalian cells for experimental purposes. These are called recombinant receptors because the receptor DNA is combined (although not fully) with the normal DNA of the cell. It is therefore translated along with the other cell proteins and expressed at the cell surface. Cells expressing the histamine receptors were homogenised in a special glass pestle and mortar, and the protein mixture from this homogenate was used for immunoblotting.
2) Histamine receptors from native tissue were also used. Native tissue just means tiny pieces of normal brain, skin, bone or whatever body part you are investigating. In this case brain tissue was used, it is homogenised in a similar way to the recombinant receptors.

To carry out immunoblotting the homogenised proteins were prepared and applied to a very thin slab of polyacrylamide gel (Fig 8). Under the influence of an electric current passed through the gel the proteins migrate from the top to the bottom. The smaller the protein the faster it will migrate so that eventually the proteins spread out down the gel according to their size. The smallest ones are at the bottom, the biggest ones still near the top. The proteins were then blotted onto a piece of special nitrocellulose paper. It is called **immuno**blotting because an immune antibody is used to identify the protein of interest. We used our purified anti-histamine receptor antibody. The antibody binds to the part of the receptor which contains the unique peptide sequence which was used to immunise the rabbit in the first place. The location of the receptor with the antibody bound to it is visualised using a special enzyme linked probe which attaches to the rabbit antibody. The enzyme on the probe is used to bring about either a colour change or a luminescent reaction which can be picked up on a photographic film. The end result is bands which correspond to the position of the histamine receptors (Fig 9).

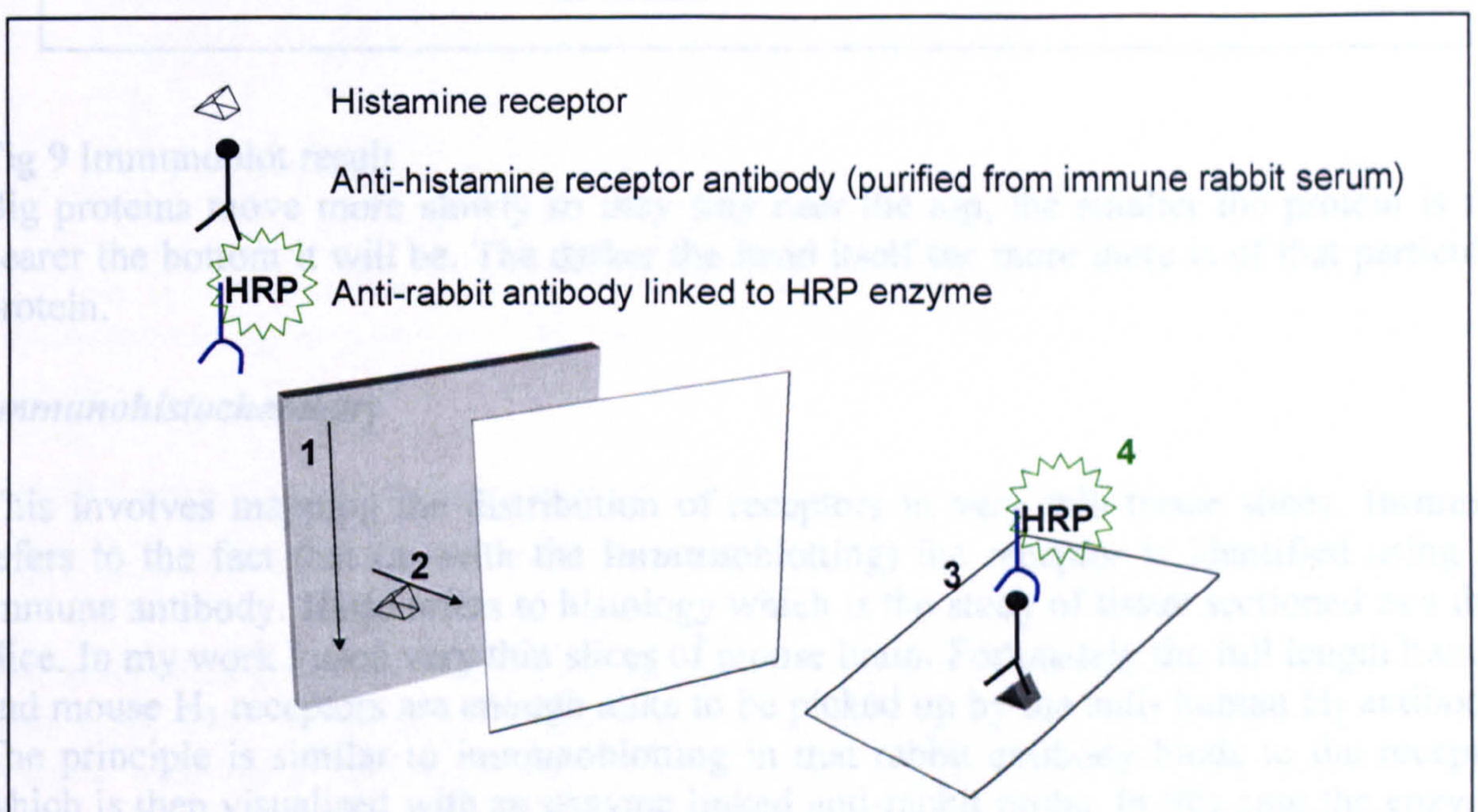

Fig 8 Steps involved in immunoblotting

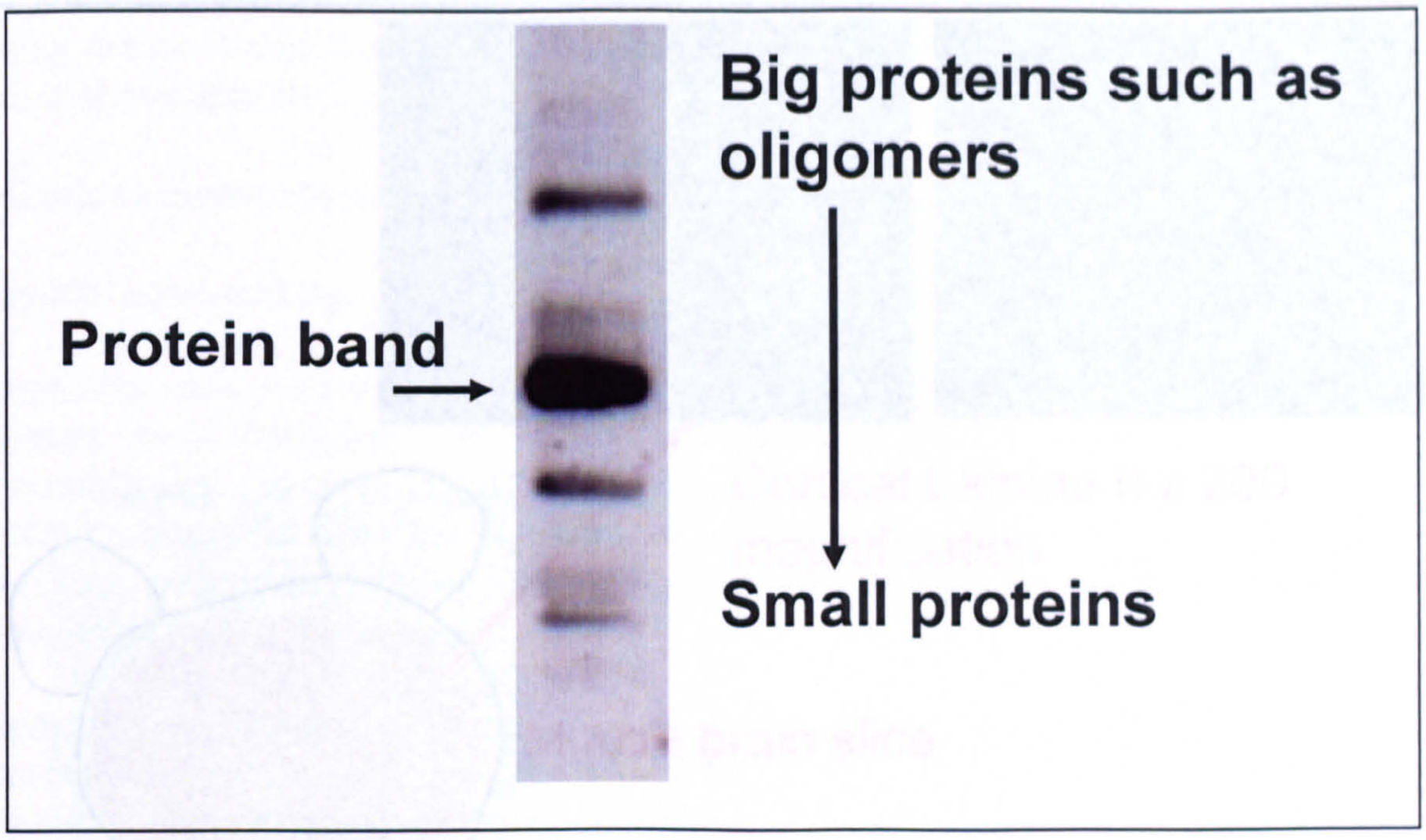

Fig 9 Immunoblot result
Big proteins move more slowly so they stay near the top, the smaller the protein is the nearer the bottom it will be. The darker the band itself the more there is of that particular protein.

Immunohistochemistry

This involves mapping the distribution of receptors in very thin tissue slices. **Immuno** refers to the fact that (as with the **immuno**blotting) the receptor is identified using an immune antibody. **Histo** refers to histology which is the study of tissue sectioned as a thin slice. In my work I used very thin slices of mouse brain. Fortunately the full length human and mouse H_3 receptors are enough alike to be picked up by the anti- human H_3 antibody. The principle is similar to immunoblotting in that rabbit antibody binds to the receptor which is then visualised with an enzyme linked anti-rabbit probe. In this case the enzyme causes a colour reaction so that areas with histamine receptors are stained brown (Fig 10). To be certain that the antibody was picking up the H_3 receptor we carried out immunohistochemistry on mouse brain slices from a normal mouse and compared them with the staining pattern on slices from mice where the H_3 gene had been artificially knocked out, so the mouse did not have any H_3 receptors. Apart from being a little overweight and showing slightly unusual circadian rhythms H_3 knock out mice appear to be perfectly healthy.

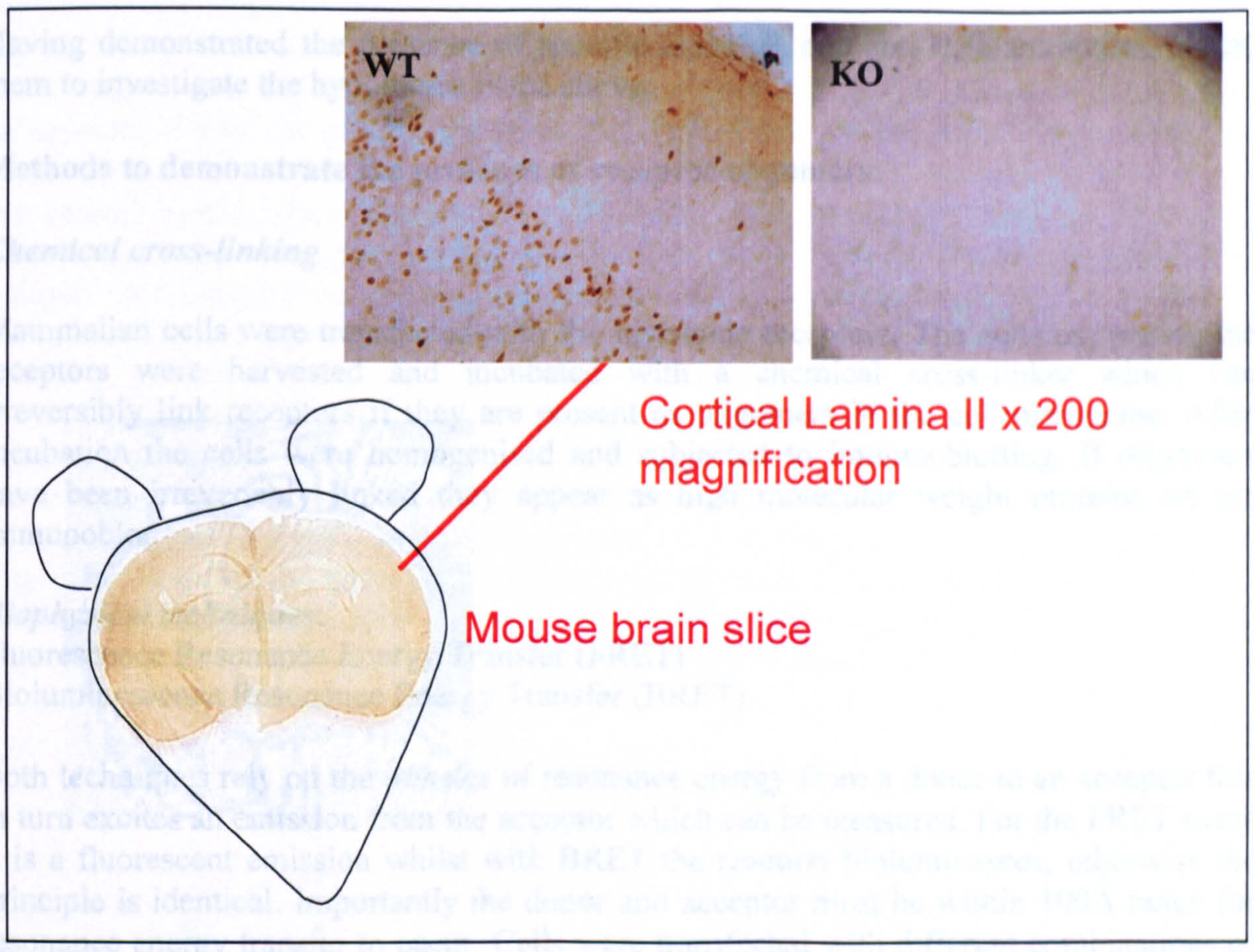

Fig 10 Immunohistochemistry on mouse brain slice. Anti-H_3Receptor antibody in Wild Type (WT) and H_3 Knockout (KO) Mouse Brain.

The antibodies generated against the H_3 and H_4 receptors were both able to reliably detect their respective receptors in immunoblots of recombinant and native tissue, and they worked well for immunohistochemistry. The anti-H_4 antibody was also tested using a technique called immunoprecipitation, described below.

Immunoprecipitation to confirm H_4R selectivity of the antibody

Mammalian cells are transfected with a histamine receptor labelled with a special tag called haemagglutinin (HA). The cells are homogenised and the proteins solubilised. The solubilised proteins are then mixed with anti-HA antibodies which bind to the HA-H_4 receptor. The protein mixture was then passed over special beads which only pulled out of solution antibody together with the proteins bound to that antibody. Proteins which do not have antibody bound to them will **not** be isolated in this way. The HA-H_4R was then eluted from the beads and subjected to immunoblotting where the protein is run out on a polyacrylamide gel and transferred to a nitrocellulose sheet as described above. Our new anti-H_4R antibody was used to test whether it could identify the HA- H_4R on the nitrocellulose paper.

Having demonstrated the presence of specific anti-H_3R and anti-H_4R antibodies, I used them to investigate the hypotheses listed above.

Methods to demonstrate the presence of receptor oligomers:

Chemical cross-linking

Mammalian cells were transfected with the histamine receptors. The cells expressing the receptors were harvested and incubated with a chemical cross-linker which can irreversibly link receptors if they are present as oligomers in the cell membrane. After incubation the cells were homogenised and subjected to immunoblotting. If oligomers have been irreversibly linked they appear as high molecular weight proteins on the immunoblot.

Biophysical techniques:
Fluorescence Resonance Energy Transfer (FRET)
Bioluminescence Resonance Energy Transfer (BRET)

Both techniques rely on the transfer of resonance energy from a donor to an acceptor this in turn excites an emission from the acceptor which can be measured. For the FRET assay it is a fluorescent emission whilst with BRET the reaction bioluminesces, otherwise the principle is identical. Importantly the donor and acceptor must be within 100Å range for resonance energy transfer to occur. Cells were transfected with different combinations of histamine receptors, either the full length receptors alone or the full length receptor together with one of the other isoforms. The receptors were differently labelled one with a donor and the other with an acceptor. Excitation of the donor generates resonance energy which can be transferred to the acceptor providing the two receptors are close enough together in the membrane (ie within 100Å range). Therefore a FRET or BRET signal will only be detected if the receptors are present as oligomers.

Nickel Column Purification

Cells were transfected with equal amounts of histamine receptors artificially tagged with either haemagglutinin (HA) or histidine (HIS). The cells were homogenised and passed over nickel beads in a column. The HIS tagged receptors were isolated on the nickel column because nickel binds strongly to histidine. If HA tagged receptors are found in the fraction immobilised on the nickel beads this will confirm the existence of HIS-H_4R/HA-H_4R oligomers.

Methods to test whether shorter isoforms can influence the full length receptors:

Saturation Binding

Here cells transfected with histamine receptors were incubated with increasing concentrations of radiolabelled histamine which is the natural ligand that binds to the

receptor in the brain. Modern drugs which target GPCRs can be thought of as synthetic ligands which manipulate the receptor in a beneficial way. Drugs which bind and activate the receptor, are called agonists, whilst those that block the receptor are termed antagonists. Some compounds do more than just block the receptor. Many receptors, including the H_3R, show some baseline (or constitutive) activity even in the absence of the natural ligand. Many compounds previously called antagonists are now known to actually decrease this constitutive activity and are known as inverse-agonists. The radiolabelled ligand I used was an antagonist called clobenpropit. It is best to use an antagonist for this type of experiment because antagonists bind to the receptor without affecting its activity. In the presence of increasing concentrations of clobenpropit increasing amounts will be bound which can be tracked by measuring the radioactivity in the samples. Eventually there is a point at which no more ligand can be bound because all the receptors are saturated (Fig 11). I used saturation binding to find out whether binding of ligand to the full length receptor could be affected by the presence of a shorter isoform. Therefore I carried out three assays in parallel: one with cells expressing the full length isoform alone, one with cells expressing the shorter isoform alone, and one with cells expressing both the full length and the shorter isoform together.

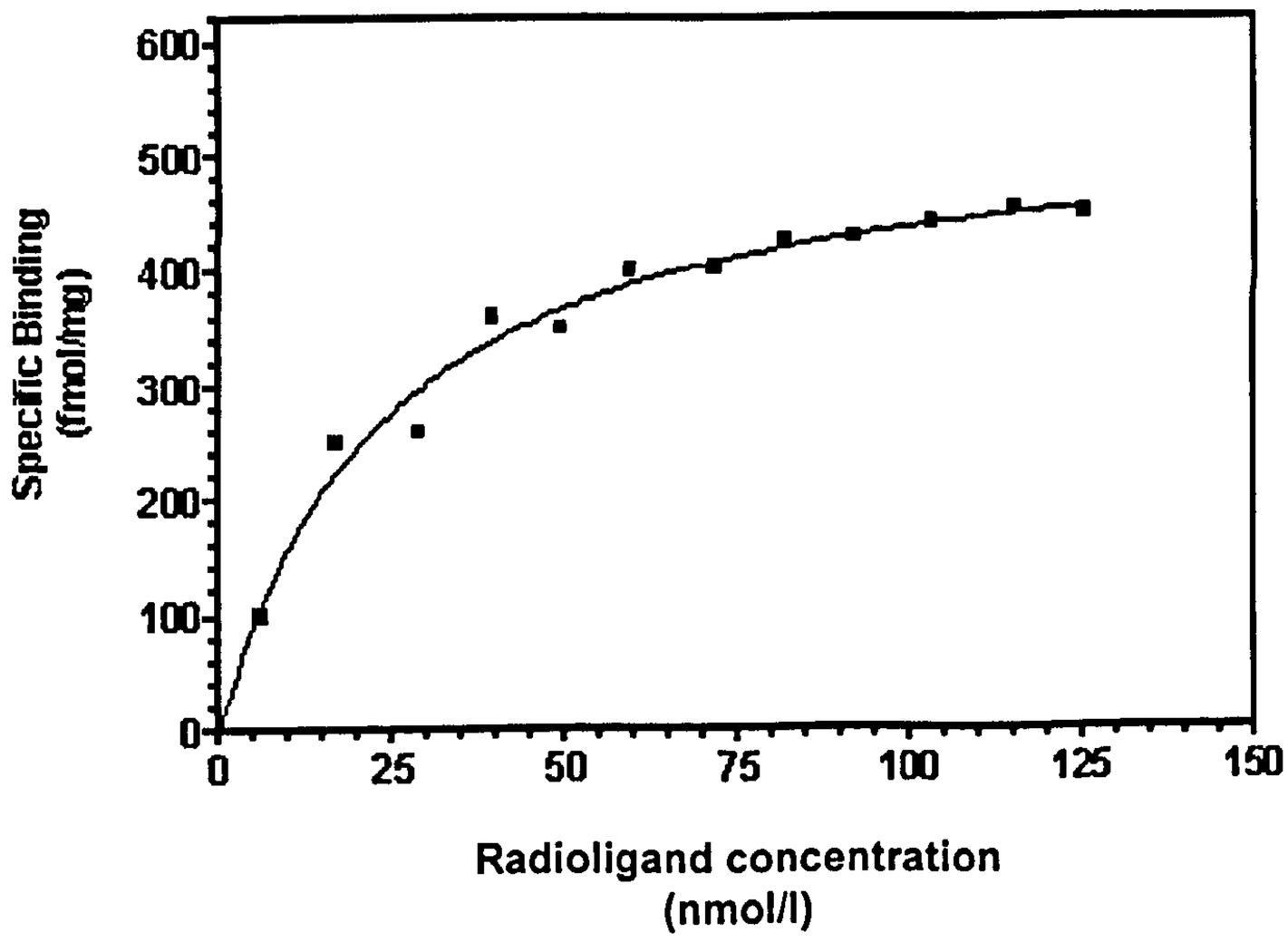

Fig 11 Saturation binding curve.

I also carried out total binding experiments on cells expressing histamine receptors which had been cultured in the presence of an antibiotic called tunicamycin. Tunicamycin inhibits receptor glycosylation. I wanted to find out whether glycosylation was necessary for ligand binding.

Surface biotinylation

This technique is used to compare how much receptor is present on the cell surface, and therefore available for ligand binding, and how much is inside the cell. Cells expressing histamine receptors were incubated in the presence of biotin (biotin is another name for the vitamin B7, here it is being used merely as a way of tagging cell surface proteins). Receptors inside the cell are not accessible to the biotin, therefore they will remain untagged. Next the cells are broken up and homogenised so that the surface receptors and the ones from inside the cell (the intracellular fraction) are all mixed up. The receptors from the surface can be separated from the intracellular fraction using beads coated with streptavidin. Streptavidin is a protein purified from *Streptomyces avidinii* that binds very tightly to the biotin. This is one of the strongest biological interactions known, and is widely taken advantage of in scientific laboratories for separating biotin labelled proteins from a mixture. In this way two different fractions are obtained one containing the surface receptors and one with the intracellular receptors. These are run out on a gel and visualised by immunoblotting in the usual way. I used this method to find out whether the amount of full length H_4R expressed at the cell surface was altered in cells transfected with the full length receptor plus one of the other truncated isoforms. This would shed light on a possible role for the shorter isoforms in regulating the amount of full length receptor available for ligand binding.

Methods to investigate whether receptors have to be glycosylated in order to form oligomers or bind ligand:

Inhibiting glycosylation

As described above receptor glycosylation can be inhibited by growing cells transfected with histamine receptors in the presence of an antibiotic called tunicamycin.

Deglycosylating mature histamine receptors

Mature receptors which are already glycosylated can be deglycosylated by treatment with an enzyme called PNGase F.

Receptors which were not glycosylated (either by preventing glycosylation or by removing sugar groups from mature receptors) were analysed by immunoblotting to find out whether oligomers were still present. In addition ligand binding experiments were carried out on unglycosylated H_3 receptors to see whether they were still able to bind ligand.

Often a number of different techniques were used to ask the same question. This is because my experimental systems are artificial, therefore the results from these experiments may not reflect what happens in a whole animal. For example, we often make use of artificially tagged receptors, and these tags may interfere with the normal functioning of the receptor. One can be more confident of a hypotheses being correct if it is supported by data from a number of different approaches.

Findings

1) Human H_3 and H_4 receptors are able to homo-oligomerise

Cross-linking experiments have confirmed the presence of homo-oligomers for human and rodent H_3R and human H_4R. Importantly these receptor oligomers were evident in native tissue as well as in the artificial recombinant expression system. In fact the H_3R was mainly found as oligomers in native tissue, similarly for endogenous H_4R (that is for H_4R in real tissue) oligomeric receptors were predominant. There is an indication that some isoforms may have a greater potential to oligomerise than others. Results suggested that the H_3 (329) formed homo-oligomers more readily than the H_3 (445). The cross-linking evidence was corroborated by FRET data for the H_3R, and by both nickel column purification and BRET assay in the case of the H_4R.

2) Human H_3 and H_4 receptors are able to hetero-oligomerise with their respective isoforms

FRET experiments also provided evidence for the existence of hetero-oligomers: oligimers consisting of the full length receptor with a shorter isoform.

Histamine H_3 and H_4 receptors are therefore able to form both homo- and hetero-oligomers. These appear to be robust, stable oligomers and histamine is not necessary for their formation.

3) Shorter isoforms can influence how the full length human H_3 and H_4 receptors work

The shorter isoforms can regulate their full length counterparts. The H_3 isoforms have different distribution patterns within the brain, however in some brain regions several variants are expressed together, therefore they could influence one another. The 445 and 329 isoforms are co-expressed in key locations including the basal ganglia, which are very important in voluntary movement. Although the 329 isoform did not itself bind the radiolabelled ligand used for saturation binding, it did dramatically reduce binding of this ligand to the full length 445 receptor. (Some of the controls in these binding experiments showed an unacceptably high background so this particular set of experiments needs to be repeated and the results verified before we can be truly confident that we are seeing a real effect.)

Message coding for all three H_4R isoforms is found in different types of white blood cell. Neither of the truncated H_4 isoforms can bind or transduce a signal. On co-expression with the full length H_4 (390) receptor the number of histamine binding sites is reduced by 55% (390 + 302 isoform) and 30% (390 + 67 isoform). The effect of the two truncated isoforms on surface expression of the full length receptor was investigated using the surface biotinylation technique. Results confirmed that the (302) and (67) isoforms decreased the surface expression of the H_4 (390) in line with the histamine binding data.

Therefore although the shorter isoforms are non-functional in regard to ligand binding and signalling they appear to have a role in regulating the activity of the full length receptors.

4) N-glycosylation is a prerequisite for receptor oligomerisation

Histamine H_3 and H_4 receptors were expressed in mammalian cells in the presence of the glycosylation inhibitor tunicamycin. Immunoblot analysis of cell homogenates confirmed that both receptors were indeed glycosylated. Furthermore inhibition of glycosylation did not remove receptor oligomers. For the H_4R deglycosylation of mature receptors using PNGase F enzyme was also undertaken. Deglycosylation did not remove receptor oligomers in either a recombinant expression system or in native tissue. However there was some indication that glycosylation may help to stabilise receptor dimers. Interestingly the molecular weights of bands seen in spleen lysates suggested that in this particular tissue H_4R receptors may not be glycosylated. For the H_3 receptor near complete prevention of glycosylation had no significant effect on radioligand binding and complete inhibition saw only a modest reduction.

In conclusion N-glycosylation is **NOT** a prerequisite for receptor dimerisation for either the H_3 or H_4 receptor. H_4 receptors might be glycosylated to varying degrees in different tissues. In the case of the H_3 receptor preventing glycosylation has only a very modest effect on ligand binding to the receptor.

5) Both H_3 and H_4 receptors are present in human brain where they serve distinct functions

As well as histamine H_3 receptors, we have been amongst the first to report that histamine H_4 receptors are also present in human brain material. The two receptors have different distribution patterns within the brain suggesting that they are doing different things. Importantly, in collaboration with a team in New Zealand, we have been the first to prove that the brain H_4 receptors are definitely working because H_4 specific drugs can affect nerve cell output from brain regions expressing the receptor.

While the H_3 and H_4 histamine receptors clearly have potential as therapeutic targets, predicting the likely effect of any new drug is difficult in the face of the complexity found both within and across different animal species. The work described in this thesis has furthered understanding of the two most recently described histamine receptors - where they are found and how they work. These are preliminary studies which will need to be extended to investigate the full range of receptor isoforms, how they are distributed within different brain areas, their molecular characteristics and how they interact with other cell components. Advances in molecular biology are enabling scientists to unravel complex systems in minute detail, and the detail itself is intriguing. However, it is essential not to lose sight of the relevance of all this to the workings of the whole animal. Advances which can transfer to the clinic will be the result of a combined effort from the fields of molecular biology, chemistry, pharmacology, animal behaviour and medicine.